2019

Old Dye, New Tricks – Diversity-Oriented Synthesis of Heterocycles from Cascade Reactions of Indigo

Nicholas Matthew Butler
University of Wollongong

UNIVERSITY OF WOLLONGONG AUSTRALIA

Old Dye, New Tricks – Diversity-Oriented Synthesis of Heterocycles from Cascade Reactions of Indigo

Nicholas Matthew Butler
Intl. B. Sc. (Hons.)

Supervisors:

Prof. Paul A. Keller
Dr. Christopher J. T. Hyland

This thesis is presented as part of the requirement for the conferral of the degree:

Doctor of Philosophy

from

The University of Wollongong
School of Chemistry and Molecular Biosciences

This research has been conducted with the support of the Australian Government Research Training Program Scholarship

March 2019

Certification

I, Nicholas Matthew Butler, declare that this thesis, submitted in fulfilment of the requirements for the conferral of the degree of Doctor of Philosophy from the University of Wollongong, is wholly my own work unless otherwise referenced or acknowledged. This document has not been submitted for qualifications at any other academic institution.

_____

Nicholas Matthew Butler
31st March, 2019

Publications

Smyth, J.E.; Butler, N.M.; and Keller, P.A. 'A twist of nature – the significance of atropisomers in biological systems.' *Nat. Prod. Rep.*, 2015, **32**, 1562-1583.

Butler, N.M.; Hendra, R.; Bremner, J.B.; Willis, A.C.; Lucantoni, L.; Avery, V.M.; and Keller, P.A. 'Cascade reactions of indigo with oxiranes and aziridines: efficient access to dihydropyrazinodiindoles and spiro-oxazocinodiindoles.' *Org. Biomol. Chem.* 2018, **16**, 6006-6016.

Keller, P.A.; Butler, N.M.; and McCosker, P.M. 'Chapter 9: Axially Chiral Natural Products and Bioactive Compounds' in Lassaletta, J.M. (Eds.), *Atropisomerism and Axial Chirality* (In Press), World Scientific Publishing (Singapore), 2019. ISBN 978-1-78634-645-2.

Butler, N.M.; Bremner, J.B.; Willis, A.C.; Lucantoni, L.; Avery, V.M.; and Keller, P.A. 'Desymmetrisation reactions of indigo with Grignard reagents for the synthesis of selective antiplasmodial [1*H*,3'*H*]-3-aryl-2,2'-diindol-3'-ones.' *Submitted*, 2019.

McCosker, P.M.; Butler N.M.; Shakoori, A.; Bremner, J.B.; Willis, A.C.; Haritakun, R.; and Keller, P.A. 'Further exploration of the heterocyclic diversity accessible from the propargylation chemistry of indigo.' *Manuscript in preparation*, 2019.

Butler N.M.; Shakoori, A.; Bremner, J.B.; and Keller, P.A. 'The purple patch – the chemistry of indigo through the ages.' *Review in preparation*, 2019.

Abstract

A diversity-oriented investigation of the chemical space associated with the ancient blue dye, indigo (**31**), was undertaken, investigating its reactivity with a variety of coupling partners, namely terminally-substituted (aryl)propargylic halides, various ring-strained epoxides and aziridines, and substituted organometallic reagents.

The reaction of indigo with 3-bromo-1-phenyl-1-propyne (**132b**) gave the new ring-expanded indolobenzonaphthryidinone **133** in 35% yield, in addition to the known azepinodiindole **122** in an improved 37% yield, and the suspected oxadiazepinodiindole **123** in 12% yield. The (4-methoxyphenyl)propargyl bromide **132a** also yielded an analogous ring-expanded indolobenzonaphthryidinone (**134**) in 21% yield. The isolation of this pair of molecules supports the hypothesis that the stronger bromide facilitates *di*-alkylation prior to *N,N′*-cyclisation, leading to increase proportions of ring-expanded materials which were subjected to biological testing.

The optimized reaction of indigo with (*S*)-epichlorohydrin (**144**) gave a mixture of the *N,N′*-cyclic pyrazinodiindole **152**, and the *N,O′*-cyclised epoxyoxazocinodiindoles **153-155** in 95% overall yield, while the reaction of indigo with the corresponding (*R*)-*N*-tosyl-2-(chloromethyl)aziridine **148** (synthesized in 3 steps from **144**) afforded exclusively the *N,N′*-cyclic pyrazinodiindoles **176-178** in a combined 63% yield. Mechanistic studies revealed that both the leaving group and the heteroatom had a significant effect on the reaction pathway, with bioxirane **149** leading exclusively to *N,O′*-cyclisation in 81% yield, while epoxides bearing strong leaving groups (**145-146**) and biaziridine **150** yielded exclusively products of *N,N′*-cyclisation in 76-93% yield. These cascade reactions proceeded without erosion of the stereochemical identity of their precursor epoxides or aziridines, allowing stereospecific access to a variety of new heterocyclic frameworks whose biological applications were then assessed.

A new methodology for the generation of non-symmetrical [1*H*,3'*H*]-3-substituted-2,2'-diindol-3'-ones was devised from a two-step addition-dehydration reaction of indigo with various Grignard reagents. Where only three examples of this scaffold had been reported previously, this method allowed chemoselective access to twenty-seven new members of this class of molecules in yields ranging 72-95%, as well as a previously-unknown 1'*H*,1''*H*,3*H*-[2,2':3',5''-terindol]-3-one in 61% yield by NMR. Using Boc_2O as a both a dehydrating and *N*-trapping agent, fifteen examples featuring alkyl, aryl, and heterocyclic substituents, of which eleven *N*-Boc materials were successfully deprotected to their free

indoles using TFA under standard conditions. Additionally, the methyl adduct **218** was isolated by a $PPh_3.I_2$-mediated dehydration in 74% yield, where Boc_2O had failed, and the collected twelve final compounds (in addition to selected *N*-Boc precursors) were subjected to biological testing.

Preliminary antiplasmodial screening of all generated final compounds revealed potent and selective *P. falciparum* inhibition down to 76 nM for **152**, and 52 nM for **218**, with SI values >100 for **152** and >1500 for **218**, making these scaffolds viable leads for further medicinal chemistry studies. A mode of action for **218** was proposed, where it undergoes hypoxia-induced reduction in parasitised erythrocytes to an active radical species, which is in agreement with previous mechanistic studies of 2-substituted-3*H*-indol-3-ones, and the preliminary SAR data from this molecule library.

Acknowledgments

Special thanks go to my supervisors, Prof. Paul Keller, and Dr. Chris Hyland for their training, mentoring and guidance over the past few years of my life, and to Dr. Steven Wales, Prof. John Bremner, and Dr. Alireza Shakoori for their valuable chemical insight. Thanks to the past and present members of the Keller research group, particularly to Jayden Gaston, Patrick McCosker, Hendris Wongso, Dr. Andrew Tague and Dr. Rudi Hendra for making a run-down, depressing building a fun place to work. Special and sincerest thanks also to the School of Chemistry at large, especially (but not limited to) Jamie Smyth, Anthony Carroll, Brett Knowles and Melanie Drew for games, drinks, and other chaos.

Special thanks to A/Prof. Glennys O'Brien, A/Prof. Michael Kelso, A/Prof. Stephen Wilson, A/Prof. Clare Murphy and Prof. Stephen Pyne for teaching opportunities throughout my PhD, and to Louisa Willdin for running the whole show.

Thanks to all technical staff for training and their maintenance of all of the ludicrously-expensive pieces of equipment we all take for granted, especially to Wilford Lie and Din Idris (NMR), Karin Maxwell, Celine Kelso and Alan Maccarone (LR-MS and HR-MS), and to Roza Dimeska, Roger Kanitz, Travis Naylor, Cathy Lancaster, Sue Butler, and Joe Daunt for their assistance with teaching. Special thanks also go to Dr. Anthony Willis (ANU) for his assistance with x-ray crystallography, and to Prof. Vicky Avery and Dr. Leo Lucantoni (Griffith University) for performing the antiplasmodial testing on all of my final compounds.

To my mum Julie, my dad Greg, and my brother Josh, for putting up with everything.

Finally, special thanks go to Erin and the Final Five for giving me a place to get away from it all. I would have burned out years ago if not for you and I love you all.

This thesis is dedicated to you all, and to Melissa, Ted, Sue, and everyone else who has had to deal with that bastard of a disease and everything that it brings.

List of Abbreviations

^{1}H NMR	Proton Nuclear Magnetic Resonance Spectroscopy
^{13}C NMR	Carbon-13 Nuclear Magnetic Resonance Spectroscopy
˚C	Degrees Celsius
Ac	Acetyl/Acetate
app (NMR)	Apparent
APT (NMR)	Attached Proton Test
Ar	Aryl
Bn	Benzyl
Boc	*tert*-butoxycarbonyl
n-Bu	*n*-Butyl
bs (NMR)	Broad singlet
δ (NMR)	Chemical shift
d (NMR)	Doublet
dd (NMR)	Doublet-of-doublets
DEPT (NMR)	Distortionless Enhancement of Polarisation Transfer
DMF	*N,N'*-dimethylformamide
DMSO	Dimethyl sulfoxide
e.g.	*Exempli gratia* – "for example"
EI-MS	Electron-impact mass spectrometry
eq.	Equivalent(s)
ESI-MS	Electrospray ionisation mass spectrometry
g	Gram(s)
h	Hour(s)
H2BC (NMR)	Heteronuclear 2-Bond Correlation Spectroscopy
HMBC (NMR)	Heteronuclear Multiple-Bond Correlation Spectroscopy
HSQC (NMR)	Heteronuclear Single-Quantum Correlation Spectroscopy
HPLC	High-Performance Liquid Chromatography
HR	High-Resolution
Hz (NMR)	Hertz
IC_{50}	Median Inhibitory Concentration
i-Pr	Isopropyl

J (NMR)	Coupling Constant
μM	Micromolar ($\times 10^{-6}$ mol/L)
Mmol	Millimole(s)
m (NMR)	Multiplet
m (IR)	Medium
M^+	Molecular Ion
Me	Methyl
mg	Milligram(s)
MIC	Minimum Inhibitory Concentration
Min	Minute(s)
mL	Millilitre(s)
Mol	Mole(s)
m/z	Mass-to-Charge Ratio
NOESY (NMR)	Nuclear Overhauser Effect Spectroscopy
nm	Nanometres
nM	Nanomolar – ($\times 10^{-6}$ mol/L)
Ms	Methanesulfonyl – "Mesyl/mesylate"
Pet Spirit	Petroleum spirit (40–60 ˚C)
Ph	Phenyl
ppm	Parts-per-million
q (NMR)	Quartet
ROESY (NMR)	Rotating-Frame Overhauser Effect Spectroscopy
s (NMR)	Singlet
s (IR)	Strong
SAR	Structure-Activity Relationship
SI	Selectivity Index
t (NMR)	Triplet
THF	Tetrahydrofuran
TLC	Thin-Layer Chromatography
TOCSY (NMR)	Total Correlation Spectroscopy
Ts	*p*-Toluenesulfonyl – "Tosyl/tosylate"
TMS (NMR)	Tetramethylsilane
TMS	Trimethylsilyl

Table of Contents

Chapter 1:
Introduction

1.1 The role of nature in modern synthetic chemistry

The design and synthesis of small-molecule inhibitors has long been at the forefront of modern drug discovery and medicinal chemistry efforts. Classically, many of these molecules have been derived from Nature, which remains an indispensable tool for the health and pharmaceutical industries. Examples range from the relatively-simple salicylates (**1**), derived from pulverised willow bark,[1] to the more complex polycyclic opioids such as morphine (**2**), derived from the dried latex of *Papaver somniferum* bulbs,[2] to the large and highly-complex vancomycin (**3**), derived from *Amycolatopsis orientalis* (formerly *Streptomyces orientalis*),[3] and used as an antibiotic of last-resort for the treatment of drug-resistant infections (Figure 1). The innate specificity of Nature in the design of highly-complex, three-dimensional molecules cannot be overstated, and remains a constant source of inspiration for the synthetic chemist, however the need for large quantities of specific inhibitors means that relying on Nature alone may only afford milli- (or micro-)grams of materials from large scale extractions. One example of this is the isolation of the kinase inhibitor staurosporine (**4**), where only 1.1 g was isolated from a 200 L *Streptomyces staurosporius* broth (5.5 ppm/volume of culture).[4] A more extreme example is the marine sponge isolate muironolide A **(5)**,[5] of which only 97 μg could be isolated from an individual *Phorbas* sp. weighing 236 g (0.41 ppm/dry wt. sponge) – as an indicative figure, the isolation of one gram of muironolide A would require the extraction of over 2.4 tonnes of dry sponge material. It is therefore imperative that new and accessible means are developed for both the discovery and synthesis of new, biologically-active molecules.

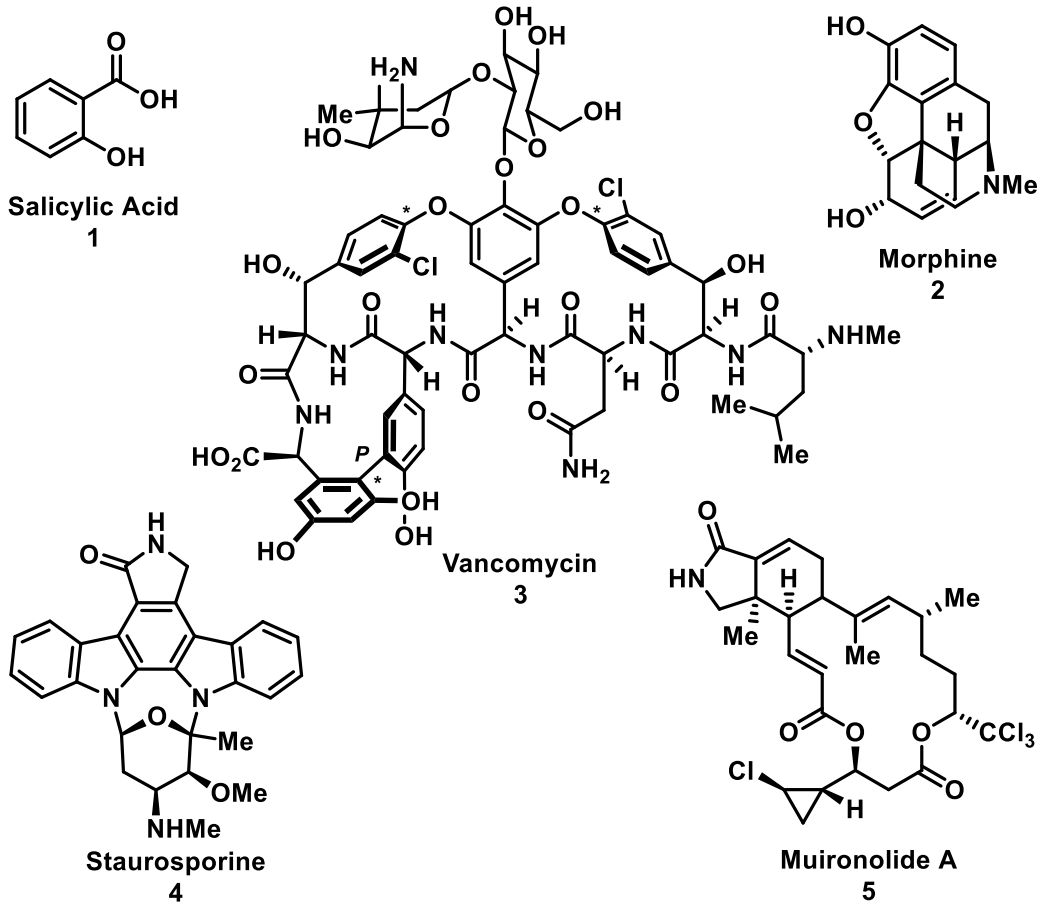

Figure 1: Selected bioactive natural products, salicyclic acid (**1**), morphine (**2**), vancomycin (**3**), stauorosporine (**4**), and muironolide A (**5**).

1.2 Target-oriented synthesis for drug discovery

The development of modern synthetic chemistry has grown upon retrosynthetic analysis, whereby a complex final product may be visualised as a series of 'disconnections' of individual fragments by simple bond-forming processes.[6] Continued disconnections, guided by simple chemical principles, allows for the design of a synthetic pathway in the forward direction, and in modern times is a process which may be automated for simple molecules.[7] These principles of target-oriented synthesis (TOS) are based on the concept of 'ideality' in chemical synthesis, first coined by Hendrickson in 1975, and refers to the minimisation of unnecessary chemical processes, such as those involving protecting groups, extraneous redox or functional group manipulations, and correction of undesired stereochemistry.[8] In short, an 'ideal' synthesis would afford "…a complex molecule from...available small molecules…in a sequence of only construction reactions involving no intermediary re-functionalisations." While an imperfect metric for the evaluation of synthetic worth (i.e. it does not consider the synthetic feasibility of particular

transformations, instead relying on a mathematical step-count), it informs a *prima facie* comparison between synthetic pathways. For example, in the synthesis of the polyketide marine natural product brevetoxin B (**6**), a comparison of the step count for the first-generation synthesis (Nicolaou *et al*, 1995 – 123 steps),[9] and later synthetic strategies toward its construction (Nakata *et al*, 2004 – 90 steps),[10] would deem the latter process the more-ideal of the two – perhaps unsurprising, since the latter relies upon synthetic disconnections made in the former synthesis to complete the natural product, though with several modifications to the upfield synthesis of the key fragments (Scheme 1).

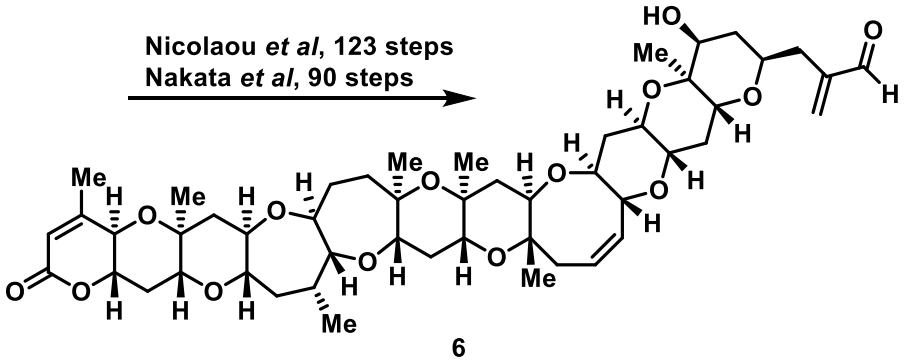

Scheme 1: Comparison of two syntheses of the marine natural product brevetoxin B (**6**) by the Nicolaou and Nakata groups.

This approach is not without its drawbacks. While the synthesis proved an herculean effort, and resulted in the development of numerous new synthetic transformations, the original Nicolaou synthesis of brevetoxin B amounted to an investment of twelve years of intensive study,[11] and resulted in the isolation of just 4.8 mg of material, in an overall process yield of 9.2×10^{-4}% due to the number of physical manipulations required. It is therefore clear that while contiguous step-wise transformations do allow access to highly complex polycyclic molecules, linear TOS does not outright solve the problems of scalability and diversity, considering that modification to the core skeleton of the natural product would likely require years of investment, assuming the desired modifications do not interfere with other key steps further downstream. Moreover, this effectively limits the structural diversity of the molecules that are able to be synthesised in this manner, as they would represent analogues of scaffolds which have already been synthesised. With respect to the discovery of new molecules for medicinal application, it is simply not practicable to adopt a linear, target-oriented approach to synthesis for all desired molecules.

1.3 Diversity-oriented synthesis for drug discovery

There is a growing appreciation for a diversity-based approach to drug discovery (diversity-oriented synthesis, DOS), particularly where the precise identity of the target is not of critical importance e.g. in medicinal or materials applications.[12] In comparison to a traditional target-based synthetic methodology, where a single precise chemical architecture is the focus, DOS aims to generate a library of diverse chemical species for rapid scaffold discovery, which may be then iteratively modified based upon the desired characteristics for the particular application, for example, in high-throughput biological screening.[13] As an orthogonal approach to TOS, DOS utilises a forward-planning approach, whereby simple molecules may be iteratively combined across multiple (usually no more than five) steps, with the aim of developing a library made up of compounds of varied frameworks and functionalities (Figure 2).

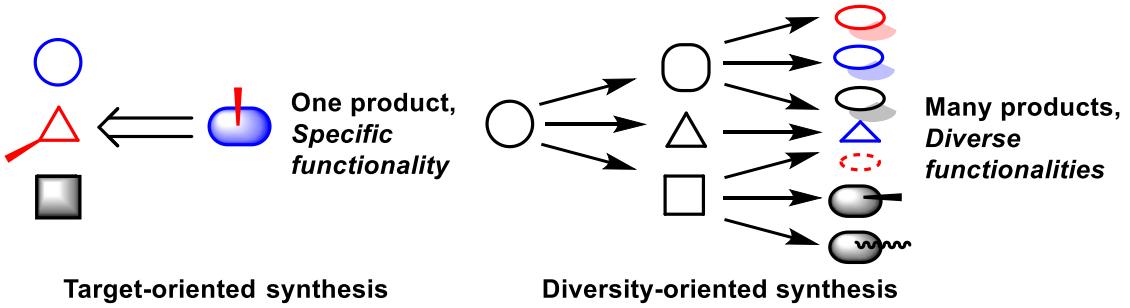

Figure 2: Comparison of the overall rationale of target-oriented (left) and diversity-oriented (right) synthesis.

The major advantage to diversity-oriented synthesis is that the process relies on coupling each fragment together iteratively, thereby allowing a vast window for derivatisation at each of the individual stages. Considering a hypothetical starting point of a single molecule, and utilising three iterative stages of 20 derivatives at each stage, this would constitute a library of up to 8,000 final compounds, which are themselves only three synthetic steps from the starting molecule but diverse in functionality. The major disadvantages of DOS are practicality, for in order for this to be a successful means of generating molecule libraries, each stage must involve reactions which must be robust and produce only the desired product with no by-products, as the necessity of intermediate purification would make this diversity-oriented process exponentially more time-consuming with each iteration. This requirement leads to a second disadvantage, owing to the scarcity of 'perfect' reactions, meaning that only specific transformations can realistically be performed in the search of diversity – thus limiting the idea of 'diversity' in the first instance. This combined with the predisposition of synthetic chemists toward

well-behaved, accessible starting materials (or privileged scaffolds as starting points)[14] leads to selection bias, and narrowing of the overall chemical diversity of the library. This is illustrated by analysis of a random selection of 'diverse' molecules, deemed to be largely comprised of products from amide coupling and Suzuki-Miyaura reactions,[15] and containing greater proportions of *para*- substituted phenyl substituents (particularly those with *para*-chloro-, fluoro-, or trifluoromethyl groups) than other substituent patterns.[16] Particularly in the case of reaction discrimination, this may result in an overall narrowing of the accessible chemical space than is idealised for diversity-oriented synthesis. Finally, a common criticism of a DOS approach is that while generating large libraries leads to greater statistical chance of identifying a 'hit', there is no overall guarantee that the generated molecule library will contain any viable leads to begin with, and may instead result in 8,000 individual iterations of how best to generate inactive molecules.

One means by which these issues may be circumvented is through collaborative efforts such as those of the European Lead Factory project,[17] where a group of 30 institutions have worked cooperatively since the project's inception in 2013, with the aim of developing a vast library (consisting of *ca.* 326,000 molecules provided by the Joint European Compound Library, in addition to a further 200,000 new molecules synthesised as part of the project – a milestone reached in June of 2018) of potential leads, which can be assessed for 'lead-likeness' and structural diversity *via* computational means,[18] as well as through ultrahigh-throughput screening methods.[19] An early analysis of a selection of the library (*ca.* 55,000 compounds) revealed considerable structural and functional diversity within typical Lipinski's rule-of-five parameters,[20] expanding into a broad region of unexplored chemical space as denoted by a low Tanimoto coefficient of 0.2 (<20% inter-collection similarity) across these compounds, as well as retaining a high degree of sp^3 character (>40% sp^3 for 86% of the library) – a desirable characteristic for drug design and specificity.[21] The project has utilised a series of methodologies, broadly classified as multicomponent reactions,[22] and divergent or combinatorial synthesis[23] to afford a broad variety of compounds – a small selection of which are depicted in Figure 3.

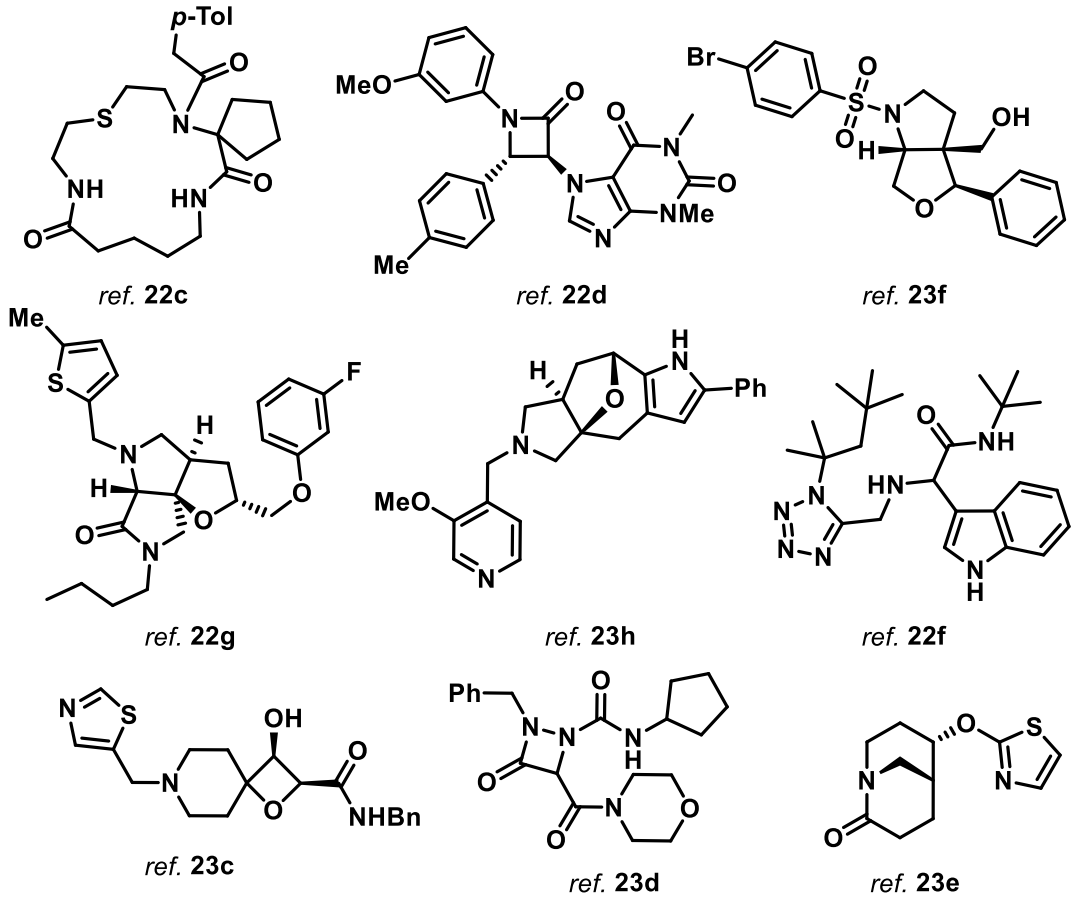

Figure 3: A selection of scaffolds synthesised as part of the European Lead Factory DOS project. References are as noted.

It is therefore the case that while 'perfect' diversity-oriented synthesis would provide significant benefits over target-oriented synthesis with respect to the rapid generation of chemical libraries, there exist significant barriers toward its widespread adoption as the major means of exploring new chemical space, which may be overcome by further exploration.

1.4 The role of cascade reactions in modern synthetic chemistry

The major pitfall for both target-oriented and diversity-oriented synthesis is the necessity of performing multiple sequential synthetic steps, most-often requiring purification of the intermediate product mixtures. While a not-insurmountable obstacle, it would be more convenient to perform multiple synthetic steps in a single reaction vessel, thus providing synthetic shortcuts to the desired architecture.[24] This demonstrates, in part, the power of cascade reactions for the construction of new molecular architectures, as they would serve to eliminate intermediate reaction steps entirely, making the overall start-to-finish process more efficient.[25] To re-invoke the idea of 'ideality' in organic synthesis,[8] cascade

reactions represent one logical endpoint, where entire processes can be circumvented, and multiple new bonds can be formed in a single reaction vessel, thus rapidly and efficiently building molecular complexity whilst eliminating intermediate isolation and purification procedures entirely.[26] In the context of current environmental concerns, cascade reactions could also offer a more environmentally-benign means of generating complex molecules, as they necessitate only a single solvent, reagent, and purification, compared with an equivalent bond-forming process over multiple sequential steps.

There are many classical examples (e.g. the Robinson 'double-Mannich' synthesis of tropinone)[27] of the use of cascade reactions as late-stage tools in synthesis, and these have been extensively-reviewed in the past.[24, 26a, 28] One particularly elegant example of the power of this approach is the Corey synthesis of the putative structure of the squalenoid natural product glabrescol (**7**), where a pentaoxirane precursor underwent Brønsted acid-mediated cyclisation with CSA (camphor-10-sulfonic acid) to afford the desired polyfuran scaffold in 31% yield (Scheme 2).[29] Based on these synthetic studies, the structure of glabrescol was revised to **8**, and confirmed by synthesis *via* a modified protocol, though this too relied on an electrophilic cascade reaction from a polyepoxide precursor.[30]

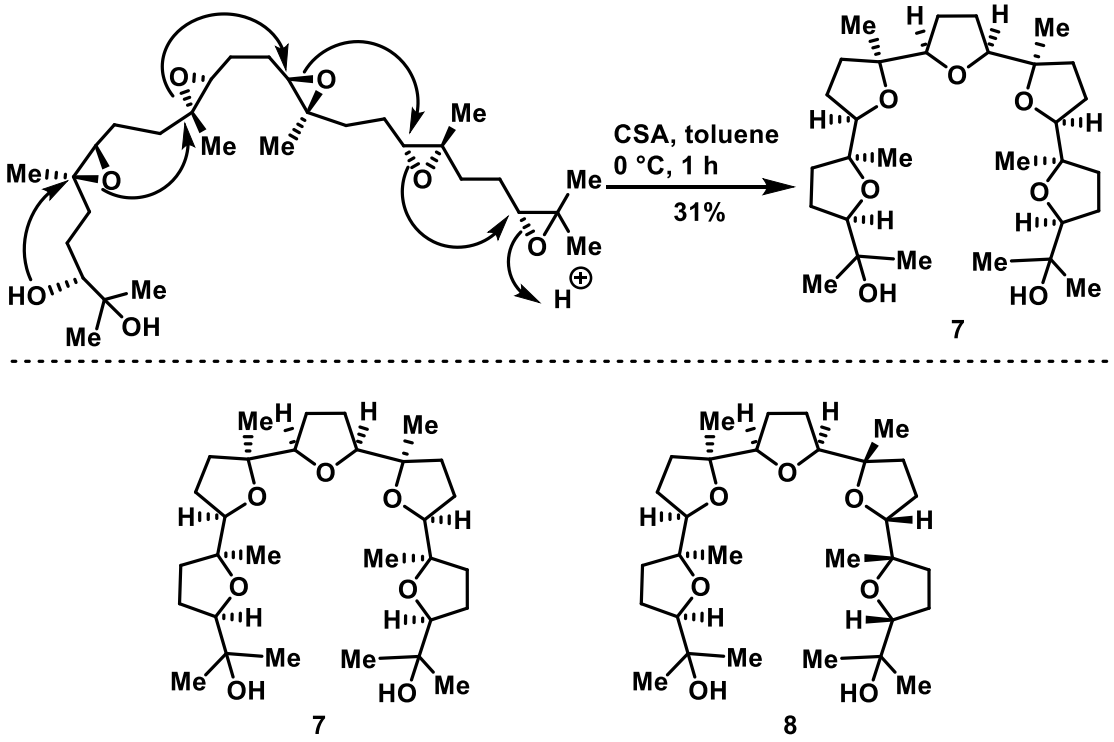

Scheme 2: Key cascade cyclisation from the Corey synthesis of the putative structure of glabrescol **7**, and the true structure of glabrescol (**8**) as confirmed by synthesis.

Cascade reactions can be broadly classified as following one of eight fundamental modes

of reactivity, as depicted in Table 1, where each sequential chemical transformation may be used as a means of discrimination. For the above example of the polycationic epoxide ring-opening to give polyfuran **7**, this could be classified as a **1a/2a/3a/4a/5a**-type cascade utilising this framework.[28a, 31]

Table 1: Classification of different types of cascade reactions. Adapted from Teitze.[28a]

First Step		Second Step		Third Step	
1a	Cationic	**2a**	Cationic	**3a**	Cationic
1b	Anionic	**2b**	Anionic	**3b**	Anionic
1c	Radical	**2c**	Radical	**3c**	Radical
1d	Pericyclic	**2d**	Pericyclic	**3d**	Pericyclic
1e	Photochemical	**2e**	Photochemical	**3e**	Photochemical
1f	Carbenoid	**2f**	Carbenoid	**3f**	Carbenoid
1g	Metal-catalysed	**2g**	Metal-catalysed	**3g**	Metal-catalysed
1h	Redox	**2h**	Redox	**3h**	Redox

This classification mode allows for modularity in describing cascade processes where the reactivity differs as the reaction proceeds. For the below example (Scheme 3), where an amine-mediated (ethylenediamine diacetate, EDDA) Knoevenagel condensation (anionic – **1b**) between Meldrum's acid (**9**) and *O*-prenylsalicylaldehyde (**10**) precedes a hetero-Diels Alder cyclisation (pericyclic – **2d**), to afford the fused-ring system **11** in 73% yield, and with >99% diastereoselectivity toward the *cis* diastereomer.[32]

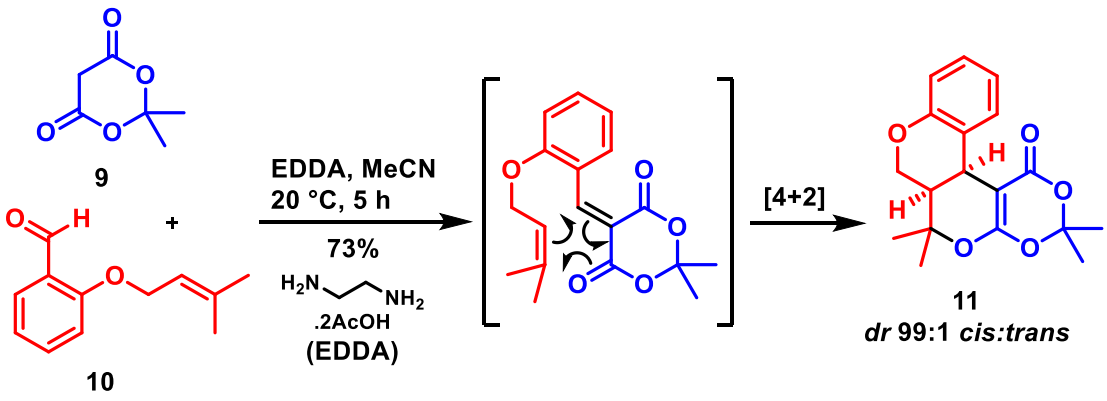

Scheme 3: Tandem Knoevenagel/hetero-Diels Alder cyclisation to produce **11** *via* a 1b/2d-type cascade reaction.

In more complex examples such as multicomponent reactions, several reagents may be combined to afford densely-functionalised systems. One key example of this is the Ugi reaction, which is typically accomplished between four coupling partners: an aldehyde or

ketone, an amine, an isocyanide, and a fourth variable component (typically a carboxylic acid, though this can be substituted for – among others – H_2O, H_2S, H_2Se, CO_2 and an alcohol, HN_3, HCNO, or HCNS).[33] A general schematic for the Ugi reaction is shown in Scheme 4.

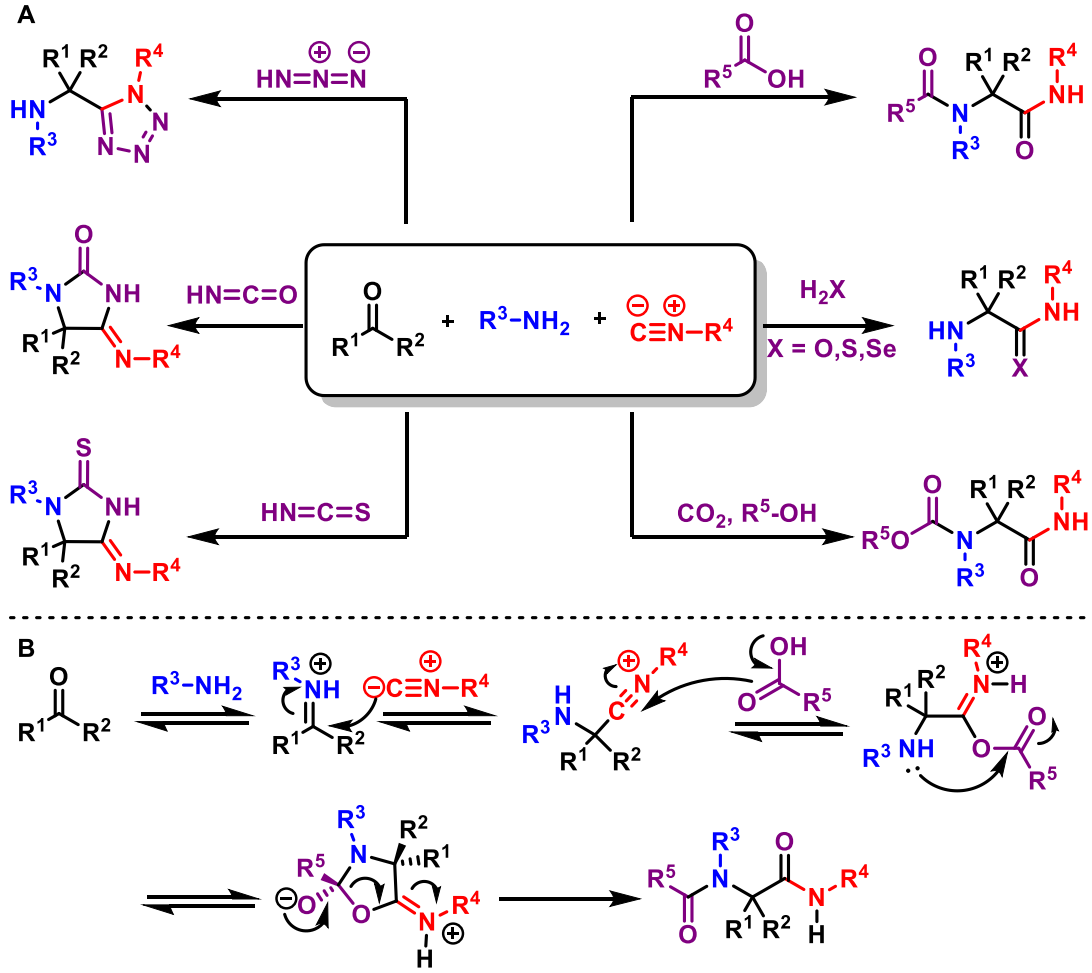

Scheme 4: The Ugi four-component reaction is one example of a cascade process with multiple coupling partners, and proceeds *via* a multi-step mechanism. General schematic and mechanism adapted from Kürti and Czacó.[34]

There are several factors to consider with the use of cascade reactions in synthesis. Cascade reactions typically require densely-functionalised starting materials, requiring multiple synthetic steps of pre-functionalisation. Additionally, as cascade reactions rely on the sequential participation of multiple functional groups, the desired product is typically only obtained in good yields where a) competing reactions are in equilibrium with the desired process (i.e. not irreversible), b) there is a considerable enthalpic or entropic benefit to the formation of the desired product, or c) where the final step in the cascade reaction is irreversible. This is exemplified in the Ugi reaction, where a) the formation of salts, hemiaminals, etc. are reversible, and b) acyl transfer occurs in the final

step to generate a pair of amide bonds – the stability of the dipeptide effectively rendering the final step irreversible. It is not to say that side-reactions can be eliminated entirely in all instances, and in many circumstances, multiple branches in the mechanism can result in undesired (or unexpected) products. Therefore, to effectively utilise cascade reactions for the construction of complex molecular frameworks, an intimate understanding of the underlying process and mechanism of the reaction must be present, as well as the desired starting point and products, to discern conditions most conducive to generating the desired endpoint.

1.5 Applications of cascade reactions to diversity-oriented and target-oriented synthesis

One of the key considerations in utilising cascade reactions as a means of either a) selectively generating the desired product *via* a TOS approach, or b) developing a library of compounds *via* a DOS approach, is the potential manipulations that are possible – ideally, the selected starting point would possess a variety of functional groups in close physical proximity, with the ability to undergo spontaneous further reactions upon addition of a second coupling partner. By moderating the coupling partners, or by using different chemical additives e.g. Lewis acids, it would therefore be possible to design specific cascade reactions to favour certain reactive pathways, and thus the formation of particular chemical scaffolds.

The application of cascade reactions to diversity-oriented synthesis is aptly demonstrated by the work of the Stockman group, where utilising the relatively-simple keto-diester **12** as the starting point, nucleophilic addition to the central ketone allowed for subsequent intramolecular cyclisation onto the outer α,β-unsaturated systems, forming a broad variety of cyclic adducts (**13**–**24**) *via* twelve unique reactive pathways, *via* both stepwise and concerted processes.[35] A summary of the major outcomes of this initial study is presented in Scheme 5.

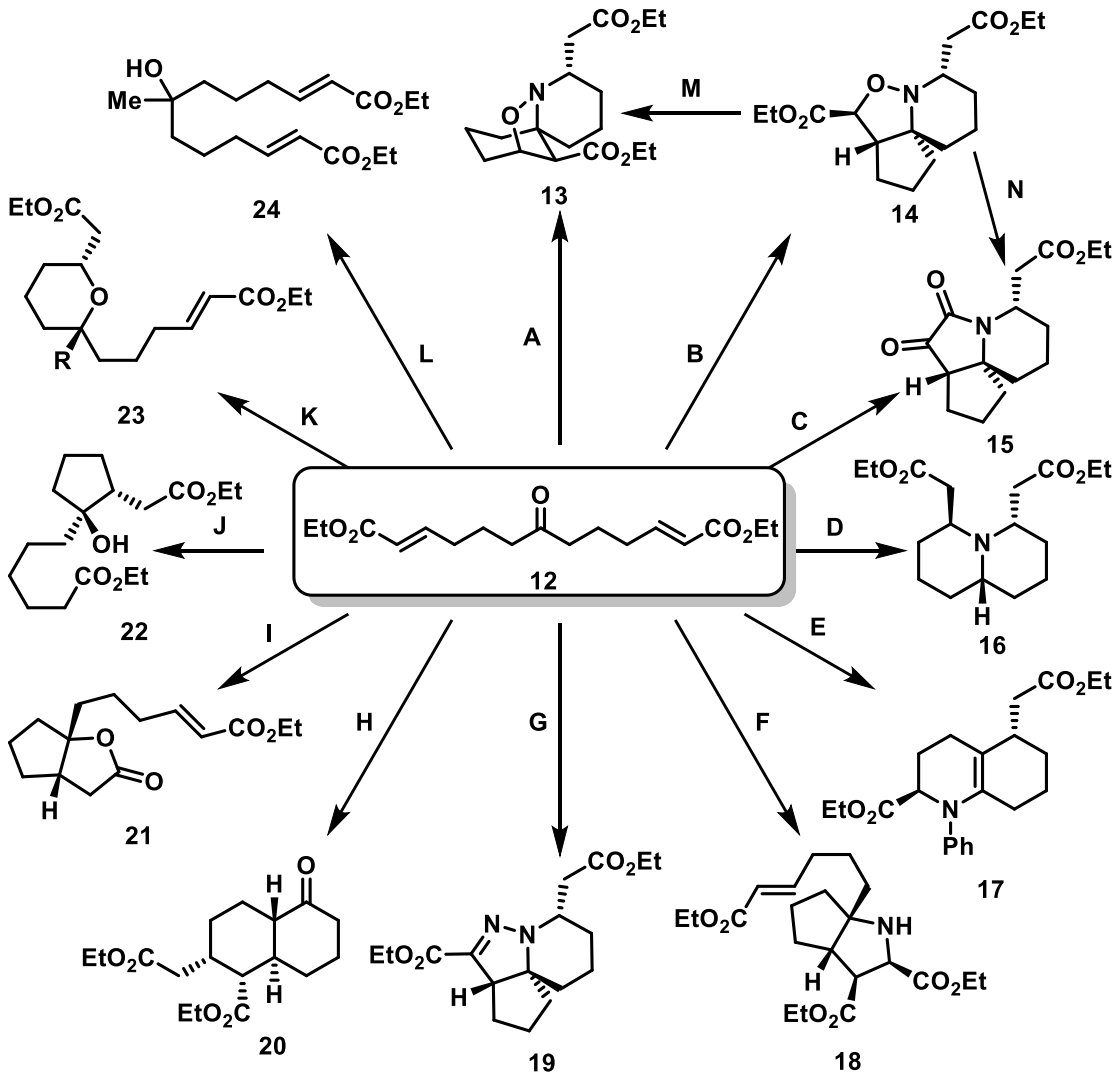

Scheme 5: Divergent synthesis of structurally-diverse products **13-24** *via* cascade reactions from common precursor **12**.

Spirocycles **13** and **14** were proposed to arise from a three-stage cascade process, where upon condensation of the central ketone with hydroxylamine, the oxime adduct underwent spontaneous Michael addition to forge the piperidine ring while generating an iminium-*N*-oxide 1,3-dipole. Subsequent nitrone [3+2]-cycloaddition to the remaining olefin gave either the *O*-internal (**13**) or *C*-internal (**14**) adducts. When oxime condensation was performed in the presence of NaOEt, compound *C*-internal adduct **14** underwent *N,O*-fragmentation and recombined to give lactone **15**,[36] while heating **14** in chlorobenzene led to the formation of *O*-internal product **13** *via* a retro-[3+2]/[3+2]

cycloaddition, indicating **14** to be the kinetic product, and **13** to be the thermodynamic product. This cascade/interconversion protocol could also be achieved utilising keto-dinitrile **25**, with the rearrangement of kinetic product **26** to thermodynamic product **27** occurring upon heating in toluene in a sealed tube, and was utilised in a short-step racemic synthesis of histrionicotoxin **28**, isolated originally from poison dart frogs (Scheme 6).[37]

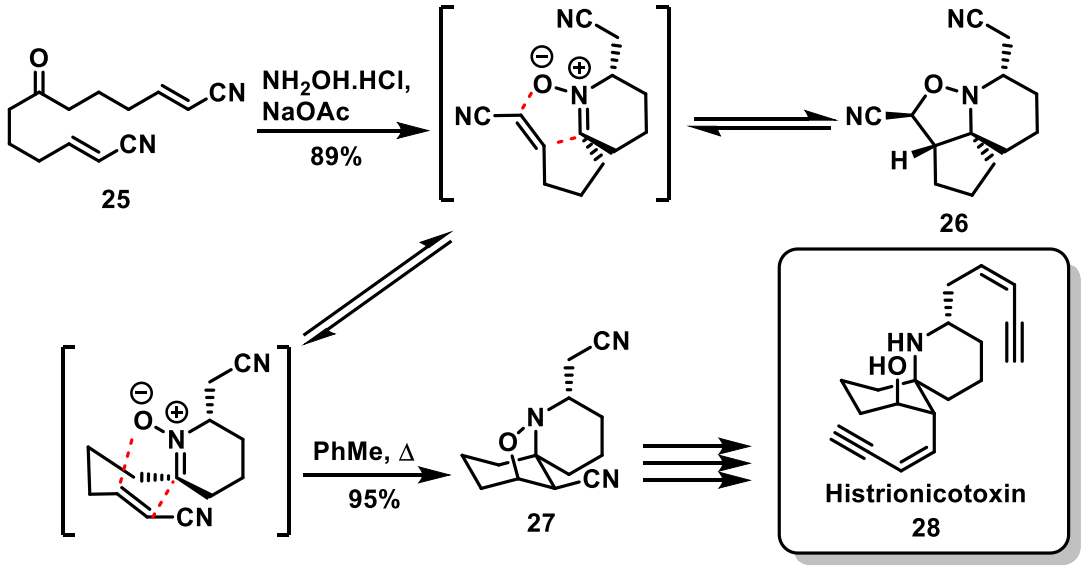

Scheme 6: Retro-[3+2]/[3+2]cycloaddition methodology toward histrionicotoxin (**28**).

An analogous hydrazone [3+2] cycloaddition also occurred using tosylhydrazine, with subsequent oxidative desulfuration affording cyclic hydrazone **19** in 41% yield. Ti(IV)-mediated reductive amination of **12** with ammonia lead to *trans*-octahydroquinolizine **16** *via* twofold aza-Michael addition in 74% yield, while aniline underwent sequential Michael/aza-Michael addition *via* an intermediate enamine, affording *trans*-octahydroquinoline **17** in 65% yield. Ethyl glycinate could also be condensed with **12** to generate an azomethine ylid *in situ*, which similarly underwent [3+2]-cycloaddition to afford the *cis*-tricarboxylate **18** in 71% yield. Interestingly, in the absence of a secondary partner, treatment of **12** with sodium hydride prompted a spontaneous, diastereospecific twofold Michael addition to afford *trans*-decalin **20**, containing four contiguous stereocentres in 70% yield.

Single-electron reduction of **12** with SmI_2 afforded either lactone **21** (using 2 eq. SmI_2) or cyclopentanol **22** (using 5 eq. SmI_2). The divergence in stereochemical outcome was proposed to be a result of the higher degree of Sm^{III}-chelation where fewer equivalents of SmI_2 were used, resulting in radical **29** with the alkyl groups positioned *trans* to one-another, while steric hindrance between samarium ions in ketyl radical **30** led to the *cis*-diastereomer (Scheme 7).

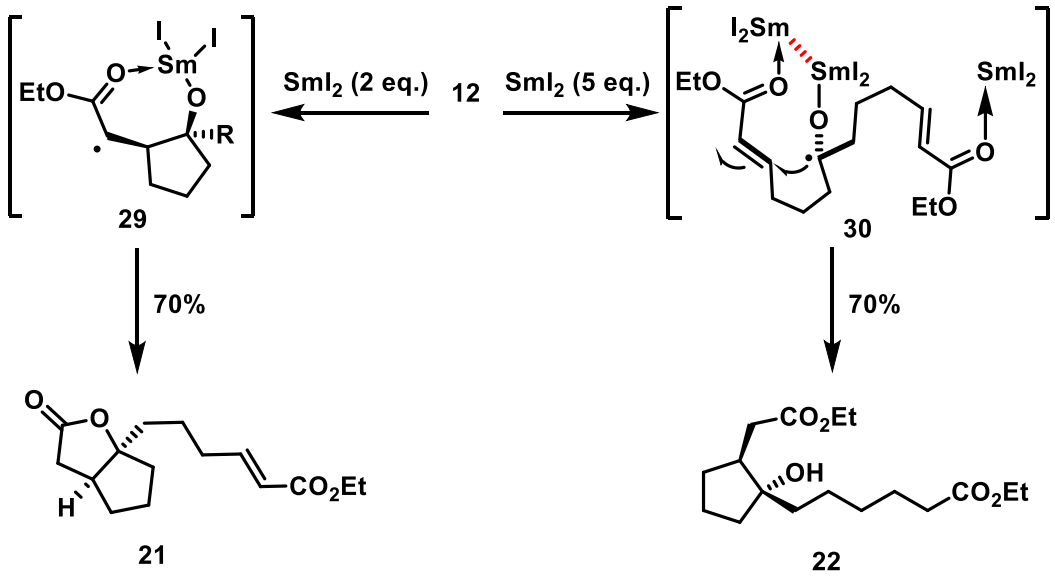

Scheme 7: Radical cyclisation of **12** to either lactone **21** or cyclopentanol **22** with SmI_2.

Finally, treatment of ketone **12** with lithium-based nucleophiles led to tetrahydropyran adduct **23** by addition to the ketone and subsequent oxa-Michael addition in 50% yield using super-hydride ($LiBEt_3H$), or 19% yield using MeLi. Comparatively, using MeMgBr in place of MeLi gave the acyclic Grignard adduct **24** in 86% yield.

Developing a fundamental understanding of the reactivity of polyfunctional materials can be a powerful tool in reaction discovery. The use of the discretely-functionalised keto-diester **12** allowed for the preparation of twelve distinct chemical scaffolds from a single precursor, lending considerable use toward a diversity-oriented approach. Moreover, modulation of the reactive species allowed specific mechanistic pathways to be favoured. Being able to control these cascade reactions can also be seen to have significant synthetic utility in target-oriented synthesis, as the products can be further elaborated to provide rapid access to highly-functionalised materials.[38] Therefore, it would be of considerable worth to explore the synthetic utility of other highly-functionalised materials, with a view toward utilising cascade reactions for both reaction discovery and diversity-oriented synthesis, as well as for the synthesis of scaffolds of particular interest.

1.6 The chemistry of indigo

Indigo (**31**) is an ancient natural dye, derived from a wide variety of plant-based sources (e.g. *Indigofera* sp., *Isatis* sp., *Persicaria* sp.), and has been used in the production of textiles and artworks for millennia.[39] The molecule itself consists of a dimeric 2,2'-biindoline core, flanked by carbonyl groups at the 3 and 3' positions. The *trans*-geometry about the central olefin is held rigid by intermolecular hydrogen bonding between the adjacent indole and ketone groups, which also contributes to indigo's characteristic intense-blue colour; hydrogen bonding and π-stacking can also occur between individual indigo molecules, leading to indigo's poor solubility in many solvents.[40]

Indigo has a rich history of international trade through the ages, forming the basis of the export industry for many countries, including as a major economic commodity in the colonial Americas. At several points throughout history, indigo was worth greater than its weight in gold, and alongside gold and spices, it was one of the primary commodities traded by the East India Company, forming the basis of the modern global economy.[41] In more recent times, indigo has become synonymous with its use in the production of blue denim jeans since their invention in 1872. The surge in demand associated with the widespread use of blue denim cultivated significant interest in the chemistry of indigo, resulting in a lab-scale synthesis of indigo by Baeyer in 1878, for which in-part he was awarded the 1905 Nobel prize for chemistry.[42] This eventually led to indigo's industrial-scale synthesis by the early 20th century.[43] Today, most of the indigo produced worldwide is synthetic,[44] though there continues to be considerable interest in developing more environmentally-conscious methods for its production.[45] The first economically-viable industrial methods were based off the second-generation Heumann process (Scheme 8),[43, 46] where anthranilic acid is alkylated with chloroacetic acid to give 2-carboxyphenylglycine (**32**), which is fused in a NaOH/KOH melt to give a salt of indoxyl-2-carboxylate **33**, which upon decarboxylation to indoxyl **34**, undergoes spontaneous air oxidation to afford indigo.

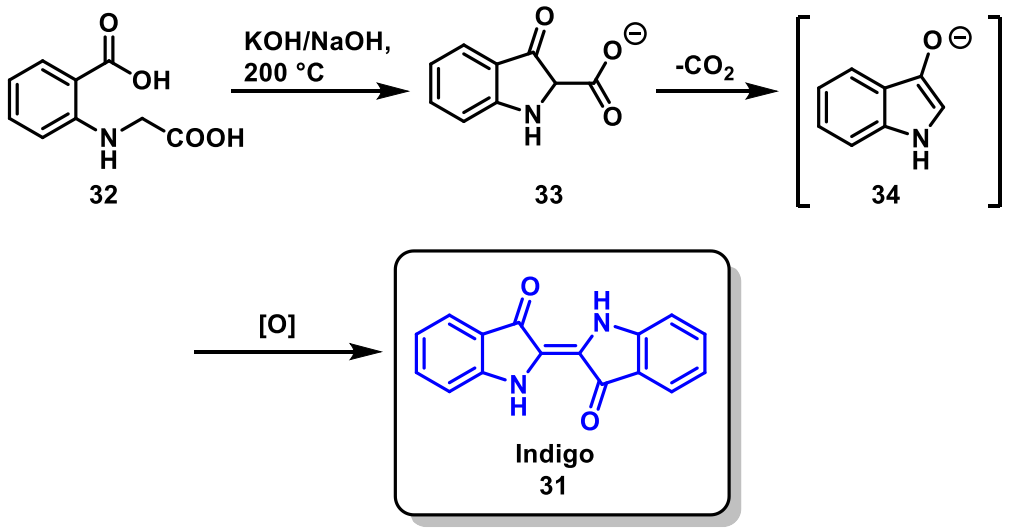

Scheme 8: Overview of the second-generation Heumann process for synthesising indigo (**31**) from anthranilic acid *via* 2-carboxyphenylglycine **32**. Counterions are not depicted for clarity.

The synthesis of indigo proved to be an important contributor to the invention of factory-scale organic chemistry, and indigo factories quickly superseded natural indigo as the dye-of-choice for many applications due to its lower price and higher quality, with fewer indigoid (isoindigo, **35** and indirubin, **36**, Figure 4) impurities. The ready availability of indigo led to the development of most of the modern understanding of the chemistry of the indigo family, including fundamentals of redox chemistry, reactions with acids and bases, electrophilic and nucleophilic chemistry, as well as tandem reactions of indigo. An overview of the known chemistry of indigo follows, however much of its history predates modern spectroscopic techniques, and thus the validity of these reported outcomes is variable.

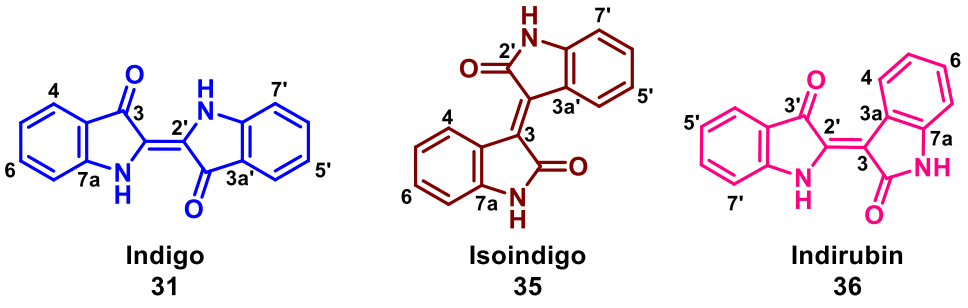

Figure 4: The indigo family: indigo, isoindigo, and indirubin with their respective colours.

1.6.1 Redox chemistry of indigo

The reduction of indigo is of particular importance to the textiles industry, as leucoindigo **37** is relatively water-soluble and adheres well to fabrics, allowing for back-oxidation to indigo upon air-drying. For this reason, the reduction of indigo is well-known, and can be achieved *via* a number of methods – most commonly using sodium dithionite or zinc

dust, or through electrochemical methods,[47] though methods involving urine, arsenic trisulfate and bacterial cultures are also known.[48] Using a Clemmensen-type reduction with zinc, iron, tin or zinc-mercury amalgam in a mixed AcOH/Ac_2O solvent, various deoxygenated and/or acetylated adducts such as **38** may be isolated (Scheme 9).[49]

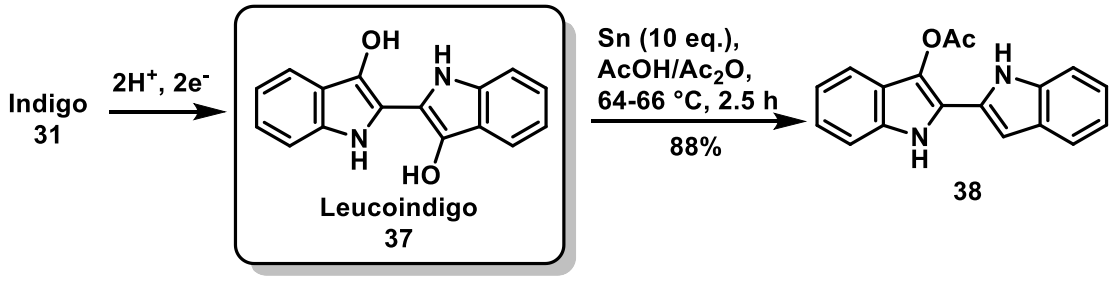

Scheme 9: Reduction of indigo to leucoindigo. Further reduction of leucoindigo is also possible in the presence of acetic anhydride.

The oxidation of indigo follows two general pathways (Scheme 10) – under aqueous acidic conditions, or under harshly oxidising conditions (e.g. with concentrated nitric or chromic acids, ozone, aqueous bromine or chlorine) indigo undergoes cleavage of the central double bond to afford isatin **39**, or under anhydrous or milder conditions (e.g. with PbO_2 or $Pb(OAc)_4$ in benzene/acetic acid, Cl_2 in CCl_4, or $KMnO_4$/AcOH then pyridine *via* 2,2'-diacetoxyindigo **40**), affords dehydroindigo **41**,[50] which is also accessible *via* electrochemical oxidation.[51] The oxidation of indigo carmine (**42**) to the corresponding isatin has also been utilised as a means of detecting ozone or superoxide in biological systems.[52]

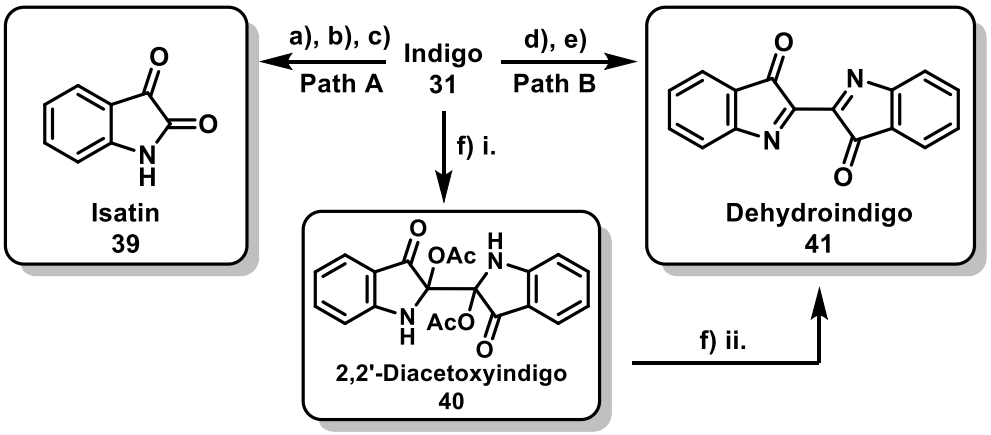

Path A: a) HNO_3(aq) **b)** $H_2Cr_2O_4$ **c)** O_3, H_2O
Path B: d) i. Cl_2, CCl_4 ii. $Ca(OH)_2$ **e)** PbO_2, $CaCl_2$, benzene, AcOH
f) i. $KMnO_4$, AcOH ii. Pyridine, PhMe

Scheme 10: Oxidation of indigo affords either isatin **39** or dehydroindigo **41**, depending on reagent choice.

1.6.2 Reactions of indigo with acids and bases

Like other indolic compounds, indigo undergoes deprotonation with a variety of strong or weak bases. Indigo was also reported to react with mineral acids to give indigo salts in 1902; i.e. treating indigo with a 5:1 mixture of acetic and sulfuric acids, and precipitation with diethyl ether yields indigo monosulfate (**43a**), while the prolonged digestion of indigo by sulfuric acid (13.5 M) under the same conditions was reported to yield indigo disulfate, **43b**.[53] Notably, indigo becomes soluble in acetic acid, benzene and chloroform when dry HCl gas passes through the suspension, while addition of ether to the solution precipitates the hydrochloride salt **44** (Figure 5).

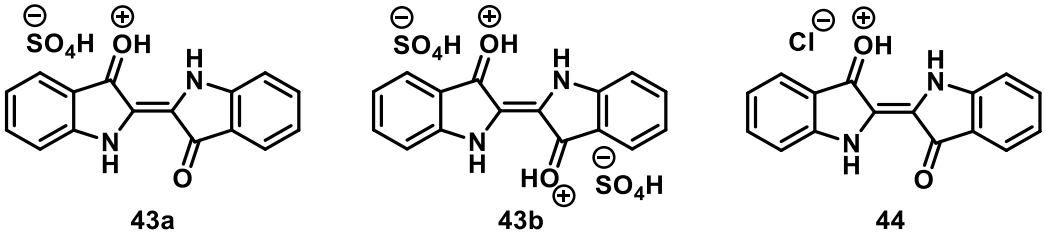

Figure 5: Salts reported from the reaction of indigo with mineral acids.

In a recent study of the closely-related 'Nindigo' (indigo-3-arylimine) family (**45**), it was determined that reversible protoisomerisation takes place upon treatment with strong acids to furnish *cis* salt adducts (**46**).[54] While both *mono*- and *di*-iminoindigoids react readily with a variety of acids, indigo was noted to be far less reactive, given the low basicity of the indigo carbonyl relative to its imine equivalent, though the reactions of indigo with triflic or sulfuric acids in chloroform were reported to give green, solvated indigo derivatives. These could not be isolated due their instability, therefore it is unknown whether indigo undergoes similar isomerisation upon acidification. The sulfuric acid adduct was observed to gradually form indigosulfonic acid products (**47**); unsurprising given the known, and controllable sulfonation of indigo with sulfuric acid/SO_3 mixtures.[55] Treatment of the *cis*-acid adduct with organic bases (e.g. DBU, NEt_3) restored the *trans*-configuration about the double bond, presumably due to restoring intramolecular H-bonding between adjacent donor-acceptor functionalities (Scheme 11).

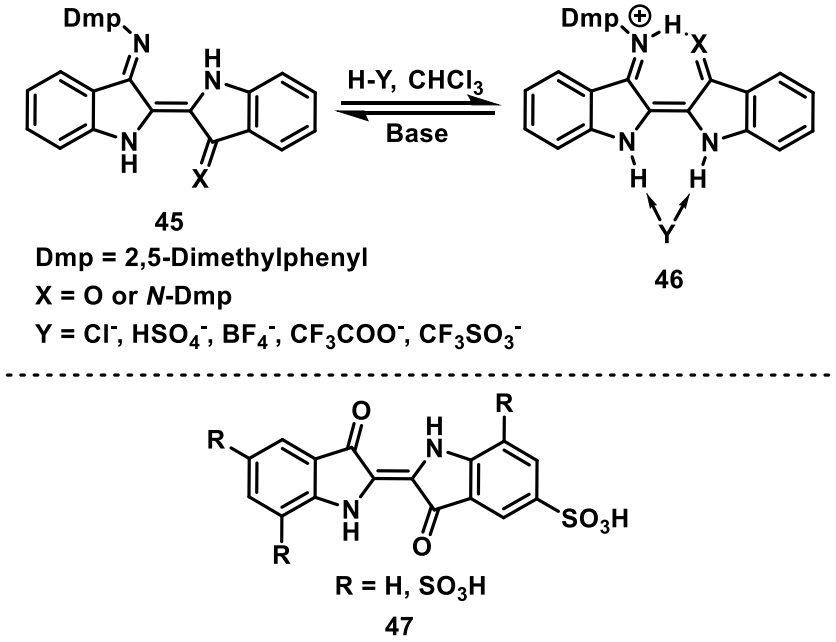

Scheme 11: Salt formation and reversible protoisomerisation of indigo-*N*-arylimines.

1.6.3 Electrophilic chemistry of indigo with nitrogen nucleophiles

Imine derivatives of indigo were first reported in 1909, by the boric acid-catalyzed condensation of indigo with aniline derivatives, affording the corresponding diimine **48** as purple needles, reported in good yields (Scheme 12).[56] In 1914, the reaction of indigo with $ZnCl_2$ and aqueous ammonia resulted in the formation of a mixture of indigo monoimine **49** and diimine **50**, separable by crystallisation from benzene. Of these, the former method has been demonstrated to be irreproducible, and no yield was reported for the latter, which prompted investigation into indigo-*N*-imines.[57]

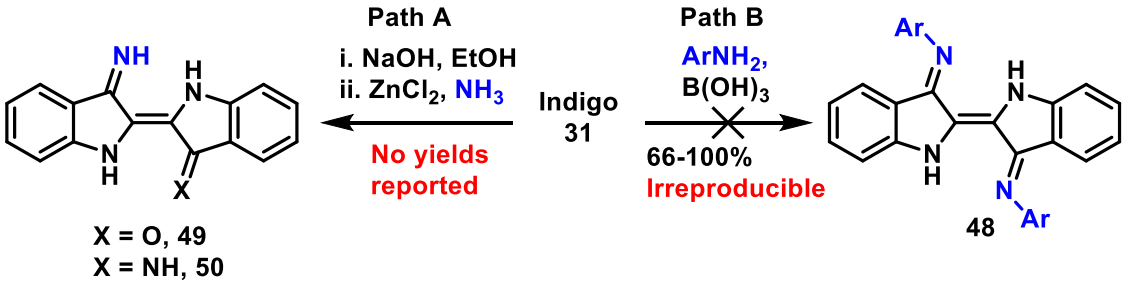

Scheme 12: Initial investigations into the formation of imines from indigo and ammonia or aniline derivatives.

A more-robust procedure for the generation of indigo-*N*-arylimines was developed in 2010 by Hicks *et al*,[58] by treating indigo with a pre-formed titanium-imido complex,[59] generated *in situ* by the addition of $TiCl_4$ to a solution of the desired amine and DABCO in bromobenzene. Heating the resulting complex at reflux led to the desired diimine 'Nindigo' **48** in good yields (Scheme 13).[60] This can then be oxidised using silver oxide,

and the resulting 'dehydroNindigo' isolated by complexation to a suitable metal, such as Pd^{II}, Ru^{II}, or Co^{II}, affording adduct **51** *via* ligand displacement of their corresponding *bis*-hexafluoroacetoacetonato (hfac) complexes.[61] Dimetallic species are then able to be transmetallated, to afford redox-active, bimetallic Nindigo-metal-boronate complexes. It is known that indigo diimines undergo facile keto-enol tautomerisation to adopt an asymmetric structure (i.e. **52**), and this process occurs by a dual proton-transfer mechanism.[62]

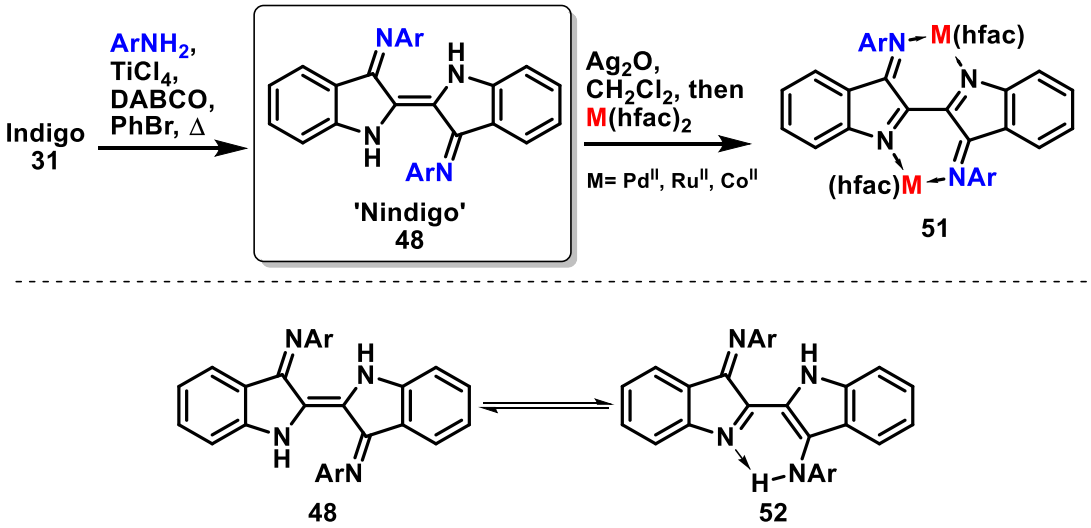

Scheme 13: Synthesis of 'Nindigo' imines (**48**) *via* nucleophilic addition of a titanium imide complex, and their use as ligands for the synthesis of transition metal complexes (**51**). Diimides such as **48** have been shown to exist as a mixture of the 'imine' form **48** and the 'enamine' **52**, and interconvert easily by proton transfer.

The Wolff-Kishner reduction of indigo was first reported in 1921, performed by heating indigo in an alkaline, alcoholic solution of phenylhydrazine.[63] This firstly generated a proposed phenylhydrazone intermediate **53**, which upon thermal decomposition gave the desired methylene compound, *mono*-desoxyindigo **54** (Scheme 12). In 1945, *mono*-desoxyindigo **54** was demonstrated to be formed by the action of hydrazine hydrate on indigo, in addition to a reported diazine side-product, **55**. In both instances however, no yields were reported, and little characterization beyond elemental analysis was undertaken.[64]

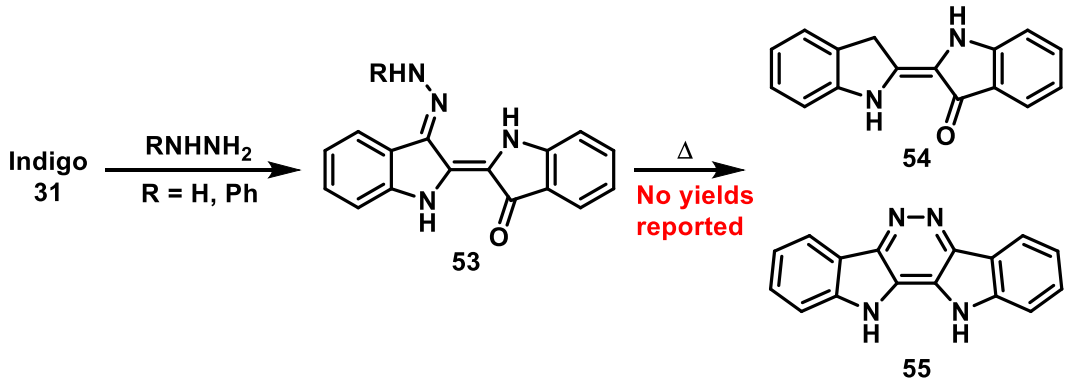

Scheme 14: The reaction of indigo with hydrazine hydrate or phenylhydrazine is reported to give the *mono*-hydrazone **53**, which is reported to either decompose into desoxyindigo **54**, or condense into diazinoindigo **55**. No yields were reported for either reaction.

Finally, indigo oxime **56** was obtained in 40% yield from the reaction of indigo with hydroxylamine.[65] Subsequently, it was found that heating an alkaline solution of indigo and hydroxylamine hydrochloride at reflux resulted in isolation of *bis*-oxime **57**, though its yield was not reported (Scheme 15).[66]

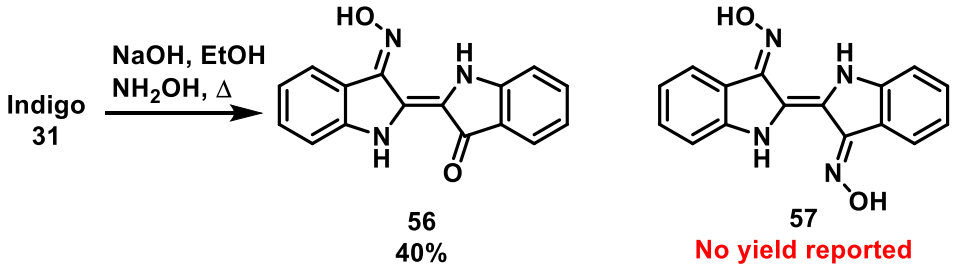

Scheme 15: Oximation of indigo with hydroxylamine afforded either **56** in modest yield, or **57**. Yields were not reported for compound **57**.

1.6.4 Electrophilic chemistry of indigo with carbon nucleophiles

Despite the development of an innumerable array of carbon-based nucleophiles in the 20th century, and the demonstrated electrophilicity of the indigo core (particularly at C3), the body of knowledge surrounding the reactions of indigo with readily-accessible carbon nucleophiles is astoundingly limited. The reaction of indigo with several Grignard reagents in diethyl ether was reported in 1909, and resulted in a handful of non-symmetrical adducts (**58**) in good to excellent yields, though yields were not reported for all compounds, and the absolute structure of these molecules was not unambiguously determined (Scheme 16).[67] The authors of this study ascertained that the Grignard reagent and indigo had reacted in a 1:1 ratio based off elemental analysis, however in the absence of then-unknown spectroscopic techniques, the only structural evidence obtained was from derivatisation of the products. It was determined that nucleophilic attack had occurred at the carbonyl group by the presence of a hydroxyl functionality, and reacting

with cold $KMnO_4$ revealed the presence of a C=C double bond. Furthermore, this molecule could be alkylated using ethyl iodide and KOH in ethanol, and subjecting this alkylated material to Zeisel's test (cleaving the alkyl groups with HI, then precipitating the iodide with $AgNO_3$) revealed the addition of two ethyl groups. The authors determined that the product was likely one of two tautomers (**58a** or **58b**), and that **58b** fit better to their observations, however they stated that "attempts to establish the constitution (did not lead) to a uniform, crystallised and well-defined connection" and "partially due to the (rest of the) molecule, did not yield unambiguous results."

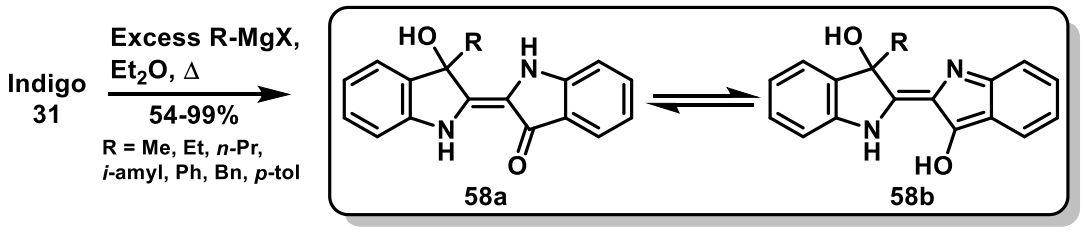

Scheme 16: Reaction of indigo with Grignard reagents to afford the corresponding tertiary alcohol adduct **58**, as one of two tautomers. The exact structure was not unambiguously determined, and yields were reported for several compounds, but not for all examples.

1.6.5 Diels-Alder chemistry of dehydroindigo

The oxidation of indigo to dehydroindigo (**41**) generates a 4π system, which is amenable to [4+2]-cycloaddition chemistry. Several examples of dehydroindigo's cycloaddition chemistry have been reported previously, and in good yields where specified. The first aza-Diels Alder reactions of dehydroindigo were reported in 1940, where a selection of electron-rich and electron-poor substrates were reported to give the expected *N,N′*-bridged cycloadducts in good yield. Further reports disclosed similar outcomes, albeit in modest yields.[68] The stereochemical outcome was not investigated in any case (Scheme 17).

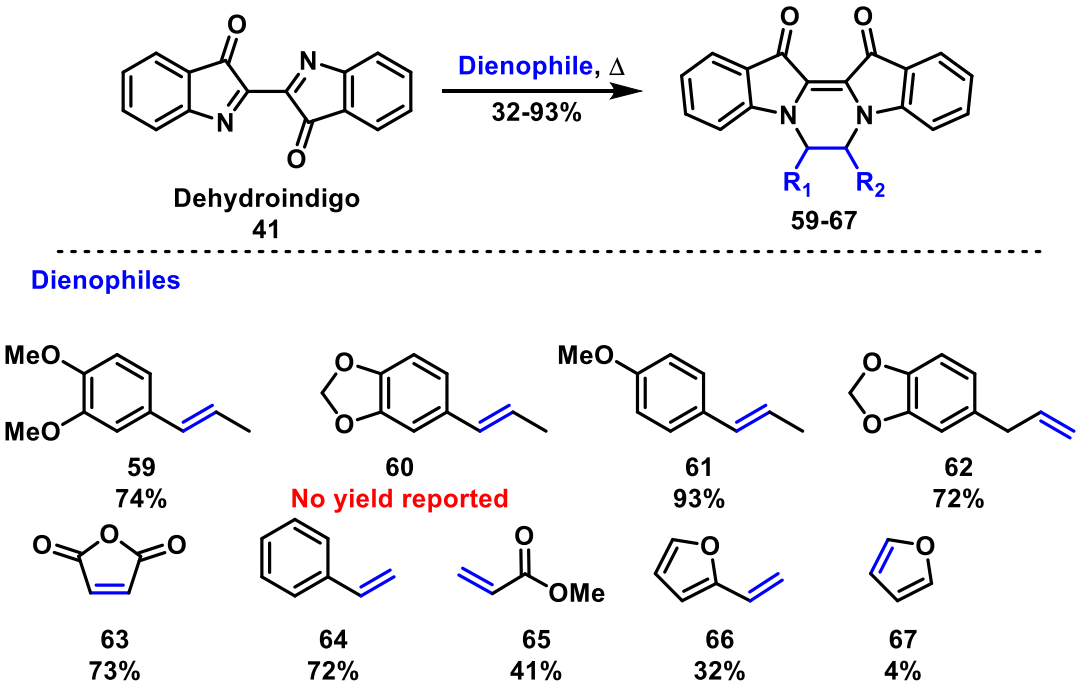

Scheme 17: Reactions of dehydroindigo with selected dienophiles *via* [4+2]-cycloaddition. The yield for compound **60** was not reported.

These bridged structures were also reported to undergo post-synthetic modifications, as in the addition of methyl propiolate to dehydroindigo, to give the expected methyl ester adduct **68**. Thermal decarboxylation of the ester gave *N,N'*-vinylindigo **69** in 22% yield, which could be oxidised by nitric acid to *N,N'*-oxalylindigo **70** in 31% yield (Scheme 18).[69]

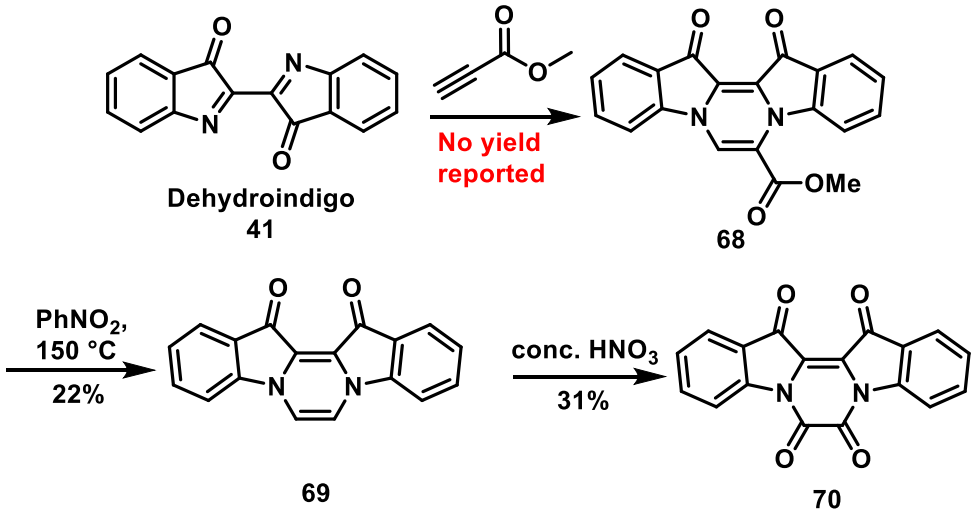

Scheme 18: Synthesis of *N,N'*-oxalylindigo **70** *via N,N'*-vinylindigo from decarboxylation of the cycloadduct **68**. The yield for compound **68** was not reported.

1.6.6 Nucleophilic chemistry of indigo – electrophilic aromatic substitution

As is typical for other 2,3-disubstituted indoles, electrophilic substitution of indigo, leucoindigo or dehydroindigo affords sulfonated, halogenated or nitro derivatives, firstly at the C5- and C5'-positions, then at C7 and C7'. It is important to re-emphasise that for the derivatives of indigo summarised here, many were reported in the early 20th century, and structural elucidation of these derivatives was based primarily on elemental analysis. Percentage yields were largely unreported, thus the validity or reproducibility of these outcomes cannot be assessed without conducting further experimentation. A summary of reported outcomes follows.

Direct halogenation of indigo using aqueous bromine or chlorine generally affords halogenated isatins from oxidation and/or hydrolysis, while halogenation in glacial acetic acid typically affords mono or di-halogenated indigo.[70] The preparation of 5-chloroindigo has been reported by direct halogenation of indigo in glacial acetic acid, and the procedure was also found to be amenable to the synthesis of 5,5'-dichloroindigo.[71] 5,5'-Dibromoindigo was obtained from the addition of bromine to a solution of indigo in nitrobenzene, under microwave-aided conditions.[72] A quantitative preparation of 5,5',7,7'-tetrabromoindigo (**71**) from the reaction of indigo with bromine and sodium nitrite in sulfuric acid has also been patented,[73] while 5,5',7,7'-tetraiodoindigo could be prepared from dehydroindigo by the action of iodine monochloride in presence of sodium bisulfate.[74]

Similarly to halogenation, nitration of indigo in water, acetic acid or sulfuric acid leads to the formation of nitroisatins, thus anhydrous media were demonstrated to be essential for the nitration of indigo to 5,5'-dinitroindigo.[75] Treatment of indigo by concentrated sulfuric acid gives indigo carmine (**42**) as a highly water-soluble blue-green powder,[76] typically isolated and handled as the disodium salt. Application of fuming sulfuric acid was also reported to produce indigo-5,5',7,7'-tetrasulfonic acid.[55, 77]

Halogenated derivatives of indigo demonstrate a variety of colours, based on the position of the halogens on the aromatic rings. For example, 5,5',7,7'-tetrabromoindigo (Ciba blue B, **71**) is electric-blue, 6-bromoindigo **72** is a deep violet colour and Tyrian purple (6,6′-dibromoindigo, **73**) is bright purple (Figure 10). Perhaps the most widely-acknowledged derivative of indigo is indigo carmine (**42**), which due to its high water solubility has found common use as a pH indicator with a range of 11.4-13.0, a redox indicator for the detection of ozone and superoxide,[52, 78] and has niche medical uses such as for the

detection of amniotic leakages, and for imaging sections of the renal and urinary tracts (Figure 6).[79]

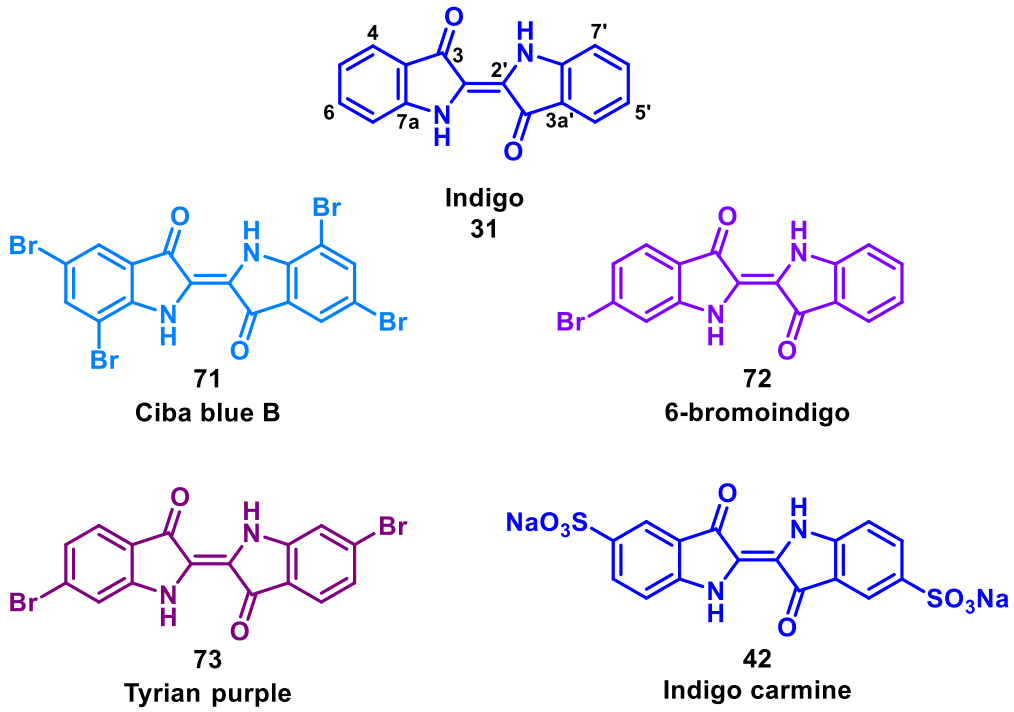

Figure 6: Selected indigo derivatives bearing substituents on the outer phenyl rings.

Tyrian purple (**73**), is an ancient pigment among the oldest of dyes, and has been used since the Iron Age by Phoenicians, Chinese and Peruvians as a sacred pigment.[80] In Rome, Emperor Nero decreed the exclusive right for the emperor to wear purple robes,[81] and the colour purple has been seen as a sign of the opulence of the British monarchy for centuries, earning the name 'Royal Purple.' Based on biblical notes, the vestments of Catholic priests are also dyed with Tyrian purple. The history of Tyrian purple is well-recorded, and it has been the subject of numerous synthetic studies.[82] Historically, the pigment could only be obtained from exposure of extracts of marine *Murex* sp. to light, and due to its low abundance, the secretions of over 10,000 individual *Murex* were required to produce a gram of the pigment.[83] This extreme scarcity, combined with its political and religious significance has meant its value has historically been 10-20 times higher than its weight in gold during different periods of time.[84] Much has been reported on the biosynthesis of Tyrian purple and its progeny – a summary of which is depicted in Scheme 19.[85]

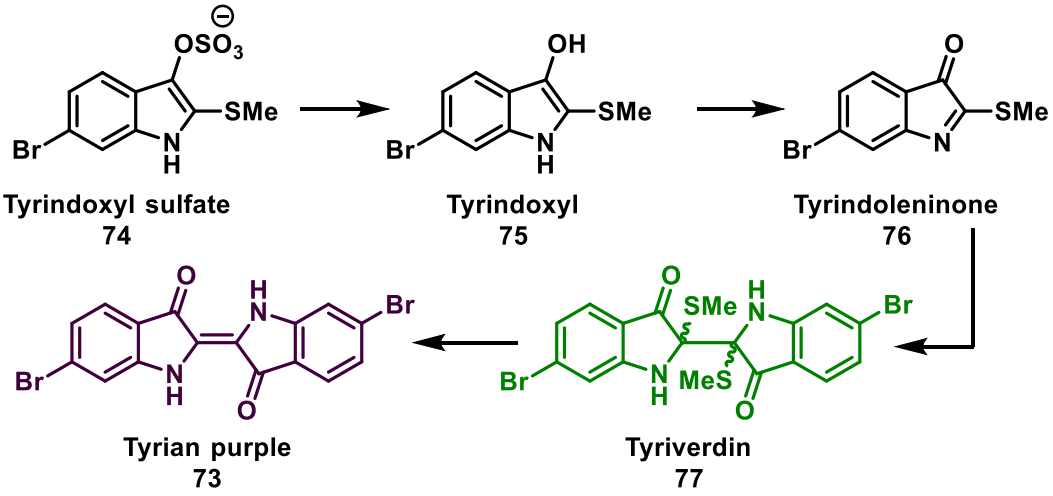

Scheme 19: Biosynthetic pathway responsible for the generation of Tyrian purple **73** from tyrindoxyl sulfate **74** *via* the antimicrobial tyriverdin **77**.

Briefly, tyrindoxyl sulfate **74** is hydrolysed under the action of either a purpurase or an arylsulfatase to give tyrindoxyl **75**. Oxidation to tyrindoleninone **76** leads to dimerization, which results in the green pigment tyriverdin **77**. Photolysis of tyriverdin gives rise to Tyrian purple, along with the elimination of odorous dimethyldisulfide.[86] Both tyriverdin and tyrindoleninone exhibit potent antimicrobial activity, though the exact mode of action is unknown, and it is unclear whether this is the result of the molecule itself acting as an inhibitor, or the ready elimination of toxic sulfides or disulfides upon UV irradiation.[87]

1.6.7 Metal complexes of indigo

There has been some interest in the complexes of indigo with metals in the past, owing to indigo's abundance, strong absorptive characteristics, and low cost. Indigo was first demonstrated to form coordination complexes with metals in 1922, forming *bis*-indigo homoleptic chelates, such as those of Cu^{II}, Zn^{II}, Ni^{II} and Co^{II} (**78**), though yields were not reported.[88] More recently, *mono*-metalated (M = Pd^{II}, Pt^{II}) adducts (**79**) were reported from the addition of chlorido-bridged $[(PBu_3)(Cl)M(\mu\text{-}Cl)]_2$ complexes to indigo salts in THF solution (Scheme 20).[89]

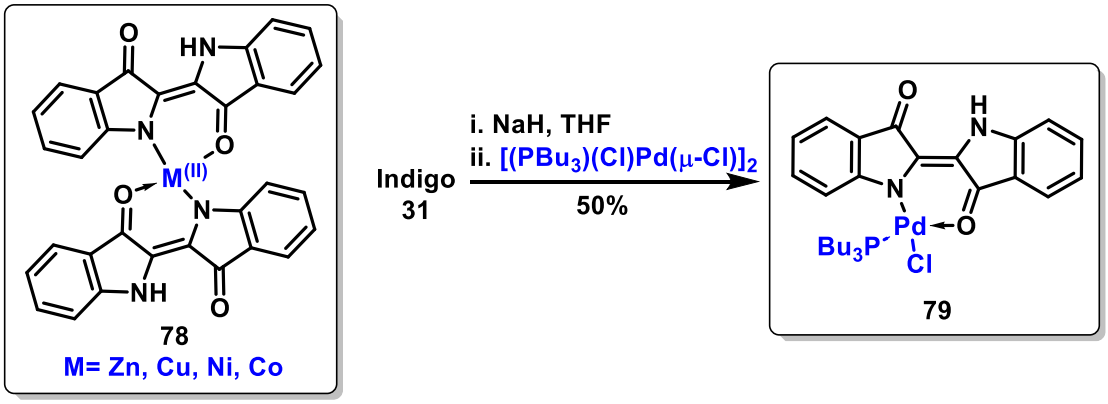

Scheme 20: Reported metal complexes of indigo. Yields were not reported for complexes of type **78**.

The recent resurgence of interest in metal-indigoid complexes, such as those of 'Nindigo' and 'thioNindigo' ligands[90] with noble metals led to the isolation of several complexes of indigo with Ru^{II} bearing acetylacetonato (acac),[91] and 2-(phenylazo)pyridinyl (pap)[92] ligands (**79**–**82**) in 2016 (Scheme 21). In subsequent studies, diruthenium complexes were also accessible using $Ru(acac)_2$.[93]

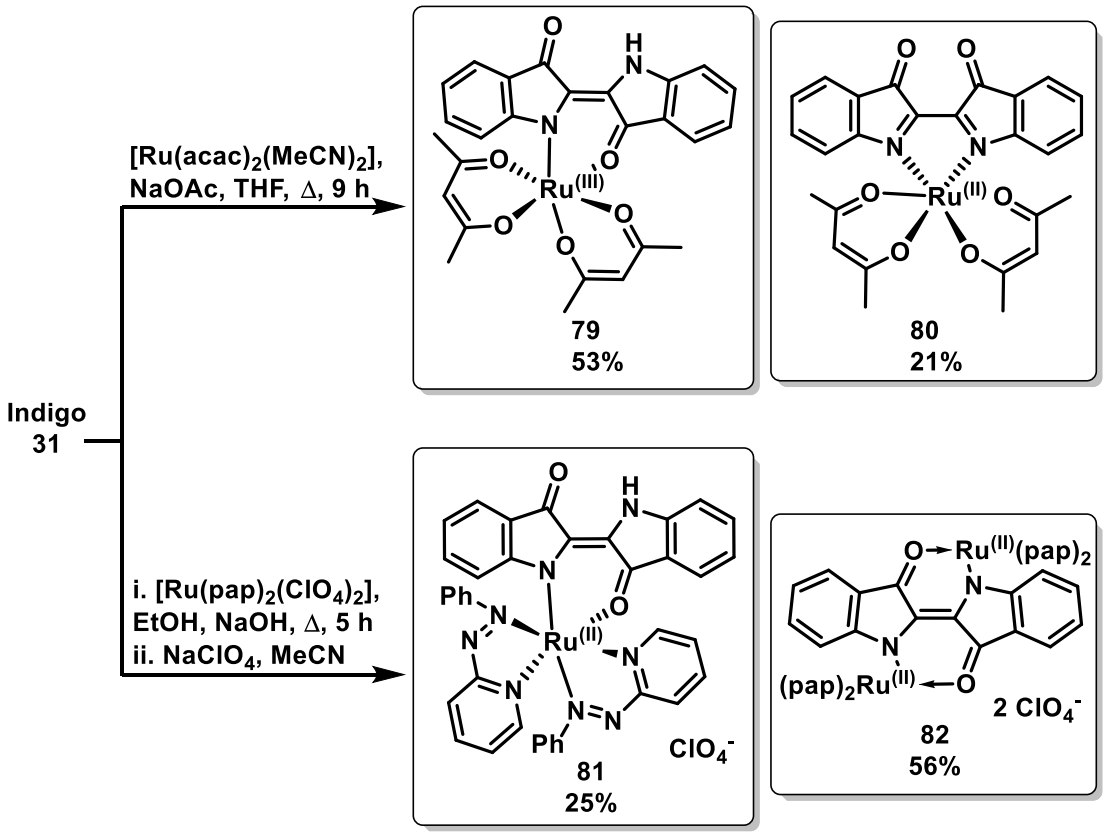

Scheme 21: Mono- and dimetallic complexes of indigo with ruthenium, bearing acac and pap ligands.

1.6.8 Nucleophilic chemistry of indigo with alkyl, acyl, and aryl halides

Early work by Baeyer suggested that indigo's poor solubility meant that it could not be alkylated.[42c] However, it was found that indigo readily undergoes *N*-alkylation in DMF solution with barium oxide and methyl iodide, affording quantitatively *N,N′*-dimethylindigo **83** (Scheme 22).[94]

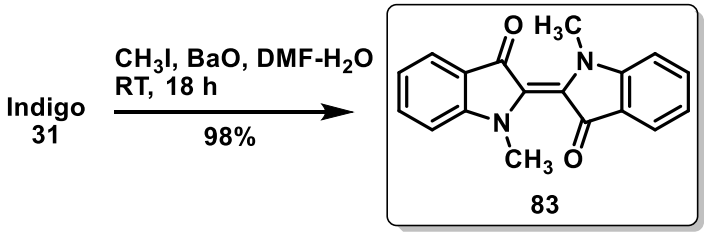

Scheme 22: Synthesis of dimethylindigo **83** *via N*-alkylation of indigo.

An alternative approach used sodium hydride in DMF, and gave **83** in 53% yield.[95] Under these conditions, *cis-N,N′*-bridged indigo derivatives **84**–**87** were synthesised in low yields from various alkyl dichlorides *via* sequential nucleophilic displacement by the indigo dianion (Scheme 23). In a similar fashion, indigo was reacted with acyl chlorides to afford cyclic scaffolds **88** and **89** in modest yields.

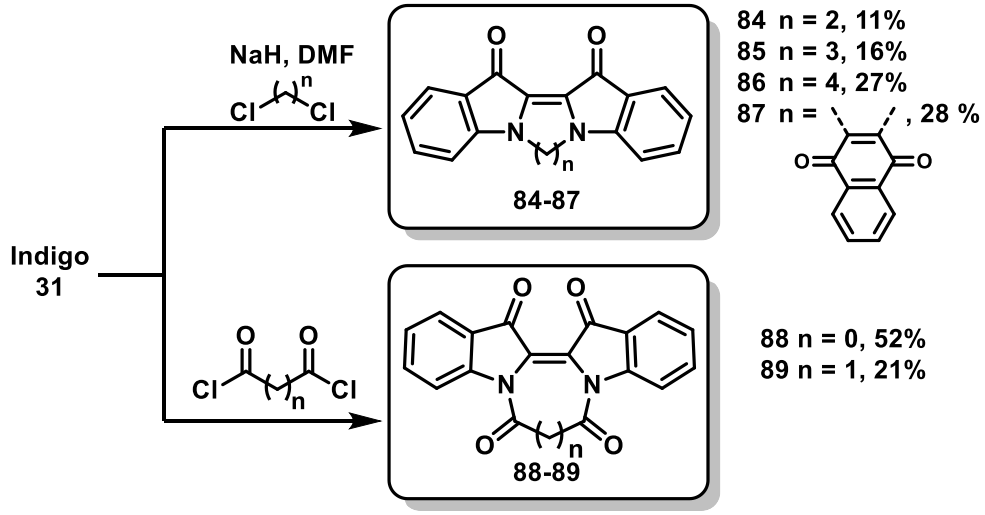

Scheme 23: Synthesis of cyclic indigo derivatives **84**–**87** *via* dual-displacement of alkyl dichlorides, or **88**–**89** *via* reaction with oxalyl (**88**) or malonyl (**89**) dichlorides.

The *N*-acylation of indigo with acyl chlorides or anhydrides has been widely utilised as a means of solubilising indigo, as well as performing subsequent chemical transformations.[96] Photochemical isomerisation between the *cis*- and *trans*- isomers of indigo derivatives occurs readily in visible light, and has been studied with a view toward the development of photosensors.[96c, 97] Interestingly, in many instances, indigo undergoes intramolecular Knoevenagel condensation upon *N*-acylation. The alkylation of

indigo with diethyl malonate, and subsequently with ethyl phenylacetate in 1926 revealed cyclic, conjugated products by the elimination of water from *N*-acylindigo intermediates.[98] Such Knoevenagel-type reactions with indigo are relatively well-known, and reliable means of generating intense red pigments containing bay-annulated systems, which have been the subject of numerous recent studies toward the synthesis of new organic semiconducting polymers due to their electron-accepting nature, and small HOMO-LUMO bandgap.[97b, 99] In one recent example, thiophene bay-annulated indigo (**90**) was synthesised in 73% yield by heating a suspension of indigo and 2-thiopheneacetyl chloride in xylene at reflux, and could be further elaborated *via* metal-mediated cross-coupling chemistry to polymers such as **91**, which have been demonstrated to have useful photophysical and charge-transporting properties (Scheme 24).[100]

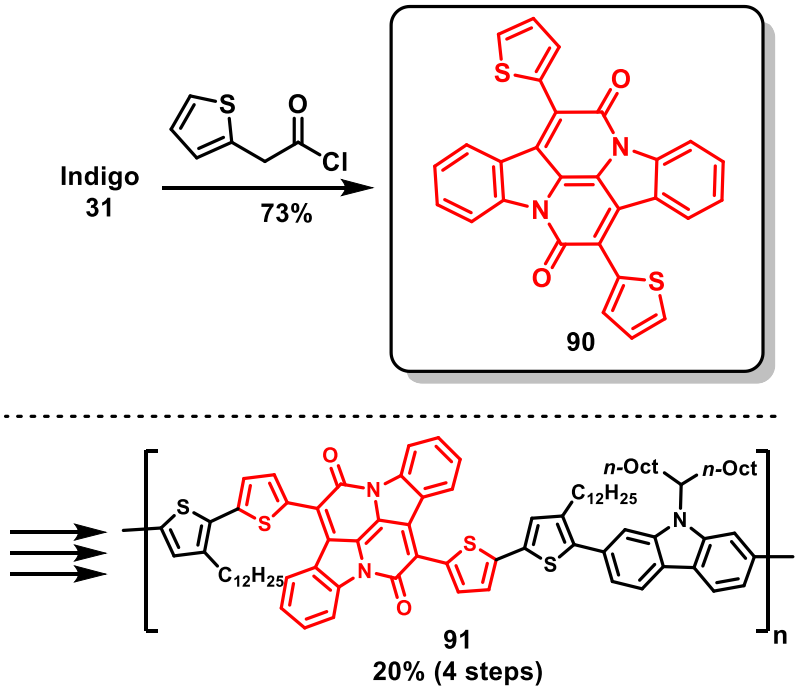

Scheme 24: Knoevenagel condensation of substituted acetyl chlorides gives bay-annulated indigo adducts such as **90**, which was converted into polymer **91** over 4 steps.

Early attempts at Ullmann-type *N*-substitution of indigo with aryl iodides under Cu^0-mediated conditions led instead to products resulting from fragmentation of indigo, and subsequent radical dimerization.[101] Reinvestigation of the reaction in 2003 revealed conditions amenable to the synthesis of a variety of *N*-aryl (**92b**–**f**) and *N,N'*-diarylindigos (**93a**–**d**) in modest to excellent yields (Scheme 25).[102]

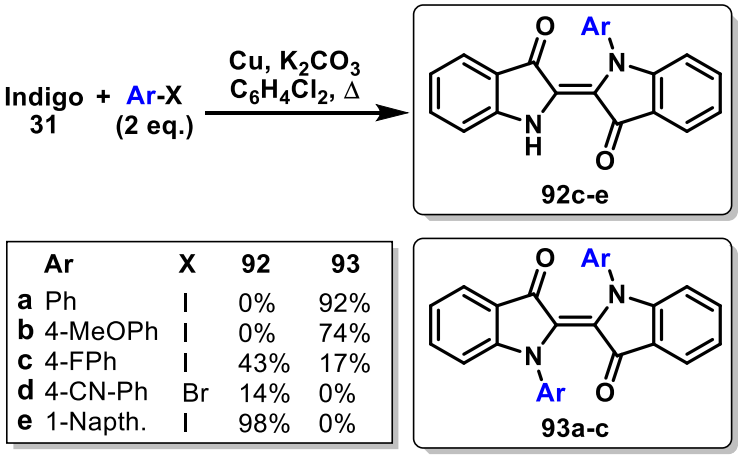

	Ar	X	92	93
a	Ph	I	0%	92%
b	4-MeOPh	I	0%	74%
c	4-FPh	I	43%	17%
d	4-CN-Ph	Br	14%	0%
e	1-Napth.	I	98%	0%

Scheme 25: Aza-Ullmann cross-coupling of indigo with aryl iodides to afford either *mono*- (**92)** or *bis*-arylated (**93**) indigo adducts.

This methodology was recently adapted toward the preparation of fullerene-free organic photodiodes (OPDs), by the synthesis of **94** from Tyrian purple (**73**),[103] which demonstrated comparable responsivity and detectivity to silicon- and fullerene-based OPDs, suggesting possible further application of solution-processable *N*-arylindigo scaffolds as semi-conducting materials (Scheme 26).

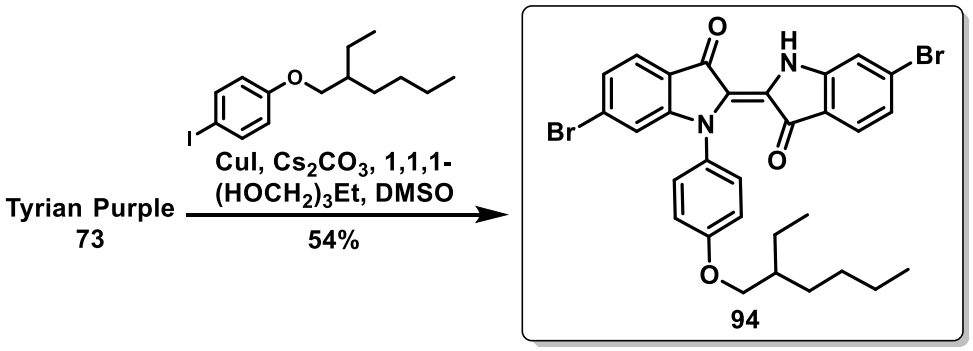

Scheme 26: Cu^{I}-catalysed cross-coupling of indigo and 1-((2-ethylhexyl)oxy)-4-iodobenzene to afford adduct **94**.

1.6.9 Summary of the fundamental chemistry of indigo

A variety of chemical transformations of indigo have been reported previously, including redox chemistry (including reduction to water-soluble substances, oxidation to reactive substances, deoxygenation, and oxidative cleavage reactions), reactions with acids and bases, nucleophilic chemistry (including alkylation, acylation, arylation, and electrophilic aromatic substitution reactions), electrophilic chemistry (including formation of imines, hydrazones, and oximes, and Grignard reactions) as well as tandem reactions of indigo (such as where *N*-acylation allows for subsequent Knoevenagel condensation). While on face-value, this seems a considerable body of knowledge, closer analysis of many publications from the early 20th century reveals that they did not disclose percentage

yields, and characterisation of derived products was solely by melting point, elemental analysis, or by derivatisation, as these works pre-date contemporary spectroscopic and/or crystallographic techniques. As a result, much of the information reported on the reactivity of indigo is of unknown validity and would require confirmation.

1.7 Cascade reactions of indigo

Where the reactivity of indigo has been re-investigated, its compact heterocyclic core has served as a useful matrix for the synthesis of biologically-relevant heterocycles,[49b, 49c, 104] though much of the fundamental chemistry of indigo remains unknown, or requires further study. There have been several reported examples of indigo undergoing cascade reactions, resulting in the generation of complex (and in many instances, unexpected) heterocycles in a one-pot setting. Indigo's extended conjugation is key to its ability to participate in these cascade reactions, as tautomerisation of the indole and carbonyl groups allows its electron density to be delocalised throughout the biindole system, resulting in rapid oscillation of localised partial positive and negative charges. The ability for multiple sites to act as potential nucleophiles (or electrophiles) as the reaction progresses toward an energetically stable product therefore allows for a complex reactivity profile. These reported cascade reactions are summarised below.

1.7.1 The hundred years' controversy: cascade reactions of indigo with benzoyl chloride

The reaction of indigo with benzoyl chloride sparked a well-catalogued dispute, the outcome of which became a point of contention for more than a century.[105] The controversy surrounding the reaction stems from independent reports from several research groups, each claiming different isolated structures from the same reaction, highlighting in part both the intricacies of indigo's chemistry, as well as a number of inconsistencies within the literature.

Initially performed in 1863, Schwartz isolated a brown amorphous solid from the prolonged reflux of indigo in excess benzoyl chloride, which was incorrectly assigned the structure *N*,*N'*-dibenzoylindigo (**95**).[106] Compound **95** was however later (correctly) reported as a crystalline violet powder by Posner, obtained from the reaction of indigo with benzoyl chloride in pyridine.[107] Hydrolysis of Posner's dibenzoylindigo was additionally known to result in the regeneration of indigo, however Schwartz's unknown compound produced different results, prompting further analysis. The empirical formula

of Schwartz's product was later found to be $C_{30}H_{17}O_3N_2Cl$, identical to that of a compound reported by Dessoulavy in 1909 (commonly referred to as 'Dessoulavy's compound,' **96**), obtained by the prolonged reflux of indigo with excess benzoyl chloride.[108] More confusingly, later reports on the reaction of indigo with benzoyl chloride in the presence of copper powder, sodium nitrate, or in nitrobenzene solution resulted in the production of Ciba Yellow G (**97**).[109] The true structure of **97** however proved evasive, and structural elucidation of Ciba Yellow G attracted the attention of organic chemists for decades, during which time a number of structures were proposed, and subsequently modified, however the correct structure was proposed in 1949,[110] and confirmed in 1986 through x-ray crystallography.[111] This final confirmation allowed ambiguities surrounding this compound to finally be put to rest over a century after its discovery (Scheme 27).

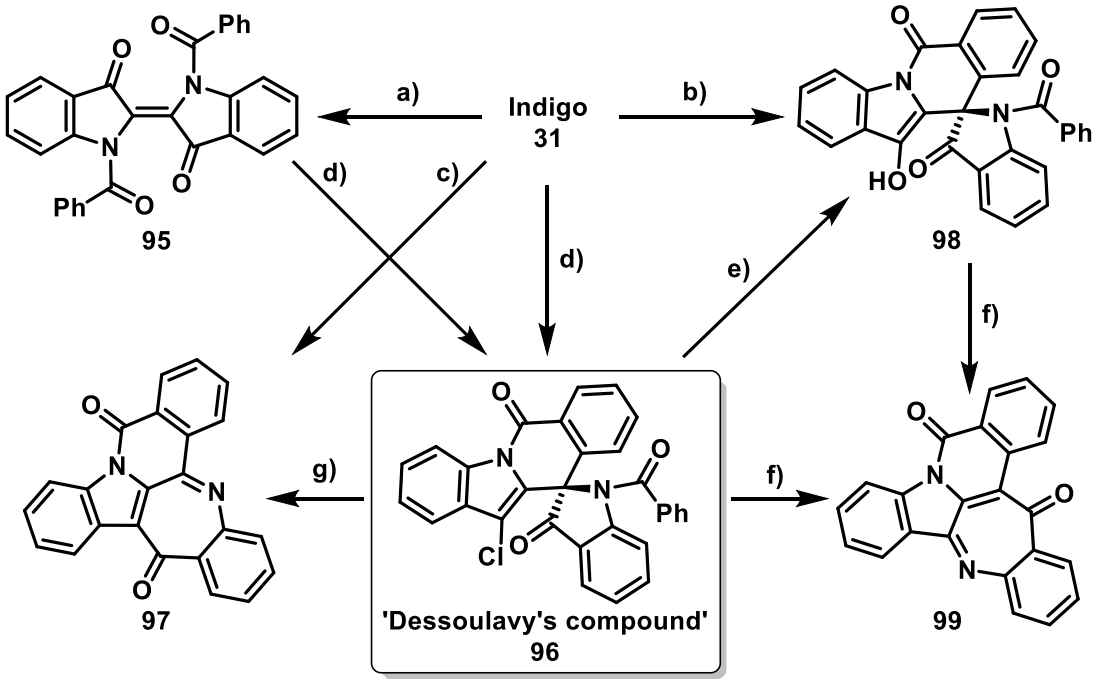

a) PhCOCl, pyridine, 75% **b)** PhCOCl, $ZnCl_2$, no yield reported. **c)** PhCOCl, Cu powder, 25% **d)** PhCOCl, Δ, no yield reported **e)** H_2SO_4, H_2O, no yield reported **f)** H_2SO_4, Δ, no yield reported **g)** Δ, no yield reported

Scheme 27: Annulation of indigo with benzoyl chloride leads to diverse structures, with compound **96** as a central intermediate. Unless specified, yields were not reported.

The chemistry of Dessoulavy's compound **96** lies at the heart of the controversy surrounding this reaction, as it serves as a divergence point for a variety of closely-related derivatives. While attempting to elucidate the structure for Ciba yellow G (**97**), Lucius reported in 1903 that Dessoulavy's compound **96** could be converted into **97** *via* expulsion of benzoyl chloride at elevated (300-380 ˚C) temperatures. Simultaneously, the reaction

of indigo with benzoyl chloride in the presence of $ZnCl_2$ as an additive gave a yellow substance (Hoscht yellow R, **98**),[112] which could also be generated from **96** by acidic hydrolysis at room temperature. Finally, upon heating either **96** or **98** with sulfuric acid, both afforded Hoscht yellow U (**99**) by elimination of benzoic acid.

In summary, the attempted benzoylation of indigo resulted in the production of five diverse structures, depending on the specific conditions under which the reactions were performed. The unanticipated complexity of this process is reflected by the timeline between the initial experiments in 1863 and the finalisation of the outcome in 1986, more than a century later.

1.7.2 Photochemical cascade reactions of *N,N′*-diacylindigos

While investigating the photochemical interconversion of *N,N′*-diacylindigo derivatives (**100**), it was observed that many underwent an irreversible photobleaching process.[113] Closer inspection revealed that the compounds underwent a photo-mediated rearrangement, generating cyclic carbamates **101a**–**e** in 40-65% yield. Mechanistically, it was proposed that stabilised diradical **102** is formed upon photoexcitation, which then underwent a 1,3-alkyl migration to give compounds **101a**–**e** (Scheme 28).

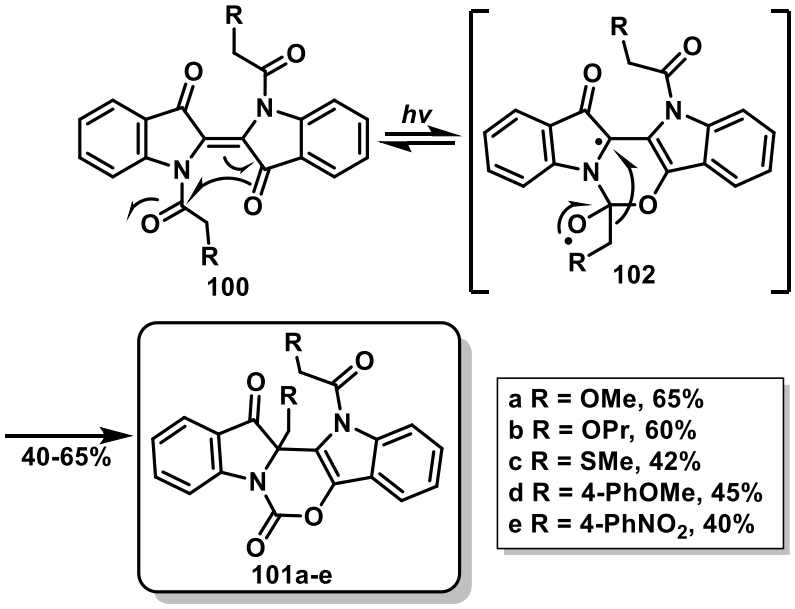

Scheme 28: Photochemical rearrangement of *N,N′*-diacylindigo to compounds **101a**–**e** *via* diradical **102**.

Performing the reaction under an oxygen atmosphere instead resulted in the formation of benzoxazinoindoles **103a**–**f** *via* molecular oxygen intercepting this radical pathway. Irradiation of the acylindigo material under an O_2 atmosphere gave peroxyl diradical **104**, which undergoes *O-O* fission to give **105** and subsequent ring-expansion to *C,O*-diradical

106. Attack of the *O*-radical on the adjacent amide leads to **107**, and subsequent *C*-*N* bond fission terminates the cascade, affording products **103a**–**f** (Scheme 29).[114]

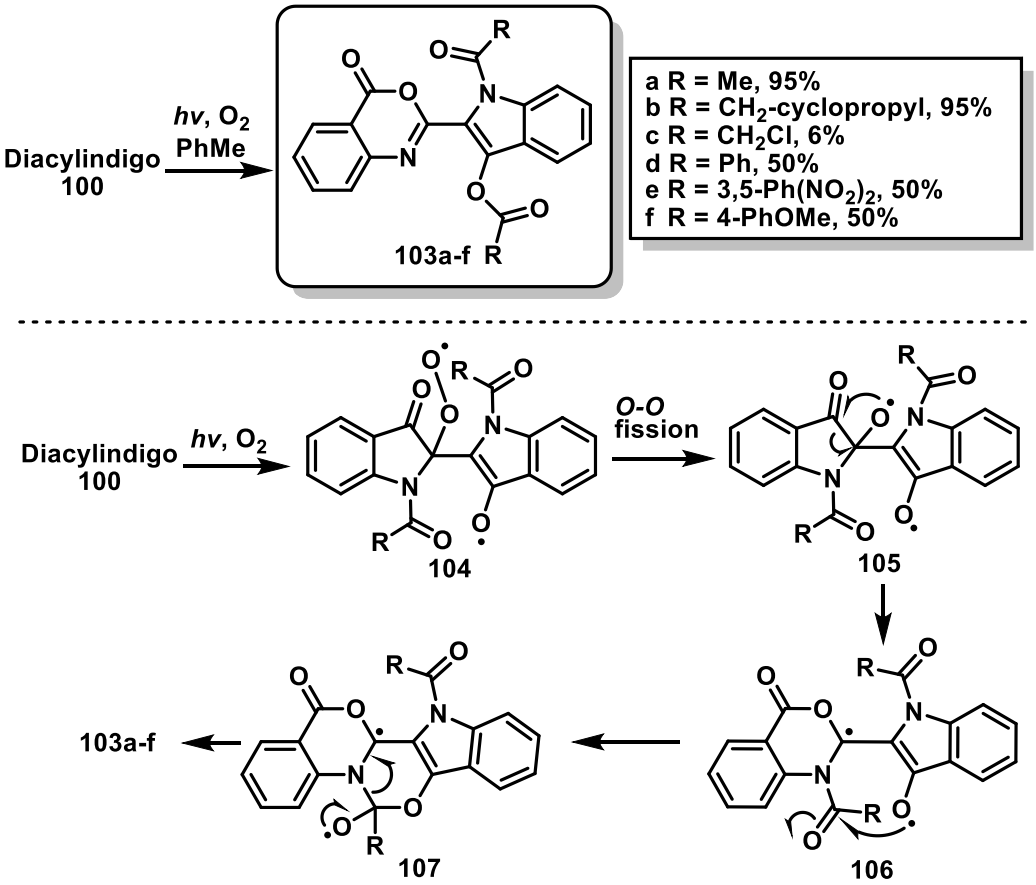

Scheme 29: Photooxidation of *N*,*N'*-diacylindigoids, resulting in ring-expansion to afford benzooxazine-indoles **103a**–**f**.

1.7.3 Cascade reactions of indigo with allylic and propargylic halides

As part of an ongoing project focused on the discovery of new cascade chemistry of indigo, our research group have previously reported on the cascade reactions of indigo with substituted allylic and propargylic halides, producing a diverse array of product heterocycles. Electrophiles with π-systems such as substituted acyl, allyl and propargyl moieties insert additional electron density to the indigo core, and the high reactivity of such systems may influence subsequent transformations. In the case of the allylation of indigo, tautomerisation of the indigo core triggers a variety of tandem cyclisation-isomerisation processes, which furnish a number of structurally complex, highly-functionalised 2,2-biindoles and spiro-bonded moieties.[115] A selection of isolated products from this series of allylation reactions is illustrated in Scheme 30.

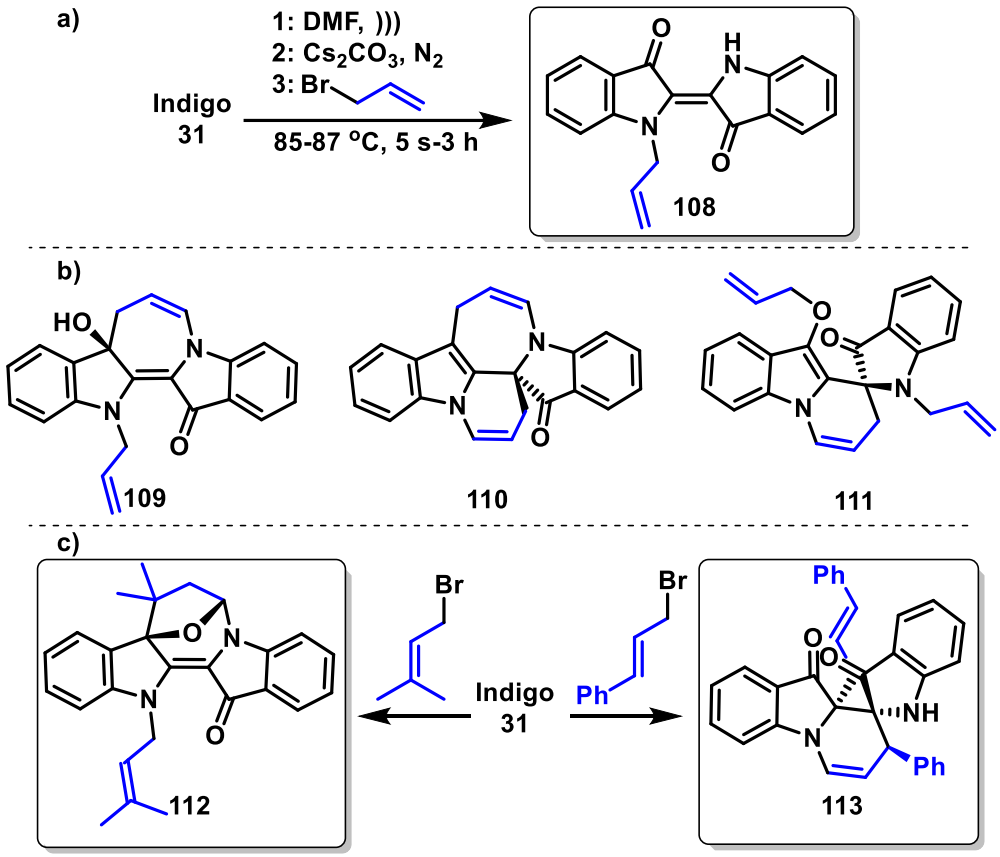

Scheme 30: Cascade reactions of indigo with allyl bromide. a) the anticipated reaction to give *N*-allylindigo **108** b) major isolated products **109**–**111** c) scaffolds accessible from substituted allylic electrophiles. Stereoindicators depict relative stereochemistry.

The structural complexity of the above scaffolds demonstrates both the novelty and the complexity of the cascade reactions that indigo undergoes. It was noted that in short (5 s) reactions that the mono-allylated product **108** predominated (83%), however this quickly undergoes further alkylation, and subsequent cyclisation to give **109** as the major product (41%) after 1 h. Increasing the reaction time to 3 h allowed for the isolation of **110** as the major product (72%), in addition to **111** in 15% yield. Significant control over the product type could also be achieved by moderating the steric environment of the inserted π-system, leading to substrate-dependent control over the cascade process. For example, the use of terminal 1,1-dimethyl and phenyl substituents was found to hinder the formation of analogues of **110**, instead affording products **111** and **112** in 26% and 16% yields, respectively.

The complexity of the mechanisms involved in these cascade processes is demonstrated further by examining the outcomes of the reaction of indigo with propargyl bromide. Over a short reaction time (5 min), indigo can be seen to have undergone a number of dramatic transformations, producing heterocycles featuring allenic and ring-expanded scaffolds as

part of a complex mixture (Scheme 31).[116] Most notably, the enhanced reactivity of the propargyl substrate promotes rapid, cascading nucleophilic processes from *N*-propargylindigo (**114**), such that the cascade reaction proceeds to over 80% completion within five minutes.

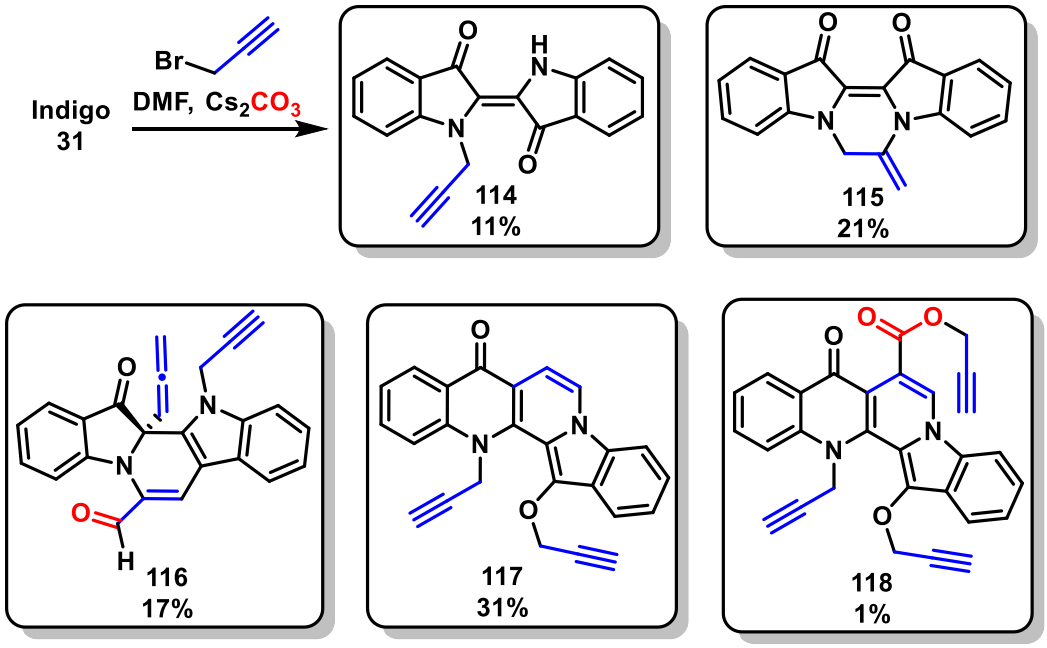

Scheme 31: The reaction of propargyl bromide with indigo results in the rapid formation of a variety of polycyclic derivatives.

In developing an understanding of the unorthodox transformations that indigo undergoes, mechanistic considerations are of considerable importance. Several mechanistic branches diverge from *N*-propargylindigo **114**, most simply where it undergoes a base-mediated 6-*exo*-dig hydroamination to afford **115**, which could also be accomplished in 98% yield by stirring **114** with Cs_2CO_3 in DMF for 5 min. Compound **116** is generated from an intermediate enol ether, which undergoes a Claisen rearrangement to generate the allene. The core heterocycles of compounds **117** and **118** are the product of three propargyl units, where nucleophilic addition to the indigo carbonyl results in a strain-driven ring-expansion from cyclic allene **119**, and simultaneous addition of a nearby electrophile – either H^+ or CO_2 for **117** and **118**, respectively. Further proton abstraction and *O*-alkylation generates the ring-expanded products (Scheme 32).

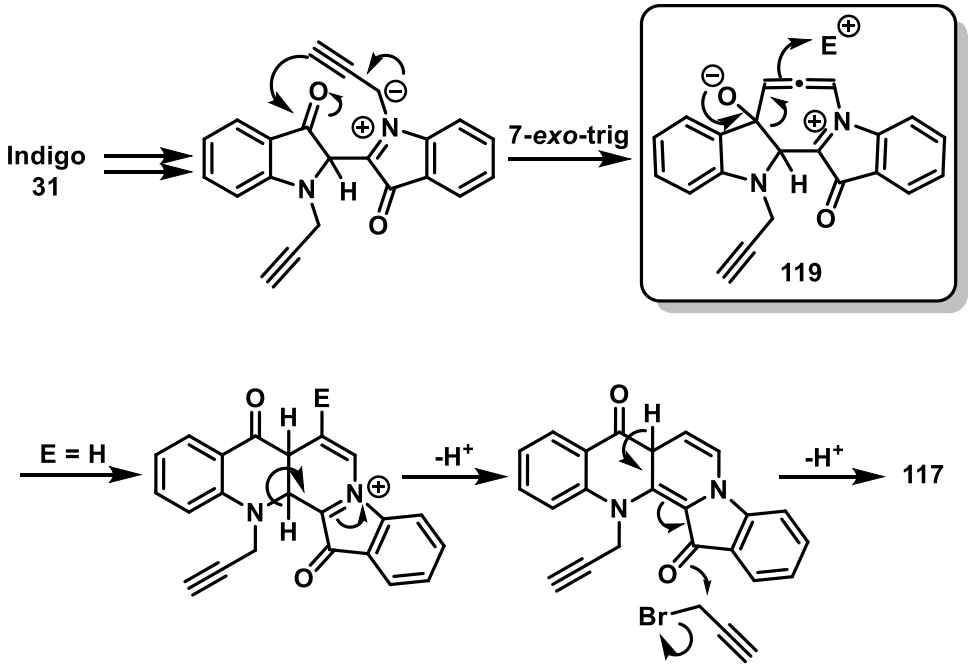

Scheme 32: Abbreviated mechanism for the formation of compound **117** from indigo *via* cyclic allene zwitterion **119**.

This propargylation reaction was observed to be affected significantly by the nature of the leaving group, where replacing the bromide with a mesylate instead led exclusively to allene **116** and naphthyridinone **117** in 28% and 59% yield, respectively. The mechanistic pathway could also be controlled by the addition of a terminal methyl substituent, which led to the formation of acyclic compound **120** and ring-expanded product **121**. Surprisingly, using 3-chloro-1-phenyl-1-propyne as the electrophile resulted in products **122** and **123**, which bear little resemblance to any of the molecules accessible from propargyl bromide. Regarding compound **123**, exhaustive NMR studies and HR-ESI mass spectral analyses have allowed the assignment of a tentative structure, however the observation of atypically-strong, apparent five-bond correlations in the HMBC spectrum from the H9-C1' would suggest this structure to be incorrect, and its precise structure is as-yet unconfirmed. Furthermore, no logical mechanism has been proposed which would account for the formation of **123** under these conditions. The use of bromoacetonitrile as an electrophile also led mostly to polymerisation over longer reaction times, though the *mono*-alkylated derivative **124** could be isolated over very short (5 s) reaction times (Scheme 33).[116b] It is apparent that the nature of both the leaving group and the terminal substituent (i.e. the substituent's steric, and electronic characteristics) have a considerable impact on the accessible mechanistic pathways of the reaction, though the full extent of these impacts have not been fully-established.

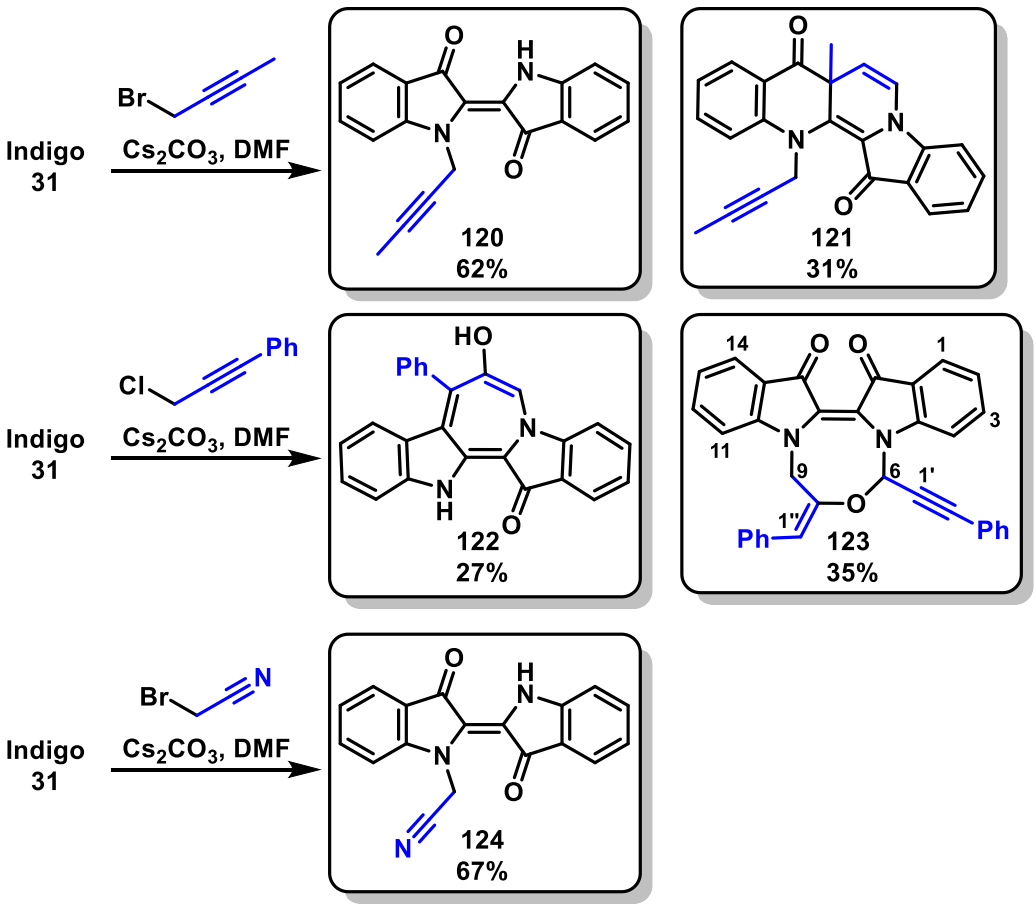

Scheme 33: Reactions of 1-bromo-2-butyne, 3-chloro-1-phenyl-1-propyne, and bromoacetonitrile with indigo to give compounds **120**–**124**. The exact structure of **123** is in doubt, due to apparent HMBC correlations from H9 to C1' through five bonds.

In summary, while there has been significant development to date of the use of cascade reactions of indigo for the synthesis of new, bioactive heterocycles, there are significant areas requiring further investigation. Our current diversity-oriented approach has allowed for the exploration of a window of chemical space, however this has been limited by the exclusive use of allylic and propargylic systems to date. Due to both the degree of unsaturation and the trigonal-planar or linear geometry of the incoming electrophile, the products from these reactions are largely two-dimensional in shape, and in the limited examples where stereogenic atoms are generated in the products – e.g. spirocycles **110** and **111** – these molecules have only been synthesised racemically. In developing a more thorough understanding of these cascade processes, it would be advantageous to probe the use of new electrophilic species with greater three-dimensionality, to determine whether the chirality of the products can be controlled by the stereochemistry of the electrophile. In the process of developing more "drug-like" architectures, it could also be advantageous to insert additional H-bonding sites to improve aqueous solubility, hence

sp^3-rich electrophiles containing heteroatoms would seem ideal.

A broad array of chemical transformations of indigo were reported in the early 20th century, however these predate many modern characterisation techniques, and in several instances, have been reported to be unreliable, or the products have been the subject of many years of repeated structural revision. While previous studies within our group have demonstrated indigo's nucleophilicity to be a starting point for cascade reactions, there are only a handful of modern reports on indigo's electrophilic potential, and none have utilised this as a platform for the construction of new, biologically-active molecules.

1.8 Project aims

Therefore, the aims of this project are:

- To further develop the chemistry of indigo with substituted propargylic halides (Chapter 2),
- To develop new nucleophilic cascade chemistry of indigo with multifunctional electrophiles (Chapter 3),
- To re-investigate the electrophilic chemistry of indigo with substituted nucleophiles (Chapter 4), and
- To establish the biological profile of derived species, toward the generation of new, bioactive heterocycles (Chapter 5).

Chapter 2:
Reactions of indigo with propargylic electrophiles

2.1 Propargylic systems in organic synthesis

2.1.1 Synthesis and properties of propargylic systems

Investigation of the synthesis and reactivity of propargylic systems has been one avenue of significant interest within the synthetic chemistry community, due to their ease of incorporation, robustness under many conditions, and unique reactivity under metal-catalysed conditions. Since the development and widespread appreciation of copper-catalysed azide-alkyne ("Click") cycloaddition chemistry in the early 2000s,[117] there has been a considerable increase in interest for propargyl units as functional handles for synthetic manipulation. A Scifinder scholar search reveals significant growth in the field of propargylic chemistry since the mid-1970s, as represented by an upward trend in the number of publications concerning propargylic systems over time (Figure 7).

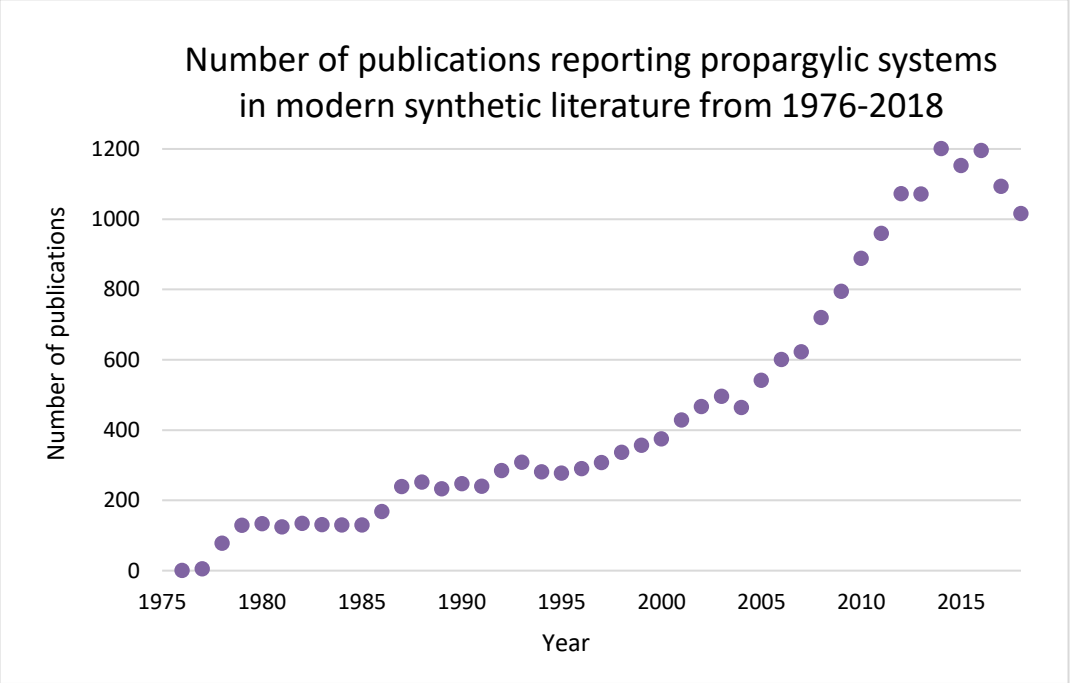

Figure 7: The growth of propargylic systems in synthetic chemistry over time. Data collected from Scifinder Scholar data.

In most instances, the propargyl unit is appended to the desired scaffold by nucleophilic substitution of propargyl bromide onto an amine, alcohol or thiol nucleophile, or by using alkyne synthetic strategies including elimination of haloalkenes or 1,2-dihaloalkanes (easily accessed by halogenation of olefins), and a broad variety of alkyne-substituted systems may be accessed in excellent yields from Sonogashira cross-coupling reactions

between terminal alkynes and aryl halides under dual Pd^0/Cu^I catalysis. Other methods include Seyferth-Gilbert homologation of ketones, nucleophilic addition of metalated acetylenes (e.g. ethynylmagnesium bromide) to aldehydes and ketones, or to alkyl halides by transmetalation with Cu^I to produce the corresponding Gilman reagent, which participate readily in S_N2 displacement reactions (Scheme 34).[118]

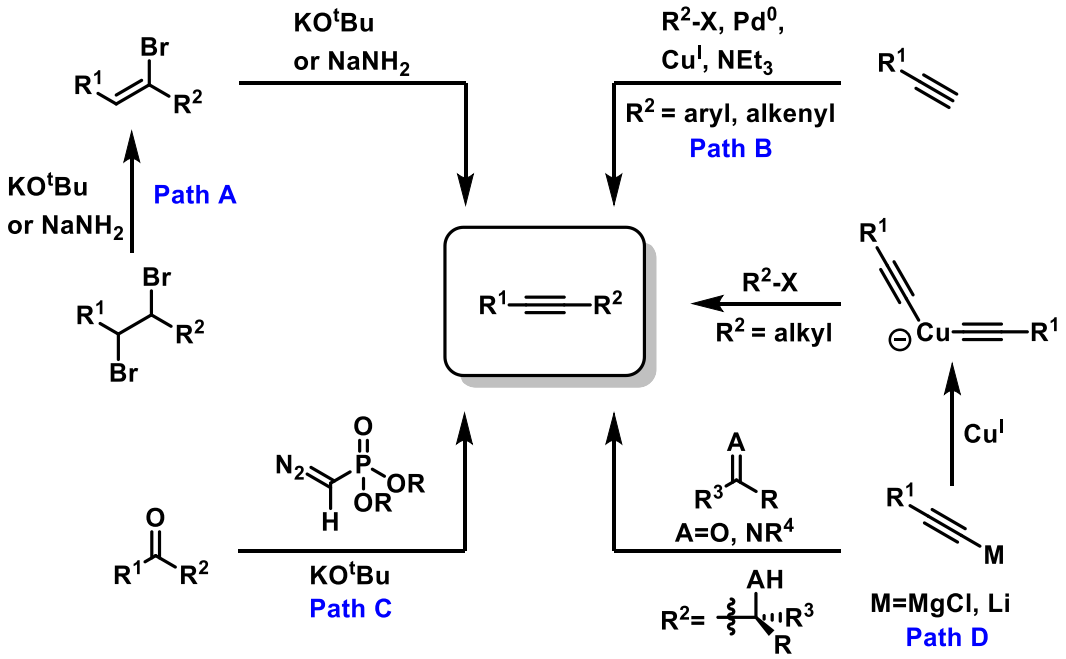

Scheme 34: Common methods for the synthesis of alkynes: **Path A**: elimination of dihaloalkanes and haloalkenes, **Path B**: Sonogashira coupling, **Path C**: Seyferth-Gilbert homologation, and **Path D**: addition of metallated acetylenes to electrophiles.

2.1.2 Reactions of propargylic systems

Much of the reactivity of propargylic systems may be attributed to the Lewis basicity of the alkyne moiety,[119] and owing to the growing popularity of propargyl units in organic synthesis, their reactivity has been the subject of several reviews.[120] Briefly, in the presence of soft Lewis acids, e.g. Ag^I, Au^I, Pd^{II} and Rh^{II} among others, the alkyne π-system can undergo reversible coordination, rendering the alkyne electrophilic – this mode of catalysis is common, though Pd and Au catalysts are of particular note due to their applicability toward carbon-carbon π-bond activation. In considering the reactivity of alkynes with various nucleophiles under Lewis acid catalysis (Scheme 35), the degree of back-bonding character that the metal possesses determines whether the Lewis pair acts primarily as a metal-stabilised carbocation (**125**) or a metallocarbene (**126**). Nucleophilic addition to carbocation **125** affords the metalated adduct **127**, which undergoes protodemetalation to give the substituted product **128**. Where the incoming nucleophile is a water molecule, the enol **128** typically tautomerises to afford a ketone –

for this reason alkyne hydration is both a robust methodology for ketone synthesis at low catalyst loading, and a common side-product from reactions not performed under anhydrous conditions.[121]

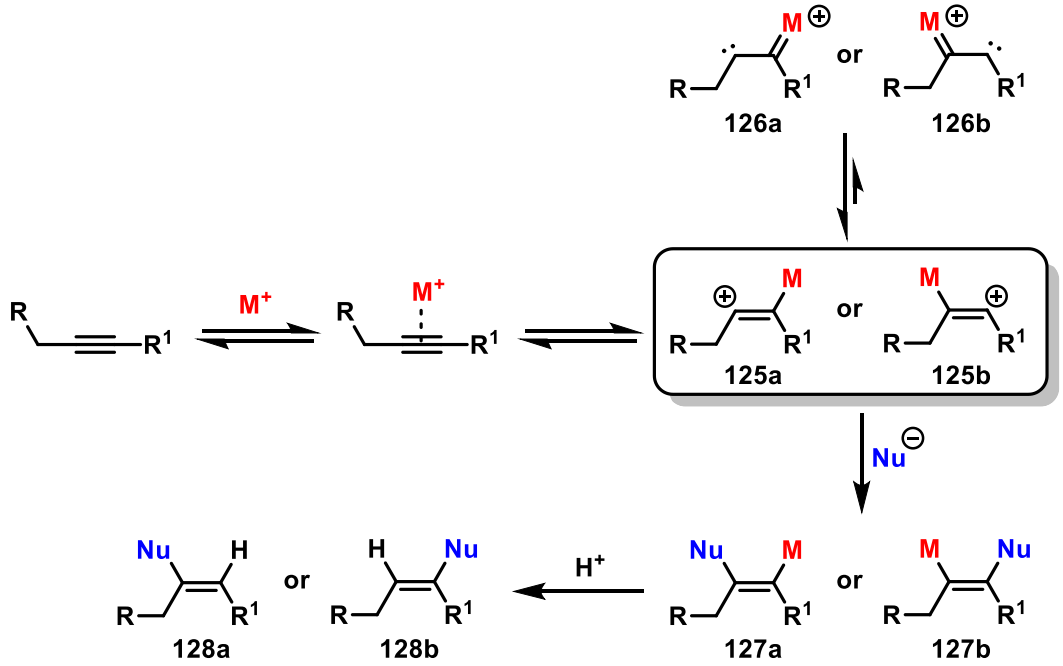

Scheme 35: Activation of alkynes toward nucleophilic addition under Lewis acid catalysis.

Intercepting this pathway is possible using various alkyne-tethered nucleophiles, leading to intramolecular cyclisation and rearrangement to afford functionalised cyclic systems. One such example involves the intramolecular cyclisation of *N*-propargylamidines to substituted imidazoles under Au^{I} catalysis (Scheme 36).[122] The reaction proceeds *via* Lewis acid activation of the pendant alkyne, which undergoes nucleophilic attack from the nearby nitrogen nucleophile. A [1,3]-hydride shift leads to aromatisation of the imidazolium ion, which affords the trisubstituted imidazole upon protodeauration.

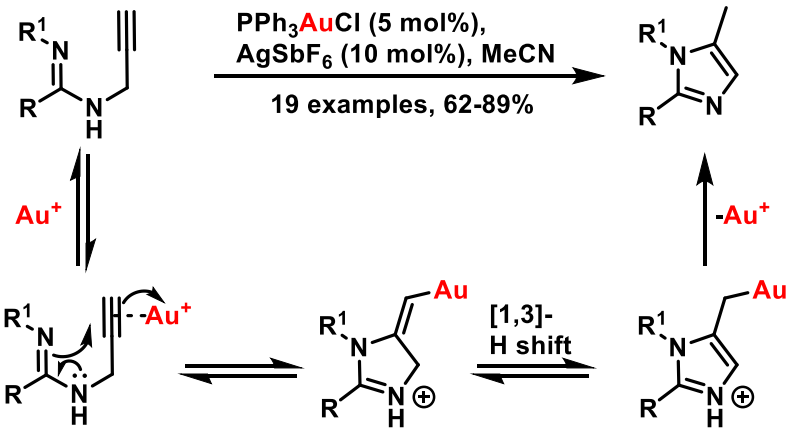

Scheme 36: Gold-catalysed cyclisation of *N*-propargylamidines to substituted imidazoles.

In similar fashion, this pathway can be intercepted by intermolecular addition to the alkyne upon Lewis acid activation. One elegant example of this is in the gold-catalysed addition of aliphatic alkynes or ynamides to anthranils by the Hashmi group, where *N*,*O*-fission of the anthranil-adduct affords a gold vinylidene ion, which undergoes regioselective Friedel-Crafts addition to the adjacent phenyl group, affording 2-substituted-7-acylindoles (**129**) in good yields and with high selectivity.[123] Interestingly, using propargylic silyl ethers under analogous conditions instead led exclusively to the formation of 3-acylquinolines (**130**) by rapid protodeauration and subsequent Mukaiyama aldol condensation due to the high nucleophilicity of the silyl enol ether pendant (Scheme 37).[124]

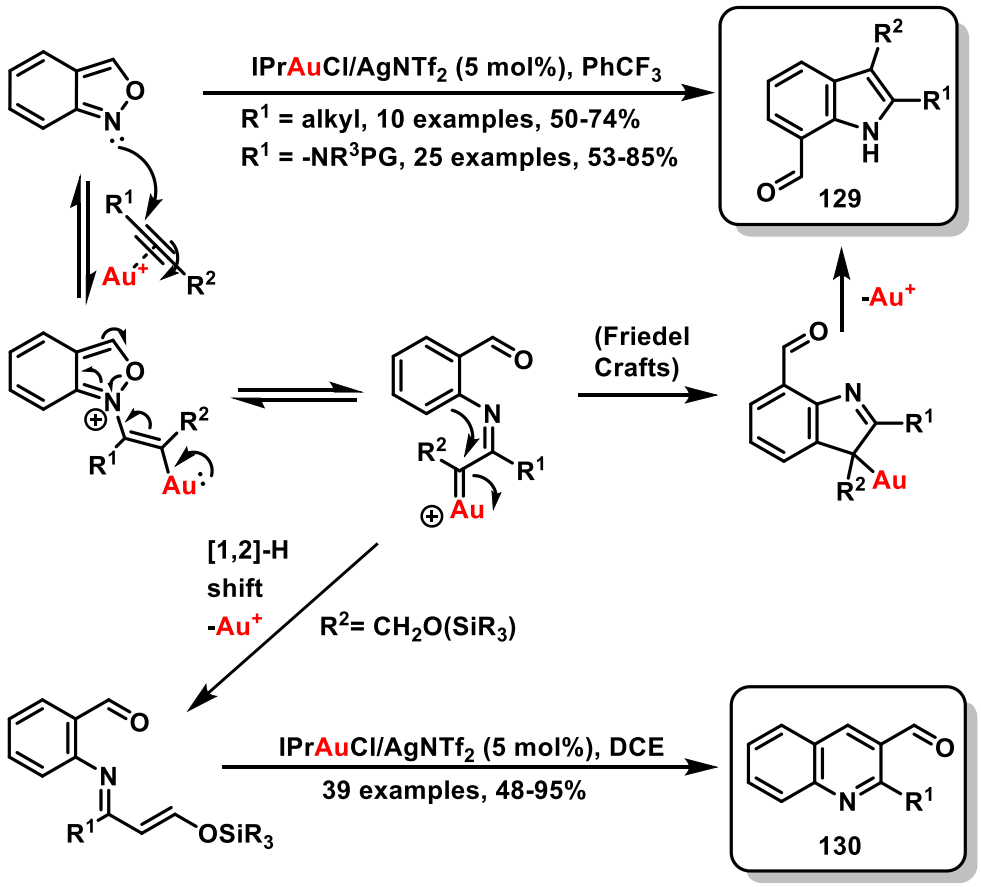

Scheme 37: Intermolecular cyclisation of anthranils with nonsymmetrical alkynes to give divergent access to either 7-acylindoles (**129**) or 3-acylquinolines (**130**) under Au^{I}-catalysis.

As could be expected from their high degree of unsaturation, alkynes readily participate in cycloaddition reactions with various coupling partners. One example which has achieved widespread acclaim and practical use is the Cu-catalysed "Click" cycloaddition of alkynes and azides to afford 4-substituted 1,2,3-triazoles. Key intermediates in this mechanism have been observed spectroscopically, computationally and

crystallographically, and as such it is known that the reaction mechanism proceeds *via* formation of a dinuclear copper acetylide,[125] with the second Cu^{I}-ion acting to both chelate the incoming azide to the alkyne, and to activate the alkyne to nucleophilic attack (Scheme 38). Elimination of a copper ion forms the triazole heterocycle and subsequent protolysis of the organocuprate leads to elimination of the product, and propagation of the catalytic cycle.[126]

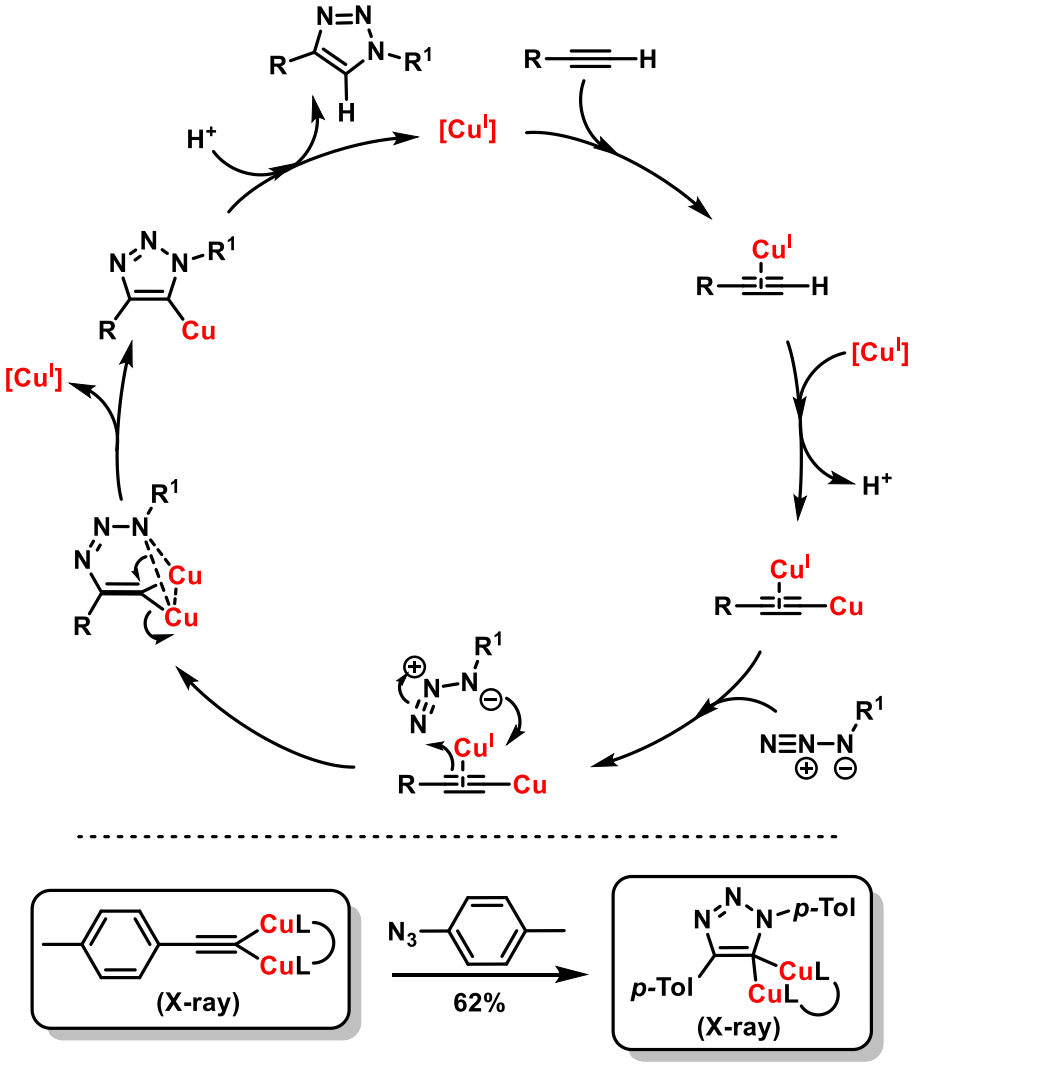

Scheme 38: Catalytic cycle for the copper-catalysed azide-alkyne "Click" cycloaddition reaction, and several key intermediates observed by crystallography.

2.2 Cascade reactions of propargylic systems with indigo

2.2.1 Limitations of previously-explored chemistry

From the established chemistry of indigo in reactions with propargylic halides, it is apparent that the nature of the leaving group has a significant effect on the reaction pathway, evidenced by the observation that exchanging the bromide leaving group for a mesylate led exclusively to products **116** and **117** in a combined 87% yield,[116b] while the corresponding chloride led instead to compounds **114** and **115** in combined 82% yield (Scheme 39).[127]

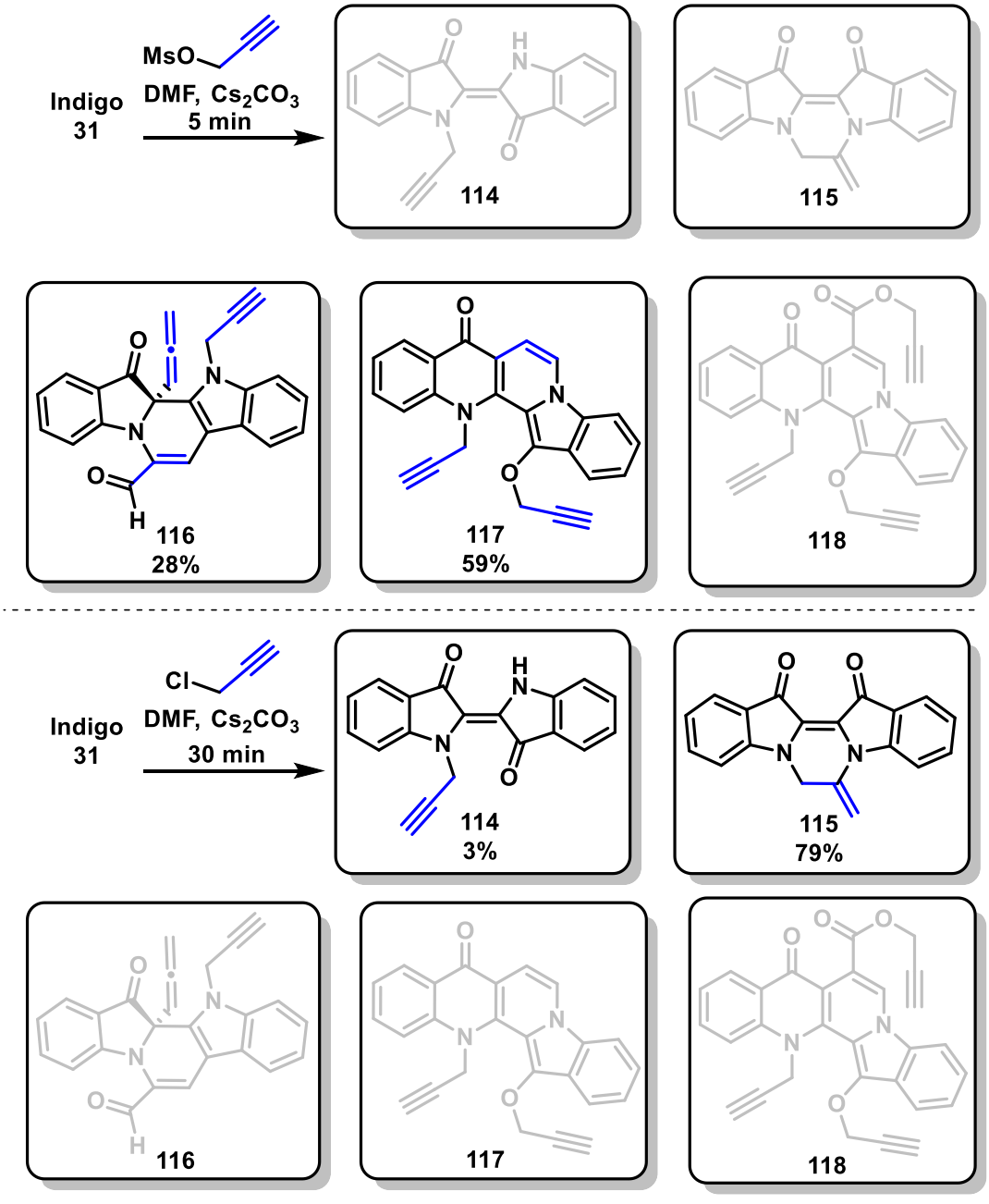

Scheme 39: The reaction of indigo with propargyl mesylate led exclusively to compounds **116** and **117** in high yield, while propargyl chloride instead gave **114** and **115** in high yield.

Our current working hypothesis is therefore that with weaker leaving groups, spontaneous *N,N′*-cyclisation occurs prior to a second *N*-alkylation, producing higher yields of **115** and related structures, while stronger leaving groups lead to more rapid *N′*-alkylation, which serves as the starting point for subsequent cascade reactions toward the more-complex heterocycles **116** and **117**. As a result, it is unknown whether the divergence in outcomes from those reported for the reaction of the methyl-substituted 1-bromo-2-butyne and the phenyl-substituted 3-chloro-1-phenyl-1-propyne are a result of the increased steric effect of the phenyl group, the conjugation of the phenyl group, the weaker chloride leaving group, or a combination of all three factors (Scheme 40). The primary reason for using the (chloro)-phenylpropargyl electrophile in previous studies was its commercial availability, and it is unknown whether the corresponding bromide would show similar or disparate reactivity with indigo. Similarly, if the conjugation of the phenyl group has a significant effect on the outcome of the reaction, it should be possible to tune this reactivity by utilising electron-donating or -withdrawing groups. This effect has not yet been adequately examined, and is the subject of this chapter.

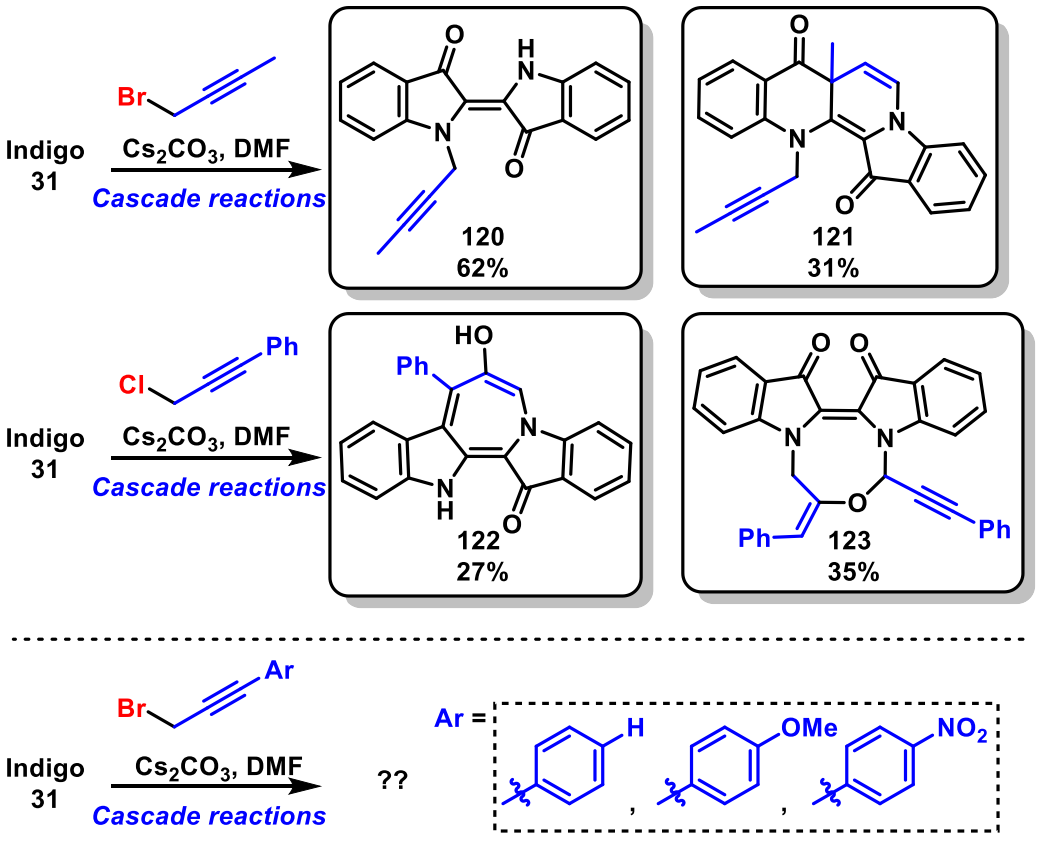

Scheme 40: Differing reactivity of the methyl- and phenyl-substituted propargyl electrophiles, and proposed methodology for determining the cause of this disparate reactivity.

2.3 Cascade reactions of (aryl)propargyl electrophiles with indigo

2.3.1 Synthesis of starting materials

The synthesis of the required aryl-substituted propargyl electrophiles was accomplished on multi-gram scale by a two-step sequence, involving Sonogashira coupling of propargyl alcohol with an aryl iodide to afford an intermediate (aryl)propargyl alcohol, which was brominated under Appel conditions using PPh_3/Br_2. The $Pd(PPh_3)_2Cl_2$ catalyst utilised for the Sonogashira coupling was prepared on multigram-scale by ligation of PPh_3 to $(PdCl_2)_n$ in benzonitrile following a previously-reported procedure;[128] the mixture was heated to reflux under an N_2 atmosphere with vigorous stirring for 20 min, then allowed to cool to room temperature overnight and the collected solids triturated with ether to furnish the desired *bis*-phosphine complex as small, bright yellow crystals in 95% yield. Initially, the cross-coupling reaction between 4-iodoanisole and propargyl alcohol was run at reflux for 3.5 h in neat diethylamine using $Pd(PPh_3)_2Cl_2$ (3 mol%) and CuBr (10 mol%),[119h] which upon workup and flash chromatography afforded the desired *p*-methoxyphenyl adduct **131a** in 62% yield. Optimal conditions were found using propargyl alcohol (5.0 eq.) and NEt_3 (7.0 eq.) in a 1:1 toluene:MeCN (v/v) mixed solvent, with CuI (10 mol%) and $Pd(PPh_3)_2Cl_2$ (2 mol%) at room temperature for 2 days, which afforded **131a** in 99% yield. This reaction proved amenable to the synthesis of various functionalised arylated substrates, affording the corresponding alcohols **131b**–**d** on gram-scale in high yield (Scheme 41).

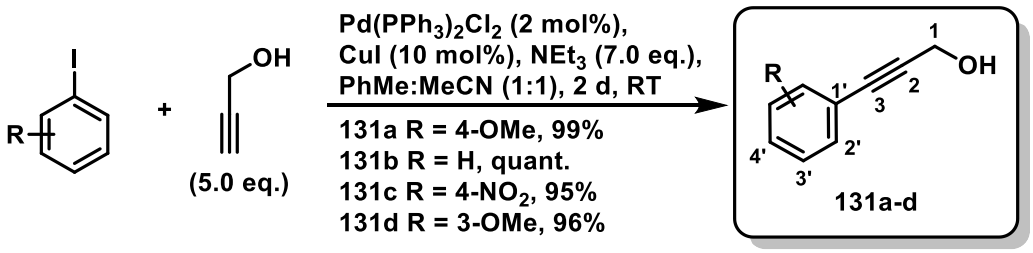

Scheme 41: Optimised conditions for the Sonogashira coupling of aryl iodides with propargyl alcohol to yield the substituted propargyl alcohols **131a**–**d**.

Analysis of the HRESI mass spectrum of **131a** revealed a peak at 163.0760, assigned to the molecular ion $[C_{10}H_{11}O_2]^+$, revealing the substitution of the iodide handle for the propargylic alcohol. Analysis of the ^1H NMR spectrum revealed a pair of 2H doublets at δ 7.37 and δ 6.84, assigned to the alkyne-adjacent H2'/H6' and methoxy-adjacent H3'/H5' respectively of the *para*-disubstituted phenyl group. Further upfield, the 2H apparent singlet at δ 4.48 was assigned to the H1 methylene protons of the propargyl fragment, which coupled to a broad singlet resonance at δ 1.68 in COSY experiments, which was

assigned to the free hydroxyl proton. The remaining 3H singlet at δ 3.81 was assigned to the *para*-methoxy group of the aryl substituent. Analysis of the ^{13}C NMR spectrum revealed a downfield quaternary resonance at δ 159.8 and an upfield quaternary resonance at δ 114.7, which were assigned to C4' and C1' of the aryl substituent, while the remaining two aromatic-range resonances at δ 133.2 and δ 114.0 were assigned to C2'/C6' and C3'/C5', respectively. A pair of adjacent quaternary resonances appeared at δ 85.6 and δ 85.9, which were assigned to the alkyne carbons C2 and C3, respectively, and the remaining resonances at δ 55.3 and δ 51.7 were assigned to the methoxy and methylene carbons, respectively.

Subjecting alcohols **131a–c** to a mixture of PPh_3/Br_2 afforded the desired alkyl bromides **132a–c** in excellent yield. Briefly, to a cooled (0 ˚C) solution of PPh_3 (1.1 eq.) in dry CH_2Cl_2 was added dropwise neat Br_2 (1.1 eq.), and the resulting bright yellow suspension warmed to room temperature over 1 h. To this was added slowly dropwise a solution of the selected propargyl alcohol (1.0 eq.) in CH_2Cl_2, and the mixture stirred at room temperature for 1 h. The resulting triphenylphosphine oxide was precipitated by adding hexanes, then either subjected to repeated recrystallisation from hexane (**131a**) or subjected to column chromatography (**131b–c**) to afford the corresponding alkyl bromides **132a–c** in excellent yield (Scheme 42).

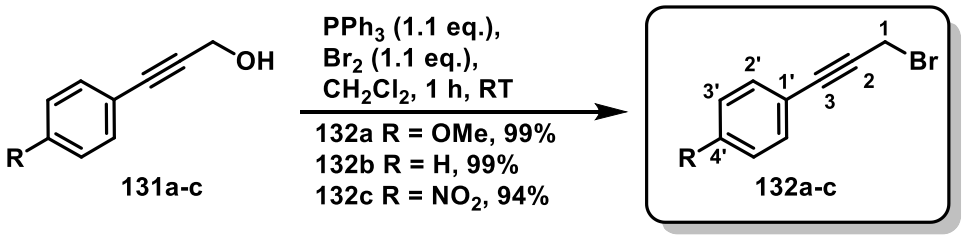

Scheme 42: Conversion of alcohols **131a–c** to alkyl bromides **132a–c** by reacting with PPh_3/Br_2.

The methoxy-substituted (phenyl)propargyl bromide **132a** was isolated in 99% yield, following repeated recrystallisation from hexane. Analysis of the EI(+) mass spectrum revealed peaks at 224^+ and 226^+ in a 1:1 ratio in 8% relative abundance, assigned to the isotopic pair of $[C_{10}H_{10}O^{79}Br]^+$ and $[C_{10}H_{10}O^{81}Br]^+$ ions, and a base peak at 145^+, corresponding to the $[M\text{-}Br^{\bullet}]^+$ fragment, demonstrating the substitution of the hydroxyl group for the alkyl bromide. Analysis of the ^1H NMR spectrum revealed a 2H singlet resonance at δ 4.17, assigned to the bromine-adjacent methylene protons H1a/b, and a 3H singlet resonance at δ 3.81, assigned to the methoxy protons of the aryl substituent. Analysis of the ^{13}C NMR spectrum revealed a highly-shielded resonance at δ 15.9, and a pair of quaternary resonances at δ 83.0 and δ 87.0, which were assigned to C1, C3 and

C2 of the propargylic moiety, respectively. Further downfield, the resonances at δ 133.6 and δ 114.1 were assigned to C2'/C6' and C3'/C5' of the 4-methoxyphenyl substituent, and the remaining resonances at δ 160.1, δ 114.3, and δ 55.5 assigned to C4', C1', and the methoxy carbon, respectively.

Under optimised conditions, this reaction proved reliable and consistently afforded the desired bromides in 90-99% yield, though it proved sensitive to the rate of alcohol addition, as evidenced by diminished yields and the formation of complex mixtures with faster addition rates to the $PPh_3.Br_2$ complex generated *in situ*. The methoxy-substituted bromide **132a** also proved unstable toward silica gel chromatography, though the phenyl- (**132b**) and 4-nitrophenyl-substituted (**132c**) propargyl bromides could be easily purified by flash chromatography.

2.3.2 Reactions with indigo

As a direct analogue to the previously-explored (phenyl)propargyl chloride, we examined the reaction between (phenyl)propargyl bromide **132b** with indigo under identical conditions to those used previously.[116b] Therefore, a sonicated suspension of indigo (1.0 mmol) in anhydrous DMF (40 mL) was transferred by cannula into a round-bottomed flask containing anhydrous cesium carbonate (3.7 mmol) and 4 Å molecular sieves under a N_2 atmosphere, and the mixture warmed in an oil bath pre-heated to strictly 85-87 ˚C for 1 h with vigorous stirring.* The N_2 flow was cut, then a solution of **132b** (5.0 mmol) in DMF (2 mL) injected through the septum, and the resulting mixture stirred for 30 min. Following aqueous workup, the crude mixture was fractionated on silica, then the individual fractions subjected to flash chromatography, affording the ring-expanded indolobenzonapthyridinone **133** in 35% yield, as well as the known compounds azepinodiindole **122** in 37% yield, and diindolooxadiazepine **123** in 12% yield (Scheme 43).

* These conditions were optimised previously by Dr. Alireza Shakoori for reactions of indigo with propargylic halides, and were used without modification to allow comparison between systems. The rationale behind this strict temperature control is that in general, the poor solubility of indigo in DMF means that at lower temperatures (e.g. 70 ˚C), more unreacted starting materials are recovered, and the slower rate of reaction leads to increased proportions of isatins and other byproducts from oxidation and/or hydrolysis.

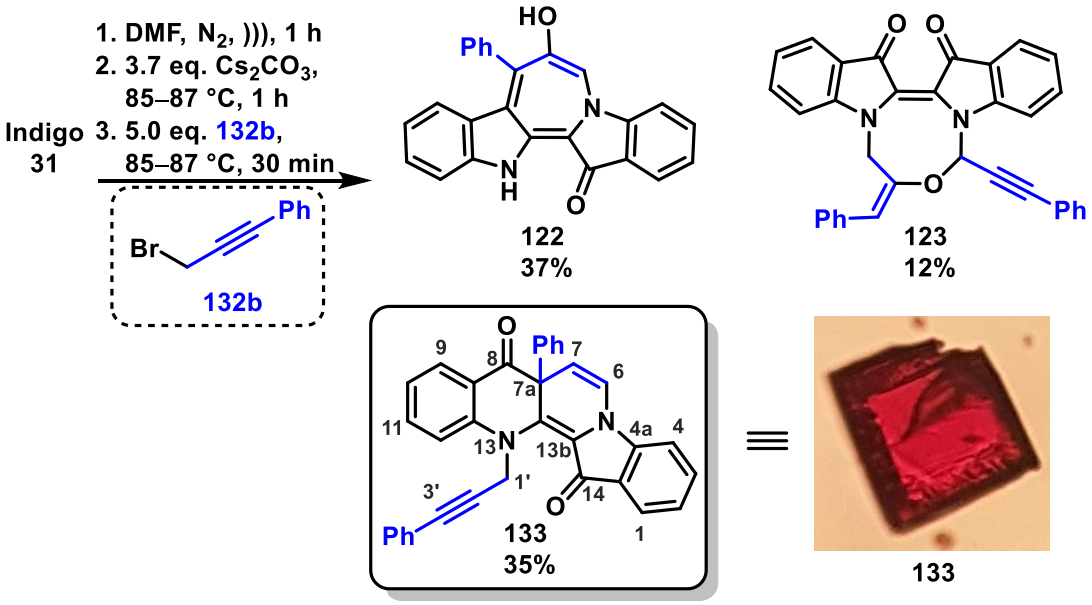

Scheme 43: Reaction of (phenyl)propargyl bromide **132b** with indigo, to afford the known products azepinodiindole **122**, oxadiazepinodiindole **123**, and the ring-expanded indolobenzonaphthyridinone **133**. Adjacent to the structure is a photograph of a single crystal of **133** grown from CH_2Cl_2/hexane, visualised under a light microscope at 40× magnification.

The ring-expanded indolobenzonaphthyridinone **133** was isolated as deep red crystals in 35% yield from indigo following fractionation on silica and flash chromatography using 10% EtOAc/hexane as eluent. Analysis of the HRESI mass spectrum revealed a peak at *m/z* 491.1762, assigned to the molecular ion $[C_{34}H_{23}N_2O_2]^+$, revealing the addition of two (phenyl)propargyl units to the indigo core, while its characteristic deep red colour qualitatively suggested through-conjugation to have been interrupted in the molecule. Analysis of the ^{1}H NMR spectrum revealed a pair of doublets at δ 5.18 and δ 4.91, which were assigned to the methylene protons of the *N*-phenylpropargyl pendant, made chemically-distinct by restricted rotation about the N13-C1' axis, as was observed in the ^{1}H spectrum for the methyl analogue **121**.[116b] This assignment was supported by analysis of the HSQC spectrum, which showed direct attachment of both doublets to a resonance at δ 44.9, assigned as C1' (Figure 8). The distinctive enamine protons H6 and H7 were assigned to a pair of doublets at δ 6.83 and δ 5.51, respectively, evidenced by COSY correlations to one-another, and the presence of a strong three-bond HMBC correlation between H6 and the quaternary ^{13}C resonance at δ 57.2, assigned to the stereogenic carbon atom C7a (Figure 9, Figure 10). Analysis of the ^{13}C NMR spectrum revealed a pair of carbonyl resonances at δ 191.6 and δ 178.9, assigned to the C8 and C14 ketone groups, respectively. Analysis of the HMBC spectrum revealed a strong correlation between C14 and a ^{1}H resonance at δ 7.77, assigned as H1, while C8 coupled strongly to a resonance

at δ 8.01, and coupled weakly to a resonance at δ 7.08, assigned as three-bond and four-bond correlations to the nearby H9 and H10, respectively. The C8 ketone group was additionally correlated to the adjacent enamine H7 through three bonds, confirming the insertion of the propargyl moiety between the indolic C2/C3 bond of the indigo precursor.

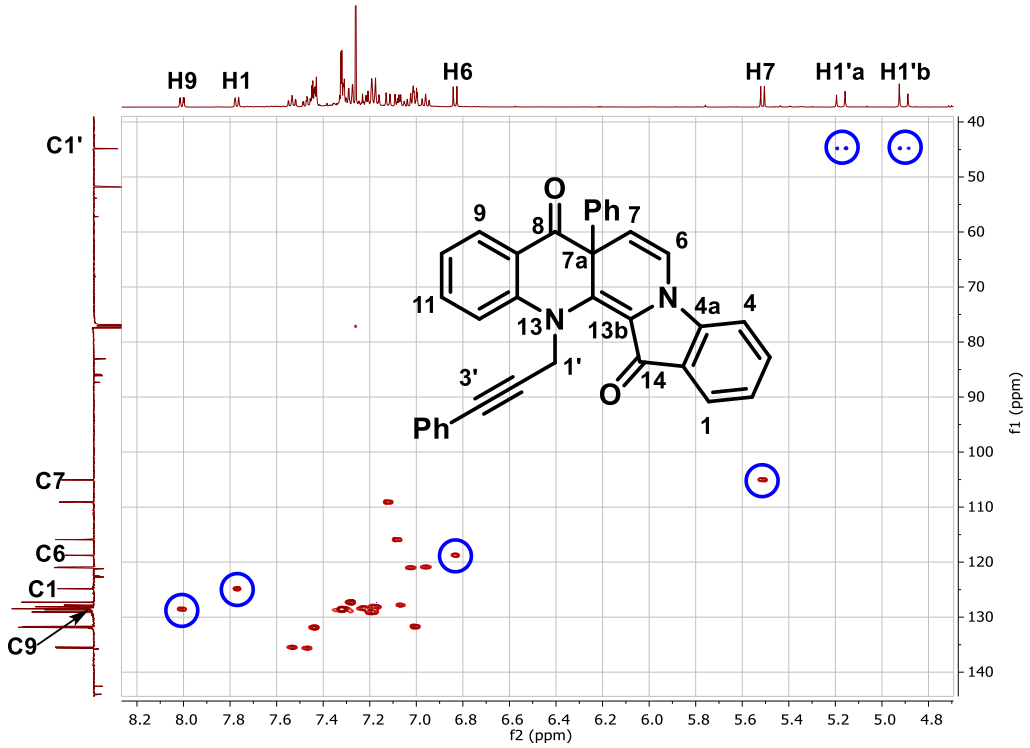

Figure 8: HSQC spectrum for compound 133, with key correlations highlighted.

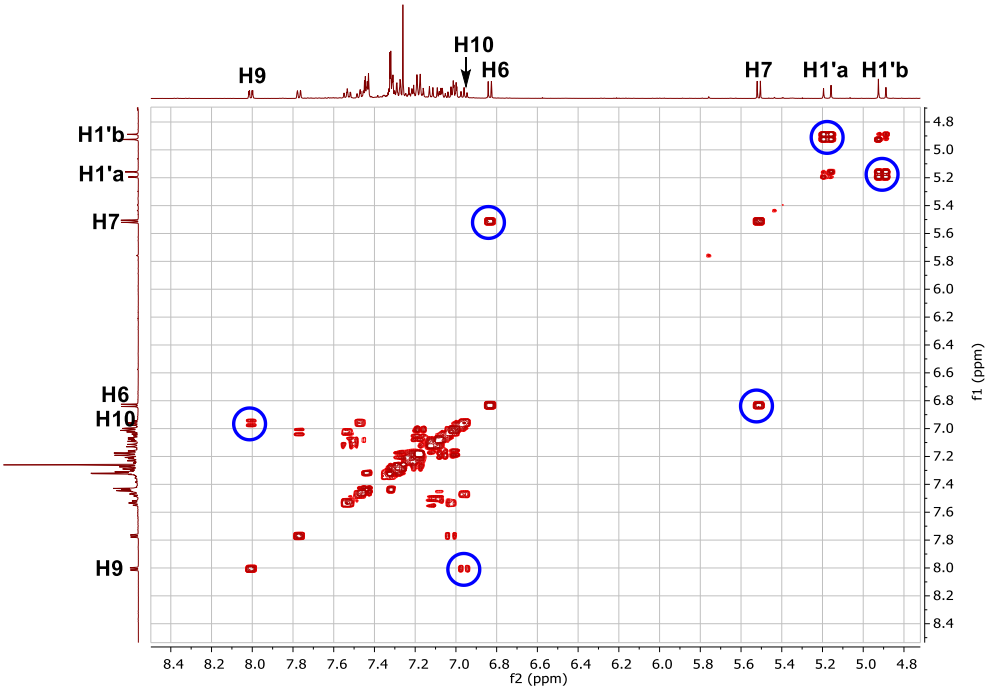

Figure 9: COSY spectrum for compound **133** with key correlations highlighted.

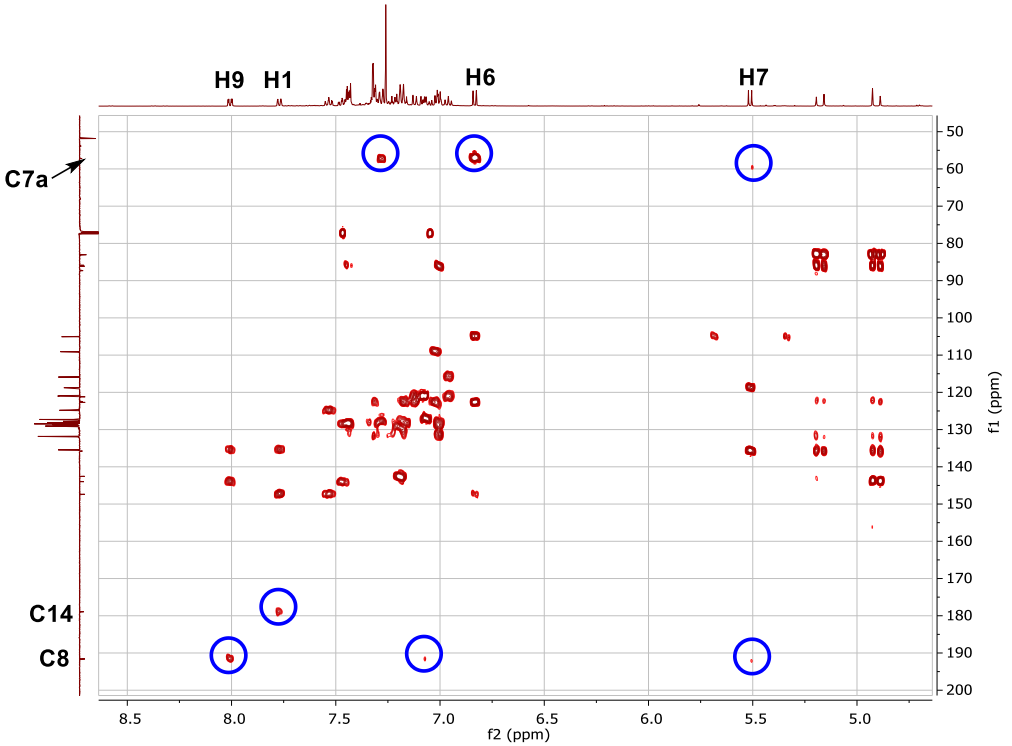

Figure 10: HMBC spectrum for compound **133**, with key correlations highlighted.

X-ray quality crystals of compound **133** were grown from slow evaporation of a hexane/CH_2Cl_2 solution, and its structure was unequivocally confirmed by x-ray crystallography (Figure 11).[†]

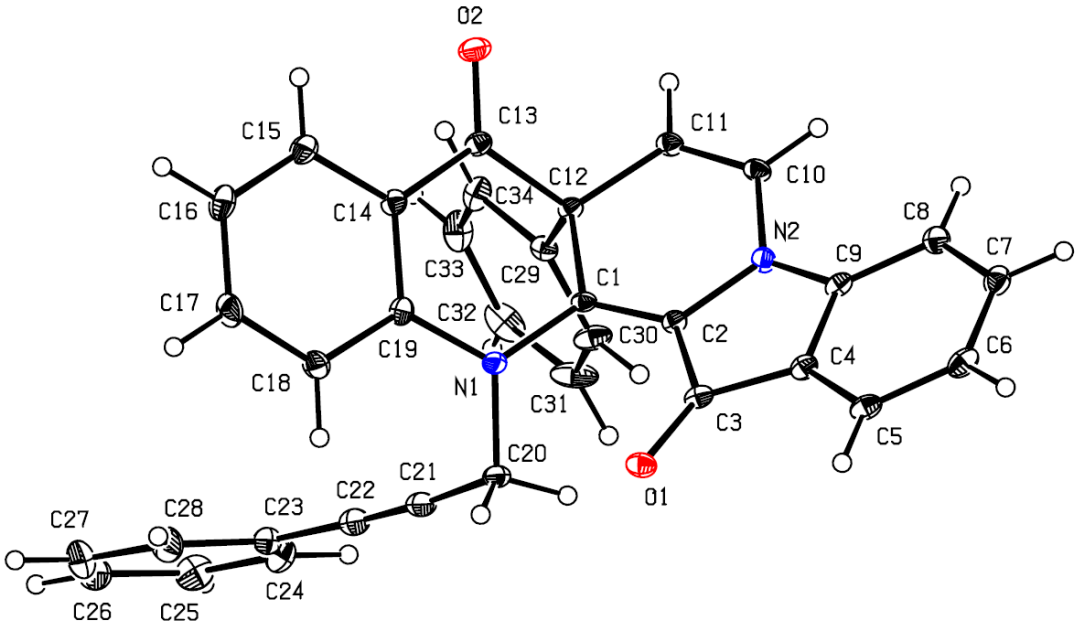

Figure 11: ORTEP depiction of compound **133**. Note that the atom numbers as denoted by x-ray crystallography do not reflect systematic numbering of atom positions.

[†] X-ray crystallography performed by Dr. Anthony Willis (ANU).

The formation of **133** by nucleophilic ring-expansion was unexpected for several reasons. Firstly, it was hypothesised that the relatively-large steric presence of the terminal phenyl substituent would hinder nucleophilic attack of the alkyne π-system to the indigo carbonyl. Furthermore, there was no evidence for the formation this compound in the previous reaction of 3-chloro-1-phenyl-1-propyne,[116b] with repeated attempts of this reaction giving similar isolated yields of compounds **122** (24%) and **123** (35%) to those reported with no **133** present. Using the bromide leaving group however, phenyl-substituted **133** was isolated in higher yield (35%) than that reported for the methyl-substituted **121** (31%), suggesting the steric effect of this substituent to be negligible. It is therefore the case that the nature of the leaving group has a significant impact on product distribution in reactions with indigo with terminally-substituted propargylic electrophiles.

To determine whether increasing the electron density of the ring system would increase the nucleophilicity of the alkyne system and lead to higher yields of ring-expanded products like **121** and **133**, we examined the reaction of indigo with 3-(4-methoxyphenyl)propargyl bromide **132a** under identical conditions to those for **132b**. Therefore, a sonicated suspension of indigo (1.0 mmol) in dry DMF (40 mL) was transferred by cannula to a round-bottomed flask containing anhydrous cesium carbonate (3.7 mmol) and 4 Å molecular sieves, and the mixture warmed in an oil bath pre-heated to strictly 85-87 ˚C for 1 h with vigorous stirring.‡ The N_2 flow was cut, then a solution of **132a** (5.0 mmol) in DMF (2 mL) injected through the septum, and the resulting mixture stirred for 30 min. Following aqueous workup, fractionation on silica and flash chromatography afforded the 4-methoxyphenyl-substituted ring-expanded product **134** in 21% yield as part of a complex mixture of polymers, baseline materials, and other decomposition products (Scheme 44).

‡ These conditions were optimised previously by Dr. Alireza Shakoori for reactions of indigo with propargylic halides, and were used without modification to allow comparison between systems.

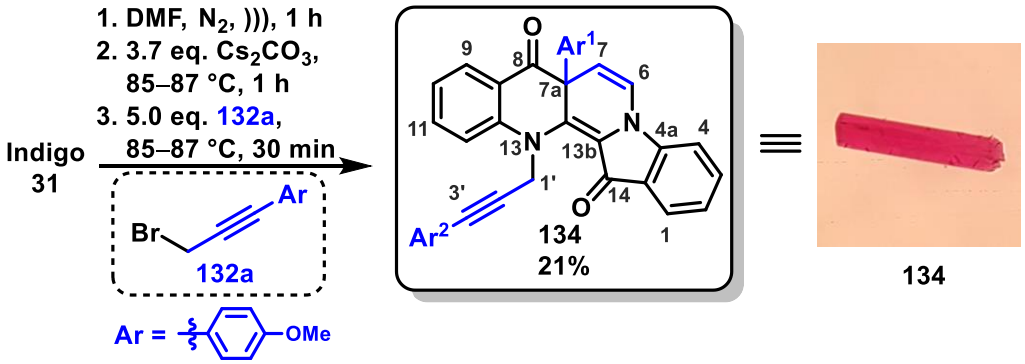

Scheme 44: Reaction of (4-methoxyphenyl)propargyl bromide **132a** with indigo, to afford the ring-expanded indolobenzonaphthyridinone **134**. Adjacent to the structure is a photograph of a single crystal of **134** grown from CH_2Cl_2/hexane, visualised under a light microscope at 40× magnification.

The methoxy-substituted indolobenzonaphthyridinone **134** was isolated as small reddish-pink crystals following repeated chromatographic separation. Analysis of the HRESI mass spectrum revealed a peak at *m/z* 551.1959, assigned to the molecular ion $[C_{36}H_{27}N_2O_4]^+$, revealing the addition of two units of the (aryl)propargyl electrophile to the indigo core. Analysis of the ^{1}H NMR spectrum revealed a pair of 3H singlet resonances at δ 3.51 and δ 3.76, assigned to the two *para*-methoxy groups attached to the unconjugated Ar^1 and conjugated Ar^2 substituents respectively. The pair of doublets at δ 5.14 and δ 4.87 were assigned to the methylene protons of the *N*-propargyl substituent due to hindered rotation about the *N-C* linkage, which were correlated to each other by both HSQC and COSY experiments (Figure 12, Figure 13). Further downfield, a pair of doublets at δ 5.49 and δ 6.82 were correlated to each other by COSY experiments, and assigned to the enamine protons H7 and H6, respectively. HMBC analysis revealed that both H6 and a 2H proton resonance at δ 7.18 assigned as H2/H6 of Ar^1 showed a strong correlation to a weak quaternary ^{13}C resonance at δ 56.4, assigned to the quaternary centre C7a, originally from the alkyne aryl-terminus (Figure 14). The H1'a/b methylene protons showed additional HMBC correlations to a pair of quaternary carbons at δ 81.5 and δ 85.8, which were assigned to C2' and C3' of the propargylic pendant.

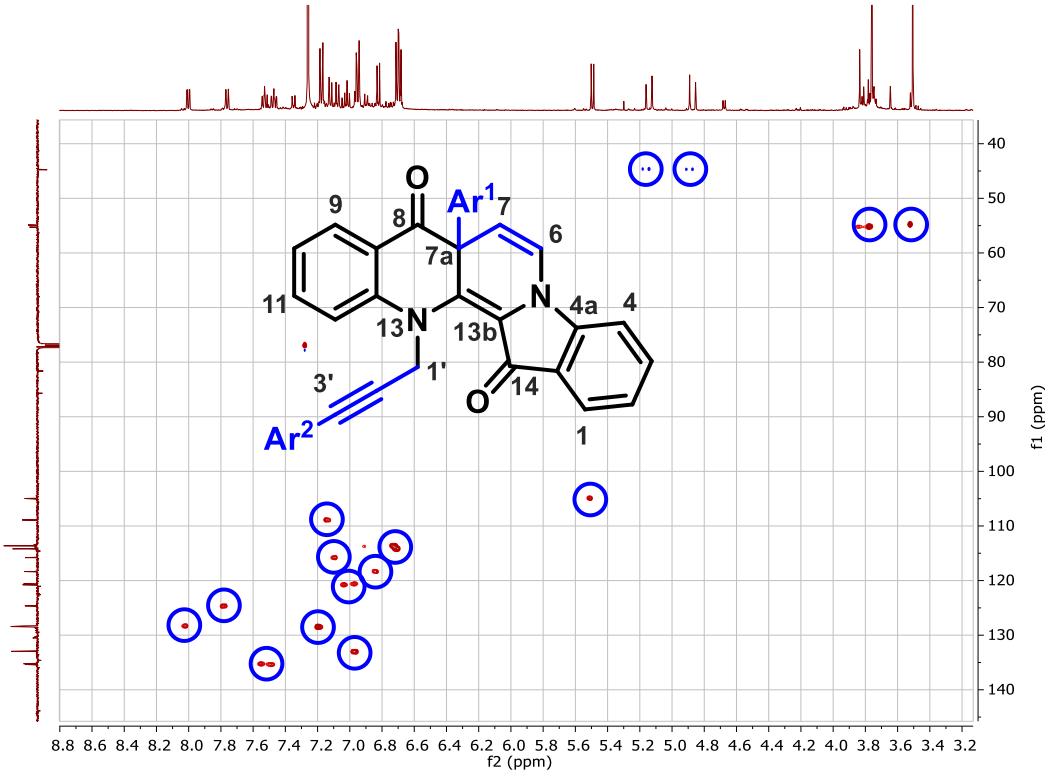

Figure 12: HSQC spectrum for compound **134** with key correlations highlighted.

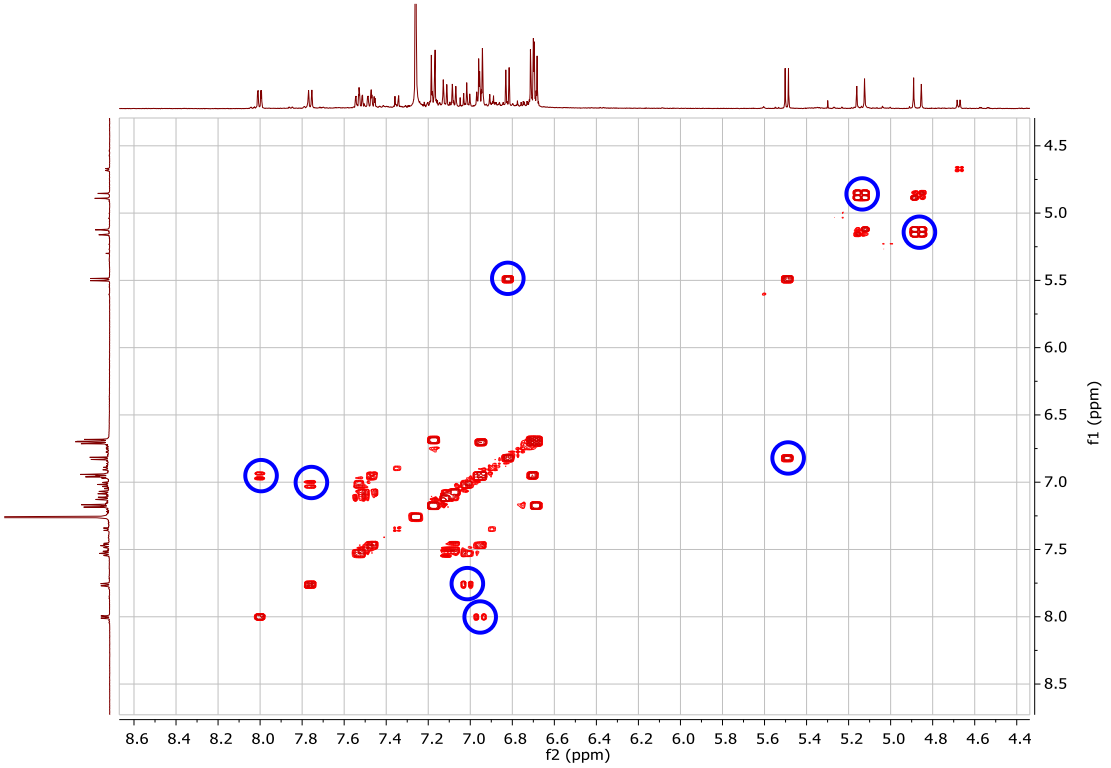

Figure 13: COSY spectrum for compound **134** with key correlations highlighted.

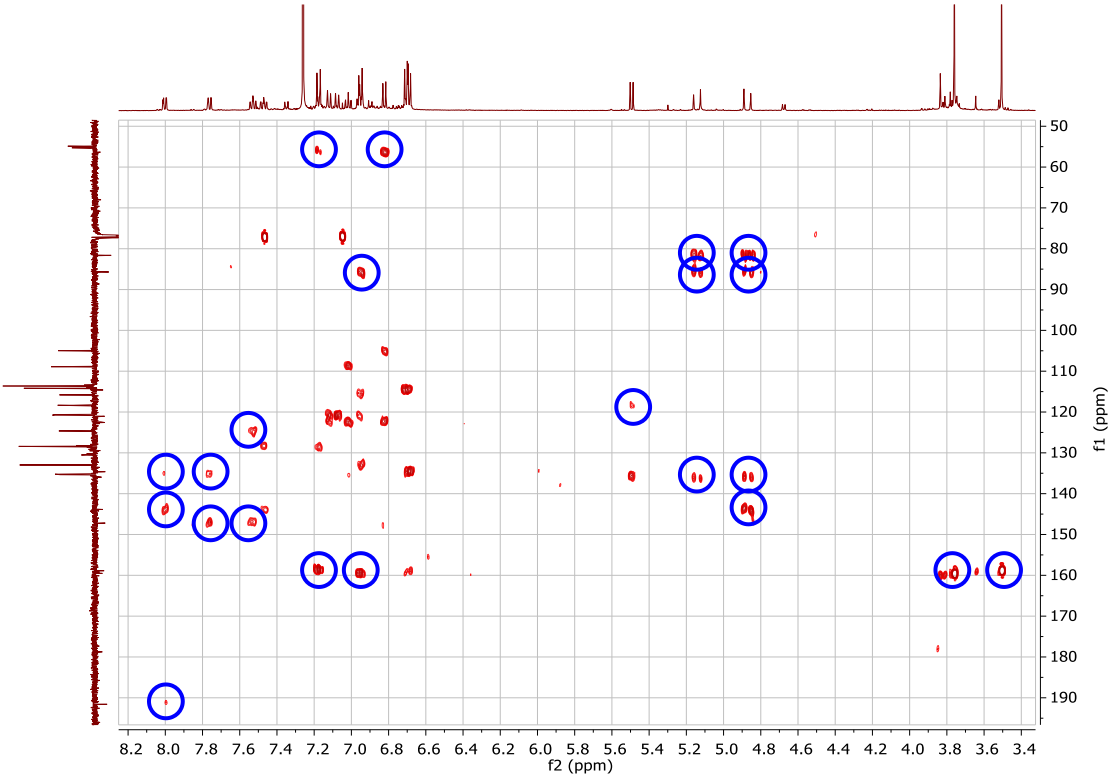

Figure 14: HMBC spectrum for compound 134 with key correlations highlighted.

X-ray quality crystals of compound **134** were grown by slow evaporation of a CH_2Cl_2/hexane solution, and its structure confirmed by x-ray crystallography (Figure 15).[§]

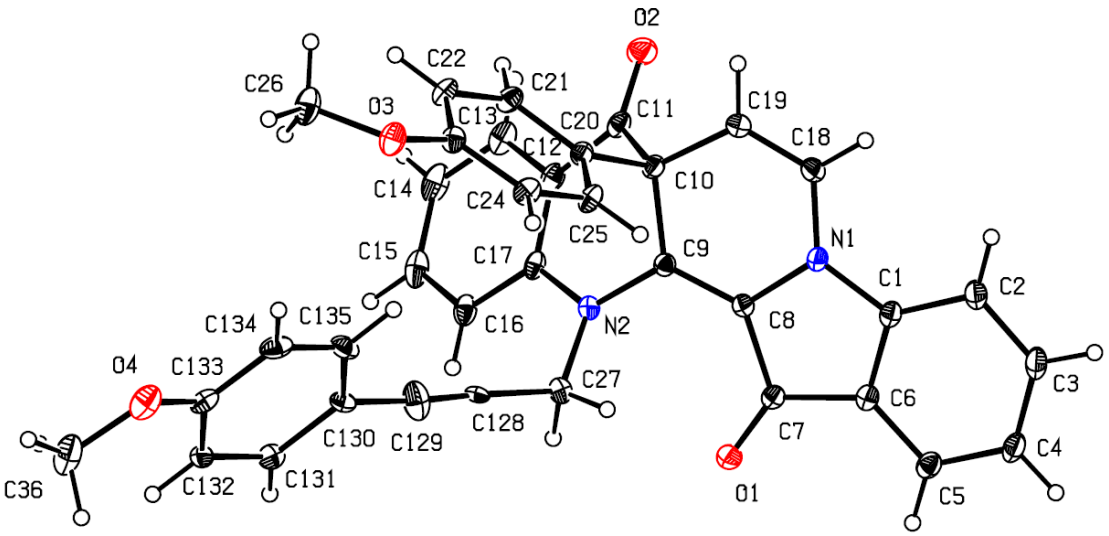

Figure 15: ORTEP depiction of compound **134**. Note that the atom numbers as denoted by x-ray crystallography do not reflect systematic numbering of atom positions.

[§] X-ray crystallography performed by Dr. Anthony Willis (ANU).

Interestingly, an additional product (**135**) arising from hydrobromination of the alkyne was also observed within the crystal matrix, though this was not observed within the crude mixture (Figure 16).[**] The incorporation of the bromide into the final molecule could be a consequence of the preceding step in its synthesis, whereby one of two pathways may lead to undesired hydrobromination. The generation of HBr from the reaction of $PPh_3.Br_2$ with alcohols occurs rapidly and in stoichiometric quantities, hence it is possible that the electron-rich propargyl bromide **132a** may undergo Markovnikov-addition of HBr to give bromostyrene **136**, promoted by the *para*-methoxy substituent. Alternatively, an ethereal $Br^{\bullet}$ radical from the decomposition of trace Br_2 in the product could result in mixtures of **132a** and **136**. This bromostyrene could also act as a competent electrophile, undergoing *N*-alkylation *in situ* to form **135** (Scheme 45), however the exact nature of the formation of **135** is unknown as it was isolated in trace quantities in a single run, and only observed crystallographically. Furthermore, the proposed bromostyrene **136** was not observed spectroscopically in any samples of **132a**, hence it is not apparent if it may have been formed *in situ* in trace quantities, or indeed whether it is involved in the formation of **135** at all.

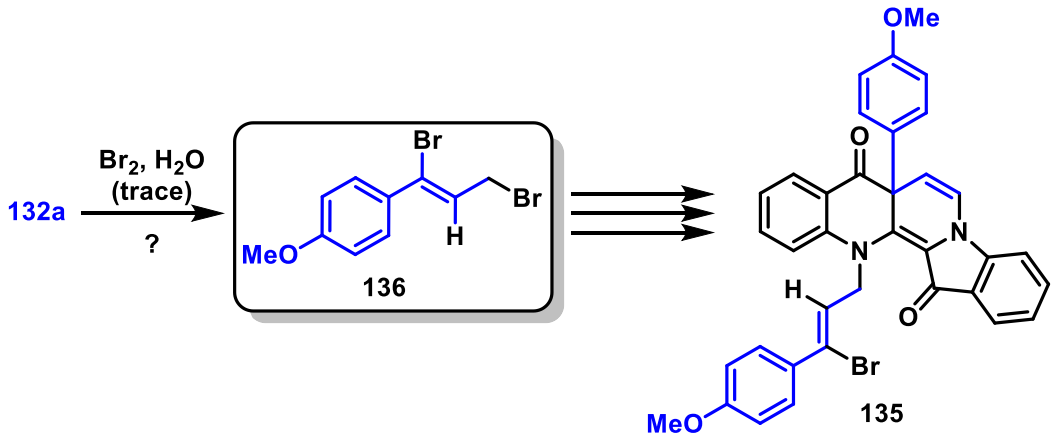

Scheme 45: Possible origin of **136** from hydrohalogenation of **132a** with residual bromine *en route* toward adduct **135**.

[**] X-ray crystallography performed by Dr. Anthony Willis (ANU).

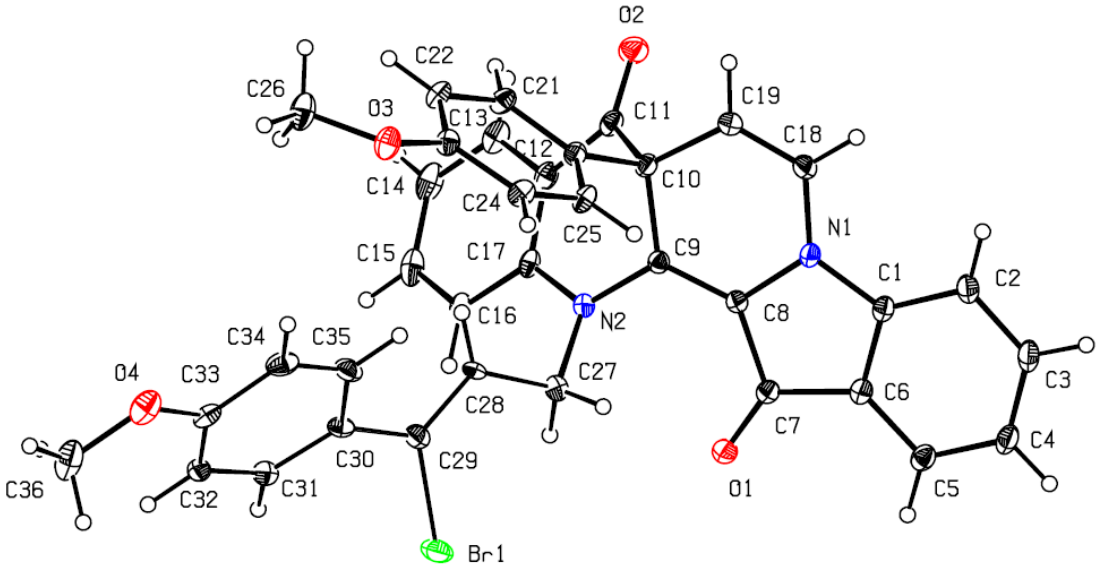

Figure 16: ORTEP depiction of compound **135**. Note that the atom numbers as denoted by x-ray crystallography do not reflect systematic numbering of atom positions.

Given the formation of both the phenyl (**133**) and 4-methoxyphenyl (**134**) substituted indolobenzonaphthyridinones from electron-rich substituted (aryl)propargyl bromides, it was of interest to probe the use of electron-poor aryl systems in these reactions. In a tandem study performed by a fellow PhD student,[127] indigo was reacted with (4-nitrophenyl)propargyl bromide (**132c**) under numerous sets of conditions, however these overwhelmingly led to decomposition and/or extensive polymerisation of the reaction mixture into uncharacterizable baseline materials, and in a control experiment, **132c** was treated with cesium carbonate in DMF, and was observed to undergo rapid autopolymerisation within minutes.[127] It is likely that the strongly electron-withdrawing nature of the nitro group led to an increase in the acidity of the methylene H1 protons, forming the resonance-stabilised carbanion **137** in the presence of the weak carbonate base. Elimination of the pendant bromide could then generate a highly-reactive propargylic carbene (**138**), which would then be susceptible to decomposition (Scheme 46). Given the rapid nature of this decomposition, electron-poor (aryl)propargyl electrophiles such as **132c** are unsuitable for application to this methodology.

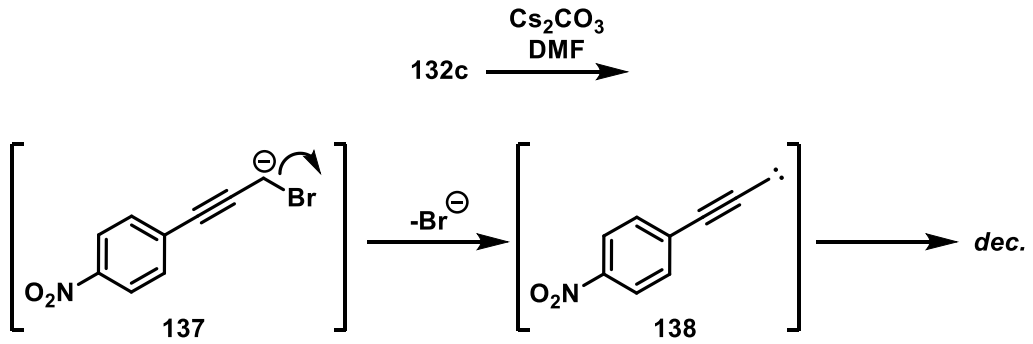

Scheme 46: Proposed mechanism for the decomposition of (4-nitrophenyl)propargyl bromide with weak base *via* carbanion **137**, and carbene **138** generated by stepwise deprotonation and halide elimination.

2.3.3 Mechanistic discussion

For both the phenyl- and 4-methoxyphenyl-substituted compounds **133** and **134**, the reaction mechanism is likely analogous to that for the formation of the methyl-substituted **123** reported previously (Scheme 47), which overlaps with the proposed mechanism for ring-expansion with unsubstituted propargyl halides (See Chapter 1, Scheme 32).[116b] Briefly, *N,N'*-dialkylation of indigo affords **139**, which in the presence of amphiprotic bicarbonate ions in solution may be protonated to give *N*-alkyliminium ion **140**. With stronger leaving groups (i.e. with R-Br, rather than R-Cl), this second alkylation would prove more favourable, accounting for the observed disparate reactivity of the phenylpropargyl chloride and bromides. Deprotonation by excess carbonate base may then afford ylid **141**, rendering the alkyne nucleophilic. Nucleophilic addition of the ylid to the adjacent carbonyl could then afford key intermediate **142**, which features a strained seven-membered ring with an internal allene, for which relief of the ring-strain energy would allow significant driving force for ring-expansion.[129] Reformation of the ketone could then promote simultaneous 1,2-migration of the indole C2 to attack the allene terminus and protonation of C7 to give the iminium ion **143**, which is deprotonated to give the isolated compounds **123**, **133**, and **134**. Where the terminal R-group is a proton, the reaction would then continue *via* enolization of the α,β-unsaturated system and *O*-alkylation to afford **117**, however this pathway does not proceed for substituted propargyl substrates as this abstraction step would require the unfavourable fragmentation of the C7a quaternary centre by loss of cationic alkyl or aryl fragments.

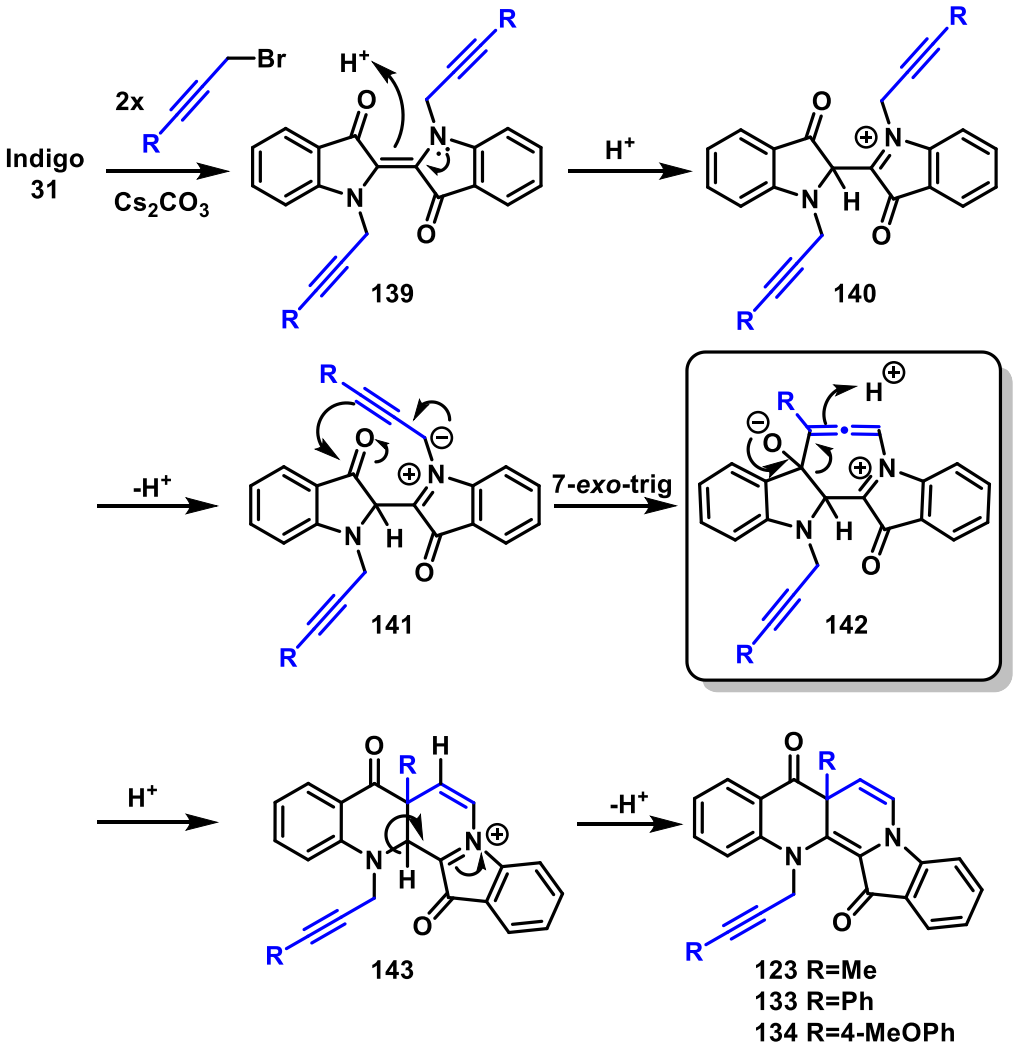

Scheme 47: Proposed mechanism for the formation of compounds **123**, **133**, and **134** from the reaction of indigo with terminally-substituted propargylic halides.

2.4 Conclusions

Indigo undergoes cascade reactions with terminally-substituted propargyl bromides to afford deep-red crystalline indolobenzonaphthyridinones in modest yields. It was found that the nature of the bromide leaving group was necessary for ring-expansion, presumably due to the faster rate of *N,N′*-dialkylation with stronger leaving groups. This would allow for tuneable and predictable access to the desired heterocycles, with the reaction pathway dictated by the leaving group. Throughout the course of this brief study, the electron-rich phenyl and 4-methoxyphenyl substituents were found to be tolerated for the reaction, however the 4-nitrophenyl equivalent proved unstable toward the reaction conditions and the desired product was not isolated.

Chapter 3:
Reactions of indigo with ring-strained electrophiles

3.1 The role of ring-strained electrophiles in organic synthesis

3.1.1 Synthesis and properties of ring-strained electrophiles

In both linear and cyclic sp^3-hybridised systems, VSEPR theory dictates that covalently-bonded atoms typically adopt a tetrahedral geometry, where four substituents are separated by an average bond angle of 109.5˚, minimizing steric and electronic interactions between atoms.[130] While this general approach has been criticised in the physical chemistry community for its oversimplification,[131] it remains the most widely-taught model for predicting structural features of simple organic molecules. In small or large ring systems where bond angles deviate from these ideal geometries, ring-strain is introduced due to unfavourable steric and/or electronic clashes between adjacent atoms. This ring-strain energy can provide significant driving force toward ring-opening reactions, and is one primary factor responsible for the high reactivity of three- and four-membered ring systems with both nucleophiles and Lewis acids.[132] The synthetic utility of substituted oxiranes, aziridines, thiiranes and cyclopropanes has been well-established, and these are widely-utilised in the synthesis of functional materials.[133] In particular, oxiranes and aziridines have found widespread use in the pharmaceutical and agrochemical industries as synthetic building blocks, and in the polymer industry as precursors in the production of plastics, resins, and adhesives.

Owing to their widespread use and high global demand, there are a broad variety of methods for the synthesis of oxiranes and aziridines from simple chemical feedstocks (Scheme 48). In general, many of these can be classified into one of two approaches – either nucleophilic ring-closing of amines or alcohols by displacement of an α-(pseudo)halide, or direct oxidation of alkenes to the strained system – though there are several alternatives, e.g. Corey-Chaykovsky epoxidation of ketones or imines with sulfur-ylids, and ring-contraction of cyclic carbonates or carbamates. Olefin epoxidation has been one avenue of particular interest due to the wide commercial availability and low cost of many alkenes, as well as their facile accessibility from cross-metathesis and Wittig- or Horner-Wadsworth-Emmons-type reactions. Classically, epoxidation reactions involve the use of either inorganic or organic peroxides (e.g. H_2O_2/NaOH, TBHP), or peroxy-acids (e.g. *m*-CPBA), though these systems typically suffer from limited enantioselectivity. The development of asymmetric alkene oxidation methods by

Sharpless was the subject of the 2001 Nobel prize for chemistry, and enantioselective allylic epoxidation featured prominently among these – as a result of this and other methods, a vast array of chiral oxiranes are now commercially-available, with many gaining broad appreciation as 'chiral pool' precursors to sp^3-rich frameworks.[134] Methods for direct aziridination of alkenes are less-common and less-general in scope than for epoxidation, though a variety of catalytic processes for asymmetric aziridination are possible using *N*-haloamines or -sulfonamides, either in the presence or absence of an external oxidant,[135] though there remain issues of stereoselectivity and generality. In practice, chiral aziridines are most-commonly accessed *via* ring-closure reactions of α-halosulfonamides or -carbamates.

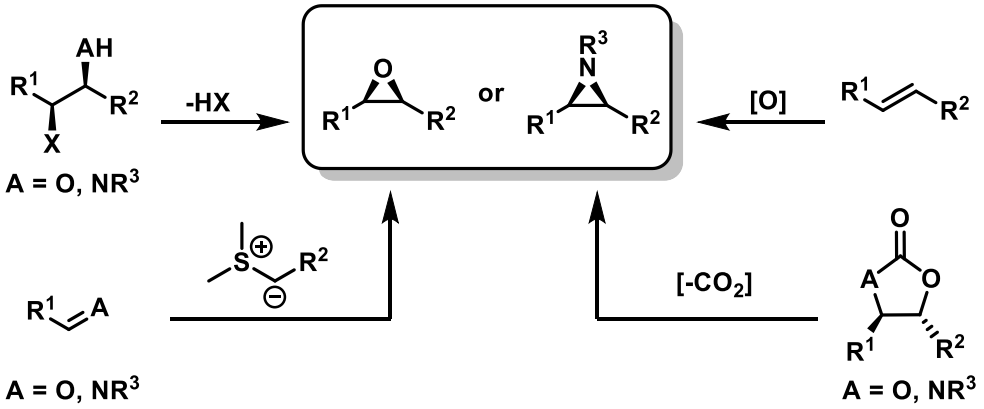

Scheme 48: Common methods used to synthesise oxiranes and aziridines: nucleophilic ring-closure, and direct oxidation of alkenes, as well as C-O or C-N insertion of sulfur ylids, and decarboxylation of carbonates and carbamates.

3.1.2 Reactions of ring-strained electrophiles

The main synthetic application of these strained systems is their use as potent electrophiles. The ring-strain energies of cyclopropane, oxirane, and aziridine have each been experimentally determined as *ca*. 27 kcal/mol, making ring-opening a highly-favourable process.[136] The high degree of polarisation of the C-O or C-N bond renders both C2 and C3 electrophilic, allowing for alkylation with a broad variety of nucleophiles (Scheme 49). Ring-opening also serves to extrude a nucleophilic heteroatom, which may be used for subsequent derivatisation, though this may also lead to undesired polymerisation.

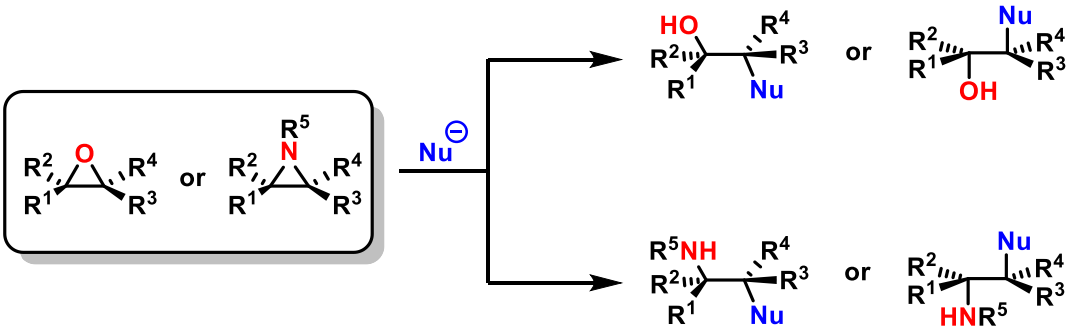

Scheme 49: Nucleophilic ring-opening of oxiranes and aziridines, leading to one of two regioisomers, depending on the steric environment of the particular substrate.

Given the bifunctional reactivity of epoxides and aziridines toward both electrophiles and nucleophiles, these would seem ideal moieties for designing new cascade reactions. As aforementioned, polyepoxide cascade reactions feature prominently in the total synthesis of various marine polyketides (see Chapter 1, Scheme 2),[137] and there are numerous examples of strained-ring species undergoing tandem reactions upon ring-opening, including Friedel-Crafts alkylation, oxa- and aza-Michael addition, hydroamination, aminohalogenation, and heterocyclisation reactions.[119a, 138] Given their high reactivity, synthetic accessibility, and applicability toward use in cascade reactions, strained-ring systems represent ideal reactive moieties for the development of new cascade chemistry of indigo.

3.2 Cascade reactions of ring-strained electrophiles with indigo

3.2.1 Substrate selection – 2-(halomethyl)oxiranes and aziridines

In establishing a fair comparison with the three-carbon allylic and propargylic electrophiles previously studied, it was important to select a range of strained electrophiles with similar chain length. For this reason, a series of chloromethyl- and bromomethyl-substituted strained systems were proposed – of these, the chiral oxiranes (*S*)-epichlorohydrin (**144**), (±)-epibromohydrin (**145**) and (*R*)-glycidyl tosylate (**146**) were available from commercial sources, while the remaining substrates were synthesised from simple materials. Additionally, while there have been previous studies into the reactivity of (±)-*N*-tosyl-2-bromomethylaziridine (**147**),[139] the related chloromethylaziridine (**148**) had neither been reported previously, nor was there an established protocol amenable to its enantioselective synthesis (Scheme 50).

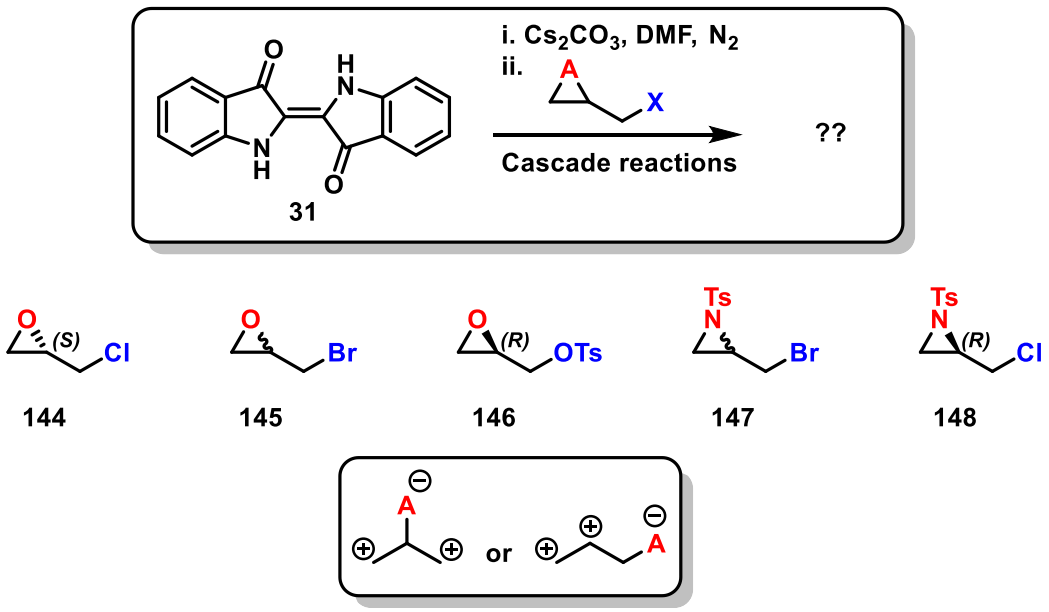

Scheme 50: Selected strained electrophiles for evaluation: (*S*)-epichlorohydrin (**144**), epibromohydrin (**145**), (*R*)-glycidyl tosylate (**146**), 2-(bromomethyl)-*N*-tosylaziridine (**147**), and *R*-2-(chloromethyl)-*N*-tosylaziridine (**148**).

As a broad class of molecules, these selected species are 1,2- or 1,3-dication synthons, bearing a potentially-nucleophilic heteroatom at C2. We anticipated that these additional electrophilic sites would facilitate twofold nucleophilic attack by indigo, allowing for controllable *N,N'*-cyclisation, allowing either six- or seven-membered heterocycles to be generated. Alternatively, liberation of the nucleophilic oxygen or nitrogen atom from the strained ring could allow for nucleophilic addition to the indigo carbonyl or *via* Michael addition to the central double bond, allowing access to spirocyclic derivatives. Assuming the stereochemical integrity of the epoxide or aziridine could be retained under the reaction conditions, these spirocycles could be accessed diastereoselectively as influenced by the set chirality of the electrophile.

3.2.2 Substrate selection – 2,2'-bioxirane and 2,2'-biaziridine

Previous work within our group has focused on the generation of vicinal diamine libraries for screening as ligands in atropselective cross-coupling reactions. For the generation of C_2-symmetric scaffolds, both 2,2'-bioxirane (**149**), and later 2,2'-biaziridine (**150**) have been utilised as synthetic starting points for further elaboration after ring-opening.[140] Accessible in enantiopure form over multiple steps from D- or L-tartaric acid,[140c, 141] both enantiomers may be accessed in multigram quantities from the common acetonide-protected dimesylate **151** by stepwise substitution and deprotection reactions (Scheme 51).

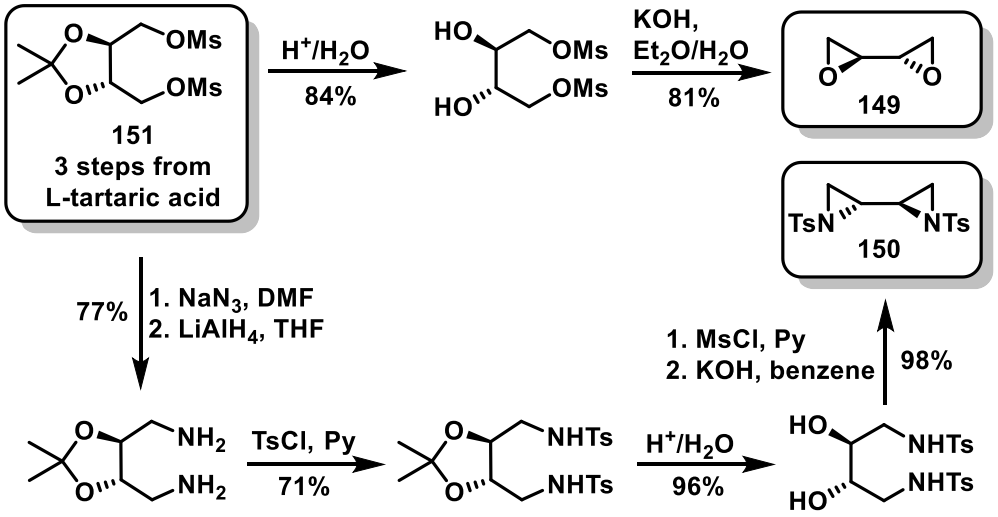

Scheme 51: Synthesis of 2,2'-bioxirane (**149**) and 2,2'-biaziridine (**150**) from common dimesylate **151**. The penultimate steps were replicated here, and are described in the experimental section (see Chapter 7).

Both dimeric species have been previously reported to undergo selective C1/C4 di-ring-opening upon treatment with various nucleophiles.[140-141] Currently, this reactivity has not been explored using di-nucleophiles, and as such it is unclear whether ring-opening these *bis*-electrophiles with indigo would proceed *via* this known 1,4 pathway to produce an eight-membered ring, or whether the formation of a more-favourable seven-membered ring would instead promote sequential 1,3-cyclisation. Alternatively, the nucleophilicity of the heteroatom may instead lead to spirocyclisation, allowing access to more complex heterocyclic frameworks.

3.3 Cascade reactions of epihalohydrins with indigo

3.3.1 Reaction discovery and structure elucidation

In developing reaction conditions for this methodology, we sought to use the previously-optimised conditions described for the allylation and propargylation of indigo as an initial basis.[††] Therefore, a suspension of indigo (1 mmol) in DMF (40 mL) was sonicated for 30 min, then transferred to a round-bottomed flask containing pre-dried Cs_2CO_3 (3.7 eq.) and 3 Å molecular sieves, and the mixture warmed in an oil bath preheated to strictly 85-87 ˚C for 1 h under nitrogen. The N_2 flow was cut, and (±)-epichlorohydrin (*rac*-**144**, 5.0 eq.) injected, and the mixture stirred vigorously for 2 h, after which TLC analysis showed complete consumption of indigo. The deep purple reaction mixture was quenched over crushed ice, and TLC analysis revealed a complex mixture of more than ten distinct

[††] Attempts to lower the reaction temperature generally led to increased recovery of unreacted starting materials, and raising the temperature increased polymerisation and isolation of baseline materials.

individual components. Fractional crystallisation of the crude mixture from 60% CH_2Cl_2/petroleum spirit, and subsequent flash chromatography on silica (gradient elution, 5%-50% EtOAc/CH_2Cl_2) afforded the *N,N'*-cyclic product **152** (43%), as well as spiroketal **153** (6%), cyclic carbonate **154** (6%), and allylic alcohol **155** (7%) in addition to polymeric baseline materials comprising 46% of the dry weight of the crude residue (Scheme 52).

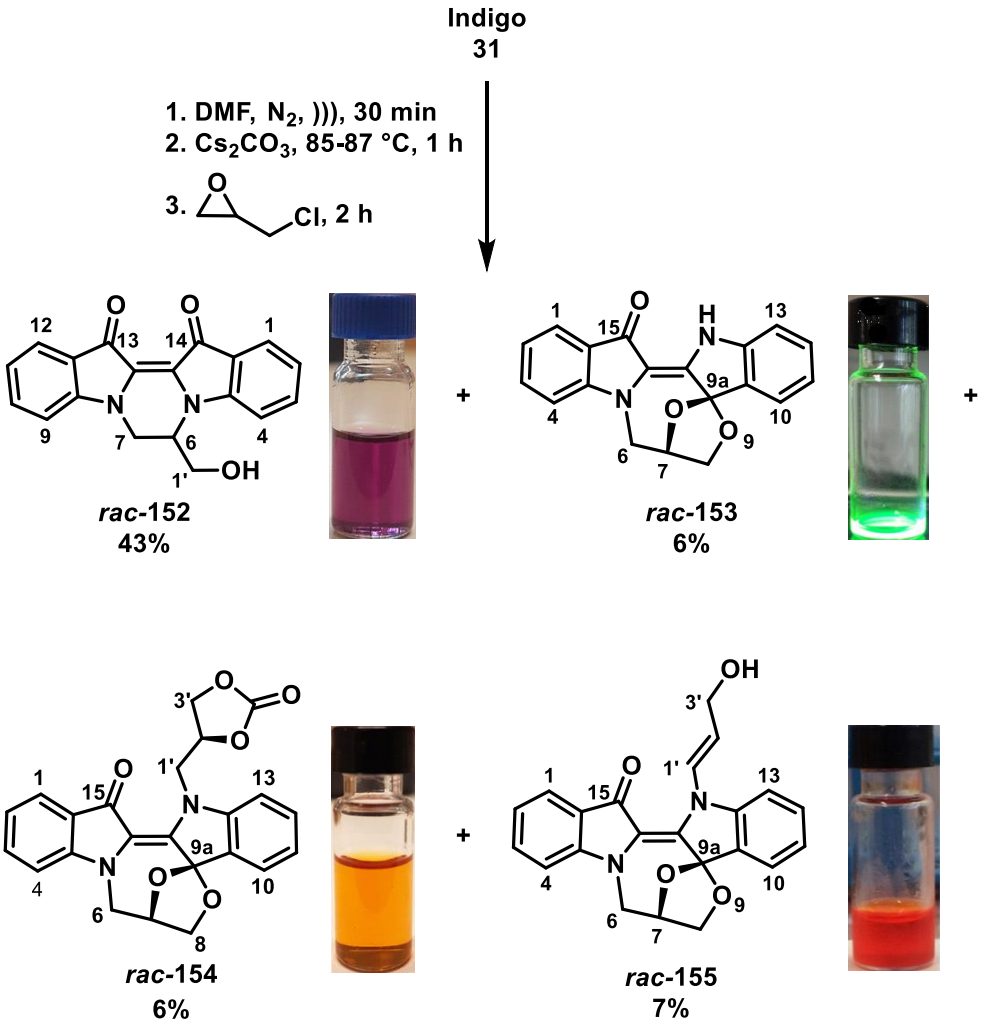

Scheme 52: Products from the cascade reaction of indigo with (±)-epichlorohydrin after 2 h. Stereoindicators show relative configuration of diastereomers.

Tetrahydropyrazinodiindole **152** was isolated as an intense dark blue powder in 43% yield from indigo. Analysis of the HRESI mass spectrum indicated a peak at *m/z* 341.0888, assigned as $[C_{19}H_{14}N_2O_3Na]^+$, revealing the addition of a single glycidyl subunit to the indigo core. The UV-Vis spectrum of **152** in CH_2Cl_2 had an intense absorption band at 303 nM (ε = 6339), and its intense deep blue-purple colour suggested that the central double bond had remained intact. Analysis of the FTIR spectrum revealed a broad absorption band centred at 3432 cm^{-1}, suggesting the presence of a hydroxyl substituent.

Analysis of the ^{13}C APT spectrum indicated the retention of both carbonyls of the parent scaffold, assigned to resonances at δ 179.9 and δ 179.7 ppm. Analysis of the ^{1}H NMR spectrum showed a broad singlet resonance at δ 5.28 which exchanged with D_2O and was assigned as the hydroxyl group. The aliphatic protons of the alkyl tether were assigned by analysis of the COSY spectrum, which revealed correlations between the hydroxyl proton and the 2H multiplet from δ 3.60-3.49, assigned as the methylene protons H1'a and H1'b of the hydroxymethyl pendant. This methylene correlated to a multiplet at δ 4.72-4.65, assigned as H6, which correlated to both a doublet at δ 4.46, and a doublet of doublets at δ 3.73, which were assigned as H7b and H7a, respectively (Figure 17). Analysis of the NOESY spectrum revealed through-space correlation of H6 and H7b to H4 and H9, respectively, while there was no apparent correlation between H9 and H7a, supporting the assignment of the diastereotopic C7 methylene protons (Figure 18). The gHMBC spectrum revealed strong, three-bond correlations between methylene H7b with both C8a, and C13a, and the alkyl chain was therefore determined to bridge both indigo nitrogen atoms (Figure 19).

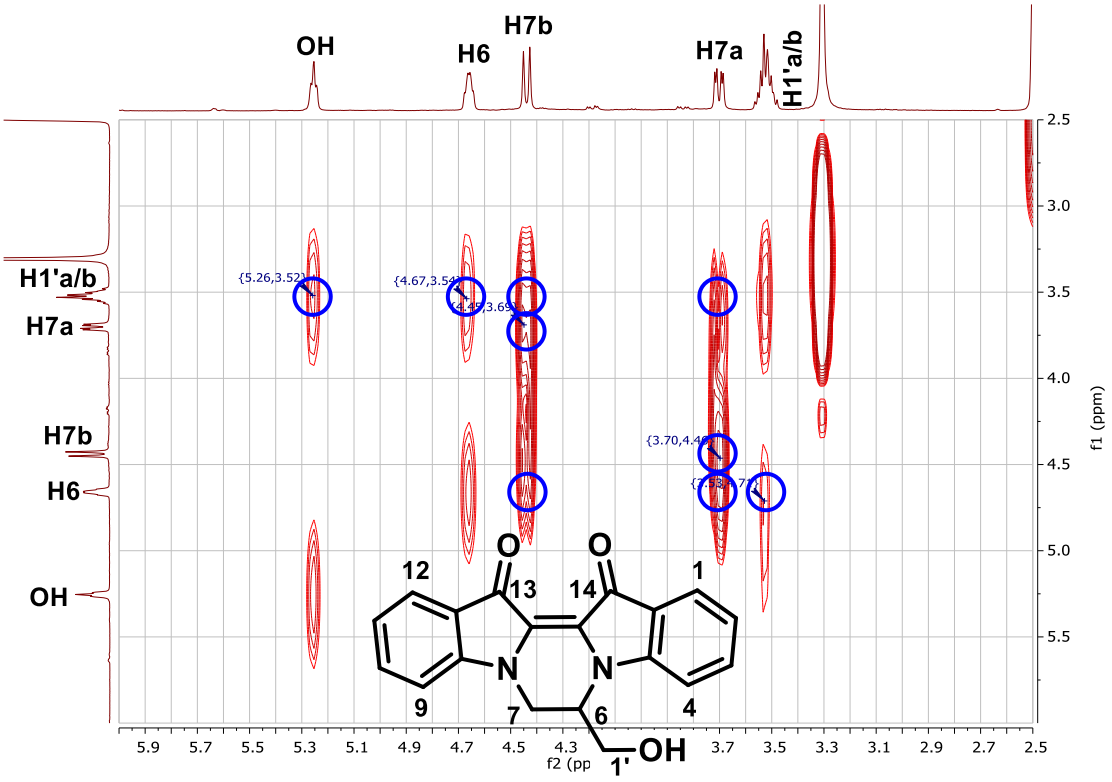

Figure 17: COSY spectrum of compound **152**, with key correlations highlighted.

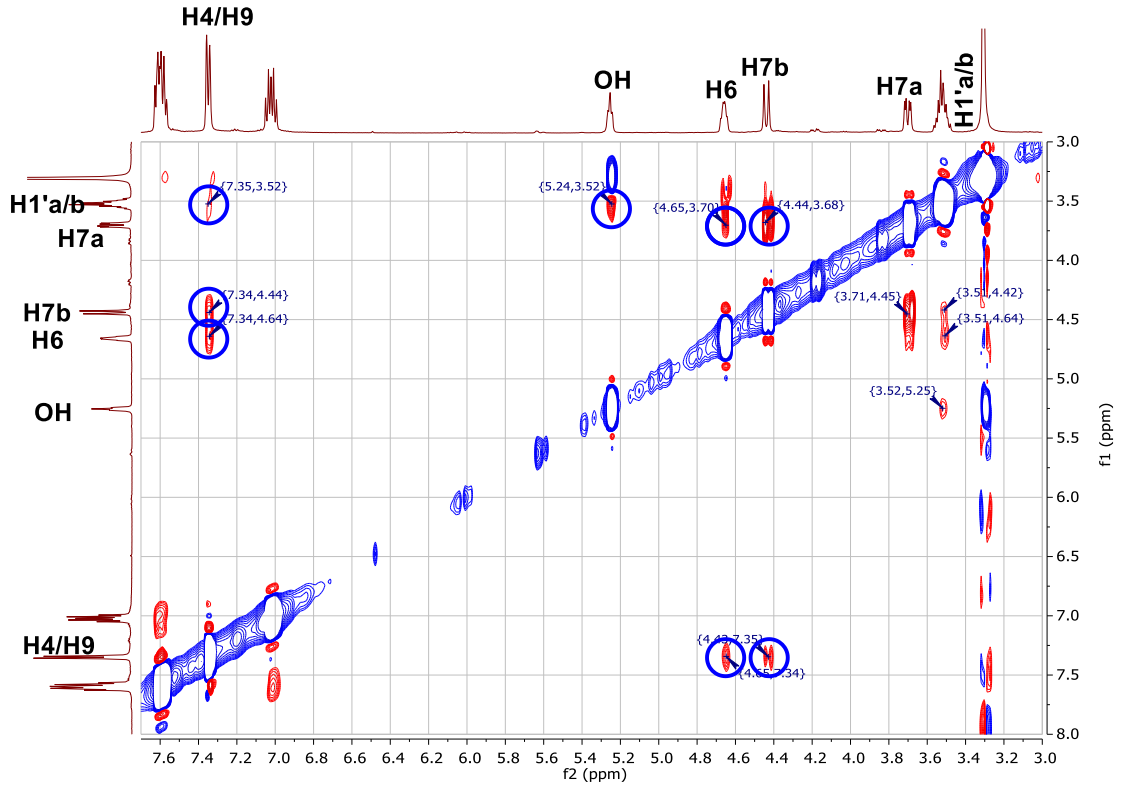

Figure 18: The NOESY spectrum of compound **152** with key correlations highlighted.

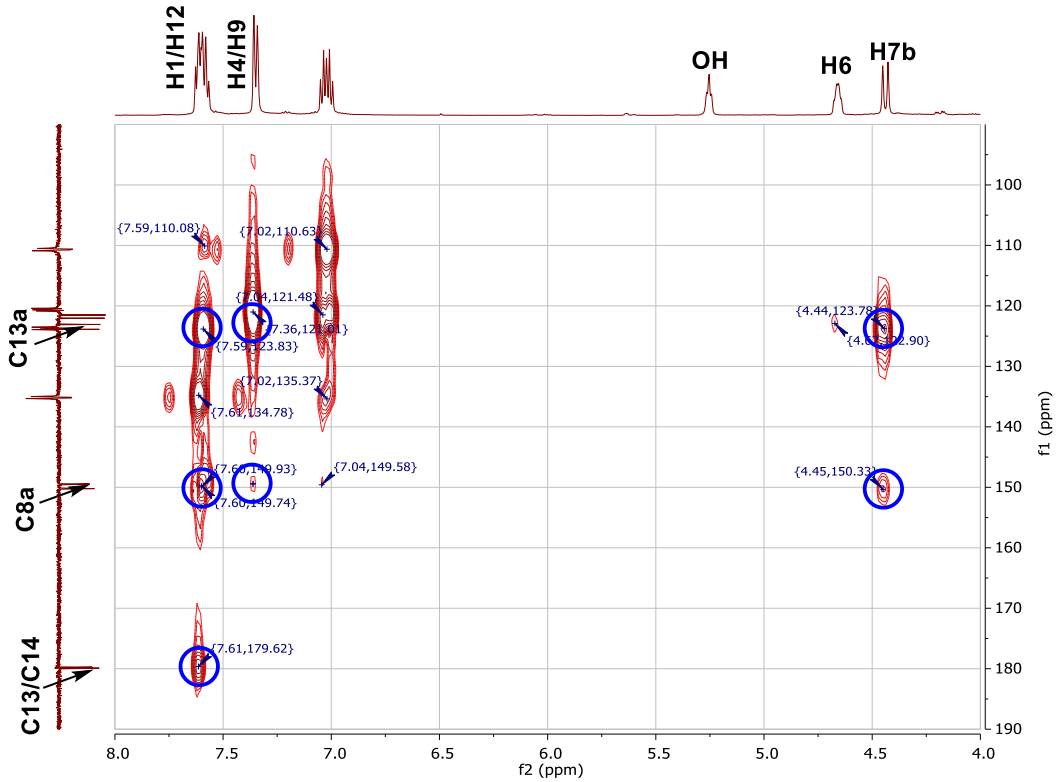

Figure 19: Partial HMBC spectrum of compound **152**.

The mother liquor from **152** was subjected to flash chromatography, resulting in the isolation of a fraction with a characteristic yellow-green fluorescence in ambient conditions, and upon irradiation with UV light. The spiroketal **153** was isolated from this fraction as bright orange crystals in 6% yield from indigo. Analysis of the HRESI mass spectrum revealed a peak at 341.0900, assigned as $[C_{19}H_{14}N_2O_3Na]^+$, and revealing the addition of a single glycidyl chain. Analysis of the FTIR spectrum revealed a sharp band at 3310 cm^{-1}, assigned to an indolic NH stretch, as well as a sharp peak at 1689 cm^{-1}, assigned as a benzylic ketone C=O stretch. Analysis of the ^1H NMR spectrum revealed the molecule to be non-symmetrical, due to the presence of eight distinct aromatic resonances, assigned as the eight aromatic peaks of the parent indigo scaffold. Further upfield, five distinct aliphatic protons were identified and assigned based on analysis of the COSY and HSQC spectra (Figure 20) – a multiplet at δ 5.16-5.09 assigned to H7, a geminal triplet at δ 4.38 and doublet of doublets at δ 4.25 assigned to the oxygen-bound methylene protons H8b and H8a respectively, and a second geminal pair of a doublet of doublets at δ 4.20 and a doublet at δ 3.74, assigned as the nitrogen-bound methylene protons H6a and H6b respectively (Figure 21). The individual assignment of the two methylenes was confirmed by analysis of the NOESY spectrum, which revealed through-space coupling of H6a and H8a *via* the rigid spirocyclic tether, suggesting a *syn* arrangement, and there was no evident correlation between H6a and H8b, suggesting these to be *anti*. This assignment was further supported by correlations between H6b and H8b, suggesting these to be *syn*. The bridgehead proton H7 also showed through-space correlation to all other aliphatic protons of the chain (Figure 22). Analysis of the ^{13}C NMR spectrum revealed the retention of a single downfield carbonyl peak at 188.2 ppm, assigned to the C15 ketone moiety. Analysis of the HMBC spectrum revealed correlations between H8a, H8b and H7 to a weak quaternary resonance in the ^{13}C NMR spectrum located at 111.5 ppm, assigned to the spiro carbon C9a (Figure 23).

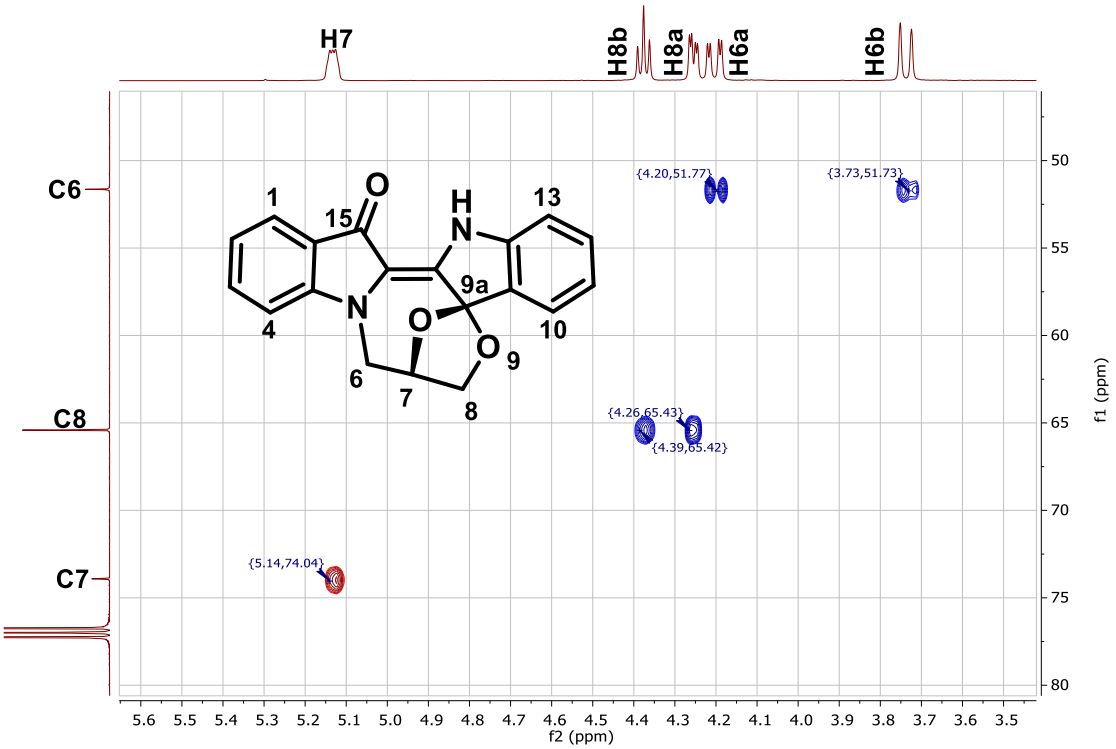

Figure 20: HSQC spectrum for compound **153**.

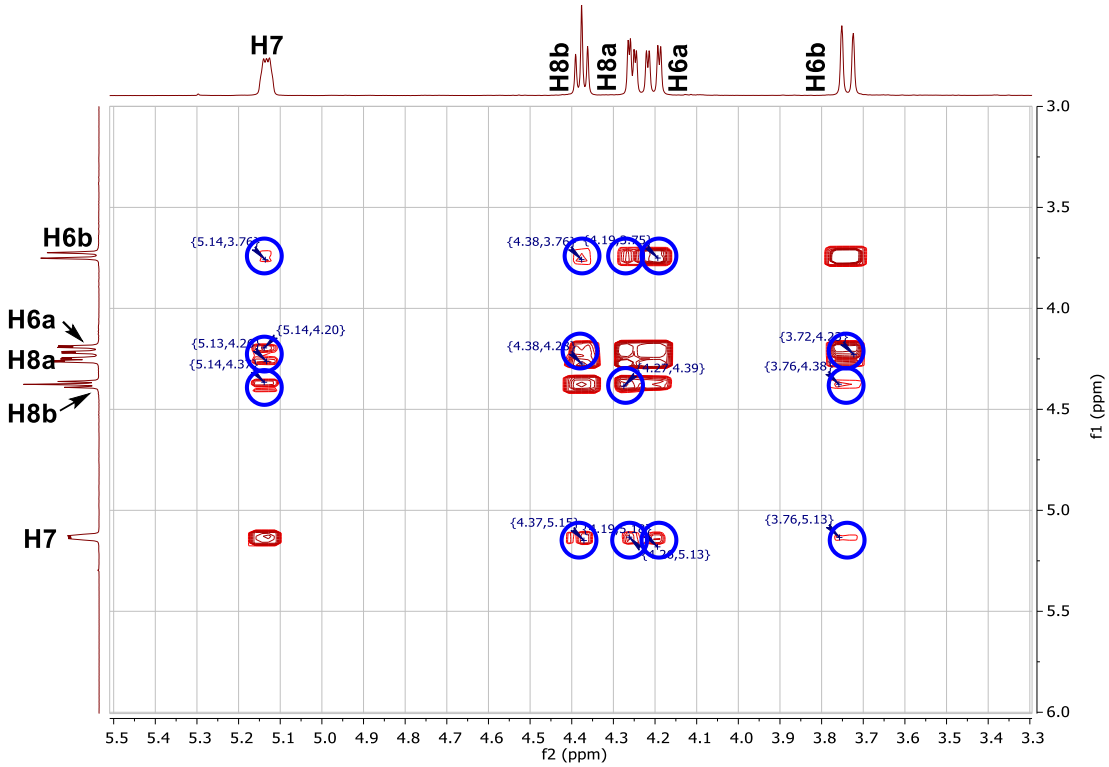

Figure 21: COSY spectrum of compound **153** with key correlations highlighted.

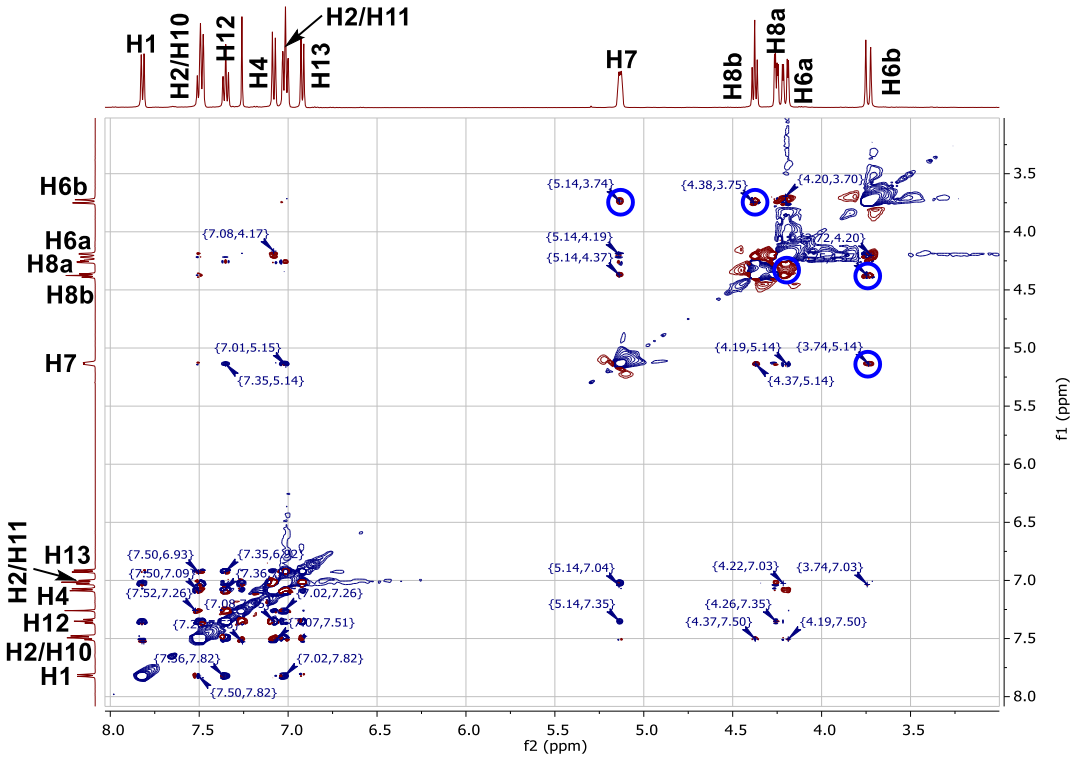

Figure 22: NOESY spectrum for compound **153** with key correlations highlighted.

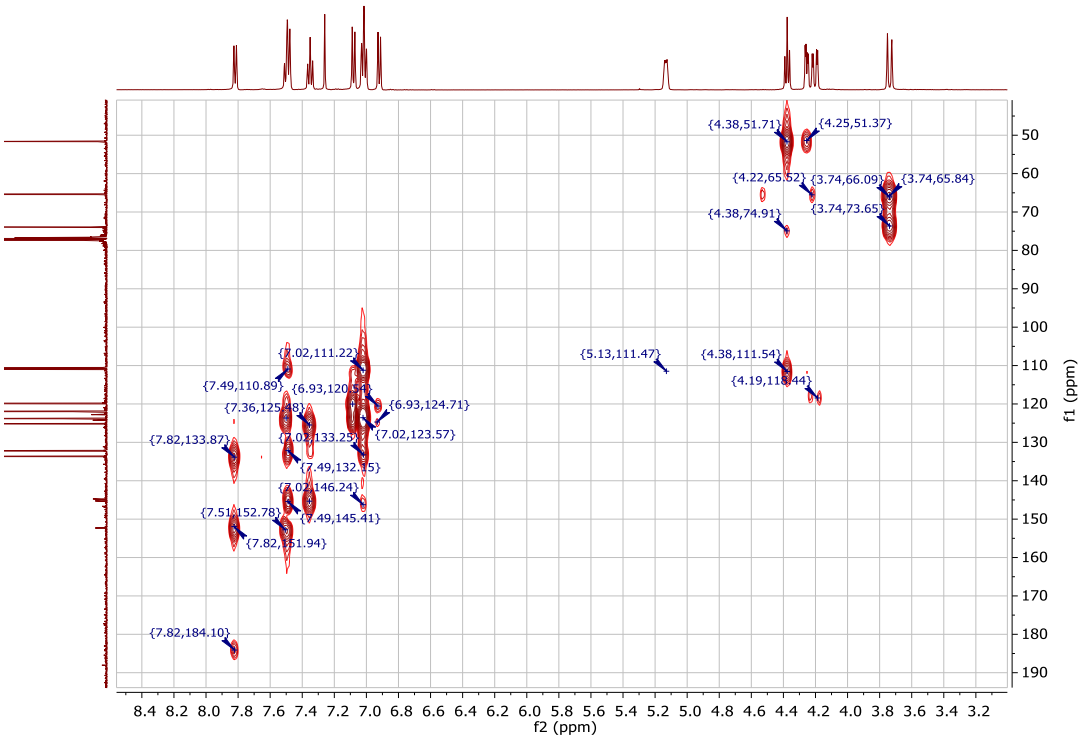

Figure 23: HMBC spectrum for compound **153**.

In a subsequent experiment using (*S*)-epichlorohydrin, orthorhombic crystals of **153** were obtained from slow evaporation of a solution in ethyl acetate, and its absolute structure and stereochemistry was confirmed by x-ray crystallography (Figure 24).[‡‡]

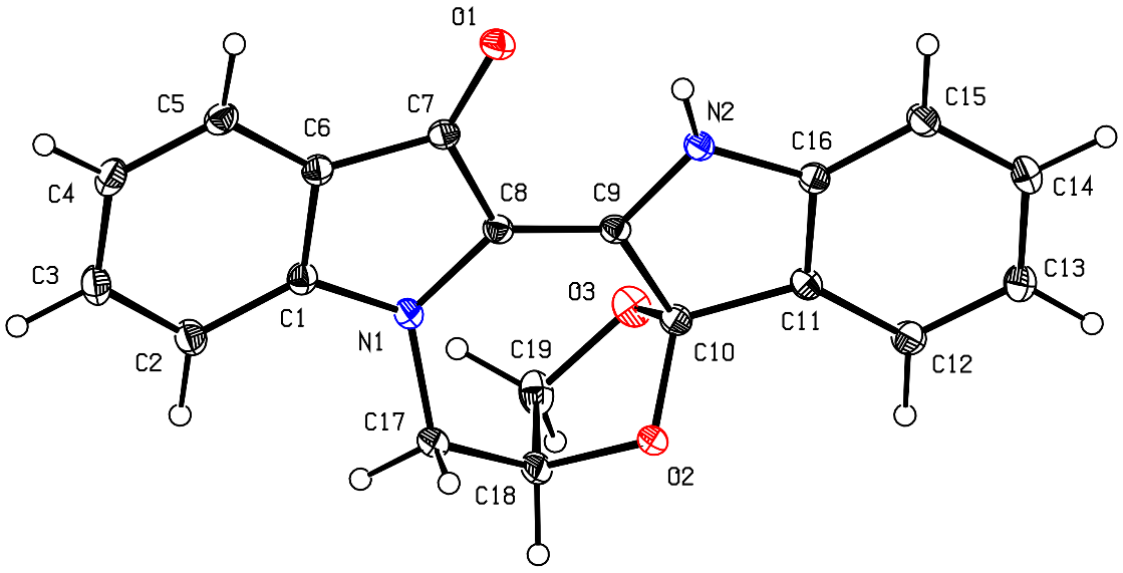

Figure 24: ORTEP depiction of compound **153**. Note that the atom numbers as denoted by x-ray crystallography do not reflect systematic numbering of atom positions.

Further elution with 30% EtOAc/CH_2Cl_2 afforded a deep orange residue. Removal of the solvent and recrystallisation from EtOAc gave the cyclic carbonate **154** as small, luminescent orange crystals in 6% yield from indigo. HRESI mass spectral analysis revealed a peak at *m/z* 441.1082, assigned to the molecular ion $[C_{23}H_{18}N_2O_6Na]^+$, showing the addition of two glycidyl subunits to the indigo core, as well as a molecule of CO_2. Analysis of the FTIR spectrum revealed two peaks at 1800 cm^{-1} and 1734 cm^{-1}, assigned as carbonate and ketone C=O stretches, respectively. Analysis of the ^1H NMR spectrum revealed ten aliphatic proton peaks, confirming the presence of two glycidyl fragments. Analysis of the ^{13}C NMR spectrum revealed a pair of carbonyl resonances at δ 182.3 and δ 178.4, assigned to C15 and the carbonate C=O, respectively. Cross-referencing the COSY spectra for compounds **153** and **154**, the spirocyclic N5-O9 linkage was identified by correlating the multiplet at δ 5.00-4.94 to the doublet at δ 3.68, assigned as H7 and H6b, respectively (Figure 25). H6b showed strong geminal coupling to part of a broad multiplet resonance at δ 4.23-4.17, assigned as H6a. The multiplet at δ 5.53-5.43 was assigned to the C2' methine, which showed strong COSY correlations to a triplet at δ 5.20, and multiplets centred at δ 4.30, δ 4.28 and δ 4.11, assigned as H3'b, H3'a, H1'b and H1'a, respectively. These assignments were supported by HSQC experiments, which

[‡‡] X-ray crystallography performed by Dr. Anthony Willis (ANU).

showed four distinct methylene carbons at δ 69.1, δ 67.9, δ 55.5 and δ 52.4, assigned as C3', C8, C1' and C6, respectively (Figure 26).

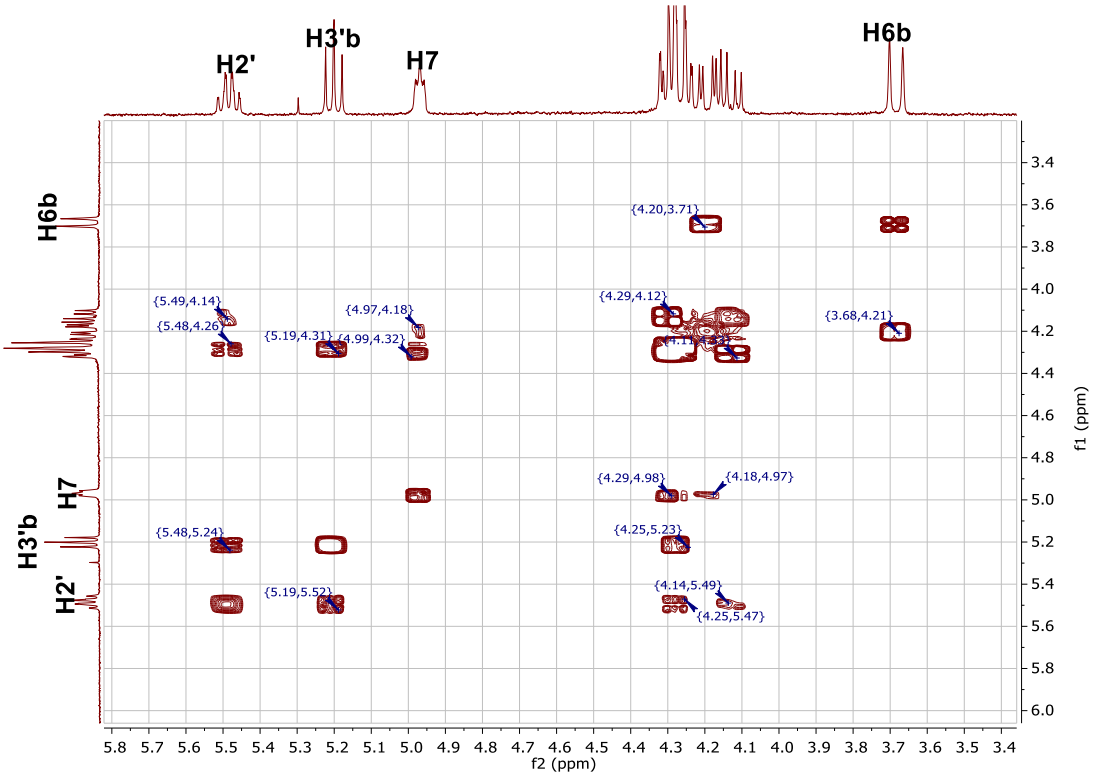

Figure 25: COSY spectrum of compound **154**.

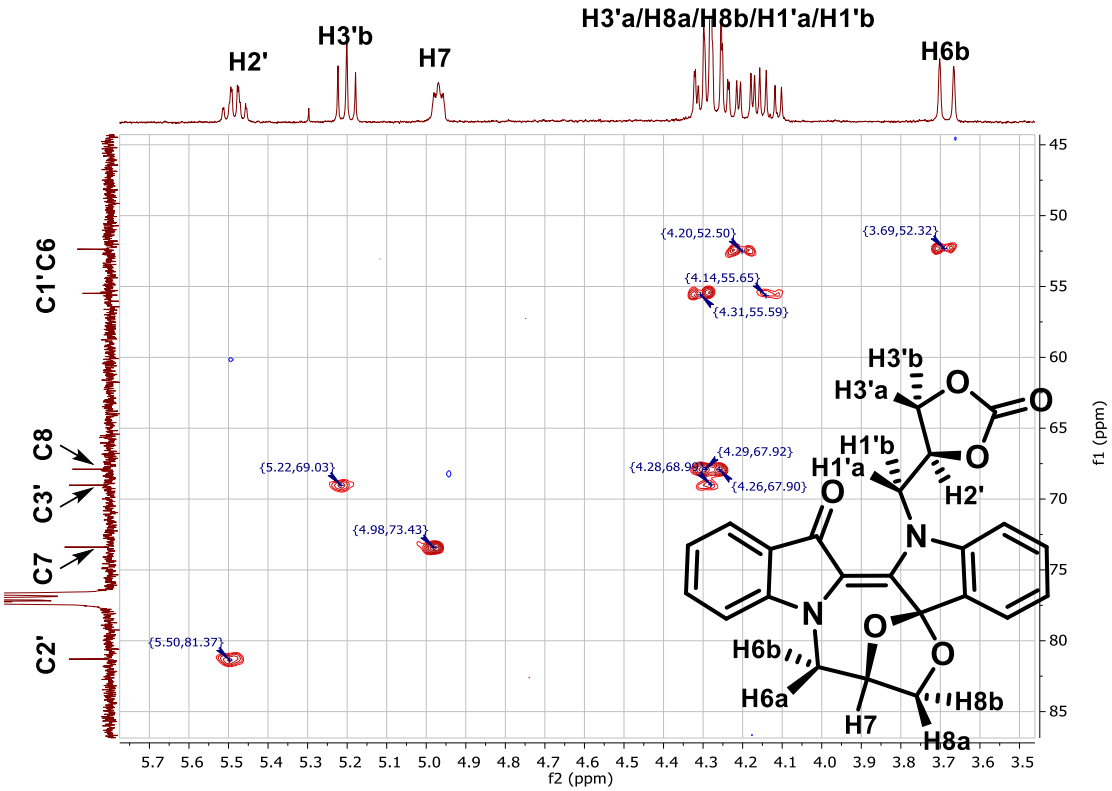

Figure 26: HSQC spectrum of compound **154**.

Monoclinic crystals of **154** were grown from slow evaporation of a CH_2Cl_2/EtOAc solution, and its structure was confirmed by x-ray crystallography (Figure 27).[§§]

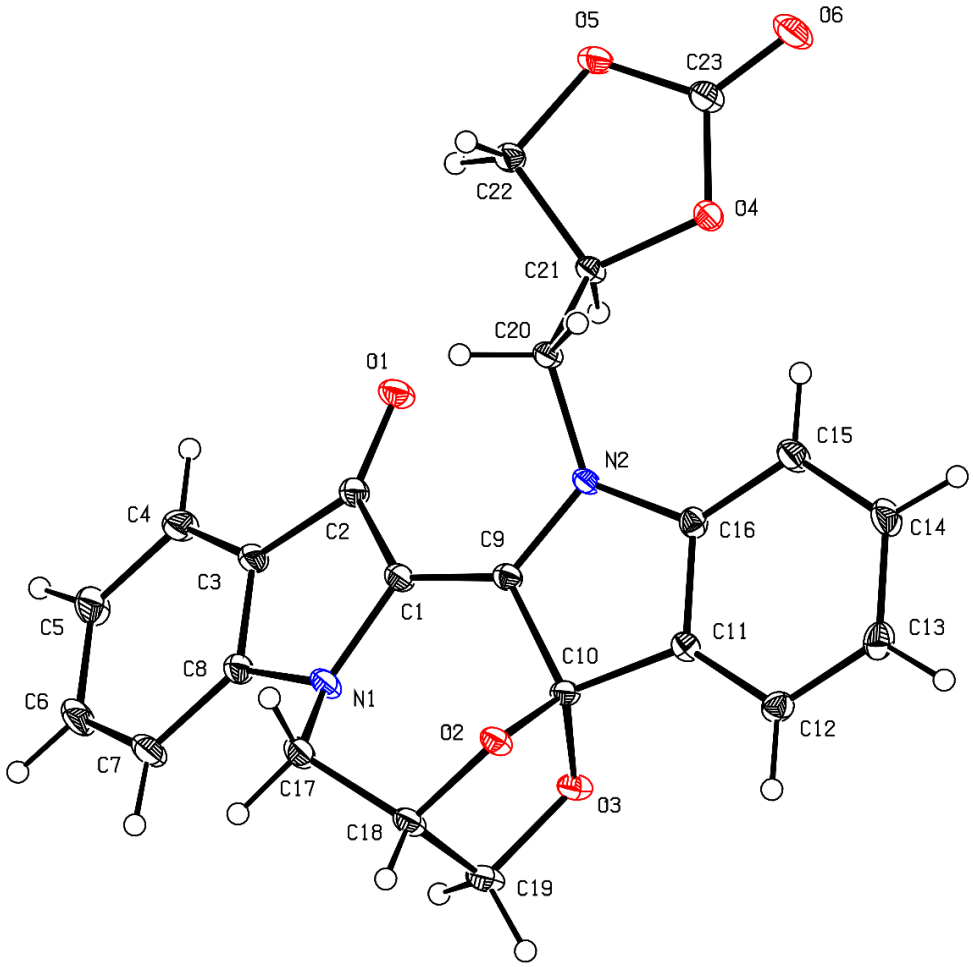

Figure 27: ORTEP depiction of compound **154**. Note that the atom numbers as denoted by x-ray crystallography do not reflect systematic numbering of atom positions.

Further elution with 50% EtOAc/CH_2Cl_2 gave a deep red-orange residue, which was separated by preparative thin-layer chromatography to afford compound **155** in 7% yield as small orange crystals. Analysis of the HRESI mass spectrum revealed a peak at *m/z* 375.1357 which was assigned to the molecular ion $[C_{22}H_{19}N_2O_4]^+$, demonstrating the addition of two glycidyl substituents to the indigo core. Analysis of the FTIR spectrum revealed a broad absorbance band centred at 3395 cm^{-1}, assigned to a hydroxyl O-H stretch, as well as a peak at 1726 cm^{-1} assigned to the ketone C=O stretch. The ^{13}C NMR spectrum did not contain all relevant resonances due to small sample quantity, however 2D HMBC analysis revealed a strong, three-bond correlation between a doublet at δ 7.78 and a ^{13}C resonance at δ 181.8, assigned to H1 and C15, respectively (Figure 28). Analysis of the HSQC spectrum revealed three methylene carbons at δ 67.6, δ 61.9, and δ 52.2,

[§§] X-ray crystallography performed by Dr. Anthony Willis (ANU).

assigned as C8, C3', and C6, respectively (Figure 29). Analysis of the TOCSY spectrum revealed long-range ^{1}H-^{1}H correlations between the doublet at δ 6.87, the doublet of triplets at δ 6.07, and part of a broad multiplet centred at δ 4.36, assigned as H1', H2', and H3' of the *trans*-enamine moiety. The spirocyclic linkage was also evident in the TOCSY spectrum, which showed correlations between the multiplet spanning δ 5.05-5.01, the doublet at δ 3.74, and a broad multiplet containing an additional three protons, assigned as H7, H6b and H6a/H8a/H8b respectively (Figure 30). The individual protons were assigned by analysis of the COSY and ROESY spectra (Figure 31, Figure 32).

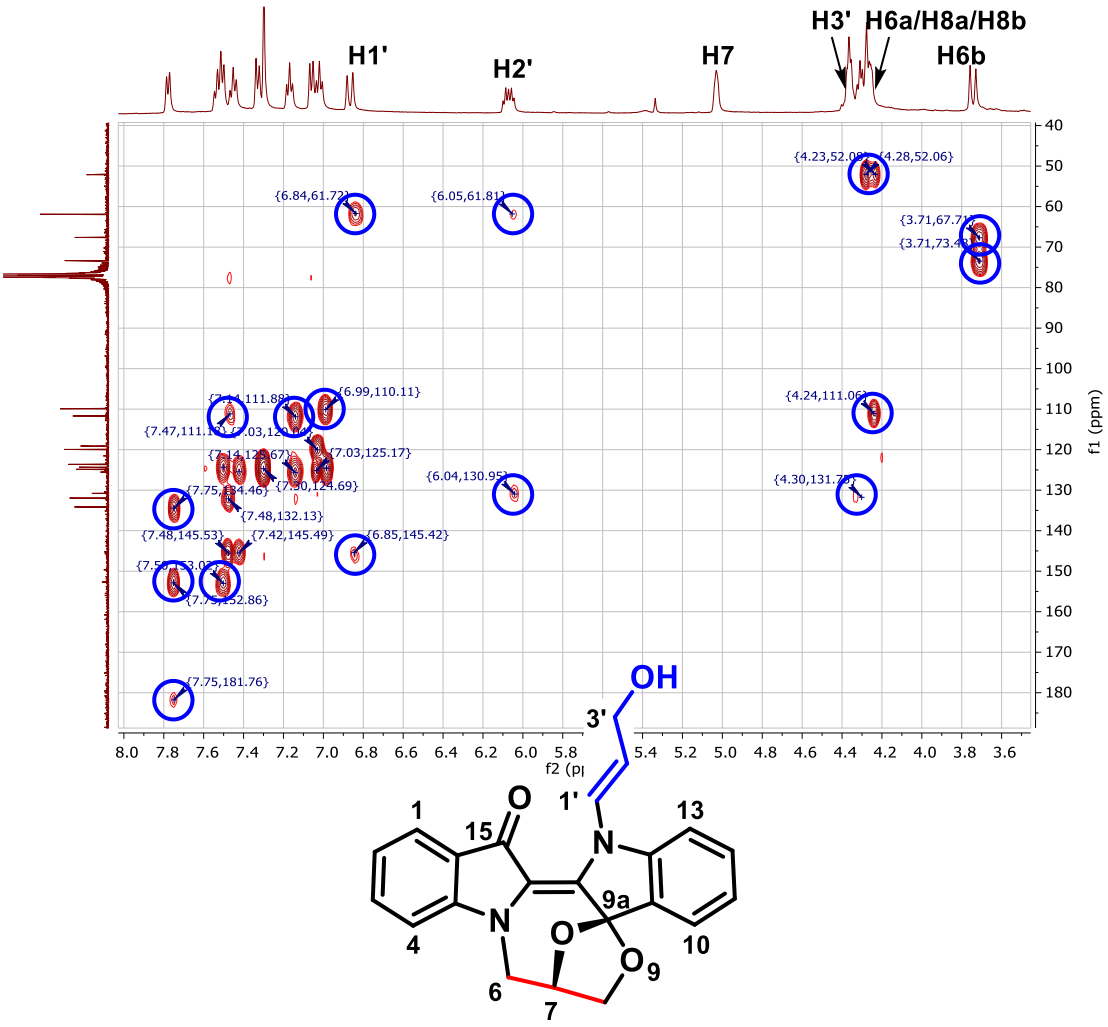

Figure 28: HMBC spectrum for compound **155** with key correlations highlighted.

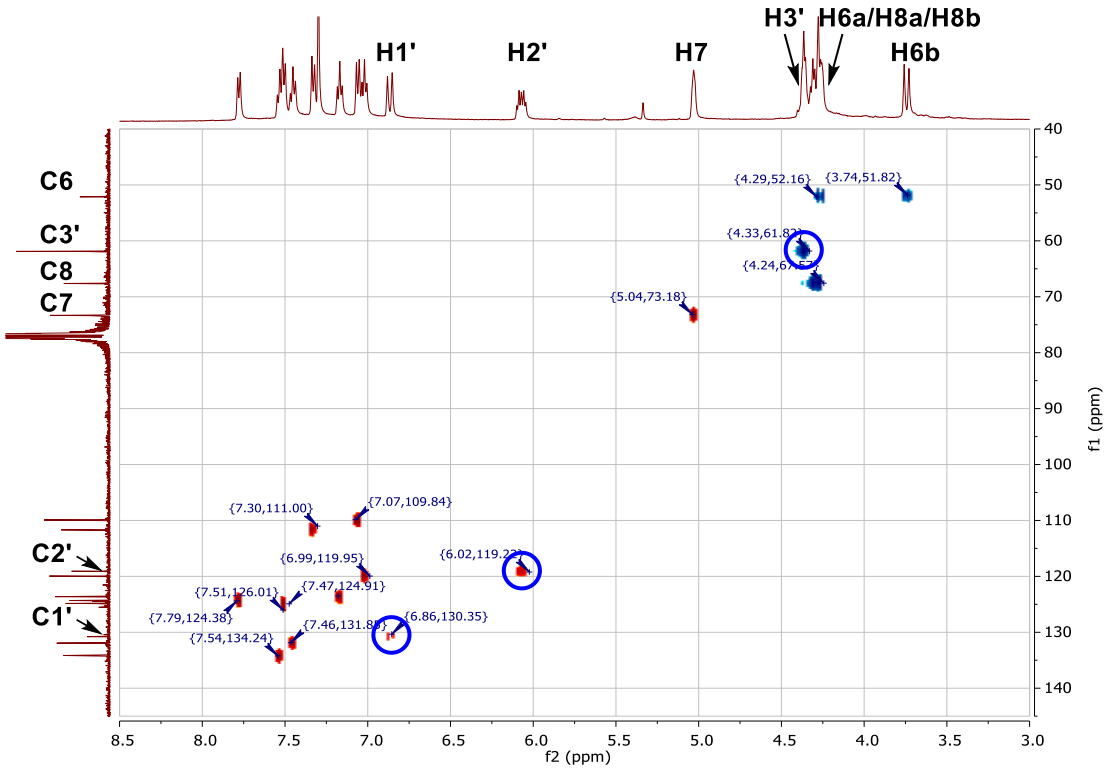

Figure 29: HSQC spectrum of compound **155** with key correlations highlighted.

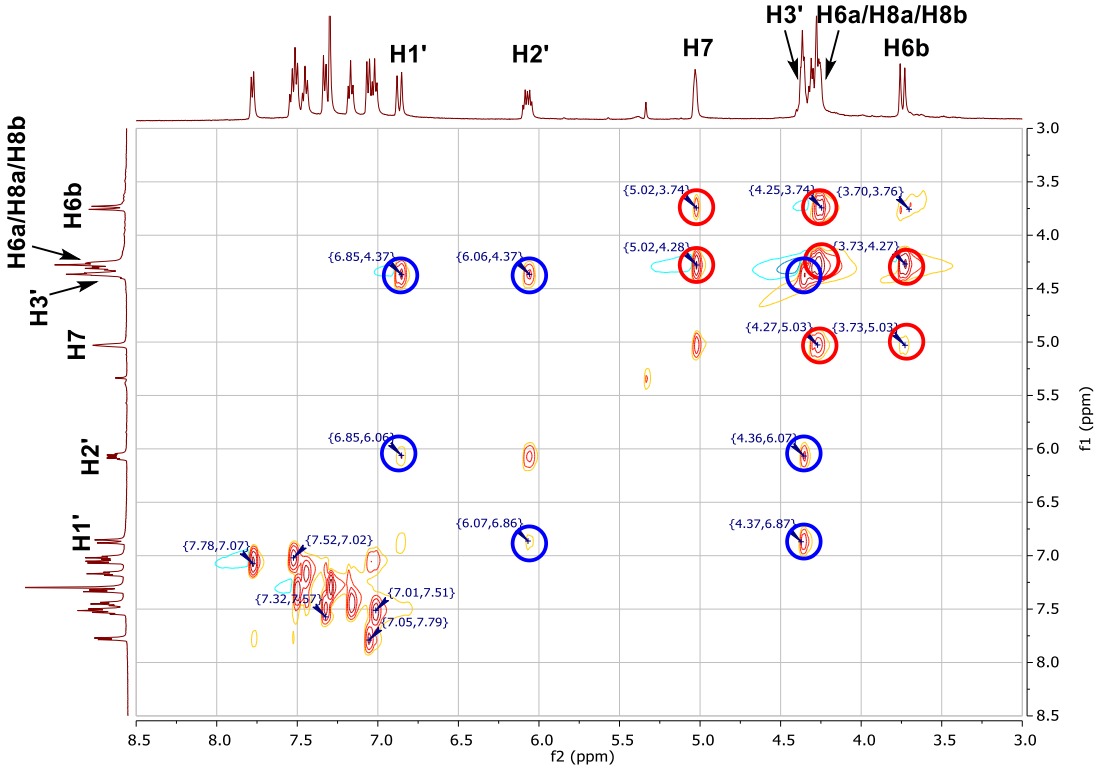

Figure 30: TOCSY spectrum of compound **155** with key correlations highlighted.

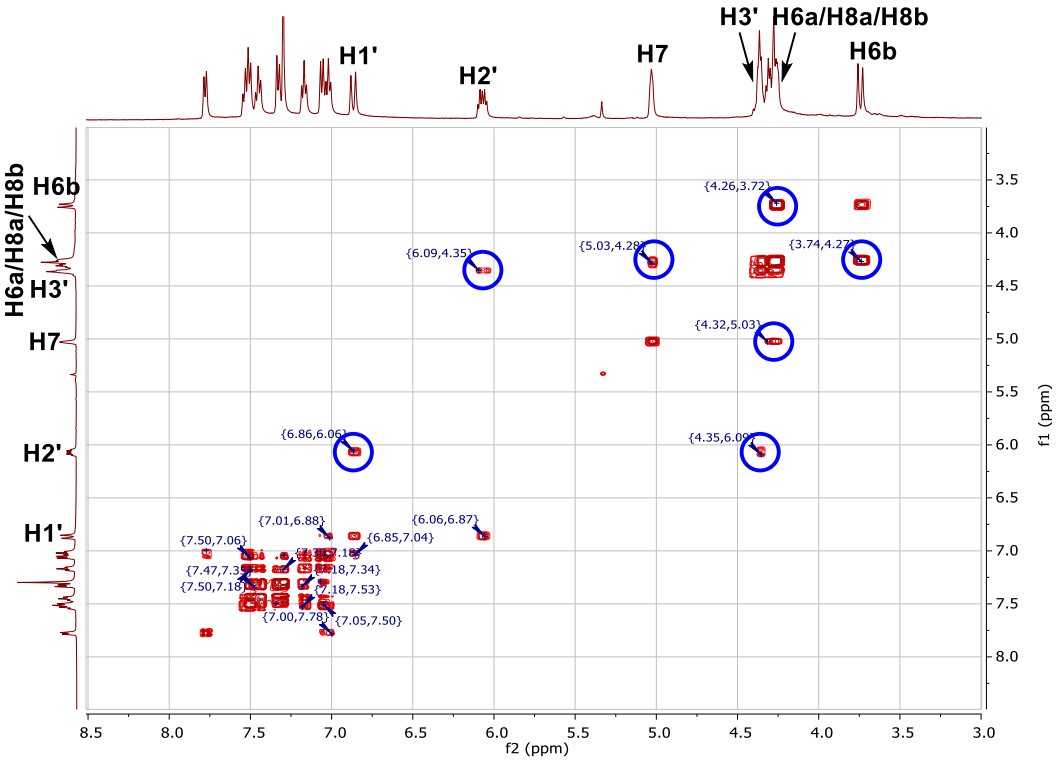

Figure 31: COSY spectrum for compound **155** with key correlations highlighted.

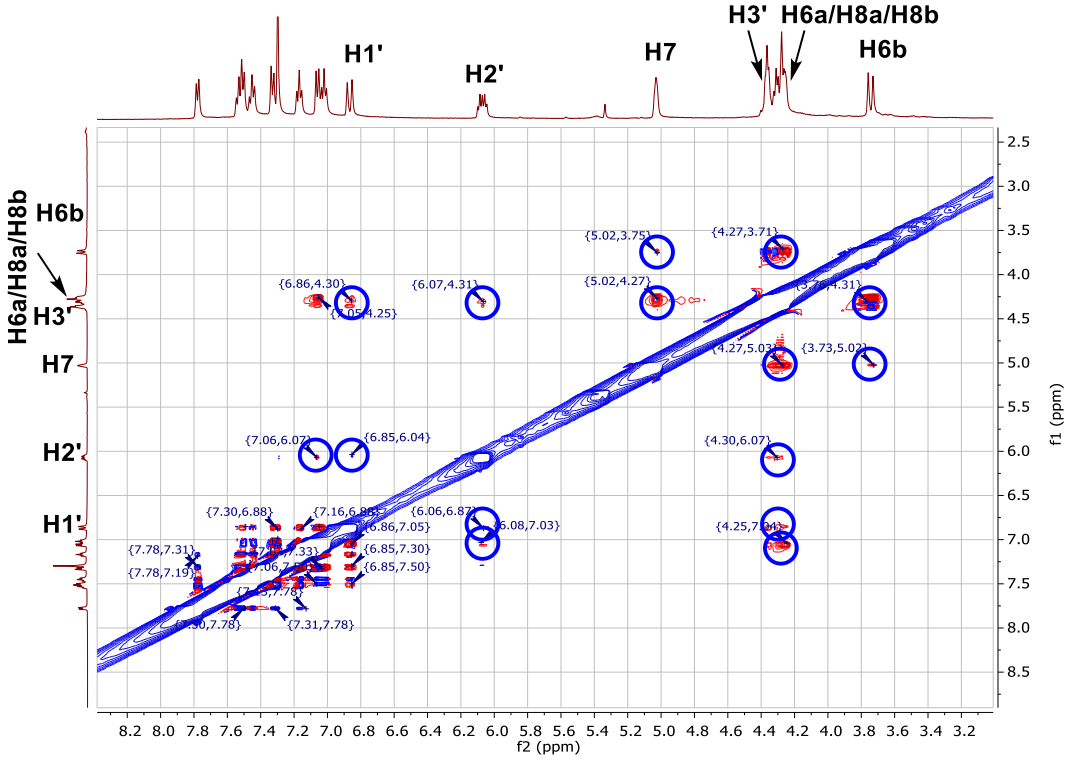

Figure 32: ROESY spectrum for compound **155** with key correlations highlighted.

In a subsequent experiment using (*S*)-epichlorohydrin **144**, x-ray quality crystals of **155** were grown by slow evaporation of a 9:1 CH_2Cl_2/hexane solution, and its absolute structure and stereochemistry were confirmed by x-ray crystallography (Figure 33).[***]

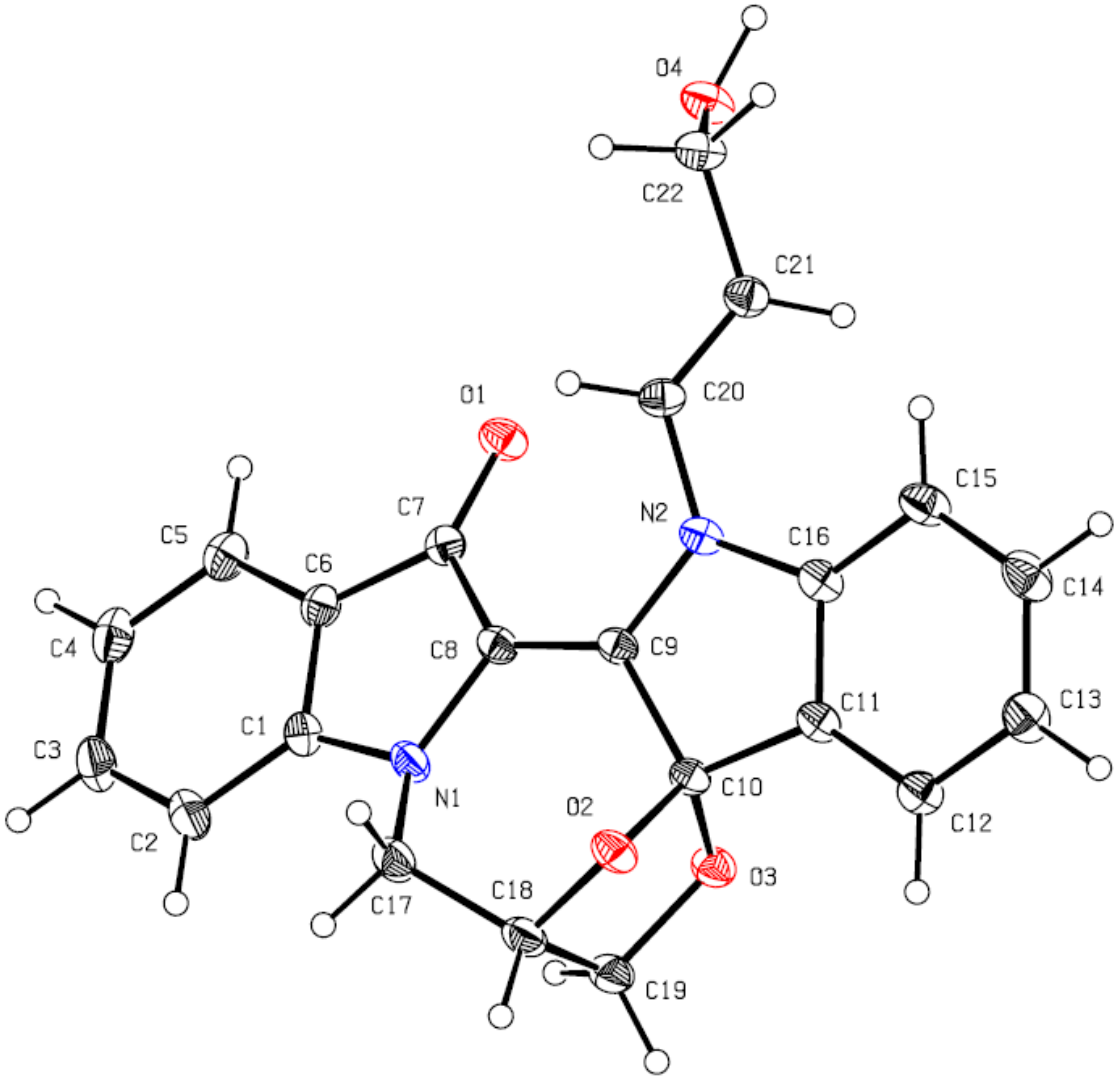

Figure 33: ORTEP depiction of compound **155** with absolute stereochemistry. Note that the atom numbers as denoted by x-ray crystallography do not reflect systematic numbering of atom positions.

3.3.2 Reaction optimisation

The initial reaction was run for 2 hours, and while it allowed access to each of the heterocycles **152**–**155**, the total mass return for the reaction was only 62%. A summary of the optimisation process for this reaction can be found in Table 2.

[***] X-ray crystallography performed by Dr. Anthony Willis (ANU).

Table 2: Summary of optimisation data for the reactions of indigo with epichlorohydrin (**144**, X=Cl), epibromohydrin (**145**, X=Br), and glycidyl tosylate (**146**, X=OTs).

	X	Time	Additives	**152** (%)	**153** (%)	**154** (%)	**155** (%)	B/L (%mass)
1	Cl[a]	2 h	3 Å Sieves	44	6	6	7	46
2	Cl[a]	1 h	3 Å Sieves	41	9	[b]	[b]	30
3	Cl[a]	30 min	3 Å Sieves	43	17		8	9
4	Cl	30 min	--	44	30		21	
5	Cl	30 min	--	41	30	20		
6[c]	Cl[a]	30 min	--	32	21		6	
7	Cl[a]	30 min	KI[d]	5	[b]			84
8	Br	30 min	--	84				
9	OTs	10 min	--	76				

B/L = Baseline materials as a percentage of the mass of the crude reaction mixture. [a]Racemic materials used. [b]Detected by TLC/ESI-MS analyses of the crude mixture, but not isolated. [c]Reaction performed using acetonitrile as solvent at reflux. [d]0.1 eq. (based on electrophile).

It was hypothesised that the high degree of polymerisation and decomposition would be reduced by using a shorter reaction time, therefore the reaction was repeated, except that the mixture was allowed to react for 1 h instead of 2 h (Table 2, Entry 2), which led to an increase in the yield of spirocycle **153** from 6% to 9%, and a small decrease in the yield of *N,N′*-cyclic **152** from 43% to 41%. Compounds **154** and **155** were evident in trace quantities by TLC and ESI-MS analysis of the crude mixture, but not isolated. Further shortening the reaction time to 30 min led to a 17% yield of **153**, in addition to a 43% yield of **152** and an 8% yield of **155** (Entry 3).

During the workup procedure, it was noted that the large surface area of the crushed 3 Å molecular sieves retained considerable quantities of the products even after repeated washing, so the reaction was repeated in the absence of molecular sieves using (*S*)-epichlorohydrin **(144**), and gratifyingly led to an improved 30% yield of **153** in addition to **152** (44%) and **155** (21%), for a total mass return of 95% based on indigo (Entry 4). Attempts to replicate this outcome however were variable, with repeated runs instead leading to mixtures of **152** (41%), **153** (30%), and **154** (20%), with no **155** evident by TLC or ESI-MS analysis (Entry 5). The exact reason for this variability is unknown, though could be related to the hygroscopicity of the DMF solvent leading to differing quantities of trace water in the absence of a drying agent (Scheme 53).

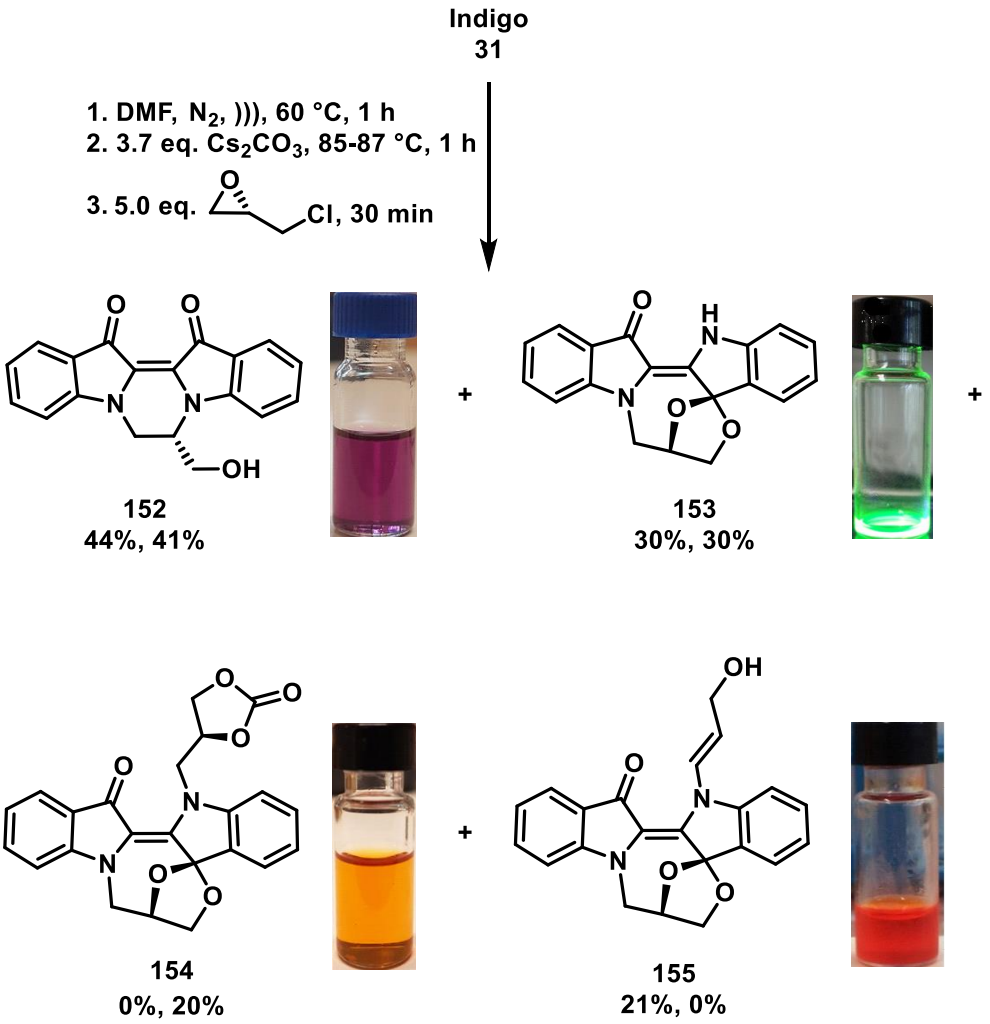

Scheme 53: Optimised reaction conditions and outcome for the reaction of indigo with (*S*)-epichlorohydrin. Yields reflect Table 2, entries 4 and 5 respectively.

Due to the low volatility, aqueous miscibility, and high boiling point of the DMF solvent, the reaction was repeated using acetonitrile as the solvent at reflux (82 ˚C), which gave a mixture of **152** (32%), **153** (21%), and **155** (6%), as well as a 26% isolated recovery of unreacted indigo due to its poor solubility in acetonitrile (Table 2, Entry 6). The overall lower yield of this process however was countered by the significantly shorter processing time for the reaction, whereby the acetonitrile solvent could be removed *in vacuo* and replaced with EtOAc and filtered prior to aqueous washing. For larger (eq. gram-scale) scale preparations this may prove a more practical approach than using larger volumes of DMF, albeit at the cost of yield due to unreacted indigo.

Yields for the *N,N′*-cyclic compound **152** were not significantly affected by changes in reaction time, and it was thought that modifying the pendant halide may affect the product distribution. Therefore, indigo was reacted with (±)-epibromohydrin (**145**) under identical conditions to those for (*S*)-epichlorohydrin (**144**), resulting in an 84% isolated yield of

152 with no other significant products detected by TLC analysis (Entry 7). Repeating this reaction using (*R*)-glycidyl tosylate (**146**), except with a reaction time of 10 min also led to a 76% isolated yield of the (*R*)-isomer of **152** (Scheme 54).

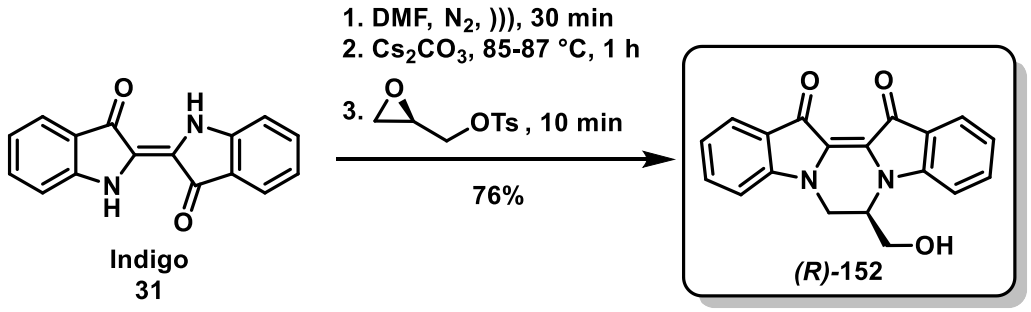

Scheme 54: Selective formation of ***(R)*-152** from the alkylation of indigo with *(R)*-glycidyl tosylate. Yields reflect Table 2, Entry 8

3.3.3 Mechanistic discussion

The regioselectivity of nucleophilic attack on halohydrins has been studied previously, where it was shown that epoxide ring-opening is up to 200 times more favourable than direct nucleophilic halide displacement in polar solvents.[142] Therefore, it is likely that ring-opening of the epoxide precedes any processes involving the pendant leaving group, as reflected by the observation that increasing the strength of the leaving group had a dramatic effect on the product distribution, and exclusively gave *N,N′*-cyclised product **152**. The identity of the halide likely plays a crucial role in determination of the mechanistic pathway of the reaction, such that nucleophilic addition of indigo to epichlorohydrin affords key intermediate **156**, which serves as a branching point between *N,N′*-cyclisation (Path A, Scheme 55) and *N,O′*-cyclisation (Path B, Scheme 56). Compound **152** is derived from **156** *via* Path A, where the leaving group is displaced by the vicinal alkoxide, resulting in a net epoxide migration from C1-C2 to C2-C3 with retention of stereochemistry. This elimination would become more favourable with better leaving groups, as reflected by the increase in the yield of **152** from 44% to 84% upon replacing X=Cl with X=Br. Reversible base-mediated prototropic isomerisation of the indigo core affords the *cis*-anion **157**, which undergoes an irreversible 6-*exo*-tet cyclisation to ring-open the newly-reformed epoxide, resulting in inversion of the C2-stereochemistry and the formation of **152** upon protonation (Scheme 55).

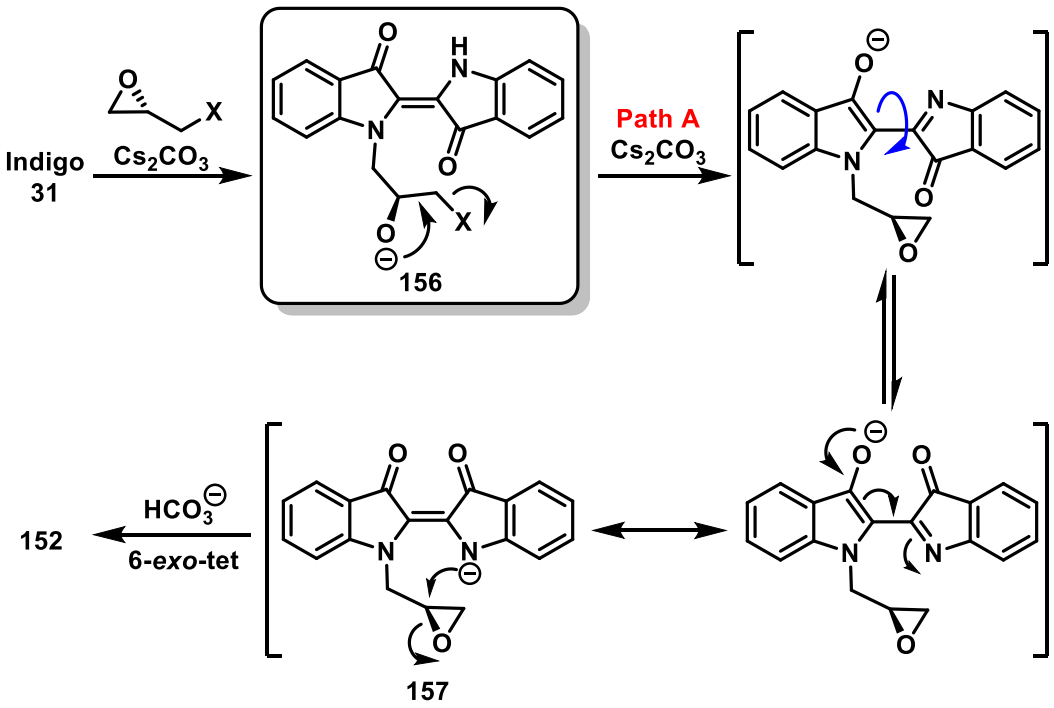

Scheme 55: Proposed mechanism for the formation of pyrazinodiindole **152** from key intermediate **156** *via* Path A. Cesium counter-ions omitted for clarity.

With weaker leaving groups, epoxide reformation would become less-favourable, and where key intermediate **156** lingers, deprotonation of the indigo nitrogen atom may instead lead to *O'*-attack on the pendant chloride *via* a dearomative 8-*exo*-tet cyclisation, leading to semi-rigid intermediate **158**. The rigidity of this macrocyclic intermediate may restrict nucleophilic attack by the adjacent alkoxide to the nearby indole C3-position to the *re*-face, thereby defining the stereochemistry of the C9a position of spirocycle **153** (Scheme 56). An alternative mechanism for ketalisation involves the halide being eliminated by water to give a diol, which undergoes condensation with the ketone, however the presence of **153** was not detected from a trialled reaction between indigo and 2-hydroxymethyloxirane (glycidol), suggesting the mechanism does not involve a diol intermediate.

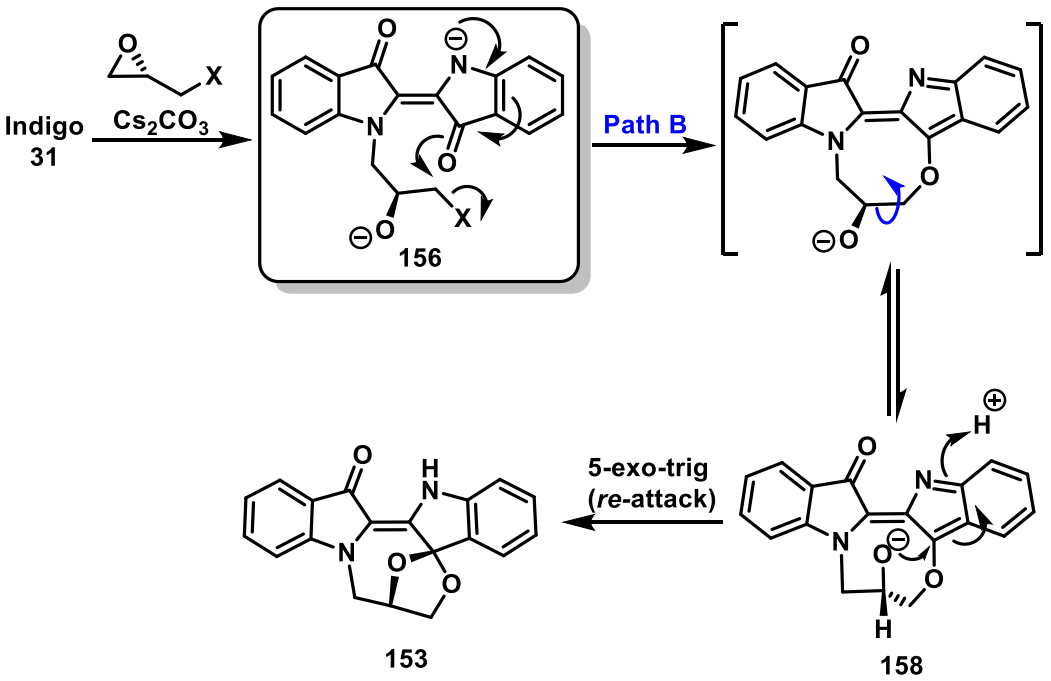

Scheme 56: Dearomative cyclisation of key intermediate **156** to macrocycle **158** by halide displacement *en route* to spiroketal product **153**.

Spirocycle **153** could then undergo further *N*-alkylation with a further equivalent of epichlorohydrin, and subsequent elimination of the halide could give the intermediate *N*-glycidyl adduct **159**. Ring-opening of this epoxide with either carbonate or bicarbonate could then give an intermediate α-hydroxycarbonate (**160**), which upon dehydration would afford cyclic carbonate **154**. Alternatively, base-mediated elimination of the epoxide **159** – or E2 elimination of the carbonate **154** – could then lead to formation of the allylic alcohol adduct **155** (Scheme 57). The precise mechanism for the formation of alcohol **155** is unknown, as despite its isolation from multiple attempts during the optimisation of the reaction, a reliable means of synthesising it could not be established. Briefly, attempted decarboxylation of carbonate **154** by treatment with potassium *tert*-butoxide in THF led to decomposition, and attempted alkylation of unsubstituted **153** with additional epichlorohydrin in the presence of cesium carbonate gave a mixture of **154** (43% yield) and polymeric baseline materials, while in the absence of cesium carbonate (e.g. using bases such as K_2CO_3, *n*-BuLi, LDA and NaH), only unreacted **153** was isolated.

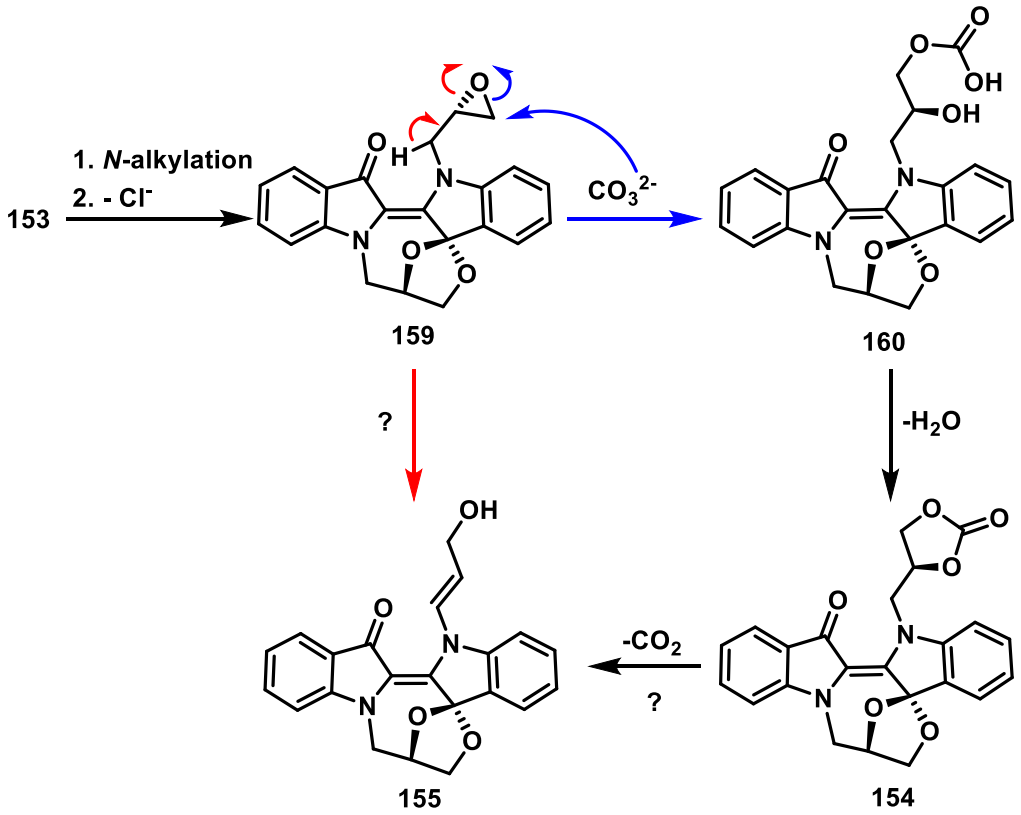

Scheme 57: Proposed divergent mechanism for the formation of *spiro*-oxazocinodiindoles **154** and **155** from indigo *via* alkylation of compound **153**.

There are several previously-reported examples of the addition of oxiranes to ketones to form ketals, though these typically proceed *via* Lewis or Brønsted acid catalysis, where the oxirane is highly-activated by coordinating to the cationic species.[143] Carboxylation of epoxides with carbon dioxide is also known, though this reaction typically proceeds under high-pressure and/or at elevated temperatures.[144] Here, the relatively-low yields (maximum 20%) of **154** are attributed to the previously-noted nucleophilicity of cesium carbonate.[116]

3.4 Cascade reactions of 2-(halomethyl)aziridines and 2-phenylaziridine with indigo

3.4.1 Synthesis of starting materials

Considering the generation of various spiroketal-containing molecules from reactions of indigo with (halomethyl)oxiranes, we sought to explore whether substituting oxiranes for aziridines would lead to further *N,N'*-cyclised pyrazinodiindoles via Path A (see Scheme 55), or instead allow access to *N,O'*-cyclised spirooxazolidines *via* Path B (see Scheme 56). The synthesis of several *N*-substituted-2-(bromomethyl)aziridines has been reported previously,[139a, 145] though these were generated racemically and by non-stereoselective means. The necessity of using chlorine gas as a reagent was also deemed prohibitive toward the synthesis of chloromethyl derivatives,[146] hence a less-hazardous, stereoselective method for the generation of chiral 2-(halomethyl)aziridines had to be devised.

Bromomethylaziridine **147** was prepared as previously reported from the acidic bromination of allylamine (**161**), and subsequent one-pot *N*-sulfonylation/ring-closure reaction in excellent yield (Scheme 58).[139a] Briefly, allylamine **161** was treated with 1.3 eq. Br_2 in aqueous HBr solution at 0 ˚C and then warmed to RT and stirred for 4 h, which upon removal of excess bromine by distillation and repeated recrystallisation of the crude mixture from isopropanol afforded the intermediate hydrobromide salt **162** in 80% yield. This brominated salt was then reacted with tosyl chloride in aqueous sodium hydroxide solution, to afford the desired aziridine product **147** in quantitative yield. This overall process was amenable to multigram-scale preparation of the desired aziridine, as no further purification was necessary. In two repeated runs, 17.7-17.9 grams of salt **162** was synthesised (79-80% yield), which was reacted over multiple 5.0-gram batches, reliably affording between 4.6-4.8 g (94-99% yield) of *N*-tosyl-2-(bromomethyl)aziridine **147**.

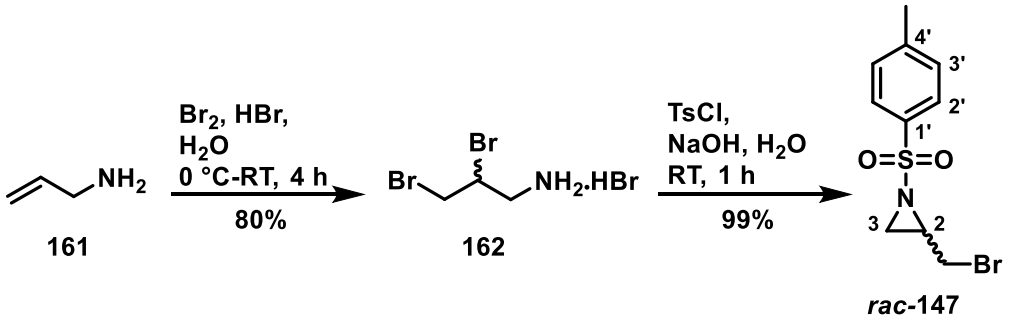

Scheme 58: Synthesis of racemic (bromomethyl)aziridine **147** on multi-gram scale from allylamine **161** *via* hydrobromide salt **162**.

Analysis of the ESI(+) mass spectrum revealed a pair of peaks at *m/z* 312^+ and 314^+ in a 1:1 ratio, assigned as the $[M+Na]^+$ molecular ion peaks for the ^{79}Br and ^{81}Br isotopes, respectively. Analysis of the ^1H NMR spectrum revealed a pair of 2H aromatic doublets at δ 7.82 and δ 7.34, assigned to H2'/H6' and H3'/H5', respectively. Further upfield, the 2H doublet at δ 3.26 was assigned to the methylene protons of the bromomethyl substituent, and the multiplet ranging from δ 3.12-3.04 was assigned to H2. The 3H singlet assigned to the tosyl methyl group was flanked on either side by a pair of doublets at δ 2.78 and δ 2.21, assigned to H3a and H3b, respectively.

Chloromethylaziridine **148** on the other hand proved more challenging to synthesise than its bromo-substituted equivalent. We sought to utilise a direct substitution of hydroxymethylaziridine **163** *via* a robust, two-step mesylation-chloridation procedure, necessitating the preparation of **163** on multigram-scale. Direct aziridination of allyl alcohol **164** with chloramine-T trihydrate (**165**) under I_2 catalysis afforded a mixture of two major products after 3 d at room temperature. Flash chromatography (40% EtOAc/pet spirit) on silica gave good resolution between the desired aziridine **163** (36% yield) and the unexpected by-product disulfonamide **166** (56% yield) from undesired ring-opening of **163** with additional **165**.

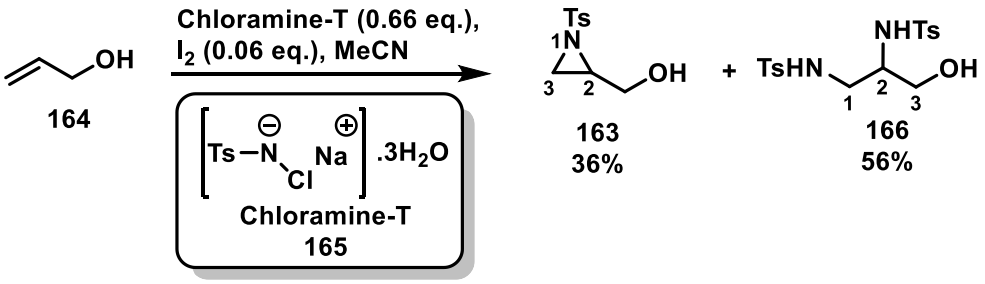

Scheme 59: Synthesis of (hydroxymethyl)aziridine **163** and the unexpected disulfonamide **166** from allyl alcohol (**164**).

Hydroxymethylaziridine **163** was isolated as a clear oil in 36% yield following flash chromatography. Analysis of the ESI(+) mass spectrum revealed a peak at *m/z* 250, corresponding to the molecular ion $[C_{10}H_{13}NO_3SNa]^+$, revealing the incorporation of a one equivalent of chloramine-T across the alkene. Analysis of the ^1H NMR spectrum revealed a pair of 2H doublets at δ 7.82 and δ 7.35, assigned as the *N*-tosyl aromatic protons. The pair of doublet-of-doublets at δ 3.81 and δ 3.54 were assigned to the diastereotopic methylene protons of the hydroxymethyl group, and the broad singlet at δ 2.18 assigned to the hydroxyl proton. The multiplet at δ 3.04-2.99 was assigned to H2, and the remaining pair of doublets at δ 2.61 and δ 2.30 assigned to the diastereotopic

methylene protons of the aziridine terminus C3.

Disulfonamide **166** was isolated as a pale cream amorphous solid in 56% yield. Analysis of the ESI(+) mass spectrum revealed a peak at *m/z* 421, assigned as the molecular ion $[C_{17}H_{22}N_2O_5S_2Na]^+$, revealing the addition of two sulfonamide units to the allylic starting material **164**. Analysis of the ^{1}H NMR spectrum revealed a pair of 2H doublets at δ 7.73 and δ 7.64 and a 4H multiplet ranging from δ 7.32-7.20, assigned to the aromatic protons of the two tosyl substituents, in addition to a 6H singlet at δ 2.39, assigned to both methyl substituents. The downfield doublet at δ 5.88 and its neighbouring triplet at δ 5.77 showed no direct ^{13}C attachment by HSQC experiments, and were assigned as the two discrete sulfonamide -NHTs groups attached to C2 and C1, respectively. The C1-adjacent sulfonamide was correlated to a broad 2H multiplet centred at δ 2.97, which was assigned as the C1 methylene protons, and the C2-adjacent sulfonamide was correlated to a multiplet ranging from δ 3.35-3.26, assigned as the C2 methine (Figure 34). The broad singlet resonance ranging from δ 3.30-3.08 was assigned as the hydroxyl proton, and the remaining multiplets located at δ 3.63-3.56 and δ 3.54-3.46 were assigned to the C3 methylene protons.

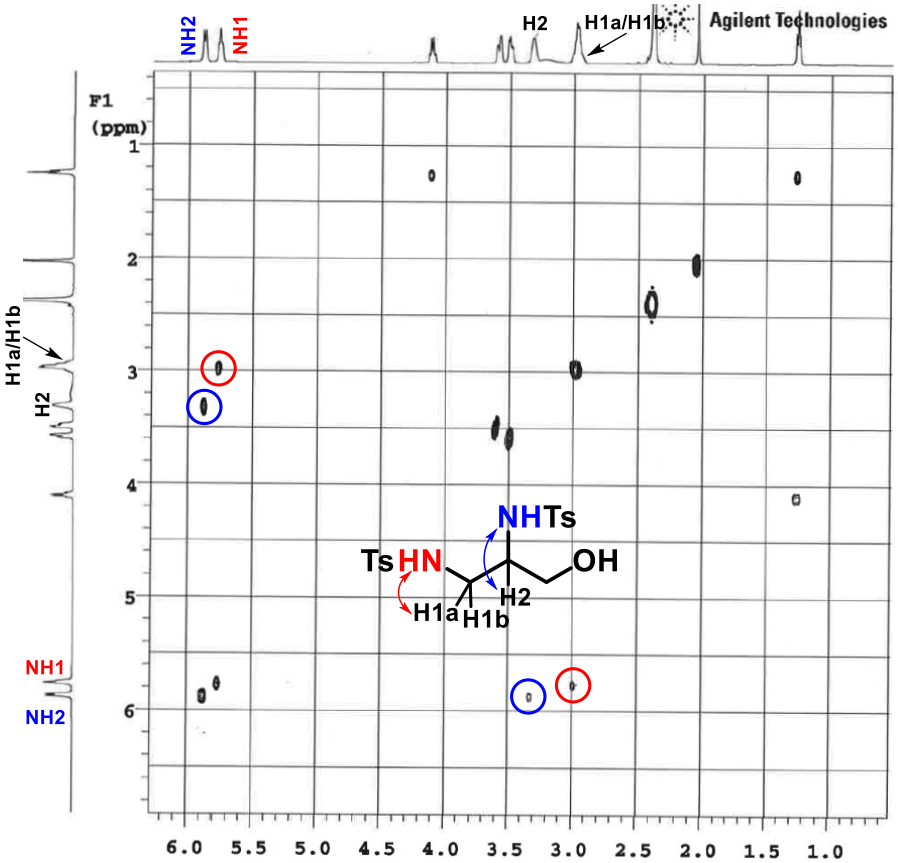

Figure 34: COSY spectrum for compound **166** with relevant crosspeaks indicated.

The desired aziridine **163** was produced initially in 36% yield alongside **166** in 56% yield. Reducing the reaction time from three days to two days produced **163** in an improved 43% yield, in addition to **166** (21%) and a mixture of products from undesired aminohalogenation in a combined crude yield of 10%. Repeated attempts did not lead to significant improvements in the yield of **163**, which was consistently isolated in 35-45% yield, though this reaction could be run at a multi-gram scale with no significant diminishing of yield, producing sufficient aziridine for our purposes.

The formation of **166** was unexpected and represents a net diamination of the olefin starting material. This was an intriguing outcome, as despite many previous attempts,[147] as well as the well-established and celebrated protocols for dihydroxylation, epoxidation and aminohydroxylation of olefins,[148] there remains no reliable method for intermolecular diamination of non-activated alkenes. This is particularly interesting given that the reaction utilises the inexpensive and environmentally-benign chloramine-T (otherwise used in water treatment, and in iodometric analysis)[149] as the nitrogen source and oxidant. Treatment of allyl alcohol with 2.1 eq. of chloramine-T gave the disulfonamide **166** in 75% yield after 16 h at room temperature, suggesting this aziridination/ring-opening process to be highly favourable.

To probe the tolerance of this method to other alkene species, the reaction was trialled for the diamination of cyclohexene (**167**) in a single unoptimized run (Scheme 60), and afforded a mixture of *meso*-aziridine **168** (78% yield) and *trans*-disulfonamide **169** (20% yield). This is therefore a promising starting point for the development of new methods for olefin diamination and despite being beyond the scope of this dissertation, warrants further examination.

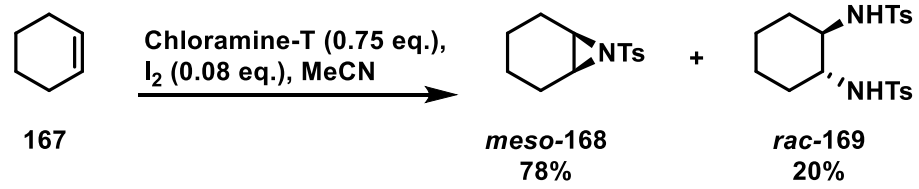

Scheme 60: Unoptimised yield for the reaction of cyclohexene (**167**) with Chloramine-T (**165**) to afford aziridine **168** and diaminated product **169**.

With the desired hydroxymethylaziridine **163** in hand, it was subjected to a two-step mesylation-chloridation. The aziridinyl alcohol was dissolved in dry CH_2Cl_2, and treated with methanesulfonyl chloride and triethylamine at 0 ˚C for 1 h, then warmed to room temperature and stirred for a further hour, at which time TLC analysis showed complete consumption of starting material. The reaction mixture was subjected to aqueous workup,

the crude mesylate combined with excess LiCl (5.0 eq.) and a phase-transfer catalyst (TBA^+Cl^-, 0.2 eq.) in THF, and the mixture stirred at 50 ˚C overnight. Aqueous workup and removal of the solvent afforded the hydrolysis product **170** in quantitative yield (Scheme 61).

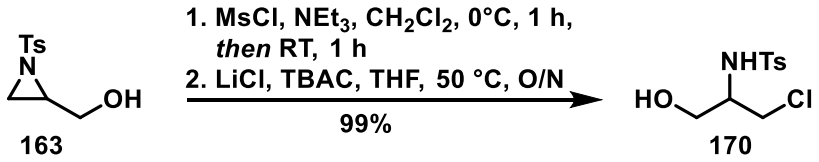

Scheme 61: Attempted synthesis of chloromethylaziridine **148** *via* mesylation/chloridation, resulting in the formation of hydrolysis product **170**.

Compound **170** was isolated as off-white crystals in 99% yield from undesired hydrolysis of the desired chloromethylaziridine on aqueous workup. Analysis of the ESI(+) mass spectrum revealed a pair of peaks at *m/z* 286 and 288 in a 3:1 ratio, assigned to the two isotopic molecular ions $[C_{10}H_{14}{}^{35}ClNO3SNa]^+$ and $[C_{10}H_{14}{}^{37}ClNO3SNa]^+$, respectively. Analysis of the ^1H NMR spectrum revealed a doublet at δ 6.05 and a broad singlet at δ 3.18, assigned to the sulfonamide and hydroxyl protons, respectively. The five remaining aliphatic protons formed a broad multiplet ranging from δ 3.78-3.44, which could not be easily disentangled.

Repeated attempts toward chlorination of **163** using this method continually resulted in **170**, as did the use of $SOCl_2$, which afforded **170** in 76% yield. Attempted Appel chloridation using PPh_3/CCl_4 led to extensive decomposition, and attempted *O*-tosylation using tosyl chloride and pyridine led to ring-opening with residual chloride ions. A successful route was identified from the acidic ring-opening of bromomethylaziridine **147** with 36% $HCl_{(aq)}$ to give the mixed bromo/chloro species **171** in 82% yield, which underwent selective bromide elimination using cesium carbonate (1.1 eq.) in anhydrous CH_2Cl_2 (0.01 M), affording the desired chloromethylaziridine **148** in 90% yield, for a total of 74% from the bromomethylaziridine.

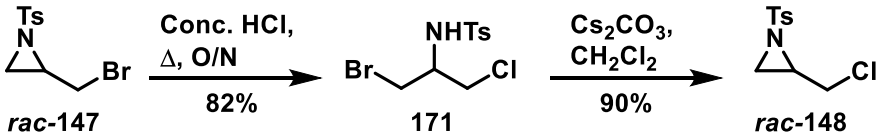

Scheme 62: Synthesis of chloromethylaziridine **148** from bromomethylaziridine **147** *via* mixed dihalide **171**.

Dihalide **171** was isolated as a white solid in 82% yield from bromomethylaziridine **147**. Analysis of the ESI(+) mass spectrum revealed a cluster of multiple peaks at *m/z* 348^+, 350^+, and 352^+ in a 3:5:2 ratio, assigned to the molecular ion $[C_{10}H_{13}NO_2BrClSNa]^+$ due

to the $^{35}Cl/^{79}Br$, $^{35}Cl/^{81}Br$, $^{37}Cl/^{79}Br$, and $^{37}Cl/^{81}Br$ isotopic pairings. Analysis of the ^{1}H NMR spectrum revealed a doublet at δ 5.03 assigned as the sulfonamide NH, in addition to a 3H multiplet ranging from δ 3.79-3.70, assigned to H2 and the chloride-adjacent H3a/H3b, and a 2H multiplet ranging from δ 3.52-3.46, assigned to the bromide-adjacent H1a/H1b methylene protons.

Chloromethylaziridine **148** was isolated in 90% yield from **171** as a colourless, viscous oil which slowly crystallised into a low-melting solid (mp. 42-44 ˚C) on standing. Analysis of the ^{1}H NMR spectrum revealed a broad doublet-of-doublet-of-doublets at δ 3.46, assigned to the methylene protons of the chloromethyl group, which showed HSQC correlation to a peak in the DEPTQ ^{13}C NMR spectrum at δ 43.5 (Figure 35). The pair of doublets at δ 2.74 and δ 2.26 were assigned to the methylene protons of the C3 aziridine terminus by HSQC analysis, which showed strong correlations between both protons and a resonance in the DEPTQ ^{13}C NMR spectrum at δ 32.8, and by COSY analysis, which revealed strong correlations between both protons and the multiplet at δ 3.09-2.99, assigned to H2 (Figure 36). Analysis of the HMBC spectrum revealed strong three-bond correlations between the chloromethyl methylene and C3, and between the 3H singlet at δ 2.44 and both C3' and C4' of the tosyl group (Figure 37).

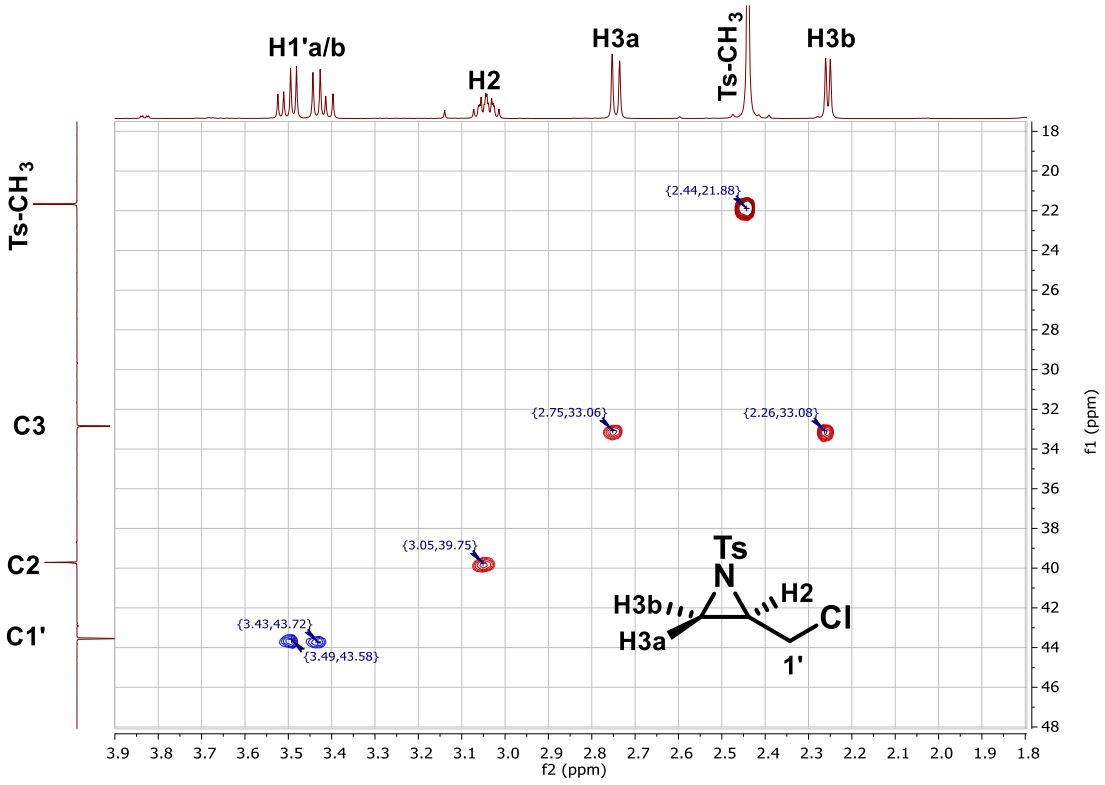

Figure 35: HSQC spectrum for chloromethylaziridine **148**.

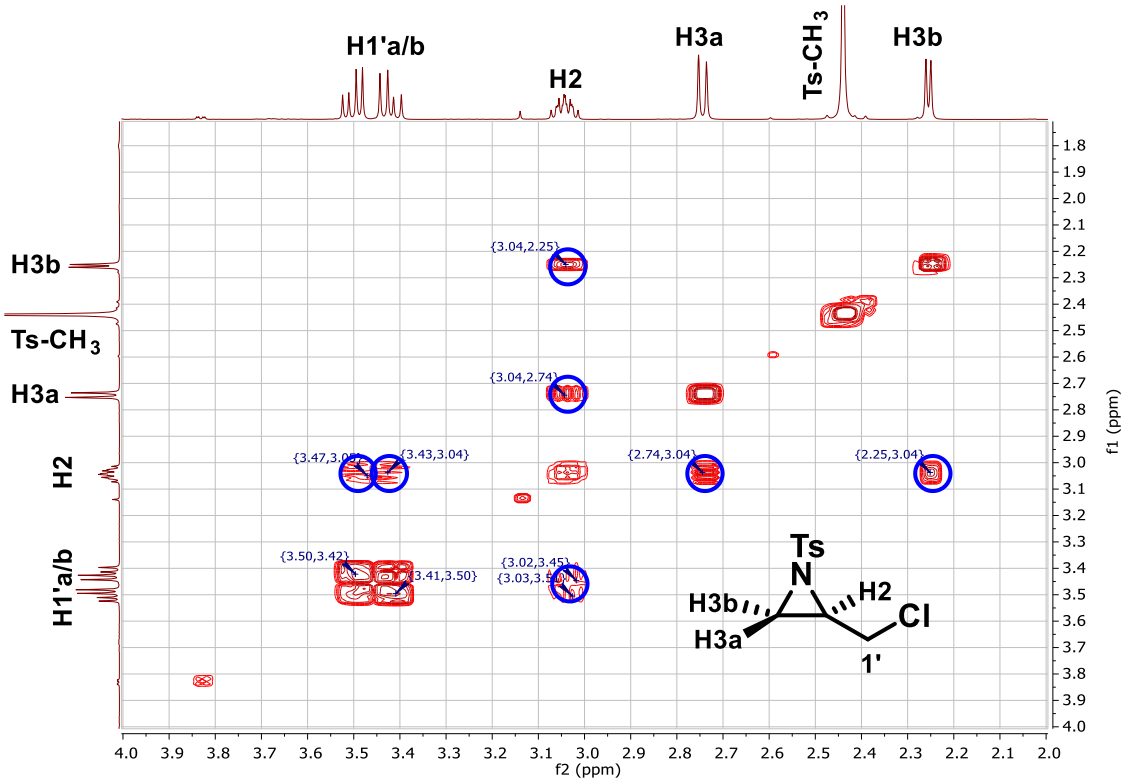

Figure 36: COSY spectrum for chloromethylaziridine **148** with key correlations highlighted.

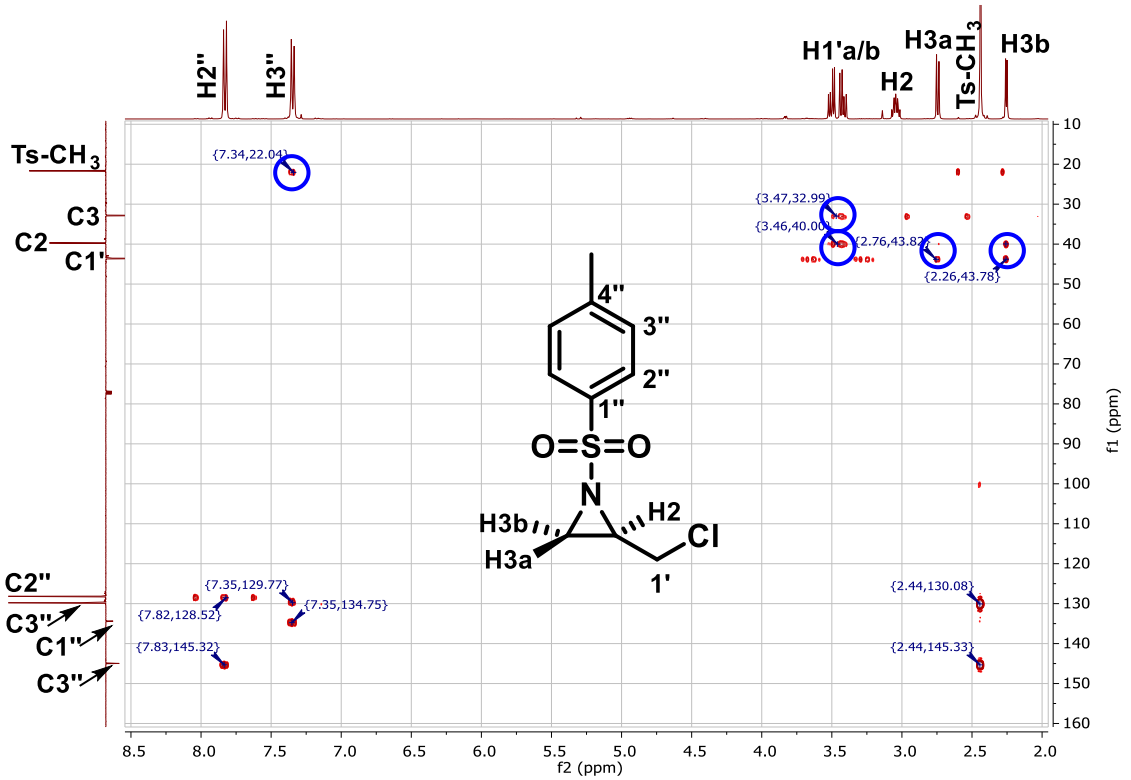

Figure 37: HMBC spectrum of chloromethylaziridine **148** with key correlations highlighted.

While this procedure proved robust, it did not solve the problem of enantioselectivity, as the precursor bromomethylaziridine **147** was generated racemically. Therefore, an alternative synthesis of **148** from (*S*)-epichlorohydrin (**144**) was devised, where the enantiopure starting material was ring-opened using chloramine-T (**165**) to afford the chiral chlorosulfonamide **172** in 97% yield upon reductive workup. This was then subjected to *O*-mesylation using MsCl/NEt_3 to give the corresponding *O*-mesylate **173** in 96% yield, followed by mesylate displacement using Cs_2CO_3 in CH_2Cl_2 (0.01 M) to afford the ring-closed enantiopure aziridine **148** in 73% yield, or 64% yield from epoxide **144** with complete stereocontrol, and only requiring a single purification step.

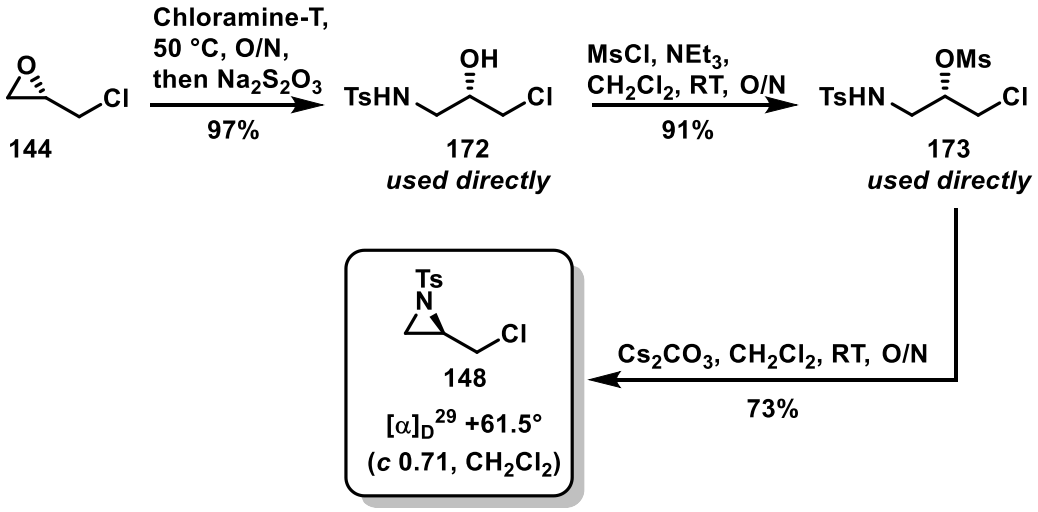

Scheme 63: Second-generation, enantiospecific synthesis of **148** from *(S)*-epichlorohydrin (**144**) over three steps.

Finally, to probe the dependence of the cascade process on the presence of a halide, we sought to synthesise *N*-tosyl-2-phenylaziridine (**174**) *via* direct aziridination of styrene (**175**). Optimal conditions were found using a slight excess of styrene (1.05 eq.), where the desired aziridine could be synthesised in 93% yield on multigram-scale (30 mmol), requiring no purification beyond hexane/acetonitrile extraction to remove unreacted styrene, and aqueous workup.

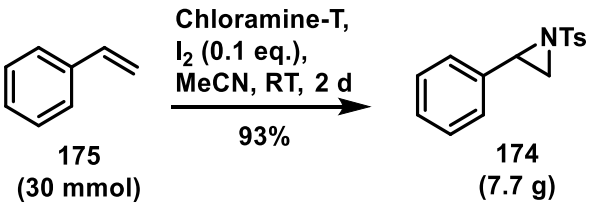

Scheme 64: Synthesis of *N*-tosyl-2-phenylaziridine on multi-gram scale under optimised conditions.

Compound **174** was isolated as a chunky, off-white amorphous solid in 93% yield after hexane/acetonitrile extraction, and aqueous workup. Analysis of the ESI(+) mass spectrum revealed a peak at *m/z* 296$^+$, assigned to the molecular ion $[C_{15}H_{15}NO_2SNa]^+$. Analysis of the ^{1}H NMR of **174** revealed a doublet of doublets at δ 3.77, assigned to the benzylic proton H2, as well as a pair of doublets at δ 2.97 and δ 2.38, assigned to the diastereotopic methylene of the aziridine.

3.4.2 Reaction discovery and structure elucidation

With optimised conditions from investigating the ring-opening reactions of halomethyloxiranes, we initially applied these conditions to the reaction of indigo and *N*-tosyl-2-(bromomethyl)aziridine (**147**), however it was quickly determined that extended reaction times (i.e. >5 min) led to extensive, uncontrollable polymerisation, hence shorter reaction times were essential. Briefly, a suspension of indigo (1.0 mmol) in DMF (40 mL) was prepared by sonicating in a 60 ˚C water bath for one hour, and transferred by cannula into a round-bottomed flask containing pre-dried Cs_2CO_3 (3.7 eq.) and a large magnetic stir bar, and the mixture stirred vigorously under N_2 in an oil bath preheated to strictly 85-87 ˚C for one hour. The N_2 flow was then cut, and **147** (5.0 eq.) injected as a solution in DMF (1 mL), and the mixture stirred vigorously for 5 seconds, then quenched over crushed ice. Aqueous workup and removal of the solvent afforded an intense blue residue which was subjected to flash chromatography, which after difficult separation resulted in the isolation of *N,N′*-cyclic products **176** and **177**, from the addition of one and two units of **147** to the indigo core, respectively (Scheme 65).

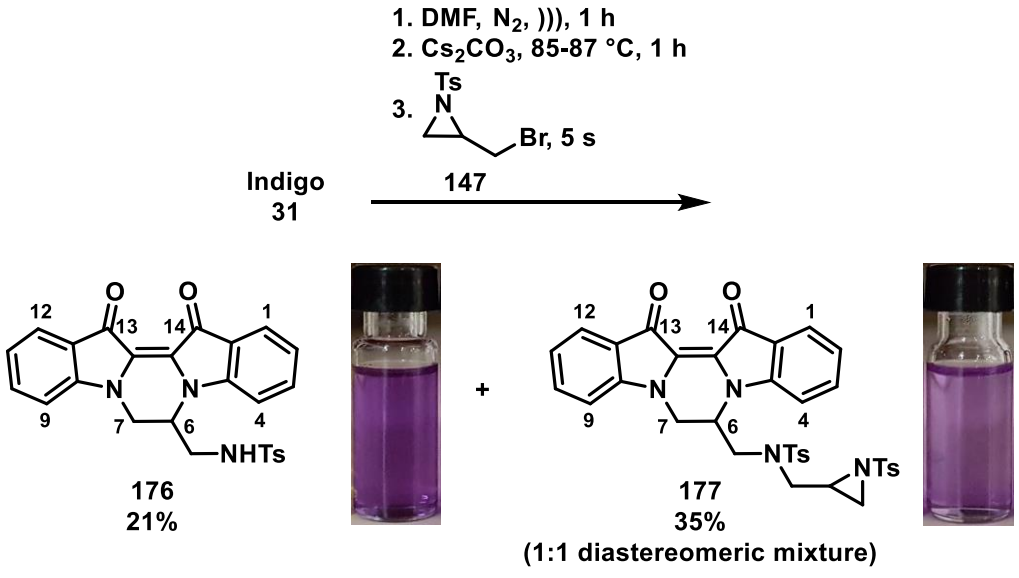

Scheme 65: Outcome of the 5 second reaction of indigo with bromomethylaziridine **147** to give *N,N′*-cyclised products **176** and **177**.

Dihydropyrazinodiindole **176** was isolated as an intense-blue, glassy amorphous solid in 21% yield following flash chromatography. Analysis of the HRESI mass spectrum revealed a peak at *m/z* 472.1319, assigned to the molecular ion $[C_{26}H_{22}N_3O_4S]^+$, revealing the addition of a single aziridinyl subunit to indigo. Its deep-blue colour and physical characteristics were similar to that of pyrazinodiindole **152**, suggesting it to be an analogue of this scaffold. The UV-Vis spectrum (CH_2Cl_2) showed a pair of broad absorption bands centred at 302 (14297) and 576 (8879) nm. Analysis of the FTIR spectrum revealed a broad absorption peak at 3385 cm^{-1}, assigned to a sulfonamide NH, and a peak at 1730 cm^{-1} assigned to the C13 and C14 carbonyls. Analysis of the ^1H NMR spectrum revealed a downfield triplet at δ 8.08 which exchanged with D_2O and was not correlated to any carbon in HSQC experiments and was assigned to the sulfonamide NH proton (Figure 38). Further upfield, the multiplet at δ 4.70-4.61 showed correlations to a pair of methylene carbons by analysis of the HSQC and COSY spectra (Figure 39), and was assigned to H6, and C6 was correlated weakly to both adjacent methylenes in HMBC experiments (Figure 40). The pair of doublets at δ 4.42 and δ 3.70 were assigned to the H6a/H6b methylene, and the broad 2H multiplet ranging δ 3.06-2.81 was assigned to the amide-adjacent methylene protons, which showed strong correlations to the sulfonamide NH in COSY experiments.

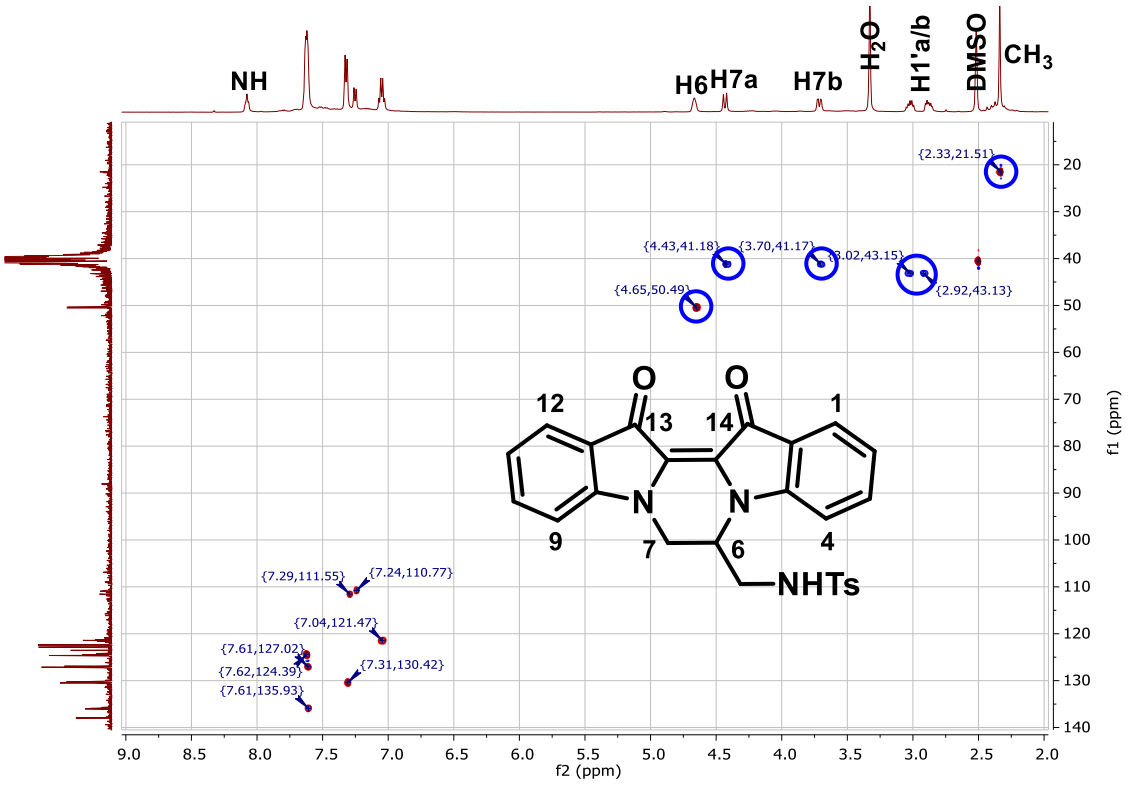

Figure 38: HSQC spectrum for compound **176** with relevant peaks highlighted.

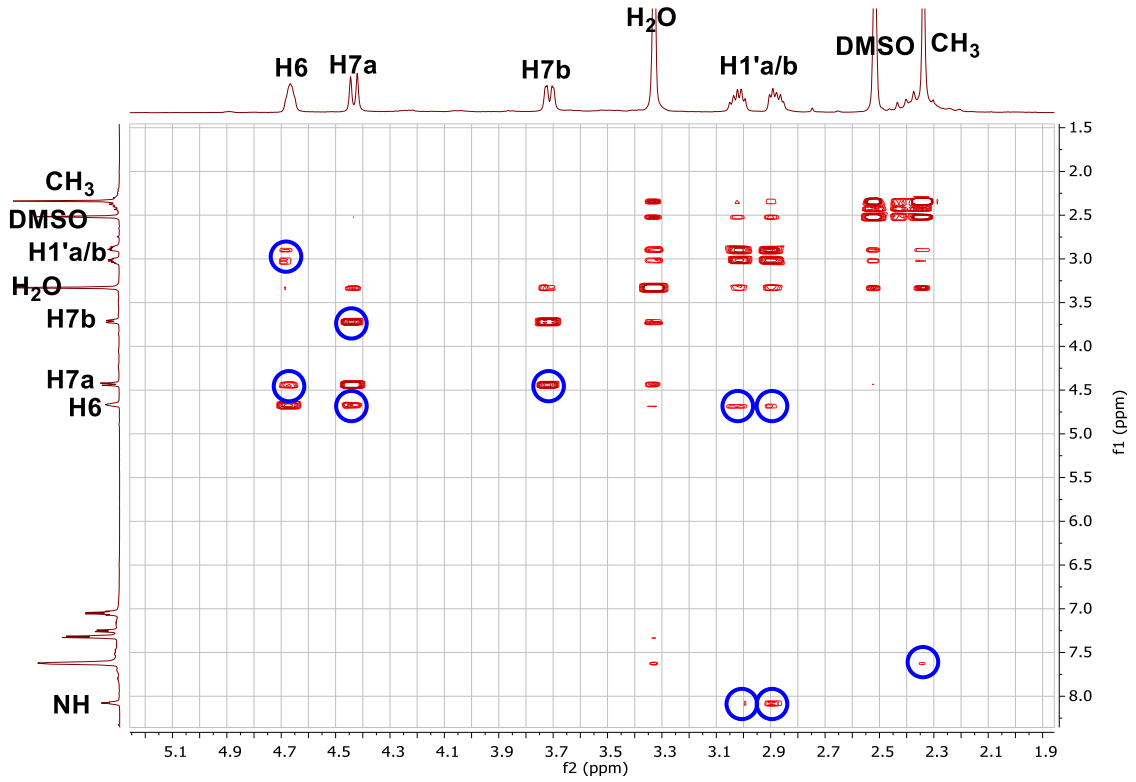

Figure 39: COSY spectrum for compound **176**.

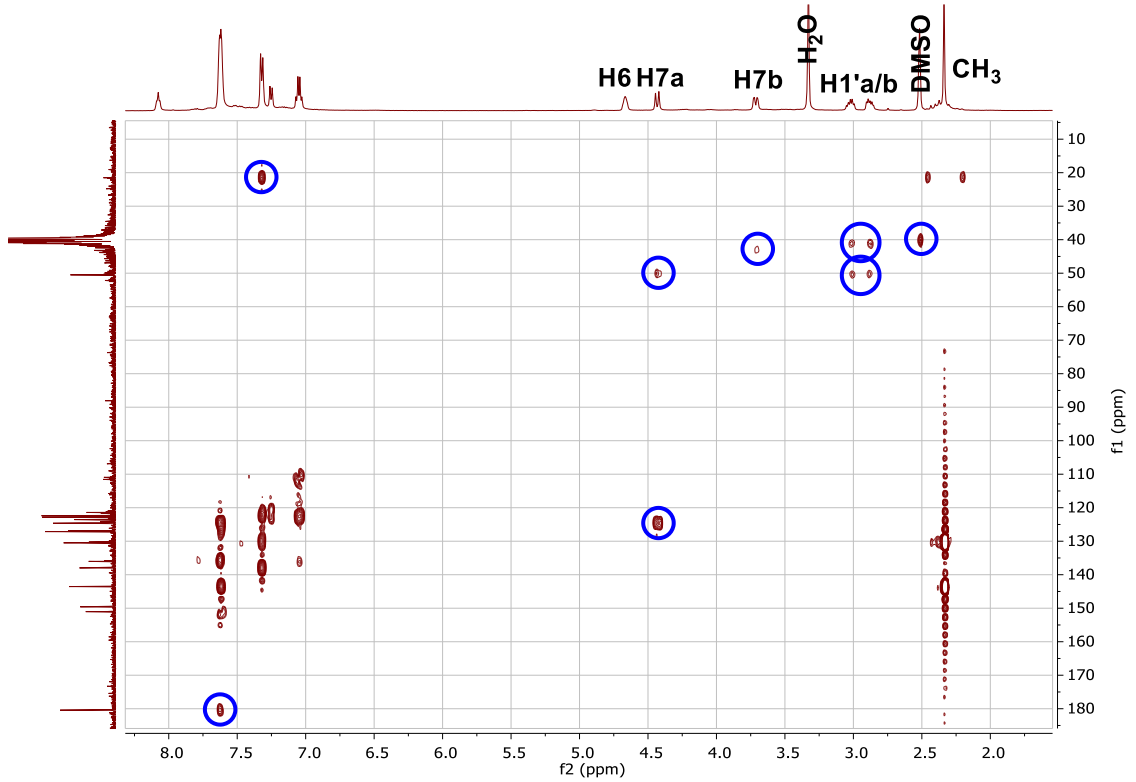

Figure 40: HMBC spectrum for compound **176**.

N,N'-Cyclic compound **177** was isolated as an intense dark blue amorphous solid following flash chromatography. Analysis of the HRESI mass spectrum revealed a peak at *m/z* 703.1661, assigned to the molecular ion $[C_{36}H_{32}N_4O_6S_2Na]^+$, revealing the addition of two aziridinyl subunits. Analysis of the ^1H and ^{13}C spectra revealed extensive peak-doubling, suggesting the presence of a 1:1 mixture of diastereomers. This is due to the proposed structure containing a pair of stereogenic atoms, and resulting from a statistical mixture of two units of the racemic starting aziridine, thus producing a 1:1 mixture of both enantiomers of the two possible diastereomers. Where both incoming aziridine molecules have the same stereochemistry, this would lead to the (*6R,2'S*)(*6S,2'R*) pair, or where both aziridines have opposite stereochemistry, this would lead to the (*6R,2'R*)(*6S,2'S*) pair, for a total of four individual stereoisomers. These isomers proved irresolute by fractional crystallisation, flash chromatography and by reverse-phase HPLC separation, hence the reported 35% yield refers to the crude yield of the mixture of diastereomers. Compound **177** was isolated in enantiopure form as the (*6R,2'S*) diastereomer from *(R)-N*-tosyl-2-chloromethylaziridine (**148**, *vide infra*), and comparing the overlaid ^1H NMR spectra for both this individual isomer and the mixture of isomers, it is evident that 50% of this mixture corresponds to the (*6R,2'S*)(*6S,2'R*) pair of diastereomers, hence it would follow that the remaining portion of the mixture corresponds to the (*6R,2'R*)(*6S,2'S*)-diastereomeric pair (Figure 41, Figure 42).

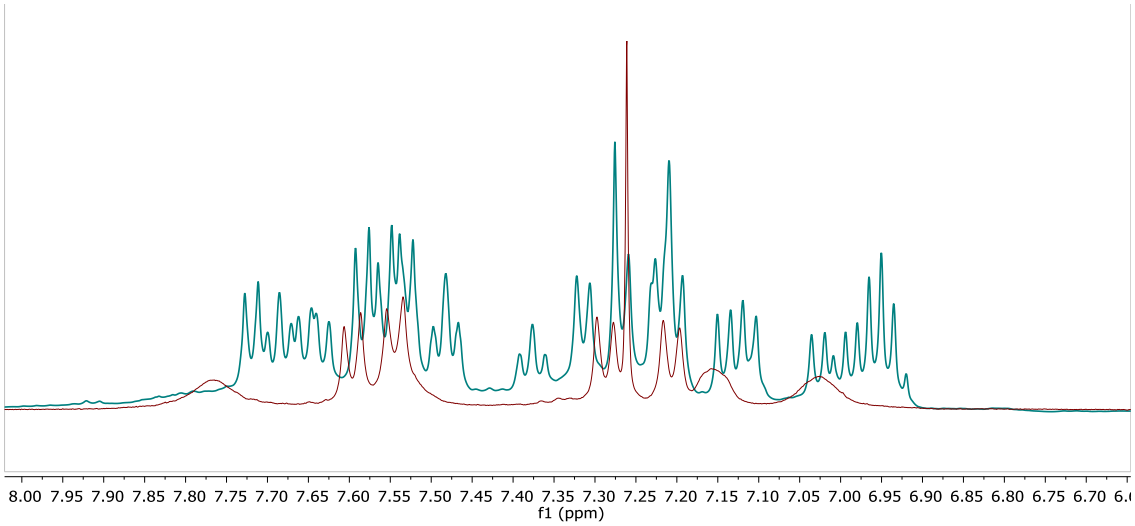

Figure 41: ^1H NMR spectral overlay from δ 8.00-6.60 for the mixture of diastereomers of **177** (teal) and the *6R,2'S* isomer of **177** (maroon),

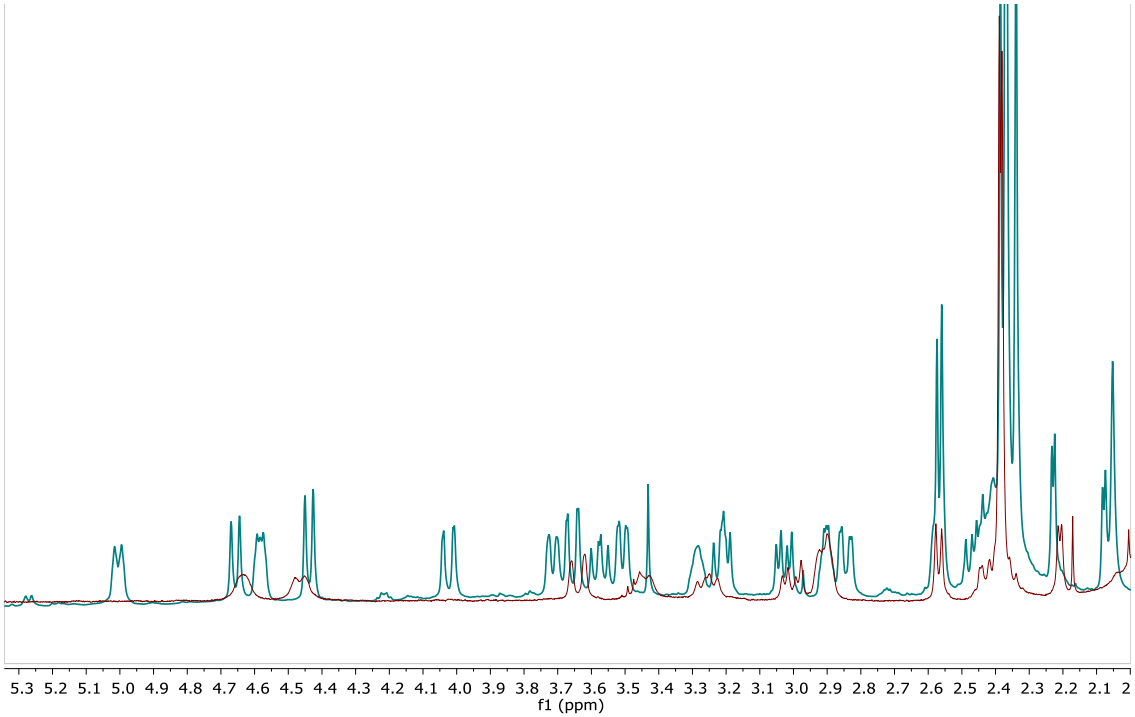

Figure 42: ^{1}H NMR spectral overlay from δ 5.30-2.00 for the mixture of diastereomers of **177** (teal) and the *6R,2'S* isomer of **177** (maroon),

3.4.3 Reaction optimisation

The isolation of a 35% yield of di-alkylated product **177** within a 5 second reaction time is testament to the high reactivity of the bromomethylaziridine **147**. This however meant that over extended reaction times, greater proportions of polymeric materials were isolated. In a repeated run, using a 30 minute reaction time, a similar diastereomeric mixture of **177** was isolated in 43% yield, with the remainder of the mixture being uncharacterisable polymer. Repeating the reaction with a 5 minute reaction time and with a reduced quantity of aziridine (3.5 eq.) afforded a 52% yield of **176**, in addition to a 38% yield of **177**. In an effort to reduce the reactivity of the aziridine, the tosyl activator was replaced with the *N*-mesyl activator, however upon treatment with indigo, this led to rapid decomposition, and the exclusive isolation of baseline materials, presumably due to the high acidity of the methyl group of the methanesulfonamide substituent, thus generating additional reactive nucleophilic sites for polymerisation.

Replacing the electrophile with *(R)-N*-tosyl-2-(chloromethyl)aziridine (**148**) and allowing the mixture to react for 30 minutes similarly afforded **176** (46%), in addition to an inseparable mixture of three additional components. The mixture was subjected to preparative RP-HPLC over 5×2.0 mL injections, and afforded three major fractions at t_R = 35 min (**177**, 8%), 37 min (**178**, 9%), and 47.7 min (polymer) (Scheme 66).

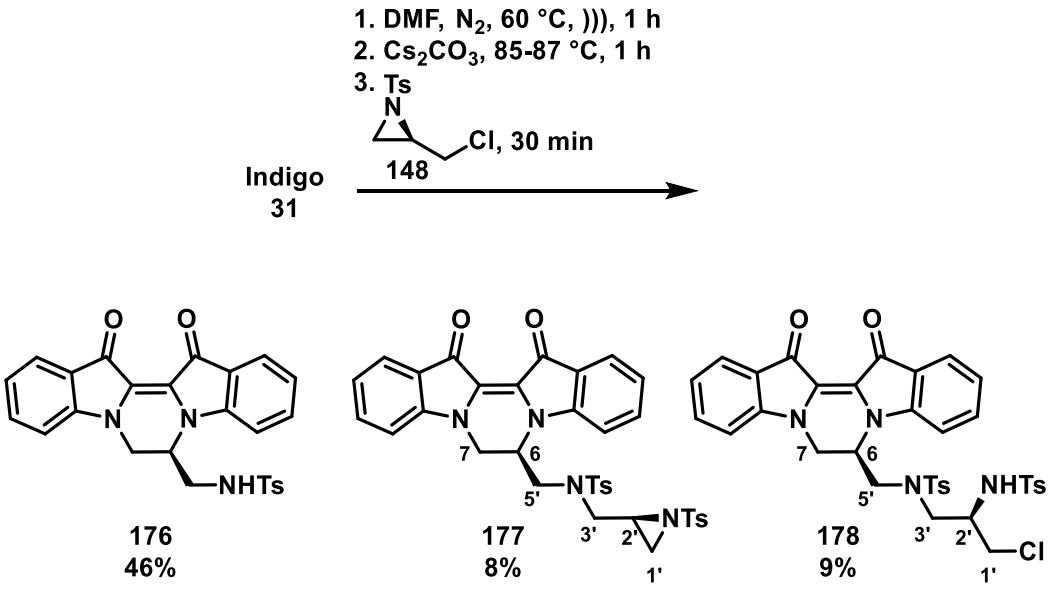

Scheme 66: Synthesis of chiral pyrazinodiindoles **176**, **177**, and **178** from the cascade reaction of indigo with (chloromethyl)aziridine **148**.

The *N*-aziridinylpyrazinodiindole **177** was isolated in 8% yield from indigo following preparative HPLC separation. Analysis of the ^{1}H NMR spectrum revealed sixteen aromatic-range protons, assigned to the two tosyl groups, and the eight indigo aryl protons. In the alkyl region, a pair of overlapping 3H singlets at δ 2.39/2.38 were assigned to the two tosyl methyl groups. Key to the structural assignment of **177** was analysis of the TOCSY spectrum, allowing for disentanglement of the ten individual proton resonances in the aliphatic range, and revealing the two individual alkyl chains (Figure 43). By cross-referencing the TOCSY, COSY and HSQC spectra, each proton and carbon resonance could be individually assigned in these two subunits.

In chain A, the multiplet ranging from δ 4.69-4.58 was assigned to H6, and showed COSY correlations to resonances at δ 3.25 and δ 2.93, assigned as the sulfonamide-adjacent methylene protons H5'a/H5'b, and δ 4.47 and δ 3.46, assigned to the indole-adjacent methylene protons H7a/H7b (Figure 45). HSQC analysis allowed for assignment of the resonances at δ 49.4, δ 49.7, and δ 40.6 to C5', C6, and C7, respectively (Figure 45). In chain B, the shielded methylene proton resonances at δ 2.21 and δ 2.57 were assigned to the terminal aziridine protons H1'a/H1'b, which showed COSY correlations to a resonance at δ 2.93, assigned to H2'. The remaining methylene protons at δ 3.64 and δ 3.00 were assigned to the amide-adjacent H3'a/H3'b couple. HSQC analysis allowed the remaining ^{13}C resonances at δ 30.9, δ 37.4, and δ 51.6 to be assigned to C1', C2', and C3', respectively.

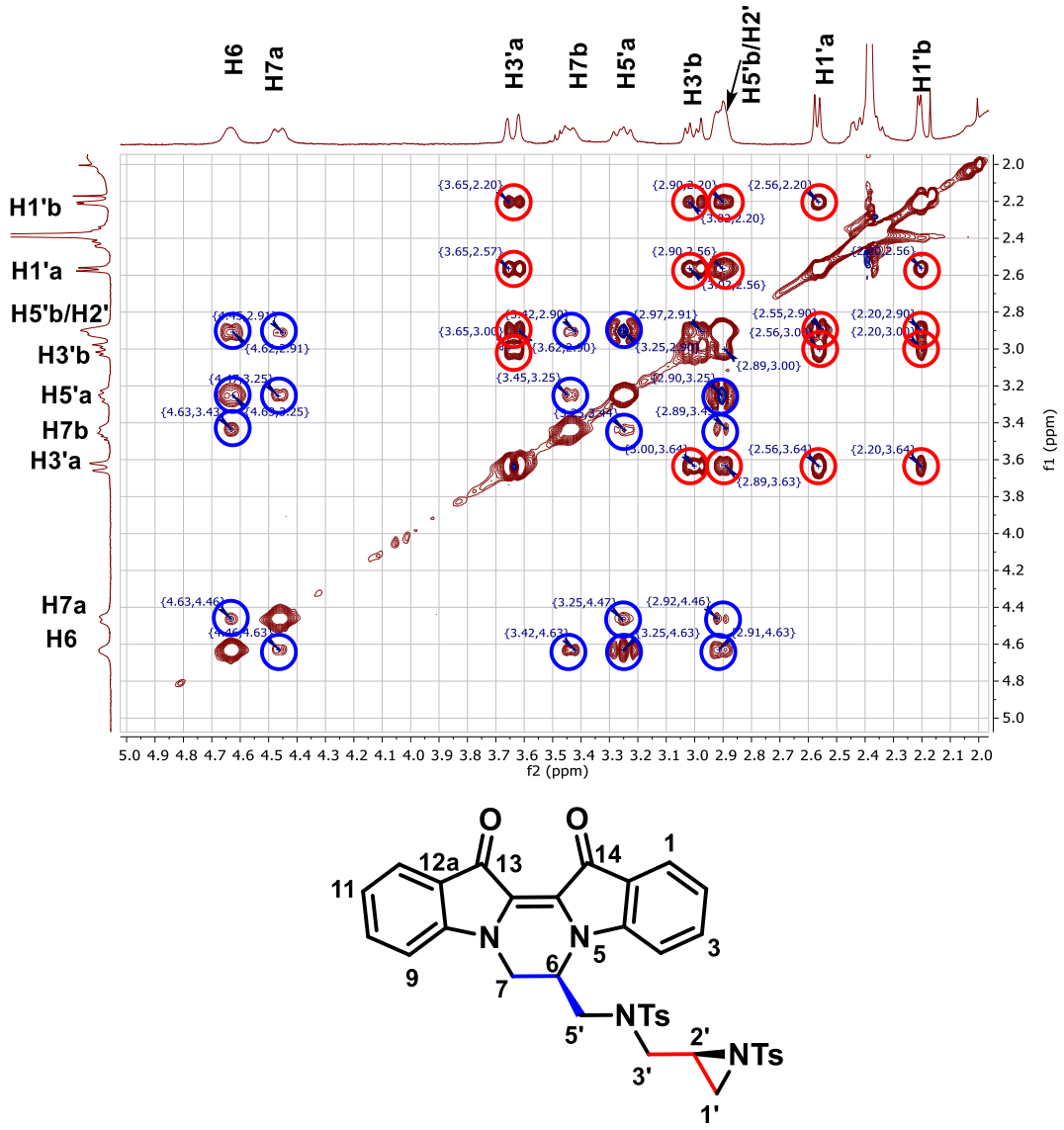

Figure 43: TOCSY spectrum for compound **177** with correlations highlighted for both chains.

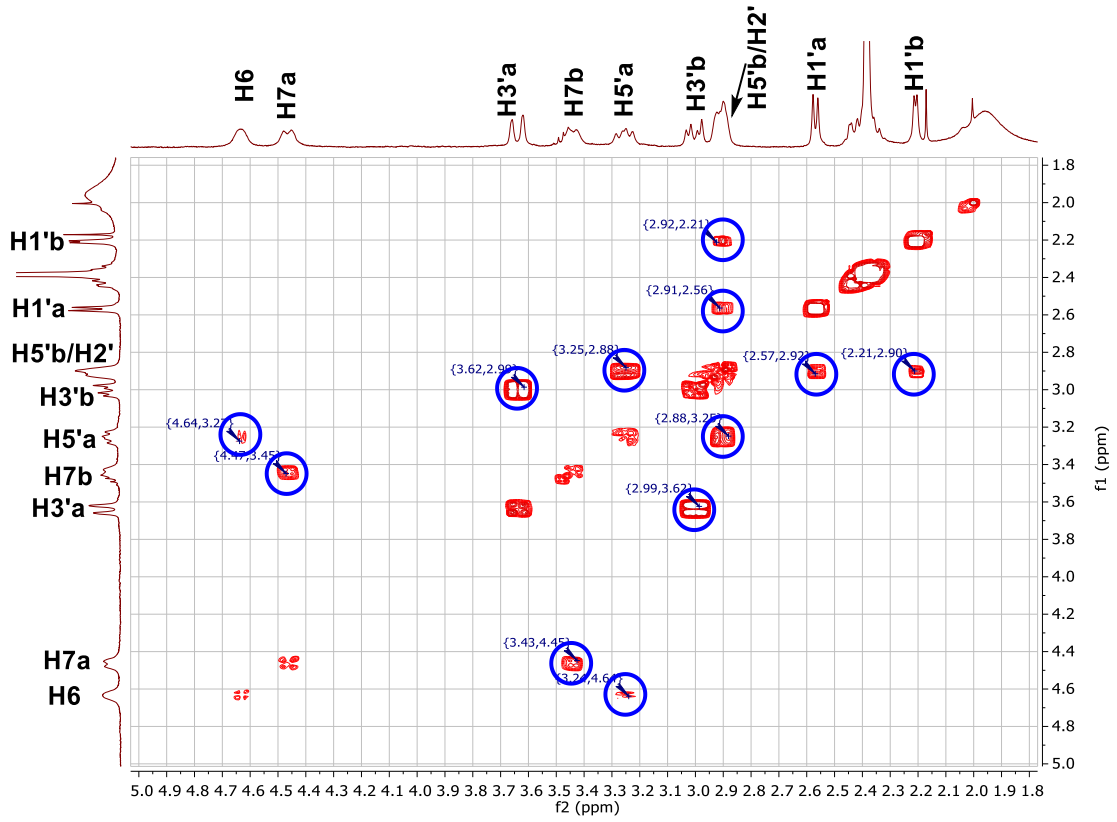

Figure 44: COSY spectrum for compound **177** with key correlations highlighted.

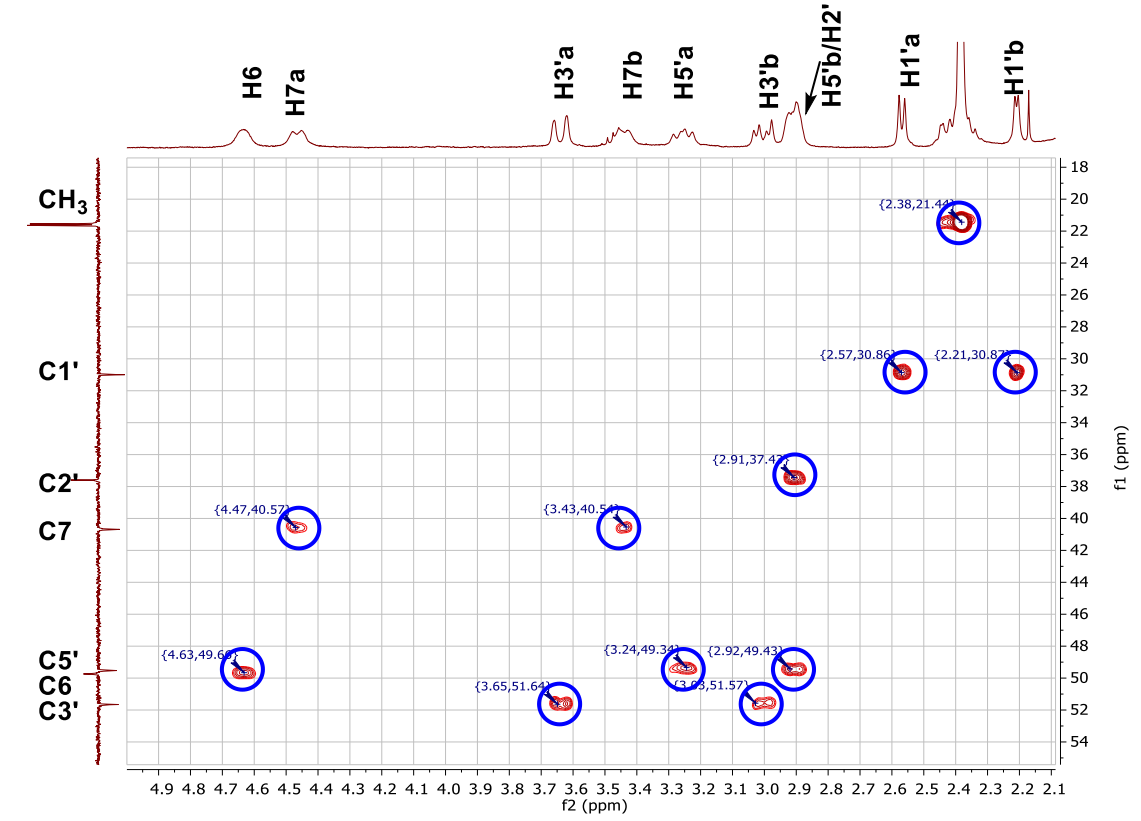

Figure 45: HSQC spectrum for compound **177**.

The *N*-chloroalkylpyrazinodiindole **178** was isolated as an intense dark-blue amorphous solid in 9% yield from indigo following RP-HPLC separation. Analysis of the HRESI mass spectrum revealed a peak at *m/z* 739.1448, assigned to the molecular ion $[C_{36}H_{33}N_4O_6S_2{}^{35}ClNa]^+$, revealing the incorporation of two aziridinyl subunits and one chlorine atom. Analysis of the ^{1}H NMR spectrum revealed a broad multiplet ranging from δ 5.71-5.60 which did not show correlation to a carbon resonance in the HSQC spectrum, and was assigned to the free N2' sulfonamide proton on the B chain. This proton showed correlations in the TOCSY spectrum to resonances at δ 3.99, δ 3.85, δ 3.42, δ 3.41 and δ 3.19, which were assigned by COSY and HSQC analysis as H2', H1'a, H1'b, H3'b and H3'a, respectively, and the ^{13}C resonances at δ 45.3, δ 53.9 and δ 53.0 assigned to C1', C2' and C3', respectively (Figure 46, Figure 47, Figure 48). The doublet at δ 4.40 showed through-space correlations to H10 in the ROESY spectrum, and was assigned as H7b of the pyrazinodiindole core (Figure 49). TOCSY analysis revealed long-range coupling to ^{1}H resonances at δ 4.61, δ 3.52, δ 3.47, and δ 2.66, which were assigned as H6, H7a, H5'a and H5'b, respectively, and the ^{13}C resonances at δ 50.9, δ 49.4, and δ 40.2 were assigned to C5', C6 and C7, respectively. The direct linkage of the two chains through N4' was supported by through-space correlation of H5'a and H3'a in the ROESY spectrum, suggesting the pair to be in close proximity.

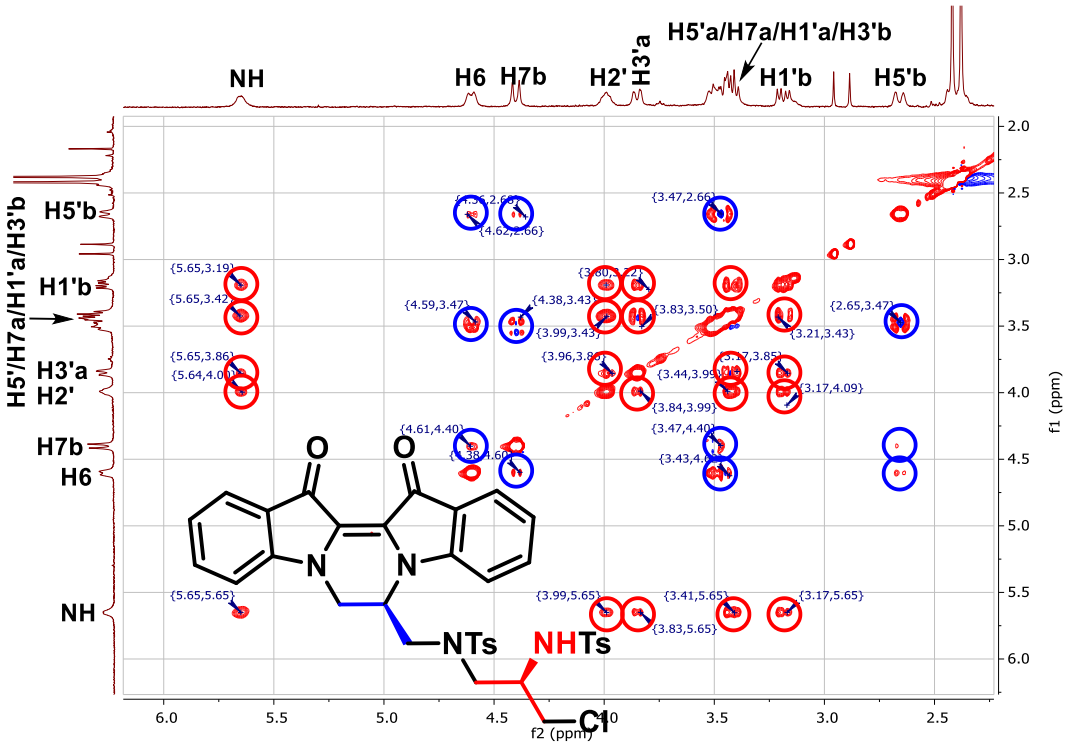

Figure 46: TOCSY spectrum of compound **178** with correlations highlighted for both chains.

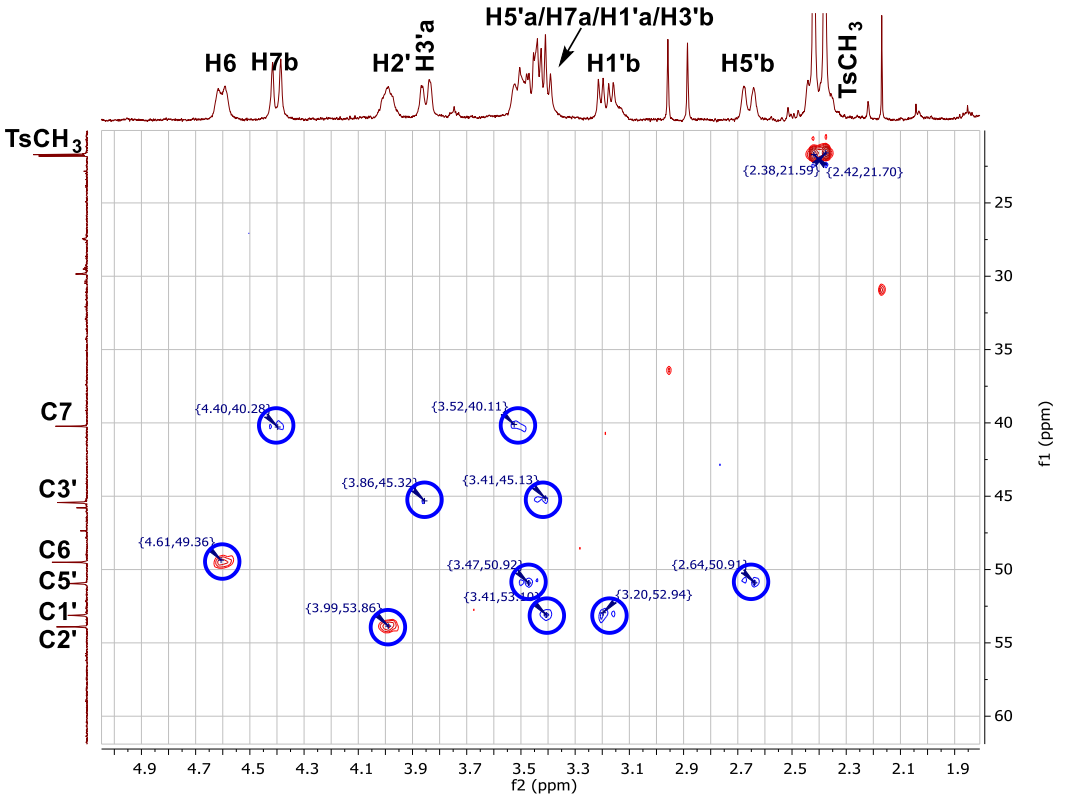

Figure 47: HSQC spectrum for compound **178**.

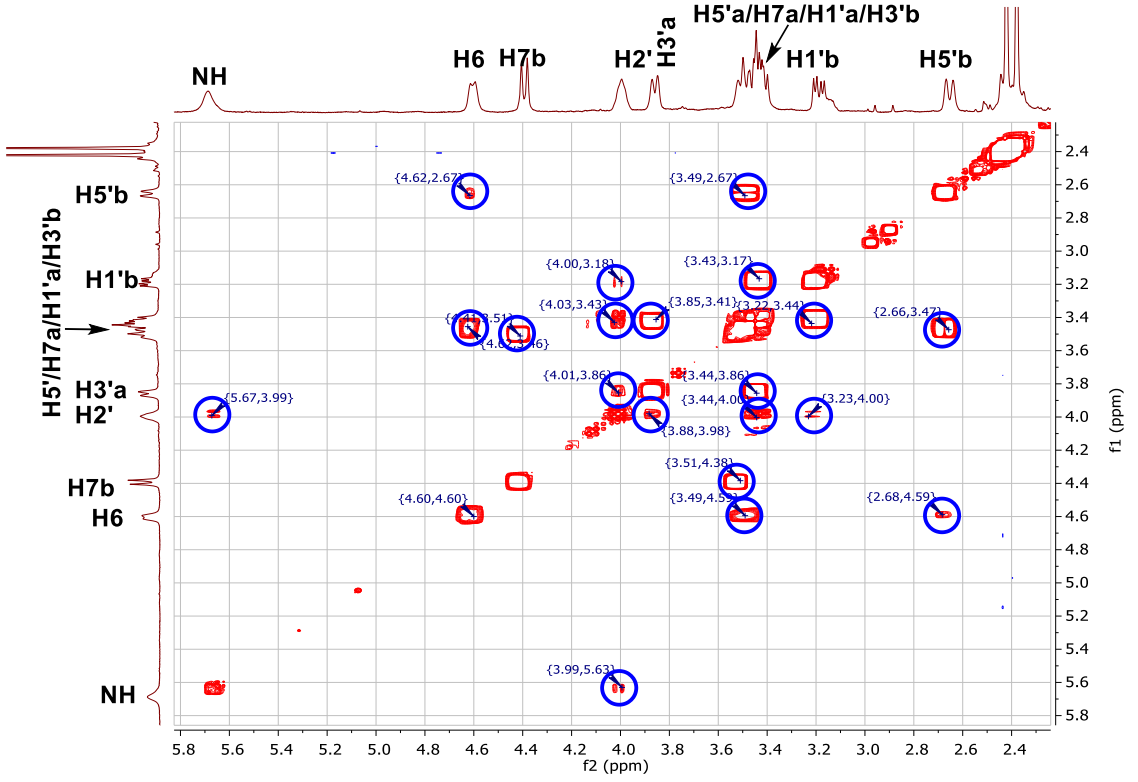

Figure 48: COSY spectrum for compound **178**.

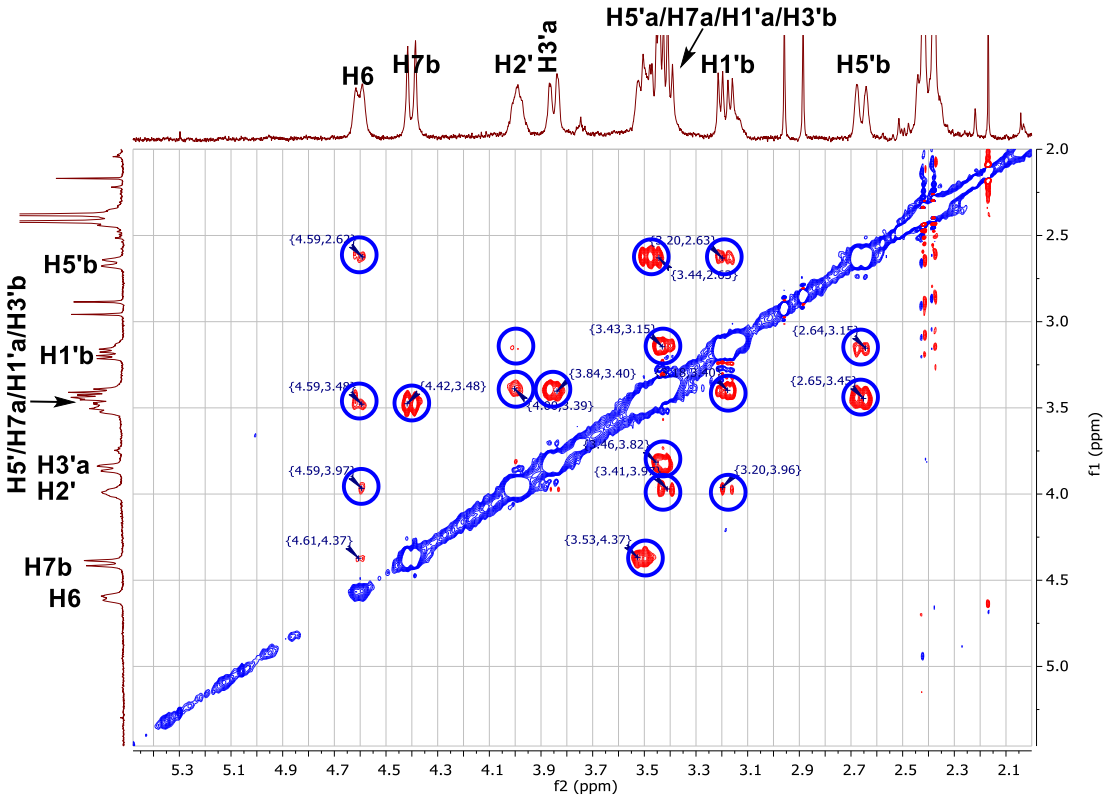

Figure 49: ROESY spectrum for compound **178**.

To examine whether indigo could undergo cascade reactions in the absence of a halomethyl substituent, it was reacted with *N*-tosyl-2-phenylaziridine (**174**) under the optimised conditions. In a single run, indigo was treated with **174** (5.0 eq.) for 10 minutes, after which TLC analysis showed complete indigo consumption. The reaction was quenched over crushed ice and subjected to aqueous workup, and subsequent flash chromatography of the deep blue-green residue afforded the acyclic, *mono*-addition products **179** and **180** in a combined 98% yield (Scheme 67).

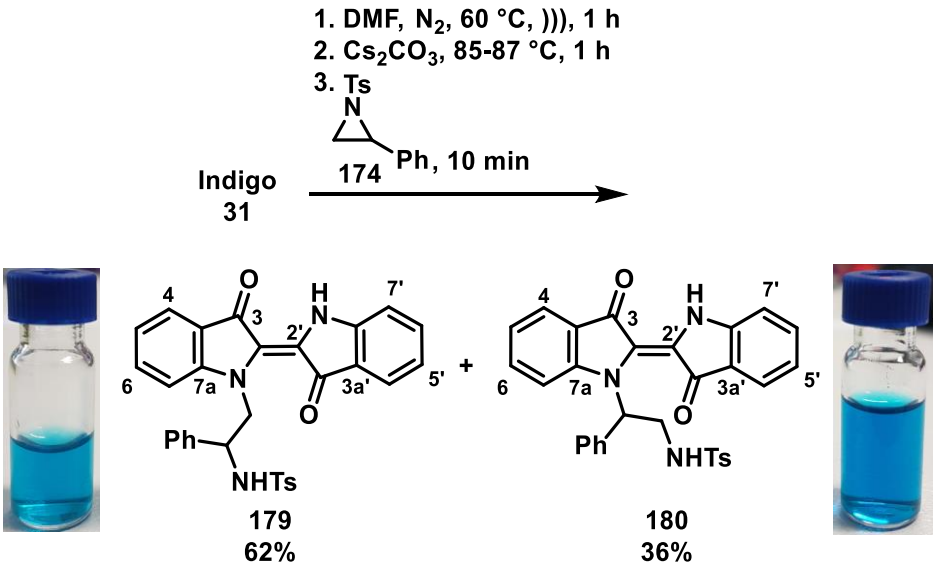

Scheme 67: Synthesis of acylic aziridine adducts **179** and **180** from phenylaziridine **174**.

The terminally ring-opened aziridine adduct **179** was isolated as a deep blue-green powder in 62% yield from indigo following flash chromatography and recrystallisation from 9:1 pet spirit/$CHCl_3$. Analysis of the HRESI mass spectrum revealed a peak at *m/z* 536.1664, assigned to the molecular ion $[C_{31}H_{26}N_3O_4S]^+$, demonstrating the addition of a single unit of the phenylaziridine. Analysis of the ^{13}C NMR spectrum revealed a pair of downfield quaternary resonances at δ 188.9 and δ 188.7, assigned as C3 and C3' respectively, showing the retention of both carbonyls. Analysis of the ^{1}H NMR spectrum revealed a deshielded sharp singlet resonance at δ 10.65, assigned to the hydrogen-bound indigo NH, which correlated with C3' by HMBC experiments, in addition to quaternary resonances at δ 151.6 and δ 119.8, assigned as C7a' and C2', respectively (Figure 51). Analysis of the HSQC spectrum showed correlations between the ^{1}H resonances at δ 5.20 and δ 3.94 and the ^{13}C resonance at δ 51.7, and the ^{1}H resonance at δ 4.95 and the ^{13}C resonance at δ 55.4, assigned to the methylene and methine groups of the pendant α-phenylethylamine, respectively (Figure 51). Further analysis of the HMBC spectrum revealed correlations between the aziridine methine group and ^{13}C resonances at δ 139.8 and δ 126.5, assigned as two- and three-bond coupling to C1" and C2" of the phenyl substituent, and COSY experiments showed coupling with the adjacent sulfonamide NH, confirming the assigned regiochemistry of the product (Figure 52).

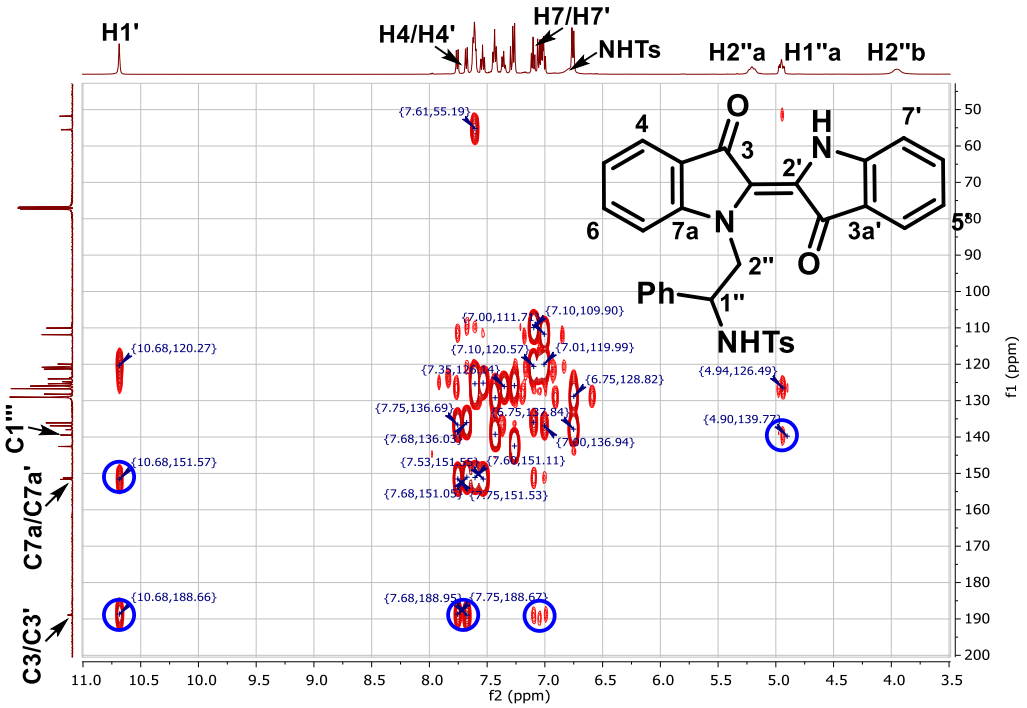

Figure 50: HMBC spectrum for compound **179** with key correlations highlighted.

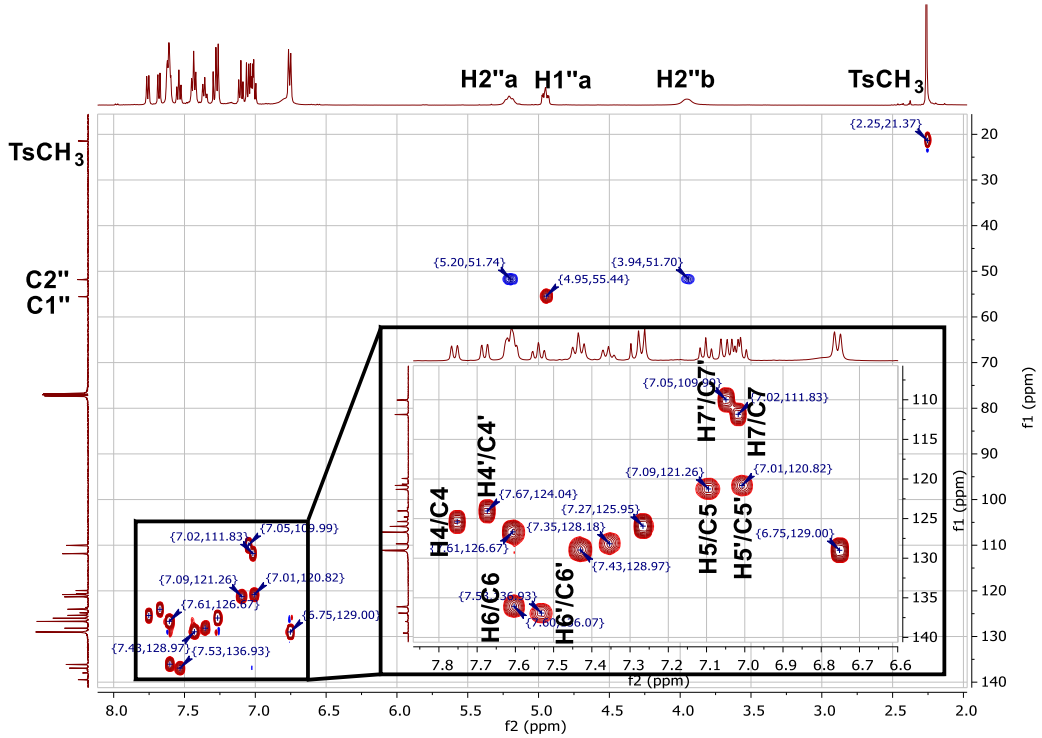

Figure 51: HSQC spectrum of compound **179** with expansion of the aromatic region (inset). Assignments for the Ph and Ts substituents are omitted for clarity.

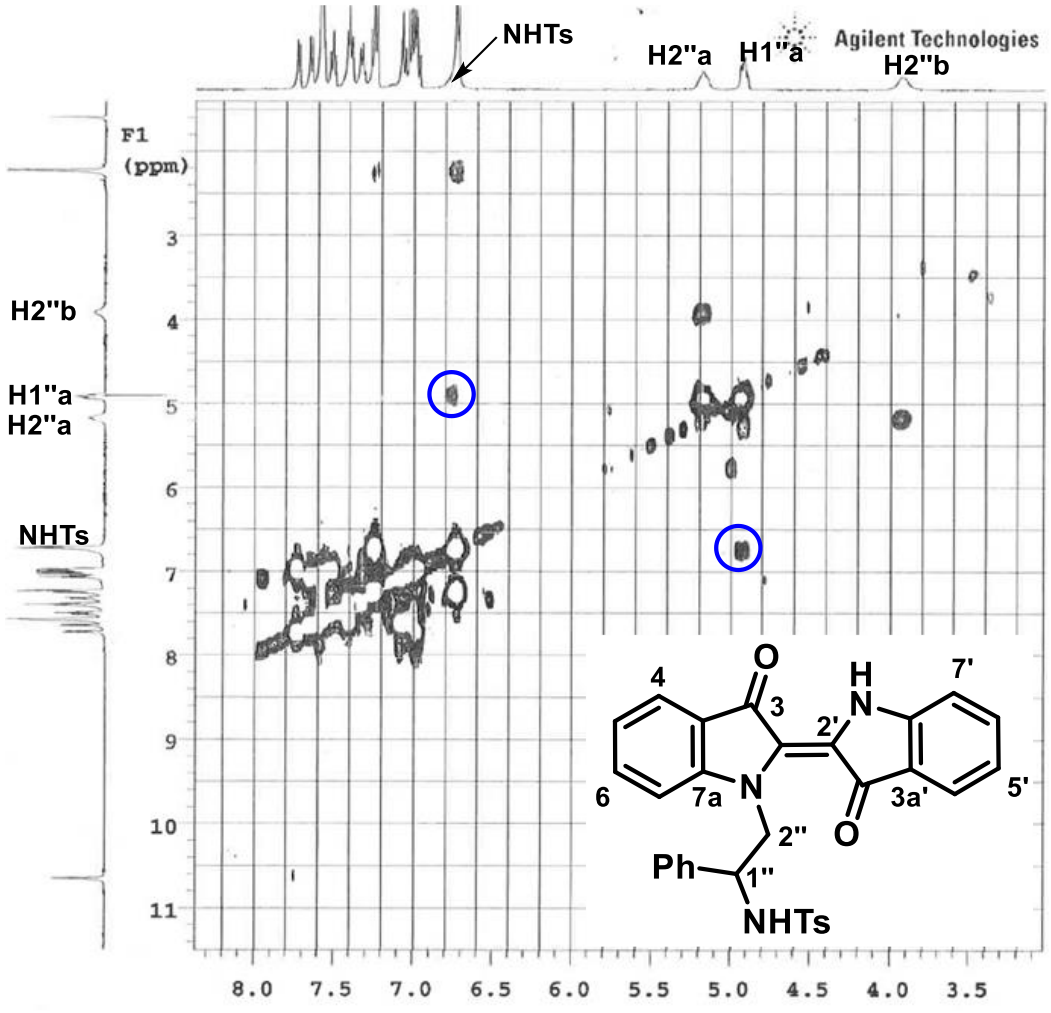

Figure 52: COSY spectrum for compound **179**, with the key correlations between H1" and the adjacent sulfonamide NH highlighted.

The benzylic aziridine adduct **180** was isolated as small, fluffy dark-blue crystals in 36% yield from indigo following flash chromatography and recrystallisation from 9:1 pet spirit/$CHCl_3$. Analysis of the HRESI mass spectrum revealed a peak at *m/z* 558.1481, assigned to the molecular ion $[C_{31}H_{25}N_3O_4SNa]^+$, revealing the addition of a single unit of the phenylaziridine. Analysis of the ^{13}C NMR spectrum revealed a pair of downfield quaternary resonances at δ 189.3 and δ 188.2, showing both indigo carbonyls to be intact, and these were assigned as C3 and C3', respectively by HMBC experiments, which showed correlations between C3' and the ^1H resonance at δ 10.74, assigned to the indolic NH proton (Figure 53). The methylene resonance at δ 4.12 was correlated to the ^{13}C resonance at δ 43.4 by HSQC experiments (Figure 54), and showed COSY correlations to both the adjacent methine proton at δ 6.56, and the sulfonamide NH proton at δ 5.89, inferring the assigned regiochemistry of the product (Figure 55).

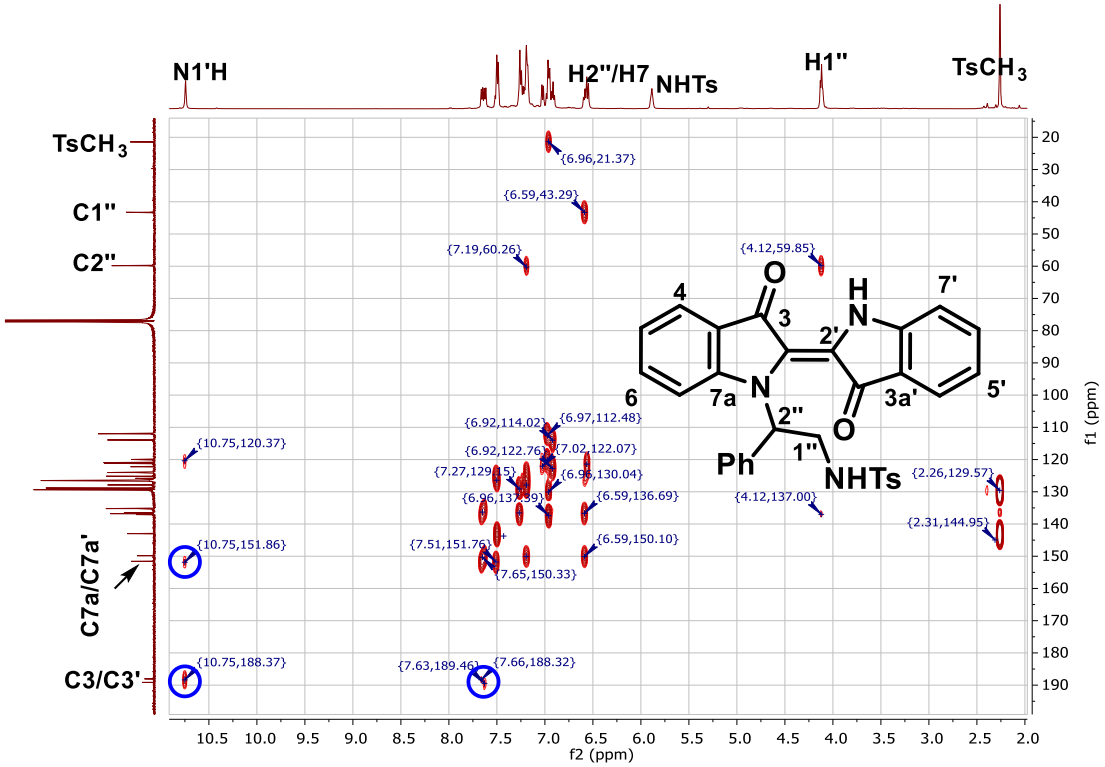

Figure 53: HMBC spectrum for compound **180** with key correlations highlighted.

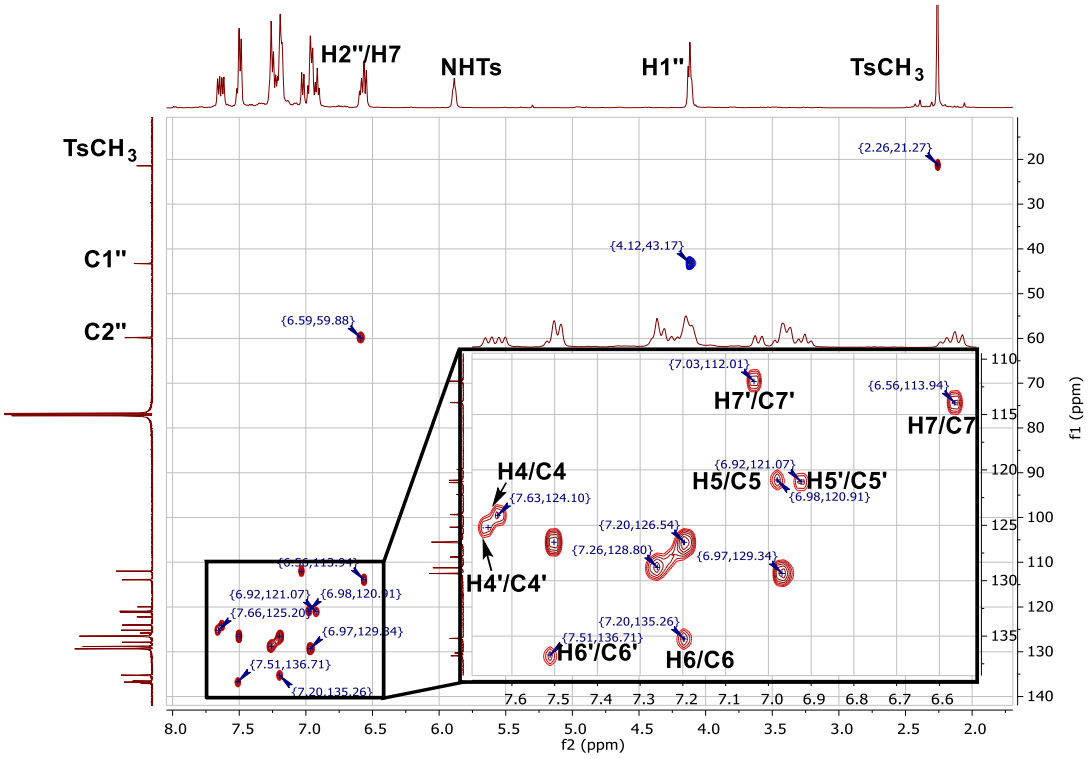

Figure 54: HSQC spectrum for compound **180** with expansion of the aromatic region (inset). Assignments for the Ph and Ts groups are omitted for clarity.

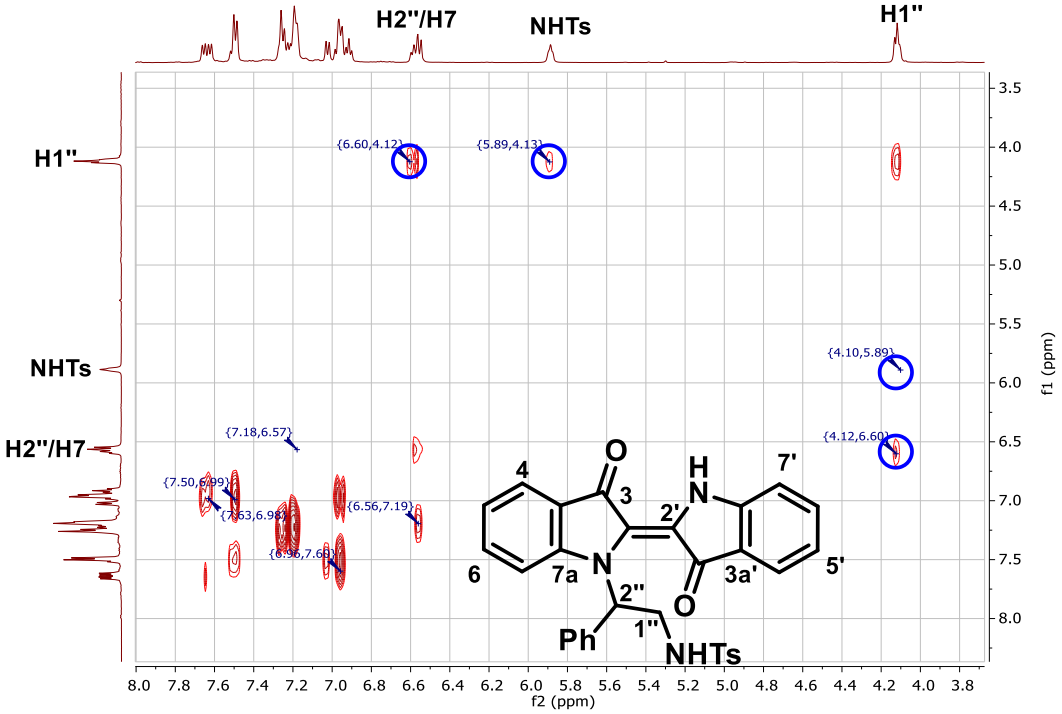

Figure 55: COSY spectrum for compound **180**, with key correlations highlighted.

X-ray quality crystals of compound **180** were grown by slow vapour-diffusion of petroleum spirit into a solution of **180** in 1:1 MeOH/$CHCl_3$ in a sealed chamber at room temperature, and its structure confirmed by x-ray crystallography (Figure 56).[†††]

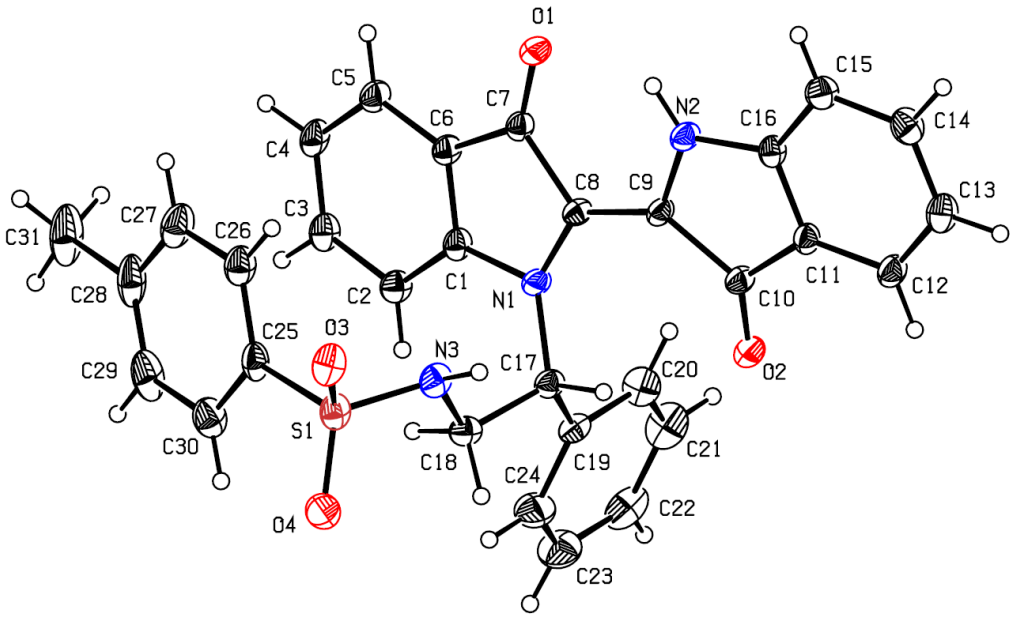

Figure 56: ORTEP depiction of compound **180**. Note that the atom numbers as denoted by x-ray crystallography do not reflect systematic numbering of atom positions.

[†††] X-ray crystallography performed by Dr. Anthony Willis (ANU).

3.4.4 Mechanistic discussion

In all reactions of indigo with (halomethyl)aziridines examined, there was no evidence of spirocyclisation having occurred, despite the high reactivity of these strained electrophiles. Presumably this is a result of the steric influence of the large tosyl activating group preventing intramolecular *N,O′*-cyclisation. This is evident for the case of the 2-phenylaziridine adducts **179** and **180**, which showed no evidence of internal cyclisation even upon prolonged heating, despite the close proximity of the nucleophilic sulfonamide and electrophilic ketone functionalities. In considering a similar divergent mechanism for the reactions of aziridines to that previously determined for reactions of oxiranes (Scheme 55, Scheme 56), it is therefore the case that contrary to oxiranes, aziridines exclusively follow Path A, where steric impedance from the *N*-tosyl group prevents halide elimination by the adjacent oxygen atom of intermediate **181**, instead leading to aziridine reformation and prototropic isomerisation to intermediate **182**. Nucleophilic inversion of the aziridine C2 leads to the final C6 stereochemistry of the pyrazinodiindole, and subsequent *N″*-alkylation of **176** leads to both *N″*-chloroalkyl **178** and *N″*-aziridinyl **177**, in addition to polymeric species from prolonged reactions.

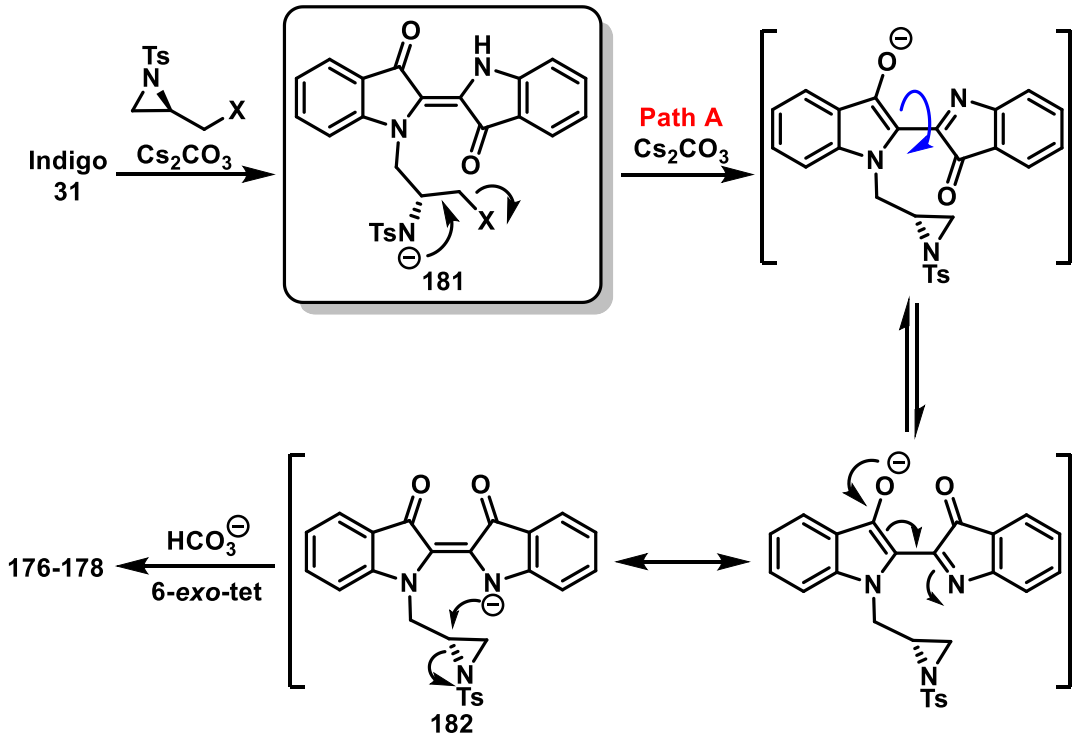

Scheme 68: Proposed mechanism for the formation of aziridine adducts **176**–**178** from Path A cyclisation of key intermediate **181** to give intermediate **182**.

Phenylaziridine adducts **179** and **180** were isolated in a 1.7:1 ratio of terminal- and benzylic ring-opened products. The preferential benzylic electrophilicity of 2-arylaziridines has been established in the presence of strong Lewis acids (e.g. $BF_3.OEt_2$ or Pd^{II}), where spontaneous ring-opening of the aziridine forms an externally-stabilised 1,3-dipole where a benzylic carbocation and a negatively-charged sulfonamide-Lewis acid complex are formed, which readily participate in [3+2]-cycloaddition, benzylic nucleophilic addition and/or dimerization reactions.[150] Under basic conditions and in the absence of transition metals, the 36% yield of compound **180** reflects the partial hindrance of C2-attack at 85 ˚C by the pendant phenyl group.

3.5 Cascade reactions of 2,2'-bioxirane and 2,2'-biaziridine with indigo

As direct, dimeric homologues of the investigated (halomethyl)-substituted aziridines and oxiranes, we sought to investigate the reactions of 2,2'-bioxirane and *N,N′*-ditosyl-2,2'-biaziridine with indigo, to determine whether these too could participate in cascade reactions, and if so, whether they follow similar trends in reactivity to their monomeric counterparts. As previously-mentioned, these are accessible on multigram-scale over several steps from D- or L-tartaric acid (see Scheme 51), and for the purposes of this investigation, both (2*S*,2'*S*)-2,2'-bioxirane (**149**) and (2*R*,2'*R*)-*N,N′*-ditosyl-2,2'-biaziridine (**150**) were synthesised in divergent fashion *via* literature methods using dimesylate **151** as the starting material, as derived from L-tartaric acid.[140c, 141]

3.5.1 Reaction discovery and structure elucidation

Indigo was reacted with 2,2'-bioxirane **149** under analogous conditions to those optimised for the reaction with *(S)*-epichlorohydrin **144**. Therefore, a suspension of indigo (1 mmol) in DMF (40 mL) was sonicated while warming to 60 ˚C for one hour, then transferred by cannula to a round-bottomed flask containing pre-dried Cs_2CO_3 (3.7 eq.) and a large magnetic stir bar, and the mixture warmed in an oil bath preheated to strictly 85-87 ˚C for one hour. The N_2 flow was cut and (2*S*,2'*S*)-2,2'-bioxirane (3.3 mmol) injected, and the bright-orange mixture stirred vigorously for 30 min. The mixture was quenched over crushed ice and separation of the crude mixture afforded spirocyclic adducts **183** and **184** in a combined 81% yield.

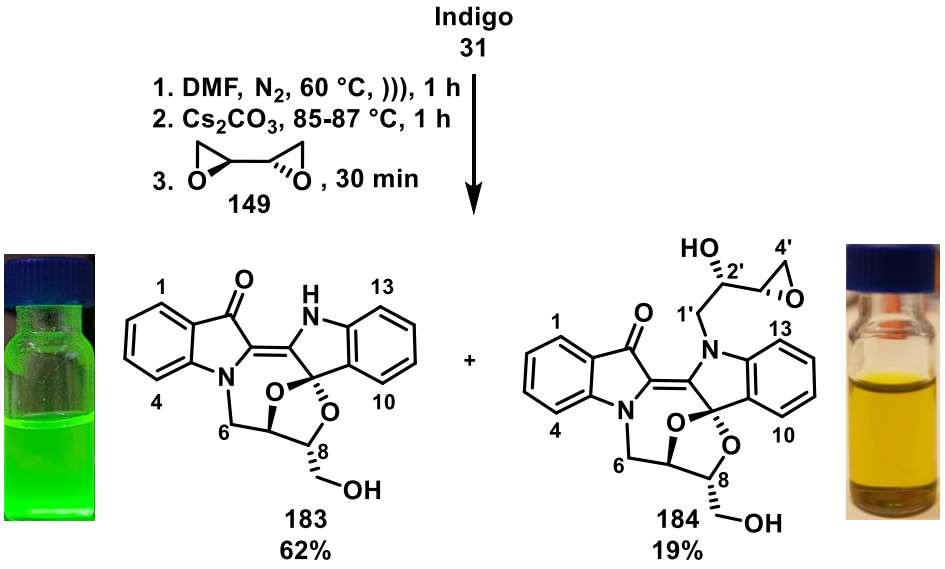

Scheme 69: Synthesis of spiroketals **183** and **184** from the reaction of indigo with 2,2'-bioxirane **149**. Adjacent to both molecules is a picture of a solution in acetone, depicting their colour. Note: The photograph of **183** shows a solution upon UV irradiation (365 nM).

The hydroxymethyl-substituted spiroketal **183** was isolated as small bright-orange crystals in 62% yield from indigo following fractionation on silica gel and subsequent flash chromatography, and exhibited a characteristic, brilliant-green fluorescence in solution under ambient conditions, or upon long-wave (λ=365 nM) UV irradiation. Analysis of the HRESI mass spectrum revealed a peak at *m/z* 349.1192, assigned to the molecular ion $[C_{20}H_{17}N_2O_4]^+$, showing the addition of a single unit of the bioxirane starting material to indigo. Analysis of the FTIR spectrum revealed a broad absorptive band centred at 3420 cm^{-1}, assigned to the hydroxyl O-H stretch of the hydroxymethyl pendant. Analysis of the ^{13}C DEPTQ spectrum revealed a single downfield resonance at δ 184.1, assigned to the C15 carbonyl, which showed correlations in the HMBC spectrum to a downfield ^1H doublet resonance at δ 7.81, assigned to H1 (Figure 57). Analysis of the COSY spectrum revealed successive correlations from H1 to a resonance at δ 7.00, which coupled to δ 7.50, which itself correlated with δ 7.10. These three resonances were assigned as H2, H3 and H4, respectively (Figure 58). Analysis of the ROESY spectrum revealed through-space coupling of H4 with a diastereotopic methylene proton at δ 4.38 assigned to H6b. Further analysis of the ROESY spectrum revealed correlations from H6b to both the doublet of doublets at δ 3.70 (assigned to H6a) and a doublet of triplets at δ 5.01, assigned to H7 (Figure 59). Methine protons H7 and H8 additionally showed strong ROESY correlations, suggesting them to be *syn* to one-another on the *cis*-dioxolane ring. The remaining diastereotopic methylene protons were assigned through HSQC analysis, which showed strong coupling between a pair of doublet-of-doublets at δ 4.17 and δ 3.96

and a ^{13}C resonance at δ 60.3, assigned as the hydroxymethyl carbon C1' (Figure 60). The spiroketal carbon was identified by analysis of the HMBC spectrum, which revealed three-bond coupling of both H10 and H7 to a weak quaternary resonance at δ 111.7, assigned to C9a.

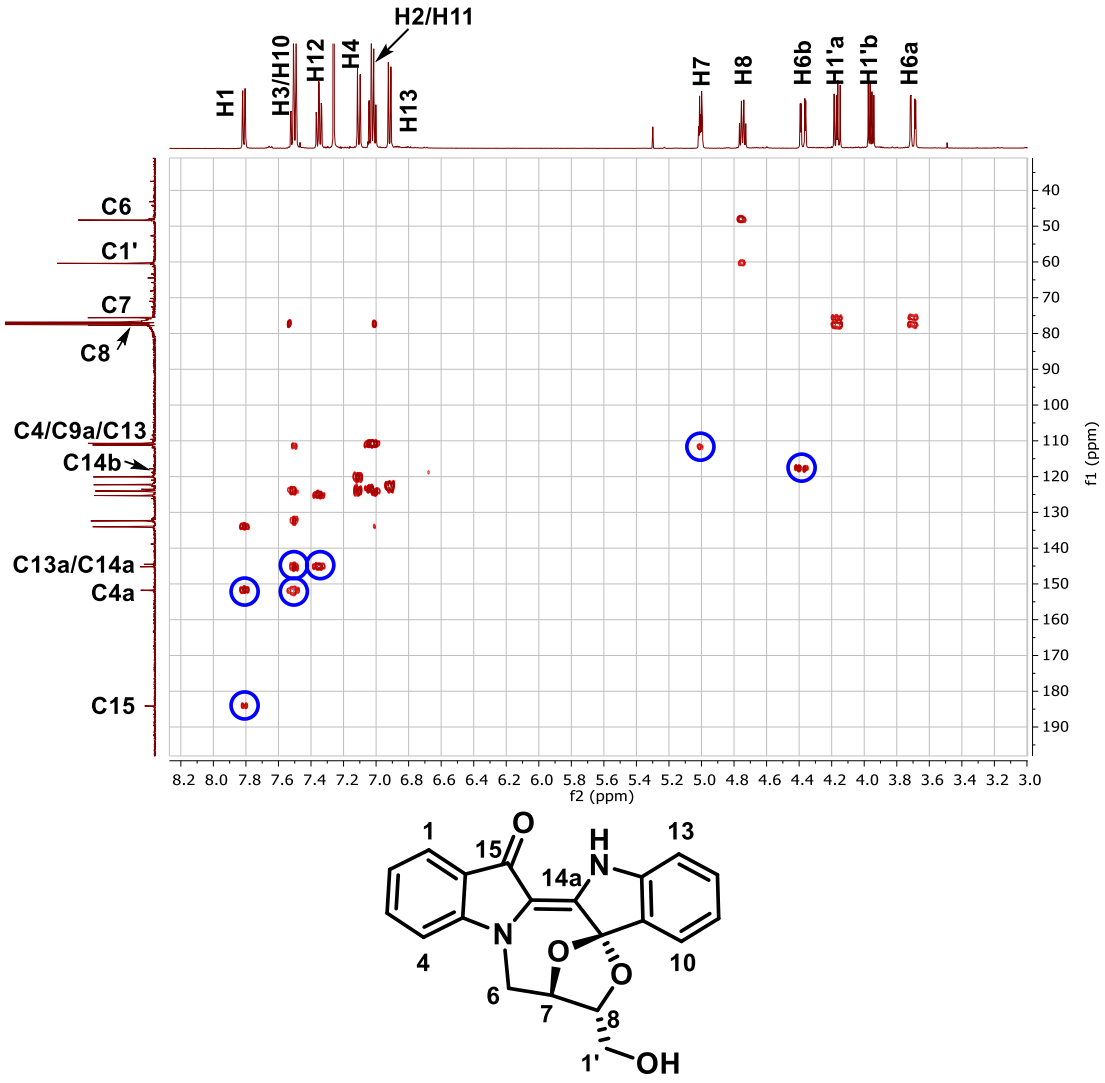

Figure 57: HMBC spectrum for compound **183** with key correlations highlighted.

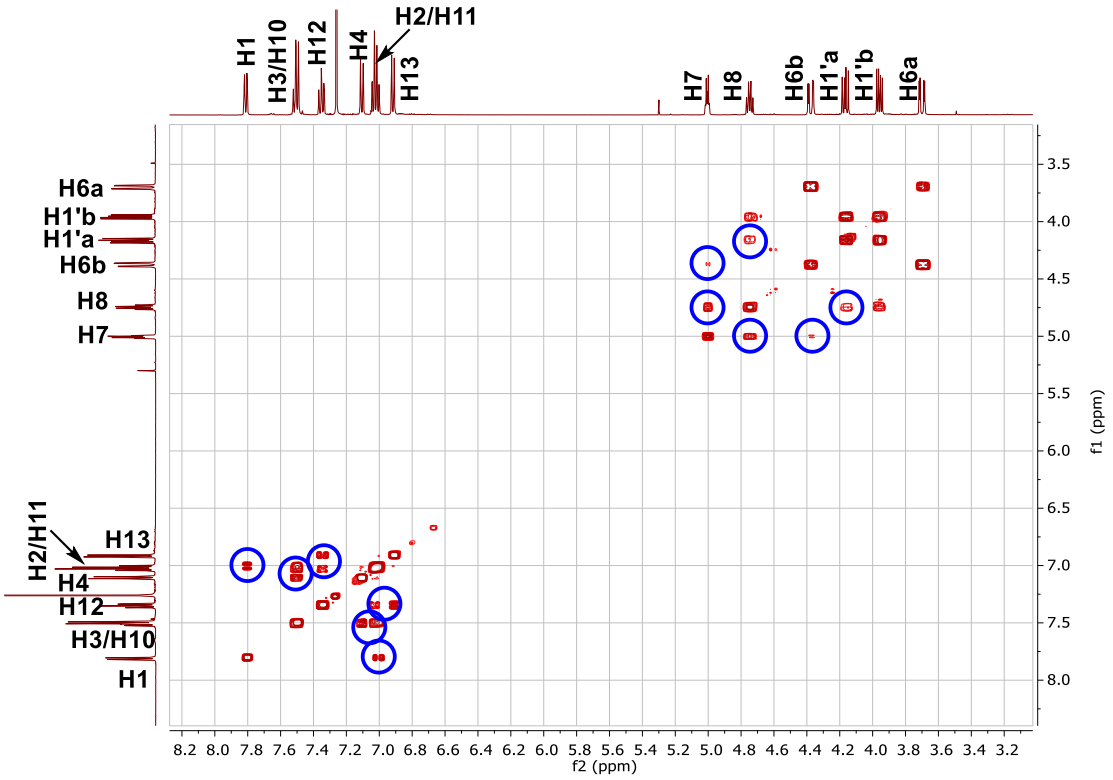

Figure 58: COSY spectrum for compound **183** with key correlations highlighted.

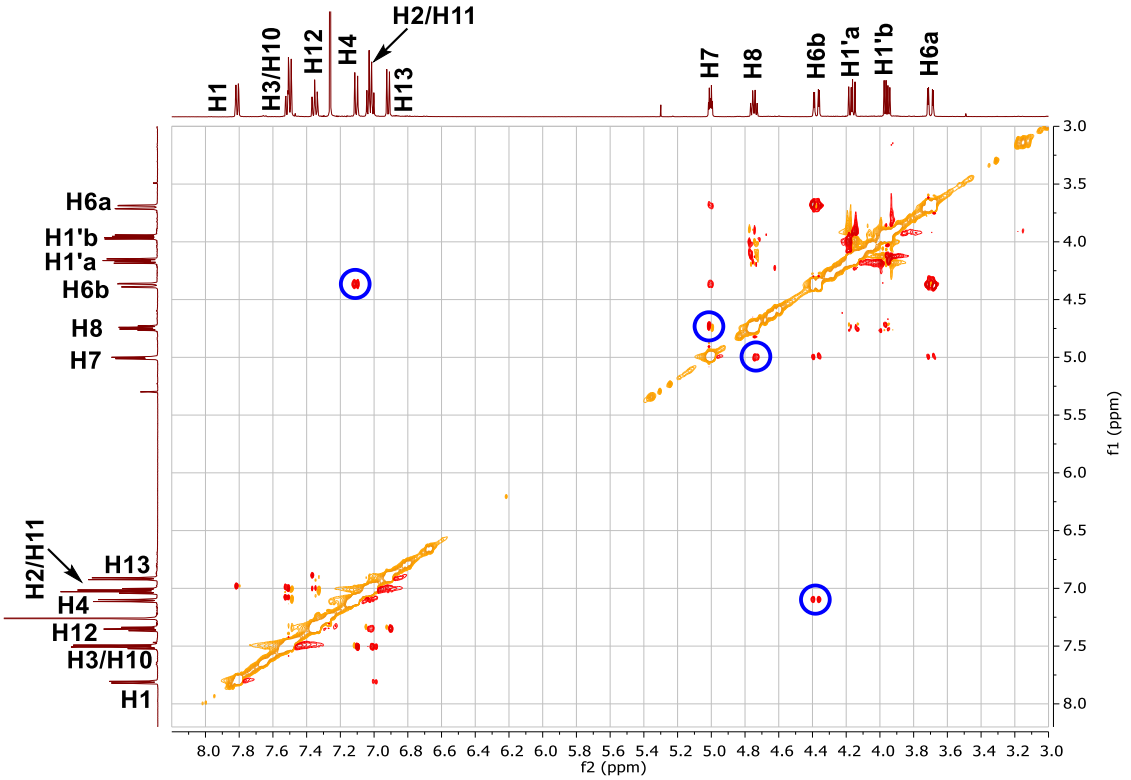

Figure 59: ROESY spectrum of compound **183** with key correlations highlighted.

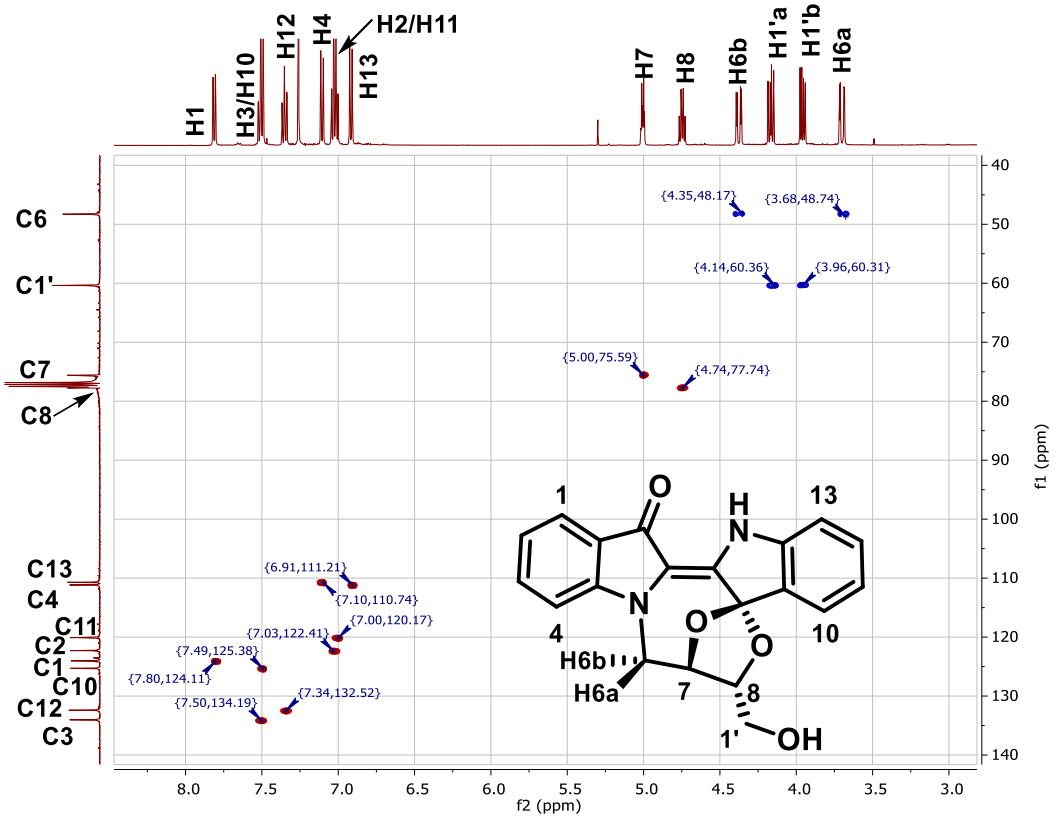

Figure 60: HSQC spectrum for compound **183** with assignments as indicated.

X-ray quality crystals of **183** were grown by slow evaporation of a saturated solution in hexane/EtOAc, and its absolute structure and stereochemistry were confirmed by X-ray crystallography (Figure 61).‡‡‡

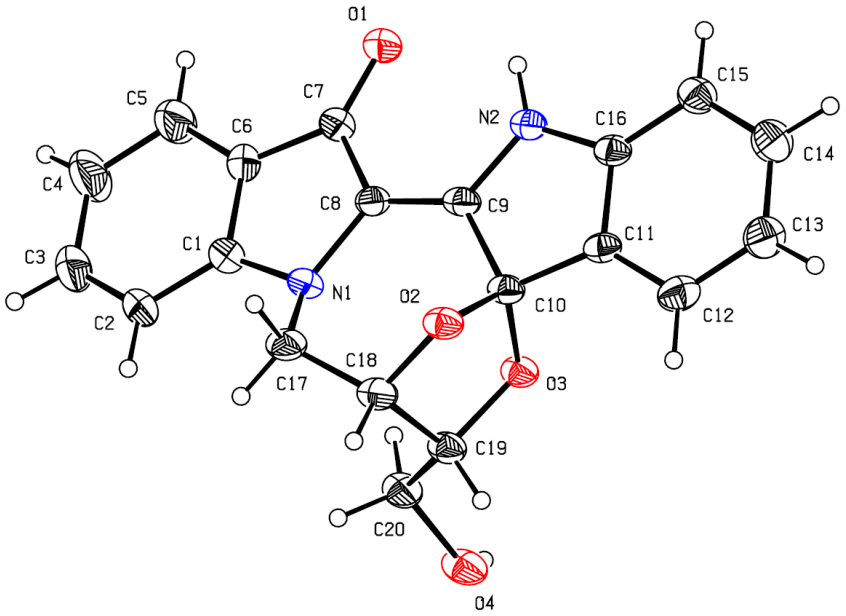

Figure 61: ORTEP depiction of compound **183**. Note that the atom numbers as denoted by x-ray crystallography do not reflect systematic numbering of atom positions.

‡‡‡ X-ray crystallography performed by Dr. Anthony Willis (ANU).

The epoxy alcohol-substituted spirocycle **184** was isolated as a pale lime-green amorphous solid in 19% yield from indigo following fractionation on silica gel and subsequent flash chromatography. Analysis of the HRESI mass spectrum revealed a peak at *m/z* 435.1556, assigned to the molecular ion $[C_{24}H_{23}N_2O_6]^+$, demonstrating the addition of two bioxirane units to the indigo core. Analysis of the ^{13}C and ^{1}H NMR spectra in $CDCl_3$ solution showed evidence of peak doubling, presumably due to slow rotation about the N14-C1" axis and/or rotational tumbling, which was eliminated by instead using d_6-DMSO for the acquisition of 1D and 2D NMR spectra.[151] Analysis of the ^{13}C DEPTQ spectrum revealed the presence of a deshielded quaternary resonance at δ 193.5, assigned to the C15 ketone. Integration analysis of the aliphatic region of the ^{1}H spectrum revealed fourteen protons, which HSQC analysis revealed to consist of four methylene groups, four methine groups, and two doublets at δ 5.83 and δ 5.22 which were not directly attached to a carbon, assigned to the two distinct hydroxyl groups at C1' and C2", respectively (Figure 62). Analysis of the TOCSY spectrum revealed long-range through-bond coupling of each distinct alkyl chain, and paired with COSY, HSQC, and ROESY analysis, allowed for the individual assignment of each proton and carbon environment (Figure 63). Briefly, the C2"-hydroxyl of the epoxy alcohol unit showed COSY correlations to a doublet-of-doublet-of-doublets at δ 3.24, assigned as H2", which was adjacent to the diastereotopic methylene protons at δ 3.83 and δ 3.73, assigned as H1"a and H1"b (Figure 64). H2" also showed COSY correlations to the multiplet spanning δ 2.73-2.66, assigned to H3", which also showed correlations to both the triplet at δ 2.57 and the doublet of doublets at δ 2.33, assigned as the geminal protons of the terminal oxirane unit at C4". On the hydroxymethyl spiroketal chain, the assigned *cis*-dioxolane stereochemistry was supported by analysis of the ROESY spectrum, which showed through-space correlation of the C1'-hydroxyl group to the doublet at δ 4.53, assigned to the nearby H6b (Figure 65). The overlap of the H1'a and H8 resonances led to difficulties in unambiguous identification from COSY and ROESY analysis alone, however HMBC analysis revealed correlations between the hydroxyl proton and ^{13}C resonances at δ 43.2, δ 62.8, and δ 70.7, assigned to C1', C8, and C7, respectively (Figure 66).

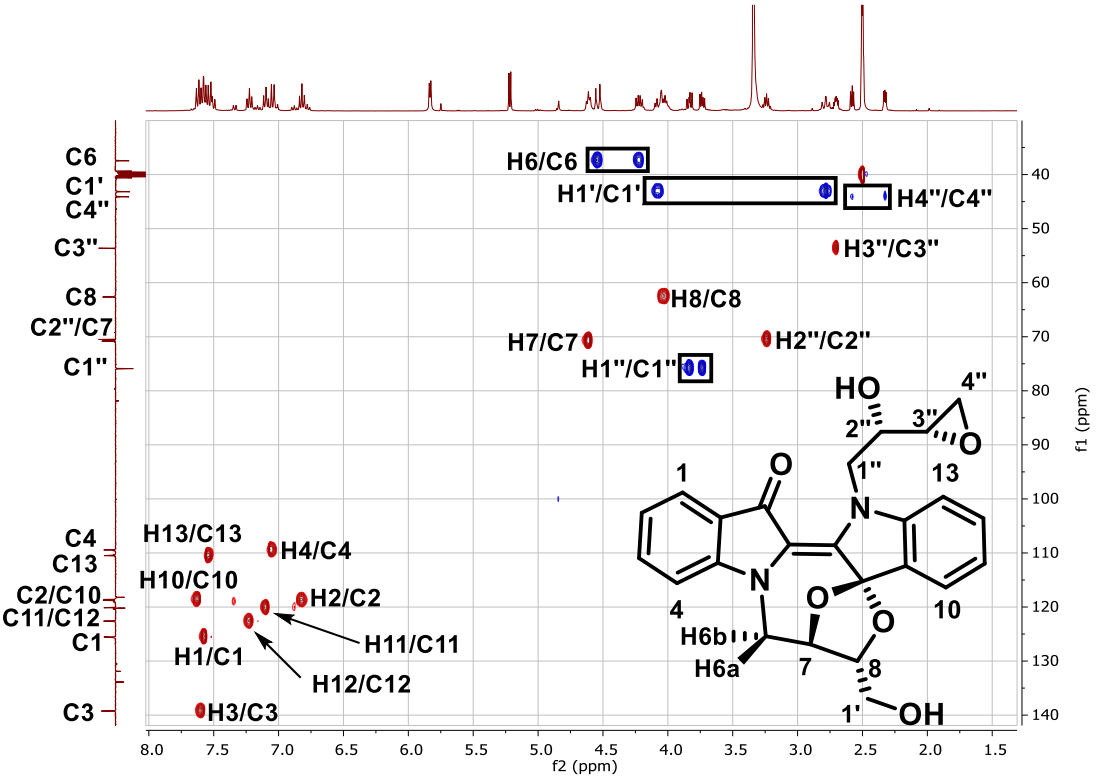

Figure 62: HSQC spectrum for compound **184**, with assignments as indicated.

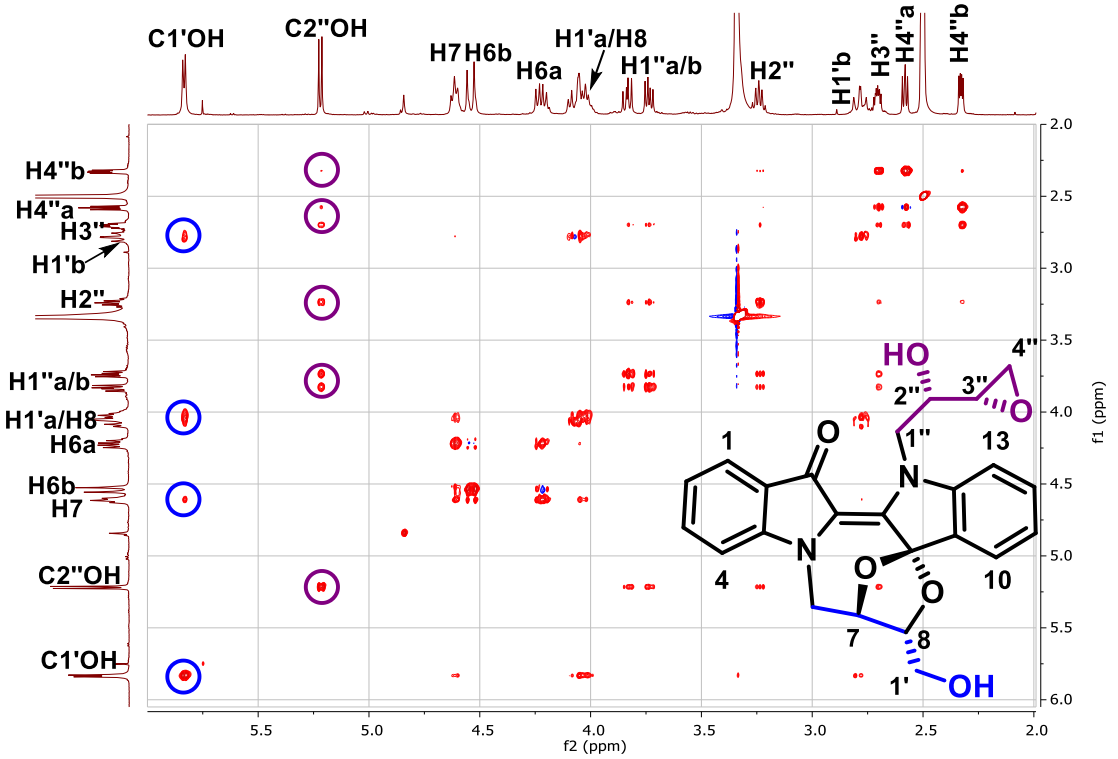

Figure 63: TOCSY spectrum for compound **184**, with key correlations of the hydroxyl protons to both chains highlighted.

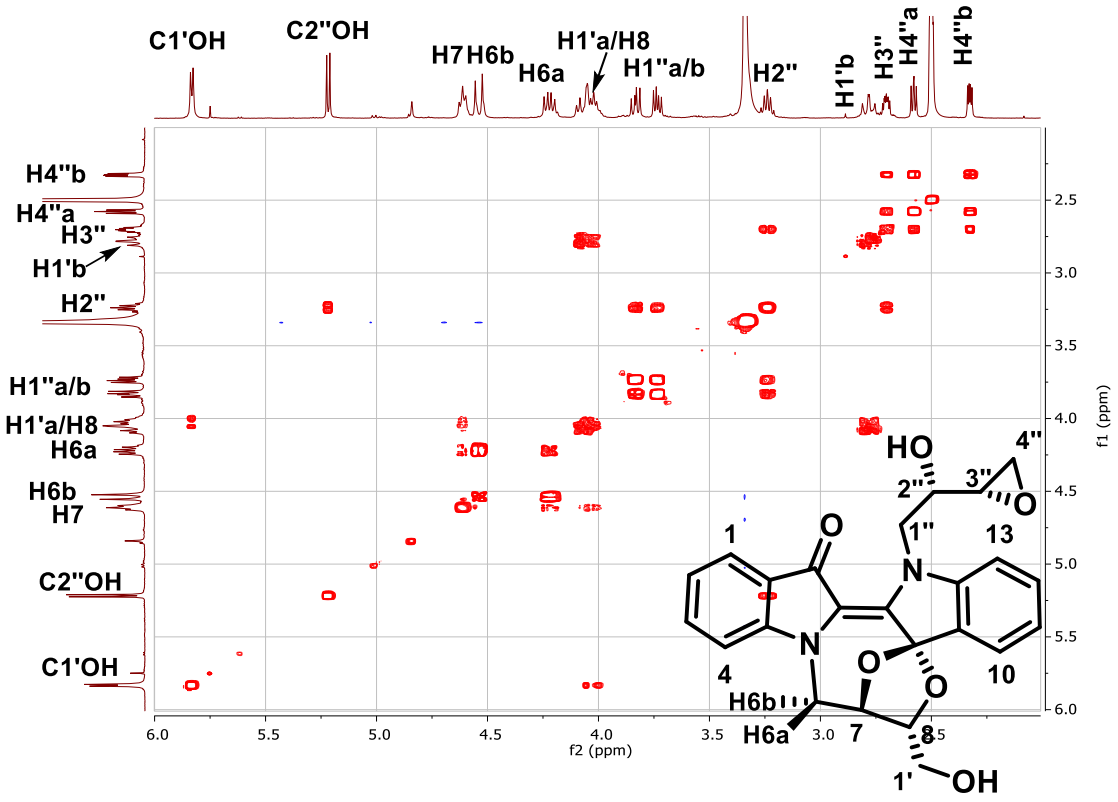

Figure 64: COSY spectrum for compound **184**.

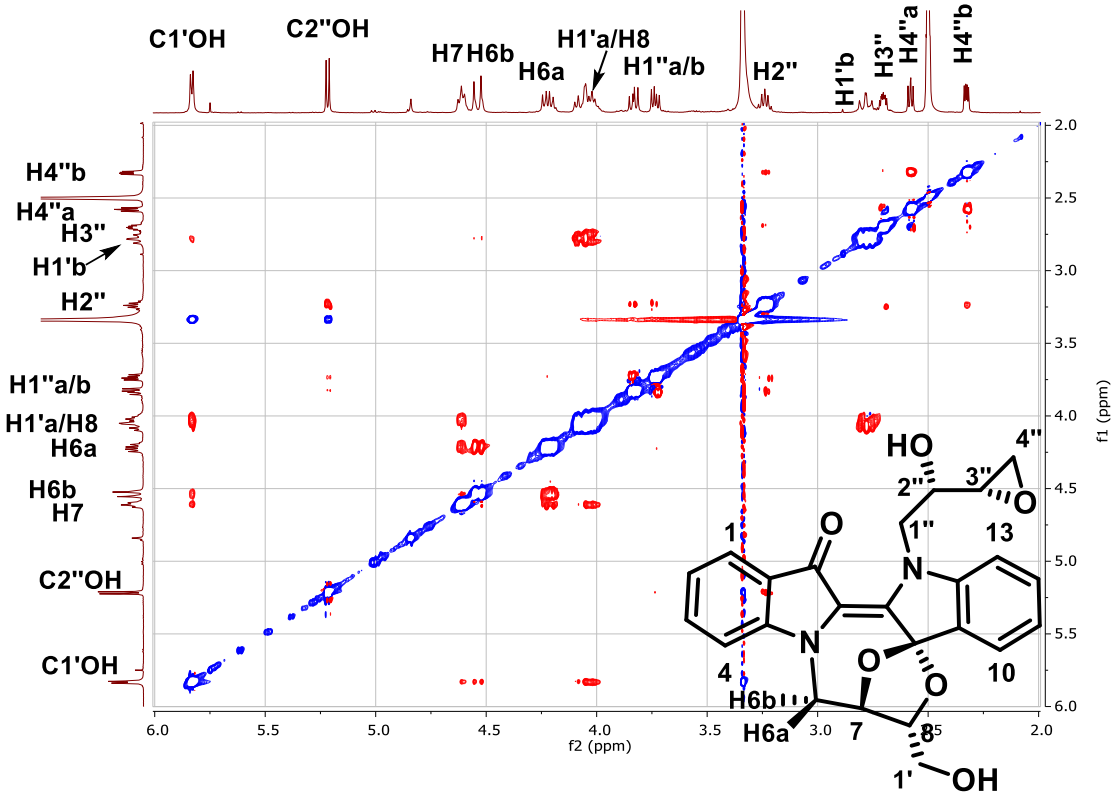

Figure 65: ROESY spectrum for compound **184**.

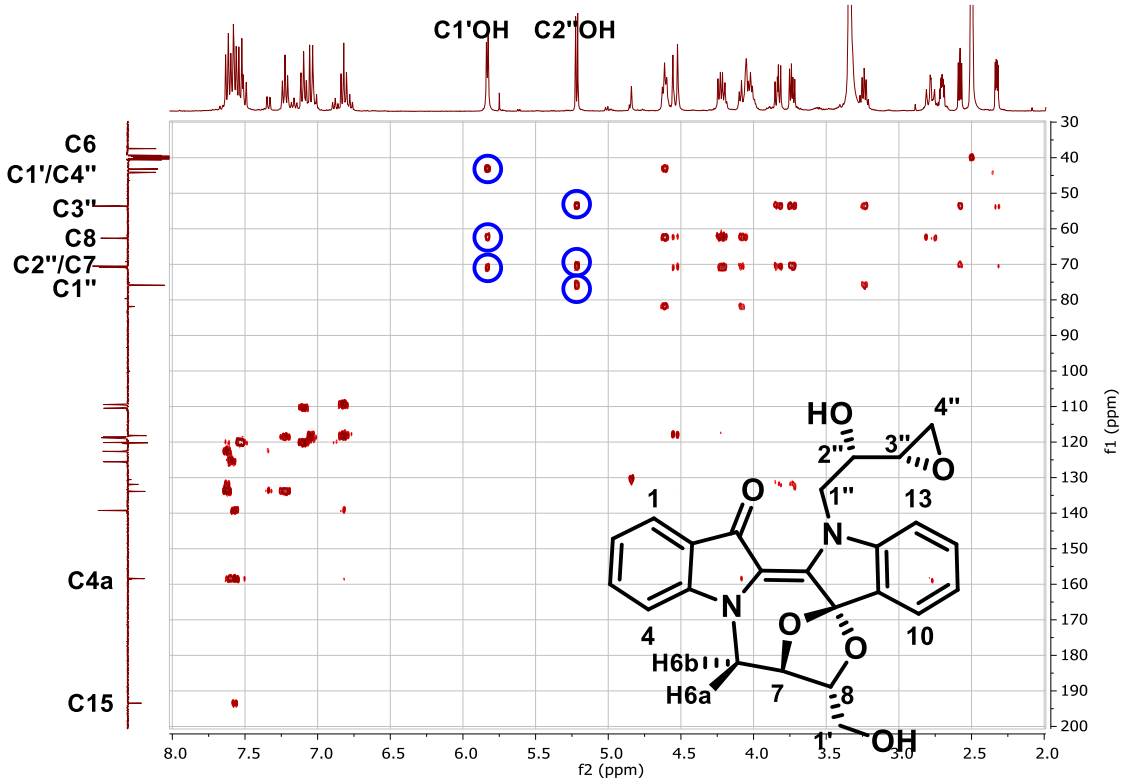

Figure 66: HMBC spectrum for compound **184** with key correlations of the two hydroxyl groups highlighted.

Given the noted tendency of the aziridines **147** and **148** to undergo Path A-type cyclisation, it was anticipated that *N,N'*-cyclic derivatives would predominate from reactions of indigo with 2,2'-biaziridine. To probe this hypothesis, indigo was reacted with (2*R*,2'*R*)-2,2'-biaziridine (**150**, 1.3 eq.) under the previously-optimised conditions for (*R*)-*N*-tosyl-2-(chloromethyl)aziridine (**148**), which afforded cleanly the diazepinodiindole **185** in excellent yield (Scheme 70).

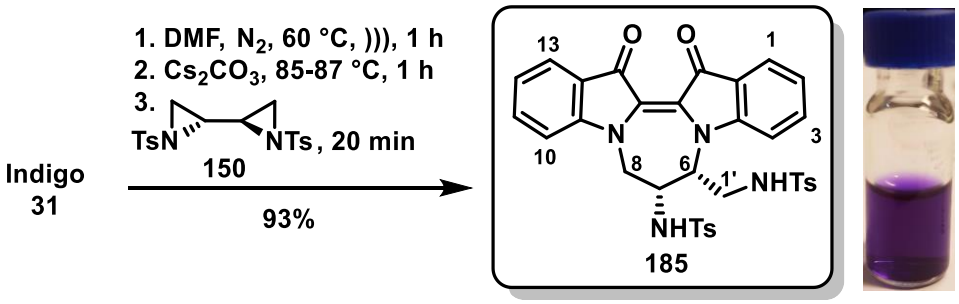

Scheme 70: Synthesis of diazepinodiindole **185** from the reaction of indigo with biaziridine **150**. Adjacent to the structure is pictured a solution in dichloromethane.

The diazepinodiindole **185** was isolated as an intense dark-blue powder in 93% yield from indigo, following repeated recrystallisation of the crude reaction mixture. Analysis of the HRESI mass spectrum revealed a peak at *m/z* 677.1513, assigned to the molecular ion $[C_{34}H_{30}N_4O_6S_2Na]^+$, revealing the incorporation of a single biaziridine fragment to the indigo core. Analysis of the ^{13}C NMR spectrum revealed a pair of downfield quaternary resonances at δ 180.9 and δ 180.8, assigned to the C14 and C15 ketone groups, and the presence of 32 peaks in the ^{13}C NMR spectrum indicated the molecule to be non-symmetrical. Analysis of the ^{1}H NMR spectrum revealed a distinct pair of 3H singlet resonances, assigned to the two tosyl methyl substituents in discrete chemical environments to each other. Analysis of the HSQC spectrum revealed a pair of methylene carbons at δ 42.4 and δ 39.4, assigned as C1' and C8, respectively, and two peaks which showed no direct attachment to a carbon at δ 6.69 and δ 5.71, which were assigned to the two sulfonamide groups at C7 and C1', respectively. Analysis of the COSY spectrum revealed coupling between the C7 sulfonamide NH and a vicinal methine proton resonance at δ 3.61, assigned as H7, which was coupled to a doublet at δ 4.63, assigned to H8a. ROESY experiments determined H7 to show strong through-space coupling to an apparent triplet methine resonance at δ 4.95, assigned to H6, supporting the assigned *cis*-stereochemistry of the C7-sulfonamide and C6-(sulfonamidomethyl) substituents. Weak through-space coupling was also observed between H8a and H6, due to their proximity in the bent 7-membered ring. The remaining methylene protons were assigned from HSQC analysis, which showed direct attachment of the diastereotopic proton resonances at δ 3.06 and δ 2.84 to C1'. Closer examination of the resonance assigned to H6 revealed a $^{3}J_{H\text{-}H}$ coupling constant of 4.7 Hz, which is consistent with axial-equatorial coupling with H7 ($^{3}J_{ax\text{-}eq}$ expected 1-6 Hz), suggesting the two protons to be *cis* to one-another and supporting the assigned stereochemistry.

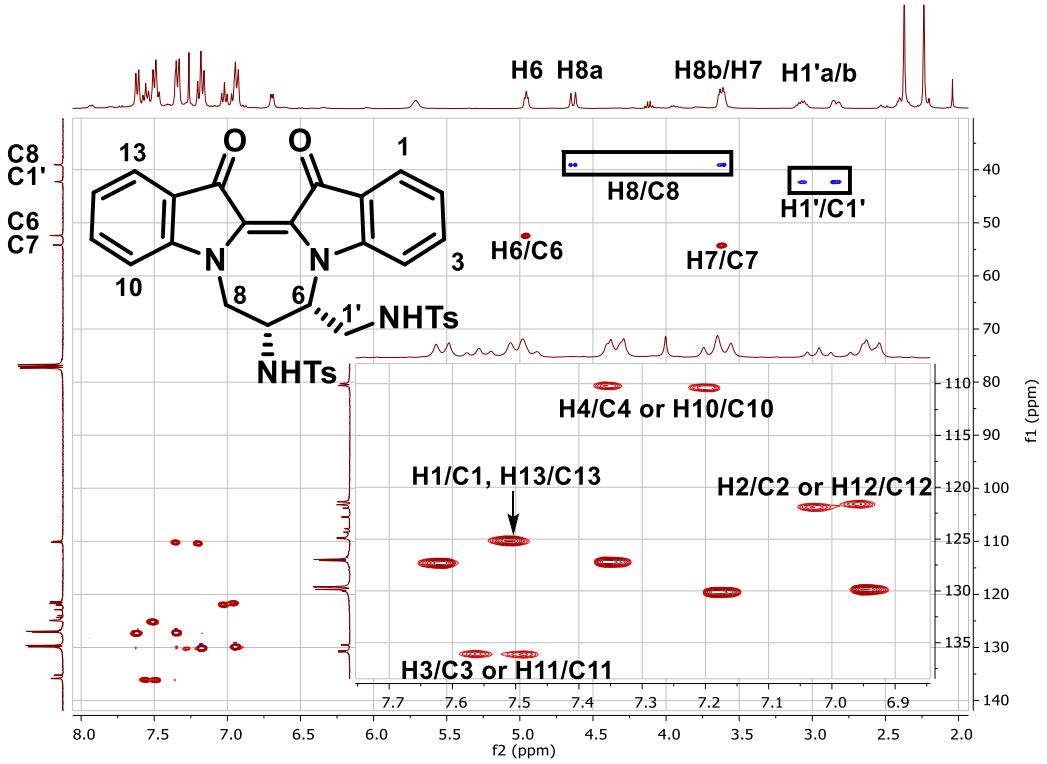

Figure 67: HSQC spectrum for compound **185** with assignments as indicated. Correlations for the Ts groups are omitted for clarity.

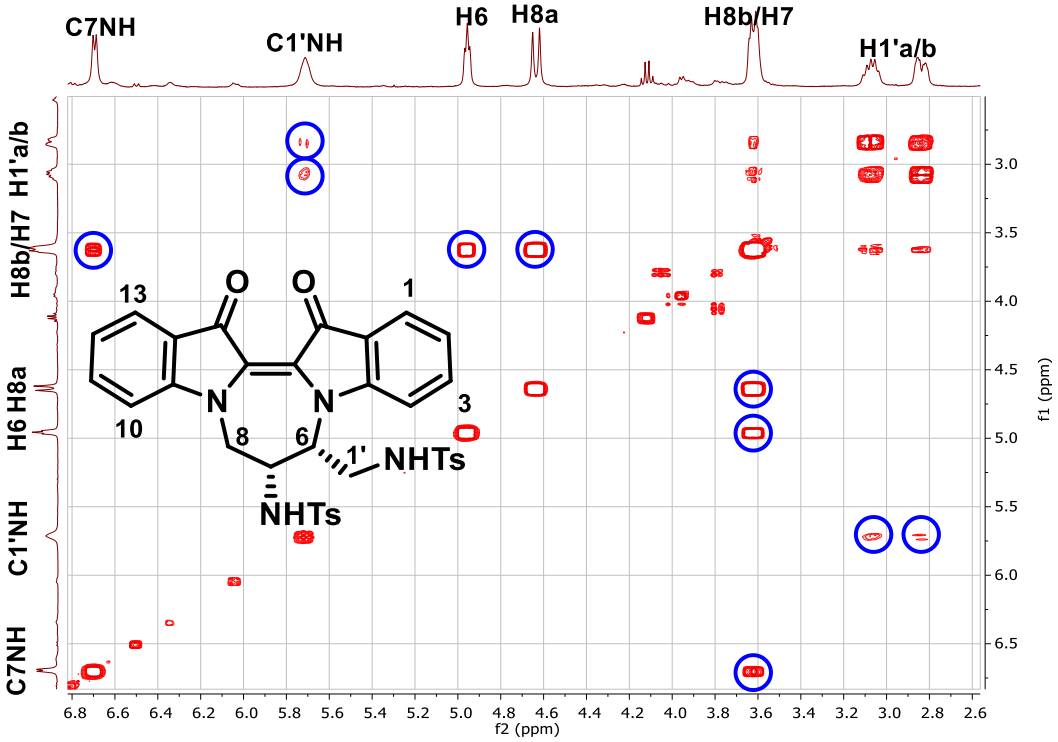

Figure 68: COSY spectrum for compound **185** with key correlations highlighted.

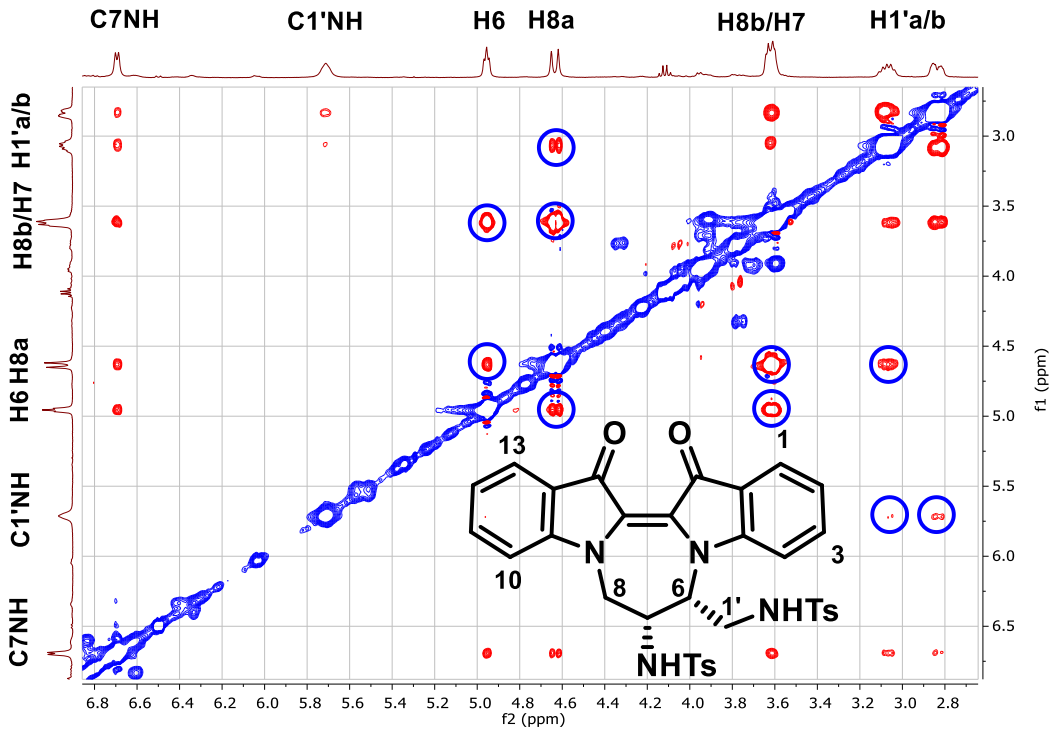

Figure 69: ROESY spectrum for compound **185**, with key correlations highlighted.

3.5.2 Mechanistic discussion

Comparing the outcomes of the 2,2'-bioxirane reaction with the reaction of epichlorohydrin, there was considerably greater preference toward Path B spirocyclisation reactions using 2,2'-bioxirane, while epichlorohydrin showed little discrimination between Path A and Path B. This is evidenced by comparing the isolated yields of compounds isolated from both mechanistic pathways in each reaction, where epichlorohydrin showed a 46:54 ratio, and bioxirane showed a 0:100 ratio of products resulting from Paths A:B, respectively. As noted previously, both the strength of the leaving group and the steric environment of the released heteroatom contribute significantly to pathway discrimination, and for the case of the bioxirane, it is apparent that both factors contribute to promote spirocyclisation. Therefore, we propose that *mono*-ring-opening of **149** generates key intermediate **186**, which undergoes *O'*-alkylation *via* an 8-*exo*-tet ring closure to give macrocycle **187**. The defined stereochemistry of the bioxirane C2 position results in facial selectivity upon re-aromatisation, and attack at the *si*-face *via* a 5-*exo*-trig hydroalkoxylation affords spirocycle **183**, which upon alkylation with a second equivalent of bioxirane **149** affords **184** (Scheme 71). The observed conservation of the stereochemical identity for spirocycle **183** in the x-ray crystal structure suggests that Payne rearrangement of intermediate **186** to an internal epoxide

(which could also undergo *O'*-nucleophilic attack to afford the *trans*-dioxolane 8-*epi*-**183** *via* the C8-epimer of intermediate **187**) had not occurred. It is also interesting to note that relative to sequential ring-opening reactions of bioxiranes reported previously (which proceed *via* nucleophilic attack at the less hindered C1 and C4),[140a, 140b, 141] intramolecular cyclisation occurs exclusively by initial C1 ring-opening, and subsequent ring-opening at the more-hindered C3 position. Attack at C4 is likely disfavoured by the entropic penalty and ring-strain of the larger nine-membered ring, making C3-attack more kinetically-favourable despite the enthalpic barrier of overcoming the increased steric bulk of internal attack.

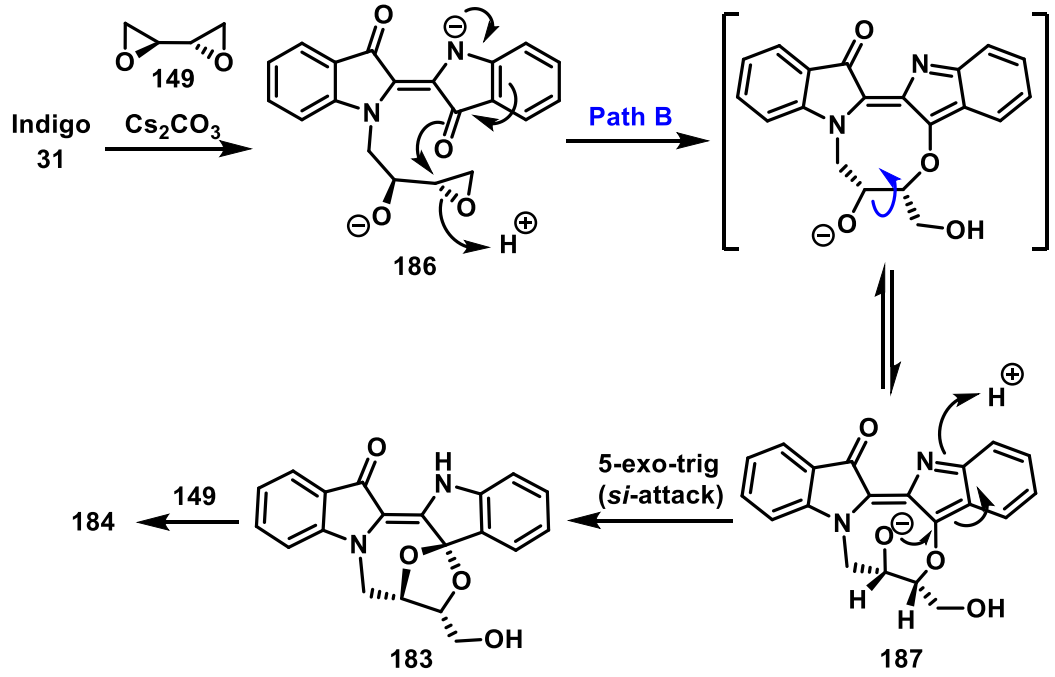

Scheme 71: Proposed mechanism for the formation of spiroketals **183** and **184** from the reaction of indigo and 2,2'-bioxirane *via* Path B.

Contrary to bioxirane **149**, the reaction of indigo with biaziridine **150** afforded exclusively the *N,N'*-cyclised product **185**, and there was no evidence of any additional products in the mixture. Therefore, upon ring-opening of biaziridine to key intermediate **188**, base-mediated protoisomerisation affords the *cis*-anion **189**, which undergoes a 7-*exo*-trig ring-closure to afford the *cis*-diazepinodiindole product **185** (Scheme 72). Similarly to the sequential C1, C3 ring-opening of bioxirane, biaziridine also underwent sequential C1, C3 ring-opening under these conditions, in contrast to its previously-established reactivity.[140b-d] Presumably this is due to both the decreased entropic cost of forming the seven-membered ring, and the considerable enthalpic barrier of orienting the C4 position

toward the indigo nitrogen due to unfavourable steric interactions between adjacent tosyl groups and the aromatic indigo core.

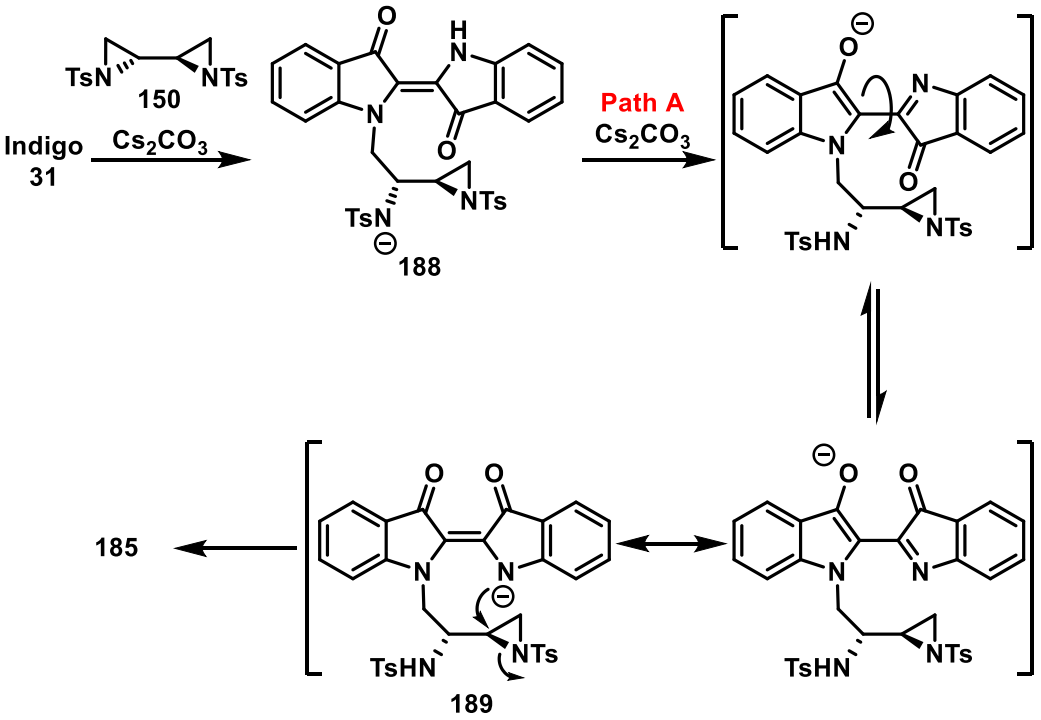

Scheme 72: Proposed mechanism for the formation of diazepinodiindole **185** from the reaction of indigo with biaziridine **150**.

3.6 Conclusions

Indigo undergoes cascade reactions with a variety of (halomethyl)oxiranes to afford mixtures of both *N,N′*- and *N,O′*-cyclic heterocycles by one of two major mechanistic pathways. By moderating the leaving group, these reactions could be optimised to either produce exclusively *N,N′*-cyclic products in up to 84% yield, or predominantly *N,O′*-cyclic products in a combined 51% yield by changing the rate of halide elimination from a common mechanistic intermediate. Under similar reaction conditions, (halomethyl)aziridines showed considerably-greater preference toward *N,N′*-cyclisation, however the high reactivity of these electrophiles led to uncontrollable polymerisation over longer reaction times. Optimal conditions afforded a combined 63% yield of enantiomerically-pure adducts bearing useful functional groups. Furthermore, optimising this reaction led to a practical synthesis of the useful chiral starting material **148** from readily-available materials, which could be used as an entry point toward the enantioselective synthesis of non-symmetrical 1,2-diamines or amino alcohols.

Reactions of indigo with the dimeric bioxirane and biaziridine had distinct mechanistic

pathway preferences to one-another, however they both followed a common trend in regioselectivity, reacting exclusively by sequential 1,3-ring opening, rather than the established 1,4-ring opening. For bioxirane, selective *N,O′*-cyclisation afforded a pair of spirocycles in 81% combined yield, while biaziridine led exclusively to a single *N,N′*-cyclic adduct in 93% yield. The observation of this 1,3-selectivity in both instances suggests that by selecting appropriate di-nucleophiles, that intramolecular cyclisation of both bioxirane and biaziridine should favour attack at C1 and C3, allowing access to enantiomerically-pure desymmetrised systems, further demonstrating the synthetic value of these simple chiral precursors.

Compared with the previously-studied reactions of indigo with allylic and propargylic electrophiles, π-nucleophiles tend to undergo cascade reactions by C2 or C3 nucleophilic attack leading to spirocyclic adducts for allylic substrates, or ring-expansion of the biindole core to indolonaphthiridinones for propargylic substrates, whereas these reactions with strained-ring systems have largely preserved the structural integrity of the indigo nucleus. These reactions proceed with conservation of the stereochemical identity of their precursors, allowing for the chemo- and stereoselective generation of desymmetrised, three-dimensional polycycles. The generation of the epoxy-oxazocinodiindole framework had not been established previously, and compounds **153**-**155**, **183** and **184** represent the first known examples of this ring system. The presence of pendant functional groups in all generated molecules moreover could allow for their incorporation into other scaffolds, allowing for rapid diversification and/or library generation with a broad variety of coupling partners.

Chapter 4:
Reactions of indigo with organometallic nucleophiles

4.1 The role of organometallic compounds in synthetic chemistry

The ubiquity of carbon in all manner of natural and synthetic molecules have rendered the formation of new carbon-carbon bonds an area of continuous interest in both methodology development, and in the design and synthesis of new molecular architectures. With a Pauling electronegativity of 2.54,[152] carbon is amphoteric and can adopt numerous oxidation states ranging ±4, hence it is rendered either an electrophile or nucleophile depending on its electronic environment. Carbon electrophiles are common (e.g. functional groups including alkyl (pseudo)halides and carboxylates) where the net oxidation state of the carbon atom is positive, while it is rendered nucleophilic when bonded to more-strongly electropositive elements such as metals.

Organometallic complexes are those which features carbon-metal bonds, and feature prominently both as reagents and as intermediates in numerous metal-catalysed cross-coupling reactions. Grignard reagents are distinguished by the presence of a carbon-magnesium bond – the strongly-electropositive magnesium atom renders the carbon atom both highly nucleophilic and strongly basic, allowing it to react with a broad variety of functional groups (Scheme 73).[153] This high reactivity however means that Grignard reagents are typically unstable toward air, moisture, and often undergo undesired reactions with even relatively-inert substituents such as esters, amides, and terminal alkynes. Nevertheless, their simple generation, low cost, and wide applicability to a broad variety of chemical transformations has made the Grignard reaction a mainstay of contemporary organic chemistry, and Victor Grignard was awarded the Nobel Prize for Chemistry in 1912 for its discovery.

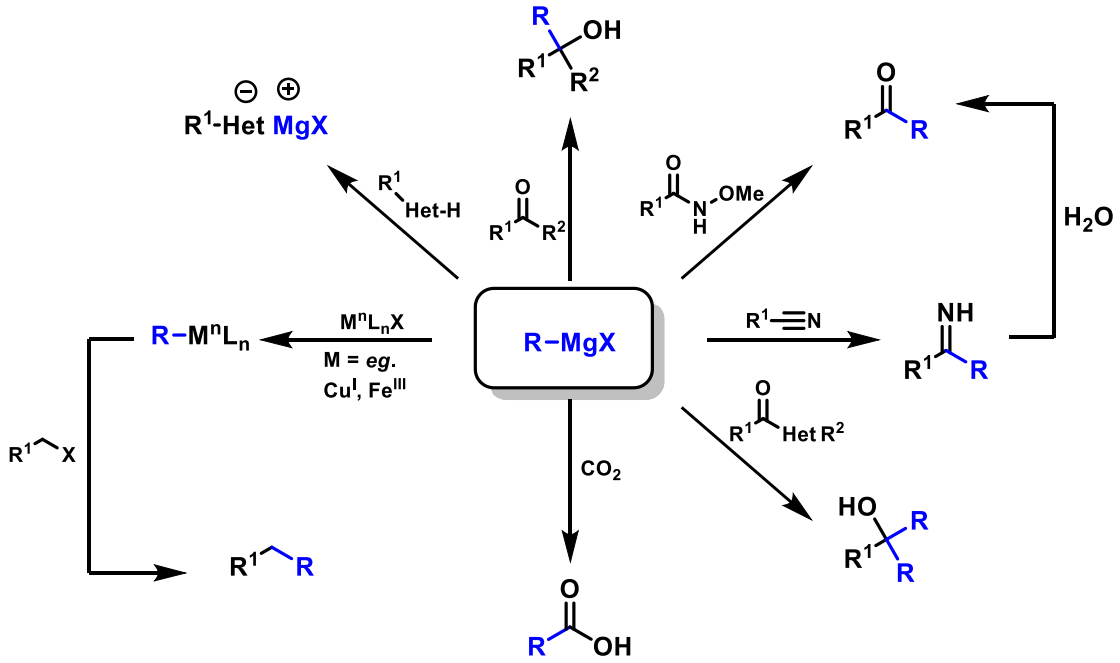

Scheme 73: A brief summary of the reactivity of Grignard reagents with various common functional groups. Clockwise from top left: deprotonation of acidic functional groups, formation of alcohols from aldehydes and ketones, ketones from Weinreb amides, imines from nitriles, alcohols from esters or amides, carboxylic acids from CO_2, and alkyl groups from transmetallation and nucleophilic substitution.

Grignard reagents can be readily generated by direct oxidative addition of Mg^0 to alkyl- or aryl halides, or by magnesium-halogen exchange with commercially-available isopropylmagnesium chloride (**190**). Of these methods, there are several advantages to the magnesium-halogen exchange as pioneered by the Knochel group, which occurs rapidly under mild conditions and allows highly-functionalised Grignard reagents to be generated *in situ* (Scheme 74).[154] These reactions can be performed at cryogenic temperatures (typically -40 ˚C), allowing functional groups such as nitriles, esters, amides and nitro groups to be tolerated, and polyhalogenated compounds may be regioselectively metalated in a predictable and reliable fashion.[155] The addition of LiCl to these reactions is typically beneficial to both reaction rate and regioselectivity, and is thought to activate the incoming Grignard reagent by formation of a lithium dichloromagnesiate "turbo-Grignard" complex (**191**),[156] which significantly enhances the nucleophilicity of the adjacent carbon atom. Addition of a suitable halogenated starting material (e.g. the tri-brominated pyridine **192**) results in metal-halogen exchange selectively at the 3-position, and the eventual formation of the desired heteroaryl "turbo-Grignard" reagent **193**. Combined with the well-established methodology for directed *ortho*-metalation,[157] and developing methods for regioselective directed *meta*- and *para*-metalation of various

substituted (hetero)aryl C-H bonds,[158] a vast array of functionalised organometallic nucleophiles are now readily-accessible.

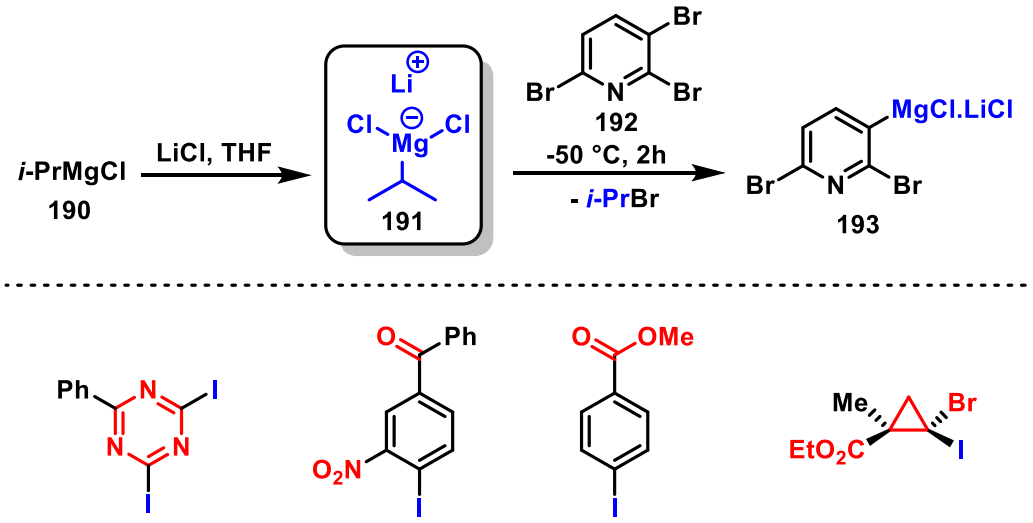

Scheme 74: The metal-halogen exchange reaction for the formation of substituted Grignard reagents. Above: an example of the reaction using "turbo-Grignard" **191** toward the formation of dibromopyridylmagnesiate **193**. Below: selected examples of tolerated functionalities to this reaction, with the metallation site highlighted in blue, and typically-incompatible functional groups highlighted in red.

4.2 Reactions of indigo with Grignard reagents

As mentioned previously, the reaction of indigo with Grignard reagents was first reported in 1909, and resulted in the isolation of eight *mono*-addition products in modest to excellent yields.[67] The authors of the original study did not unambiguously assign a structure to the products, however they proposed the structure to be one of a pair of tautomeric species (**58a** and **58b**) on the basis of elemental analysis and synthesis of derivatives. The reported selectivity for *mono*-addition to indigo is intriguing, as this allows for desymmetrisation of the biindole nucleus. The high functional density of indigo could therefore allow for the facile and selective synthesis of various 3-aryl-2,2'-diindoles (**194**) from a conceptually-simple dehydration of the tertiary alcohol adduct (Scheme 75). This reaction was serendipitously re-discovered through the course of our exploration, though it was quickly recognised to be a useful starting point for the development of new methods toward the synthesis of functional diindoles (see Section 4.2.1 Reaction discovery and structural assignment, *vide infra*).

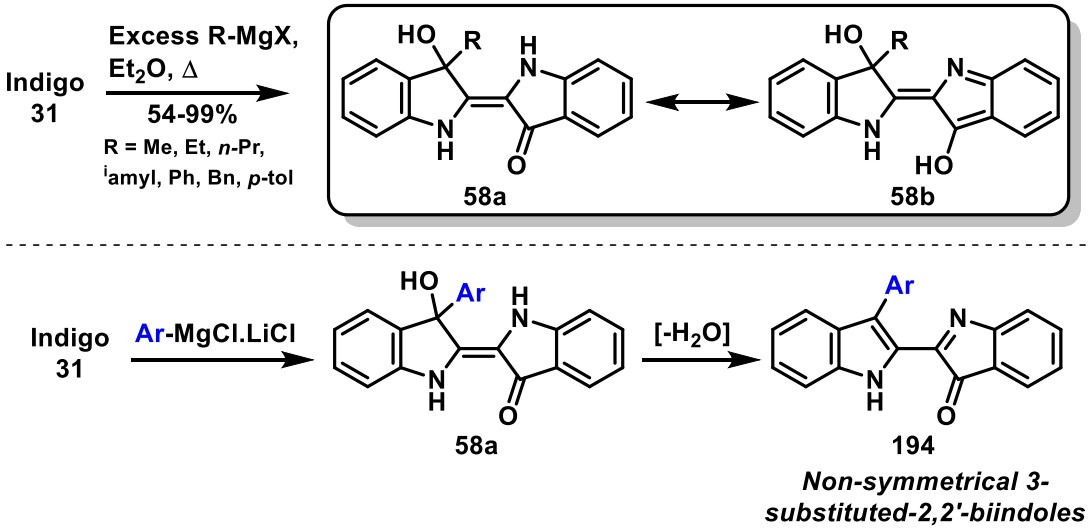

Scheme 75: Above: the previously-reported (1909) synthesis of *mono*-Grignard adducts from indigo, and the proposed possible structures of the product: **58a** and **58b**. Below: the overall synthetic strategy of this study, involving a two-step addition-dehydration procedure toward the synthesis of desymmetrised adducts such as **194**.

Non-symmetrical 2,2'-diindole moieties are a key component of numerous natural products and pharmaceuticals (Figure 70). These include the natural product staurosporine (**4**), and its derivatives lestaurtinib (**195**), and midostaurin (**196**), which are highly-potent and selective kinase inhibitors – midostaurin recently gained FDA approval for the treatment of FLT3+ acute myeloid leukaemia under the name Rydapt.[159] Other significant examples of the 2,2'-biindole moiety include the natural products iheyamine A (**196**) and indimicins A-D (**197**–**200**), as well as the clinical lead birinapant (**201**), investigated for the treatment of myelodysplastic syndrome and chronic myelomonocytic leukaemia. Furthermore, while 1*H*-3'*H*-2,2'-biindoles have received sporadic attention as synthetic intermediates[104b, 104c, 160] and oxidation products,[161] there are only three reported examples of 3'-oxoindolenine-indoles – the natural product bisindigotin (**202**) and two synthetic precursors (**203** and **204**) encountered in Sperry's 2016 total synthesis of iheyamine A and a *des*-methoxy analogue.[162] Neither the innate biological profile, nor the synthetic value of these molecules has been adequately established, therefore making this an avenue worthy of closer examination. Furthermore, this would allow a simple means of exploring the chemistry of indigo's carbonyl groups, which until now has been an area of very limited study.

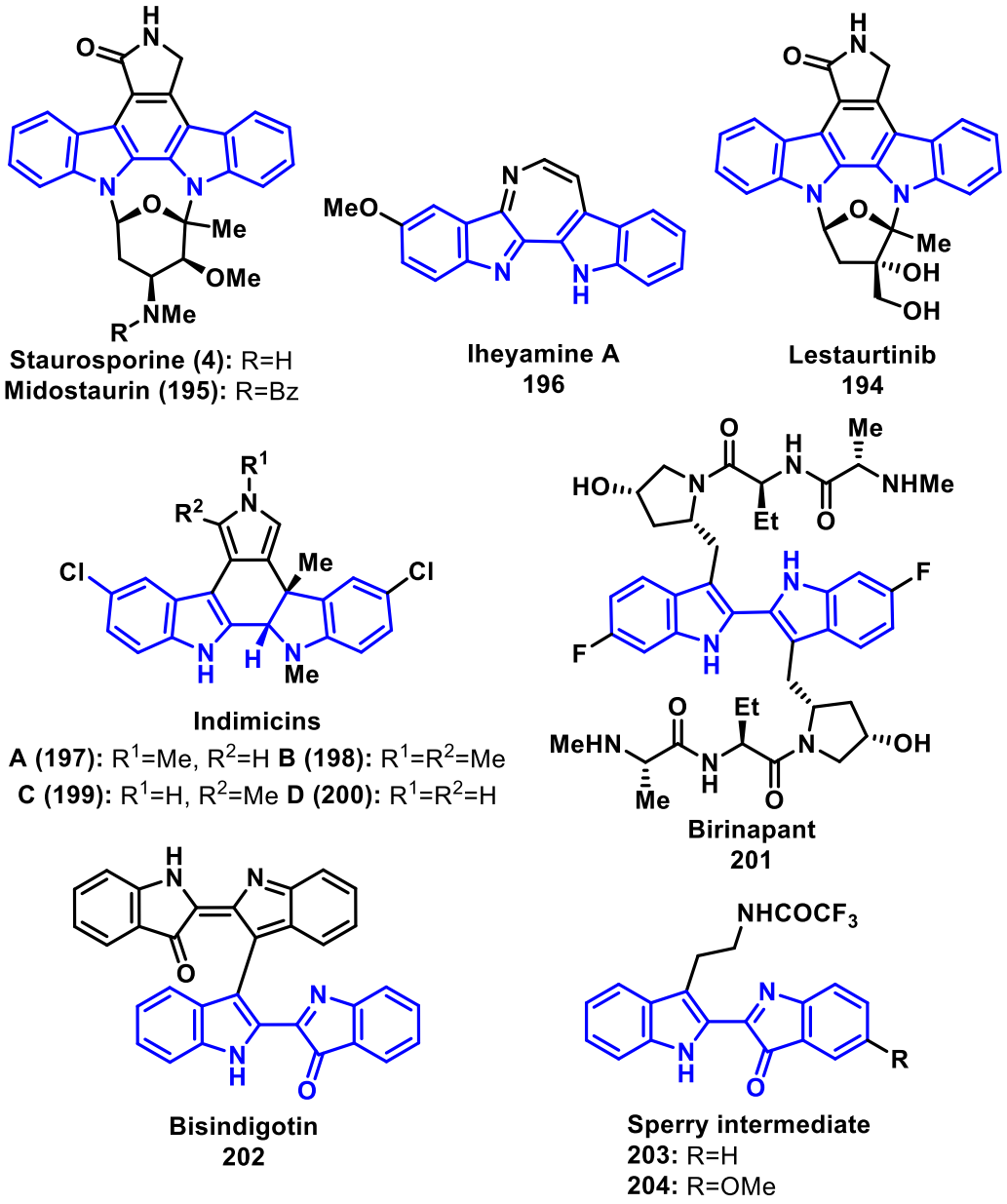

Figure 70: Selected significant examples of the 2,2'-biindoline scaffold (highlighted in blue), as exhibited in natural products, clinical leads, and synthetic intermediates.

4.2.1 Reaction discovery and structural assignment

During the course of our exploration of the chemistry of indigo in reactions with strained-ring systems (see Chapter 3, *vide supra*), we sought to examine the reactivity of the doubly-strained 1-azabicyclo[1.1.0]butane (**205**).[163] Highly-strained molecules such as these have been used recently by the Baran group for the direct azetidinylation, cyclobutylation (**206**) and "propellerisation" (**207**) of secondary amines in the presence of *i*-PrMgCl.LiCl (**191**) as an activator – generating a highly nucleophilic R_2N-MgCl.LiCl "turbo-amide" intermediate species *in situ* (Scheme 76, **A**).[164] Given the vast substrate scope reported for this transformation, we sought to replicate the reaction of **205** using

indigo in place of the secondary amine to determine whether the appended azetidine ring would be sufficiently-strained to undergo further reactions with the indigo core. Therefore, to a cooled (-84 ˚C) suspension of dibromoamine hydrobromide salt **162** (3.0 mmol) in dry THF (10 mL) was added a freshly-titrated (0.98 M) solution of phenyllithium in THF (9.0 mmol) slowly dropwise, and the mixture stirred for 2 h. Meanwhile, to a vigorously-stirred suspension of indigo (1.0 mmol) and LiCl (2.5 mmol) in THF (10 mL) was added a freshly-titrated (0.87 M) solution of *i*-PrMgCl in THF (2.5 mmol), and the mixture stirred at room temperature for 2 h. The resulting indigo/turbo-Grignard solution was transferred by cannula into the azabicyclobutane solution at -84 ˚C, and the intense-red mixture allowed to warm to room temperature overnight. This mixture was then cooled to 0 ˚C, and a solution of Boc_2O (6.0 mmol) in THF (5 mL) added slowly, and the resulting red-brown solution stirred for 3 h. Aqueous workup and subsequent flash chromatography afforded a mixture of four major components – the deep burgundy *mono*-*N*-Boc indigo **208**, the deep purple *N*-H isopropyl adduct **209**, and the bright orange *N*-Boc isopropyl **210** and phenyl **211** adducts in a combined 77% yield, with no azetidine incorporation (Scheme 76, **B**).

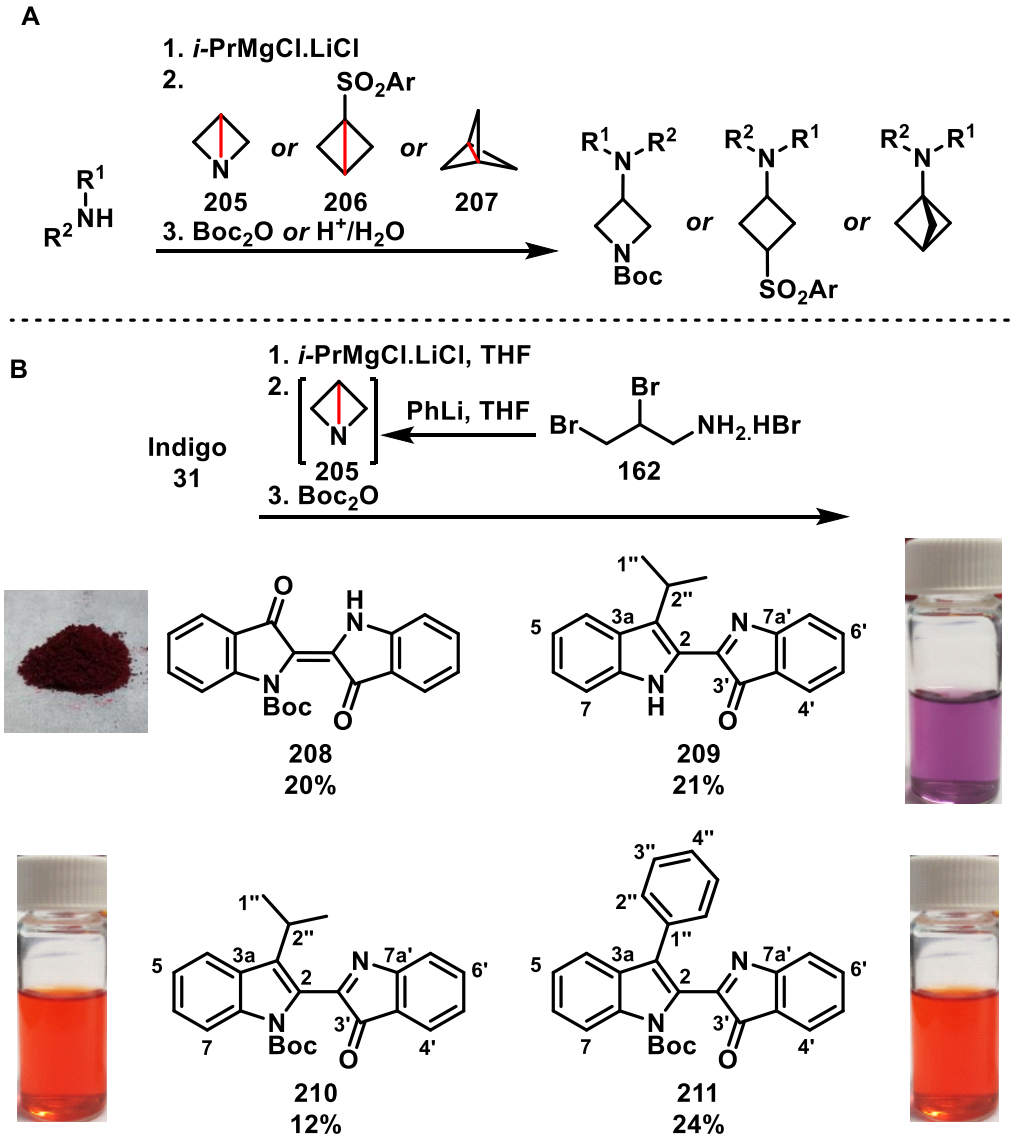

Scheme 76: **A**: Literature protocol for 'strain-release' functionalisation of amines by addition across the highlighted (red) bond,[164] **B**: Outcome of the attempted 'strain-release' azetidinylation of indigo, producing *N*-Boc indigo **208** and Grignard adducts **209**–**211**. Adjacent to the structure of **208** is a photograph showing its colour in its crystalline form. Adjacent to **209**–**211** is a photograph of a solution in acetone at a concentration of approximately 0.1 mM.

Mono-N-Boc indigo **208** was isolated as small burgundy crystals in 20% yield following flash chromatography. Analysis of the HRESI mass spectrum revealed a peak at *m/z* 363.1342, assigned to the molecular ion $[C_{21}H_{19}N_2O_4]^+$, revealing the addition of a Boc substituent to the indigo molecule, and its deep red-purple colour in solution qualitatively suggested the indigo core to have remained intact. Analysis of the ^{1}H spectrum revealed eight distinct aromatic resonances, and a pair of carbonyl resonances were evident in the ^{13}C NMR spectrum, suggesting the molecule to be unsymmetrical. The 9H singlet at δ 1.62 was assigned to the degenerate methyl groups of the *N*-Boc substituent, while the broad singlet at δ 10.02 was assigned to the free NH group.

Isopropyl adduct **209** was isolated as small, dark purple crystals in 21% yield following flash chromatography, with its deep purple colour qualitatively suggesting the retention of intramolecular hydrogen bonding. Analysis of the HRESI mass spectrum revealed a peak at *m/z* 289.1349, assigned to the molecular ion $[C_{19}H_{17}N_2O]^+$, revealing the net substitution of one oxygen atom for an isopropyl group. Analysis of the ^{1}H NMR spectrum revealed a 1H heptet at δ 4.55, which showed COSY correlations to a 6H doublet at δ 1.54, assigned to H2" and the adjacent H1" methyl groups, respectively (Figure 71). Further downfield, the broad singlet at δ 10.11 exchanged with D_2O, and was therefore assigned to the free NH of the indole. Analysis of the ROESY spectrum revealed through-space correlation of the H1" methyl groups with a doublet at δ 7.92, assigned to H4 of the adjacent aromatic ring (Figure 72). Having identified H4, this was used as an entry point to this ring, and analysis of the COSY spectrum allowed the assignment of H5, H6 and H7 to resonances at δ 7.08, δ 7.29, and δ 7.41, respectively, therefore allowing for the assignment of C4, C5, C6 and C7 to ^{13}C resonances at δ 122.6, δ 119.8, δ 125.7, and δ 112.2, respectively, by analysis of the HSQC spectrum (Figure 73). These assignments were confirmed by HMBC experiments, which showed strong, three-bond coupling between H4-C6, H6-C4, H5-C7, and H7-C5 (Figure 74). Both H4 and H6 additionally showed three-bond coupling to a quaternary ^{13}C resonance at δ 138.8, assigned to the indole C7a, and both H5 and H7 were coupled to a quaternary resonance at δ 126.6, assigned to C3a, which also showed three-bond coupling to the isopropyl H2". The remaining positions of the indole were assigned by identifying HMBC correlations to the isopropyl substituent – both H1" and H2" were coupled to a quaternary resonance at δ 135.0, assigned to C3, however only H2" was coupled to the resonance at δ 123.8, assigned to C2.

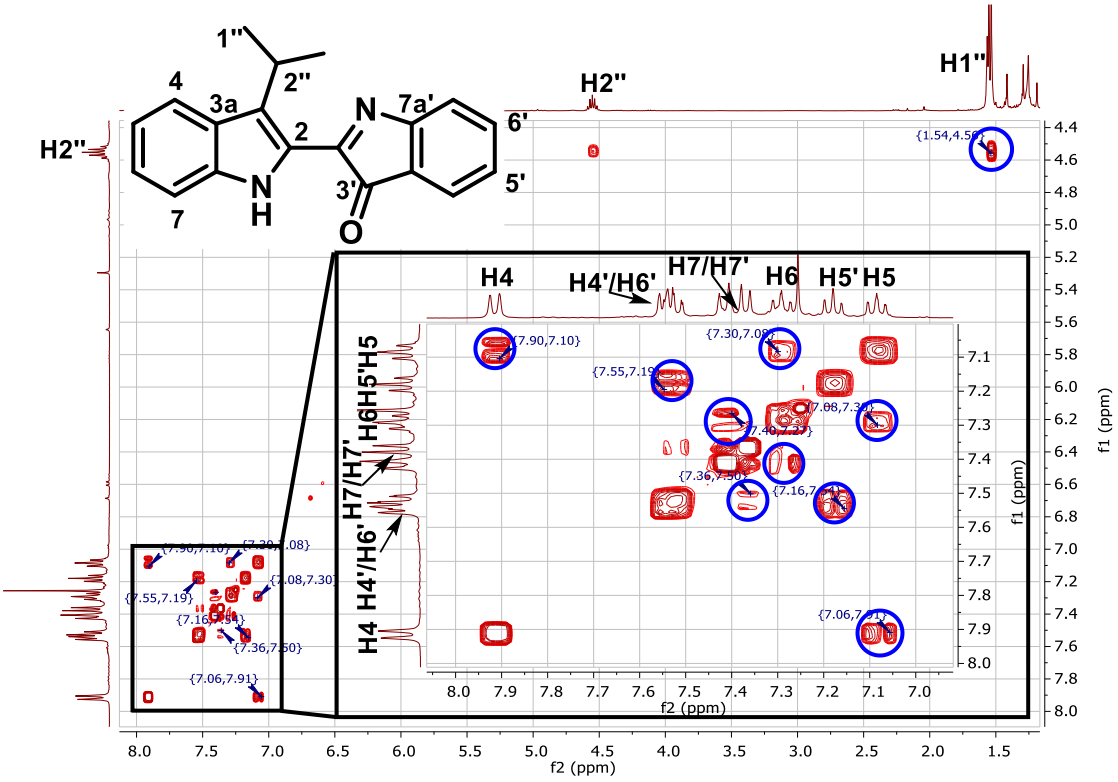

Figure 71: COSY spectrum for compound **209**, with expansion of the aromatic region (inset), and key correlations highlighted.

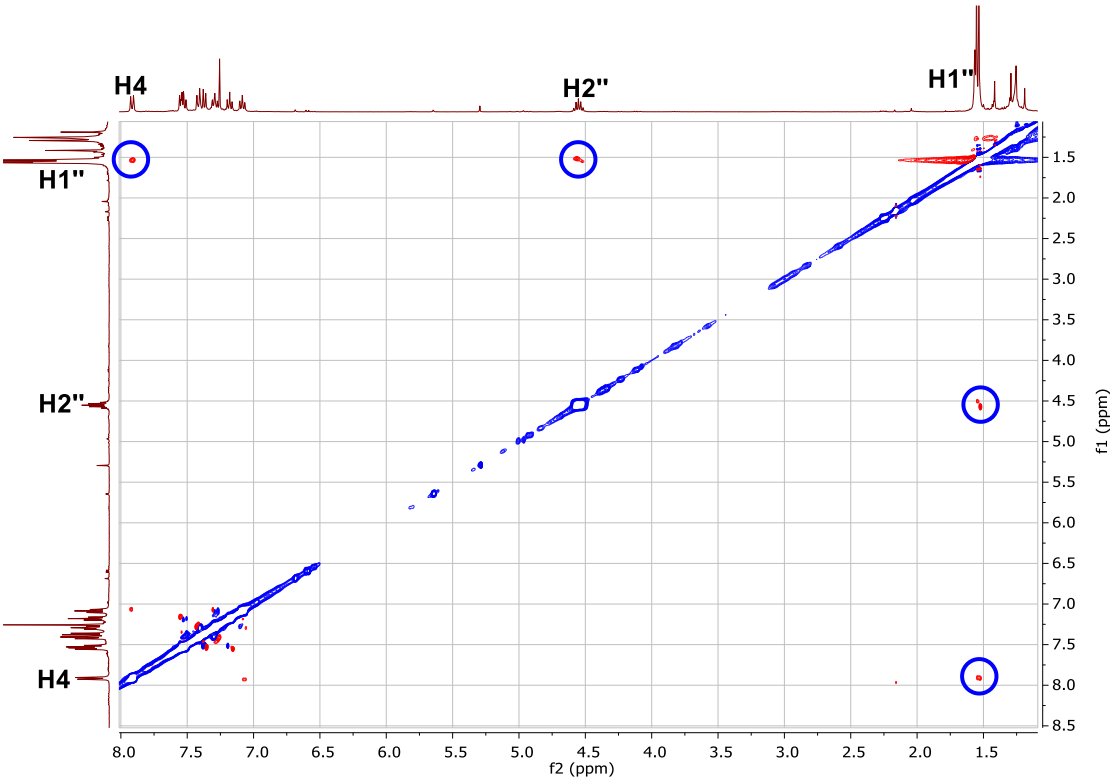

Figure 72: ROESY spectrum for compound **209** with key correlations highlighted.

On the opposite hemisphere, the remaining C3' carbonyl was assigned to the resonance at δ 197.1, and showed HMBC correlations to a ^{1}H resonance at δ 7.54, assigned to H4'. This was coupled to a protic ^{13}C resonance at δ 137.6, and a quaternary resonance at δ 162.7, assigned to C6' and C7a', respectively. The C2' C=N group was assigned to a quaternary resonance at δ 154.6, and while its remoteness meant it did not show any correlations in the HMBC spectrum, in the twelve synthesised examples of this scaffold (*vide infra*), the indolenine C2' was always observed within the range of δ 156.3±2.8. The chemical shift of this position, as well as the considerable downfield shift of the C6' and C7' positions (*cf.* C6 and C7a on the opposite ring, located at δ 125.7 and δ 138.8, respectively) is typical of other reported 2-aryl-3*H*-indol-3-ones,[165] supporting the assignment of this ring system. Therefore, we were able to definitively assign all proton and carbon environments of the molecule (Figure 75).

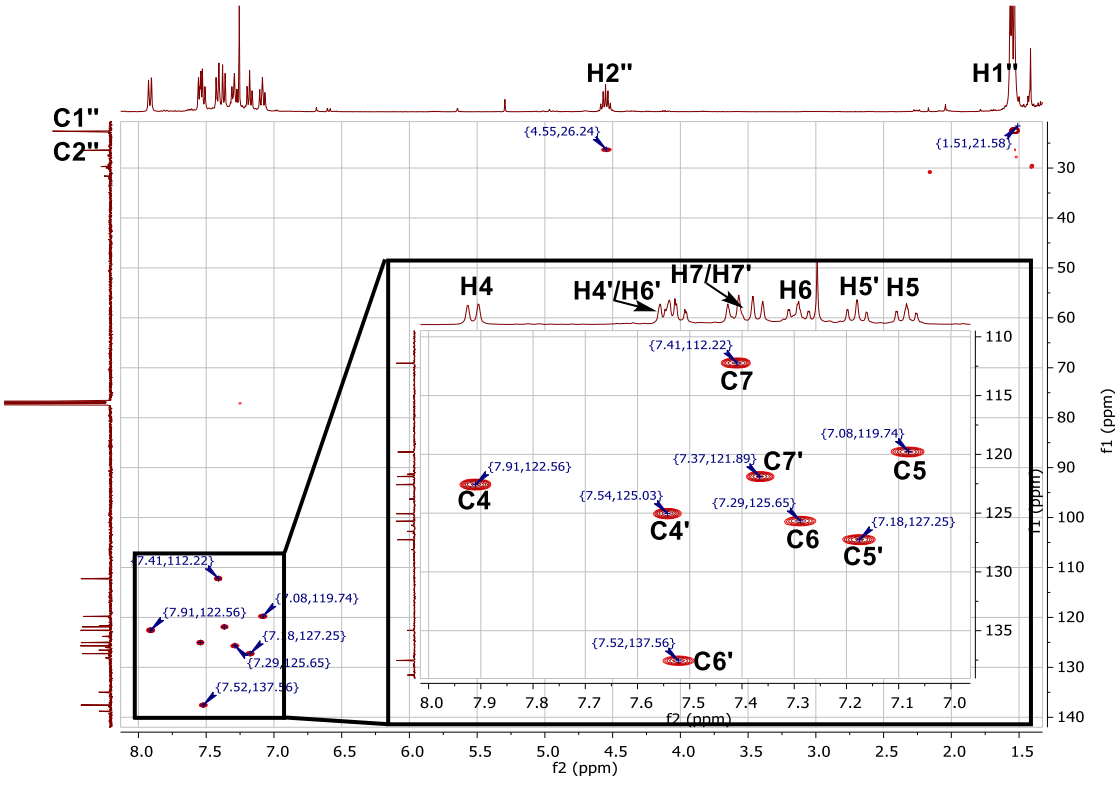

Figure 73: HSQC spectrum for compound **209** with expansion of the aromatic region (inset) and assignments as indicated.

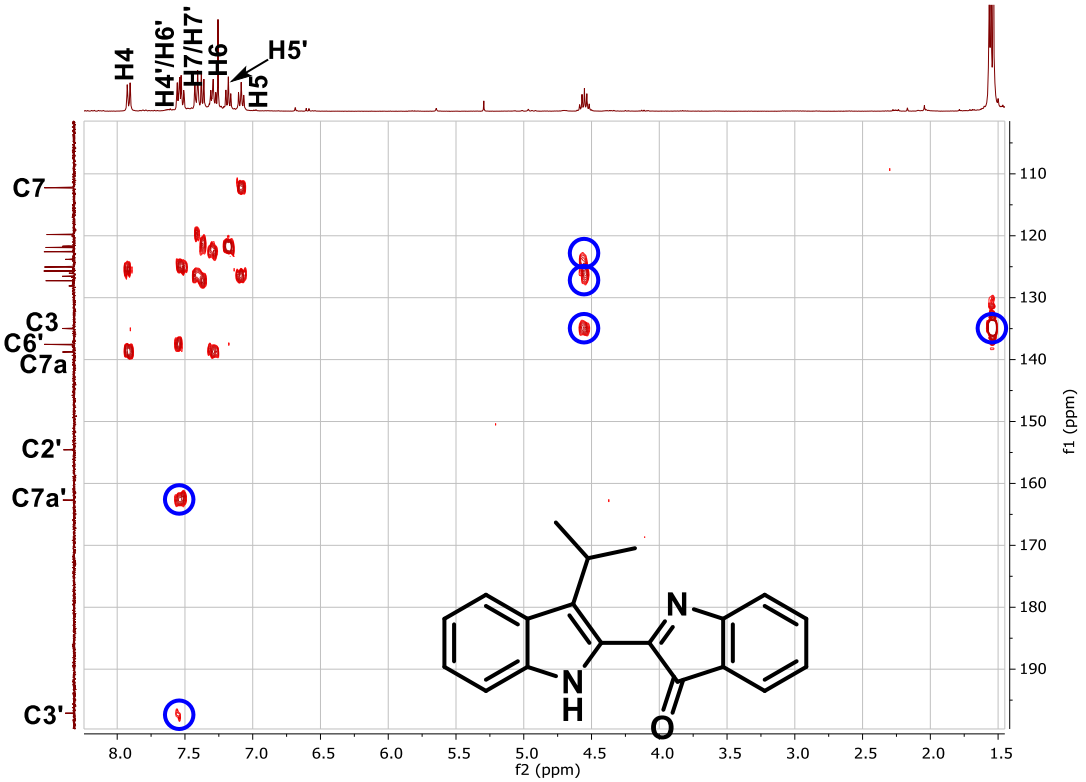

Figure 74: HMBC spectrum for compound **209** with key correlations highlighted.

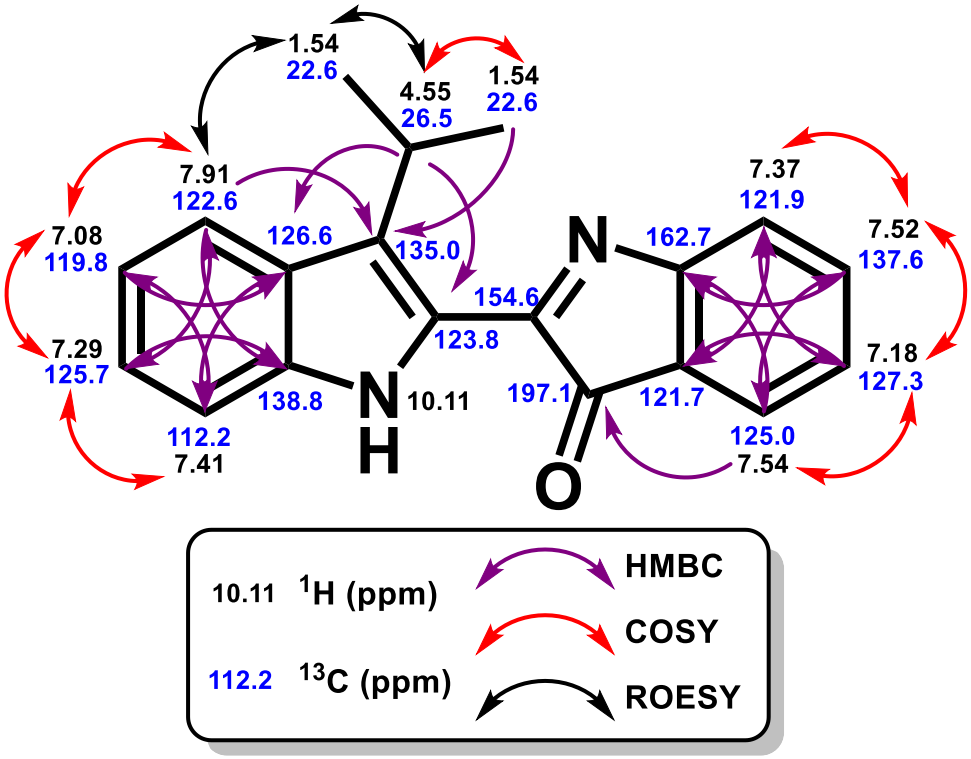

Figure 75: Summary of correlations from 2D NMR data allowing the structural assignment of compound **209**.

The *N*-Boc isopropyl adduct **210** was isolated as bright orange crystals in 12% yield following flash chromatography on silica gel. Analysis of the HRESI mass spectrum revealed a peak at *m/z* 389.1860, assigned to the molecular ion $[C_{24}H_{25}N_2O_3]^+$, revealing the substitution of one oxygen for an isopropyl unit, and the addition of a Boc substituent. Analysis of the ^{1}H NMR spectrum revealed a 9H singlet at δ 1.49, assigned to the degenerate methyl groups of the Boc group, as well as a 1H heptet at δ 3.58 and a 6H doublet at δ 1.46 which correlated strongly to one-another in the COSY spectrum, and were assigned to H2" and H1" of the isopropyl unit, respectively (Figure 76). Analysis of the ROESY spectrum revealed through-space correlation between the Boc CH_3 group and a heavily-deshielded doublet at δ 8.21, assigned to the nearby H7, as well as correlations of the isopropyl protons H2" and H1" with a doublet at δ 7.83, assigned to H4 (Figure 77). H4 showed correlations in the COSY spectrum to an apparent triplet at δ 7.25, assigned to H5, and both H5 and H7 showed correlations with the apparent triplet at δ 7.38, which was assigned to H6. With H4-H7 unambiguously assigned, HSQC analysis allowed assignment of C4, C5, C6, and C7 to the ^{13}C resonances at δ 121.8, δ 122.7, δ 126.1, and δ 115.9, respectively. Of the remaining carbons of the indole moiety, C2, C3, and C7a were assigned to carbon resonances at δ 124.0, δ 134.0, and δ 137.6, respectively, by analysis of the HMBC spectrum (Figure 79). The precise chemical shift of C3a was ambiguous due to peak overlap in the ^{13}C NMR spectrum. The shape of the overlapped ^{13}C resonance ranging δ 128.54–128.47 was broadened and asymmetric in the 1D spectrum, and the HMBC spectrum demonstrated correlations to both H7 and H7' which are chemically-distinct and separated by a shortest path of nine covalent bonds, therefore correlation of either H7-C3a' or H7'-C3a are highly unlikely. Therefore, the broad resonance at δ 128.54–128.47 was assigned as a pair of overlapped resonances at δ 128.51 and δ 128.50, with both peaks belonging to either C3a or C3a'.

The 3*H*-indol-3-one fragment of the *N*-Boc indole **210** showed similar chemical shifts and 2D connectivity to the *N*-H indole **209**, with the exceptions of C2', which was relatively-deshielded by Δδ +6.1 in the ^{13}C NMR spectrum (δ 160.7 in **210**, *cf.* δ 154.6 in **209**), and C3', which was relatively-shielded by Δδ -5.0 (δ 192.1 in **210** *cf.* δ 197.1 in **209**). These values are consistent across fifteen derivatives of this *N*-Boc scaffold (*vide infra*), and lie within the range of δ 160.4±0.9 at C2' and δ 191.9±1.2 at C3'. We can therefore confidently assign each proton and carbon environment of **210** (Figure 80).

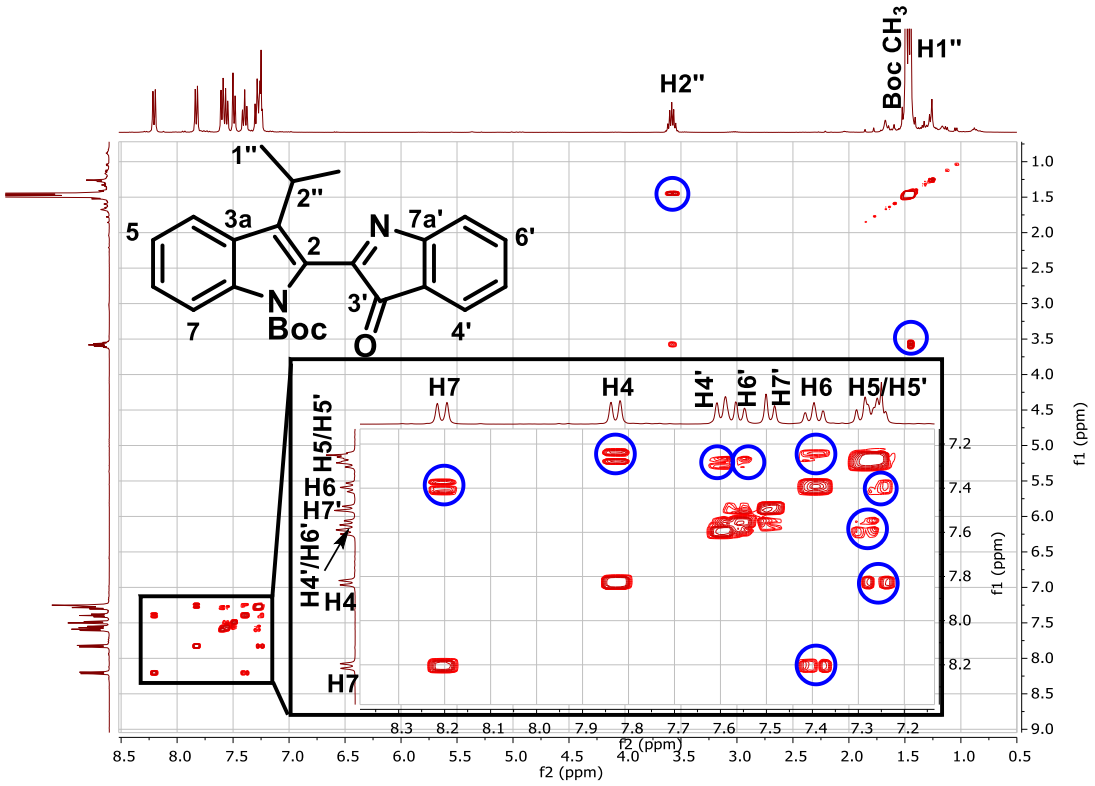

Figure 76: COSY spectrum for **210**, with expansion of the aromatic region (inset) and key correlations highlighted.

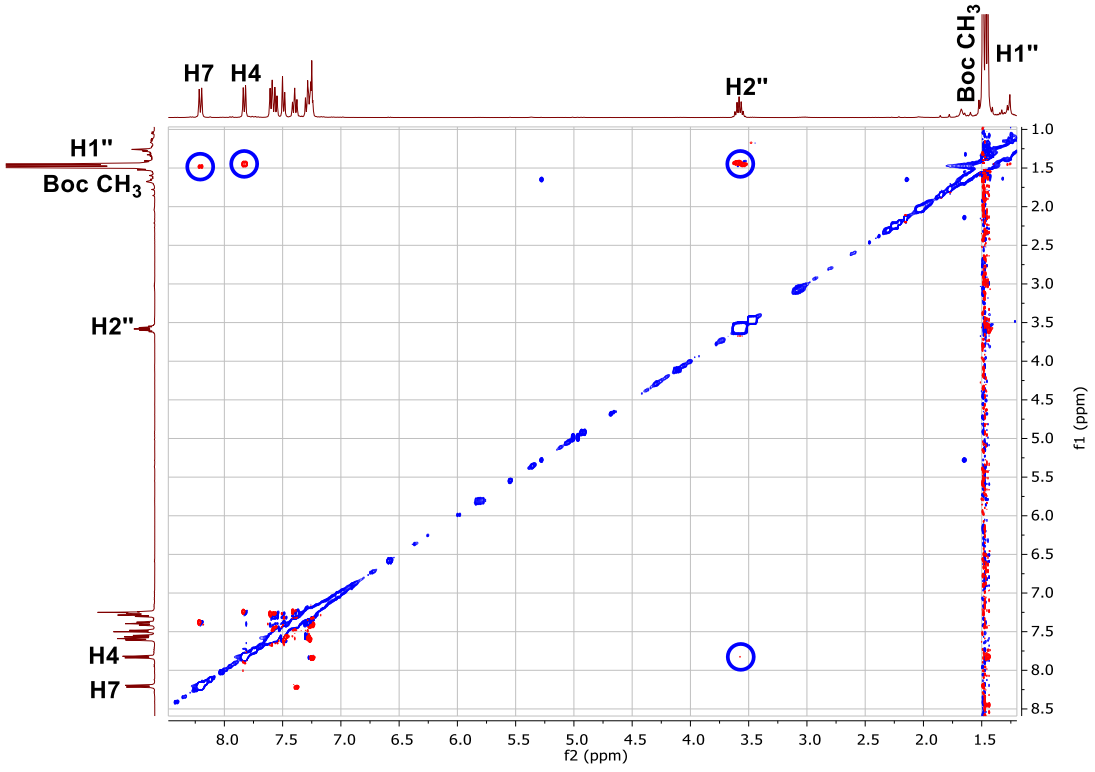

Figure 77: ROESY spectrum for compound **210**, with key correlations highlighted.

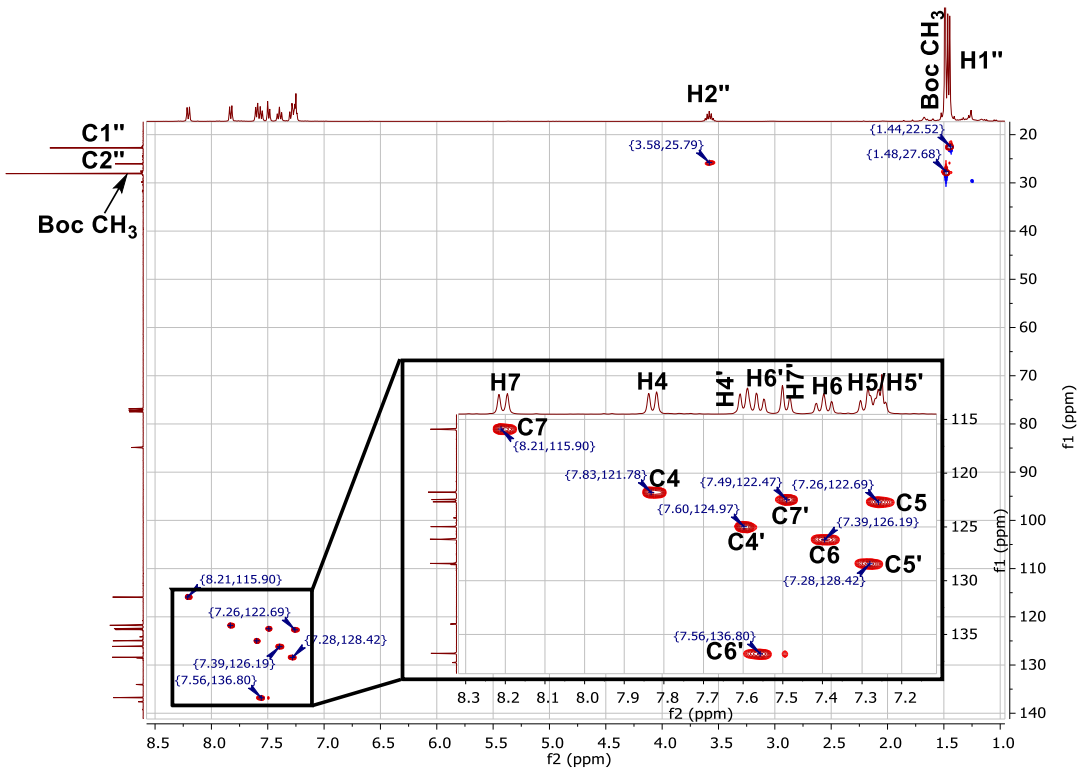

Figure 78: HSQC spectrum for compound **210** with expansion of the aromatic region (inset) and assignments labeled.

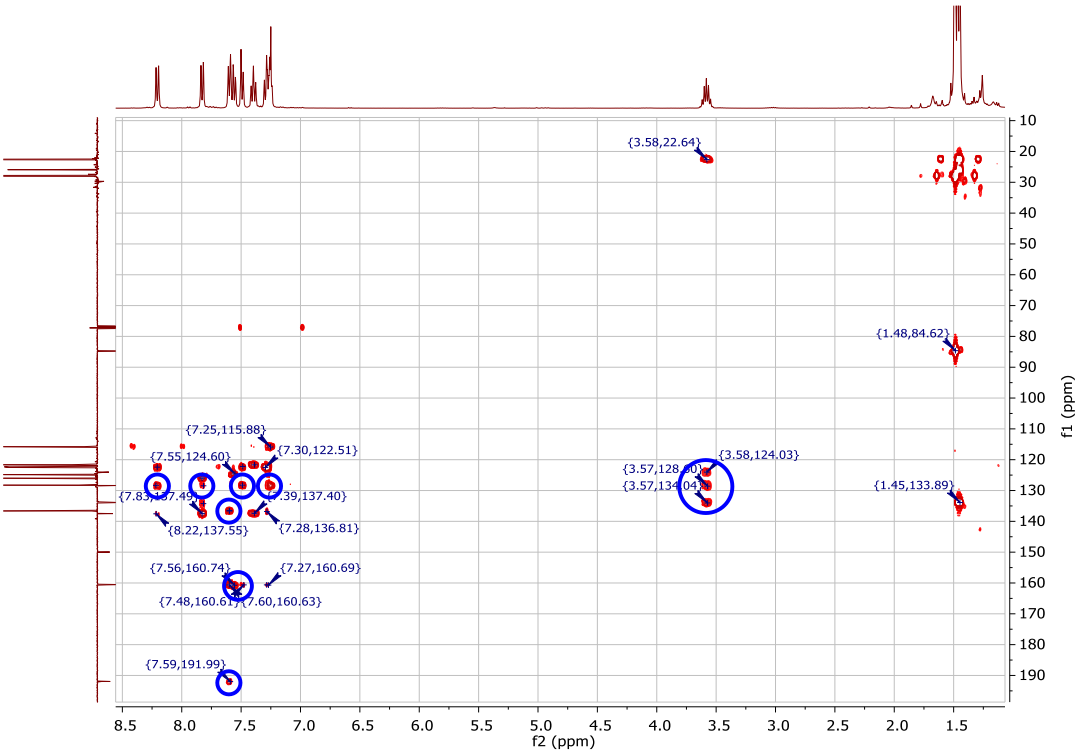

Figure 79: HMBC spectrum for compound **210**, with key correlations highlighted.

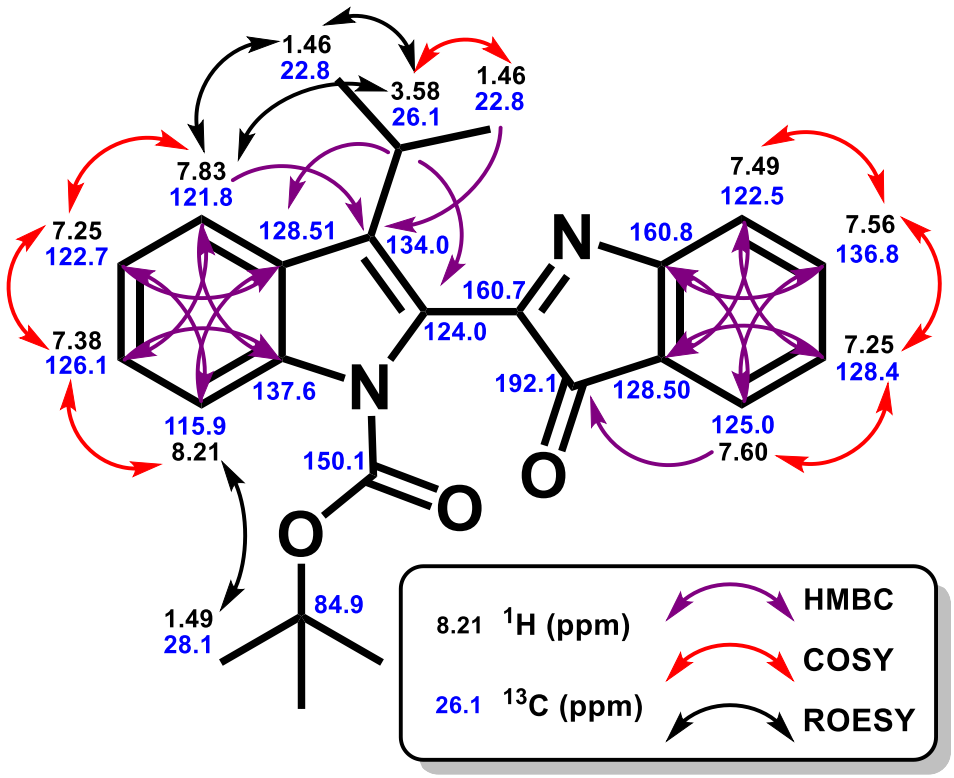

Figure 80: Summary of correlations from 2D NMR data allowing the structural assignment of compound **210**.

The *N*-Boc phenyl adduct **211** was isolated in 24% yield as small, bright orange crystals following flash chromatography. Analysis of the HRESI mass spectrum revealed a peak at *m/z* 423.1702, assigned to the molecular ion $[C_{27}H_{23}N_2O_4]^+$, demonstrating the substitution of a phenyl group for one oxygen atom, and the addition of an *N*-Boc substituent to the indigo core. Analysis of the ^{1}H spectrum revealed a lone doublet resonance at δ 8.24 which was correlated to the Boc group in the ROESY spectrum, and therefore assigned to H7 (Figure 81). The ^{13}C resonance at δ 191.8 was assigned to C3', which showed a strong three-bond correlation in the HMBC spectrum to the doublet at δ 7.54, assigned to H4'. Using the H7 and H4' protons as entry points to both rings, the remaining proton and carbon environments were assigned from analysis of the COSY (Figure 82), HMBC (Figure 83), and HSQC spectra (Figure 84). The H2"/H6" and H3"/H5" protons of the phenyl substituent were assigned to a pair of multiplets at δ 7.44-7.38 and δ 7.66-7.60, respectively, and H4" was assigned to a multiplet at δ 7.38-7.34. The ^{13}C resonances at δ 128.3, δ 131.0, and δ 122.7 were therefore assigned to carbon atoms C2"/C6", C3"/C5", and C4", respectively, and H3"/H5" showed strong three-bond coupling to a quaternary resonance at δ 128.1 in the HMBC spectrum, and was therefore assigned to C1".

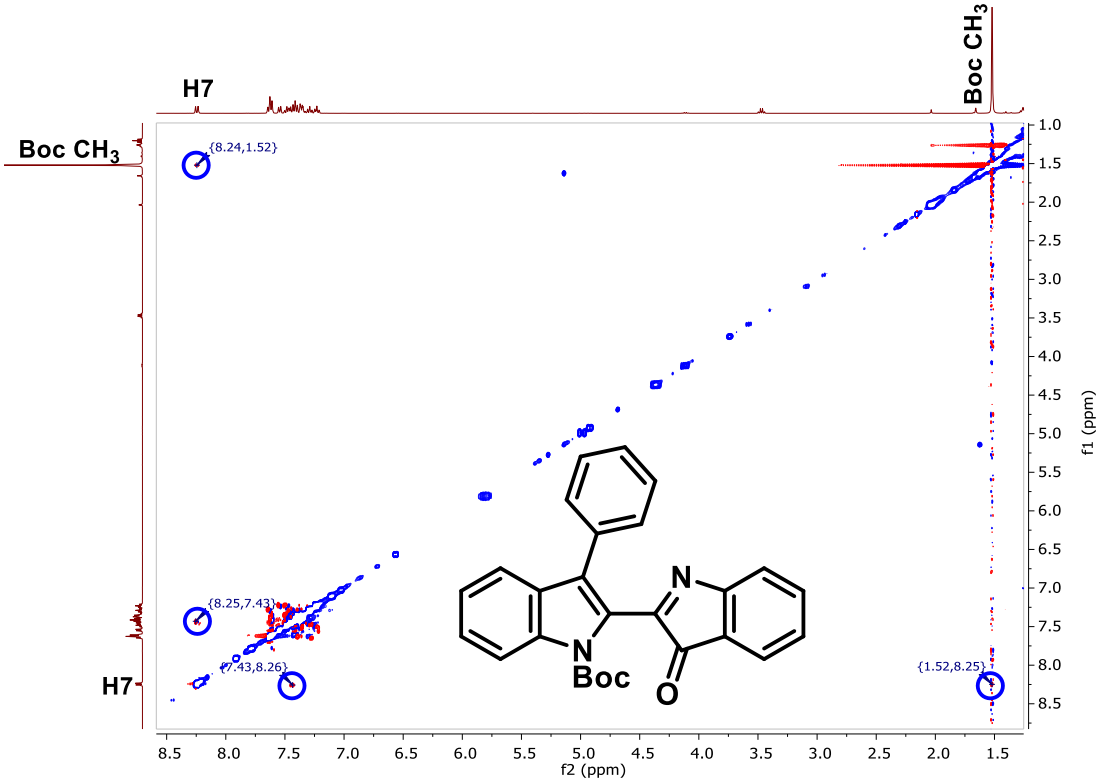

Figure 81: ROESY spectrum for compound **211** with key correlations highlighted.

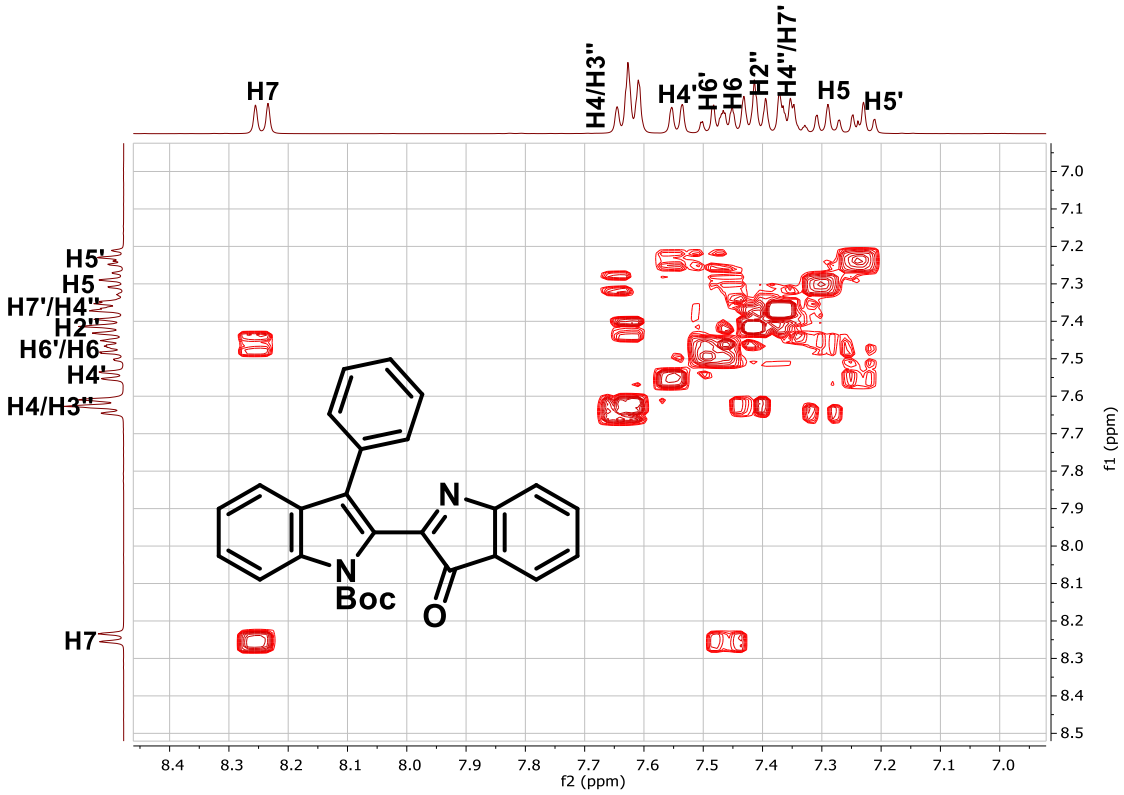

Figure 82: COSY spectrum for compound **211** with assignments.

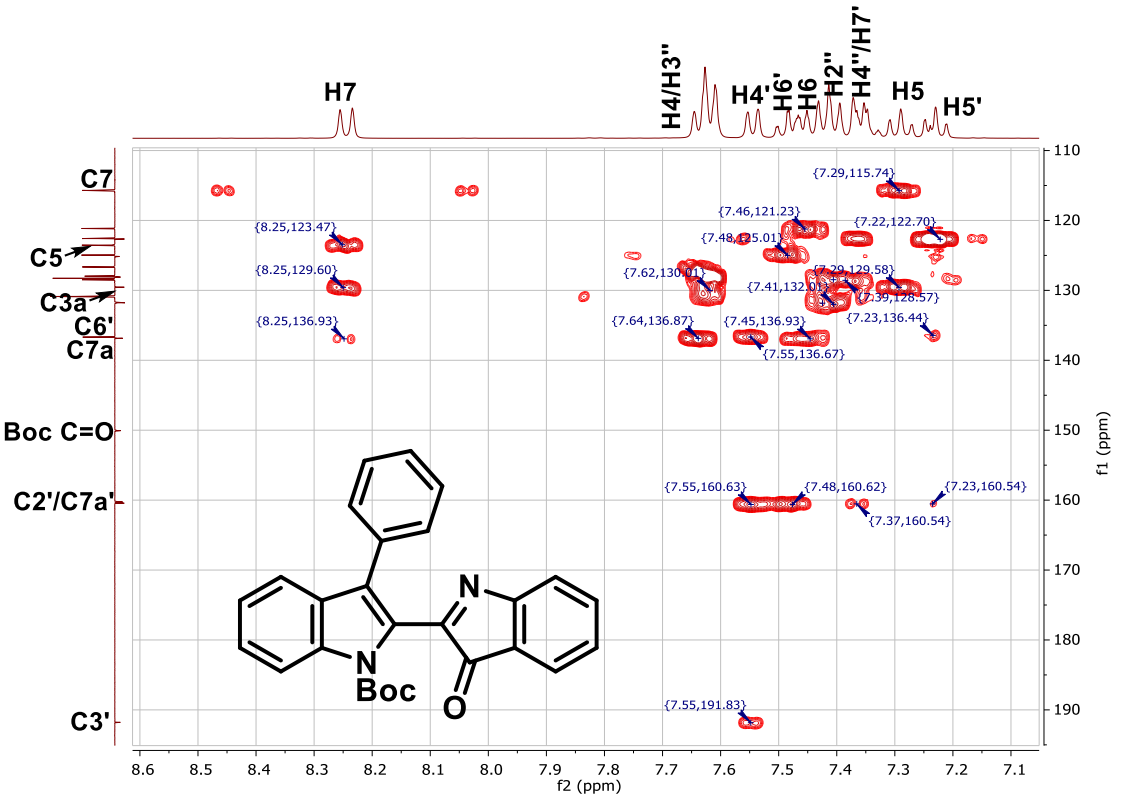

Figure 83: HMBC spectrum for compound **211** with assignments listed.

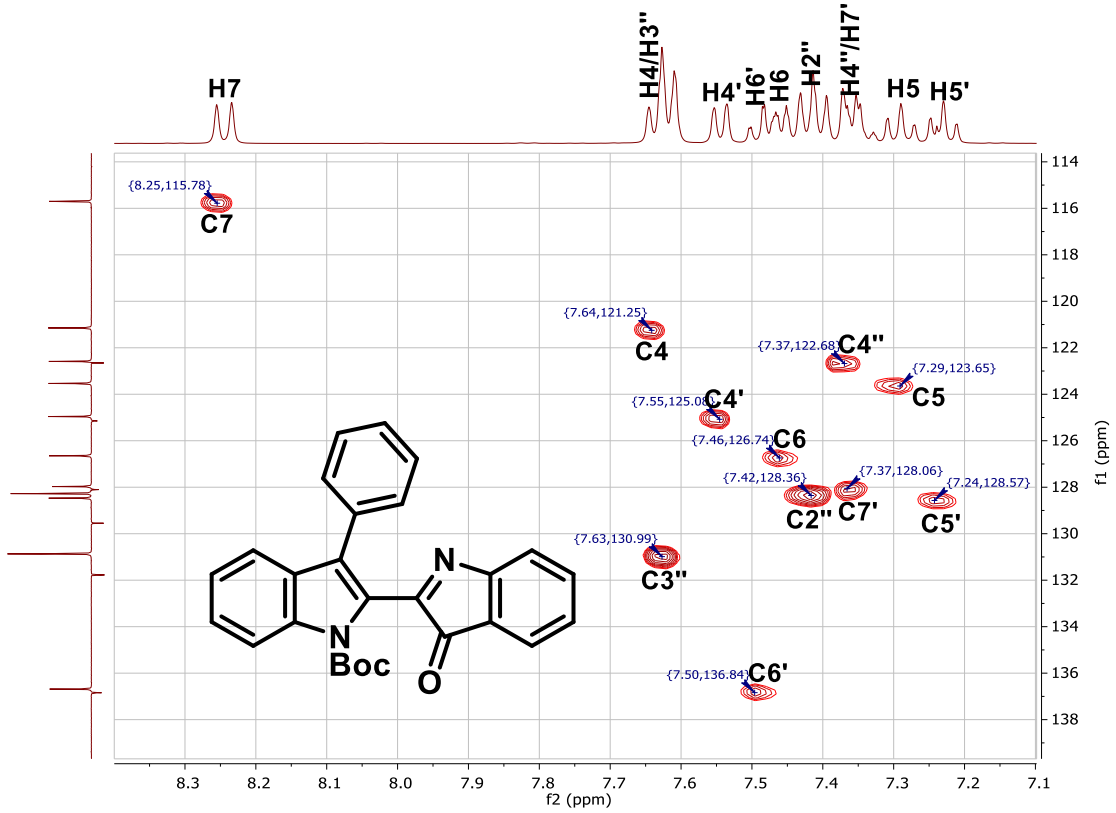

Figure 84: HSQC spectrum for compound **211** with assignments listed.

Large crystals of **211** were grown by slow evaporation of a hexane solution, and its structure was therefore unambiguously determined by x-ray crystallography (Figure 85).[§§§] Of note is the loss of planarity despite the retained conjugation of the system, as a result of the steric repulsion of the *N*-*tert*-butylcarbamate group. The N1-C8-C9-C10 linkage exhibits a dihedral angle of 60.3˚ in the solid state,[166]**** thus preventing orbital overlap and limiting electronic interaction between the 3*H*-indole and 1*H*-indole moieties.

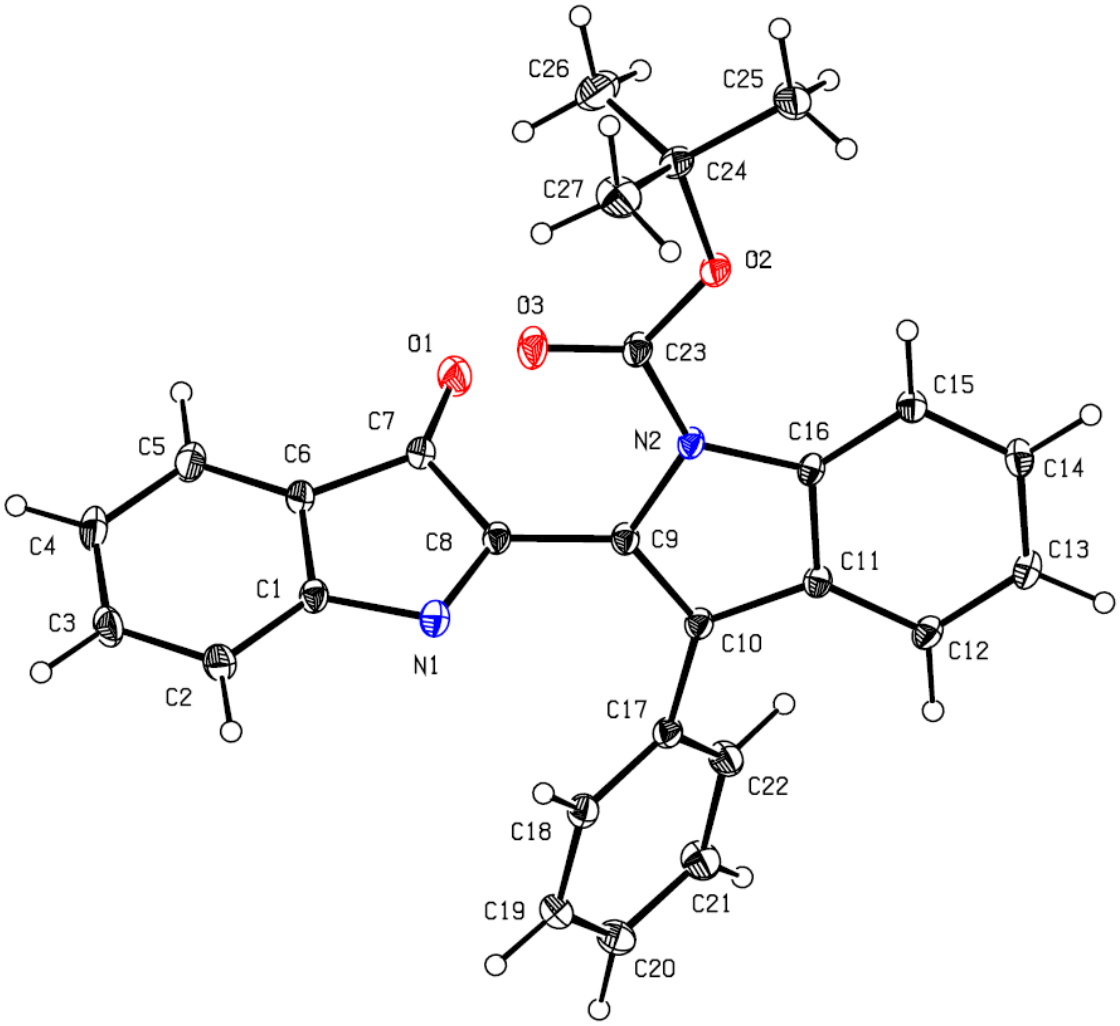

Figure 85: ORTEP depiction of compound **211**. Note that the atom numbers as denoted by x-ray crystallography do not reflect systematic numbering of atom positions.

4.2.2 Reaction optimisation

Despite indigo's poor solubility in THF and the presence of numerous extraneous reagents, the combined 57% yield of Grignard adducts suggested nucleophilic addition of the organometallic species to the indigo core to be highly favourable. Using *i*-PrMgCl.LiCl **191** as a model substrate (5.0 eq.), we sought to optimise the reaction by

[§§§] X-ray crystallography performed by Dr. Anthony Willis (ANU).

[****] Calculated using Mercury v. 3.9, © Cambridge Crystallographic Data Centre.

removing both the competing phenyllithium and the extraneous dibromoammonium salt (**162**) and repeating the reaction under identical conditions in a one-pot setting. We observed complete consumption of the indigo, however despite the presence of excess Boc_2O, dehydration of the intermediate alcohol (**212**) to **209** was sluggish, and only *di*-Boc indigo (**213**) was isolated in 19% yield, as identified by analysis of the LRESI mass spectrum ($M+H^+$ = *m/z* 463^+), comparison of the ^1H NMR and ^{13}C NMR spectra with those previously-reported,[167] and x-ray crystallographic analysis of crystals grown from CH_2Cl_2 (Figure 86).††††

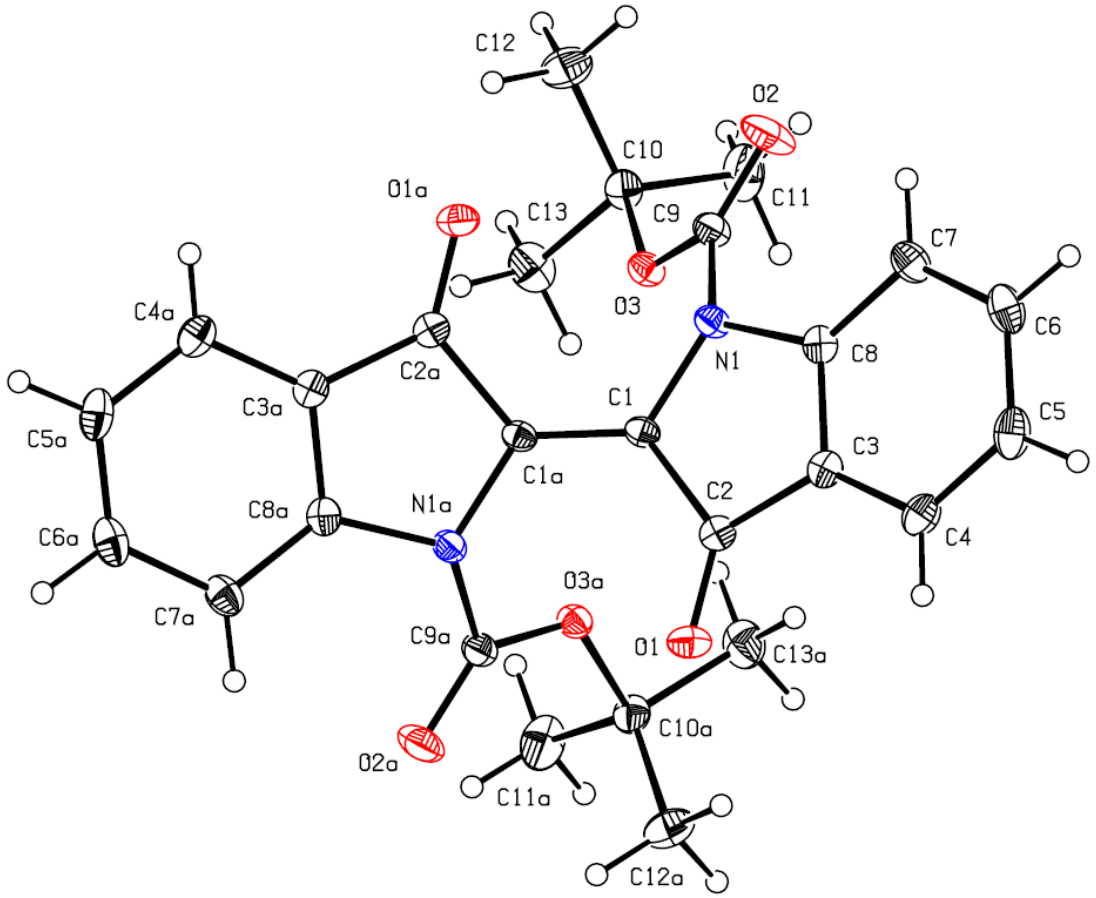

Figure 86: ORTEP depiction of *di*-Boc indigo **213**. Note that the atom numbers as denoted by x-ray crystallography do not reflect systematic numbering of atom positions.

We surmised that the amine's absence may have slowed the rate of dehydration, and thus repeated the reaction in the presence of TMEDA (6.0 eq.), however this gave inconsistent yields ranging 20-40% on repeated attempts, and considerable quantities of the intermediate alcohol remained unreacted, as detected by TLC analysis. Therefore, to determine the best conditions for displacing the oxygen atom, a variety of dehydration

†††† X-ray crystallography performed by Dr. Anthony Willis (ANU).

reactions were trialled on small-scale using the crude isopropyl alcohol adduct (**212**, *ca.* 5 mg), and the outcomes of this are presented in Table 3.

Table 3: Summary of small-scale attempts at dehydration (dehyd.) of isopropyl adduct **212**. Reactions were performed on *ca.* 5 mg of material, and the outcome determined by TLC and/or ESI-MS analysis. Decomposition is denoted as dec.

	Solvent	**Reagent**	**Temp.**	**Dehyd.?**	**Dec.?**
1	MeOH	$HCl_{(aq)}$	Δ	✕	✓
2	MeOH	NaOMe	RT	✕	✓
3	CH_2Cl_2	--	Δ	✕	✕
4	CH_2Cl_2	$BF_3.OEt_2$	RT	✓	✓
5	CH_2Cl_2	$SOCl_2$	RT	✕	✓
6	CH_2Cl_2	MsCl[a]	RT	✓	✓
7	CH_2Cl_2	Boc_2O[b]	RT	✓	✕
8	CH_2Cl_2	$TiCl_4$	RT	✕	✓
9	CH_2Cl_2	$PPh_3.I_2$[c]	RT	✕	✓
10	Toluene	--	Δ	✓	✕
11	Toluene	H_2SO_4	RT	✓	✓
12	Toluene	P_2O_5	RT	✕	✓
13	Pyridine	--	Δ	✕	✓
14	H_2SO_4	--	RT	✓	✓
15	THF	PCl_3	Δ	✕	✓

[a]NEt_3 added [b]DMAP added [c]Imidazole added

Of these trialled conditions, dehydration was observed with $BF_3.OEt_2$ (Entry 4), MsCl/NEt_3 (Entry 6), and H_2SO_4 (Entry 14), however only Boc_2O/DMAP (Entry 7), and heating in toluene (Entry 10) did not lead to significant decomposition. On full-scale (0.5 mmol), attempted dehydration using toluene in the presence of 3 Å molecular sieves showed moderate progression by TLC analysis after heating at reflux for 3 h, however the dehydrated material decomposed after leaving at reflux overnight, and trace products from undesired Wurtz coupling of *i*-PrMgCl.LiCl with 4- or 7-metallated indigo were isolated. We hypothesised that the inconsistency of the one-pot addition/dehydration with Boc_2O may be due to the remaining strongly-coordinating Li^+ or Mg^{2+} ions, which were not present in the small-scale reaction, therefore the reaction was repeated with an additional aqueous workup between the Grignard addition and Boc_2O addition. Treatment with Boc_2O/DMAP in CH_2Cl_2 quickly led to the formation of **210**, which was isolated in 80% yield following flash chromatography (Scheme 77).

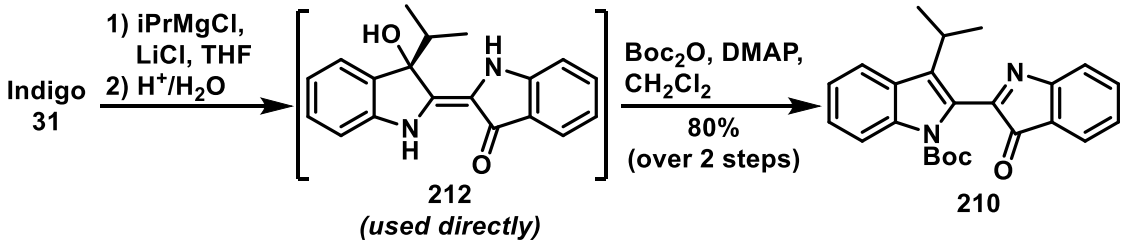

Scheme 77: Optimised reaction outcome for the two-step isopropylation/Boc-mediated dehydration of indigo with *i*-PrMgCl.LiCl (**191**).

Treating indigo with PhMgCl under these conditions gave a combined 92% yield of *N*-Boc phenyl adduct **211** and *N*-H phenyl adduct **214**, and while this yield was somewhat diminished by using PhLi in place of PhMgCl (71%), it suggested that both organolithium and organomagnesium aryl nucleophiles were tolerated in the first instance (Scheme 78). It was later found that the dehydration reaction could be greatly accelerated by the addition of NEt_3, and while this did not lead to an increase in isolated yield, the reaction was typically deemed to be complete within 20 min by TLC analysis.

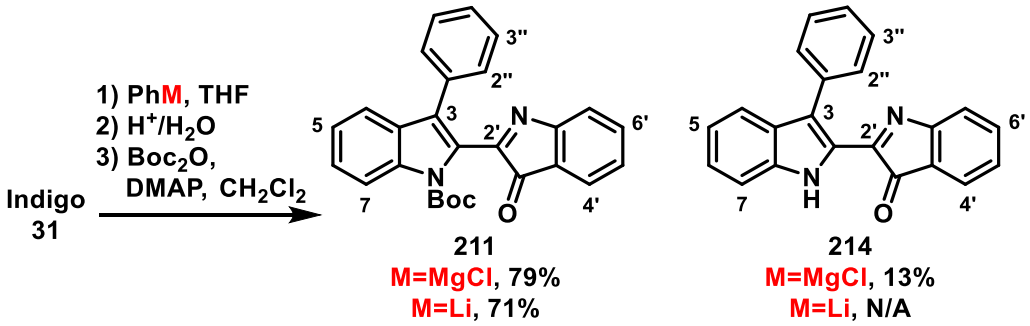

Scheme 78: Reaction of indigo with PhMgCl and PhLi under optimised conditions.

The phenyl adduct **214** was isolated as an intense, dark-purple powder in 13% yield from indigo, following fractionation on silica and subsequent flash chromatography. Analysis of the HRESI mass spectrum revealed a peak at *m/z* 323.1187, assigned to the molecular ion $[C_{22}H_{15}N_2O]^+$, revealing the net substitution of the phenyl group for one oxygen atom, and analysis of the FTIR spectrum revealed a sharp absorbance band at 3370 cm^{-1}, assigned to the N-H stretch. Analysis of the ^1H NMR spectrum revealed a broad singlet resonance at δ 10.25 which exchanged with D_2O and was assigned to the free NH group, and analysis of the ^{13}C NMR spectrum revealed a resonance at δ 196.1, assigned to the C3' ketone group. The considerable degree of overlap of the proton environments made disentanglement of the individual protons difficult, however cross-referencing the HMBC and HSQC spectra for **214** with those acquired for **209** allowed for identification of distinctive ^{13}C resonances at δ 112.0 and δ 137.4, assigned to C7 and C6', respectively

(Figure 87, Figure 88). The phenyl protons H2"/H6", H3"/H5", and H4" were assigned to resonances at δ 7.54, δ 7.70, and δ 7.41, thus allowing assignment of C2"/C6", C3"/C5", and C4" to ^{13}C resonances at δ 128.1, δ 131.0, and δ 127.7.

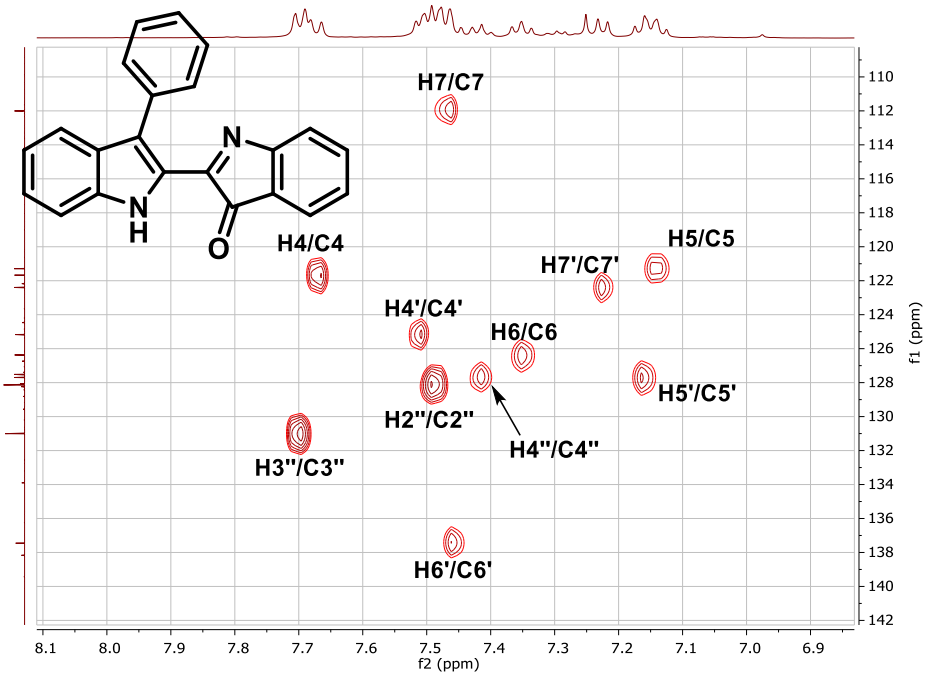

Figure 87: HSQC spectrum for compound **214** with assignments as indicated.

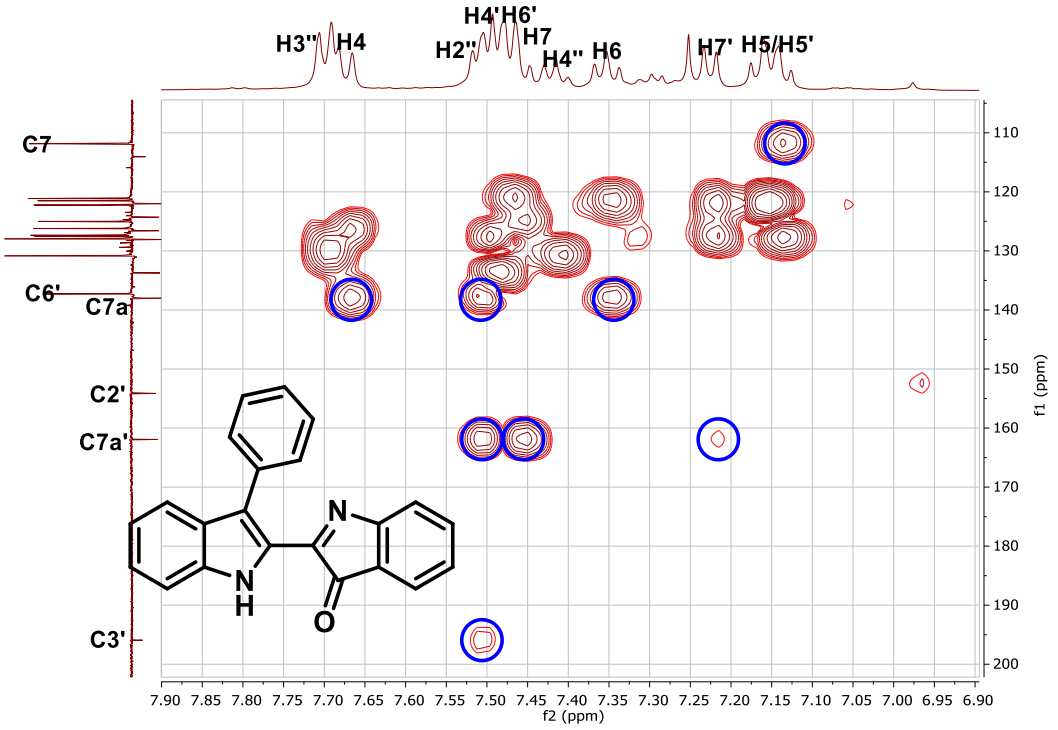

Figure 88: HMBC spectrum for **214** with key assignments highlighted.

4.3 Substrate scope

4.3.1 Substrate scope – alkyl nucleophiles

Having determined the optimal conditions for this reaction, we sought to explore the use of a small selection of simple, commercially-available organometallics. The good yield of isopropyl adduct **210** suggested moderate steric bulk was not detrimental to the reaction, hence a handful of alkyl substituents – namely methyl, allyl, benzyl, and butyl – were selected to generate a selection of small-to-moderate steric impactors. Given the applicability of organolithium reagents to this reaction, we elected to utilise the methyllithium and *n*-butyllithium reagents we had on-hand, activated *in situ* by complexing with TMEDA, while the allylmagnesium bromide and benzylmagnesium chloride solutions were pre-activated by stirring with flame-dried LiCl.

Treating a well-dried suspension of indigo (0.5 mmol) in anhydrous THF with *n*-butyllithium (5.0 eq.) at -84 ˚C in the presence of TMEDA (1.1 eq. based on BuLi) gave an intense dark-red complex which was warmed to room temperature over one hour with vigorous stirring, and stirred at room temperature for a further hour. Aqueous workup afforded a deep golden residue, which was dissolved in CH_2Cl_2, to which DMAP (2.2 eq.), NEt_3 (2.0 eq.), and Boc_2O (3.0 eq.) were added sequentially in air, and the mixture stirred for one hour. Aqueous workup and flash chromatography afforded the *n*-butyl adduct **215** in 80% yield (Scheme 79).

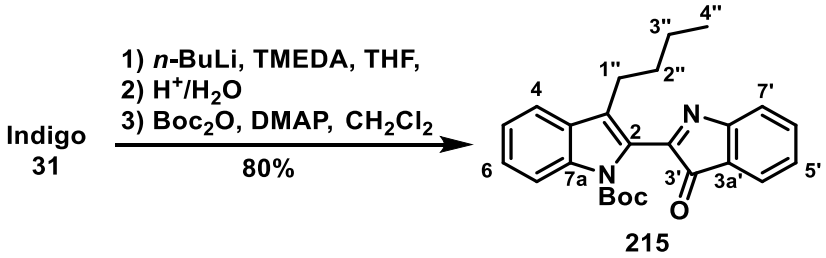

Scheme 79: Synthesis of *n*-butyl adduct **215** from the addition of *n*-BuLi to indigo.

Analysis of the HRESI mass spectrum for **215** revealed a peak at *m/z* 403.2036, assigned to the molecular ion $[C_{25}H_{27}N_2O_3]^+$, demonstrating the net substitution of the butyl moiety for one oxygen atom, and the addition of a Boc group. Analysis of the ^{1}H NMR spectrum revealed the expected eight distinct aromatic resonances, which were assigned on the basis of COSY (Figure 89) and HMBC experiments (Figure 90). Further upfield, four distinct aliphatic multiplets were identified at δ 2.93 (dd), δ 1.70 (dq), δ 1.36 (dq), and δ 0.90 (t), which were assigned to H1", H2", H3", and H4", respectively, based on HMBC, COSY and H2BC analyses (Figure 91). Analysis of the ^{13}C DEPTQ spectrum revealed a

trio of negatively-phased aliphatic resonances at δ 32.7, δ 24.1, and δ 22.6, in addition to a single positively-phased resonance at δ 13.8, which were assigned to C2", C1", C3" and C4" by analysis of the HSQC spectrum (Figure 92).

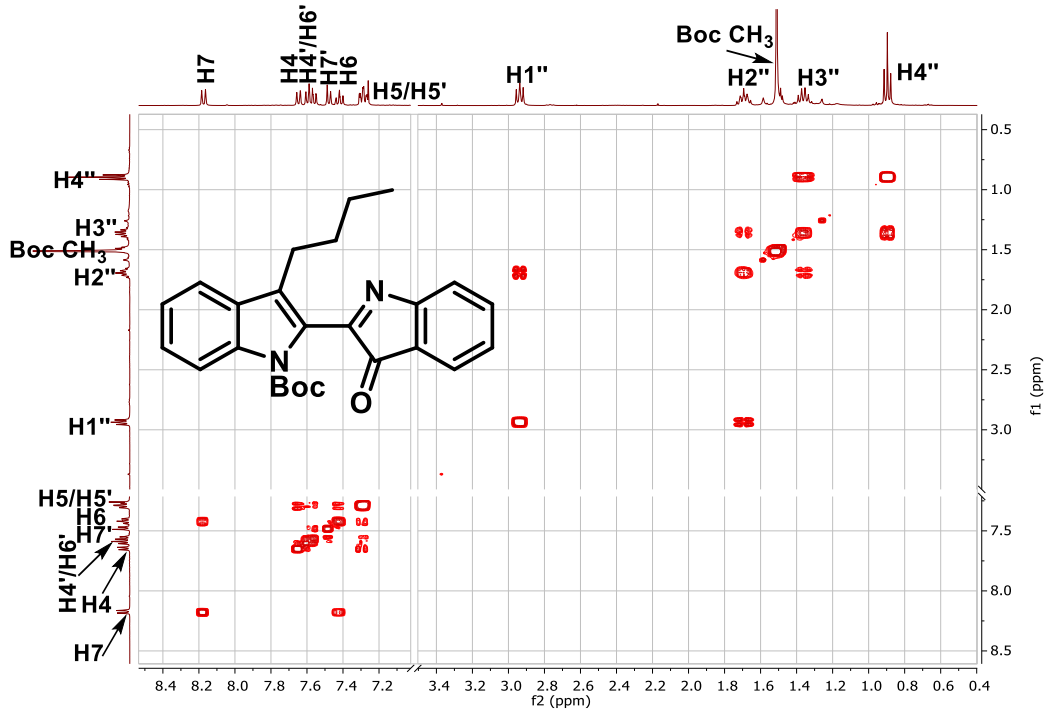

Figure 89: COSY spectrum for compound **215** with assignments as indicated.

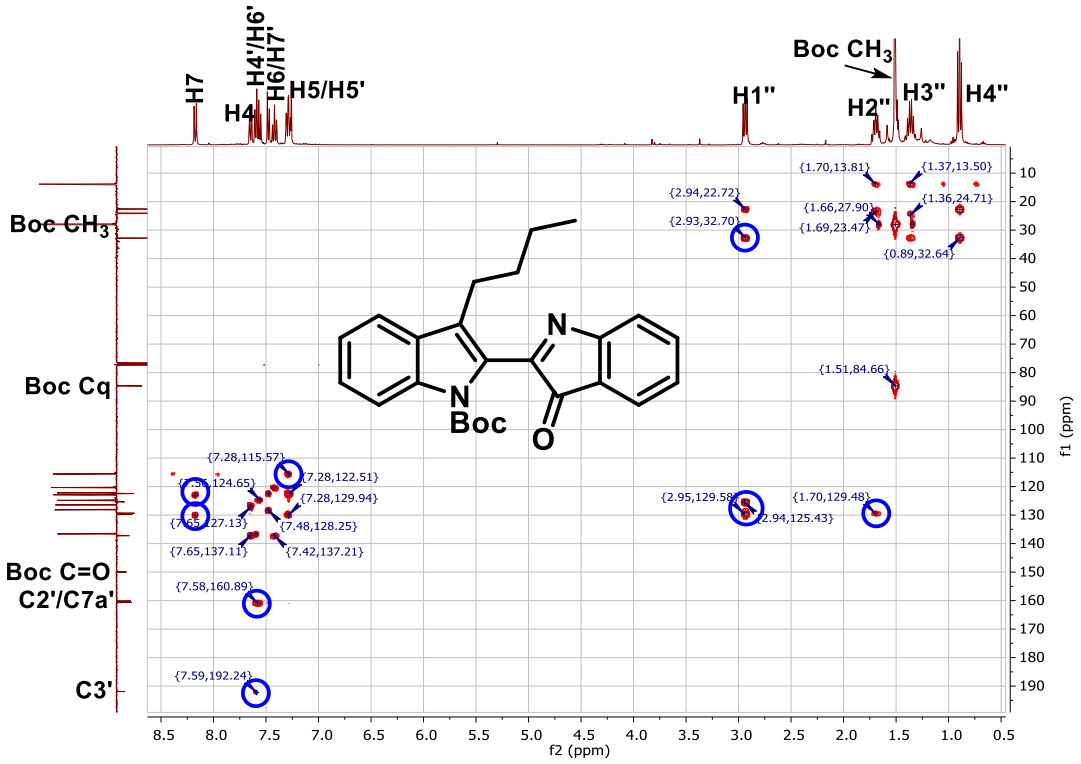

Figure 90: HMBC spectrum for compound **215** with key correlations highlighted.

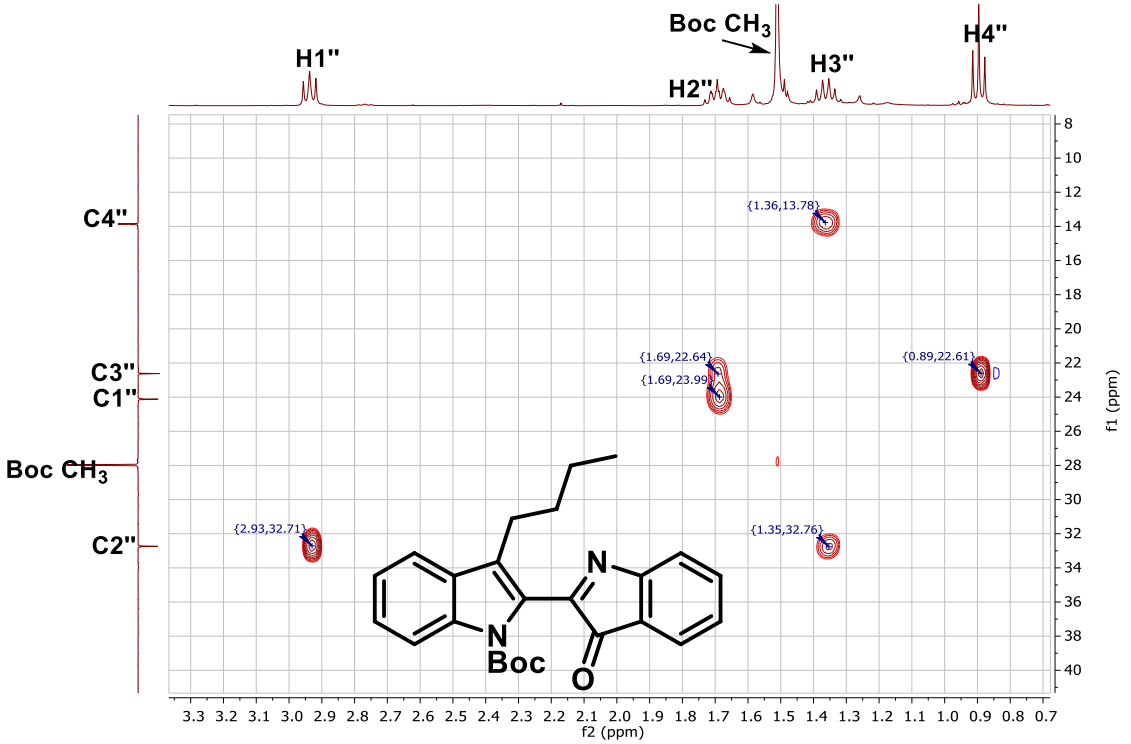

Figure 91: H2BC spectrum for compound **215**, showing two-bond correlations in the aliphatic region, demonstrating the connectivity of the alkyl chain.

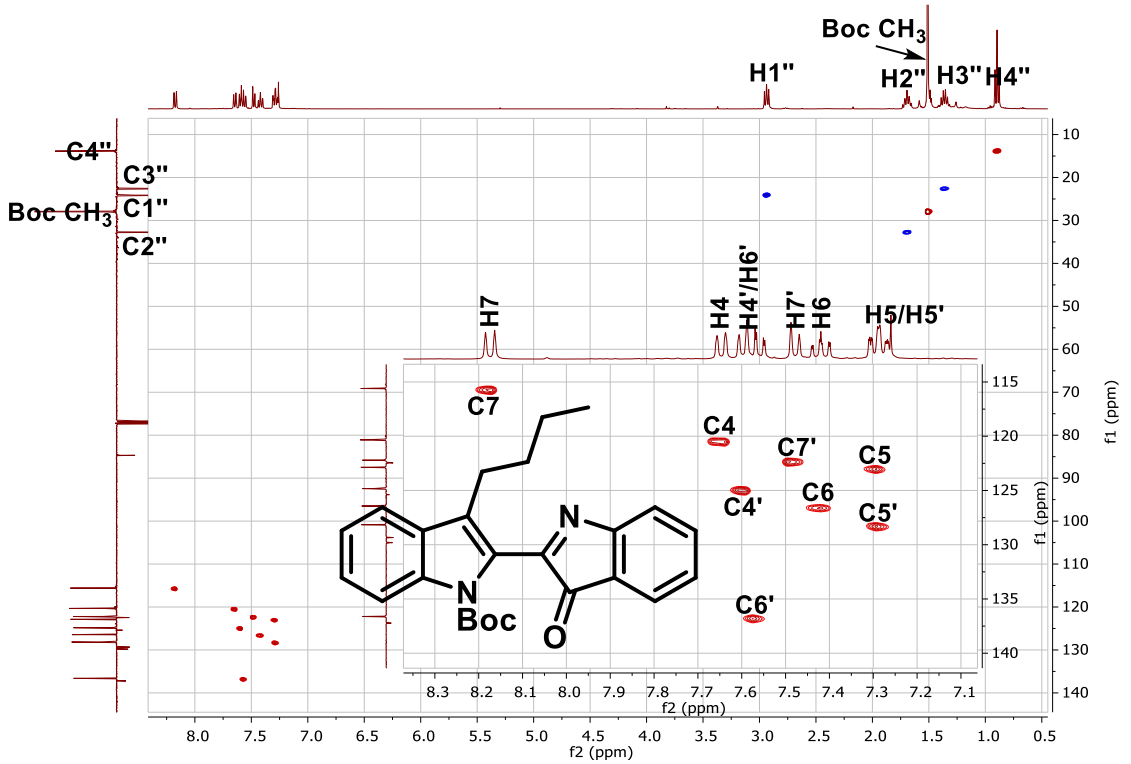

Figure 92: HSQC spectrum for compound **215** with expansion of the aromatic region (inset).

With two aliphatic examples in hand, we aimed toward the synthesis of the *N*-Boc methyl adduct **216** from the substitution of methyllithium to indigo. We quickly found however that the reduced steric effect of the methyl-substituted alcohol **217** precluded dehydration with Boc_2O, and did not lead to the desired product, instead leading to mixtures of *N*-acylated and *O*-acylated materials (Scheme 80). Therefore, a series of small-scale trial reactions were conducted to determine a suitable dehydrating agent for less sterically-encumbered adducts – the outcomes of which are presented in Table 4.

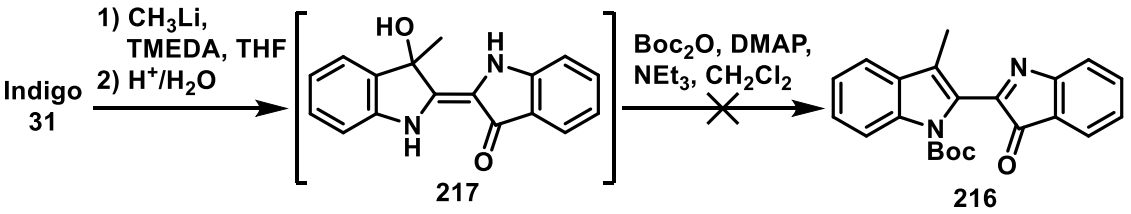

Scheme 80: The attempted dehydration of methyl adduct **217** to **216** using Boc_2O was unsuccessful, and the desired product was not obtained.

Table 4: Summary of small-scale attempts at dehydration (dehyd.) of methyl adduct **217**. Reactions were performed on *ca*. 5 mg of material, and the outcome determined by TLC and/or ESI-MS analysis. Decomposition is denoted as dec.

	Solvent	**Reagent**	**Temp.**	**Dehyd.?**	**Dec.?**
1	MeCN	CF_3COOH	RT	✓	×
2	MeCN	H_2SO_4	RT	✓	×
3	CH_2Cl_2	--	Δ	×	×
4	CH_2Cl_2	$BF_3.OEt_2$	RT	×	✓
5	CH_2Cl_2	$SOCl_2$	RT	×	✓
6	CH_2Cl_2	$MsCl^a$	RT	×	✓
7	CH_2Cl_2	Boc_2O^b	RT	×	✓
8	CH_2Cl_2	$TiCl_4$	RT	×	✓
9	CH_2Cl_2	$PPh_3.I_2{}^c$	RT	✓	×
10	Toluene	--	Δ	✓	✓
11	Toluene	H_2SO_4	RT	✓	✓
12	Toluene	P_2O_5	RT	×	✓
13	Pyridine	$POCl_3$	Δ	×	✓
14	H_2SO_4	--	RT	✓	✓
15	THF	PCl_3	Δ	×	✓

[a]NEt_3 added [b]DMAP added [c]Imidazole added

Of these trialled methods, the three best outcomes were noted in entries 1, 2, and 9, using either TFA or H_2SO_4 in MeCN, or with $PPh_3.I_2$ and imidazole in CH_2Cl_2. Of these, the outcomes for TFA on small-scale could not be replicated on 0.5 mmol scale, and though H_2SO_4 led to decomposition, it afforded the dehydrated adduct **218** in 33% yield over 2 steps. This method however was surpassed by the use of $PPh_3.I_2$/imidazole, which led exclusively to the dehydrated product **218** in 93% yield from **217**, or 74% from indigo over two steps.

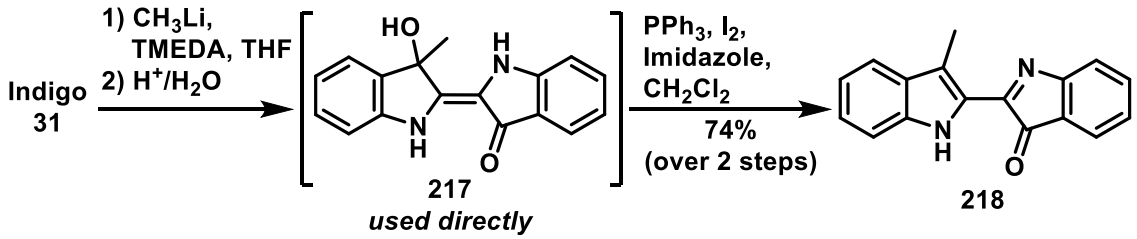

Scheme 81: Synthesis of dehydrated methyl adduct **218** from Appel dehydration of alcohol **217**.

The methyl adduct **218** was isolated as feathery, dark purple crystals in 74% yield from indigo. Analysis of the UV-Vis spectrum (acetone) revealed a pair of broad absorptive bands centred at λ(ε) 326 (8389) and 538 (4881) nM, and FTIR analysis revealed a sharp absorptive band at 3376 cm^{-1}, assigned to a N-H stretch. Analysis of the HRESI mass spectrum revealed a peak at *m/z* 261.1022, assigned to the molecular ion $[C_{17}H_{13}N_2O]^+$, confirming the net substitution of the methyl group for one oxygen atom. Analysis of the ^{1}H NMR spectrum revealed a broad singlet at δ 9.98, assigned to the NH, and a 3H singlet at δ 2.84, assigned to the *pseudo*-benzylic methyl group. Analysis of the ^{13}C NMR spectrum revealed quaternary resonances at δ 196.9 and δ 154.8, assigned to C3' and C2', respectively, and an upfield resonance at δ 11.6, assigned to the methyl group.

The addition of BnMgCl.LiCl to indigo afforded the benzylic adduct **219** in 91% yield, following Boc-mediated dehydration and flash chromatography (Scheme 82). Analysis of the HRESI mass spectrum revealed a peak at *m/z* 437.1880, assigned to the molecular ion $[C_{28}H_{25}N_2O_3]^+$, demonstrating the net substitution of the benzyl group for one oxygen atom, as well as the addition of the *N*-Boc substituent. Analysis of the ^{1}H NMR spectrum revealed thirteen aromatic protons, and a 2H singlet at δ 4.32, assigned to the benzylic methylene group. The characteristic quaternary ^{13}C resonances at δ 191.9, and δ 160.5, and the protic resonance at δ 136.8 were assigned to C3', C7a' and C6' of the 3-oxo-3*H*-indole moiety, and the resonances at δ 150.1, δ 85.1, and δ 28.1 were assigned to the C=O, C_q and CH_3 carbons of the *N*-Boc substituent.

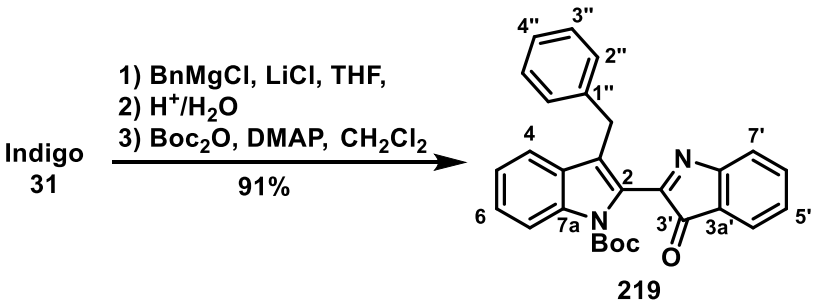

Scheme 82: Synthesis of Boc-protected benzyl adduct **219** from the addition of BnMgCl.LiCl to indigo.

We next turned our attention to allyl adduct **220**, though despite its comparable steric presence to the successful *n*-butyl addition, compound **220** proved evasive due to the low observed reactivity of the lithium-ate complex, and only unreacted starting materials were recovered as *N*-Boc and *N,N'-di*-Boc indigo adducts (Scheme 83). The reason for this low reactivity is unknown, as the precursor allylmagnesium bromide solution was titrated immediately prior to its use, however given the water sensitivity and hygroscopic nature of lithium-ates, trace water or oxygen in the nitrogen line, the LiCl salt or the THF solvent may have prematurely quenched the reagent. The comparatively-lower reactivity of organomagnesium bromides (*cf.* organomagnesium chlorides) is known, however under these circumstances, this does not sufficiently explain its poor reactivity, and requires further exploration.

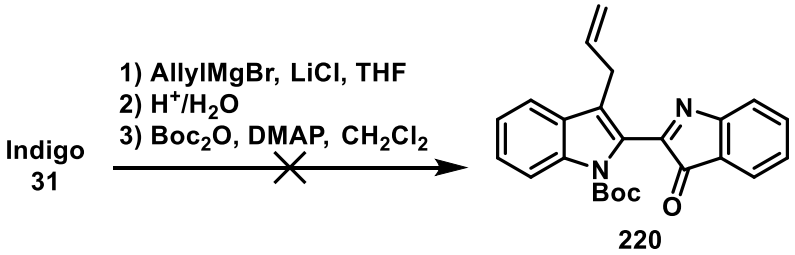

Scheme 83: Unsuccessful attempted allylation of indigo with allylmagnesium bromide to give **220**. Compound **220** was not detected, and only unreacted starting materials were recovered.

4.3.2 Substrate scope – aryl nucleophiles

Having determined that aryl and alkyl Grignard reagents can be readily inserted into the indigo core, we sought to explore the accessible space from metal-halogen insertion, to generate substituted aryl Grignard reagents. We initially chose 4-iodoanisole as a model substrate for magnesium-halogen exchange using *i*-PrMgCl (**190**) as the metal donor, and adapting conditions reported previously for the *in situ* preparation of complex **221**, where the metal-halogen insertion was performed using a 10% molar excess of **190** at room temperature for 1 h.[168] Under these conditions, a 41% yield of the desired 4-

methoxyphenyl adduct **222** was isolated, in addition to the undesired isopropyl adduct **210**. This insertion step was optimised by use of excess iodoanisole (1.25 eq.), the addition of LiCl (1.25 eq.), and extending the reaction time to 1.5 h to encourage the complete consumption of *i*-PrMgCl. Under these modified conditions, an improved 72% yield of **222** was obtained, in addition to the isopropylated **210**, isolated in 11% yield (Scheme 84).

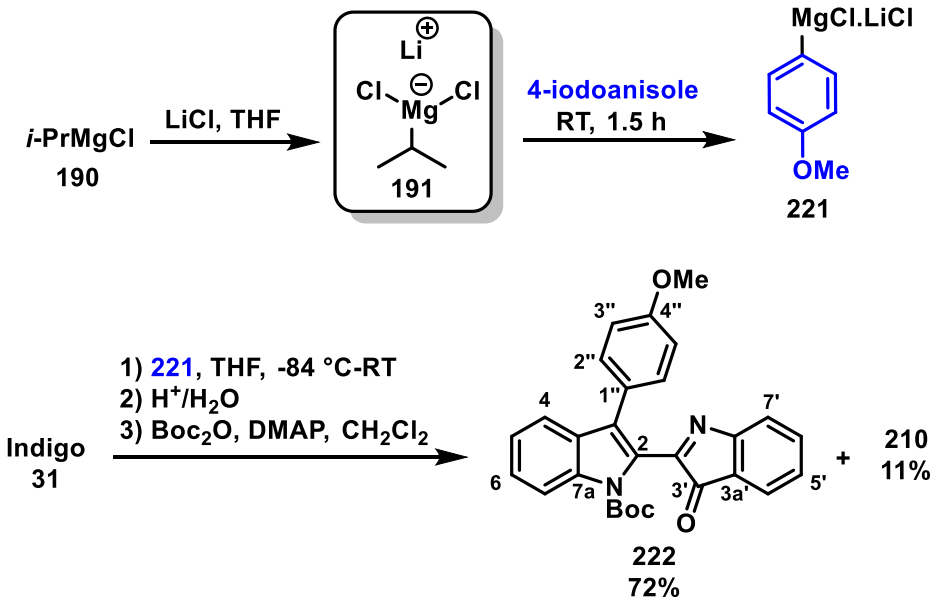

Scheme 84: Optimised conditions for the synthesis of *p*-methoxyphenyl adduct **222** from indigo.

The *para*-methoxyphenyl adduct **222** was isolated as a bright-orange powder in 72% yield from indigo. Analysis of the HRESI mass spectrum revealed a peak at *m/z* 453.1807, assigned to the molecular ion $[C_{28}H_{25}N_2O_4]^+$, revealing the net substitution of one oxygen atom for the anisole moiety, and the addition of an *N*-Boc substituent. Analysis of the ^{1}H NMR spectrum revealed a pair of 2H doublet resonances at δ 7.59 and δ 6.96, and a 3H singlet at δ 3.83, assigned to H2"/H6", H3"/H5", and the pendant methoxy substituent of the newly-incorporated aryl ring, respectively. H2"/H6", H3"/H5" and the methoxy protons all showed strong correlations in the HMBC spectrum to a quaternary ^{13}C resonance at δ 159.5, assigned to C4" (Figure 93). H3"/H5" also correlated to a resonance at δ 124.0, assigned to C1", and H2"/H6" showed a correlation to a resonance at δ 128.0, assigned to the indole C3. Further downfield, the resonance at δ 191.9 was assigned to C3', and showed HMBC correlation to the doublet resonance at δ 7.55 *via* three bonds, assigned to H4'. The chemical shifts of C2" and C3" were determined by HSQC analysis, and were assigned to the resonances at δ 132.2 and δ 113.7, respectively (Figure 94).

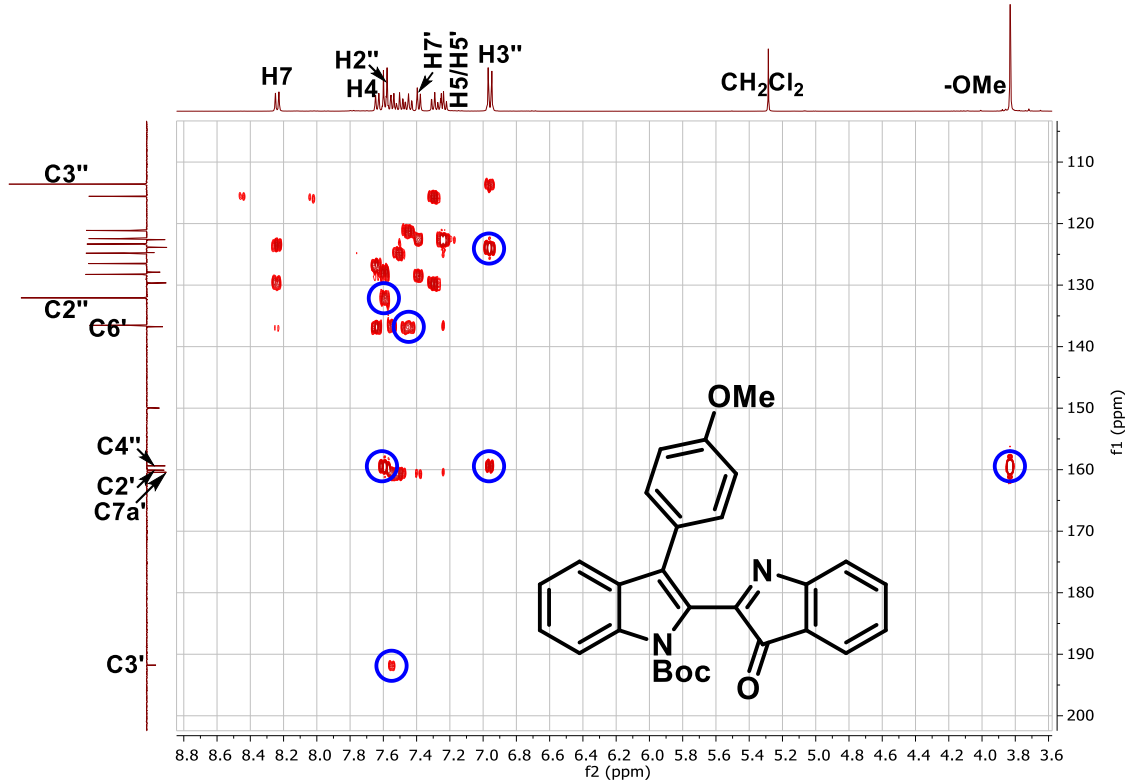

Figure 93: HMBC spectrum for compound **222** with key assignments highlighted.

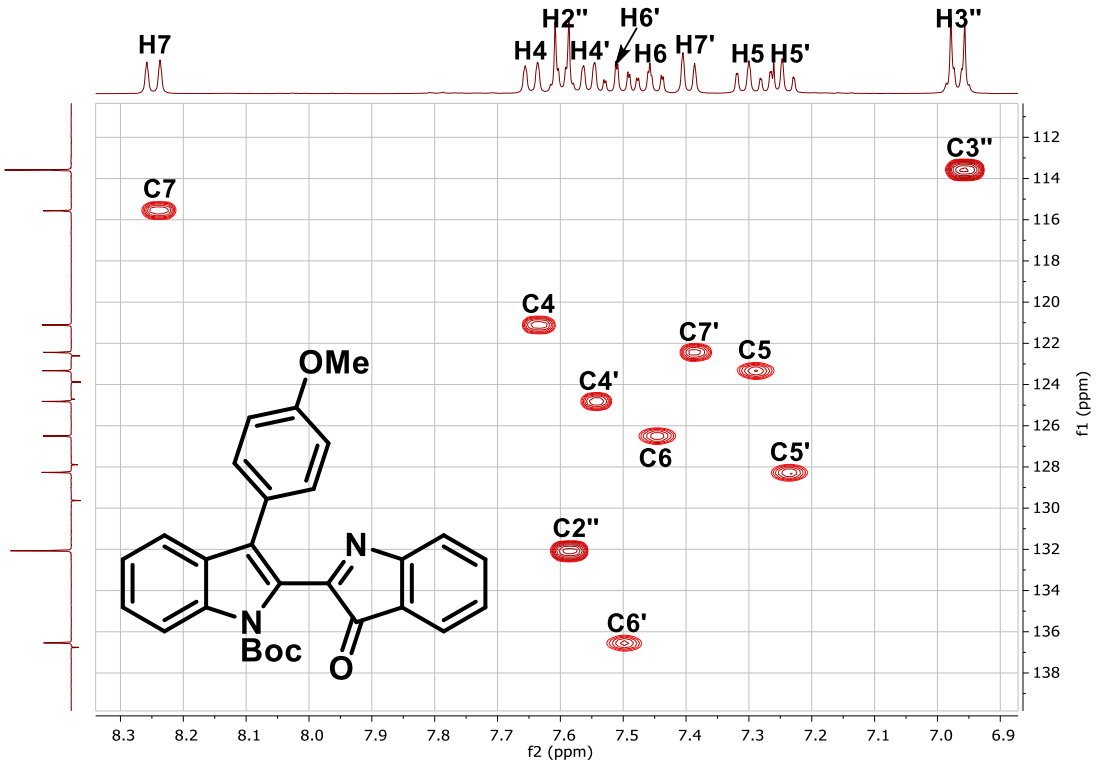

Figure 94: HSQC spectrum for compound **222** with assignments as indicated.

The *meta*-methoxy **223** and *ortho*-methoxy **224** adducts were prepared *via* identical means, and were isolated in 72% yield and 94% yield, respectively (Scheme 85). The considerably-higher yield of the *ortho*-methoxy adduct **224** is here attributed to the favourable interaction of a lone pair from the methoxy group of 2-iodoanisole **225** and the *i*-PrMgCl.LiCl complex **191**, with the formation of the Lewis acid-base pair **226** stabilising the interaction between the magnesium atom and the adjacent aryl iodide, increasing the probability of orbital overlap and eventual metalation of the C-I bond.

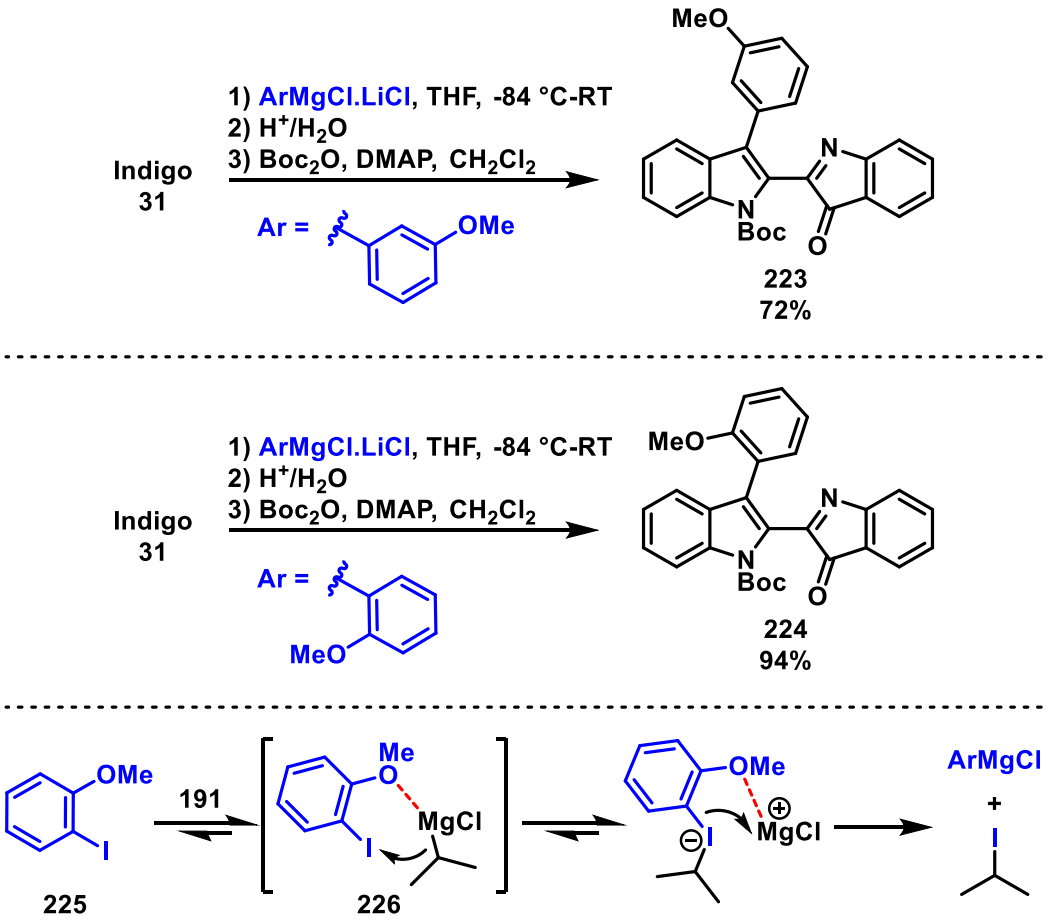

Scheme 85: Synthesis of the *meta*- and *ortho*-methoxy substituted adducts **223** and **224** from indigo under optimised conditions, and mechanism for the *ortho*-assisted metalation of 2-iodoanisole, with Li^+ and Cl^- ions omitted for clarity.

Monoclinic crystals of **224** were grown by evaporation of a saturated CH_2Cl_2/hexane solution, and its structure confirmed by x-ray crystallography (Figure 95).[‡‡‡‡] Interestingly, relative to the unsubstituted phenyl **211**, the magnitude of the dihedral angle of the two indole hemispheres was reduced from 60.3˚ (**211**) to 55.3˚ (**224**), possibly due

[‡‡‡‡] X-ray crystallography performed by Dr. Anthony Willis (ANU).

to orbital interactions between C3' and the nearby oxygen of the methoxy group, which were separated by a distance of 3.01 Å in the crystalline matrix.[§§§§]

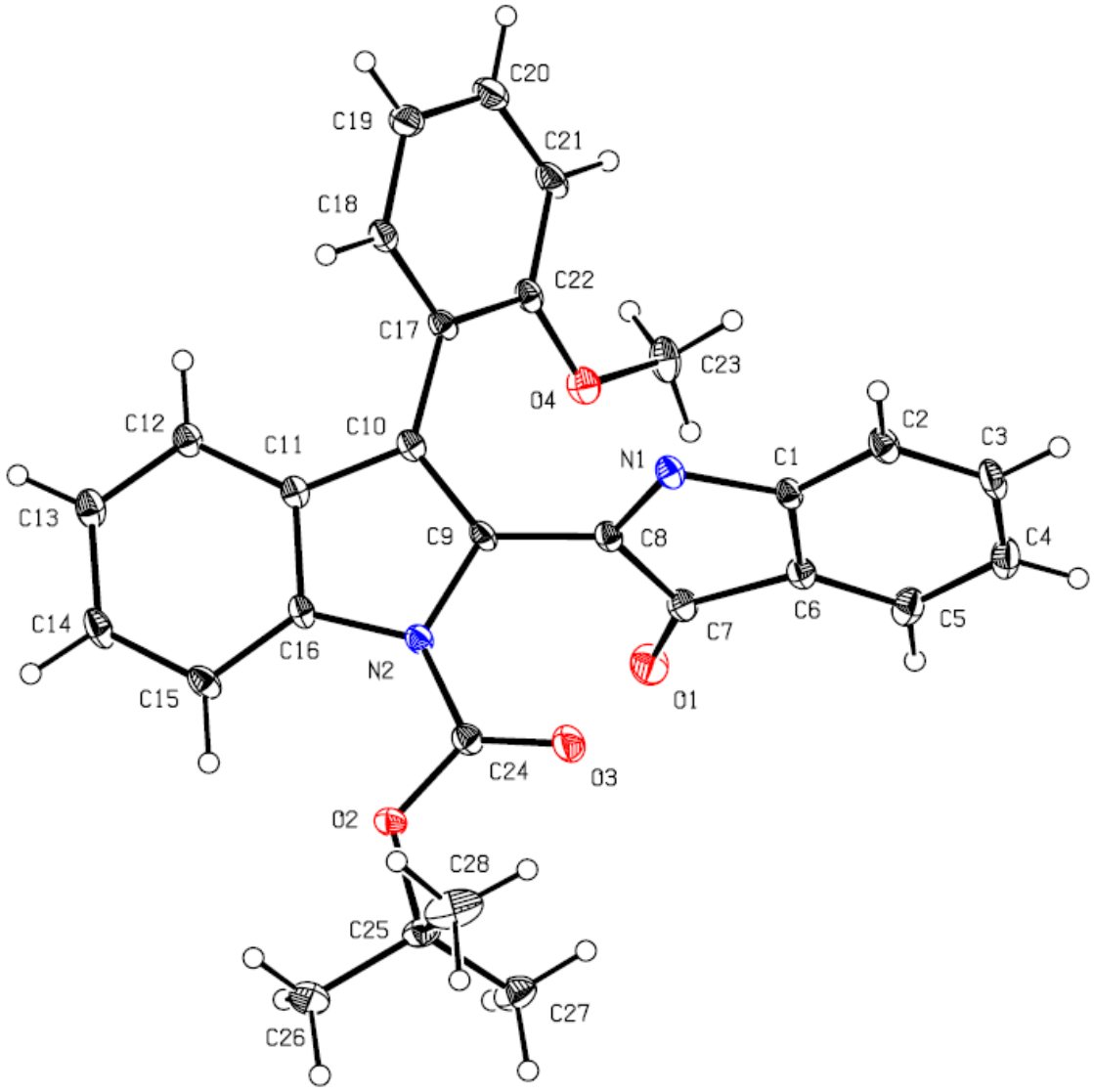

Figure 95: ORTEP depiction of compound **225**. Note that the atom numbers as denoted by x-ray crystallography do not reflect systematic numbering of atom positions.

To determine whether di-substituted aryl Grignard reagents were tolerated, 1-iodo-2,4-dimethoxybenzene (**227**) was metalated with *i*-PrMgCl.LiCl (**191**) at 0 ˚C for 2 h, and the resulting Grignard reagent combined with indigo. Subsequent Boc-mediated dehydration afforded the desired 2,4-dimethoxyphenyl adduct **228** in 72% yield as a deep orange powder (Scheme 86). Analysis of the HRESI mass spectrum revealed a peak at *m/z* 483.1914, assigned to the molecular ion $[C_{29}H_{27}N_2O_5]^+$, demonstrating the net substitution of the dimethoxyphenyl group for one oxygen atom, and the incorporation of the *N*-Boc group. Analysis of the ^{1}H NMR spectrum revealed a pair of 3H singlets at δ

[§§§§] Calculated using Mercury v. 3.9, © Cambridge Crystallographic Data Centre.

3.83 and δ 3.36, assigned to the C4"-adjacent and C2"-adjacent methoxy groups, respectively. The 1H doublet at δ 6.40 had a coupling constant of $^{4}J_{H3"\text{-}H5"}$ = 2.4 Hz, indicative of *meta*-coupling to the doublet of doublets at δ 6.63, and these resonances were assigned to H3" and H5" of the aryl substituent, respectively. Analysis of the COSY spectrum revealed coupling of H5" to part of an overlapped 2H multiplet at δ 7.50-7.45, which HSQC experiments revealed was due to the incidental overlap of two aryl carbons at δ 132.5 and δ 136.5, assigned to C6" and C6', respectively. Interestingly, H3" overlapped with a minor resonance which appeared to show COSY correlations to an extraneous resonance at δ 7.29 (Figure 96), which correlated weakly in the HSQC spectrum to a ^{13}C resonance at δ 128.9 (Figure 97). This was attributed to the hindered rotation about the C3-C1" biaryl axis due to the presence of three *ortho*-substituents, giving rise to major and minor rotamers in equilibrium.[151, 169] The extraneous resonances at ^{1}H δ 7.29 and ^{13}C δ 128.9 were therefore assigned to H6" (min) and C6" (min), respectively. This assignment was also supported by the presence of additional HSQC correlations of H4 and H5 to weak ^{13}C resonances at δ 123.1 and δ 126.1, assigned to C4 (min) and C5 (min) respectively. This suggests that the orientation of the overhanging aryl group has an appreciable deshielding effect on the chemical shift of the adjacent C4 and C5 positions of the indole in **228**, however this phenomenon was not observed for any other Grignard reagents examined.

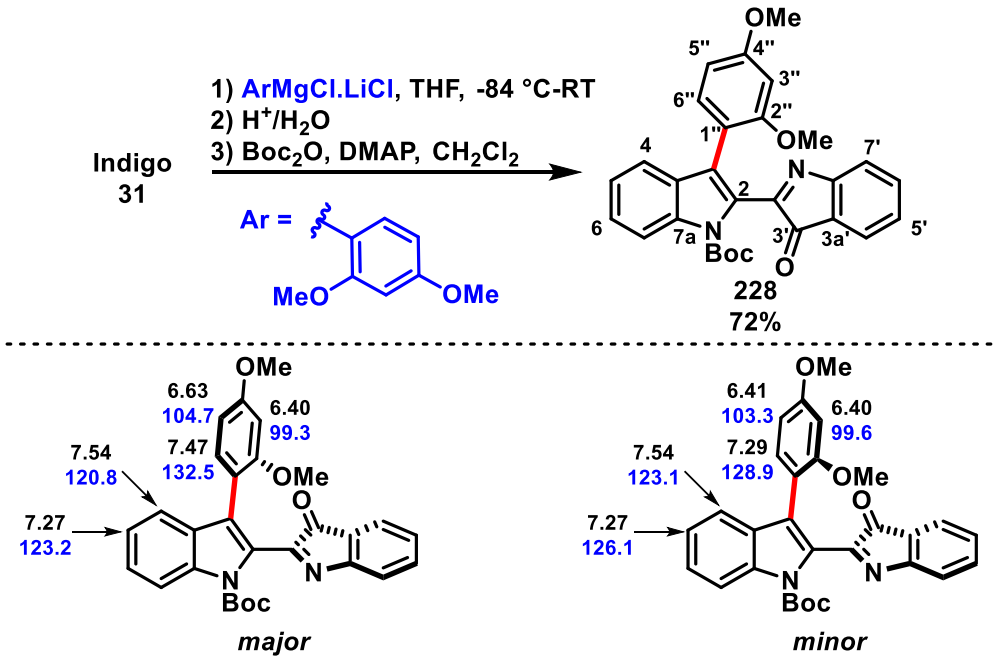

Scheme 86: Synthesis of dimethoxyphenyl adduct **228**, with the biaryl axis highlighted in red. Below are depicted the proposed major (where the C3' carbonyl and C2" methoxy are *syn*) and minor (where the C3' carbonyl and C2" methoxy are *anti*) rotameric conformations, and the ^{1}H (black) and ^{13}C (blue) chemical shifts for the affected positions.

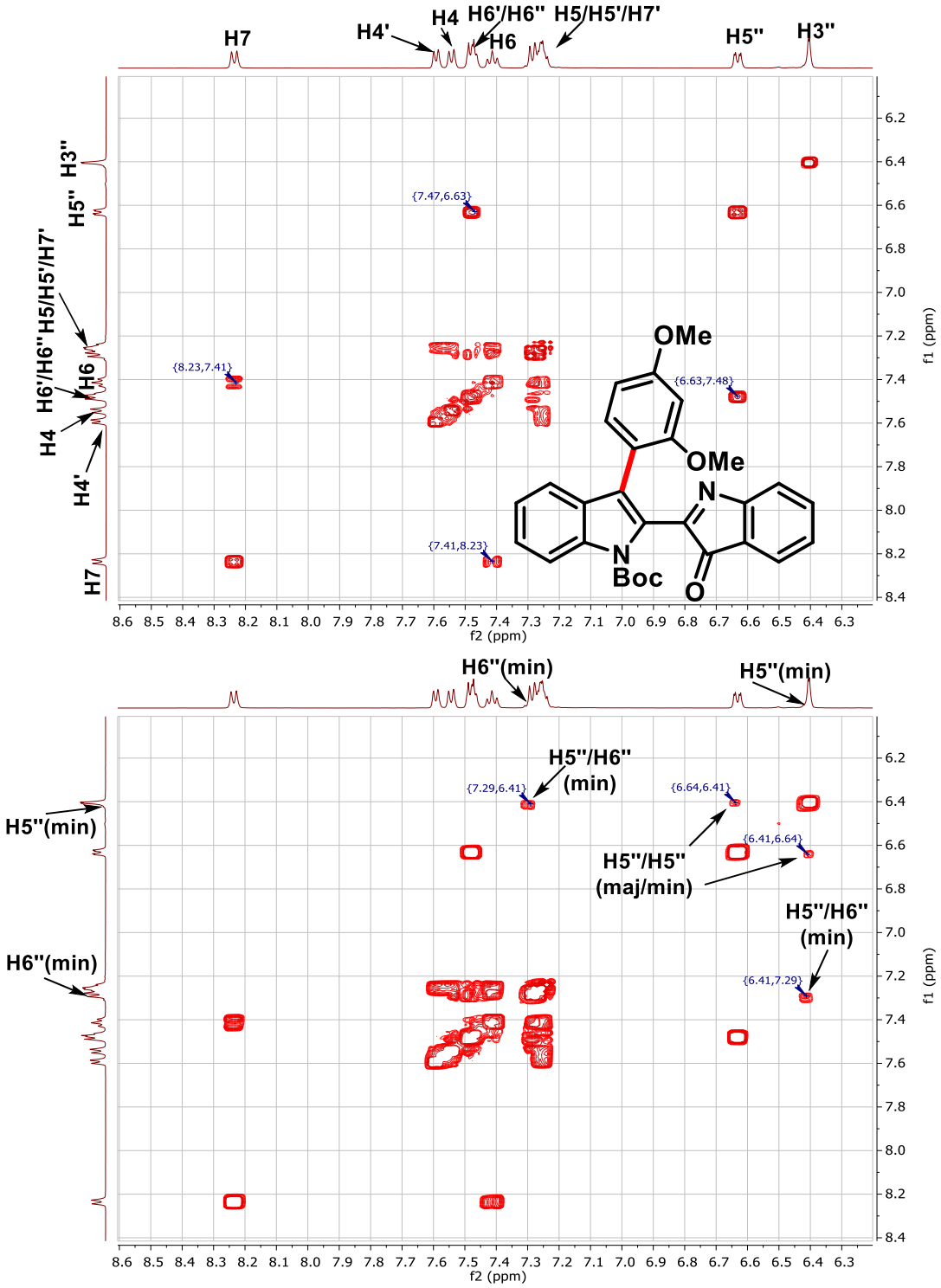

Figure 96: COSY spectrum of compound **228** at low (top) and high (bottom) intensities, showing the appearance of additional peaks corresponding to the minor rotamer.

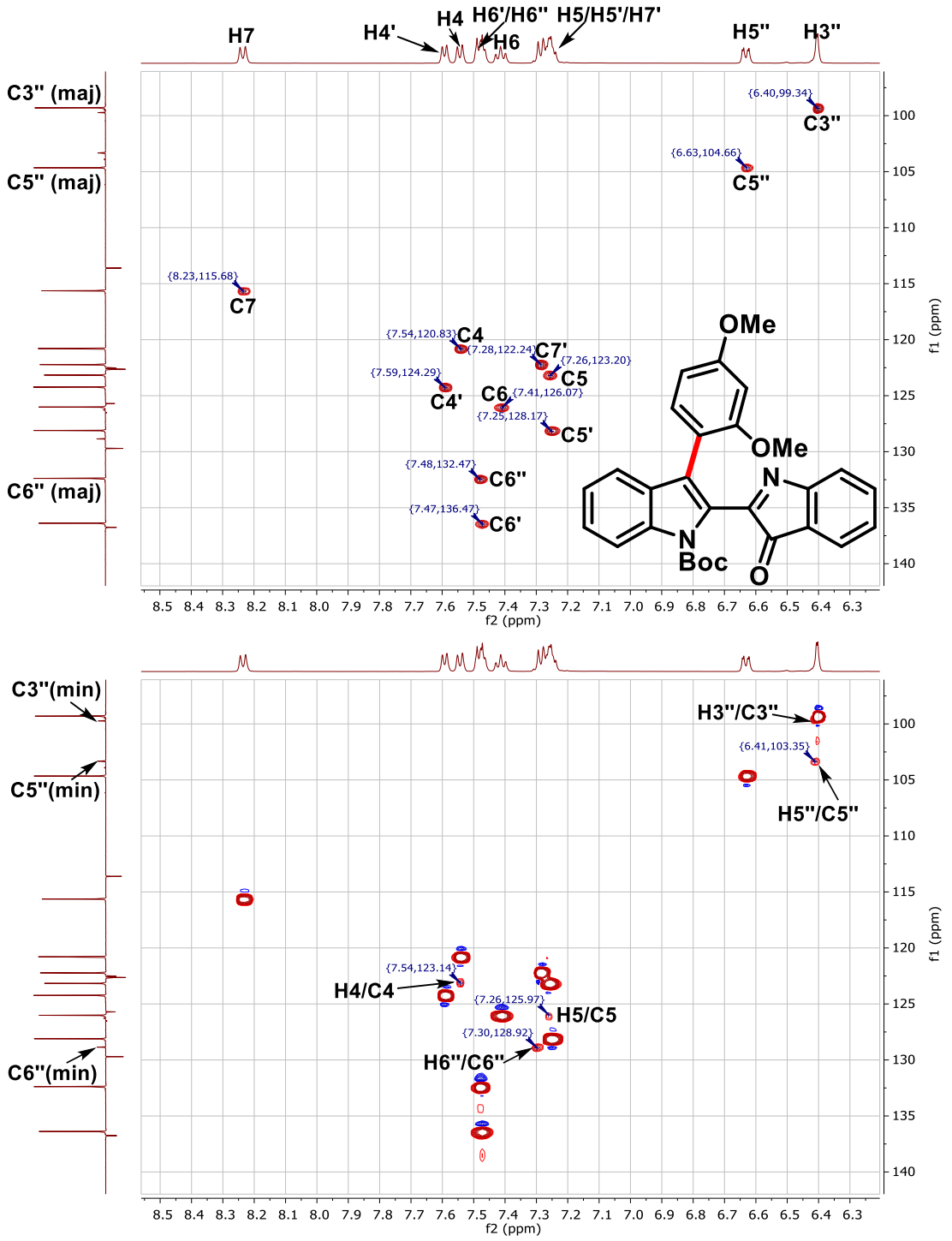

Figure 97: HSQC spectrum of compound **228** at low (top) and high (bottom) intensities, showing the appearance of additional peaks corresponding to the minor rotamer.

Next, the incorporation of halogenated substrates was investigated. Therefore, using *para*-fluoroiodobenzene (**229**) and *ortho*-chloroiodobenzene (**230**) as coupling partners, the corresponding fluorinated **231** and chlorinated **232** adducts were isolated in good yields (Scheme 87).

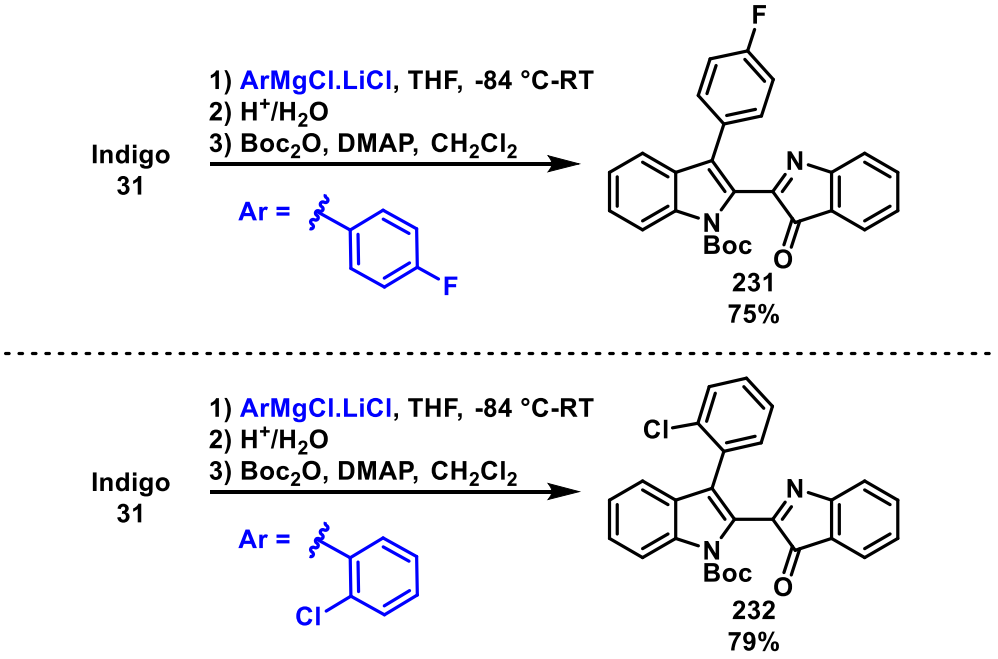

Scheme 87: Synthesis of halogenated desymmetrised diindoles **231** and **232** from their corresponding halogenated Grignard reagents.

Analysis of the HRESI mass spectrum for the fluorophenyl adduct **231** revealed a peak at *m/z* 441.1608, assigned to the molecular ion $[C_{27}H_{22}N_2O_3F]^+$, demonstrating the net substitution of the fluorophenyl moiety for an oxygen atom, and the addition of the *N*-Boc group, and the ^{1}H-decoupled ^{19}F spectrum revealed a single resonance at δ -114.0, typical of the aryl C-F moiety. Characteristic ^{19}F-^{13}C spin-coupling was also apparent in the ^{13}C NMR spectrum, causing splitting of the C4" ($^1J_{C\text{-}F}$ = 248.2 Hz), C3" ($^2J_{C\text{-}F}$ = 21.3 Hz), C2" ($^3J_{C\text{-}F}$ = 8.1 Hz) and C1" ($^4J_{C\text{-}F}$ = 2.5 Hz) resonances, in decreasing magnitude as the C-F distance increased.

Analysis of the HRESI mass spectrum for the chlorophenyl adduct **232** revealed a 3:1 ratio of two peaks at *m/z* 457.1313 and 459.1285, assigned to the isotopic molecular ions $[C_{27}H_{22}N_2O_3{}^{35}Cl]^+$ and $[C_{27}H_{22}N_2O_3{}^{37}Cl]^+$, confirming the insertion of the chlorophenyl moiety and the addition of the *N*-Boc group. The x-ray crystal structure for **232** additionally revealed a dihedral angle of 44.5˚ and an intramolecular Cl···C3' distance of 3.54 Å (Figure 98).[*****]

[*****] Calculated using Mercury v. 3.9, © Cambridge Crystallographic Data Centre.

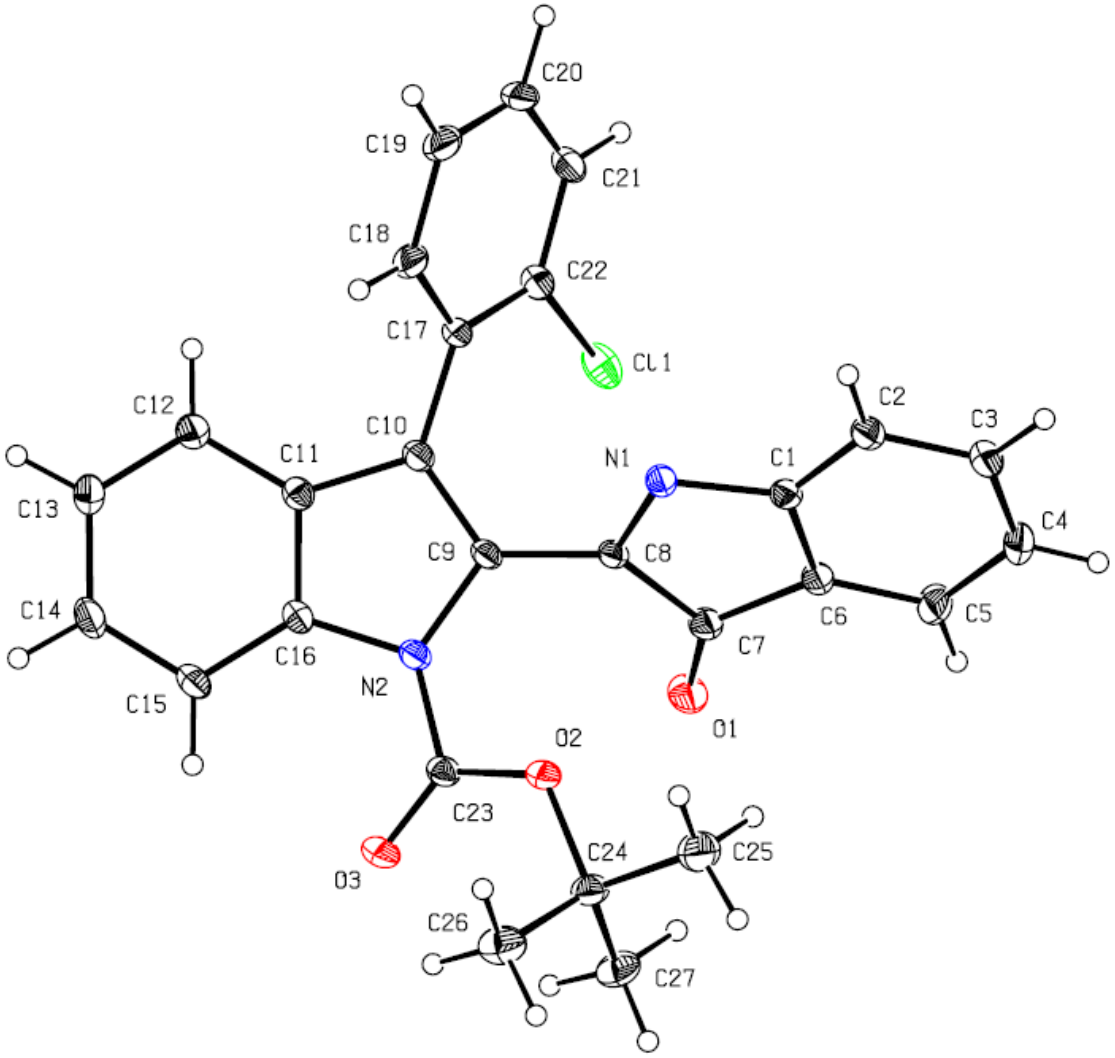

Figure 98: ORTEP depiction of compound **232**. Note that the atom numbers as denoted by x-ray crystallography do not reflect systematic numbering of atom positions.

4.3.3 Substrate scope – heterocyclic nucleophiles

To assess the applicability of heterocyclic substrates to this transformation, we selected five simple heterocycles containing a variety of N, O, and S heteroatoms – pyridyl, *N*-methylimidazolyl, thiophenyl, benzofuranyl, and *N*-methylindolyl moieties were selected to determine whether these were tolerated by the reaction. The magnesium-iodine exchange reaction of 3-iodopyridine was therefore initially investigated as a direct 3-aza analogue of the phenyl system. Early difficulties were encountered where, despite the use of scrupulously-anhydrous conditions, distilled and dried solvent and meticulously-purified starting materials, the generated Grignard reagent was rendered inactive by the presence of water, resulting in the exclusive isolation of unreacted indigo. Systematic troubleshooting of each component in the closed system determined that despite the efficacy of the gas drying tube (assessed using self-indicating desiccant in the tube), the

in-house nitrogen gas line still contained sufficient water to prematurely quench the generated Grignard reagent. Gratifyingly, repeating the reaction under identical conditions – except for the addition of a second drying tube containing activated $CaCl_2$ to the nitrogen line – afforded exclusively the desired 3-pyridyl diindole **233** in 89% yield (Scheme 88).

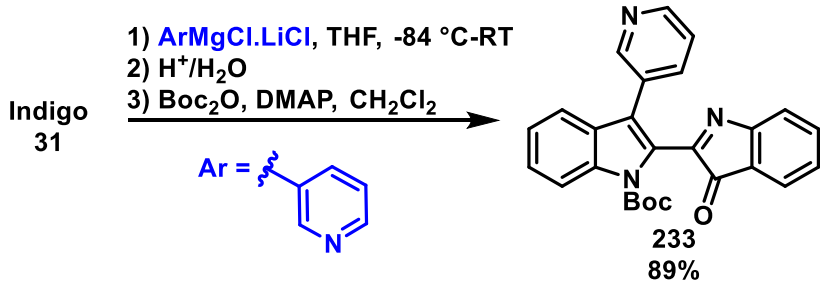

Scheme 88: Synthesis of the 3-pyridyl-substituted diindole **233** from indigo.

Analysis of the HRESI mass spectrum for **233** revealed a peak at *m/z* 424.1656, assigned to the molecular ion $[C_{26}H_{22}N_3O_3]^+$, confirming the incorporation of the pyridyl moiety and the addition of a Boc group. Analysis of the ^{1}H NMR spectrum revealed three deshielded resonances at δ 8.90, δ 8.60, and δ 8.02, assigned to H2", H4", and H6" of the 3-pyridyl ring, in addition to a doublet at δ 8.26, assigned to the Boc-adjacent H7. Analysis of the COSY spectrum revealed correlation of both H4" and H6" to a resonance at δ 7.38, assigned to H5" (Figure 99). Coupling this information with HSQC experiments therefore revealed the chemical shift of the protic C2", C4", C5", and C6" carbon atoms, which were assigned to the resonances at δ 151.3, δ 148.9, δ 123.0, and δ 138.2, respectively (Figure 100). Analysis of the ROESY spectrum, revealed correlations between both H2" and H6" and a doublet at δ 7.60, assigned to H4 of the nearby indole, confirming the regioselectivity of the metalation reaction to exclusively C3 of the iodopyridine (Figure 101).

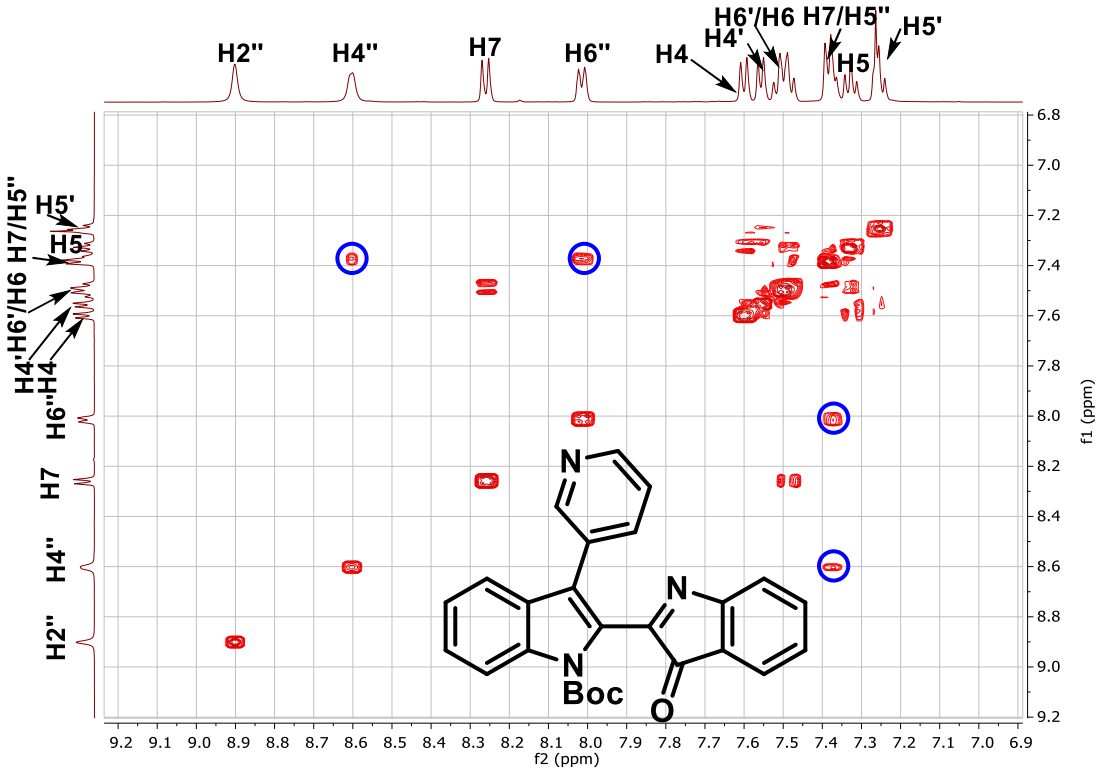

Figure 99: COSY spectrum for compound **233**, with key correlations about from H4"-H5"-H6" on the pyridyl ring highlighted (blue).

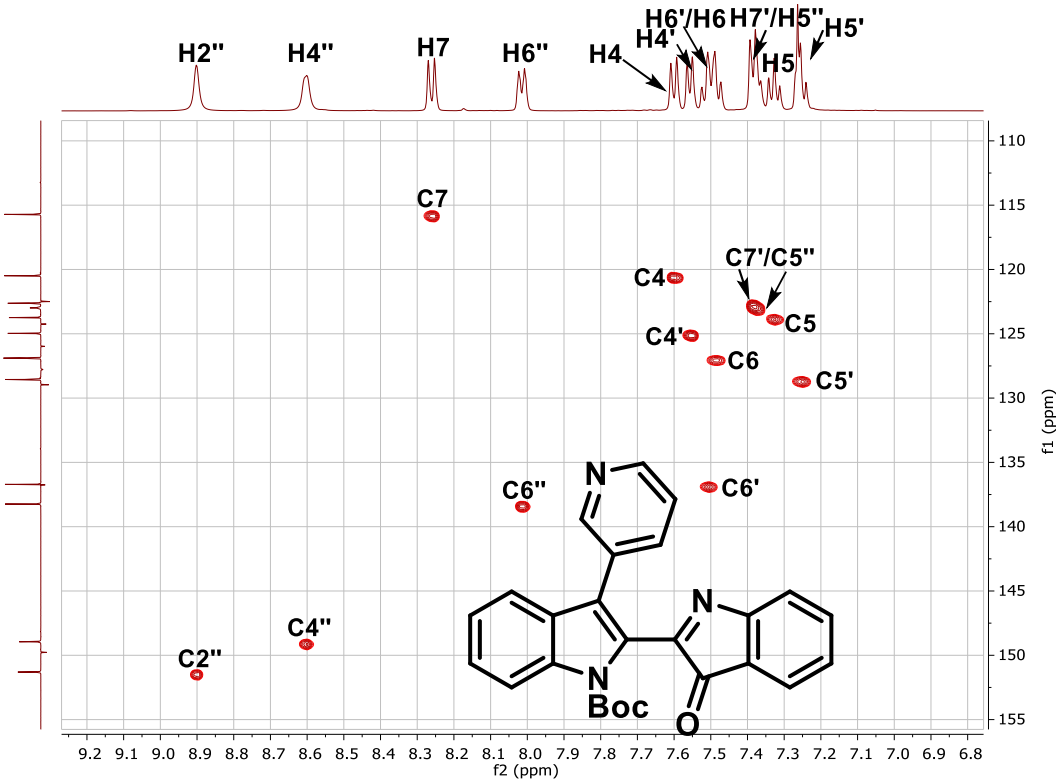

Figure 100: HSQC spectrum for compound **233**, with assignments as listed. Note that the C7'-H7' and C5"-H5" correlations overlap at the 2D resolution of the experiment, however the pair are resolved in the 1D ^{13}C NMR spectrum.

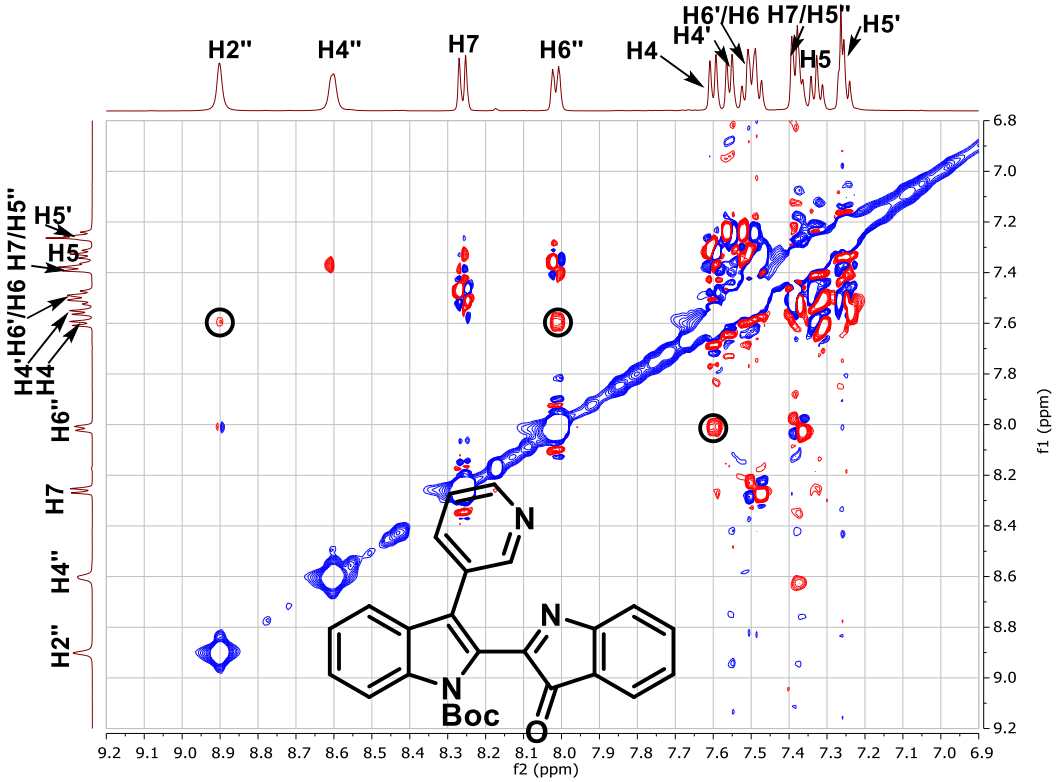

Figure 101: Weak through-space correlations in the ROESY spectrum from H2" and H6" to H4 confirm the regiochemical identity of the pyridine moiety. Key correlations are highlighted (black).

With the successful incorporation of a basic nitrogen heterocycle, we next turned our attention to the analogous *N*-methylimidazolyl system. Given that the desired 2-metalated imidazole **234** is commonly generated *in situ* from directed metalation of *N*-methylimidazole with *n*-BuLi, a 0 ˚C solution of *N*-methylimidazole (2.5 mmol) in THF was treated with *n*-BuLi (2.2 mmol), and the mixture stirred at 0 ˚C for 1.5 h. The resulting pale-golden solution of **234** was transferred to a vigorously-stirred suspension of indigo in THF at -84 ˚C, and the mixture allowed to warm to room temperature over one hour. After stirring at room temperature for a further hour, the reaction was worked up and the residue subjected to Boc-mediated dehydration, affording exclusively the desired 3-(*N*-methylimidazol-2-yl)-diindole **235** in 94% yield (Scheme 89).

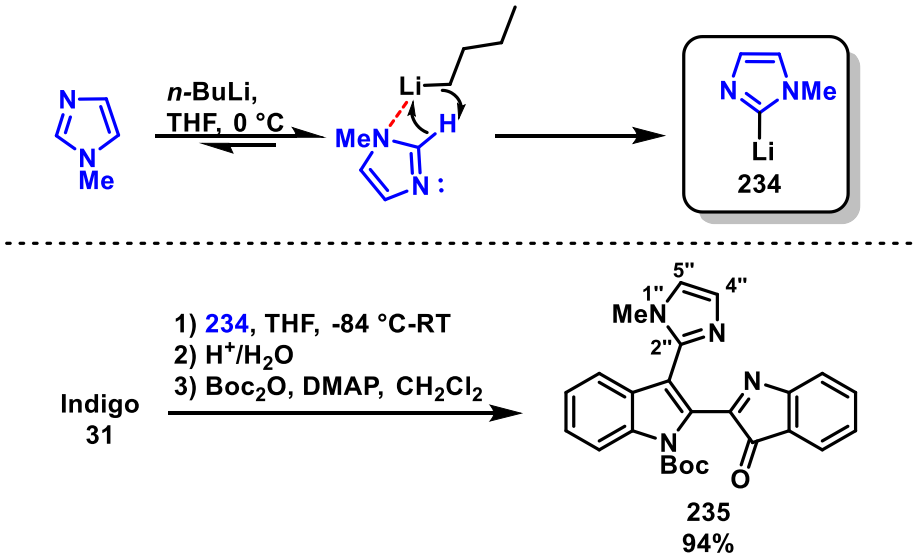

Scheme 89: Regiospecific metalation of *N*-methylimidazole to give lithioimidazole **234**. Combining **234** with indigo afforded the desired diindole **235** in excellent yield.

Analysis of the HRESI mass spectrum for **235** revealed a peak at *m/z* 427.1264, assigned to the molecular ion $[C_{25}H_{23}N_4O_3]^+$, corresponding to the insertion of the imidazole moiety and the addition of a Boc group. Analysis of the ^{1}H NMR spectrum revealed a 3H singlet at δ 3.68, assigned to the *N*-methyl substituent, in addition to a pair of apparent singlet resonances at δ 7.16 and δ 7.04, assigned to the imidazole protons H4" and H5", respectively. Closer inspection revealed an unusually-low $^3J_{H4\text{-}H5}$ coupling constant of 0.9 Hz, however this has been observed previously in the ^{1}H NMR spectra for various substituted *N*-methylimidazoles, and imidazole coupling constants are known to be pH-dependent.[23h, 170] This weak $^3J_{H4\text{-}H5}$ coupling was accompanied by an unusually-weak 3-bond correlation in the COSY spectrum (Figure 102), however the *ortho*-configuration of these two protons was confirmed by analysis of the HMBC spectrum, which showed strong 3-bond correlations from the *N*-methyl group protons, H4", and H5" to the quaternary ^{13}C resonance at δ 140.0, assigned to the imidazole C2" (Figure 103).

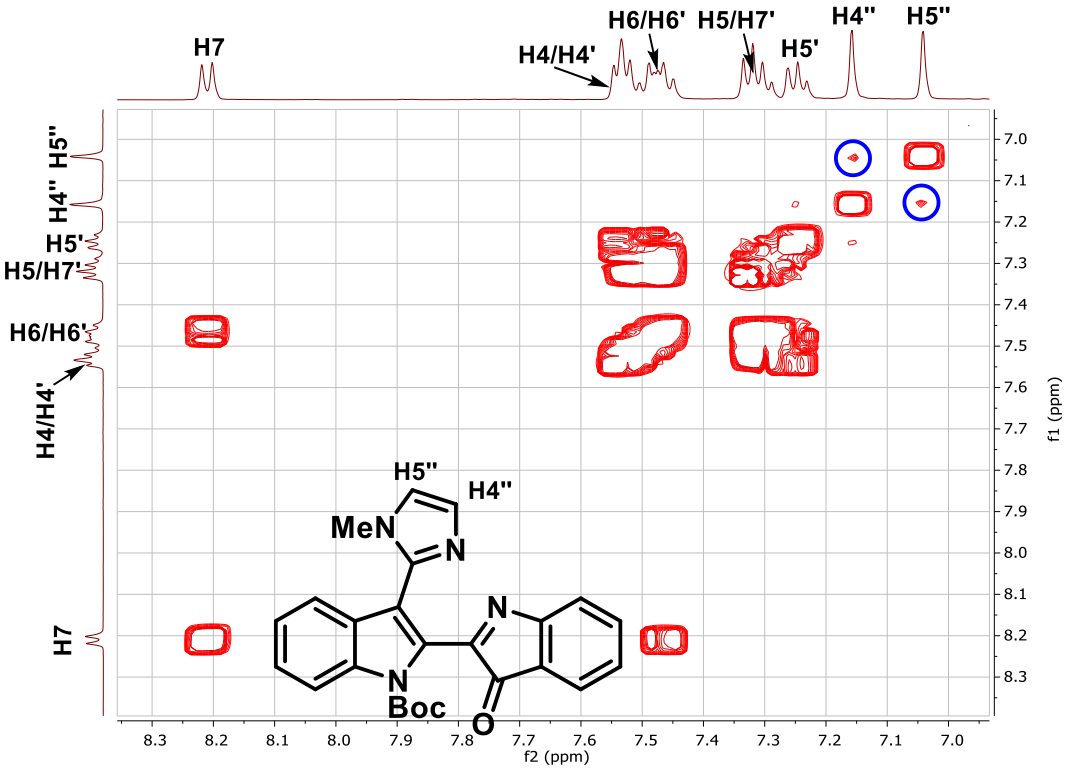

Figure 102: COSY spectrum for compound **235** at high intensity. Unusually-weak coupling was observed for the imidazole protons H4" and H5" (highlighted in blue).

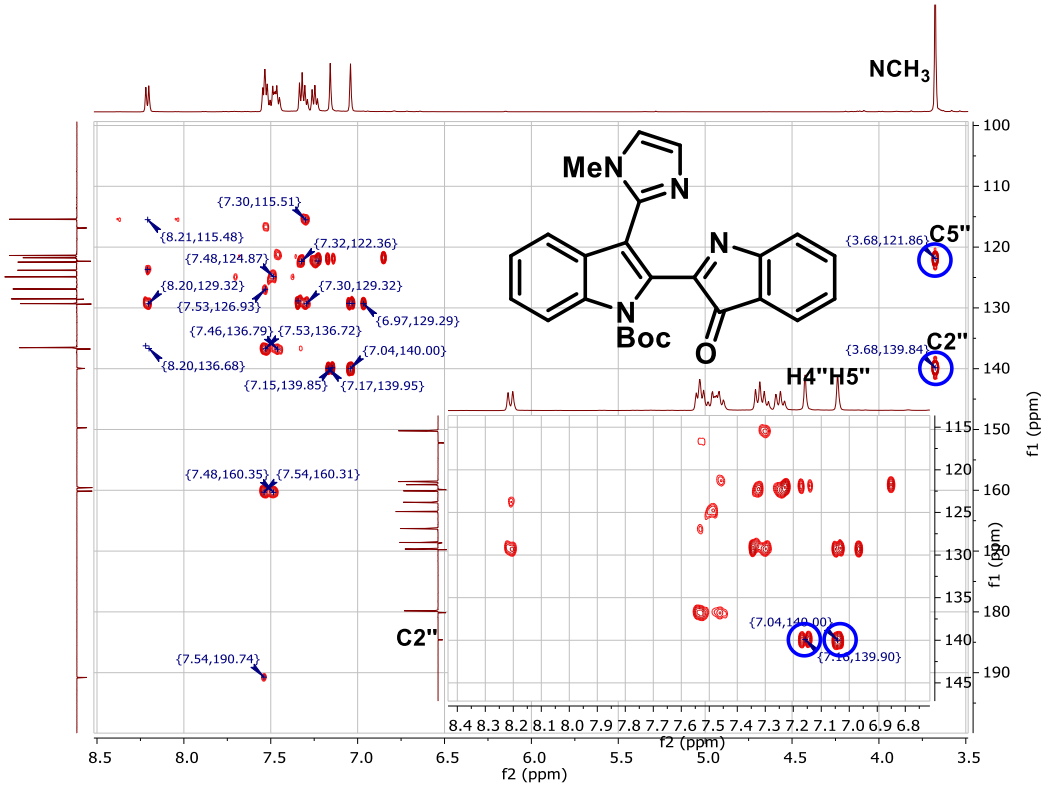

Figure 103: HMBC spectrum for compound **235**, with expansion of the aromatic region (inset) and key correlations highlighted.

Next, the sulfur-containing heterocycle thiophene was investigated, and rapid conversion of 2-iodothiophene to lithium dichloro(thiophen-2-yl)magnesate (**236**) was observed upon treatment with *i*-PrMgCl.LiCl at 0 ˚C. The pale gold solution of the ate complex was combined with indigo and warmed from -84 ˚C to room temperature over one hour, then the intense yellow solution stirred for an additional hour prior to quenching. Boc-mediated dehydration of the resulting golden residue afforded cleanly the thiophene adduct **237** in 95% yield (Scheme 90).

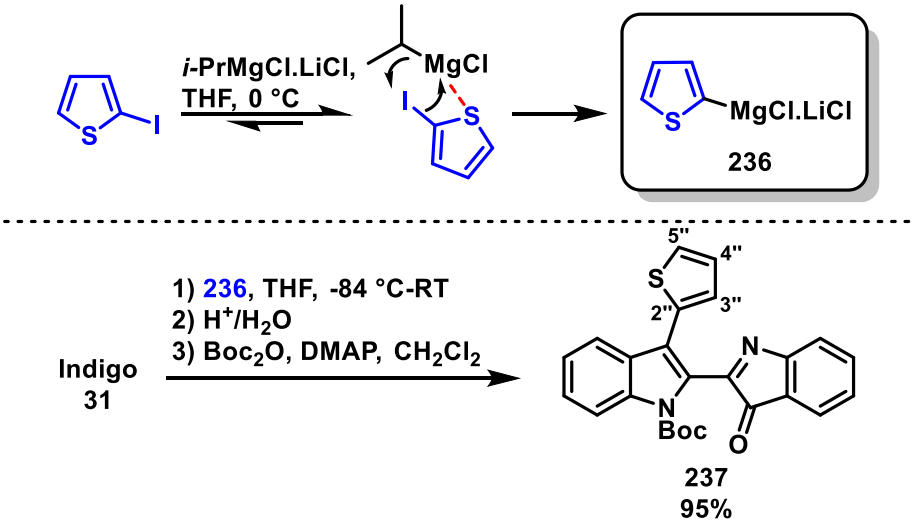

Scheme 90: Synthesis of thiophene adduct **237** from 2-thiophenyl Grignard reagent **236**. Li^+ and Cl^- ions omitted for clarity.

Analysis of the HRESI mass spectrum of **237** revealed a peak at *m/z* 429.1267, assigned to the molecular ion $[C_{25}H_{21}N_2O_3S]^+$, corresponding to the net substitution of the thiophene moiety for an oxygen atom, and the addition of the *N*-Boc substituent. Analysis of the ^{1}H NMR spectrum revealed a characteristic doublet-of-doublets at δ 7.14, which showed COSY correlations to two sets of doublet-of-doublets at δ 7.40 and δ 7.60 (Figure 104), which were assigned to H4", H5", and H3" of the thiophene moiety, respectively – this assignment was supported by through-space correlation of H5" to a doublet at δ 7.94 in the ROESY spectrum (Figure 105), assigned to H4 of the adjacent indole ring. Analysis of the HMBC spectrum revealed strong, three-bond coupling of H4" and H5" to a quaternary ^{13}C resonance at δ 132.4 which also showed weak, two-bond coupling to H3", and was therefore assigned to C2" (Figure 106). H3" additionally was coupled through three bonds to a quaternary resonance at δ 121.0, assigned to the indole C3. The oxoindolenine fragment was confirmed by the lone carbonyl resonance at δ 191.4 assigned to C3' and the characteristic ^{13}C resonances at δ 159.6, δ 136.6 and δ 160.3, assigned to C2', C6' and C7a', respectively.

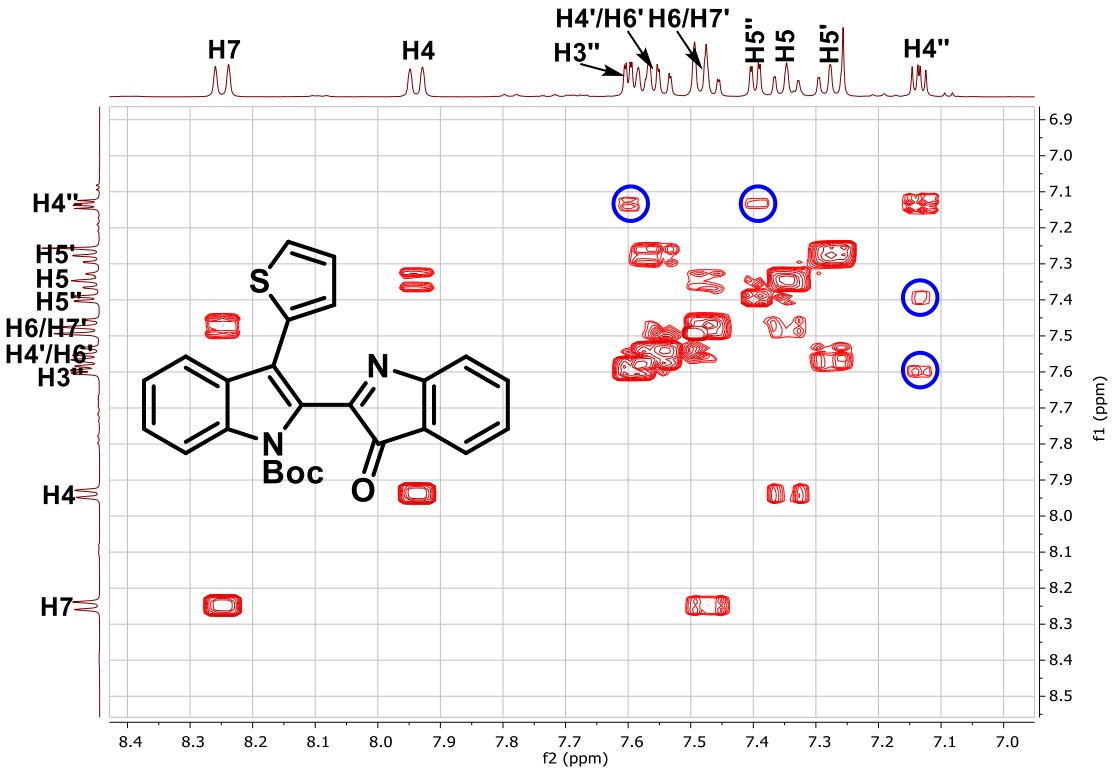

Figure 104: COSY spectrum for **235**, with relevant assignments. Key correlations of the thiophene moiety are highlighted (blue).

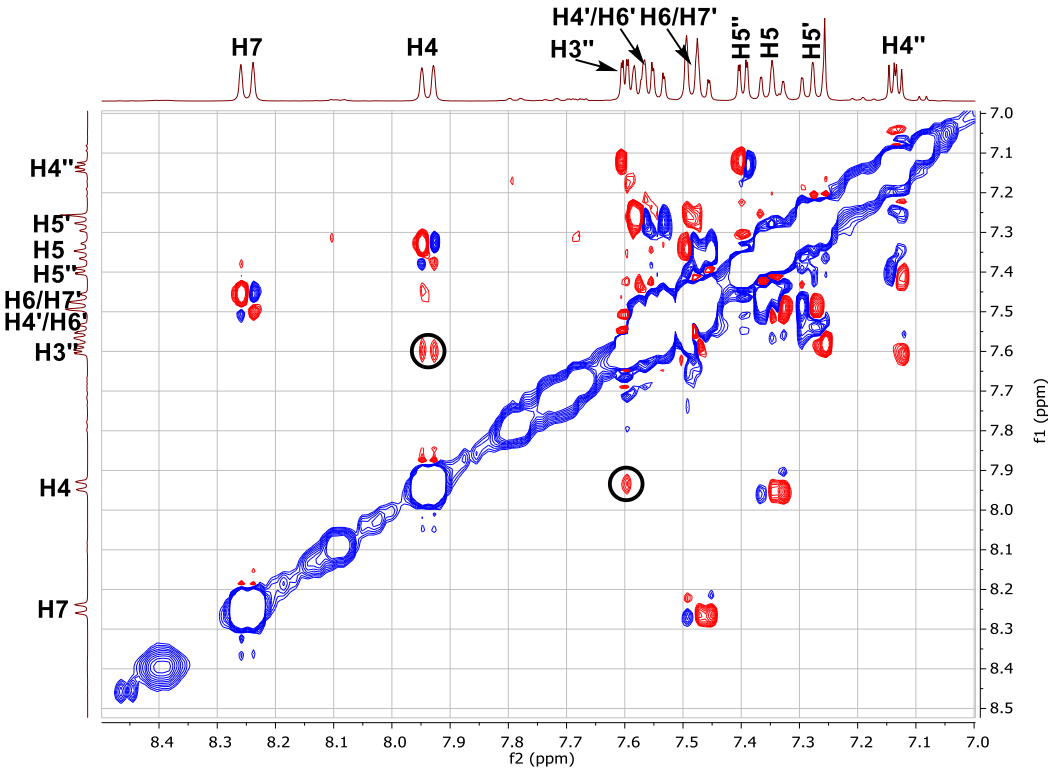

Figure 105: ROESY spectrum for compound **237** with relevant assignments and key correlations between H3" and H4 highlighted (black).

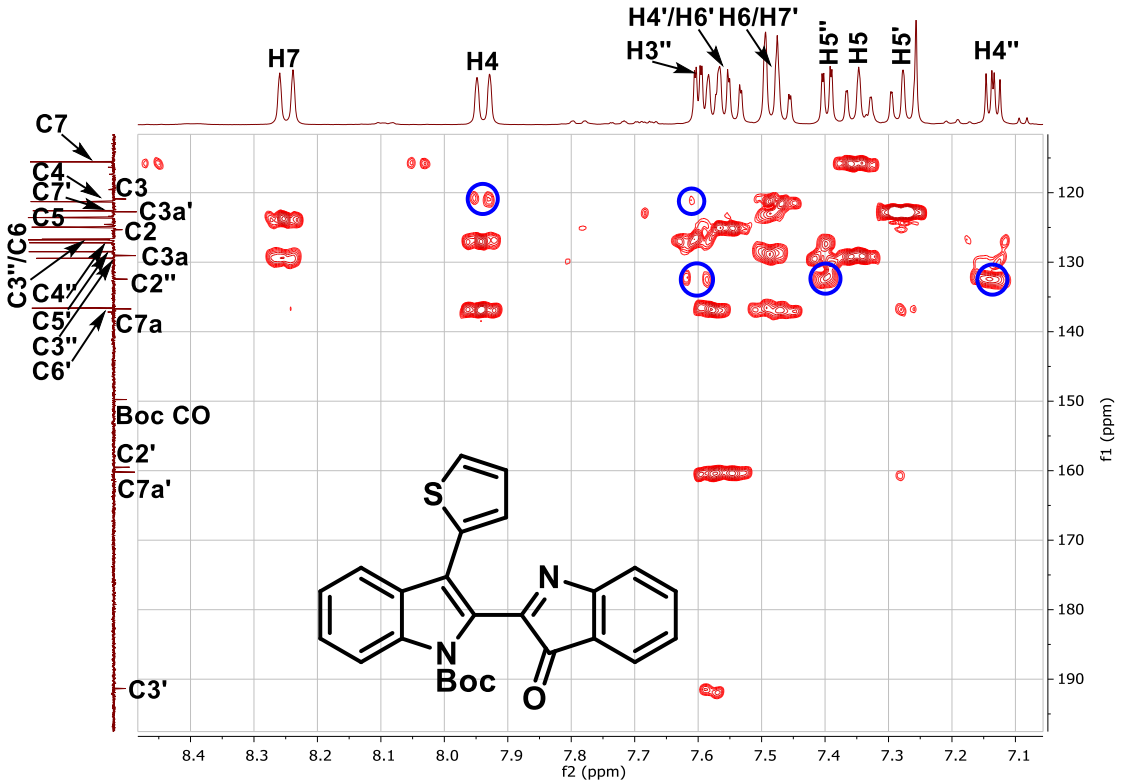

Figure 106: HMBC spectrum for compound **237**. Key correlations of the thiophene protons H3", H4" and H5" to C2", and H3" and H4 to C3 are highlighted (blue).

Crystals of **237** were grown by slow evaporation of a saturated hexane/CH_2Cl_2 solution, and the structure unambiguously confirmed by x-ray crystallography (Figure 107).[†††††] The thiophene moiety showed disordered packing in the solid state, where the two possible rotational isomers about the biaryl axis (i.e. **237a**, where the sulfur atom is oriented toward the indole fragment, and **237b** where the sulfur atom is oriented toward the indolenine fragment) were observed in a 4:1 ratio, respectively. The central axis of the molecule was observed to be twisted by an angle of 56.5˚,[‡‡‡‡‡] and there was no apparent interaction between the thiophene moiety and the C3' ketone group.

[†††††] X-ray crystallography performed by Dr. Anthony Willis (ANU).
[‡‡‡‡‡] Calculated using Mercury v. 3.9, © Cambridge Crystallographic Data Centre.

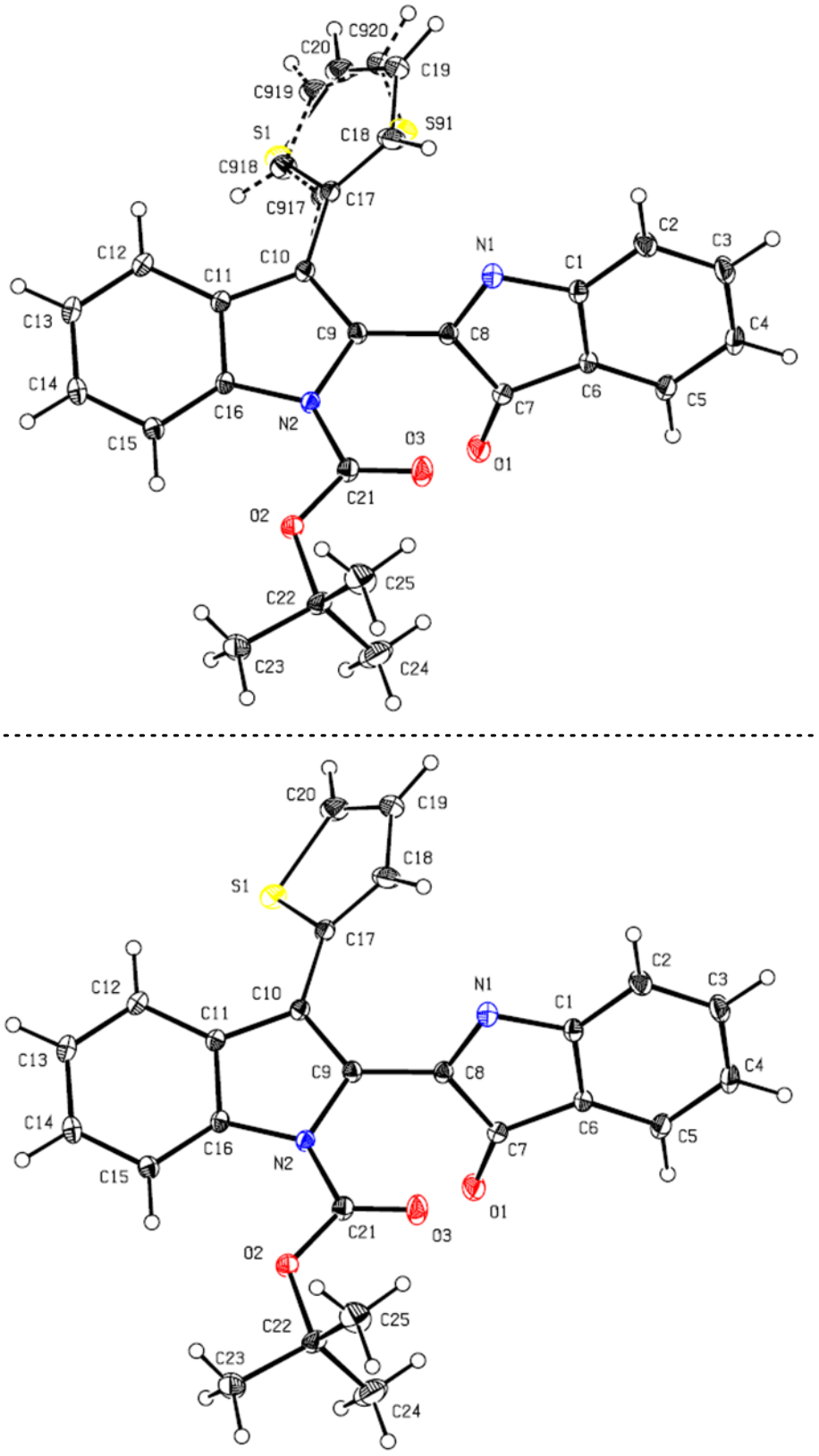

Figure 107: ORTEP depiction of compound **237**. Top: superposition of the two isomers (**237a** and **237b**) resulting from disordered packing of the thiophene moiety. Bottom: The major isomer **237a**, where the sulfur atom is oriented toward the 1*H*-indole moiety.

Directed metalation of benzofuran has been reported to exclusively afford 2-lithiobenzofuran (**328**),[157a] which was utilised as a means of probing the reaction's tolerance for oxygen heterocycles. Therefore, a solution of benzofuran (2.5 mmol) in THF was cooled to -84 ˚C, then *n*-BuLi solution (2.2 mmol) added slowly, and the mixture allowed to warm to room temperature over one hour. The resulting lithiobenzofuran solution was added to indigo at -84 ˚C, and the deep red solution warmed to room temperature over one hour, then stirred vigorously for a further hour. Aqueous workup and Boc-mediated dehydration of the deep golden residue afforded a dark orange mixture, which was separated by flash chromatography to yield the benzofuran adduct **329** in 85% yield (Scheme 91).

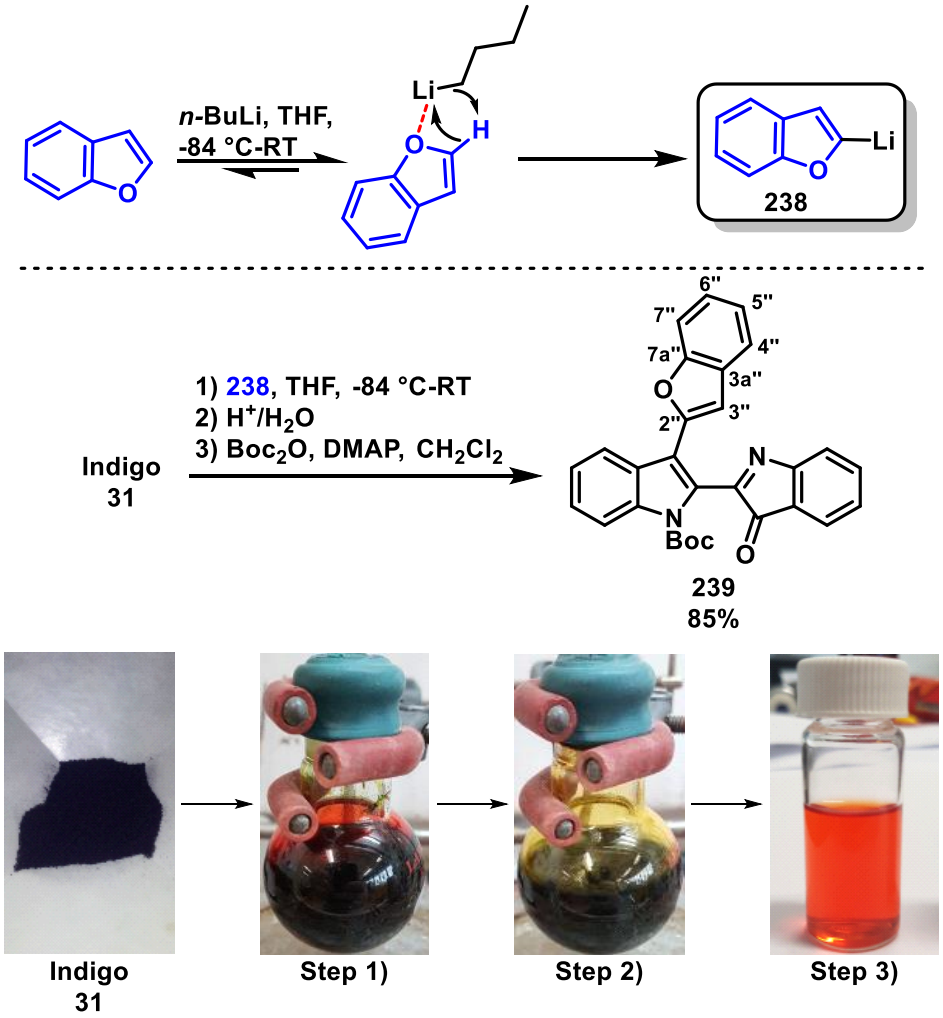

Scheme 91: Regiospecific metalation of benzofuran to afford 2-lithiobenzofuran **238**, used to synthesise the benzofuran-indigo adduct **239** via Boc-mediated dehydration. Below are pictured indicative colour changes at each point of the reaction. Steps 1), 2), and 3) are as denoted above the reaction arrow.

Finally, the insertion of a third indole moiety was investigated, to determine whether this reaction would allow access to substituted terindole scaffolds. Direct lithiation of *N*-methylindole afforded 2-lithio-*N*-methylindole (**240**), which upon combining with indigo gave a deep golden adduct which underwent Boc-mediated dehydration to an unstable product (presumably **241**), which rapidly decomposed upon attempted purification by flash chromatography, producing various polymeric materials and no viable products. Therefore, starting from 5-iodoindole **242**, *N*-methylation on gram-scale afforded the corresponding *N*-methylindole **243** in quantitative yield. Magnesium-halogen exchange using *i*-PrMgCl.LiCl gave a solution of Grignard reagent **244**, which was combined with indigo, then subjected to Boc-mediated dehydration, affording **245** in 78% crude yield after repeated purification (Scheme 92).

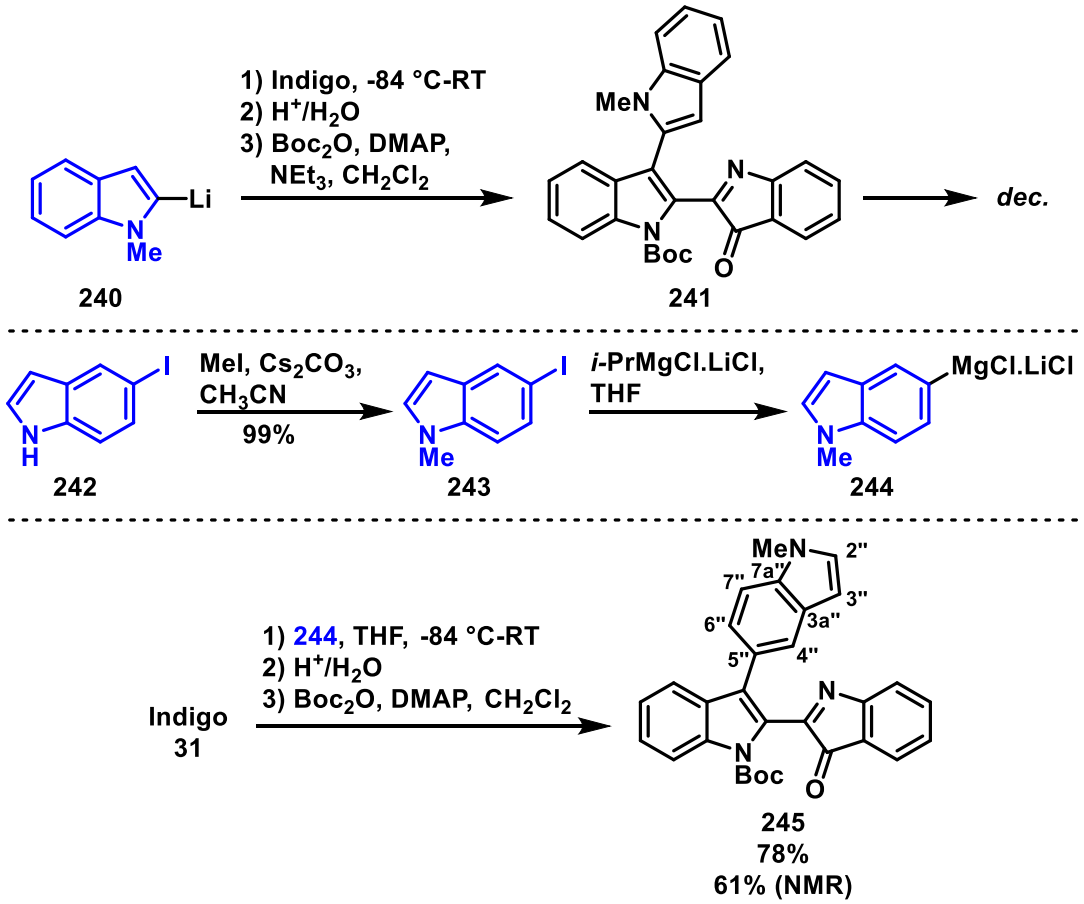

Scheme 92: Attempts toward the synthesis of terindoles from indigo. Top: direct lithiation of *N*-methylindole to give **241**, which decomposed rapidly upon attempted purification. Middle: preparation of indol-5-ylmagnesium chloride reagent **244**. Bottom: Reaction of **244** with indigo to give 2,2':3',5"-terindole **245**.

Terindole **245** was isolated as a crude mixture and degraded upon attempted further purification by flash chromatography, however its structure was able to be definitely assigned based on the isolated sample. Analysis of the HRESI mass spectrum of terindole **245** revealed a peak at 476.1968, assigned to the molecular ion $[C_{30}H_{26}N_3O_3]^+$, revealing the substitution of the oxygen atom for an *N*-methylindolyl moiety, and the incorporation of the *N*-Boc substituent. Analysis of the ^{1}H NMR spectrum revealed the sample to be 78% pure, consisting of a 4:1 ratio of the desired product and an unknown impurity which could not be resolved by chromatographic separation, and elevated-temperature NMR experiments (DMSO-d_6, 60 ˚C) demonstrated that these additional peaks were not attributable to previously-encountered rotamers about the biaryl and/or carbamate axes. The sample and impurity resonances however were able to be disentangled by numerous 2D NMR experiments, allowing the structure of the major component to be confirmed. Analysis of the ^{1}H NMR spectrum revealed a 3H singlet at δ 3.79, assigned to the *N*-methyl substituent of the indole moiety. Further downfield, the doublet at δ 6.52 showed correlations in the COSY spectrum to the doublet at δ 7.06, assigned to H3" and H2", respectively (Figure 108). Analysis of the HMBC spectrum revealed correlations between both H2" and H3" to a pair of quaternary ^{13}C resonances at δ 128.1 and δ 136.4, assigned to C3a" and C7a", respectively (Figure 109). C7a" was also correlated to a doublet resonance at δ 7.93, which showed *meta*-coupling ($^4J_{H4"\text{-}H6"}$ = 1.0 Hz) to a resonance at δ 7.44, assigned to H4" and H6", respectively. The remaining H7" was assigned to part of a multiplet at δ 7.34, and showed strong three-bond coupling to a quaternary resonance at δ 122.6, assigned to C5", therefore confirming both the presence of the additional 1*H*-indole moiety and the regiochemistry of the C3-C5" biaryl linkage. Therefore, despite the presence of significant impurity in the sample, every individual ^{1}H and ^{13}C resonance could be confidently assigned.

4.3.4 Substrate scope – summary of outcomes

Under the trialled conditions, this newly-discovered two-stage addition/dehydration reaction of indigo with numerous alkyl, aryl, and heterocyclic organometallics afforded rapid access to a variety of densely-functionalised desymmetrised 2,2'-diindoles, with good functional tolerance, and in good-to-excellent yields ranging 61–95%. A summary of the preceding outcomes of this work is provided in Figure 110.

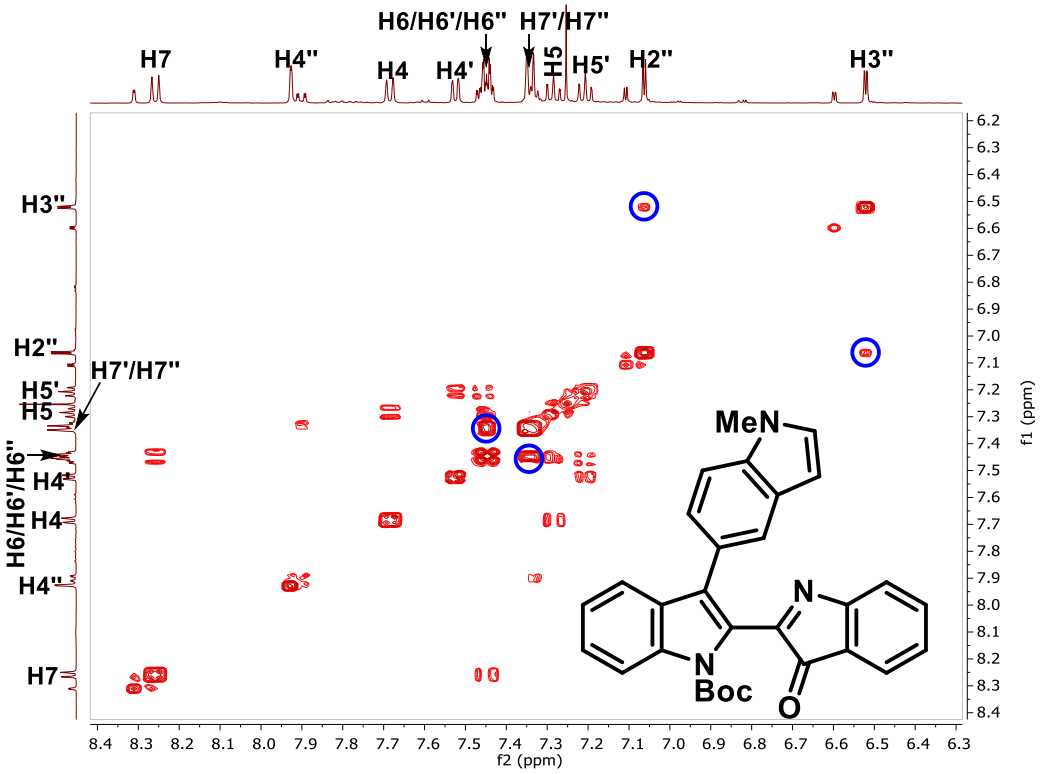

Figure 108: COSY spectrum for compound **245** with relevant assignments and key correlations of the *N*-methylindol-5-yl moiety highlighted.

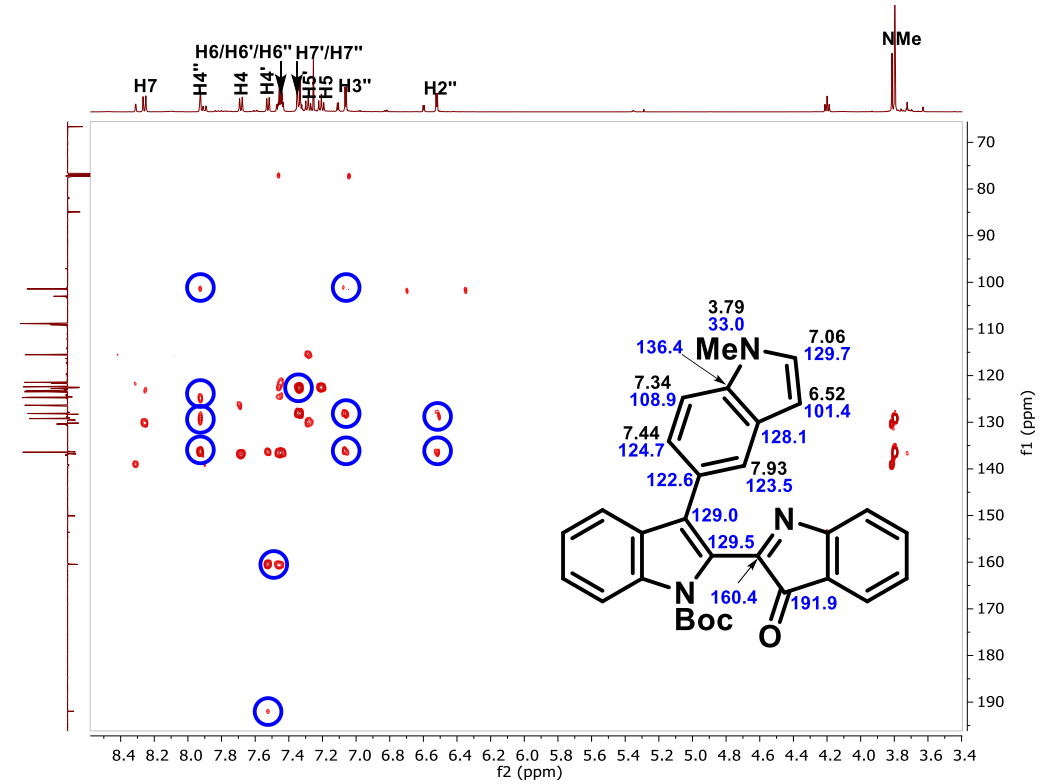

Figure 109: HMBC spectrum of compound **245**, with key proton (black) and carbon (blue) assignments as annotated on the molecule.

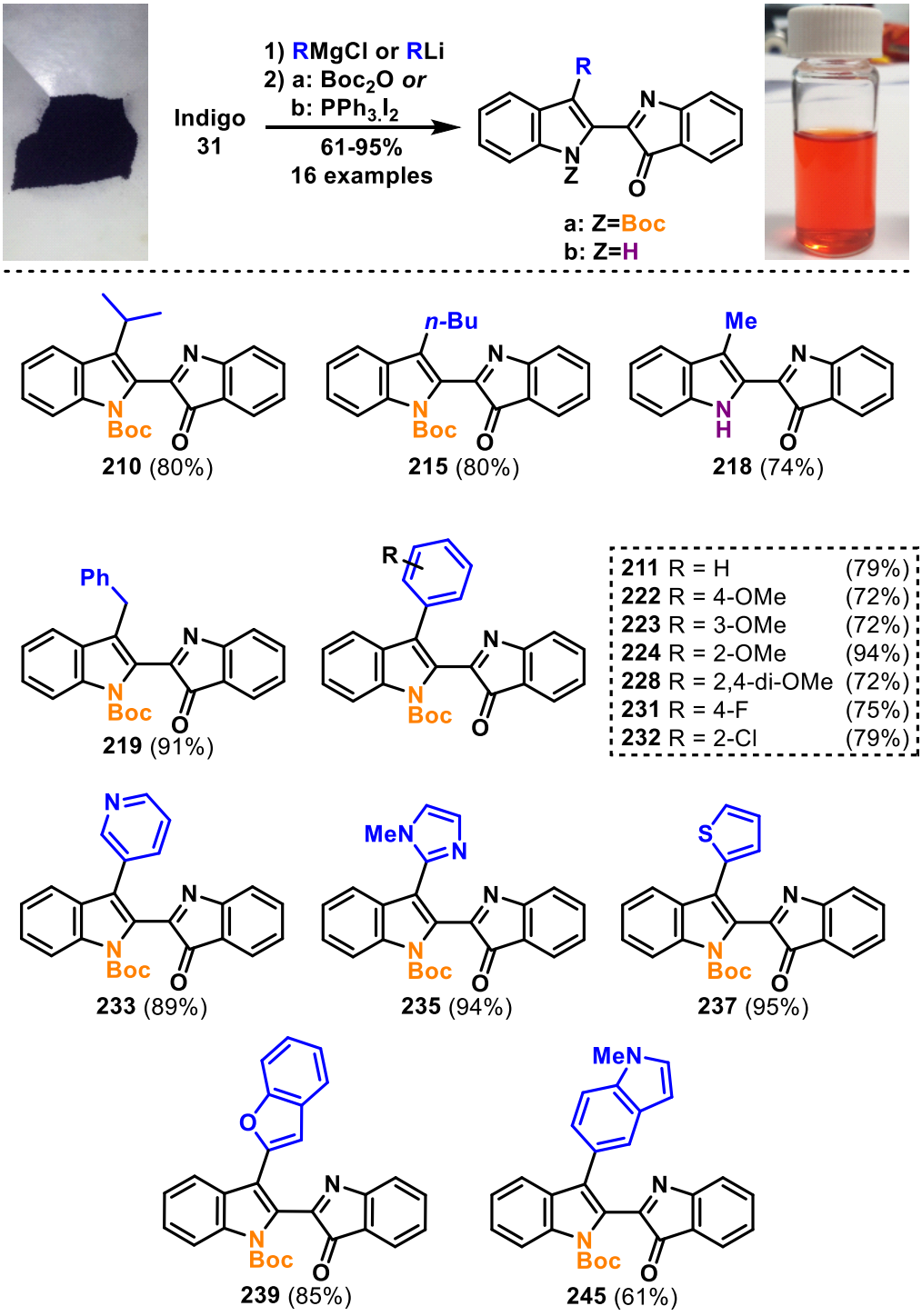

Figure 110: Summary of heterocyclic compounds accessed directly from indigo *via* this two-stage addition/dehydration methodology.

4.4 Mechanistic discussion

Given both the modularity and consistency of this transformation, it is likely that all reactions explored herein proceed *via* an identical mechanism, though the question remains as to why indigo only undergoes a single nucleophilic addition, despite the presence of both: a) two electrophilic carbonyl moieties, and b) a considerable excess (4.0–5.0 eq.) of powerful organometallic nucleophiles. A simple answer to this question is the considerable acidity of the indole NH groups depleting the excess reagent, however this would only account for the loss of 2.0 equivalents of the incoming Grignard, leaving sufficient nucleophile remaining that twofold addition would appear facile. One explanation is related to the self-indicating nature of the reaction, where the mixture turned an intense scarlet colour upon addition of the nucleophilic species at low temperature. It is therefore proposed that the indigo di-anion forms a stable six-membered chelate complex (**246**), where the hard Lewis acidic lithium or magnesium atoms are bonded to the indigo core *via* one nitrogen atom and one oxygen atom, thus sequestering the negative charges to one hemisphere of the diindole and deactivating one ketone group by converting it to a stable enolate. Nucleophilic attack of the residual Grignard reagent on the active carbonyl on the opposite hemisphere therefore would generate adduct **247**, which is hydrolysed to alcohol **58a** upon aqueous workup (Scheme 93). This proposed mechanism is consistent with our own observations, and also with the observed *mono*-selectivity from the original 1909 study.[67]

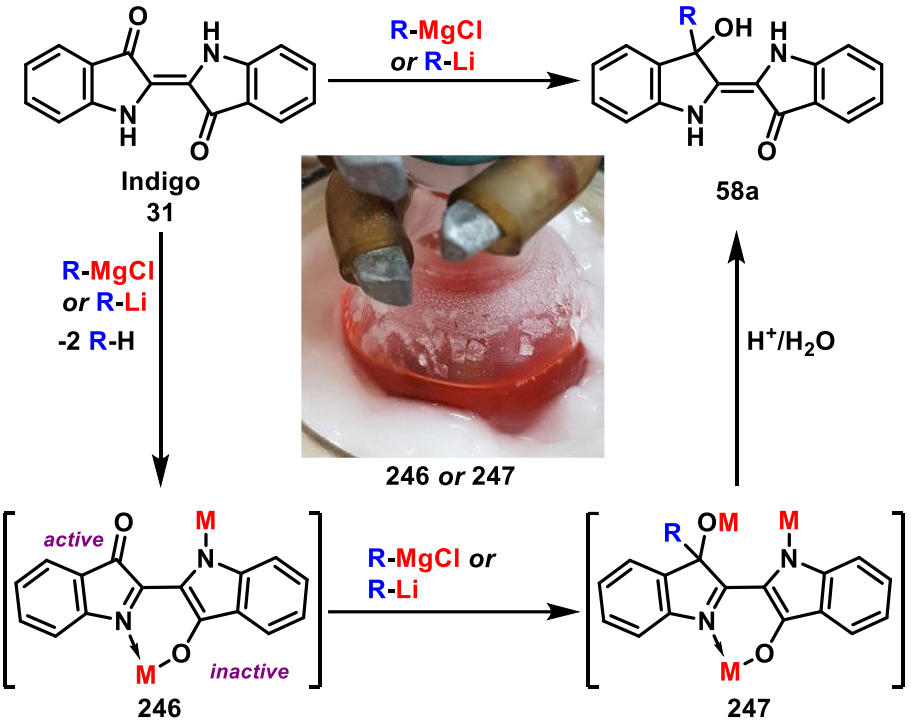

Scheme 93: Proposed mechanism for selective *mono*-Grignard addition to indigo, proceeding *via* chelate complexes **246** and **247**, and photographic depiction of an observed, brightly-coloured complex (inset), showing its colour in solution at -84 ˚C.

In most cases, treatment of the resulting alcohol **58a** with Boc_2O resulted in rapid dehydration, with the isolation of mixtures of *N*-H and *N*-Boc adducts **210** and **211** from the reaction of PhMgCl suggesting that dehydration either occurs prior or independently of *N*-acylation. Upon adding Boc_2O to the solution of the alcohol, DMAP and NEt_3, gas evolution and an immediate endotherm were observed, and NMR analysis revealed the presence of *tert*-butanol in the crude reaction mixture. This suggested that elimination of the alcohol necessitated the formation of CO_2 gas and *t*-BuOH as by-products, explained by the *in-situ* generation and decomposition of a *tert*-butyl carbonate ester moiety (**248**) by condensation of the alcohol with Boc anhydride. Conjugate 1,4-elimination would then give the non-symmetrical *N*-H diindole **194**, which could undergo *N*-acylation to give the corresponding *N*-Boc diindole (Scheme 94). The high isolated yields and rapid reactions of aryl Grignard reagents, combined with the failed dehydration of the methyl adduct **217** suggests that Boc-mediated dehydration requires at least moderate steric buttressing between the substrate and the carbonate ester to proceed, and/or to prevent competing acylation of the pro-indolenine nitrogen atom *N′*. Conversely, the optimal dehydration using $PPh_3.I_2$ was only possible for the methyl adduct (see Section 4.3.1), presumably due to the steric demands of the phosphonium species (**249**) generated *in situ*, which extrudes PPh_3O to give diindole **218**.

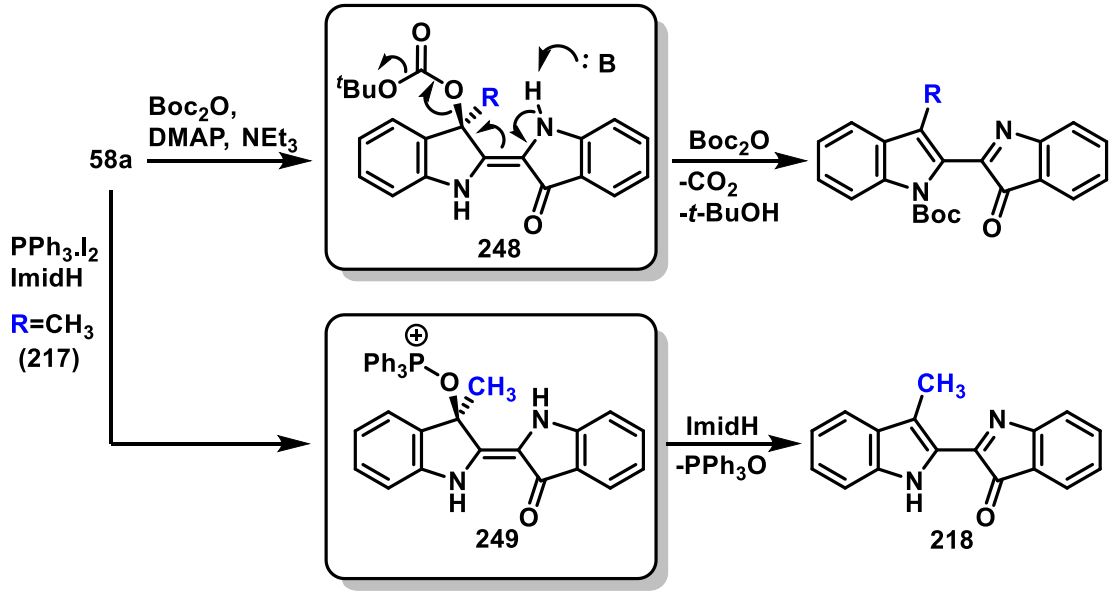

Scheme 94: Proposed mechanism for the Boc-mediated dehydration of alkyl- and aryl-Grignard adducts, and the phosphine-mediated dehydration toward the methyl adduct **218**.

4.5 Boc-deprotection of isolated scaffolds

With our sights set on evaluating the biological potential of these newly-accessed heterocyclic scaffolds, the derived *N*-Boc indoles required deprotection to their corresponding free *N*-H indoles. This could be accomplished by the action of TFA, either neat or in CH_2Cl_2 solution, typically affording the free indole cleanly, and in good yields (Scheme 95). The reaction progress was monitored by TLC analysis and by monitoring the colour change of the reaction mixture from orange to deep blue-green, and royal purple upon aqueous workup. In most cases, the reaction was deemed to be complete within 2 h, however several substrates required longer reaction times in order for complete consumption of the starting material. In addition, treatment of the *N*-Boc 3-methoxyphenyl (**223**), *N*-methylimidazol-2-yl (**235**), and benzofuran-2-yl (**239**) adducts (as well as the crude *N*-methylindol-5-yl adduct **245**) led to rapid and extensive decomposition under these conditions, and the desired free indoles were not isolated. The exact reason for this is unknown as degradation was non-specific and led mostly to polymeric tars and anthranilic acid derivatives, offering little information as to why it had occurred. One common element of these substrates is their high electron density, which may have led to acid-catalysed intramolecular cyclisation onto the adjacent carbonyl or imine functionalities, however electron density alone does not account for the reaction's discrimination between the successful 2-methoxy (**224**), 4-methoxy (**222**), and 2,4-dimethoxy (**228**), and the unsuccessful 3-methoxy (**223**) substrates. Degradation also

occurred rapidly upon attempted neutral deprotection (using TBAF.H_2O in THF), hence the absence of an acid catalyst did not hinder this reactivity. The exact cause for decomposition thus remains elusive, and requires further investigation.

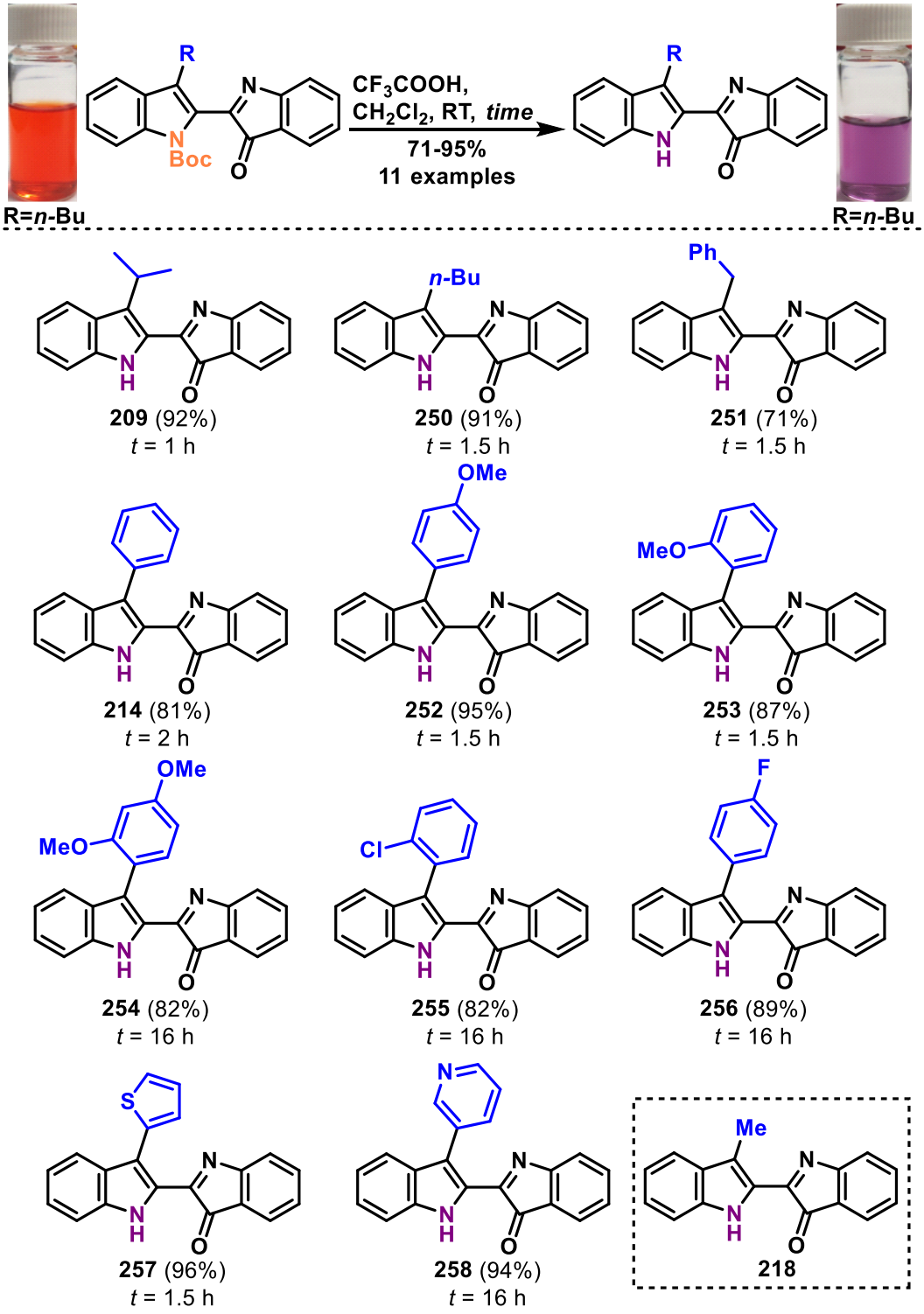

Scheme 95: Isolated yields from *N*-Boc deprotection of synthesised substrates.

4.6 Conclusions

As was first reported more than a century ago, indigo reacts rapidly with a variety of Grignard reagents and organolithium species to yield tertiary alcohol adducts in excellent yields.[67] Herein, we have re-investigated and utilised this robust reaction as a starting point for methodology development toward the generation of diverse, functionalised, and desymmetrised 2,2'-biindoles in high yields from this cheap and plentiful starting material. We determined that the formation of an intramolecular chelate complex is key for the specific insertion of a single equivalent of the desired nucleophile, and it is this predictability and reliability that lends it toward the target-oriented synthesis of functional materials. Where previously there were only three previously-reported examples of 3'-oxo-1*H*-3'*H*-2,2'-biindoles, we have developed new chemistry which has allowed for the synthesis of a total of twenty-seven novel molecules of this class, bearing either *N*-H or *N*-Boc substituents, and featuring an array of useful functional moieties for both incorporation into new chemical scaffolds, and for drug discovery purposes.

Chapter 5:
Biological activity testing of indigo derivatives

5.1 Biological activity of indigo derivatives

Despite the vast body of knowledge regarding the biological activity of the isomeric 2,3'-linked indirubin (**36**) and its derivatives as kinase inhibitors and apoptotic agents,[171] there has been very little investigation of the biological application of the corresponding 2,2'-linked indigo (**31**) and its derivatives. The 5,5'-dichloroindigo-*N*-glycosides akashines A-C (**259**–**261**) showed potent *in vitro* inhibition of numerous tumour cell lines with reported IC_{50} values of 5.1–5.9 μM against human CCL-HT29 (colon carcinoma), MEXF-514L (melanoma), LXFA-526L (lung carcinoma), MCF-7 (breast cancer), and RXF-631L (kidney tumour) lines, among others.[172] The pseudo-dimeric natural product bisindigotin (**202**) was found to inhibit dioxin-mediated ethoxyresorufin-*O*-deethylase (EROD) activity for the Hep-G2 (immortalised human liver cancer) cell line (IC_{50} = 0.8 μM), moderating toxicity versus untreated cells,[173] and showed dual activity as an inhibitor of both EROD and CYP1A1 (Cytochrome P450, 1-A1) induction in H4IIE (rat hepatoma) cells.[174] Previous studies into the cascade chemistry of indigo also revealed several potent inhibitors of the NCI-H187 (human lung cancer), and KB (human oral cancer) cell lines, as well as the malarial vector *P. falciparum* K1 (drug-susceptible) parasites. The *N,N'*-cyclised propargyl adduct **115** in particular showed IC_{50} values of 6.24 μM, 4.36 μM and 0.85 μM, respectively, against these three targets (Figure 111). We therefore sought to examine the biological profile of all final synthesized species from the preceding chapters. The low-micromolar inhibitory activity against *P. falciparum* parasites was particularly promising, hence we sought primarily to investigate the antiplasmodial activity of these compounds to identify potential leads for future elaboration.

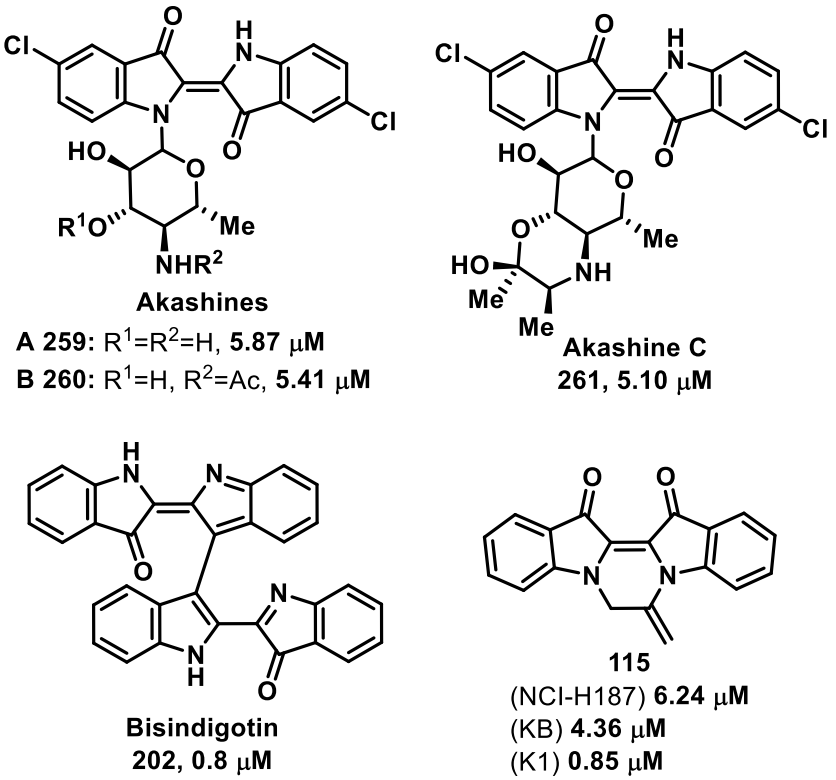

Figure 111: Previously-reported biological activity of indigo derivates. All concentrations listed represent IC_{50} values. For akashines A-C (**259**–**261**) these represent inhibition of the CCL-HT29 cell line, while for bisindigotin **202**, this represents inhibition of EROD in the Hep-G2 cell line. IC_{50} values for the propargyl adduct **115** are as listed for the assigned cell lines.

5.2 Antiplasmodial activity of propargylic and strained-ring adducts

The fourteen final derived species from Chapters 2 and 3 were assessed against *Plasmodium falciparum* 3D7 (chloroquine sensitive) and Dd2 (drug resistant) parasite strains, and preliminary cytotoxicity assessment was carried out using Human Embryonic Kidney (HEK293) cells, with reference standards of artesunate, dihydroartemisinin (DHA), chloroquine, puromycin and pyrimethamine, and 0.4% DMSO and 5 μM puromycin used as negative and positive in-plate controls, respectively.[§§§§§] The outcomes of these assays are presented in Table 5.

[§§§§§] All biological assays were performed by collaborators at Griffith University (Prof. Vicky Avery and Dr. Leonardo Lucantoni).

Table 5: Summary of outcomes from antiplasmodial and toxicity assays for compounds derived from cascade reactions of indigo, as synthesised in Chapters 2 and 3.

Entry	#	Compound	3D7 (nM)[a]	Dd2 (nM)[a]	HEK293 (nM)[a]	SI (HEK/3D7)
1	**133**	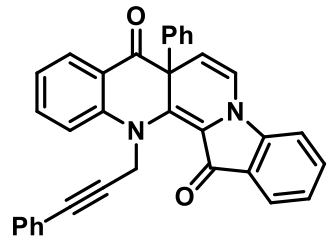	11000 ±8000	14000 ±6000	5.6% at 80 μM[b]	>7
2	**134**	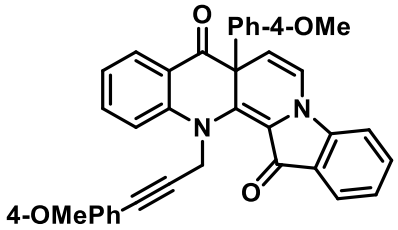	28.4% at 80 μM[b]	IA	-31.4% at 80 μM[b]	--
3	***rac*-152**	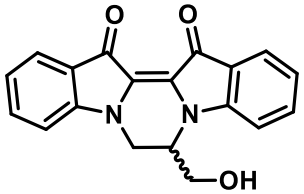	76.6 ±4.0	201.7 ±7.4	7726 ±467	101
4	***S*-152**	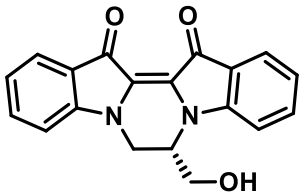	105.6 ±37.4	195.5 ±0.2	10361 ±1028	98.1
5	***R*-152**	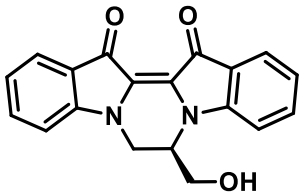	88.6 ±16.3	164.5 ±32.2	10708 ±1090	120.9
6	**153**	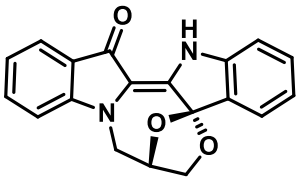	17.4% at 80 μM[b]	IA	-30.7% at 80 μM[b]	--

7	**154**	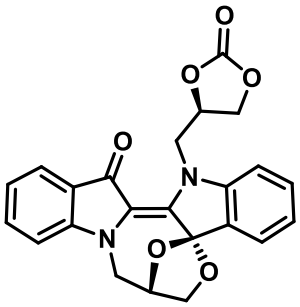	10000 ±3000	22000 ±6000	34.1% at 80 μM[b]	>8
8	**155**	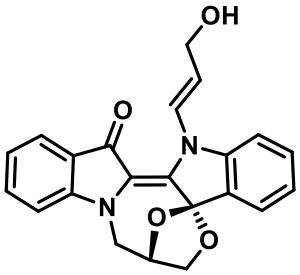	98.7% at 160 μM[b]	73.2% at 160 μM[b]	25.5% at 160 μM[b]	--
9	**176**	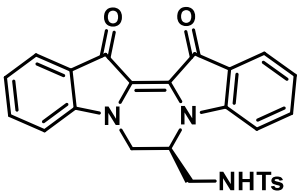	6000 ±2000	25000 ±5000	14.9% at 80 μM[b]	>14
10	**177**	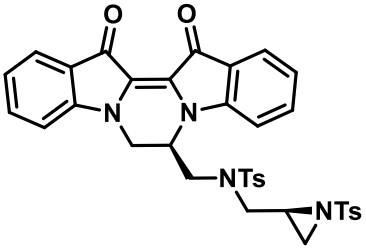	3100 ±600	4000 ±2000	65.9% at 80 μM[b]	--
11	**178**	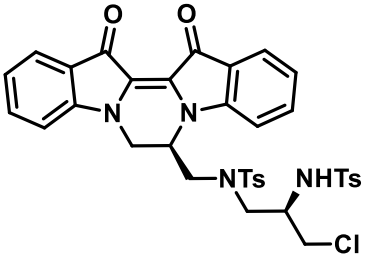	5000 ±2000	8000 ±6000	47.3% at 80 μM[b]	>17
12	**179**	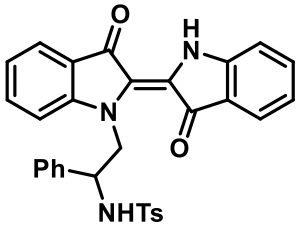	3700 ±700	6000 ±2000	12.5% at 80 μM[b]	>21

13	**180**	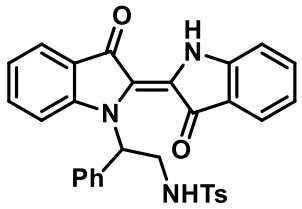	4000 ±800	8120 ±60	6.0% at 80 μM[b]	>20
14	**183**	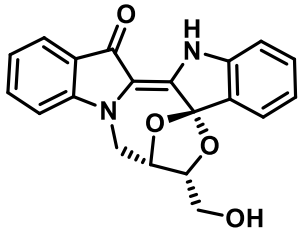	98.6% at 80 μM[b]	97.7% at 80 μM[b]	65.4% at 80 μM[b]	--
15	**184**	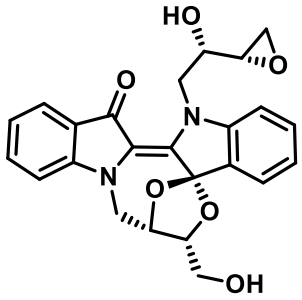	9000 ±2000	16000 ±4000	64.0% at 80 μM[b]	--
16	**185**	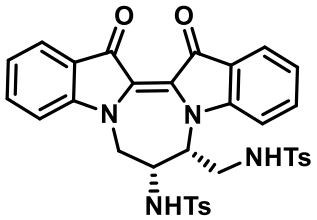	2800 ±700	5000 ±2000	15000 ±2000	5.3
17		**Artesunate**	1.1 ±0.0	1.7 ±0.5	70.7% at 10 μM[b]	--
18		**Chloroquine**	5.8 ±0.1	94.6 ±24.9	67.4% at 40 μM[b]	--
19		**Dihydroartemisinin**	0.4 ±0.1	0.6 ±0.1	62.3% at 10 μM[b]	--
20		**Puromycin**	141.9 ±12.7	147.4 ±23.3	1202 ± 2.8	8.5
21		**Pyrimethamine**	4.0 ±0.1	5.0% at 40 μM[b]	72.8% at 40 μM[b]	--

[a]Concentrations reflect calculated IC_{50} values. [b]Percentage inhibition is given where an IC_{50} value could not be calculated due to the dose-response curve not reaching a full inhibition plateau at the maximum concentration. IA = inactive.

Of the molecules submitted for testing, the *N,N'*-cyclic compounds **152**, **176**–**178**, and **185** were considerably more-active than both the *N,O'*-cyclic molecules **153**–**155** and **183**–**184**, and the propargylic adducts **133**–**134**, which showed weak inhibitory activity >10 μM. There was no significant difference in the activity of the isomeric hydroxymethylpyrazinodiindoles ***rac*-152**, ***S*-152** and ***R*-152**, which showed IC_{50} values of 77.6–105.6 nM for the 3D7 parasite strain – an eight-fold improvement from the previous benchmark **115**. The structural homology of **152** and **115** (differing only by the net hydration of the exocyclic olefin) supports the hypothesis that the incorporation of new heteroatoms could lead to an improvement in the biological profile of the indigo derivatives (see Chapter 3). Notable for all trialled compounds is their low cell toxicity, with only compounds **152** and **185** showing appreciable HEK293 inhibition at their maximum concentrations. The calculated IC_{50} values for **152** demonstrate it to be two orders-of-magnitude more-potent against the 3D7 line than HEK293 line, leading to high selectivity (SI 100-120) for the parasites over the human control. There was a noted decrease in activity against the resistant Dd2 parasites, with IC_{50} ratios Dd2:3D7 of *ca.* 1.5–2, however this discrepancy falls within the accepted parameters of equipotency for this assay and does not indicate cross-species resistance.

5.3 Antiplasmodial activity of non-symmetrical 2,2'-diindoles

The non-symmetrical 2,2'-diindoles synthesised in Chapter 4 were also subjected to the same assays, to assess their antiplasmodial potency and toxicity. Where the final deprotected *N*-H indoles were unable to be synthesised, their precursor *N*-Boc-protected diindoles (i.e. the 3-methoxyphenyl adduct **223**, imidazole adduct **235** and benzofuran adduct **239**) were tested, and their relative activity benchmarked against a small selection of other Boc-protected diindoles (i.e. the isopropyl adduct **210**, phenyl adduct **211**, 2-methoxyphenyl adduct **224** and thiophene adduct **237**) to determine the relative effect of the induced substituent.[******] The outcomes of this testing are summarised in Table 6.

[******] All biological assays were performed by collaborators at Griffith University (Prof. Vicky Avery and Dr. Leonardo Lucantoni).

Table 6: Summary of outcomes from antiplasmodial and toxicity assays for compounds derived from addition-dehydration reactions of indigo, as synthesised in Chapter 4.

Entry	#	Compound	3D7 (nM)[a]	Dd2 (nM)[a]	HEK293 (nM)[a]	SI (HEK/3D7)
1	**209**	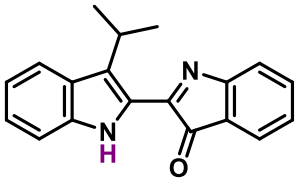	610.2 ±39.7	811.1 ±72.2	22394 ±1432	36.7
2	**210**	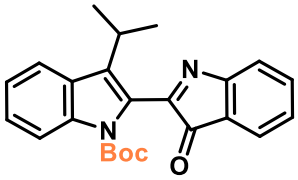	2207 ±1043	2832 ±1142	10356 ±994	4.7
3	**211**	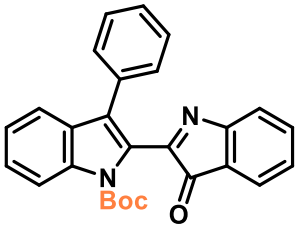	7485 ±2512	9690 ±2331	66.1% at 80 μM[b]	--
4	**214**	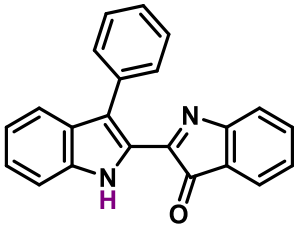	6911 ±637	8236 ±1321	4.2% at 80 μM[b]	>12
5	**218**	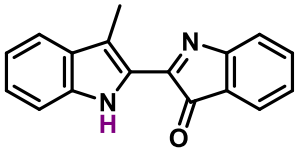	51.8 ±4.2	84.7 ±11.1	22.9% at 80 μM[b]	>1544
6	**223**	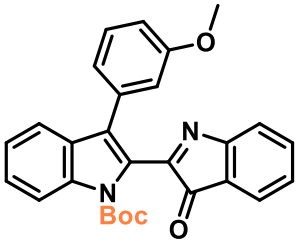	3958 ±423	4694 ±1044	20.1% at 80 μM[b]	>20
7	**224**	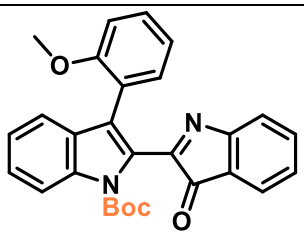	7036 ±1221	7561 ±1695	55.8% at 80 μM[b]	--

8	**235**	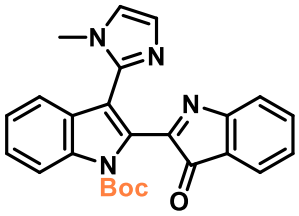	6380 ±1321	6160 ±1127	9.7% at 80 μM[b]	>12
9	**237**	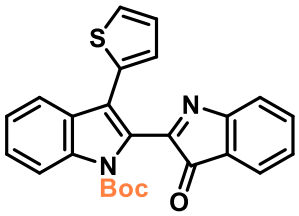	2724 ±674	2582 ±577	53.1% at 80 μM[b]	--
10	**239**	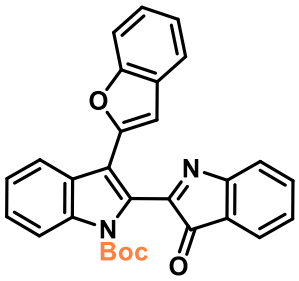	2344 ±1122	2642 ±818	35.1% at 80 μM[b]	>34
11	**250**	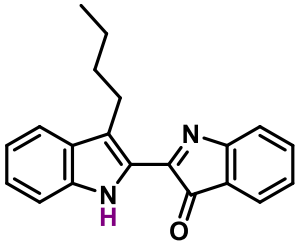	951 ±289	841 ±80	2.1% at 80 μM[b]	>84
12	**251**	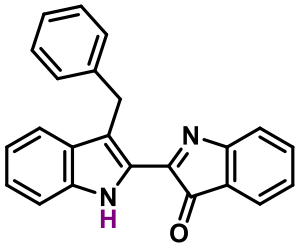	800 ±167	747 ±55.7	17.2% at 80 μM[b]	>100
13	**252**	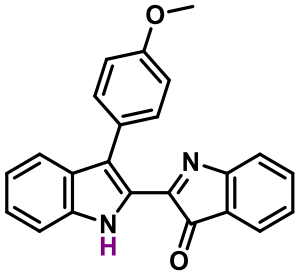	1449 ±264	1686 ±311	1.1% at 80 μM[b]	>70
14	**253**	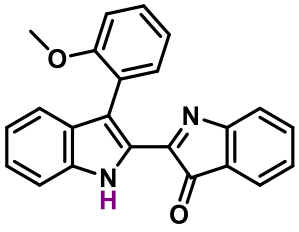	5003 ±1511	6543 ±1018	3.2% at 80 μM[b]	>16

15	**254**	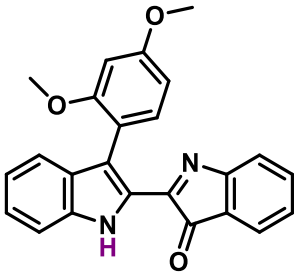	3617 ±173	4000 ±544	4.7% at 80 μM[b]	>22
16	**255**	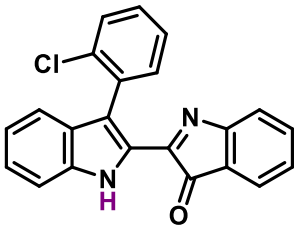	5770 ±1620	4948 ±339	7.9% at 80 μM[b]	>14
17	**256**	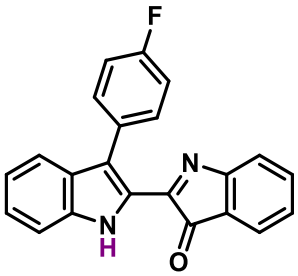	765 ±128	733 ±111	-0.6% at 80 μM[b]	>104
18	**257**	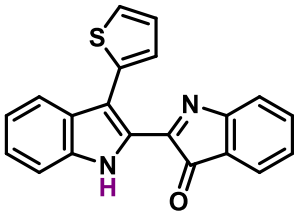	4145 ±1115	3923 ±255	3.6% at 80 μM[b]	>19
19	**258**	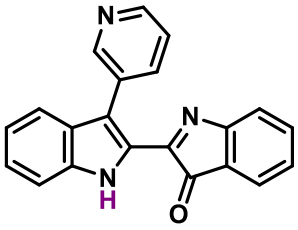	5103 ±1373	4207 ±528	7.1% at 80 μM[b]	>15
20		**Artesunate**	6.0 ±2.5	6.4 ±2.2	35.7% at 10 μM[b]	>1666
21		**Chloroquine**	29.3 ±7.5	308.8 ±82.7	56.2% at 40 μM[b]	--
22		**Puromycin**	100.4 ±29.5	75.1 ±22.5	819.6 ±84.8	8.16
23		**Pyrimethamine**	14.5 ±2.8	17.3% at 40 μM[b]	56.2% at 40 μM[b]	--
24		**Pyronaridine**	14.4 ±4.6	14.7	3572 ±349	248

[a]Concentrations reflect calculated IC_{50} values. [b]Percentage inhibition is given where an IC_{50} value could not be calculated due to the dose-response curve not reaching a full inhibition plateau at the maximum concentration. IA = inactive.

The free indoles **209**, **214**, **218**, and **250**–**258** exhibit a broad array of IC_{50} values against the 3D7 line, ranging 51.8 nM (**218**) to 6.91 μM (**214**). In general, compounds with smaller alkyl substituents were more-active than those bearing aromatic substituents, however notable substituent effects were observed for the substituted aryl adducts. Aryl adducts bearing *para*-substituents (e.g. the 4-fluorophenyl **256** – 0.765 μM; and 4-methoxyphenyl **252** – 1.44 μM) led to increased potency as compared with the parent phenyl compound. The exceptionally-low toxicity of all tested compounds (evidenced by low percentage inhibition of HEK293 at the maximum concentration 80 μM) is notable, and led to the outstanding selectivity of **218** (SI >1544).

5.4 Proposed mechanism of action

Previous study into the synthesis and mode-of-action of other 2-substituted-3*H*-indol-3-ones and indolone-*N*-oxides against *P. falciparum* (FcB1 strain) suggested that these readily undergo single-electron reduction of the C=N functionality to give persistent carbon-centred radicals,[165a] which may activate a redox signalling pathway, leading to eventual haemolysis and death of the nascent parasites.[175] The substituents examined largely consist of substituted-phenyl (typically electron-donating, e.g. the 4-dimethylaminophenyl **262** and **263** or 4-isopropoxyphenyl **264** and **265**, though the 4-nitrophenyl-substituted **266** showed similar potency) moieties at the 2-position, providing stabilisation to the indolyl C2 radical generated.[176] The nature of the stabilisation is likely mesomeric, as the replacement of the phenyl substituent with alkyl groups led to complete loss of activity (e.g. the *n*-propyl adduct **267**, which showed three orders-of-magnitude lower potency). Many of these molecules exhibit similar potency and specificity against *P. falciparum* to the lead methyl compound **218**, therefore it is hypothesised that these share a common mode-of-action, whereby the rapid reduction of the C=N group under hypoxic conditions (in the presence of cysteine- and methionine-rich reductases or glutathione, both of which are prevalent in red blood cells) leads to the stable radical **268**.[176] The oxidising potential of **268** leads to hyperphosphorylation of tyrosine residues in the cell membrane and consequent membrane-cytoskeleton decoupling.[177] The high concentration of reactive oxygen species (e.g. H_2O_2) in infected haemocytes have also been hypothesised to participate in pseudo-catalytic recycling of the pro-radical, possibly contributing to its high potency.[165a]

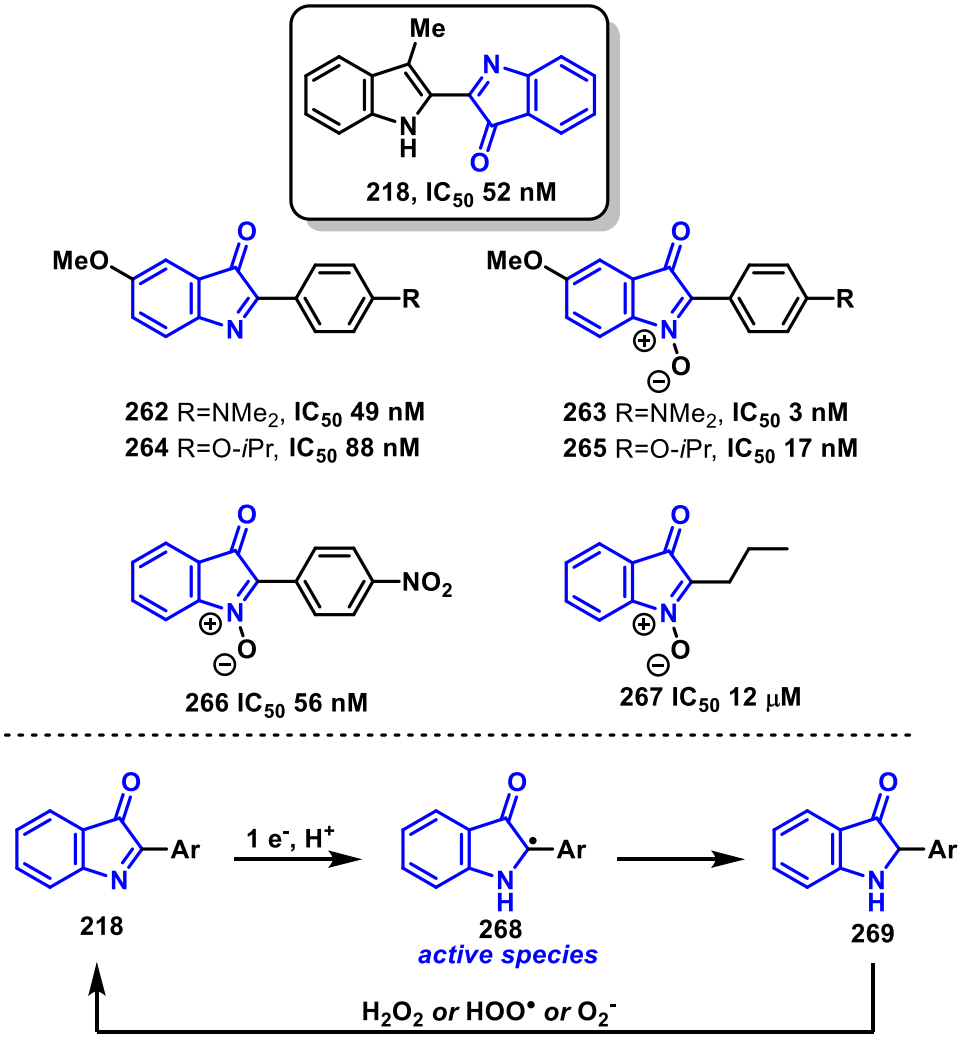

Scheme 96: Comparison of the lead compound **218** with previously-investigated 2-substituted-3*H*-indol-3-ones with similar biological activity against *P. falciparum* (FcB1), and the proposed mechanism-of-action of the methyl adduct **218**.[165a, 175-177]

It is demonstrated here that the 3-methyl-2-indolyl substituent shows similar activity, presumably due to the extended conjugation of the diindole system, and the stabilising effect of the methyl substituent.[178] This radical mode-of-action also explains the unexpected potency of the 4-fluorophenyl (**256**) and 4-methoxyphenyl (**252**) adducts relative to the corresponding phenyl adduct **214**, with both the *para*-fluoro and methoxy groups acting as strong radical stabilisers.

In summary, of the thirty-five compounds subjected to biological testing, thirty-one showed micromolar activity against *P. falciparum* (3D7), and of these, seven showed sub-micromolar IC_{50} values, with the pyrazinodiindole **152** and the 3-methyl-2,2'-biindol-3-one **218** emerging as promising leads with exceptional activity and selectivity.

Chapter 6:
Conclusions and future directions

The pursuit of diversity in small-molecule libraries is of paramount importance to the discovery and development of new heterocyclic molecules for pharmaceutical, industrial, and material applications. We have utilised the unique, multi-faceted reactivity of the ancient dye indigo as the foundation for the development of new heterocyclic libraries and synthetic methodologies, employing both its ability to undergo cascade reactions, and its overlooked ability to undergo Grignard reactions to generate new, highly-potent and selective leads for drug discovery.

6.1 Reactions of indigo with propargylic electrophiles (Chapter 2)

This brief study into the reactivity of substituted arylpropargyl bromides was intended to supplement both previous and parallel studies within our group.[116b, 127] Previous study of the reaction of 3-chloro-1-phenyl-1-propyne with indigo resulted in the isolation of compounds **122** (27%) and **123** (35%), however it was unclear whether these arose from the conjugated phenyl group or the weaker chloride leaving group. Using the bromide leaving group under optimised conditions, compounds **122** (37%) and **123** (12%) were isolated in addition to the new ring-expanded adduct **133** in 35% yield (Scheme 97). The disparate outcomes of the two reactions indicate the nature of the leaving group to play a pivotal role in pathway discrimination for these cascade reactions. The methoxy-substituted arylpropargyl bromide gave a 21% yield of the ring-expanded **134**, though parallel studies have shown that the presence of electron-withdrawing substituents leads to rapid polymerisation, making these unsuitable substrates. Initial biological studies of **133** and **134** suggested these to be nontoxic, however their poor aqueous solubility contributed to their mediocre antiplasmodial activity *in vitro*, suggesting that aryl substituents do not confer favourable characteristics.

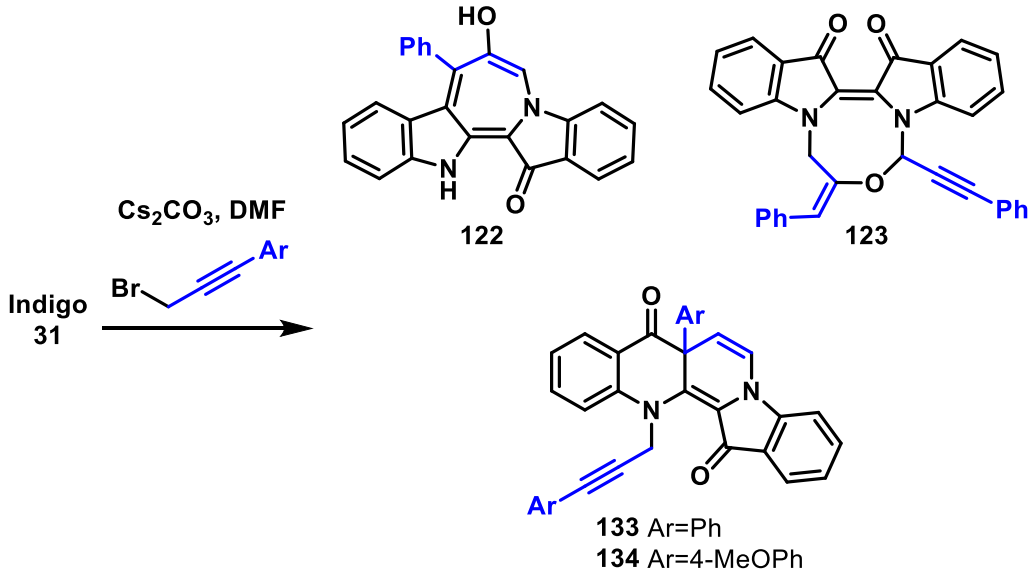

Scheme 97: Cascade reactions of aryl-substituted propargyl bromides gave access to **122**, **123** and **133-134**.

While there has been considerable progression in understanding of the cascade reactions of indigo with propargylic systems, there are several remaining avenues worthy of exploration. One involves a two-step protocol, whereby treating indigo with propargyl chloroformate (**270**) would give *N,N′-di*-proc indigo (**271**), which could undergo decarboxylation using Pd(0), as has been previously-explored with *N,N′-di*-alloc indigo (**272**). Under these conditions, **272** underwent transformation firstly to *N,N′-di*-allyl indigo (**273**), then to the azepinodiindole **274** in quantitative yield by *N,O′*-cyclisation. The corresponding transformation of **271** could afford selective access to *N,N′-di*-propargyl indigo (**275**) *in situ*, which may then undergo further cyclisation and/or derivatisation to more-complex chemical scaffolds.

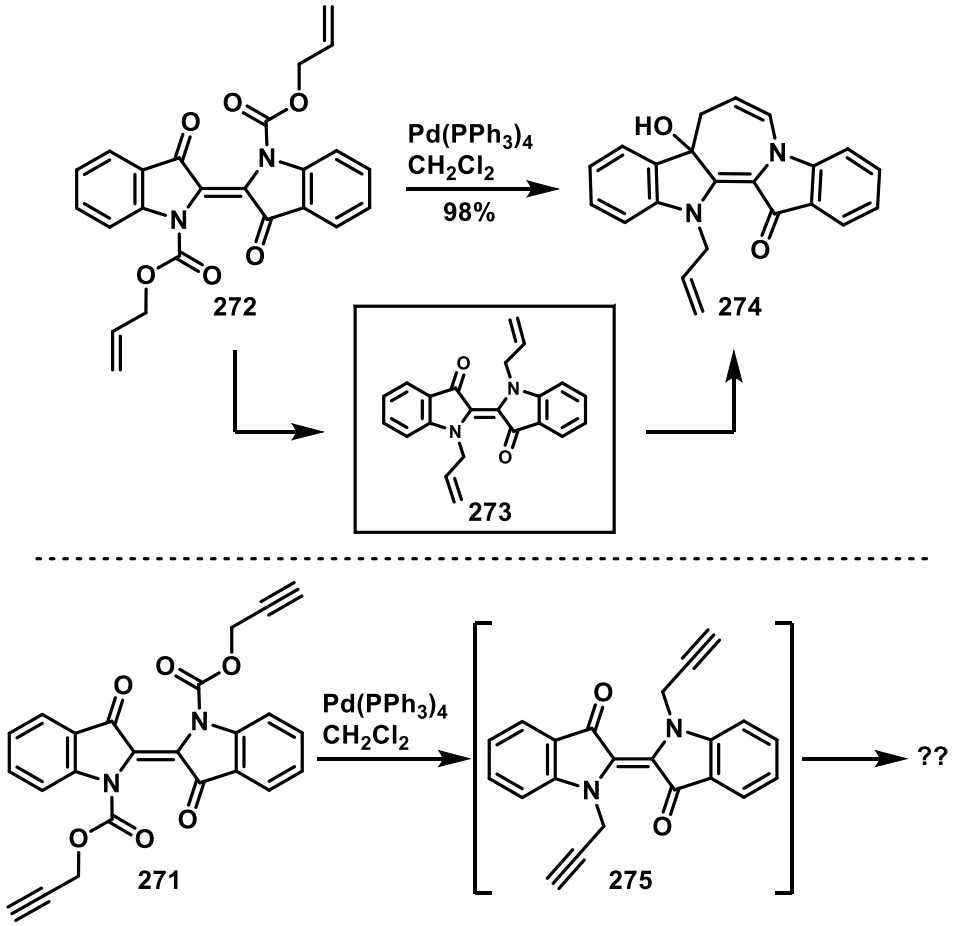

Scheme 98: Proposed future development of decarboxylative rearrangement of diproc indigo **271** to dipropargyl indigo **275**, which may be derivatised into other useful molecules.

6.2 Reactions of indigo with ring-strained electrophiles (Chapter 3)

Our study into the cascade reactions of indigo with ring-strained electrophiles revealed a pair of divergent mechanisms, whereby a heteroatom-dependent *N,N′*- or *N,O*-cyclisation gave rise to either substituted pyrazinodiindoles and/or spirocyclic epoxyoxazocinodiindoles in good yields in a one-pot setting (Scheme 99). The reaction of indigo with (*S*)-epichlorohydrin (**144**) was optimised to give the *N,N′*-cyclic **152** and *N,O′*-spirocyclic **153**, and the allylic alcohol **155** in a combined 95% yield, or instead to give mixtures of **152**, **153** and the cyclic carbonate **154** in similar yields. Replacing the halide pendant with a bromide or tosylate led to exclusive formation of **152**, in 84% and 76% yield, respectively. Compound **152** showed potent and selective *P. falciparum* inhibition, with IC_{50} values as low as 76 nM and SI values >100. This was an order-of magnitude more-active than the non-hydroxylated analogue **115**, suggesting the additional heteroatom to be beneficial toward its antiplasmodial activity.

The (chloromethyl)aziridine **148** was synthesised in enantiopure fashion in 64% yield over three steps from (*S*)-epichlorohydrin (**144**), or in 74% yield over two steps from

racemic (bromomethyl)aziridine **147** *via* a mixed bromo-chloro species (**171**). Treatment of indigo with (*R*)-**148** gave complex mixtures of the pyrazinodiindoles **176-178** in a combined 63% yield following flash chromatography and subsequent RP-HPLC separation. Using the racemic (bromomethyl)aziridine **147** led to rapid polymerisation, however the racemic **176** was isolated in 52% yield, alongside a statistical mixture of the diastereomers of *N*-aziridinyl adduct **177** in 38% yield. Treatment of indigo with phenylaziridine **174** afforded a 1.7 : 1 ratio of the terminal adduct **179** and the benzylic adduct **180** in a combined 98% yield, suggesting that cyclisation could not occur in the absence of a halide pendant.

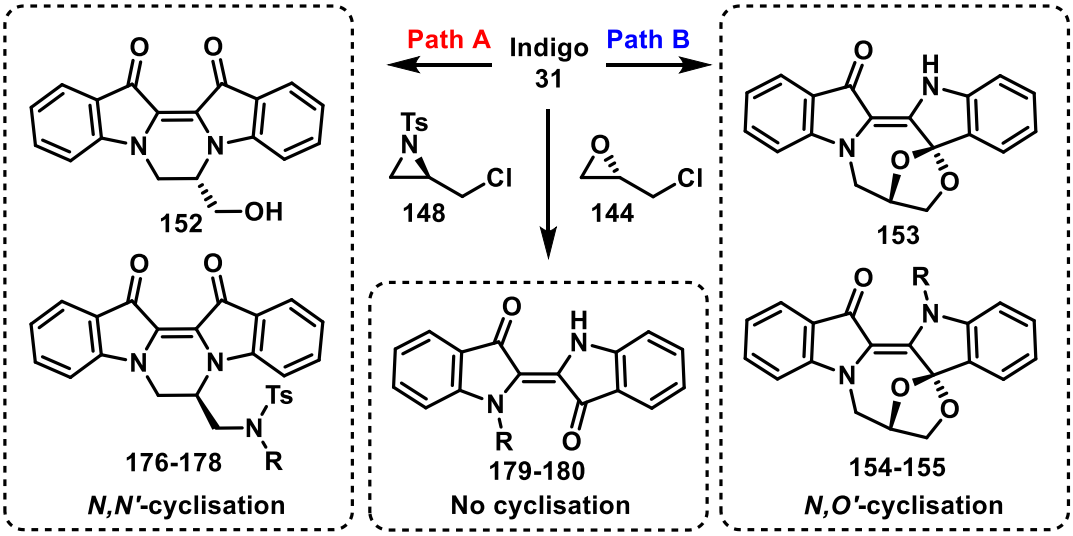

Scheme 99: Major mechanistic pathways from the reactions of indigo with ring-strained electrophiles – Path A involves *N,N′*-cyclisation and Path B involves *N,O′*-cyclisation, or no cyclisation was observed.

The dimeric bioxirane **149** and biaziridine **150** were synthesised according to literature procedures, and treatment of indigo with bioxirane **149** led exclusively to the *N,O′*-spirocyclic adducts **183** and **184** in 62% and 19% yield, respectively, while the reaction of indigo with biaziridine **150** gave a 93% yield of the lone *N,N′*-cyclic diazepinodiindole **185**. Given that there is an established protocol for the synthesis of mixed epoxy-aziridine species **276**,[179] preferential oxirane ring-opening could lead to an intermediate epiminoalkoxide (**277**), which could then lead to the formation of aminomethyl-substituted *N,O′*-cyclised spiroketals such as **278**. Derivatisation of **278** (e.g. *via* bidirectional *N*- or *N′*-alkylation) could allow for tuning of its fluorescent properties for bioconjugative applications (Scheme 100).

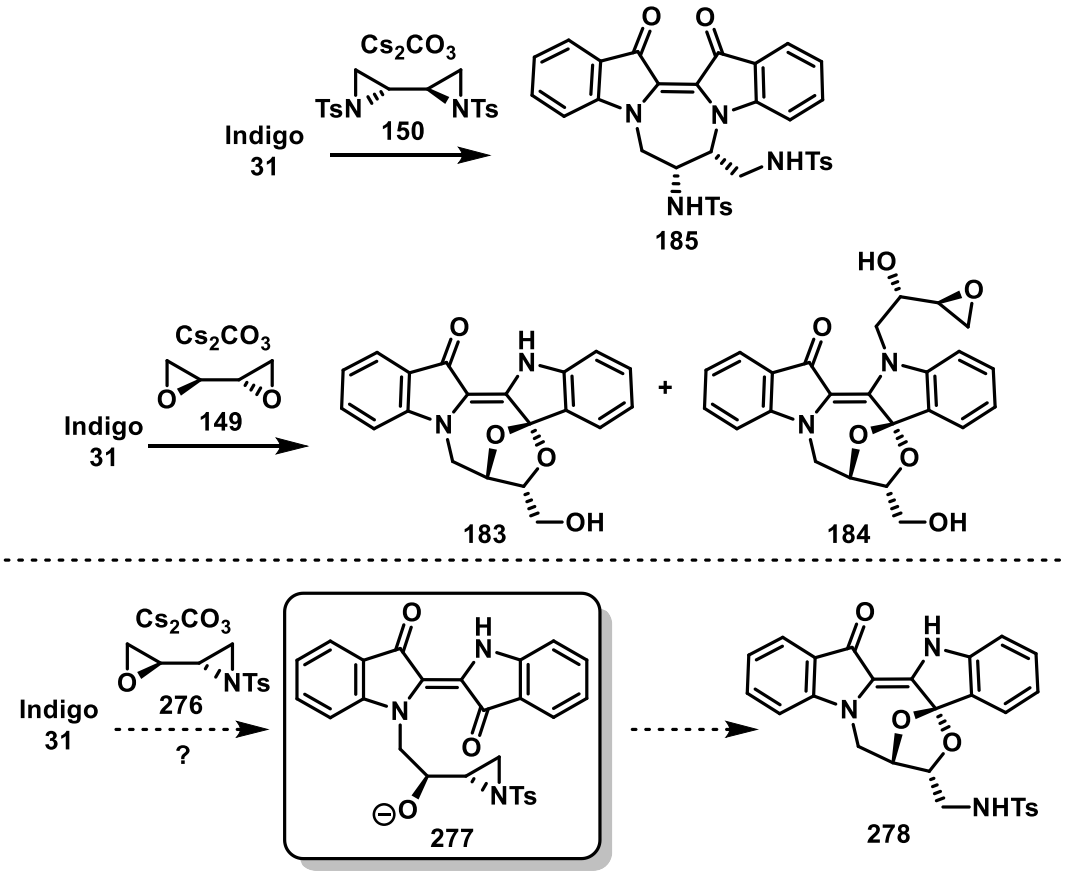

Scheme 100: The dimeric biaziridine exclusively afforded *N,N'*-cyclic compound **185** while bioxirane instead gave exclusively products **183** and **184** *via N,O'*-spiroketalisation. The proposed epoxyaziridine **276** could allow access to amino-substituted spiroketals (**278**) from the putative alkoxide **277** by dearomative cylisation.

While attempting to synthesise the (chloromethyl)aziridine **148**, a potentially-useful synthetic route toward intermolecular di-sulfonamidation of olefins was serendipitously discovered using chloramine-T under iodine-catalysed conditions. Under unoptimized conditions using allyl alcohol as a model substrate, a 1 : 1.5 ratio of aziridine **163** : diamide **166** was obtained, which could be improved to give a 75% isolated yield of the di-adduct **166**. Under unoptimized conditions, this reaction was also applied to cyclohexene to give diamide **169** in 20% yield, presumably due to the low reactivity oaf the azabicyclo[1.1.0]heptane intermediate **168**, which was also isolated in 78% yield. Therefore, while this represents an important net transformation, further optimisation is necessary to provide a robust methodology for the diamination of alkenes. Given the success of copper-catalysed asymmetric olefin aziridination using amino acid-derived box ligands,[180] similar catalyst systems could be utilised as a starting point toward generating chiral aziridine intermediates (**279**) *in situ*, which could be ring-opened to disulfonamides (**280**), and chiral diamines (**281**) upon *N*-deprotection (Scheme 101).

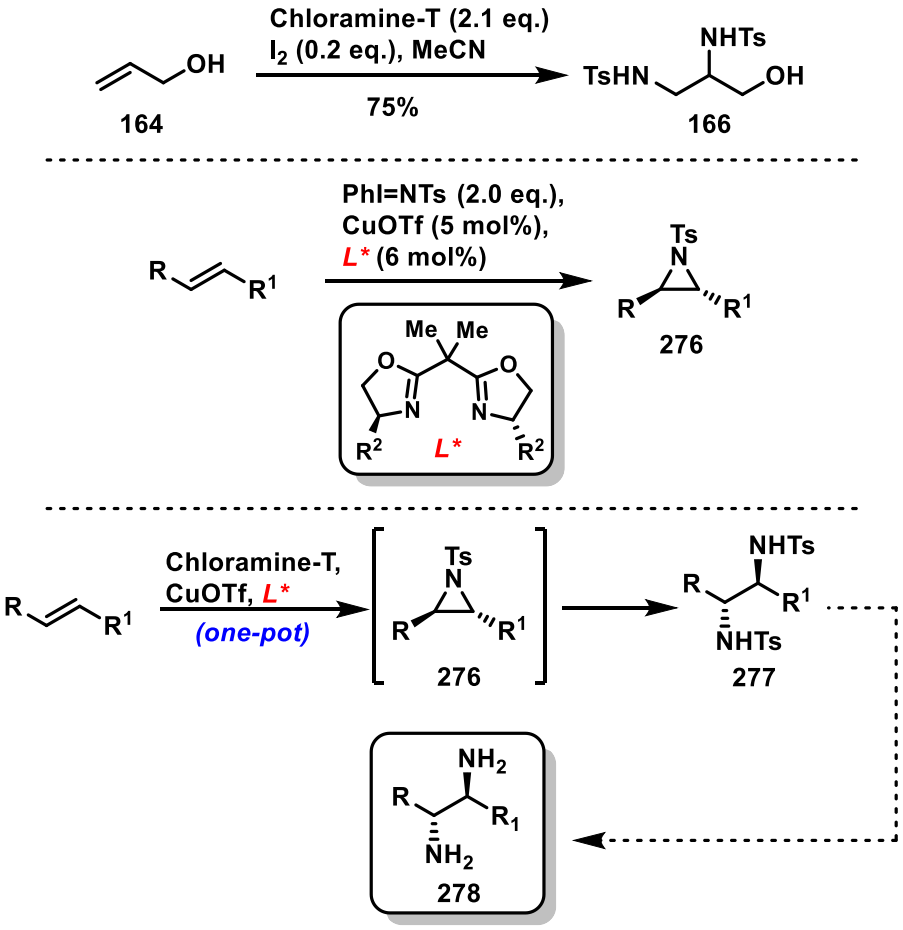

Scheme 101: Proposed methodology for diamination of alkenes, stemming from an observed diamidation of allyl alcohol upon attempted aziridination.

Additionally, the initial (chloromethyl)aziridine target (*R*)-**148** or its enantiomer (*S*)-**148** could themselves be used as a foundation for chiral amine synthesis, by chemoselective bidirectional ring-opening and subsequent halide-displacement. This could allow application toward analogues of the spiroindolone drug cipargamin (**282**), which is currently under investigation for the treatment of malaria (Scheme 102).[181] Briefly, this could involve selective indole-3-functionalisation *via* an indolylcuprate,[182] followed by displacement of the chloride (e.g. by F^-, amines, alkoxides, thiolates, etc.), reductive deprotection of the *N*-tosyl group with Mg^0, and condensation with 5-chloroisatin to give the desired cipargamin analogues. The initial ring-opening reaction could also be adapted toward the synthesis of various other tryptamine-containing natural products, thus making **148** a valuable chiral building block.

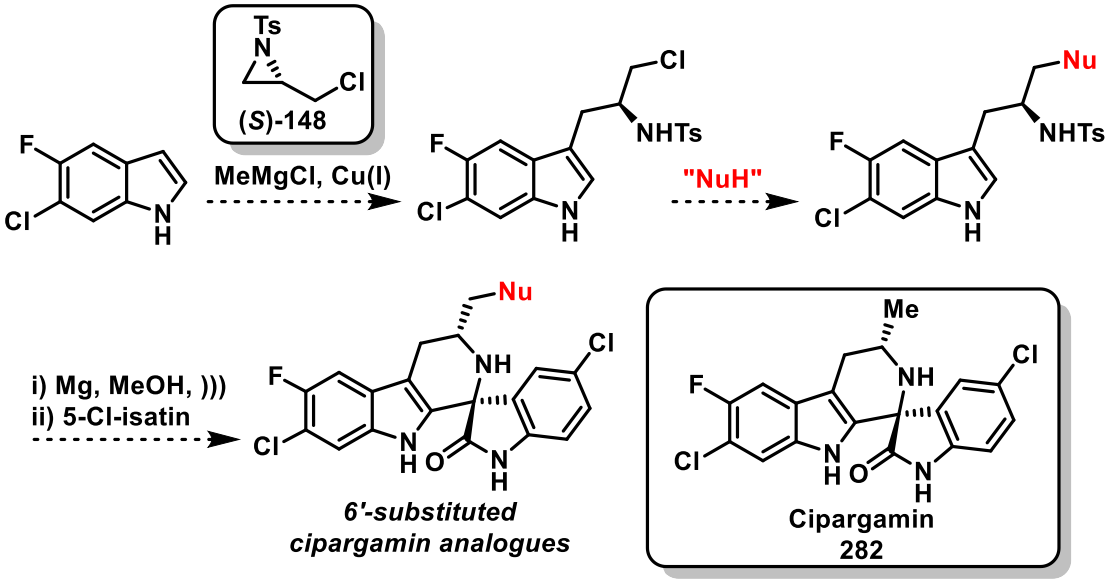

Scheme 102: Proposed synthesis of analogues of the antimalarial drug candidate cipargamin (**282**) from (*S*)-**148**.

6.3 Reactions of indigo with organometallic nucleophiles (Chapter 4)

Throughout the course of this work, we have developed a new methodology for the desymmetrisation of indigo by Grignard addition and subsequent dehydration to a variety of non-symmetrical [1*H*,3'*H*]-2,2'-diindole-3'-ones in excellent yields over two steps. Twenty-seven derivatives of this class were synthesised, where previously there had only been three reported derivatives – one natural product and two synthetic intermediates. The reaction proved tolerant to alkyl (methyl **218**, isopropyl **210**, butyl **215**, and benzyl **219**), phenyl (**211**) and substituted phenyl (4-methoxy **222**, 3-methoxy **223**, 2-methoxy **224**, 2,4-dimethoxy **228**, 2-chloro **232**, and 4-fluoro **231**) and heteroaryl (3-pyridyl **233**, *N*-methylimidazol-2-yl **235**, 2-thiophenyl **237**, and 2-benzofuranyl **239**) substrates, with all compounds isolated in 72-95% yield from indigo (Scheme 103). The *N*-methylindol-5-yl adduct **245** was also synthesised in 78% crude yield (61% by ^{1}H NMR), however it was isolated alongside an irresolute impurity which could not be removed.

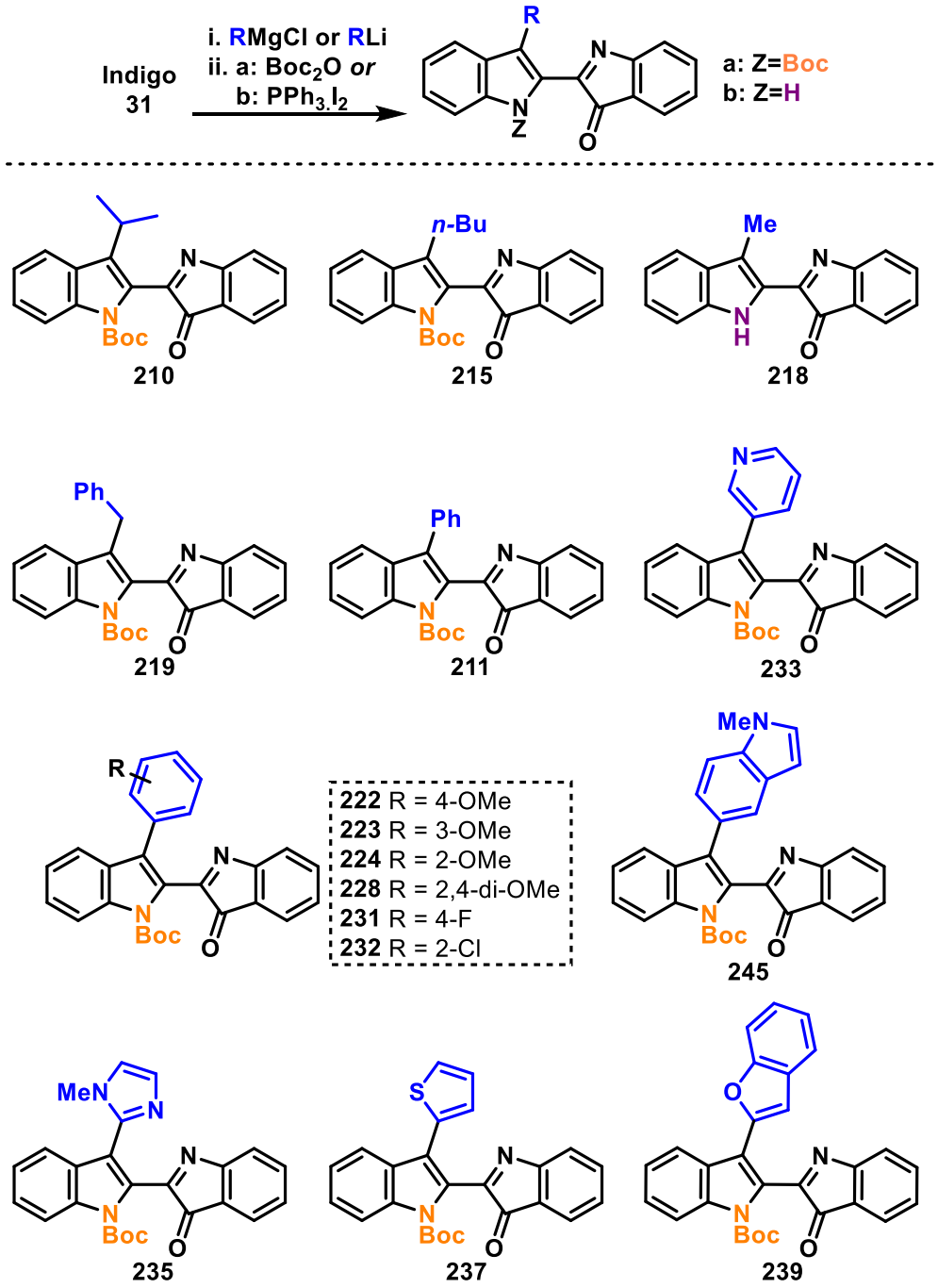

Scheme 103: The sixteen isolated scaffolds from reactions of Grignard reagents with indigo.

Of the fifteen isolated *N*-Boc indoles synthesised, eleven were able to be deprotected to their corresponding free indoles (**209**, **214**, and **250**–**258**), while the methyl adduct **218** was isolated as the free indole. Evaluation of the biological activity of these twelve free indoles revealed that **218** exhibited potent and highly-selective antiplasmodial activity, with IC_{50} values against *P. falciparum* of 52 nM, and SI values >1500 *in vitro*. The structural homology and similar biological profile of **218** to other 2-aryl-3-oxoindolenines suggest a similar mechanism of action, where *P. falciparum* propagation is inhibited by a

hypoxia-induced single-electron reduction, leading to stable radical intermediates which trigger hyperphosphorylation and eventual haemolysis of infected blood cells prior to parasite maturation.[165a] This mechanism of action was supported by SAR trends, where the strongly-stabilising benzyl **251**, 4-fluorophenyl **256** and 4-methoxyphenyl **252** moieties presumably led to increased radical stabilisation,[178] evidenced by their lower IC_{50} values of 0.80 μM, 0.77 μM and 1.44 μM, respectively, compared with the parent phenyl **214** (IC_{50} 6.91 μM) (Scheme 104).

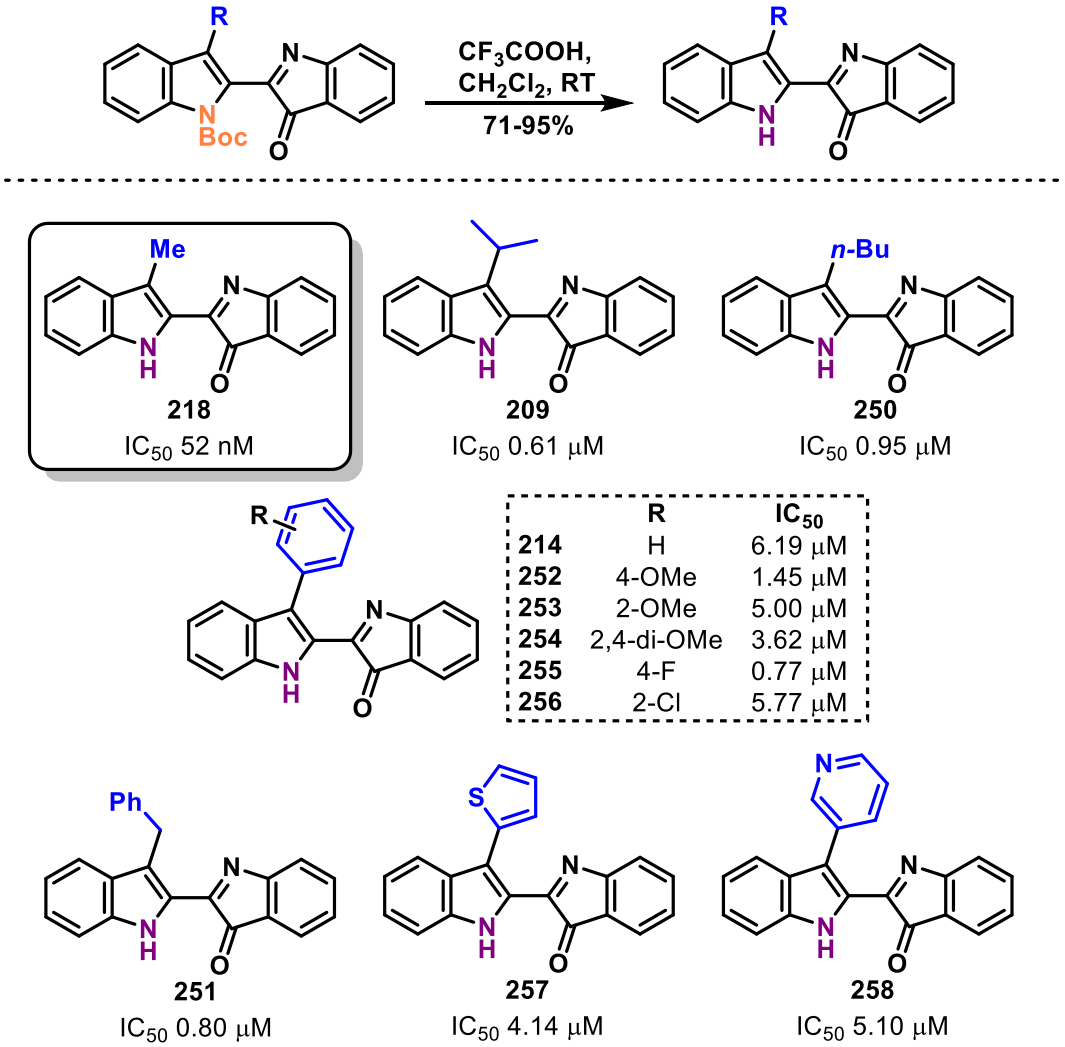

Scheme 104: The twelve isolated free indoles from this study, with comparison of their IC_{50} values against *P. falciparum* (3D7) parasites *in vitro*.

Given that 2-aryl-3-oxoindolenine-*N*-oxides have previously showed increased activity against *P. falciparum* relative to their parent heterocycle,[165a, 175-177] an obvious direction for future development would be to examine the biological properties of the *N*-oxides of the diindoles synthesised as part of this study. Chemoselective oxidation of nitrogen heterocycles (e.g. pyridines to pyridine-*N*-oxides) is well-known using numerous reagents (e.g. *m*-CPBA, H_2O_2-urea complex),[183] and the corresponding transformation

has been previously-adapted to simple 2,3,3-trisubstituted-3*H*-indoles by reduction to the corresponding indoline, and back-oxidation with *m*-CPBA to yield the *N*-oxide species.[184] As the indigo core has previously been demonstrated to be susceptible to oxidative cleavage, it is unknown whether the conditions required for *N*-oxide formation (i.e. to **283**) would also trigger C2-C2'-cleavage to substituted isatins and/or anthranilic acid derivatives.[116b] Further derivatives with vinyl (**284**), fluoromethyl (**285**), and difluoromethyl (**286**) substituents could also be explored to improve the stability of the active radical species, while additional substituents about the indigo core could also improve its membrane permeability, which in previous studies of 5-methoxy-3-oxoindolenines (e.g. **287**) was observed to increase antiplasmodial activity relative to their non-substituted counterparts (**288**). The 5'-methoxy and 5,5'-dimethoxy species **289** and **290** would therefore be attractive scaffolds for further derivatisation (Scheme 105).

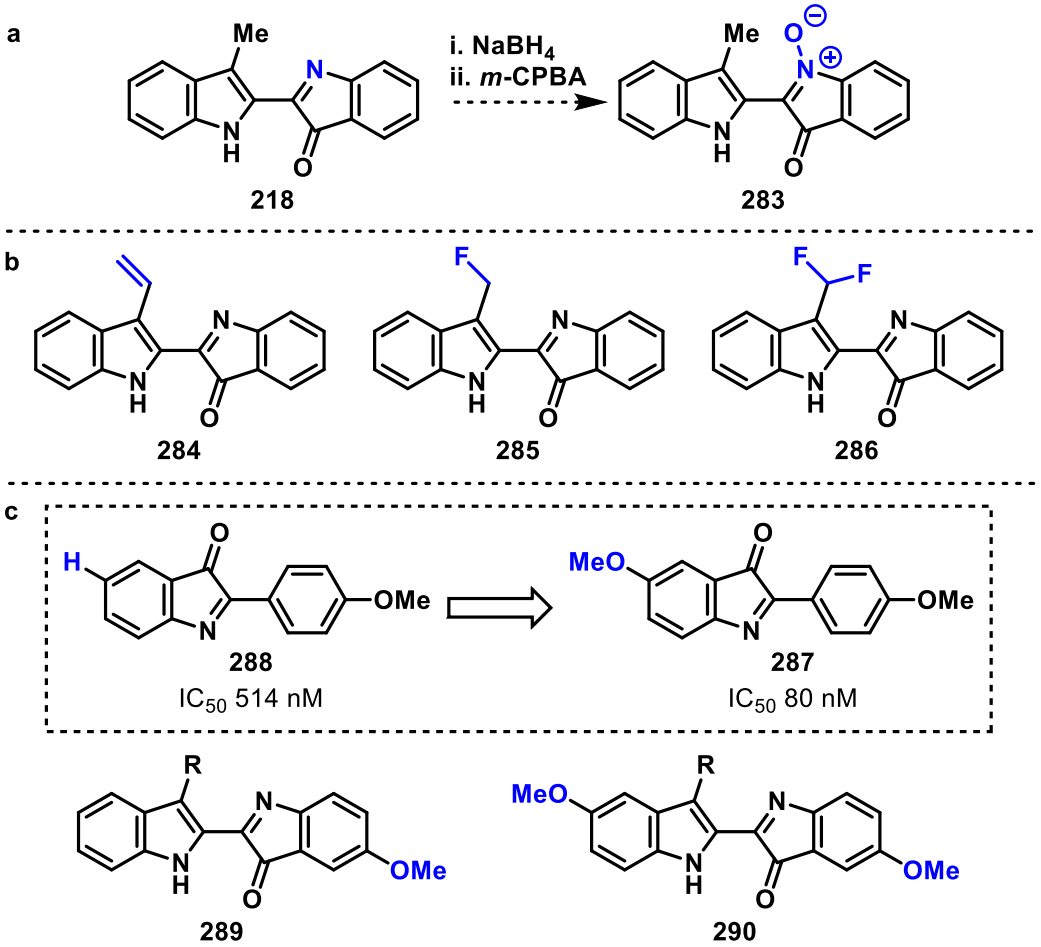

Scheme 105: Proposed derivatives for further biological evaluation and optimisation: a) *N*-oxide formation, b) new radical-stabilising adducts such as the vinyl **284**, and fluorinated adducts **285** and **286**, and c) methoxylated adducts **289** and **290**.

This methodology could also be applied as a starting point for the synthesis of complex polycyclic structures. The natural product indimicin A (**197**) features a non-symmetrical 2,2'-diindole core, with a fused *N*-methylpyrrole substituent, and has not been synthesised previously.[185] The addition-dehydration of *N*-methylpyrrol-3-ylmagnesium chloride **291** to 5,5'-dichloroindigo (**292**) could give access to the desymmetrised *N*-Boc adduct **293**, which could then undergo *N*-methylation and selective reduction of the iminium ion to give the racemic *N*-methylindoline **294**. Nucleophilic addition to the carbonyl on the less-hindered face with methyllithium could then afford the tertiary alcohol **295**, which upon treatment with TfOH could undergo both Boc deprotection and dehydration of the alcohol group, leading to cationic intermediate **296**, and subsequent Friedel-Crafts alkylation of the nearby pyrrole at the *syn*-face to afford the desired diastereomer of indimicin A (Scheme 106). Using alternatively-substituted pyrroles in the first step could also give access to indimicins B, C, and D (**198**–**200**) following this pathway.

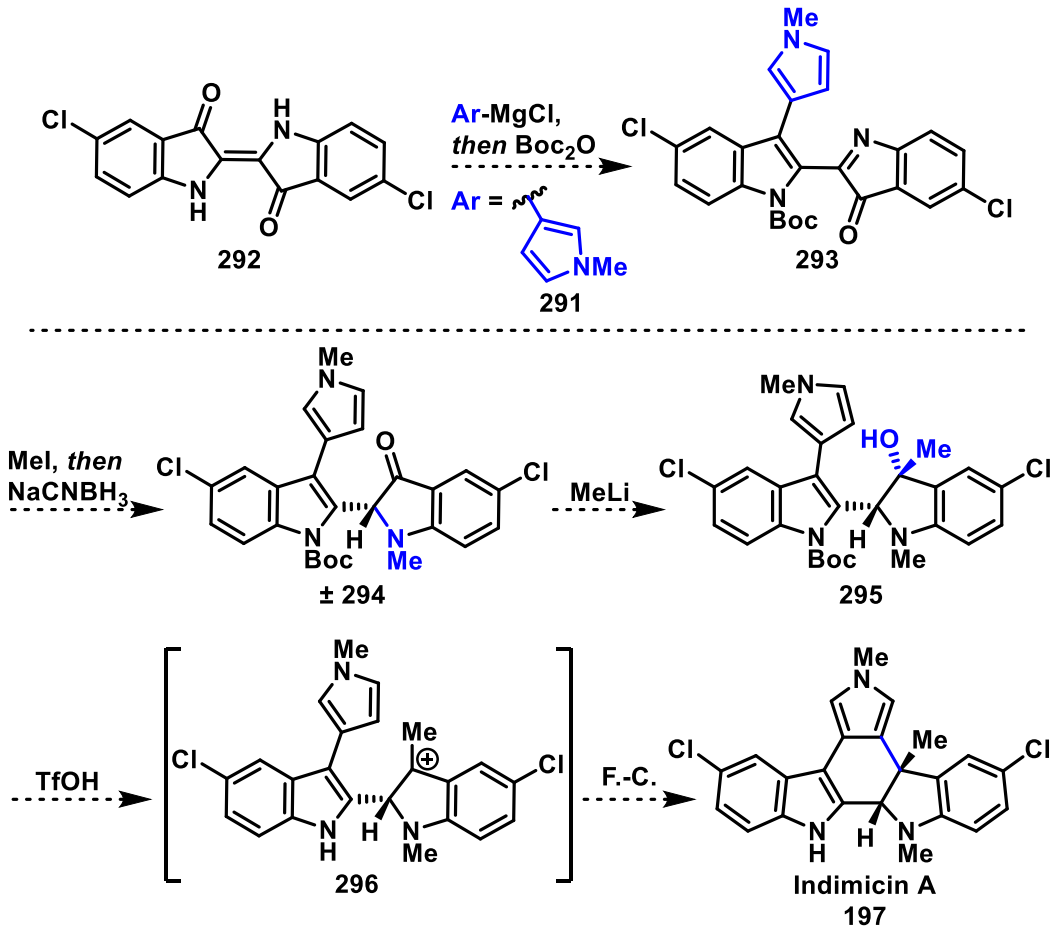

Scheme 106: Proposed synthesis of indimicin A (**197**) using this developed methodology, following the addition of a pyrrole substituent to dichloroindigo **292** in the intial step to give the desymmetrised adduct **293**.

6.4 Conclusion

Throughout the course of this investigation, we have a) examined the cascade reactions of indigo with propargylic electrophiles to produce various fused-ring and ring-expanded adducts, b) investigated cascade reactions with ring-strained electrophiles to generate a variety of *N,O′*-spirocyclic and *N,N′*-cyclic molecules, and c) developed new methodology for the construction of non-symmetrical 2,2'-diindoles by reacting indigo with various organometallic nucleophiles. Where previously it was thought that indigo was relatively inert,[50d] we have established a variety of methods for its rapid derivatisation into highly-functionalised and biologically-active materials. Indigo's unique reactivity is a result of the functional density of its core, and our proposed reaction mechanisms demonstrate that the conjugation of the indigo moiety allows its reactivity to change between individual steps in the cascade process, rapidly building molecular complexity. This unusual and rapidly-oscillating reactivity however remains unpredictable, and we still do not possess a complete understanding of the reactivity of indigo. These investigations have revealed numerous key pieces of information, however there is much that requires further exploration, and we have only begun to scratch the surface of indigo's unique chemistry.

Chapter 7:
Experimental Data

7.1. General experimental information

Reagents and solvents were purchased reagent grade and used without further purification unless otherwise stated. All reactions were performed in standard oven-dried glassware under $CaCl_2$-dried nitrogen gas unless otherwise stated. Anhydrous DMF (99.9%) was purchased from Sigma Aldrich and used without further purification. Indigo dye was purchased from Sigma Aldrich, or from AK Scientific and used without further purification. THF was dried by distillation from Na/benzophenone and stored over 3 Å molecular sieves prior to use. All solutions of Grignard reagents or organolithium reagents were titrated prior to use, using either 2-butanol or menthol in THF with 1,10-phenanthroline as indicator. Melting point temperatures are expressed in degrees Celsius (˚C) and are uncorrected. ^{1}H and ^{13}C NMR spectra ($CDCl_3$/DMSO) were recorded either at 500 MHz and 125 MHz, or 400 MHz and 101 MHz, respectively, with chemical shifts (δ) reported as parts per million relative to TMS (δ = 0.00 ppm), $CDCl_3$ (δ = 7.26; 77.0 ppm) or DMSO-d_6 (δ = 2.50 ppm; 39.51 ppm). ^{19}F NMR spectra ($CDCl_3$) were recorded at 470 MHz or 377 MHz, with chemical shifts (δ) reported as parts per million relative to $CFCl_3$ (δ = 0.00 ppm). Coupling constants (J) are reported in Hertz (Hz). Multiplicities are reported as singlets (s), doublets (d), triplets (t), doublet of doublets (dd), quartets (q), hextets (h), heptets (hept), or multiplets (m). Electrospray (ESI single quadrupole) mass spectra have their ion mass to charge values (m/z) stated with their relative abundances as a percentage in parentheses. Peaks assigned to the molecular ion are denoted as $[M+H]^+$ or $[M+Na]^+$. HR-ESI mass spectra were recorded using a XEVO QToF instrument, with LeuEnk as internal standard. Infrared (IR) spectra were recorded neat. UV-visible absorption spectra were recorded as solutions in CH_2Cl_2 or acetone at room temperature. Optical rotations were recorded in $CHCl_3$ or CH_2Cl_2 at room temperature. Thin layer chromatography (TLC) was performed using silica gel F254 aluminium sheets. Column chromatography was performed using silica gel 60 (0.063-0.200 mm). Eluents are reported in volume to volume (v:v) ratios. Solvent extracts and chromatographic fractions were concentrated by rotary evaporation *in vacuo*. Petroleum spirit had a bp range of 40-60 ˚C.

7.2 Reactions of indigo with propargylic electrophiles

7.2.1. Synthesis of starting materials

***bis*-(triphenylphosphine)palladium (II) chloride [$Pd(PPh_3)_2Cl_2$]**[128]

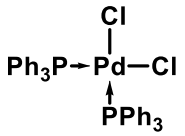

A suspension of palladium(II) chloride (1.02 g, 5.75 mmol) and triphenylphosphine (3.26 g, 12.4 mmol) in benzonitrile (30 mL) was heated at 180 °C with vigorous stirring for 20 min under dry N_2, then allowed to cool to RT overnight. The resulting bright-yellow crystals were collected by vacuum filtration, washed with ether (3×50 mL) and dried *in vacuo* to give *bis*-(triphenylphosphine)palladium(II) chloride (3.85 g, 95%) as fine, bright yellow needles.

3-(4-methoxyphenyl)prop-2-yn-1-ol (131a)

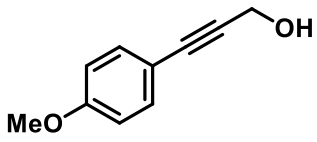

A 250 mL round-bottomed flask equipped for magnetic stirring was charged with 4-iodoanisole (5.03 g, 21.5 mmol), $Pd(PPh_3)_2Cl_2$ (300 mg, 0.43 mmol, 2 mol%), and CuI (410 mg, 2.15 mmol, 10 mol%), then evacuated and backfilled thrice with dry nitrogen. The solids were suspended in toluene (40 mL) and MeCN (40 mL), and the mixture cooled to 0 ˚C, then NEt_3 (14.5 g, 143 mmol) and propargyl alcohol (6.00 g, 107 mmol) were added slowly. The ice bath was removed, and the resulting thick emulsion stirred vigorously for 2 d under a nitrogen balloon, then the solvent removed *in vacuo*. The dark-brown, tarry residue was taken up in EtOAc (200 mL), and filtered over a plug of silica (eluting with EtOAc, 200 mL), and the combined fractions washed sequentially with 1 M HCl (4×50 mL), and sat. $NaHCO_3$ (4×50 mL), dried ($MgSO_4$), and the solvent removed to afford the desired arylpropargyl alcohol **131a** (3.48 g, 99%) as pale amber crystals, mp. 74–76 ˚C, lit. 77–78 ˚C.[186] R_f (20% EtOAc/pet spirit) 0.37. ^{1}H NMR ($CDCl_3$, 500 MHz) δ 7.37 (d, J = 8.5 Hz, 2H, H2', H6'), 6.84 (d, J = 8.5 Hz, 2H, H3', H5'), 4.47 (s, 2H, H1), 3.81 (s, 3H, OCH_3), 1.68 (bs, 1H, OH). ^{13}C NMR (126 MHz) δ 159.8 (C4'), 133.2 (C2', C6'), 114.7 (C1'), 114.0 (C3', C5'), 85.9 (C3), 85.6 (C2), 55.3 (-OCH_3), 51.7 (C1). HRESI-MS calcd. for $C_{10}H_{11}O_2^+$ 163.0754, found 163.0760.

3-phenylprop-2-yn-1-ol (131b)

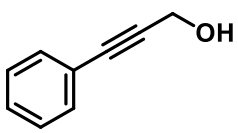

Prepared as **131a**, except using iodobenzene (4.38 g, 21.5 mmol), and a lower catalyst loading of $Pd(PPh_3)_2Cl_2$ (147 mg, 0.209 mmol, 1 mol%). Following aqueous workup, the residue was subjected to flash chromatography (45 g silica, 20% EtOAc/hexane), affording the desired arylpropargyl alcohol (2.83 g, 100%) as a pale amber oil. R_f (60% CH_2Cl_2/pet spirit) 0.50.

^{1}H NMR ($CDCl_3$, 400 MHz) δ 7.39 (d, *J* = 8.0 Hz, 2H, H2', H6'), 7.30 – 7.20 (m, 3H, H3', H4', H5'), 4.43 (s, 2H, H1), 1.71 (bs, 1H, OH). ^{13}C NMR (101 MHz) δ 131.5 (C2', C6'), 128.3 (C4'), 128.2 (C3', C5'), 122.5 (C1'), 87.3 (C3), 85.4 (C2), 51.2 (C1). HRESI-MS calcd. for $C_9H_9O^+$ 133.0648, found 133.0643.

3-(4-nitrophenyl)prop-2-yn-1-ol (131c)

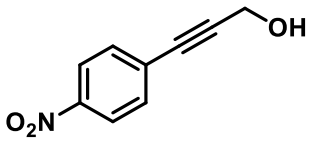

Prepared as **131a**, except using 4-iodonitrobenzene (5.33 g, 21.4 mmol). Following aqueous workup, the residue was passed through a plug of silica using EtOAc as eluent, and the desired arylpropargyl alcohol was isolated (3.60 g, 95%) as tan crystals, mp. 109–110 ˚C, lit. 113–114 ˚C.[187] R_f (60% CH_2Cl_2/pet spirit) 0.12. ^{1}H-NMR ($CDCl_3$, 500 MHz) δ 8.18 (d, *J* = 8.5 Hz, 2H, H3', H5'), 7.57 (d, *J* = 8.5 Hz, 2H, H2', H6'), 4.53 (s, 2H, H1), 1.69 (bs, 1H, OH). ^{13}C NMR (101 MHz, $CDCl_3$): δ 147.3 (C4'), 132.4 (C2', C6'), 129.4 (C1'), 123.6 (C3', C5'), 92.5 (C3), 83.8 (C2), 51.5 (C1). HRESI-MS calcd. for $C_9H_8O_3N^+$ 178.0499, found 178.0494.

3-(3-methoxyphenyl)prop-2-yn-1-ol (131d)

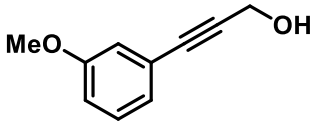

Prepared as **131a,** except using 3-iodoanisole (0.47 g, 2.0 mmol). Following aqueous workup, the desired arylpropargyl alcohol was isolated (0.31 g, 96%) as a brown oil. R_f (10% EtOAc/pet spirit) 0.21. ^{1}H NMR ($CDCl_3$, 400 MHz): δ 7.21 (dd, *J* = 8.4 Hz, 7.6 Hz, 1H, H5'). 7.04 (d, *J* = 7.6 Hz, 1H, H6'), 7.01 – 6.97 (m, 1H, H2'), 6.88 (dd, *J* = 8.4 Hz, 2.0 Hz, 1H, H4'), 4.51 (s, 2H, H1), 3.82 (s, 3H, OCH_3), 1.55 (bs, 1H, OH). ^{13}C NMR ($CDCl_3$, 101 MHz): δ 158.7 (C3'), 128.9 (C5'), 123.8 (C1'), 123.1 (C2'), 116.1 (C6'), 114.5 (C4'), 86.8 (C3), 84.9 (C2), 54.8 (-OCH_3), 50.9 (C1). HRESI-MS calcd. for $C_{10}H_{11}O_2^+$ 163.0754, found 163.0763.

3-bromo-1-(4-methoxyphenyl)-1-propyne (132a)

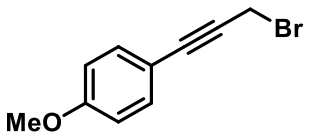

A solution of triphenylphosphine (1.91 g, 7.3 mmol) in CH_2Cl_2 (20 mL) was cooled to 0 ˚C, then bromine (1.17 g, 7.3 mmol) added slowly. The resulting yellow suspension was stirred vigorously for 30 min at 0 ˚C, then a solution of **131a** (0.962 g, 5.93 mmol) in CH_2Cl_2 (20 mL) added dropwise over 15 min. The mixture was stirred for 1 h, then diluted with hexanes (70 mL) and filtered through silica to remove precipitated PPh_3O. The collected filtrate was concentrated *in vacuo*, and the residue taken up in a minimum of Et_2O and

passed through a plug of silica, eluting with pet spirit.[††††††] Removal of the solvent gave the corresponding arylpropargyl bromide **132a** (1.32 g, 99%) as a yellow oil. R_f (10% EtOAc/pet spirit) 0.79. ^{1}H NMR ($CDCl_3$, 500 MHz) δ 7.38 (d, J = 8.5 Hz, 2H, H2', H6'), 6.84 (d, J = 8.5 Hz, 2H, H3', H5'), 4.17 (s, 2H, H1), 3.81 (s, 3H, -OCH_3). ^{13}C NMR (125 MHz) δ 160.1 (C4'), 133.6 (C2', C6'), 114.3 (C1'), 114.1 (C3', C5'), 87.0 (C3), 83.0 (C2), 55.5 (-OCH_3), 15.9 (C1). EI-MS (+) 226^+ (8%, $^{81}BrM^+$), 224^+ (8%, $^{79}BrM^+$), 145^+ (100%, $[M - Br^\bullet]^+$).

3-bromo-1-phenyl-1-propyne (132b)

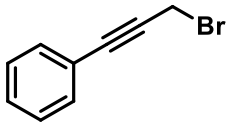

Prepared as **132a**, except using **131b** (0.661 g, 5.00 mmol), triphenylphosphine (1.46 g, 5.56 mmol) and bromine (0.889 g, 5.56 mmol), and the mixture stirred at 0 ˚C for 1 h. The solvent was removed *in vacuo* and hexane (10 mL) added, and the precipitated solids washed with further hexane (2×5 mL). The combined filtrates were concentrated *in vacuo*, and subjected to flash chromatography (25 g silica, 60% CH_2Cl_2/pet spirit), to afford the desired arylpropargyl bromide (0.968 g, 99%) as a pale-yellow oil. R_f (10% EtOAc/pet spirit) 0.70. ^{1}H NMR (400 MHz, $CDCl_3$): δ 7.51 – 7.42 (m, 2H, H3', H5'), 7.40 – 7.29 (m, 3H, H2', H4', H6'), 4.18 (s, 2H, H1). ^{13}C NMR (101 MHz, $CDCl_3$): δ 131.8 (C1'), 128.8 (C3', C5'), 128.3 (C2', C6'), 122.1 (C4'), 86.7 (C3), 84.2 (C2), 15.3 (C1). EI-MS (+) 196^+ (8%, $^{81}BrM^+$), 194^+ (8%, $^{79}BrM^+$), 115^+ (100%, $[M - Br^\bullet]^+$).

3-bromo-1-(4-nitrophenyl)-1-propyne (132c)

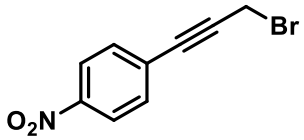

Prepared as **132a**, except using **131c** (0.885 g, 5.00 mmol), triphenylphosphine (1.44 g, 5.49 mmol) and bromine (0.870 g, 5.44 mmol), and the mixture stirred at 0 ˚C for 1 h. The solvent was removed *in vacuo* and hexane (10 mL) added, and the precipitated solids washed with further hexane (2×5 mL). The combined filtrates were concentrated *in vacuo*, and subjected to flash chromatography (25 g silica, 60% CH_2Cl_2/pet spirit), to afford the desired arylpropargyl bromide (1.13 g, 94%) as a bright yellow powder. R_f (30% CH_2Cl_2/pet spirit) 0.62. ^{1}H NMR (400 MHz, $CDCl_3$): δ 8.19 (d, J = 8.5 Hz, 2H, H3', H5'), 7.59 (d, J = 8.5 Hz, 2H, H2', H6'), 4.17 (s, 2H, H1). ^{13}C NMR (101 MHz, $CDCl_3$): δ 147.4 (C4'), 132.6 (C3', C5'), 128.9 (C1'), 123.6 (C2', C6'), 89.3 (C3), 84.3 (C2), 14.0 (C1). EI-MS (+) 241^+ (8%, $^{81}BrM^+$), 239^+ (8%, $^{79}BrM^+$), 160^+ (100%, $[M - Br^\bullet]^+$).

[††††††]Alternatively, the crude mixture could be stirred overnight with anhydrous $ZnCl_2$ (2.0 eq.) in EtOAc, and the $ZnCl_2/PPh_3O$ complex removed by filtration. The isolated yield for this procedure was 72%.

7.2.3. ***General Procedure A*** for alkylation of indigo

A suspension of indigo (262 mg, 1.00 mmol) in anhydrous DMF (40 mL) was sonicated at 60 ˚C for one hour. The resulting hot suspension was transferred by cannula under positive pressure of nitrogen into a 100 mL round-bottomed flask containing a magnetic stir bar, pre-dried and ground Cs_2CO_3 (1.206 g, 3.700 mmol), and fitted with a rubber septum. The resulting dark-green to amber solution was stirred for one hour in an oil bath, pre-heated to strictly 85-87 ˚C under dry nitrogen. The nitrogen flow was cut, and the electrophile (5.0 mmol) injected through the septum either neat, or as a solution in DMF (2 mL), and the mixture stirred at 85-87 ˚C for the required time. The resulting intensely-coloured solution was quenched over crushed ice (ca. 100 g), and the flask rinsed with EtOAc (ca. 10 mL) to remove adhered products. Upon warming to RT, the emulsion was saturated with solid NaCl, and extracted with EtOAc (4×60 mL) or $CHCl_3$ (4×60 mL) until the aqueous phase became clear. The combined organic fractions were condensed to ca. 150 mL, then extracted with brine (4×40 mL), dried ($MgSO_4$), and filtered through a 2 cm plug of celite, and the solvent removed *in vacuo*.

7.2.4. Reaction of indigo with 3-bromo-1-phenyl-1-butyne (**131b**)

7-hydroxy-8-phenylazepino[1,2-*a*:3,4-*b'*]diindol-14(13*H*)-one (122)

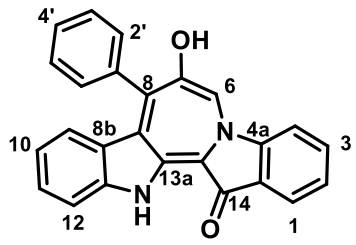

Prepared following ***General Procedure A*** (see Section 7.2.3), using arylpropargyl bromide **131b** (0.985 g, 5.05 mmol), and 4 Å molecular sieves (*ca.* 0.5 g) and a 30 min reaction time. The crude residue was fractionated on silica gel (80 g), eluting sequentially with 1) 60% CH_2Cl_2/hexane (**Fraction 1**), 2) CH_2Cl_2 (**Fraction 2**), 3) 10% EtOAc/CH_2Cl_2 (**Fraction 3**), and the column stripped using EtOAc (**Fraction 4**). Removal of the solvent from **Fraction 1** afforded the known azepinodiindolone **122** (139 mg, 37%) as a bright yellow powder, mp 149-151 ˚C. Spectral and physical characteristics were identical to those previously reported.[116b] R_f (10% EtOAc/hexane) 0.47. ^{1}H NMR ($CDCl_3$) δ 8.76 (d, *J* = 7.8 Hz, 1H, H9), 8.22 (d, *J* = 7.6 Hz, 1H, H12), 8.03 (dd, *J* = 7.9, 1.4 Hz, 1H, H1), 7.85-7.82 (m, 1H, H3), 7.73 – 7.66 (m, 2H, H2, H11), 7.60 (d, *J* = 8.0 Hz, 1H, H4), 7.53 – 7.46 (3H, m, H3', H5', H10), 7.39 – 7.35 (3H, m, H2', H4', H6'), 6.91 (1H, s, H6). ^{13}C NMR ($CDCl_3$) δ 184.6 (C14), 159.3 (C7), 152.2 (C12a), 144.5 (C8b), 143.0 (C14a), 137.8 (C8a), 135.7 (C8), 135.1 (C13a), 133.8 (C11), 133.5 (C4), 133.0 (C3), 130.9 (C2), 129.7 (C1), 129.0 (C2', C6'), 128.8 (C1'), 128.5 (C4'), 127.4 (C3', C5'), 127.1 (C10), 127.0 (C13b), 123.2 (C9),

121.8 (13b), 118.0 (C12). IR (neat) 3282 (br, m), 1656 (s), 1601 (s), 1585 (s), 1394 (m), 1119 (s), 734 (s) cm^{-1}. HRESI-MS calcd. for $C_{25}H_{17}N_2O_2^+$ 377.1291, found 377.1286.

7a-phenyl-13-(3-phenylprop-2-yn-1-yl)benzo[*b*]indolo[1,2-*h*][1,7]naphthyridine-8,14(7a*H*,13*H*)-dione (133)

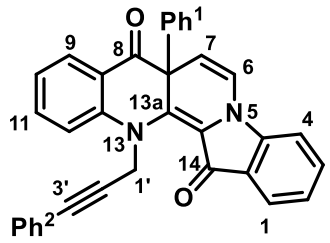

Fraction 2 was condensed and subjected to flash chromatography (80 g silica, 10% EtOAc/hexane). Removal of the solvent from the major band afforded the benzoindolonaphthyridine-dione **133** (171 mg, 35%) as deep red crystals, dec. 161 ˚C. X-ray quality crystals were grown by slow evaporation of a saturated solution in CH_2Cl_2. R_f (10% EtOAc/hexane) 0.17. ^{1}H NMR (500 MHz, $CDCl_3$) δ 8.01 (dd, *J* = 7.8, 1.7 Hz, 1H, H9), 7.77 (ddd, *J* = 7.7, 1.3, 0.7 Hz, 1H, H1), 7.53 (ddd, *J* = 8.4, 7.2, 1.3 Hz, 1H, H3), 7.51 – 7.41 (m, 3H, H11, Ph^1 or Ph^2 H3/H5), 7.35 – 7.27 (m, 4H, Ph^1 or Ph^2 H3/H5, Ph^1 or Ph^2 H2/H6), 7.25 – 7.15 (m, 3H, H4, Ph^1 or Ph^2 H3/H5), 7.12 (d, *J* = 7.5 Hz, 1H, H4), 7.10 – 7.06 (m, 1H, H12), 7.04 – 6.99 (m, 3H, H2, Ph^1 H4, Ph^2 H4), 6.96 (ddd, *J* = 7.9, 7.2, 0.9 Hz, 1H, H10), 6.83 (d, *J* = 7.9 Hz, 1H, H6), 5.51 (d, *J* = 7.9 Hz, 1H, H7), 5.18 (d, *J* = 18.4 Hz, 1H, H1'b), 4.91 (d, *J* = 18.5 Hz, 1H, H1'a). ^{13}C NMR (126 MHz, $CDCl_3$) δ 191.6 (C8), 178.9 (C14), 147.4 (C4a), 144.0 (C12a), 142.6 (Ph^1 C1), 135.8 (C13a), 135.6 (C11), 135.5 (C3), 131.8 (Ph^2 C1), 131.7 (Ph^1 or Ph^2 C3/C5), 129.1 (Ph^1 or Ph^2 C3/C5), 128.7 (Ph^1 or Ph^2 C2/C6), 128.4 (C9), 127.8 (Ph^1 or Ph^2 C2/C6), 127.3 (Ph^1 or Ph^2 C4), 124.8 (C1), 122.7 (C14a), 122.5 (C13b), 121.2 (C8a), 121.0 (C2), 120.9 (C10), 118.8 (C6), 115.9 (C12), 109.1 (C4), 105.1 (C7), 86.1 (C3'), 83.0 (C2'), 57.2 (C7a), 44.9 (C1'). IR (neat) 1690 (m), 1595 (m), 1571 (m), 1465 (s), 1332 (s), 1148 (m), 1001 (m), 743 (s) cm^{-1}. HRESI-MS calcd. for $C_{34}H_{23}N_2O_2^+$ 491.1754, found 491.1762.

(*Z*)-8-((*E*)-benzylidene)-6-(phenylethynyl)-8,9-dihydro-6*H*-[1,3,6]oxadiazocino[3,4-*a*:6,5-*a'*]diindole-15,16-dione (123)‡‡‡‡‡‡

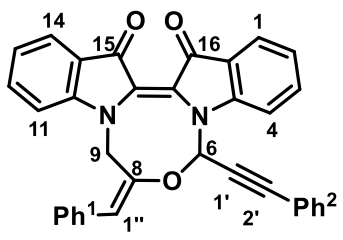

Fraction 3 and **Fraction 4** were combined and subjected to flash chromatography (80 g silica, 10% EtOAc/CH_2Cl_2), and removal of the solvent from the major dark blue fraction gave the proposed dihydrooxadiazocinodiindole **123** (61 mg, 12%) as an intense dark-blue powder, mp 295-297 ˚C. Spectral and physical characteristics were identical to those previously

‡‡‡‡‡‡ Assignments for compound **123** are based on the given structure as previously-reported, however further 2D NMR studies have suggested this structure to be incorrect.

reported.[116b] R_f (10% EtOAc/CH_2Cl_2) 0.51. ^{1}H NMR ($CDCl_3$) δ 7.81 (d, *J* = 7.5 Hz, 1H, H14), 7.75 (d, *J* = 7.6 Hz, 1H, H1), 7.46 (d, *J* = 7.3 Hz, 1H, H11), 7.45 – 7.33 (m, 4H, H3, H12, H13, Ph^2H), 7.17 – 6.98 (m, 10H, H2, 4×Ph^2H, 5×Ph^1H), 6.86 (d, *J* = 8.1 Hz, 1H, H4), 6.72 (s, 1H, H1''), 5.67 (s, 1H, H6), 4.75 (ABq, *J* = 36.9, 16.0 Hz, 2H, H9). ^{13}C NMR ($CDCl_3$) δ 180.9 (C15), 180.2 (C16), 149.4 (C4a), 148.2 (C10a), 135.4 (C13), 134.5 (C1''), 134.1 (C15b), 132.0 (C11), 129.4 (C12), 129.3 (3×Ar''C), 129.0 (C14a), 128.9 (C3'), 128.7 (Ar'C), 128.5 (Ar''C), 128.0 (C16a), 125.9 (3C, 2×Ar'C, 1×Ar''C), 125.6 (C14), 124.4 (C1), 123.4 (C14a), 122.9 (15a), 121.7 (Ar'C), 121.5 (Ar'C), 117.5 (C9), 114.6 (C2), 109.6 (C4), 89.0 (C2'), 83.0 (C1'), 61.2 (C8), 56.8 (C6). IR (neat) 3076 (m), 1735 (m), 1689 (m), 1459 (m), 1243 (m), 1162 (m), 1102 (s), 761 (s) cm^{-1}. HRESI-MS calcd. for $C_{34}H_{23}N_2O_3^+$, 507.1714, found 507.1720.

7.2.5. Reaction of indigo with 3-bromo-1-(4-methoxyphenyl)-1-butyne (**131a**)

7a-(4-methoxyphenyl)-13-(3-(4-methoxyphenyl)-prop-2-yn-1-yl)benzo[*b*]indolo[1,2-*h*][1,7]naphthyridine-8,14(7a*H*,13*H*)-dione (134)

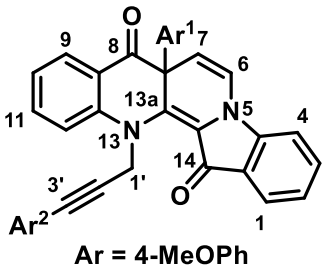

Prepared following ***General Procedure A*** (see Section 7.2.3), using arylpropargyl bromide **131a** (1.13 g, 5.02 mmol), and 4 Å molecular sieves (*ca.* 0.5 g) and a 30 min reaction time. The crude residue was fractionated on silica gel (20% EtOAc/pet spirit), and the major red fraction condensed and subjected to flash chromatography (80 g silica, gradient elution with 10-25% EtOAc/pet spirit). Removal of the solvent from the major deep-red fraction afforded the *bis*-methoxyphenylbenzoindolonaphthyridine **134** (114 mg, 21%) as small, bright pink crystals, dec. 140 ˚C. X-ray quality crystals were grown by slow evaporation of a solution in EtOAc/pet spirit. R_f (20% EtOAc/pet spirit) 0.33. ^{1}H NMR (500 MHz, $CDCl_3$) δ 8.00 (dd, *J* = 7.8, 1.6 Hz, 1H, H9), 7.76 (d, *J* = 7.7 Hz, 1H, H1), 7.53 (ddd, *J* = 8.4, 7.3, 1.3 Hz, 1H, H3), 7.47 (ddd, *J* = 7.2, 6.8, 1.7 Hz, 1H, H11), 7.19 – 7.16 (m, 2H, Ar^1 H2/H6), 7.12 (d, *J* = 8.2 Hz, 1H, H4), 7.08 (d, *J* = 8.4 Hz, 1H, H12), 7.02 (app t, *J* = 7.2 Hz, 1H, H2), 6.98 – 6.93 (m, 3H, H10, Ar^2 H2/H6), 6.82 (d, *J* = 7.9 Hz, 1H, H6), 6.72 – 6.67 (m, 4H, Ar^1 H3/H5, Ar^2 H3/H5), 5.49 (d, *J* = 7.9 Hz, 1H, H7), 5.14 (d, *J* = 18.4 Hz, 1H, H1'a), 4.87 (d, *J* = 18.4 Hz, 1H, H1'b), 3.76 (s, 3H, Ar^2 OMe), 3.51 (s, 3H, Ar^1 OMe). ^{13}C NMR (126 MHz, $CDCl_3$) δ 191.6 (C8), 178.7 (C14), 159.5 (Ar^1C4), 158.9 (Ar^2 C4), 147.2 (C4a), 143.9 (C12a), 136.0 (C13a), 135.4 (C11), 135.2 (C3), 134.6 (Ar^1 or Ar^2 C1), 133.6 (Ar^1 or Ar^2 C1), 133.0 (Ar^2 C2/C6), 128.4 (Ar^1

C2/C6), 128.3 (C9), 124.6 (C1), 122.6 (C14a), 121.0 (C8a), 120.8 (C2), 120.6 (C10), 118.4 (C6), 115.8 (C12), 114.6 (C13b), 114.2 (Ar^1 or Ar^2 C3/C5), 113.6 (Ar^1 or Ar^2 C3/C5), 108.9 (C4), 105.0 (C7), 85.7 (C3'), 81.6 (C2'), 56.4 (C7a), 55.3 (Ar^1-OMe), 54.9 (Ar^2-OMe), 44.8 (C1'). IR (neat) 1688 (m), 1597 (m), 1572 (m), 1469 (s), 1336 (s), 1152 (m), 1002 (m), 743 (s) cm^{-1}. HRESI-MS calcd. for $C_{36}H_{27}N_2O_4^+$ 551.1965, found 551.1959.

7.3 Reactions of indigo with ring-strained electrophiles

7.3.1. Synthesis of starting materials

2,3-dibromopropan-1-ammonium bromide (162)[139a]

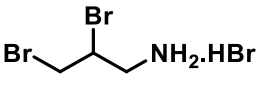

To a solution of allylamine (4.28 g, 75.0 mmol) in water (50 mL) was added 48% $HBr_{(aq)}$ (9.6 mL, 82.5 mmol) and bromine (18.0 g, 113 mmol) at 0 ˚C, and the mixture stirred at room temperature for 4 h. The mixture was warmed in a 70 ˚C water bath, at which point the remaining bromine was distilled off,[§§§§§§] then the solution was cooled, and the water removed *in vacuo*. The off-white residue was recrystallised from hot *i*-PrOH (*ca.* 50 mL) and the collected crystals dried *in vacuo* to afford 2,3-dibromopropan-1-ammonium bromide **162** (17.9 g, 80%) as shiny, white needles, mp 168–170 ˚C, lit. 170–172.5 ˚C.[188]

(±)-*N*-tosyl-2-bromomethylaziridine (147)[139a]

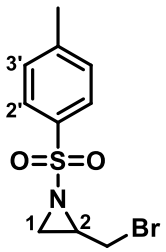

Tosyl chloride (3.36 g, 17.6 mmol) was added to a solution of hydrobromide salt **162** (5.00 g, 16.8 mmol) in water (20 mL), then NaOH (3.43 g, 85.8 mmol) in water (20 mL) was added with vigorous stirring. The mixture was stirred for 1 h, then extracted with CH_2Cl_2 (4×50 mL) and the combined organic layers washed with brine (2×50 mL), dried ($MgSO_4$) and concentrated to afford the desired bromomethylaziridine **147** (4.83 g, 99%) as a clear, refractive oil. R_f (20% EtOAc/pet spirit) 0.42. ^{1}H NMR (500 MHz, $CDCl_3$) δ 7.82 (d, *J* = 8.0 Hz, 2H, H2', H6'), 7.33 (d, *J* = 8.0 Hz, 2H, H3', H5'), 3.26 (d, *J* = 6.5 Hz, 2H, CH_2Br), 3.05 (dt, *J* = 6.5 Hz, 4.0 Hz, 1H, H2), 2.78 (d, *J* = 6.5 Hz, 1H, H1b) 2.44 (s, 3H, $TsCH_3$), 2.22 (d, *J* = 4.0 Hz, 1H, H1a). ^{13}C NMR (125 MHz) δ 144.9 (Ar C1'), 134.4 (Ar C4'), 129.7 (Ar C2', C6'), 128.6 (Ar C3', C5'), 39.8 (C1), 34.3 (C2), 30.6 (CH_2Br), 21.6 ($TsCH_3$). ESI-MS (+) 292 (100%, [^{81}Br]M+H^+), 290 (100%, [^{79}Br]M+H^+].

[§§§§§§]Care should be taken to avoid exposure to bromine vapour during this step. Excess bromine was distilled into a Schlenk tube containing $Na_2S_2O_3$ solution, and all glassware washed with dilute NaOH after use.

(±)-*N*-tosyl-2-hydroxymethylaziridine (163)[189]

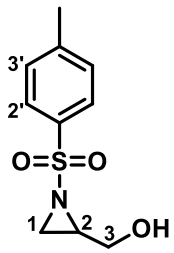

To a vigorously-stirred suspension of chloramine-T trihydrate (8.46 g, 30.0 mmol) and iodine (0.777 g, 3.06 mmol, 10 mol%) in dry MeCN (90 mL) was added allyl alcohol (2.56 g, 44.1 mmol), and the mixture stirred at room temperature for 3 d. The mixture was filtered, then the solvent removed *in vacuo*, and the residue taken up in EtOAc (100 mL) and washed with sat. $Na_2S_2O_3$ solution (20 mL) and brine (3×50 mL), and the solvent removed. Flash chromatography (80 g silica, 40% EtOAc/pet spirit) afforded the desired hydroxymethylaziridine **163** (2.43 g, 36%) as a clear, viscous oil. R_f (40% EtOAc/pet spirit) 0.25. ^{1}H NMR (500 MHz, $CDCl_3$) δ 7.82 (d, *J* = 8.0 Hz, 2H, H2', H6'), 7.35 (d, *J* = 8.0 Hz, 2H, H3', H5'), 3.81 (dd, *J* = 12.5 Hz, 3.0 Hz, 1H, H3a) 3.54 (dd, *J* = 12.0 Hz, 5.5 Hz, 1H, H3b), 3.08 – 2.96 (m, 1H, H2), 2.61 (d, *J* = 7.0 Hz, 1H, H1b) 2.45 (s, 3H, $TsCH_3$), 2.30 (d, *J* = 4.5 Hz, 1H, H1a), 2.18 (bs, 1H, OH). ^{13}C NMR (125 MHz) δ 145.0 (Ar C1'), 134.5 (Ar C4'), 130.0 (Ar C2', C6'), 128.2 (Ar C3', C5'), 61.1 (C3), 40.7 (C1), 31.2 (C2), 21.8 ($TsCH_3$). ESI-MS (+) 250 (100%, M+Na^+), 228 (26%, M+H^+).

***N,N'*-(3-hydroxypropane-1,2-diyl)bis(4-methylbenzenesulfonamide) (166)**[*******]

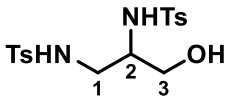

Further elution afforded a second major fraction, and removal of the solvent afforded the *bis*-sulfonamide **166** (3.32 g, 56%) as a bone-coloured amorphous solid. R_f (40% EtOAc/pet spirit) 0.13. ^{1}H NMR (500 MHz, $CDCl_3$) δ 7.73 (d, *J* = 8.0 Hz, 2H, Ts^1 H2', H6'), 7.64 (d, *J* = 8.0 Hz, 2H, Ts^2 H2', H6'), 7.29 – 7.20 (m, 4H, Ts^1/Ts^2 H3', H5'), 5.88 (d, *J* = 7.5 Hz, 1H, C2-NH), 5.77 (t, *J* = 5.0 Hz, 1H, C1-NH) 3.63 – 3.56 (m, 1H, H3a) 3.54 – 3.46 (m, 1H, H3b), 3.35 – 3.26 (m, 1H, H2), 3.22 (bs, 1H, OH), 3.04 – 2.90 (m, 2H, H1a/b) 2.39 (s, 6H, 2×$TsCH_3$). ^{13}C NMR (125 MHz) δ 143.70 (Ts^1 C1'), 143.66 (Ts^2 C1'), 137.1 (Ts^1 C4'), 136.3 (Ts^2 C4'), 129.86 (Ts^1 C2', C6'), 129.83 (Ts^2 C2', C6'), 127.1 (Ts^1 C3', C5'), 127.0 (Ts^2 C3', C5'), 61.7 (C3), 54.1 (C2), 43.6 (C1), 21.56 (Ts^1 CH_3), 21.53 (Ts^2 CH_3). ESI-MS (+) 421 (100%, M+Na^+), 399 (26%, M+H^+).

***meso*-*N*-tosyl-7-azabicyclo[4.1.0]heptane (168)**

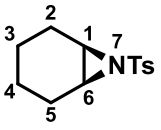

Prepared as per **163** using cyclohexene **167** (1.70 g, 20.7 mmol), chloramine-T (4.25 g, 15.1 mmol) and iodine (385 mg, 1.51 mmol, 10 mol%) in MeCN (45 mL), and the mixture stirred for 2 d. The crude residue was subjected to flash chromatography (45 g silica, 40% EtOAc/pet spirit), and

[*******]Repeating the reaction on a 7 mmol scale but increasing the amount of chloramine-T to 2.1 eq. gave a 75% isolated yield of **166**.

removal of the solvent from the major fraction afforded the azabicyclo[4.1.0]heptane **168** (2.94 g, 78%) as white crystals, mp 54–56 ˚C. R_f (40% EtOAc/pet spirit) 0.82. ^{1}H NMR (500 MHz, $CDCl_3$) δ 7.84 (d, *J* = 8.0 Hz, 2H, H2', H6'), 7.35 (d, *J* = 8.0 Hz, 2H, H3', H5'), 3.00 (app s, 2H, H1, H6), 2.47 (s, 3H, $TsCH_3$), 1.85 – 1.78 (m, 4H, H2a, H5a, H3a, H4a), 1.48 – 1.38 (m, 2H, H2b, H5b), 1.32 – 1.20 (m, 2H, H3b, H4b). ^{13}C NMR (125 MHz) δ 144.0 (Ar C1'), 135.9 (Ar C4'), 129.6 (Ar C2', C6'), 127.6 (Ar C3', C5'), 39.8 (C1/C6), 22.8 (C2/C5), 21.6 ($TsCH_3$), 19.4 (C3/C4). ESI-MS (+) 274 (100%, $M+Na^+$), 252 (26%, $M+H^+$).

***N,N'*-(*trans*-cyclohexane-1,2-diyl)bis(4-methylbenzenesulfonamide) (169)**

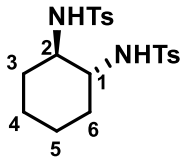

Further elution afforded a second fraction, and removal of the solvent afforded the *bis*-sulfonamide **169** (0.624 g, 20%) as a white amorphous solid, mp 178–179 ˚C. ^{1}H NMR (500 MHz, $CDCl_3$) δ 7.76 (d, *J* = 8.3 Hz, 4H, 2×Ts H2', H6'), 7.31 (d, *J* = 8.3 Hz, 4H, 2×Ts H3', H5'), 4.98 (br s, 2H, 2×NHTs), 2.78 – 2.73 (m, 2H, H1, H2), 1.83 – 1.79 (m, 2H, H3a, H6a), 1.54 – 1.52 (m, 2H, H4a, H5a), 1.12 – 1.06 (m, 4H, H3b, H4b, H5b, H6b). ^{13}C NMR (125 MHz) δ 143.3 (2×TsC1'). 139.6 (2×TsC4'), 129.7 (2×TsC2', C6'), 127.3 (2×TsC3', C5'), 66.3 (C1 or C2), 54.9 (C1 or C2), 35.3 (C3 or C6), 31.0 (C3 or C6), 26.5 (C4 or C5), 24.0 (C4 or C5), 21.9 (Ts^1CH_3), 21.7 (Ts^2CH_3). ESI-MS (+) 445 (100%, $M+Na^+$), 423 (26%, $M+H^+$).

***N*-(1-chloro-3-hydroxypropan-2-yl)-4-methylbenzenesulfonamide (170)**

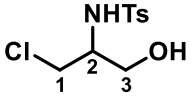

To a 0 ˚C solution of hydroxymethylaziridine **163** (0.407 g, 1.79 mmol) in CH_2Cl_2 (5 mL) was added NEt_3 (0.435 g, 4.30 mmol) and MsCl (0.444 g, 3.88 mmol), and the mixture stirred at 0 ˚C for 1 h, then allowed to warm to room temperature over 1 h. The mixture was quenched with sat. NH_4Cl solution (5 mL), then transferred to a separatory funnel and the organic layer washed with sat. NH_4Cl (20 mL) and sat. $NaHCO_3$ (20 mL), dried ($MgSO_4$), and the solvent removed. The resulting crude *O*-mesylate (0.579 g) was dried *in vacuo*, then dissolved in THF (10 mL), and TBAC.$2H_2O$ (0.104 g, 0.331 mmol) and LiCl (0.353 g, 8.33 mmol) added, and the mixture stirred overnight at 50 ˚C under nitrogen. The mixture was taken up in ether (30 mL) and washed with water (20 mL) and brine (20 mL), dried ($MgSO_4$) and the solvent removed to afford the chloro-substituted hydroxyl adduct **170** (0.436 g, 99%) as off-white crystals. R_f (20% EtOAc/pet spirit) 0.62. ^{1}H NMR (500 MHz, $CDCl_3$) δ 7.73 (d, *J* = 8.3 Hz, 2H, TsH3', H5'), 7.25 (d, *J* = 8.0 Hz, 2H, TsH2', H6'), 6.04 (t, *J* = 6.2 Hz, 1H, NH), 3.78 – 3.44 (m, 5H, H1a/b, H2, H3a/b), 3.18 (bs, 1H, OH), 2.35 (s, 3H, Ts CH_3). ^{13}C

NMR (125 MHz, $CDCl_3$) δ 144.1 (TsC1'), 137.6 (TsC4'), 130.1 (TsC2', C6'), 127.2 (TsC3', C5'), 59.1 (C3), 55.1 (C2), 44.1 (C1), 21.8 ($TsCH_3$). ESI-MS (+) 286 (100%, $[^{35}Cl]M+Na^+$), 288 (33%, $[^{37}Cl]M+Na^+$).

***N*-(1-bromo-3-chloropropan-2-yl)-4-methylbenzenesulfonamide (171)**

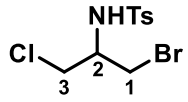

To a solution of bromomethylaziridine **147** (3.15 g, 10.9 mmol) in EtOH (50 mL) was added 36% $HCl_{(aq)}$ (15 mL, 150 mmol), and the mixture heated at reflux overnight. The mixture was cooled to room temperature, then diluted with water (50 mL) and EtOAc (50 mL), and the aqueous phase extracted with EtOAc (3×30 mL), then the combined organic fractions washed with sat. $NaHCO_3$ solution (3×40 mL), dried ($MgSO_4$) and the solvent removed to afford the mixed bromo-chloro species **171** (2.90 g, 82%) as an off-white amorphous solid, mp 82–85 ˚C. R_f (20% EtOAc/pet spirit) 0.50. ^{1}H NMR (500 MHz, $CDCl_3$) δ 7.76 (d, *J* = 8.3 Hz, 2H, TsH3', H5'), 7.32 (d, *J* = 8.0 Hz, 2H, TsH2', H6'), 5.03 (d, *J* = 8.0 Hz, 1H, NH), 3.79 – 3.70 (m, 3H, H2, H3a/b), 3.52 – 3.46 (m, 2H, CH_2Cl), 2.43 (s, 3H, $ArCH_3$). ^{13}C NMR (125 MHz, $CDCl_3$) δ 144.4 (TsC1'), 137.4 (TsC4'), 130.2 (TsC2', C6'), 127.3 (TsC3', C5'), 54.5 (C2), 43.9 (C3), 32.9 (C1), 21.8 ($TsCH_3$). ESI-MS (+) 348 (60%, $[^{35}Cl/^{79}Br]M+Na^+$), 350 (100%, $[^{37}Cl/^{79}Br]M+Na^+$ or $[^{35}Cl/^{81}Br]M+Na^+$), 352 (20%, $[^{37}Cl/^{81}Br]M+Na^+$).

(*S*)-*N*-(3-chloro-2-hydroxypropyl)-4-methylbenzenesulfonamide (172)

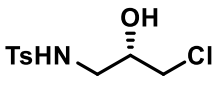

To a well-stirred suspension of chloramine-T trihydrate (3.59 g, 12.8 mmol) in dry acetonitrile (20 mL) in a 50 mL round-bottomed flask fitted with a rubber septum was injected (*S*)-epichlorohydrin **144** (2.36 g, 25.5 mmol). The mixture was warmed to 50 ˚C in an oil bath, and stirred vigorously for 24 h. Sat. $Na_2S_2O_3$ solution (5 mL) was added and the acetonitrile removed *in vacuo*, then the wet residue was diluted with EtOAc (40 mL) and extracted with water (40 mL). The aqueous phase was extracted with further EtOAc (3×20 mL) and the combined organic fractions washed sequentially with sat. $Na_2S_2O_3$ solution (2×10 mL), water (2×10 mL) and brine (2×40 mL). The organic fraction was dried ($MgSO_4$) and the solvent removed to give a clear syrup, which solidified upon standing to give a pale ivory solid. The resulting chlorohydrin **172** (3.25 g, 97%) was used directly for subsequent steps. R_f (9:1 CH_2Cl_2/EtOAc) 0.25. ^{1}H NMR (400 MHz, $CDCl_3$) δ 7.75 (d, *J* = 8.3 Hz, 2H, TsH3', H5'), 7.33 (d, *J* = 8.0 Hz, 2H, TsH2', H6'), 4.79 (t, *J* = 6.2 Hz, 1H, NH), 3.94 (dq, *J* = 10.7, 5.2 Hz, 1H, H2), 3.63 – 3.47 (m, 2H, CH_2Cl), 3.22 – 3.14 (m, 1H, H1a), 3.07 – 2.99 (m, 1H, H1b), 2.58 (d, *J* = 5.2 Hz, 1H, OH), 2.44 (s, 3H, $ArCH_3$). ^{13}C NMR (101 MHz, $CDCl_3$) δ 143.9 (TsC1'), 136.4 (TsC4'), 130.1 (TsC2', C6'), 127.2 (TsC3', C5'), 70.0 (C2), 46.8 (C3),

45.9 (C1), 21.6 ($TsCH_3$). ESI-MS (+) 286 (100%, $[^{35}Cl]M+Na^+$), 288 (33%, $[^{37}Cl]M+Na^+$). $[\alpha]_D^{21}$ = -19.7 ˚ (*c* 0.64, CH_2Cl_2).

(*S*)-1-chloro-3-((4-methylphenyl)sulfonamido)propan-2-yl methanesulfonate (173)

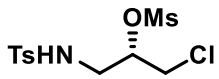

To a solution of **172** (1.331 g, 5.05 mmol) and NEt_3 (1.1 mL, 7.9 mmol) in dry CH_2Cl_2 (30 mL) was added slowly dropwise methanesulfonyl chloride (0.58 mL, 7.5 mmol) at 0 ˚C, and the resulting pale golden solution allowed to warm to room temperature overnight with stirring. The mixture was partitioned with 1 M HCl solution (10 mL) and the resulting organic phase washed with 1 M HCl (2×20 mL), then sat. $NaHCO_3$ solution (1×20 mL), and the resulting solution dried ($MgSO_4$) and the solvent removed to give chloromesylate **173** (1.566 g, 91%) as a clear yellow oil. NMR showed the mesylate to be >90% pure, and was used directly for the next step. R_f (9:1 CH_2Cl_2/EtOAc) 0.62. ^{1}H NMR (400 MHz, $CDCl_3$) δ 7.74 (d, *J* = 8.3 Hz, 2H, TsH3', H5'), 7.34 (d, *J* = 8.1 Hz, 2H, TsH2', H6'), 4.93 (d, *J* = 6.5 Hz, 1H, NH), 4.89 – 4.80 (m, 1H, H2), 3.77 (d, *J* = 5.4 Hz, 2H, H1a, H1b), 3.68 (s, 3H, SO_2CH_3), 3.37 – 3.29 (m, 2H, H3a, H3b), 2.44 (s, 3H, $TsCH_3$). ^{13}C NMR (101 MHz, $CDCl_3$) δ 144.2 (TsC1'), 135.7 (TsC4'), 130.2 (TsC2', C6'), 127.1 (TsC3', C5'), 78.9 (C2), 52.6 ($MsCH_3$), 44.5 (C3), 43.1 (C1), 21.6 ($TsCH_3$). ESI-MS (+) 364 (100%, $[^{35}Cl]M+Na^+$), 366 (33%, $[^{37}Cl]M+Na^+$]. $[\alpha]_D^{21}$ = +14.1˚ (*c* 0.22, CH_2Cl_2).

(*R*)-*N*-tosyl-2-chloromethylaziridine (148)[†††††††]

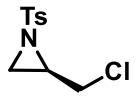

To a 0 ˚C solution of **173** (621 mg, 1.82 mmol) in dry CH_2Cl_2 (160 mL) was added pre-dried and ground cesium carbonate (976 mg, 3.00 mmol), and the mixture stirred vigorously for 2 h at 0 ˚C, then allowed to warm to room temperature overnight. The mixture was partitioned with water (100 mL), and the resulting organic layer separated and washed with brine (2×50 mL), dried ($MgSO_4$), and the solvent removed to give a clear, bluish oil. Flash chromatography (20 g silica, 20% EtOAc/pet spirit) gave the desired aziridine **148** (325 mg, 73%) as a colourless oil which slowly crystallised on standing, mp 42–44 ˚C. R_f (20% EtOAc/pet spirit) 0.40. ^{1}H-NMR ($CDCl_3$, 500 MHz) δ 7.82 (d, *J* = 8.0 Hz, 2H, TsH2', H6'), 7.33 (d, *J* = 8.0 Hz, 2H, TsH3', H5'), 3.39-3.50 (m, 2H, CH_2Cl), 3.04 (quint, *J* = 5.0 Hz, 1H, H2), 2.74 (d, *J* = 7.0 Hz, 1H, H1b) 2.43 (s, 3H, $TsCH_3$), 2.24 (d, *J* = 4.5 Hz, 1H, H1a). ^{13}C NMR (125 MHz) δ 145.2 (TsC1'), 134.6 (TsC4'), 130.0 (TsC2', C6'), 128.4 (TsC3', C5'), 43.7 (CH_2Cl), 39.9 (C3),

††††††† *rac*-**148** was also synthesised from the mixed bromo-chloro species **171** under identical conditions to those for the chloro-mesylate **173**. The isolated yield for this reaction was 90% on 8.88 mmol scale.

33.1 (C2), 21.9 ($TsCH_3$). ESI-MS (+) 268 (100%, $[^{35}Cl]M+Na^+$), 270 (33%, $[^{37}Cl]M+Na^+$). $[\alpha]_D^{21}$ = +61.5° (*c* 0.71, CH_2Cl_2).

(±)-*N*-tosyl-2-phenylaziridine (174)[189]

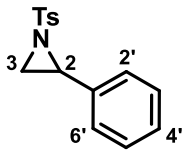

To a solution of chloramine-T trihydrate (8.46 g, 30 mmol) and iodine (381 mg, 1.50 mmol, 5 mol%) in dry MeCN (90 mL) was added styrene **175** (3.6 mL, 31.6 mmol) with stirring under nitrogen at RT. The flask was wrapped in aluminium foil, and stirred vigorously under static nitrogen for 2 days. The resulting orange mixture was filtered through a pad of celite (eluted with MeCN, 3×20 mL), and the filtrate extracted with pet. spirit (3×50 mL) to remove unreacted styrene. The solvent was removed *in vacuo*, then the residue dissolved in ethyl acetate (100 mL) and washed with sat. $Na_2S_2O_3$ solution (2×40 mL) and brine (50 mL), dried ($MgSO_4$) and the solvent removed. The resulting crystalline solid was triturated with hexane (50 mL) and collected by vacuum filtration to give phenylaziridine **174** (7.66 g, 93%) as off-white crystals, mp 93–95 ˚C. R_f (10% EtOAc/pet spirit) 0.32. ^{1}H NMR (500 MHz, $CDCl_3$) δ 7.86 (d, *J* = 8.3 Hz, 2H, TsH2", H6"), 7.32 (d, *J* = 8.0 Hz, 2H, TsH3", H5"), 7.30 – 7.12 (m, 5H, PhH2', H3', H4', H5', H6'), 3.77 (dd, *J* = 7.2, 4.5 Hz, 1H, H2), 2.97 (d, *J* = 7.2 Hz, 1H, H3a), 2.42 (s, 3H, $TsCH_3$), 2.38 (d, *J* = 4.5 Hz, 1H, H3b). ^{13}C NMR (125 MHz, $CDCl_3$) δ 144.8 (TsC1"), 135.14 (TsC4" or PhC1'), 135.07 (TsC4" or PhC1'), 129.9 (TsC2", C6"), 128.7 (PhC3', C5'), 128.4 (Ph C4'), 128.0 (TsC3", C5"), 126.7 (PhC2', C6'), 41.1 (C2), 36.0 (C3), 21.8 (Ts CH_3). ESI-MS (+) 274 (32%, $M+H^+$), 296 (100%, $M+Na^+$).

(2*S*,3*S*)-2,3-dihydroxybutane-1,4-diyl dimethanesulfonate[141]

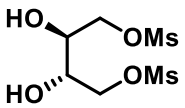

To a solution of the acetonide-protected dimesylate **131** (6.24 g, 21.5 mmol)‡‡‡‡‡‡‡ in 95% EtOH (70 mL) was added methanesulfonic acid (0.1 mL), and the mixture heated at reflux for 4 h, then allowed to cool to room temperature overnight. The solution was chilled to 0 ˚C, and the crystalline product collected by vacuum filtration and dried *in vacuo* to yield the desired diol (2.56 g, 48%) as fluffy white crystals, mp 100–102 ˚C, lit 101–102 ˚C.[141] This was used directly for the next step without further purification.

(2*S*,2'*S*)-2,2'-bioxirane (149)[141]

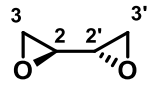

A 100 mL twin-necked round-bottomed flask equipped with a pressure-equalised addition funnel and a nitrogen gas adaptor was charged with a

‡‡‡‡‡‡‡Prepared over 3 steps from L-tartaric acid by Mr. Jamie Smyth.

solution of the deprotected dimesylatediol (3.71 g, 13.3 mmol) in ether (30 mL), and a solution of $KOH_{(aq)}$ (1.91 g in 6 mL, 34.1 mmol) added over 15 min *via* the dropping funnel, and the mixture stirred vigorously for 1 h. The upper ether layer was collected, and the aqueous layer extracted with ether (3×10 mL), and the combined organic layers washed with brine (2×10 mL), dried ($MgSO_4$) and the solvent removed to give the desired bioxirane **149** (1.07 g, 93%) as a colourless oil. ^{1}H NMR (400 MHz, $CDCl_3$) δ 2.68 (m, 4H, H3a/b, H3'a/b), 2.56 (m, 2H, H2, H2'). ^{13}C NMR (101 MHz, $CDCl_3$) δ 51.0 (C2, C2'), 44.4 (C3, C3'). $[\alpha]_D^{25}$ +24.9 ˚ (*c* 0.62, $CHCl_3$), lit. +25.7 ˚.[141]

(2*R*,2'*R*)-2,2'-biaziridine (150)[140c]

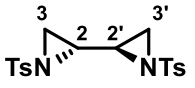

To a solution of the disulfonamido-diol *N*,*N*'-((2*S*,3*S*)-2,3-dihydroxybutane-1,4-diyl) bis(4-methylbenzenesulfonamide) (15.2 g, 35.5 mmol)§§§§§§§ in pyridine (65 mL) was added dropwise MsCl (11.8 g, 103 mmol) at 0 ˚C, and the mixture allowed to warm to room temperature overnight under nitrogen. The mixture was diluted with 1 M HCl (300 mL) and EtOAc (500 mL), and the aqueous phase repeatedly extracted with EtOAc (3×250 mL). The combined organic fractions were washed with 1 M HCl (2×500 mL), water (8×500 mL), then $NaHCO_3$ (2×100 mL), and the solution dried ($MgSO_4$) and the solvent removed to afford an intermediate dimesylate (19.2 g, 92% crude yield) as a dark tan powder which was used directly.

The crude dimesylate was suspended in benzene (200 mL), and 10% KOH solution (100 mL) added slowly. The mixture was stirred vigorously at room temperature overnight, then diluted with EtOAc (400 mL) and water (100 mL), and the aqueous phase extracted with EtOAc (4×50 mL). The combined organic layers were washed with water (100 mL) and $NaHCO_3$ (4×50 mL), then dried ($MgSO_4$) and the solvent removed. Flash chromatography (150 g silica, 30% EtOAc/pet spirit) afforded a highly-crystalline major fraction, which was condensed and recrystallised from $CHCl_3$/pet spirit to afford the desired biaziridine **150** (9.18 g, 67% over two steps) as fluffy, white crystals, mp 120–121 ˚C, lit. 128–129.5 ˚C.[190] R_f (20% EtOAc/pet spirit) 0.26. ^{1}H NMR ($CDCl_3$, 400 MHz) δ 7.75 (d, *J* = 8.4 Hz, 4H, 2×TsH2", H6"), 7.32 (d, *J* = 8.4 Hz, 4H, 2×TsH3", H5"), 2.90-2.96 (m, 2H, H2, H2'), 2.54 (d, *J* = 6.9 Hz, 2H, H3a, H3'a), 2.45 (s, 6H, 2×$TsCH_3$), 2.08 (d, *J* = 3.9 Hz, 2H, H3b, H3'b). ^{13}C NMR ($CDCl_3$, 101 MHz) δ 144.8 (2×TsC1"), 134.2 (2×TsC4"), 129.7 (2×TsC2", C6"), 127.9 (2×TsC3", C5"), 36.6 (C2), 31.7 (C3), 21.6 ($TsCH_3$). ESI-MS (+) 415 (27%, M+Na^+), 393 (100%, M+H^+). $[\alpha]_D^{20}$ = +97.0 ˚ (*c*

§§§§§§§Prepared over 7 steps from L-tartaric acid by Mr. Jamie Smyth.

0.69, $CHCl_3$), lit. +110 °.[140c]

7.3.2. Reaction of indigo with (*S*)-epichlorohydrin (**144**)

(*S*)-6-(hydroxymethyl)-6,7-dihydropyrazino[1,2-*a*:4,3-*a*']diindole-13,14-dione (152)

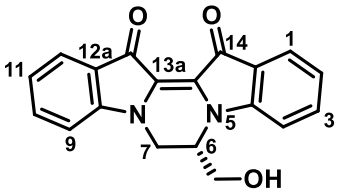

Prepared following ***General Procedure A*** (see Section 7.2.3), using (*S*)-epichlorohydrin (462 mg, 5.0 mmol), and a 30 min reaction time. The resulting crude residue was dissolved in a minimum of hot $CHCl_3$, and gradual dilution with a tenfold volume of hot pet. spirit precipitated an intense blue powder, which was collected on a Hirsch funnel and combined with **Fraction 5** (see below). The combined solids were dried *in vacuo* to furnish the dihydropyrazinodiindole **152** (141 mg, 44%) as a dark blue powder, mp >350 ˚C. R_f (9:1 CH_2Cl_2/EtOAc) 0.14. UV-Vis (CH_2Cl_2) λ_{max}/nm (ε, $M^{-1}cm^{-1}$) 241 (12773), 303 (6339), 579 (2819). ^{1}H-NMR (DMSO-d_6, 500 MHz) 7.56-7.64 (m, 4H, H1, H3, H10, H12), 7.35 (d, *J* = 8.0 Hz, 2H, H4, H9), 6.99-7.06 (m, 2H, H2, H11), 5.28 (s, 1H, CH_2<u>OH</u>), 4.66 (s, 1H, H6), 4.44 (d, *J* = 12.0 Hz, 1H, H7a), 3.71 (dd, *J* = 3.5, 12.0 Hz, 1H, H7b), 3.47-3.57 (m, 2H, <u>CH_2</u>OH). ^{13}C NMR (126 MHz) δ 179.9 (C13 or C14), 179.7 (C13 or C14), 150.2 (C4a or C8a), 149.4 (C4a or C8a), 135.3 (C3 or C10), 135.0 (C3 or C10), 123.9 (C13b), 123.5 (C1 or C12), 123.1 (C13a), 122.0 (C12a or C14a), 121.5 (C12a or C14a), 120.8 (C1 or C12), 120.6 (C2 or C11), 120.4 (C2 or C11), 110.9 (C4 or C9), 110.5 (C4 or C9), 59.9 (<u>C</u>H_2OH), 51.2 (C6), 51.1 (C7). IR (neat) 3432 (br, m), 2937 (w), 2876 (w), 1689 (s), 1607 (s), 1561 (s), 1470 (m), 1465 (m), 1369 (m), 1340 (w), 1298 (s), 1180 (s), 1158 (m), 1144 (s), 743 (s). HRESI-MS calcd. for $C_{19}H_{14}N_2O_3Na^+$ 341.0902, found 341.0888. $[\alpha]_D^{29}$ = -6.4 ˚ (*c* 0.10, $CHCl_3$).

(7*S*,9a*R*)-7,8-dihydro-6*H*-7,9a-epoxy[1,5]oxazocino[5,4-*a*:3,2-*b*']diindol-15(14*H*)-one (153)

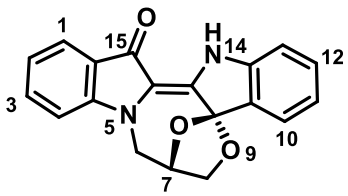

The mother liquor from compound **152** was concentrated, and subjected to flash chromatography (gradient elution, 5-50% EtOAc:CH_2Cl_2) to afford five major fractions. **Fraction 1** was subjected to PTLC (10% EtOAc/CH_2Cl_2), and the selected band scraped off and soaked in EtOAc. The silica was removed by filtration and the luminescent, yellow solution was combined with **Fraction 2** and the solvent removed to furnish the title compound **153** as small, bright orange crystals (101 mg, 32%), mp 189–191 ˚C (dec). X-ray quality crystals were grown by slow evaporation of a saturated solution in EtOAc at -20 ˚C. R_f (9:1 CH_2Cl_2/EtOAc) 0.57. UV-Vis (CH_2Cl_2) λ_{max}/nm (ε, $M^{-1}cm^{-1}$) 236 (8964), 287 (5169), 364 (2651), 483 (3573). ^{1}H NMR (500 MHz,

$CDCl_3$) δ 7.81 (d, *J* = 7.7 Hz, 1H, H1), 7.49 (m, 2H, H3, H10), 7.35 (app t, *J* = 7.7 Hz, 1H, H12), 7.08 (d, *J* = 8.3 Hz, 1H, H4), 7.02 (app t, *J* = 7.5 Hz, 2H, H2, H11), 6.92 (d, *J* = 7.9 Hz, 1H, H13), 5.16 – 5.08 (m, 1H, H7), 4.37 (t, *J* = 7.2 Hz, 1H, H8b), 4.26 (dd, *J* = 7.0 Hz, 3.0 Hz, H8a) 4.20 (dd, *J* = 14.0, 3.0 Hz, 1H, H6a), 3.74 (d, *J* = 14.0 Hz, 1H, H6b). ^{13}C NMR (126 MHz, $CDCl_3$) δ 184.1 (C15), 152.6 (C4a), 145.5 (C13a), 145.1 (C14a), 133.9 (C3), 132.4 (C12), 125.4 (C10), 124.5 (C9b), 124.1 (C1), 123.1 (C15a), 122.2 (C2), 120.1 (C11), 118.5 (C14b), 111.6 (C9a), 111.2 (C13), 110.9 (C4), 74.2 (C7), 65.6 (C8), 51.9 (C6). IR (neat) 3310 (br, w) 2966 (w), 2953 (w), 2893 (w), 1689 (s), 1614 (s), 1576 (s), 1098 (m), 995 (s), 747 (s). HRESI-MS calcd. for $C_{19}H_{14}N_2O_3Na^+$ 341.0902, found 341.0900. $[\alpha]_D^{27}$ = -6.5 ˚ (*c* 0.17, $CHCl_3$).

(7*R*,9a*R*)-14-((*E*)-3-hydroxyprop-1-en-1-yl)-7,8-dihydro-6*H*-7,9a-epoxy[1,5] oxazocino[5,4-*a*:3,2-*b*']diindol-15(14*H*)-one (155)

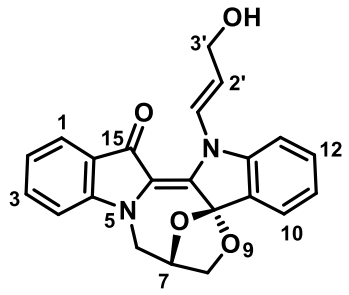

Fraction 3 was subjected to PTLC (developed twice; 20% EtOAc:CH_2Cl_2, then EtOAc) and the selected band scraped off and soaked in EtOAc. The silica was removed, and the solution combined with **Fraction 4** to give the title compound **154** as red-orange crystals (75.2 mg, 21%), mp 152–154 ˚C (dec.). X-ray quality crystals were grown by slow evaporation of a saturated solution in 9:1 CH_2Cl_2/hexane. R_f 0.21 (20% EtOAc/CH_2Cl_2). UV-Vis (CH_2Cl_2) λ_{max}/nm (ε, $M^{-1}cm^{-1}$) 243 (18482), 274 (20838), 355 (1472), 500 (1174). ^{1}H NMR (500 MHz, $CDCl_3$) δ 7.78 (d, *J* = 7.6 Hz, 1H, H1), 7.55 – 7.48 (m, 2H, H3, H10), 7.45 (t, *J* = 7.7 Hz, 1H, H12), 7.36 – 7.30 (m, 1H, H13), 7.17 (t, *J* = 7.4 Hz, 1H, H11), 7.06 (d, *J* = 8.3 Hz, 1H, H4), 7.02 (t, *J* = 7.4 Hz, 1H, H2), 6.87 (d, *J* = 14.2 Hz, 1H, H1'), 6.07 (dt, *J* = 6.5, 14.0 Hz, 1H, H2'), 5.05 – 5.01 (m, 1H, H7), 4.44 – 4.21 (m, 6H, H6b, H8a, H8b, H3'a, H3'b, OH), 3.74 (d, *J* = 14.3 Hz, 1H, H6a). ^{13}C NMR (125 MHz, $CDCl_3$) δ 181.5 (C15), 152.7 (C4a), 149.7 (C14a), 145.9 (C13a), 134.2 (C3), 131.9 (C12), 130.8 (C1'), 125.5 (C9b), 125.2 (C15a), 124.9 (C10), 124.5 (C14b), 124.3 (C1), 123.6 (C11), 120.0 (C2), 119.1 (C2'), 111.7 (C13), 111.1 (C9a), 109.9 (C4), 73.4 (C7), 67.6 (C8), 61.9 (C3'), 52.2 (C6). IR (neat) 3349 (br, m), 1726 (m), 1466 (s), 1265 (s), 702 (s). HRESI-MS calcd. for $C_{22}H_{19}N_2O_4^+$ 375.1345, found 375.1357. $[\alpha]_D^{29}$ = -6.7 ˚ (*c* 0.11, $CHCl_3$).

14-((2-oxo-1,3-dioxolan-4-yl)methyl)-7,8-dihydro-6*H*-7,9a-epoxy[1,5]oxazocino[5,4-*a*:3,2-*b'*]diindol-15(14*H*)-one (154)

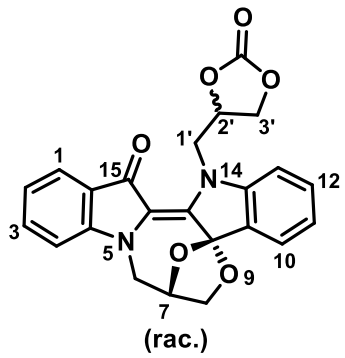

Prepared following ***General Procedure A***, using (±)-epichlorohydrin (5.0 mmol, 462 mg), and a 2 h reaction time. Following the above separation protocol, the racemic products (±)-**152** (134.4 mg, 43%), (±)-**153** (19.8 mg, 6%), and (±)-**155** (27.9 mg, 7%) were isolated. **Fraction 4** was condensed, and recrystallisation from a minimum volume of EtOAc afforded cyclic carbonate **154** (27 mg, 6%) as luminescent orange crystals, mp 146–149 ˚C (dec.). X-ray quality crystals were grown from slow evaporation of a saturated solution in 9:1 EtOAc/pet spirit at 4 ˚C. R_f (10% EtOAc/CH_2Cl_2) 0.45. UV-Vis (CH_2Cl_2) λ_{max}/nm (ε, $M^{-1}cm^{-1}$) 238 (17364), 344 (5999), 499 (2531). ^{1}H NMR (400 MHz, $CDCl_3$) δ 7.68 (d, *J* = 7.1 Hz, 1H, H1), 7.52 – 7.41 (m, 3H, H3, H10, H12), 7.33 (d, *J* = 8.1 Hz, 1H, H13), 7.13 (td, *J* = 7.4, 0.8 Hz, 1H, H11), 7.04 – 6.94 (m, 2H, H2, H4), 5.53 – 5.43 (m, 1H, H2'), 5.20 (d, *J* = 9.2 Hz, 1H, H3'a), 5.00 – 4.94 (m, 1H, H7), 4.33 – 4.22 (m, 4H, H6a, H8a, H8b, H3'b), 4.22 – 4.08 (m, 2H, H6a, H1'b), 3.68 (d, *J* = 14.3 Hz, 1H, H6b). ^{13}C NMR (101 MHz, $CDCl_3$) δ 182.2 (C15), 155.2 (O=<u>C</u>OO), 152.9 (C4a), 148.0 (C14a), 146.6 (C13a), 134.3 (C3), 132.7 (C12), 128.3 (C15a), 124.8 (C9b), 124.6 (C10), 124.2 (C1), 123.4 (C11), 120.7 (C14b), 119.9 (C2), 112.0 (C9a), 111.1 (C13), 110.2 (C4), 81.3 (C2'), 73.4 (C7), 69.0 (C3'), 67.9 (C8), 55.5 (C1'), 52.4 (C6). IR (neat) 3431 (w), 1799 (m), 1734 (s), 1611 (s), 1466 (s), 1065 (s), 774 (m). HRESI-MS calcd. for $C_{23}H_{18}N_2O_6Na^+$ 441.1063, found 441.1082; calcd. for $C_{23}H_{19}N_2O_6^+$ 419.1243, found 419.1257.

(7*R*,9a*R*)-(((*S*)-2-oxo-1,3-dioxolan-4-yl)methyl)-7,8-dihydro-6*H*-7,9a-epoxy[1,5]oxazocino[5,4-*a*:3,2-*b'*]diindol-15(14*H*)-one (154)

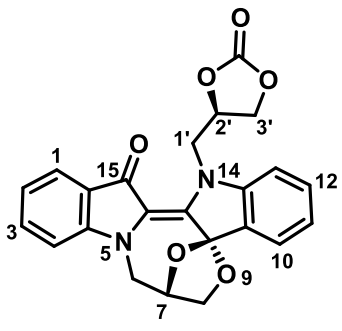

Prepared following ***General Procedure A***, using *(S)*-epichlorohydrin (462 mg, 5.0 mmol) and a 30 min reaction time. Following the above separation protocol, products **152** (133 mg, 41%), and **153** (97 mg, 30%) were isolated. **Fraction 4** was subjected to PTLC (20% EtOAc/CH_2Cl_2). Recrystallisation from a minimum volume of EtOAc afforded cyclic carbonate **154** (87 mg, 20%) as luminescent orange crystals. $[\alpha]_D^{29}$ = -6.1 ˚ (*c* 0.09, $CHCl_3$).

(±)-6-(hydroxymethyl)-6,7-dihydropyrazino[1,2-*a*:4,3-*a*']diindole-13,14-dione (*rac*-152)

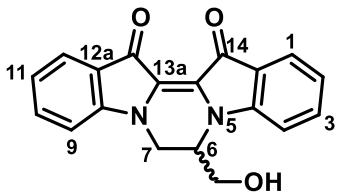

Prepared following ***General Procedure A***, using (±)-epibromohydrin **145** (685 mg, 5.0 mmol), and a 10 min reaction time. The crude residue was dissolved in a minimum of hot $CHCl_3$, and gradual dilution with a tenfold volume of hot pet spirit precipitated an intense blue powder, which was collected on a Hirsch funnel. The mother liquor was condensed, and a second recrystallization of the residue afforded a second crop of product. The combined solids were dried *in vacuo* to furnish the title compound *rac*-**152** as a dark blue powder (266.9 mg, 84%). Spectral characteristics (excepting optical rotation) were identical to those reported for (*S*)-**152**.

(*R*)-6-(hydroxymethyl)-6,7-dihydropyrazino[1,2-*a*:4,3-*a*']diindole-13,14-dione (*R*-152)

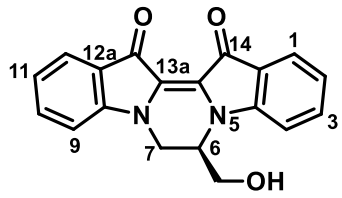

Prepared following ***General Procedure A***, using of (*R*)-glycidyl tosylate **146** (1.141 g, 5.0 mmol), and a 10 min reaction time. The crude residue was dissolved in a minimum of hot $CHCl_3$, and gradual dilution with a tenfold volume of hot pet spirit precipitated an intense blue powder, which was collected on a Hirsch funnel. The mother liquor was condensed, and a second recrystallization of the residue afforded a further crop of product. The combined solids were dried *in vacuo* to furnish the title compound *(R)*-**152** as a dark blue powder (242.3 mg, 76%). Spectral characteristics (excepting optical rotation) were identical to those obtained from its enantiomer. $[\alpha]_D^{29} = +3.7^\circ$ (*c* 0.33, CH_2Cl_2).

7.3.3. Reaction of indigo with (*R*)-*N*-tosyl-2-chloromethylaziridine (**148**)

(*R*)-*N*-((13,14-dioxo-6,7,13,14-tetrahydropyrazino[1,2-*a*:4,3-*a*']diindol-6-yl)methyl)-4-methylbenzenesulfonamide (176)

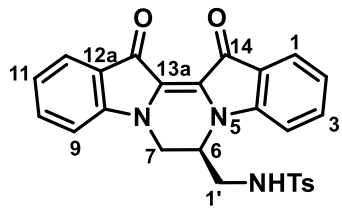

A suspension of indigo (131 mg, 0.500 mmol) in anhydrous DMF (20 mL) was sonicated at 60 ˚C for one hour. The resulting hot suspension was transferred by cannula under positive pressure of nitrogen into a 50 mL round-bottomed flask containing a magnetic stir bar, pre-dried and ground Cs_2CO_3 (603 mg, 1.85 mmol), and fitted with a rubber septum. The resulting dark-green to amber solution was stirred for one hour in an oil bath, pre-heated to strictly 85-87 ˚C under dry nitrogen. The nitrogen flow was cut, and a solution of (*R*)-*N*-tosyl-2-chloromethylaziridine **148** (627 mg, 2.56 mmol) in DMF (2 mL) was injected through the septum, and the mixture stirred at 85–87

˚C for 30 min. The resulting intensely-coloured solution was quenched over crushed ice (ca. 50 g), and the flask rinsed with EtOAc (ca. 10 mL) to remove adhered products. Upon warming to RT, the emulsion was extracted with EtOAc (5×40 mL) until the aqueous phase became clear. The combined organic fractions were washed with brine (4×40mL), dried ($MgSO_4$), and filtered through a 2 cm plug of celite, and the solvent removed *in vacuo*. The crude residue was fractionated on silica (60 g) using $CHCl_3$ as eluent to afford two major fractions. Removal of the solvent from **Fraction 2** afforded the *N,N*-cyclised *mono*-adduct **176** (108.2 mg, 46%) as a glassy, intense-blue solid, mp 165–167 ˚C (dec.). R_f (9:1 $CHCl_3$/MeCN) 0.23. UV-VIS (CH_2Cl_2) λ_{max}/nm (ε, $M^{-1}cm^{-1}$) 236 (18847), 302 (14297), 380 (2329), 576 (8879). ^{1}H NMR (500 MHz, DMSO) δ 8.06 (t, *J* = 5.9 Hz, 1H, NH), 7.64 – 7.57 (m, 6H, H1, H3, H10, H12, H3", H5"), 7.34 – 7.27 (m, 3H, H9, H2", H6"), 7.24 (d, *J* = 8.3 Hz, 1H, H4), 7.07 – 6.98 (m, 2H, H2, H11), 4.68 – 4.59 (m, 1H, H6), 4.42 (d, *J* = 12.3 Hz, 1H, H7a), 3.70 (d, *J* = 9.4 Hz, 1H, H7b), 3.06 – 2.81 (m, 2H, H1'), 2.30 (s, 3H, $TsCH_3$). ^{13}C NMR (126 MHz, DMSO) δ 179.71 (C13 or C14), 179.69 (C13 or C14), 150.4 (C9a), 148.9 (C4a), 142.8 (C4"), 135.3 (C3 or C10), 135.2 (C3 or C10), 134.9 (C1"), 129.6 (C2", C6"), 126.2 (C3", C5"), 125.4 (C12a), 124.6 (C13b), 123.9 (C13a), 123.7 (C1 or C12), 123.5 (C1 or C12), 122.8 (C14a), 122.1 (C2 or C11), 121.7 (C2 or C11), 110.8 (C9), 110.2 (C4), 49.6 (C6), 42.5 (C1'), 40.5 (C7), 20.8 ($TsCH_3$). IR (neat) 3566 (w), 2987 (w), 1737 (w), 1697 (m), 1609 (s), 1159 (s), 1132 (s) 754 (s). HRESI-MS calcd. for $C_{26}H_{21}N_3O_4SNa^+$ 472.1331, found 472.1319. $[\alpha]_D^{25}$ = -9.3˚ (*c* 0.41, $CHCl_3$).

Fraction 1 was concentrated to dryness then dissolved in acetonitrile (20.0 mL), of which 10.0 mL was subjected to preparative RP-HPLC over 5×2.0 mL injections, using a Prominence Preparatory Liquid Chromatograph (Shimadzu) with PDA detector, and a Shim-Pack GIS C18 5 μm column (Shimadzu) with 150×20 mm I.D. Gradient elution from 80% to 0% Solvent A (0.1% TFA in H_2O) in 60 minutes with Solvent B (0.1% TFA in MeCN) at a flow rate of 10.0 mL/min afforded three major fractions at t_R 35 min, 37 min, and 47.7 min, and their purity was confirmed by analytical RP-HPLC, using a Prominence LC-2030C 3D system (Shimadzu) with PDA detector, and a Shim-Pack GIS C18 5 μm column (Shimadzu) with 4.6×150 mm I.D. Gradient elution from 80% to 0% Solvent A (0.1% TFA in H_2O) in 30 minutes with Solvent B (0.1% TFA in MeCN) at a flow rate of 1.0 mL/min showed the three fractions (t_R 16.5, 17.2, and 21.4 min, respectively) to be free of neighbouring impurities.

_N_-(((_R_)-13,14-dioxo-6,7,13,14-tetrahydropyrazino[1,2-_a_:4,3-_a_']diindol-6-yl)methyl)-4-methyl-_N_-(((_S_)-1-tosylaziridin-2-yl)methyl)benzenesulfonamide (177)

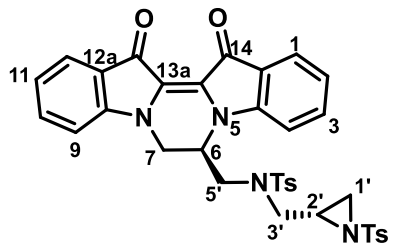

Removal of the solvent from the fraction collected at t_R 35 min afforded the *di*-substituted *N,N'*-cyclised indigo derivative **177** (27.4 mg, 8%) as an intense blue-purple solid, mp 121–123 ˚C (dec.). R_f (9:1 $CHCl_3$/MeCN) 0.49. UV-Vis (CH_2Cl_2) λ_{max}/nm (ε, $M^{-1}cm^{-1}$) 281 (37018), 360 (2022), 578 (7659). ^{1}H NMR (400 MHz, $CDCl_3$) δ 7.81 – 7.71 (m, 2H, H1, H12), 7.60 (d, *J* = 8.1 Hz, 2H, Ts^1 or Ts^2 H3/H5), 7.57 – 7.48 (m, 4H, H3, H10, Ts^1 or Ts^2 H3/H5), 7.29 (d, *J* = 8.1 Hz, 2H, Ts^1 or Ts^2 H2/H6), 7.21 (d, *J* = 8.0 Hz, 2H, Ts^1 or Ts^2 H2/H6), 7.16 (s, 2H, H2, H11), 7.02 (s, 2H, 2×ArH, H4, H9), 4.63 (s, 1H, H6), 4.47 (d, *J* = 10.8 Hz, 1H, H7a), 3.64 (d, *J* = 15.8 Hz, 1H, H3'a), 3.51 – 3.37 (m, 1H, H7b), 3.31 – 3.19 (m, 1H, H5'a), 3.05 – 2.95 (m, 1H, H3'b), 2.95 – 2.86 (m, 2H, H5'b, H2'), 2.57 (d, *J* = 6.9 Hz, 1H, H1'a), 2.39 (s, 3H, Ts^1 or Ts^2 CH_3), 2.38 (s, 3H, Ts^1 or Ts^2 CH_3), 2.21 (d, *J* = 4.1 Hz, 1H, H1'b). ^{13}C NMR (126 MHz, DMSO) δ 180.4 (C13 or C14), 180.1 (C13 or C14), 150.9 (C4a or C8a), 149.0 (C4a or C8a), 145.4 (Ts^1 or Ts^2 C4), 144.5 (Ts^1 or Ts^2 C4), 136.0 (Ts^1 or Ts^2 C1), 135.8 (Ts^1 or Ts^2 C1), 135.7 (C3 or C10), 133.9 (C3 or C10), 130.6 (Ts^1 or Ts^2 C2/C6), 130.3 (Ts^1 or Ts^2 C2/C6), 130.1 (C13b), 128.0 (Ts^1 or Ts^2 C3/C5), 127.7 (Ts^1 or Ts^2 C3/C5), 127.0 (C13a), 124.7 (C1 or C12), 124.4 (C1 or C12), 124.2 (C12a or C14a), 124.1 (C12a or C14a), 121.4 (C2 or C11), 121.3 (C2 or C11), 111.6 (C4 or C9), 110.9 (C4 or C9), 60.6 (C3'), 54.4 (C6), 49.5 (C5'), 48.9 (C7), 47.3 (C2'), 40.8 (C1'), 21.5 (Ts^1 or Ts^2 CH_3), 21.4 (Ts^1 or Ts^2 CH_3). IR (neat) 2987 (w), 1738 (w), 1697 (m), 1609 (s), 1132 (s), 754 (s). HRESI-MS calcd. for $C_{36}H_{32}N_4O_6S_2Na^+$ 703.1655, found 703.1661. $[\alpha]_D^{25}$ = -12.6˚ (*c* 0.11, $CHCl_3$).

_N_-((_R_)-3-chloro-2-((4-methylphenyl)sulfonamido)propyl)-_N_-(((_R_)-13,14-dioxo-6,7,13,14-tetrahydropyrazino[1,2-_a_:4,3-_a_']diindol-6-yl)methyl)-4-methylbenzenesulfonamide (178)

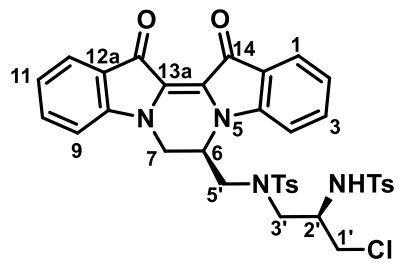

Removal of the solvent from the fraction collected at t_R 37 min afforded the *di*-substituted *N,N'*-cyclised indigo derivative **178** (33.3 mg, 9%) as an intense blue-purple solid, mp 132–134 ˚C (dec.). R_f (9:1 $CHCl_3$/MeCN) 0.49. UV-Vis (CH_2Cl_2) λ_{max}/nm (ε, $M^{-1}cm^{-1}$) 574 (8850). ^{1}H NMR (500 MHz, $CDCl_3$) δ 7.82 (d, *J* = 7.9 Hz, 2H, Ts^1 or Ts^2 H3/H5), 7.78 – 7.71 (m, 2H, H1, H12), 7.58 – 7.52 (m, 3H, Ts^1 or Ts^2 H3/H5, H3 or H10), 7.49 (t, *J* = 7.7 Hz, 1H, H3 or H10), 7.36 (d, *J* = 7.9 Hz, 2H, Ts^1 or

Ts^2 H2/H6), 7.27 (d, 2H, Ts^1 or Ts^2 H2/H6), 7.12 (d, *J* = 8.1 Hz, 1H, H4 or H9), 7.09 – 6.94 (m, 3H, H4 or H9, H2, H11), 5.69 (s, 1H, NH), 4.60 (app d, *J* = 10.3 Hz, 1H, H6), 4.39 (d, *J* = 12.1 Hz, 1H,), 4.07 – 3.94 (m, 1H, H2'), 3.86 (d, *J* = 11.6 Hz, 1H, H1'a), 3.57 – 3.37 (m, 4H, H7b, H1'b, H3'a, H5'a), 3.19 (dd, *J* = 15.1, 6.8 Hz, 1H, H3'b), 2.65 (d, *J* = 14.3 Hz, 1H, H5'b), 2.42 (s, 3H, Ts^1 or Ts^2 CH_3), 2.38 (s, 3H, Ts^1 or Ts^2 CH_3). ^{13}C NMR (126 MHz, $CDCl_3$) δ 181.2 (C13 or C14), 180.5 (C13 or C14), 150.7 (C4a or C8a), 148.4 (C4a or C8a), 145.2 (Ts^1 or Ts^2 C4), 144.3 (Ts^1 or Ts^2 C4), 137.3 (Ts^1 or Ts^2 C1), 135.8 (C3 or C10), 135.7 (C3 or C10), 133.2 (Ts^1 or Ts^2 C1), 130.4 (Ts^1 or Ts^2 C2/C6), 130.2 (Ts^1 or Ts^2 C2/C6), 127.7 (Ts^1 or Ts^2 C3/C5), 127.4 (Ts^1 or Ts^2 C3/C5), 125.7 (C1 or C12), 125.2 (C13a), 125.1 (C1 or C12), 123.1 (C12a or C14a), 123.0 (C13b), 122.9 (C12a or C14a), 121.8 (C2 or C11), 121.6 (C2 or C11), 110.7 (C4 or C9), 108.9 (C4 or C9), 53.9 (C2'), 53.1 (C3'), 51.0 (C5'), 49.5 (C6), 45.4 (C1'), 40.2 (C7), 21.8 (Ts^1 or Ts^2 CH_3), 21.7 (Ts^1 or Ts^2 CH_3). IR (neat) 3013 (w), 1743 (w), 1608 (m), 1304 (m), 756 (s). HRESI-MS calcd. for $C_{36}H_{33}N_4O_6S_2{}^{35}ClNa^+$ 739.1428, found 739.1448. $[\alpha]_D{}^{25}$ = -11.4˚ (*c* 0.12, $CHCl_3$)

(±)-*N*-((13,14-dioxo-6,7,13,14-tetrahydropyrazino[1,2-*a*:4,3-*a*']diindol-6-yl)methyl)-4-methylbenzenesulfonamide (*rac*-176)

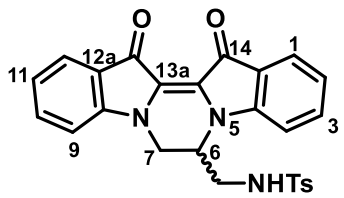

Prepared following ***General Procedure A***, using (±)-*N*-tosyl-2-bromomethylaziridine (1.00 g, 3.45 mmol), and a 5 min reaction time.******** The crude residue was fractionated on silica (80 g) using 5% MeCN:$CHCl_3$ as eluent. Removal of the solvent from **Fraction B** afforded the *N*,*N*-cyclised *mono*-adduct ***rac*-176** (247.2 mg, 52%) as a glassy, intense-blue solid. Spectral and physical characteristics (excepting optical rotation) were identical to those reported above for (*R*)-**176**.

Fraction A was condensed and assessed by analytical RP-HPLC (80%-0% H_2O/MeCN; 1.0 mL/min), which showed the presence of small amounts of **177**, though this was not quantified.

******** Longer reaction times typically led to extensive polymerisation

7.3.4. Reaction of indigo with *N*-tosyl-2-phenylaziridine (**174**)

(*E*)-*N*-(2-(3,3'-dioxo-[2,2'-biindolinylidene]-1-yl)-1-phenylethyl)-4-methylbenzenesulfonamide (179)

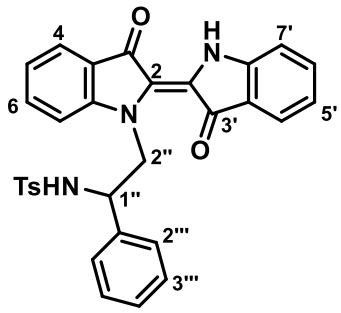

Prepared following ***General Procedure A***, using phenylaziridine **174** (1.363 g, 4.99 mmol) and a 5 min reaction time. The crude residue was fractionated on silica (60 g) by sequential elution with 1) 10% pet spirit/CH_2Cl_2 (**Fraction 1**), 2) CH_2Cl_2 (**Fraction 2**), and the column stripped with 10% EtOAc/CH_2Cl_2 (**Fraction 3**). The solvent was removed from **Fraction 1** to give a dark blue residue, which was re-dissolved in a minimum of hot $CHCl_3$, and precipitated with a tenfold volume of pet. spirit. The resulting solid was collected on a Hirsch funnel, and dried *in vacuo* to give the terminally ring-opened aziridine adduct **179** (333.4 mg, 62%) as a dark teal powder, mp 211–213 ˚C. R_f (10% pet spirit/CH_2Cl_2) 0.43. UV-Vis (CH_2Cl_2) λ_{max}/nm (ε, $M^{-1}cm^{-1}$) 294 (24346), 341 (9142), 645 (13774). ^{1}H NMR (500 MHz, $CDCl_3$) δ 10.65 (s, 1H, NH), 7.72 (d, *J* = 7.6 Hz, 1H, H4), 7.64 (d, *J* = 7.5 Hz, 1H, H4'), 7.61 – 7.55 (m, 3H, H6, H3'''', H5''''), 7.50 (t, *J* = 7.4 Hz, 1H, H6'), 7.40 (t, *J* = 7.5 Hz, 2H, H3''', H5'''), 7.32 (t, *J* = 7.3 Hz, 1H, H4'''), 7.23 (d, *J* = 8.0 Hz, 2H, H2''', H6'''), 7.06 (t, *J* = 7.4 Hz, 1H,), 7.04 – 6.94 (m, 3H, H7, H5', H7'), 6.72 (d, *J* = 7.9 Hz, 2H, H2'''', H6''''), 5.23 – 5.11 (m, 1H, H2''a), 4.96 – 4.85 (m, 1H, H1''), 3.97 – 3.87 (m, 1H, H2''b), 2.22 (s, 3H, $TsCH_3$). ^{13}C NMR (126 MHz, $CDCl_3$) δ 189.0 (C3'), 188.8 (C3), 151.8 (C7a'), 151.3 (C7a), 142.7 (TsC4''''), 139.6 (C1''' or TsC1''''), 138.1 (C1''' or TsC1''''), 137.0 (C6'), 136.2 (C6), 129.2 (TsC2'''', C6''''), 129.1 (TsC3'''', C5''''), 128.3 (C4'''), 126.8 (C3''', C5'''), 126.1 (C2''', C6'''), 125.5 (C4), 124.9 (C3a or C3a'), 124.1 (C4'), 123.7 (C2 or C2'), 121.4 (C5), 120.9 (C3a or C3a'), 120.8 (C5'), 120.0 (C2 or C2'), 112.0 (C7), 110.2 (C7'), 55.6 (C1''), 51.9 (C2''), 21.6 ($TsCH_3$). IR (neat) 3288 (w), 1630 (m), 1607 (s), 1026 (s). HRESI-MS calcd. for $C_{31}H_{26}N_3O_4S^+$ 536.1644, found 536.1664.

(*E*)-*N*-(2-(3,3'-dioxo-[2,2'-biindolinylidene]-1-yl)-2-phenylethyl)-4-methylbenzenesulfonamide (180)

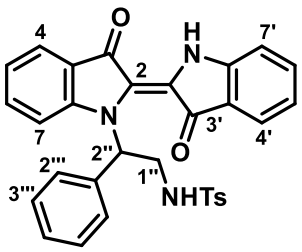

Fraction 2 was combined with **Fraction 3** and condensed to give a dark blue-green residue, which was dissolved in a minimum of hot $CHCl_3$, then diluted with a tenfold volume of hot pet spirit. The solution was chilled, and the resulting precipitate collected by vacuum filtration and dried *in vacuo* to give the title compound **180** (191.9 mg, 36%) as a dark blue powder, mp 194–196 ˚C. X-ray quality crystals were grown by gradual diffusion of pet spirit into a saturated solution in 1:1 $CHCl_3$/MeOH in a sealed vapour chamber at room temperature. R_f (10% pet spirit/CH_2Cl_2) 0.31. UV-Vis (CH_2Cl_2) λ_{max}/nm (ε, $M^{-1}cm^{-1}$) 292 (23907), 340 (7457), 637 (9167). ^{1}H NMR (500 MHz, $CDCl_3$) δ 10.74 (s, 1H, N1'-H), 7.65 (d, *J* = 7.7 Hz, 1H, H4') 7.62 (d, *J* = 7.7 Hz, 1H, H4), 7.54 – 7.46 (m, 3H, H6', TsH3''', H5'''), 7.29 – 7.16 (m, 6H, H6, 5×Ph-H'''), 7.02 (d, *J* = 8.0 Hz, 1H, H7'), 7.00 – 6.94 (m, 3H, H5', TsH2'''', H6''''), 6.91 (t, *J* = 7.3 Hz, 1H, H5), 6.63 – 6.50 (m, 2H, H7, H2''), 5.93 – 5.84 (m, 1H, C1''-NH), 4.19 – 4.04 (m, 2H, H1''), 2.26 (s, 3H, $TsCH_3$). ^{13}C NMR (126 MHz, $CDCl_3$) δ 189.3 (C3), 188.2 (C3'), 151.8 (C7a'), 150.0 (C7a), 143.1 (TsC4''''), 136.9 (Ts C1''''), 136.7 (C6'), 135.5 (C1'''), 135.2 (C6), 129.4 (TsC2'''', C6''''), 128.8 (C3''', C5'''), 127.8 (C4'''), 126.53 (C2''', C6'''), 126.51 (TsC3'''', C5''''), 125.8 (C2 or C2'), 125.2 (C4), 125.1 (C2 or C2'), 124.2 (C4'), 122.2 (C3a), 121.2 (C5), 120.9 (C5'), 120.1 (C3a'), 114.1 (C7), 112.1 (C7'), 60.0 (C2''), 43.4 (C1''), 21.6 ($TsCH_3$). IR (neat) 3254 (w), 1628 (m), 1605 (s), 1069 (s). HRESI-MS calcd. for $C_{31}H_{25}N_3O_4SNa^+$ 558.1463, found 558.1481.

7.3.5. Reaction of indigo with (2*S*,2'*S*)-2,2'-bioxirane (**149**)

(7*S*,8*R*,9a*S*)-8-(hydroxymethyl)-7,8-dihydro-6*H*-7,9a-epoxy[1,5]oxazocino[5,4-*a*:3,2-*b*']diindol-15(14*H*)-one (183)

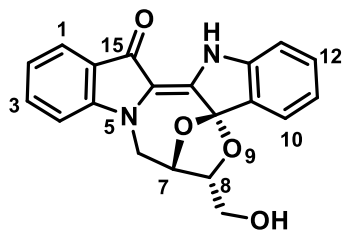

Prepared following ***General Procedure A***, using (2*S*,2'*S*)-2,2'-bioxirane (281 mg, 3.3 mmol), and a 30 min reaction time. The crude residue was separated into five fractions on a plug of silica (70 g), eluting sequentially with 1) CH_2Cl_2 (250 mL each) 2) 20% EtOAc/CH_2Cl_2 3) 40% EtOAc/CH_2Cl_2 4) 60% EtOAc/CH_2Cl_2 5) 80% EtOAc/CH_2Cl_2. **Fractions 2** and **3** were combined, and subjected to flash chromatography on 25 g silica, and elution with 20% EtOAc:CH_2Cl_2 afforded the *mono*-substituted spirocycle **183** (216 mg, 62%) as a luminescent orange powder, mp 155–156 ˚C (dec.). X-ray quality crystals were grown

from slow evaporation of a hexane/ethyl acetate solution. R_f (20% EtOAc/CH_2Cl_2) 0.33. UV-Vis (CH_2Cl_2) λ_{max}/nm (ε, $M^{-1}cm^{-1}$) 244 (12573), 365 (2296), 485 (2882). ^{1}H NMR (500 MHz, $CDCl_3$) δ 7.81 (d, *J* = 7.0 Hz, 1H, H1), 7.54 – 7.48 (m, 2H, H3, H10), 7.35 (td, *J* = 7.7, 1.3 Hz, 1H, H12), 7.11 (d, *J* = 8.3 Hz, 1H, H4), 7.06 – 6.99 (m, 2H, H2, H11), 6.92 (dt, *J* = 7.8, 0.8 Hz, 1H, H13), 5.04 – 4.97 (m, 1H, H7), 4.79 – 4.71 (m, 1H, H8), 4.38 (dd, *J* = 14.1, 2.8 Hz, 1H, H6b), 4.17 (dd, *J* = 11.3, 7.3 Hz, 1H, H1'a), 3.96 (dd, *J* = 11.2, 5.7 Hz, 1H, H1'b), 3.70 (dd, *J* = 14.0, 2.4 Hz, 1H, H6a), 1.26 (s, 1H, OH). ^{13}C NMR (101 MHz, $CDCl_3$) δ 184.1 (C15), 151.8 (C4a), 145.2 (C13a), 144.5 (C14a), 134.0 (C3), 132.4 (C12), 125.3 (C10), 124.2 (C15a), 124.0 (C1), 123.5 (C9b), 122.3 (C11), 120.1 (C2), 117.8 (C14b), 111.7 (C9a), 111.2 (C13), 110.7 (C4), 77.7 (C8), 75.6 (C7), 60.4 (C1'), 48.3 (C6). IR (neat) 3420 (w), 2922 (w), 1715 (m), 1612 (s), 1317 (m), 735 (s). HRESI-MS calcd. for $C_{20}H_{17}N_2O_4^+$ 349.1188, found 349.1192. $[\alpha]_D^{25}$ = -7.2° (*c* 0.21, CH_2Cl_2).

(7*S*,8*R*,9a*S*)-14-((*S*)-2-hydroxy-2-((*S*)-oxiran-2-yl)ethyl)-8-(hydroxymethyl)-7,8-dihydro-6*H*-7,9a-epoxy[1,5]oxazocino[5,4-*a*:3,2-*b*']diindol-15(14*H*)-one (184)

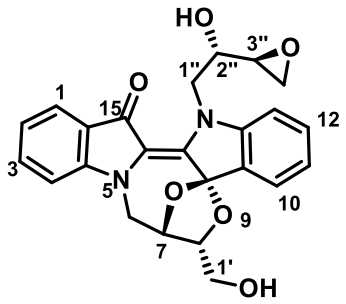

Further elution of **Fractions 2** and **3** with 40% EtOAc:CH_2Cl_2 gave a residue which was combined with **Fractions 4** and **5** and concentrated, and flash chromatography of this residue (20% EtOAc/CH_2Cl_2; 20 g silica) gave the *di*-alkylated spirocycle **184** (82 mg, 19%) as a pale green, amorphous solid. R_f (40% EtOAc/CH_2Cl_2) 0.63. UV-Vis (CH_2Cl_2) λ_{max}/nm (ε, $M^{-1}cm^{-1}$) 323 (3820), 350 (4772), 425 (1723). ^{1}H NMR (400 MHz, DMSO) δ 7.65 – 7.46 (m, 4H, H1, H3, H10, H13), 7.26 – 7.19 (m, 1H, H12), 7.12 – 7.00 (m, 2H, H4, H11), 6.82 (t, *J* = 7.3 Hz, 1H, H2), 5.83 (d, *J* = 4.8 Hz, 1H, C1'-OH), 5.22 (d, *J* = 5.7 Hz, 1H, C2"-OH), 4.61 (t, *J* = 6.0 Hz, 1H, H7), 4.54 (d, *J* = 12.6 Hz, 1H, H6a), 4.21 (dt, *J* = 11.6, 5.8 Hz, 1H, H6b), 4.11 – 3.96 (m, 2H, H8, H1'a), 3.83 (dd, *J* = 9.2, 6.4 Hz, 1H, H1"a), 3.73 (dd, *J* = 9.2, 5.0 Hz, 1H, H1"b), 3.24 (dt, *J* = 11.6, 5.9 Hz, 1H, H2"), 2.78 (dd, *J* = 12.3, 10.3 Hz, 1H, H1'b), 2.73 – 2.68 (m, 1H, H3"), 2.61 – 2.54 (m, 1H, H4"a), 2.33 (dd, *J* = 5.2, 2.7 Hz, 1H, H4"b). ^{13}C NMR (101 MHz, DMSO) δ 193.5 (C15), 158.4 (C4a), 139.2 (C3), 133.9 (C13a), 130.6 (C14a), 125.7 (C14b), 125.5 (C1), 122.6 (C12), 120.2 (C9b), 120.1 (C11), 118.8 (C2), 118.6 (C10), 118.1 (C15a), 110.7 (C13), 110.3 (C9a) 109.4 (C4), 75.9 (C1"), 70.8 (C7), 70.5 (C2"), 62.8 (C8), 53.7 (C3"), 44.1 (C4"), 43.2 (C1'), 37.4 (C6). IR (neat) 3566 (w), 2922 (w), 1737 (m), 1608

(m), 1155 (s), 748 (s). HRESI-MS (+) calcd. for $C_{24}H_{23}N_2O_6^+$ 435.1556, found 435.1575. $[\alpha]_D^{25}$ = -8.5˚ (*c* 0.32, CH_2Cl_2).

7.3.6. Reaction of indigo with (2*R*,2'*R*)-*N,N'*-ditosyl-2,2'-biaziridine (**150**)

4-methyl-*N*-(((6*R*,7*R*)-7-((4-methylphenyl)sulfonamido)-14,15-dioxo-7,8,14,15-tetrahydro-6*H*-[1,4]diazepino[1,2-*a*:4,3-*a*']diindol-6-yl)methyl)benzenesulfonamide (185)

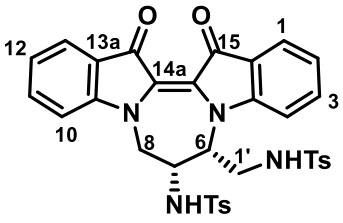

Prepared following ***General Procedure A*** using (2*R*,2'*R*)-*N,N'*-ditosyl-2,2'-biaziridine **150** (512 mg, 1.30 mmol) in DMF (3 mL) over a 20 min reaction time. The crude residue was dissolved in a minimum of hot $CHCl_3$, and gradual dilution with a tenfold volume of hot pet. spirit precipitated an intense dark blue powder. The suspension was cooled to 0 ˚C overnight, and the fine dark blue precipitate was collected on a Hirsch funnel and dried *in vacuo* to give the 1,3-*di*-ring-opened biaziridine adduct **185** (610 mg, 93%) as an intense dark blue-black powder, mp 135–136 ˚C (dec.). R_f (10% EtOAc/CH_2Cl_2) 0.29. UV-Vis (CH_2Cl_2) λ_{max}/nm (ε, $M^{-1}cm^{-1}$) 573 (6647). ^{1}H NMR (400 MHz, $CDCl_3$) δ 7.62 (d, *J* = 8.1 Hz, 2H, Ts^1 or Ts^2 H3/H5), 7.56 (t, *J* = 7.6 Hz, 1H, H3 or H11), 7.52 – 7.45 (m, 3H, H1, H3 or H11, H13), 7.38 – 7.31 (m, 3H, H4 or H10, Ts^1 or Ts^2 H3/H5), 7.22 – 7.13 (m, 3H, H4 or H10, Ts^1 or Ts^2 H2/H6), 7.02 (t, *J* = 7.4 Hz, 1H, H2 or H12), 6.99 – 6.90 (m, 3H, H2 or H12, Ts^1 or Ts^2 H2/H6), 6.69 (d, *J* = 5.9 Hz, 1H, C7-NH), 5.71 (br s, 1H, C1'-NH), 4.96 (app t, *J* = 4.7 Hz, 1H, H6), 4.64 (d, *J* = 12.9 Hz, 1H, H8a), 3.69 – 3.54 (m, 2H, H8b, H7), 3.15 – 2.98 (m, 1H, H1'a or H1'b), 2.90 – 2.78 (m, 1H, H1'a or H1'b), 2.36 (s, 3H, Ts^1 or Ts^2 CH_3), 2.24 (s, 3H, Ts^1 or Ts^2 CH_3). ^{13}C NMR (101 MHz, $CDCl_3$) δ 180.9 (C14 or C15), 180.8 (C14 or C15), 149.9 (C4a or C9a), 149.3 (C4a or C9a), 144.1 (Ts^1 or Ts^2 C4), 143.8 (Ts^1 or Ts^2 C4), 136.0 (Ts^1 or Ts^2 C1), 135.9 (C3 or C11), 135.8 (C3 or C11), 135.4 (Ts^1 or Ts^2 C1), 129.9 (Ts^1 or Ts^2 C2/C6), 129.6 (Ts^1 or Ts^2 C2/C6), 127.1 (Ts^1 or Ts^2 C3/C5), 127.0 (Ts^1 or Ts^2 C3/C5), 125.0 (C1 or C13), 124.9 (C1 or C13), 124.3 (C14a), 124.0 (C14b), 123.0 (C13a or C15a), 122.2 (C13a or C15a), 121.7 (C2 or C12), 121.4 (C2 or C12), 110.3 (C4 or C10), 110.1 (C4 or C10), 54.3 (C7), 52.5 (C6), 42.4 (C1'), 39.4 (C8), 21.7 (Ts^1 or Ts^2 CH_3), 21.6 (Ts^1 or Ts^2 CH_3). IR (neat) 3253 (w), 1741 (w), 1697 (w), 1609 (m), 1304 (m), 745 (s). HRESI-MS calcd. for $C_{34}H_{30}N_4O_6S_2Na^+$ 677.1499, found 677.1513. $[\alpha]_D^{29}$ = -15.0 ˚ (*c* 0.04, $CHCl_3$).

7.4 Reactions of indigo with organometallic nucleophiles

7.4.1. ***General Procedure B*** for Grignard Addition

A solution of the Grignard reagent (2.50 mmol) in THF (5 mL) was added to a flame-dried round-bottomed flask, equipped with a magnetic stir bar and pre-dried LiCl (106 mg, 2.50 mmol), and the mixture stirred vigorously at room temperature for 30 min. The resulting complex was added slowly dropwise to a cooled (0 ˚C) suspension of indigo (131 mg, 0.500 mmol) in THF (15 mL) with vigorous stirring, and the resulting mixture allowed to warm to room temperature over 1 h, then stirred at room temperature overnight. To the mixture was added sat. aq. $NaHCO_3$ (3 mL) and transferred to a separatory funnel containing further $NaHCO_3$ solution (40 mL). The aqueous phase was extracted with EtOAc (4×40 mL), and the combined organic phases washed with further $NaHCO_3$ solution (40 mL) and brine (40 mL), dried ($MgSO_4$), and the solvent removed. The residue was used directly for subsequent dehydration reactions.

7.4.2. ***General Procedure C*** for Grignard Addition

A solution of isopropylmagnesium chloride (titrated at 0.40–1.10 M, 2.00 mmol) in THF was added to a flame-dried round-bottomed flask, equipped with a magnetic stir bar and finely-powdered, pre-dried LiCl (106 mg, 2.50 mmol), and the mixture stirred vigorously at room temperature for 30 min. The solution was cooled to 0 ˚C, and a solution of the desired aryl iodide (2.50 mmol) in THF (3 mL) added dropwise, and the mixture stirred for the indicated time. The resulting aryl Grignard reagent was added slowly dropwise to a cooled (-84 ˚C – EtOAc/N_2) suspension of indigo (131 mg, 0.500 mmol) in THF (15 mL) with vigorous stirring, and the resulting mixture allowed to warm to room temperature over 1 h and stirred at room temperature for a further hour. The reaction was quenched by addition of sat. aq. $NaHCO_3$ (3 mL) and the mixture transferred to a separatory funnel containing further $NaHCO_3$ solution (40 mL). The aqueous phase was extracted with EtOAc (4×40 mL), and the combined organic phases washed with further $NaHCO_3$ solution (40 mL) and brine (40 mL), dried ($MgSO_4$), and the solvent removed. The residue was used directly for subsequent dehydration reactions.

7.4.3. ***General Procedure D*** for Grignard Addition

A flame-dried round-bottomed flask, equipped with a magnetic stir bar was charged with a solution of the desired aryl iodide (2.50 mmol) in THF (1 mL), and cooled to 0 ˚C. Isopropylmagnesium chloride lithium chloride complex (titrated at 0.51 M, 2.00 mmol) in THF was added slowly dropwise, and the mixture stirred for the indicated time. The

resulting aryl Grignard reagent was added slowly dropwise to a cooled (-84 ˚C – EtOAc/N_2) suspension of indigo (131 mg, 0.500 mmol) in THF (15 mL) with vigorous stirring, and the resulting mixture allowed to warm to room temperature over 1 h and stirred at room temperature for a further hour. The reaction was quenched by addition of sat. aq. $NaHCO_3$ (3 mL) and transferred to a separatory funnel containing further $NaHCO_3$ solution (40 mL). The aqueous phase was extracted with EtOAc (4×40 mL), and the combined organic phases washed with further $NaHCO_3$ solution (40 mL) and brine (40 mL), and dried ($MgSO_4$), and the solvent removed. The residue was used directly for subsequent dehydration reactions.

7.4.4. ***General Procedure E*** for Organolithium Addition

A flame-dried round-bottomed flask, equipped with a magnetic stir bar was charged with a solution of the desired heterocycle (2.50 mmol) in THF (1 mL), and cooled to -84 ˚C (EtOAc/N_2). A solution of *n*-BuLi in hexane (titrated at 1.95 M, 2.00 mmol) was added slowly dropwise, and the mixture allowed to warm to room temperature over the indicated time. The resulting organolithium reagent was added slowly dropwise to a cooled (-84 ˚C) suspension of indigo (131 mg, 0.500 mmol) in THF (15 mL) with vigorous stirring, and the resulting deep red mixture allowed to warm to room temperature over 1 h, and stirred at room temperature for a further hour. The reaction was quenched by addition of sat. aq. $NaHCO_3$ (3 mL), and the mixture transferred to a separatory funnel containing further $NaHCO_3$ solution (40 mL). The aqueous phase was extracted with EtOAc (4×40 mL), and the combined organic phases washed with further $NaHCO_3$ solution (40 mL) and brine (40 mL), dried ($MgSO_4$), and the solvent removed. The residue was used directly for subsequent dehydration reactions.

7.4.5. ***General Procedure F*** for Boc-mediated Dehydration:

The crude tertiary alcohol residue (*ca.* 0.5 mmol) was suspended in CH_2Cl_2 (100 mL), then DMAP (131 mg, 1.1 mmol), NEt_3 (0.2 mL) and di-*tert*-butyl dicarbonate (327 mg, 1.5 mmol) were added sequentially in air, and the mixture stirred vigorously at room temperature for 1 h. The resulting intense orange solution was diluted with 0.2 N HCl (50 mL), and the lower organic layer collected and washed with a further 0.2 N HCl (50 mL), sat. $NaHCO_3$ (40 mL) and brine (40 mL), dried (Na_2SO_4) and the solvent removed.

7.4.6. Isolated scaffolds

tert-butyl 3-isopropyl-3'-oxo-1*H*,3'*H*-[2,2'-biindole]-1-carboxylate (210)

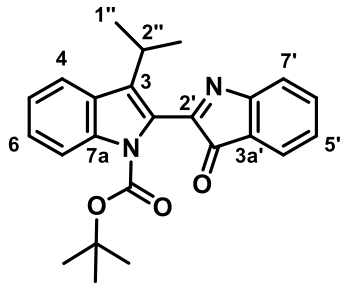

Prepared *via* ***General Procedure B***, using isopropylmagnesium chloride (0.598 M, 3.3 mL, 1.97 mmol) and LiCl (106 mg, 2.50 mmol). Subsequent Boc-mediated dehydration (***General Procedure F***) of the crude product afforded a red residue, which was fractionated on silica (75 g, using 60% CH_2Cl_2/pet spirit as eluent) and recrystallised from hexane to afford the *N*-Boc indole **210** (153 mg, 80%) as shiny, bright-orange crystals, mp 62–64 ˚C. R_f (10% EtOAc/pet spirit) 0.56. UV-Vis (acetone) λ_{max}/nm (ε, $M^{-1}cm^{-1}$) 333 (5448), 434 (1702), 509 (1275). ^{1}H NMR (400 MHz, $CDCl_3$) δ 8.21 (d, *J* = 8.4 Hz, 1H, H7), 7.83 (d, *J* = 8.0 Hz, 1H, H4), 7.60 (d, *J* = 7.4 Hz, 1H, H4'), 7.56 (app t, *J* = 7.5 Hz, 1H, H6'), 7.49 (d, *J* = 7.5 Hz, 1H, H7'), 7.40 (app t, *J* = 7.6 Hz, 1H, H6), 7.31 – 7.21 (m, 2H, H5, H5'), 3.58 (hept, *J* = 7.1 Hz, 1H, H2''), 1.49 (s, 9H, 3×Boc CH_3), 1.46 (d, *J* = 7.1 Hz, 6H, H1'', H3''). ^{13}C NMR (101 MHz, $CDCl_3$) δ 192.1 (C3'), 160.8 (H7a'), 160.7 (C2'), 150.1 (Boc C=O), 137.6 (C7a), 136.8 (C6'), 134.0 (C3), 128.52 (C3a or C3a'), 128.50 (C3a or C3a'), 128.4 (C5'), 126.1 (C6), 125.0 (C4'), 124.2 (C2), 122.7 (C5), 122.5 (C7'), 121.8 (C4), 115.9 (C7), 84.9 (Boc Cq), 28.1 (Boc CH_3), 26.1 (C2''), 22.8 (C1'', C3''). IR (neat) 2962 (w), 2929 (w), 2630 (w), 2339 (w), 1734 (s), 1575 (m), 1452 (s), 1369 (s), 1344 (s), 1321 (s), 1234 (s), 1145 (s), 761 (s), 744 (s) cm^{-1}. HRESI-MS calcd. for $C_{24}H_{25}N_2O_3^+$ 389.1860, found 389.1860.

3-phenyl-1*H*,3'*H*-[2,2'-biindol]-3'-one (214)

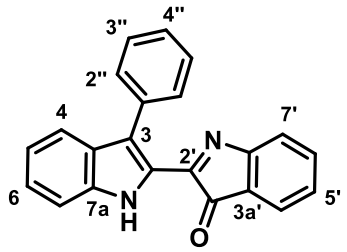

Prepared *via* ***General Procedure B*** using phenylmagnesium chloride (0.805 M, 2.50 mL, 2.01 mmol) and LiCl (106 mg, 2.50 mmol). Subsequent Boc-mediated dehydration (***General Procedure F***) of the crude product afforded a dark brown residue, which was fractionated on silica (40 g, using 60% CH_2Cl_2/pet spirit as eluent). Removal of the solvent from the first fraction afforded the free indole **214** (22 mg, 13%) as an intense black-purple powder, mp 190–192 ˚C. R_f (60% CH_2Cl_2/pet spirit) 0.58. UV-Vis (acetone) λ_{max}/nm (ε, $M^{-1}cm^{-1}$) 326 (2627), 538 (1491). ^{1}H NMR (500 MHz, $CDCl_3$) δ 10.25 (s, 1H, NH), 7.70 (d, *J* = 7.6 Hz, 2H, H3'', H5''), 7.67 (d, *J* = 8.1 Hz, 1H, H4), 7.54 – 7.45 (m, 5H, H4', H7, H2'', H6'', H6'), 7.42 (t, *J* = 7.4 Hz, 1H, H4''), 7.35 (t, *J* = 7.6 Hz, 1H, H6), 7.23 (d, *J* = 7.6 Hz, 1H, H7'), 7.19 –

7.11 (m, 2H, H5, H5'). ^{13}C NMR (126 MHz, $CDCl_3$) δ 196.1 (C3'), 162.1 (C7a'), 154.3 (C2'), 138.2 (C7a), 137.5 (C6'), 133.9 (C1''), 131.0 (C3'', C5''), 128.1 (C2'', C6''), 127.7 (C4''), 127.5 (C5'), 126.7 (C3a), 126.4 (C6), 125.2 (C4'), 124.5 (C3), 122.4 (C3a'), 122.2 (C3a'), 121.7 (C4), 121.3 (C5), 114.2 (C2), 112.0 (C7). IR (neat) 3370 (br w), 2922 (s), 2850 (m), 1734 (m), 1558 (s), 1168 (m), 747 (m) cm^{-1}. HRESI-MS calcd. for $C_{22}H_{15}N_2O^+$ 323.1184, found 323.1187.

tert-butyl 3'-oxo-3-phenyl-1*H*,3'*H*-[2,2'-biindole]-1-carboxylate (211)

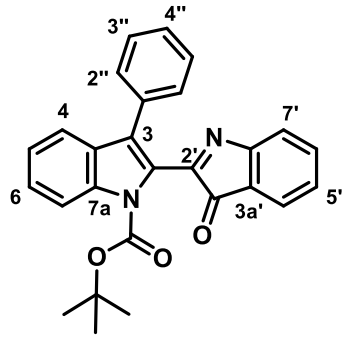

Further elution afforded a red-orange fraction, which was subjected to flash chromatography (20 g silica, 10% EtOAc/pet spirit), and removal of the solvent gave the *N*-Boc indole **211** (174 mg, 79%) as shiny, bright orange crystals, mp 132–133 ˚C (dec.). X-ray quality crystals were grown by slow evaporation from hexane. R_f (60% CH_2Cl_2/pet spirit) 0.56. UV-Vis (acetone) λ_{max}/nm (ε, M^{-1}cm^{-1}) 323 (7900), 329 (2917), 499 (1440). ^{1}H NMR (400 MHz, $CDCl_3$) δ 8.24 (d, J = 8.4 Hz, 1H, H7), 7.66 – 7.60 (m, 3H, H2'', H6'', H4), 7.53 (d, J = 7.1 Hz, 1H, H4'), 7.51 – 7.33 (m, 6H, H3'', H4'', H5'', H6, H6', H7'), 7.28 (app t, J = 7.2 Hz, 1H, H5), 7.23 (app t, J = 7.4 Hz, 1H, H5'), 1.52 (s, 9H, 3×Boc CH_3). ^{13}C NMR (101 MHz, $CDCl_3$) δ 191.8 (C3'), 160.4 (C7a'), 160.3 (C2'), 150.1 (Boc C=O), 136.8 (C7a), 136.7 (C6'), 131.8 (C3), 130.9 (C3'', C5''), 129.6 (C3a), 128.5 (C5'), 128.3 (C2'', C6''), 128.1 (C1''), 128.0 (C7'), 126.7 (C6), 125.2 (C2), 125.0 (C4'), 123.5 (C5), 122.7 (C3a'), 122.6 (C4''), 121.2 (C4), 115.7 (C7), 85.3 (Boc Cq), 28.1 (Boc CH_3). IR (neat) 2978 (w), 2920 (w), 2360 (m), 1734 (s), 1576 (m), 1319 (s) 1149 (s), 746 (s), 699 (s) cm^{-1}. HRESI-MS calcd. for $C_{27}H_{23}N_2O_3^+$ 423.1703, found 423.1702.

tert-butyl 3-butyl-3'-oxo-1*H*,3'*H*-[2,2'-biindole]-1-carboxylate (215)

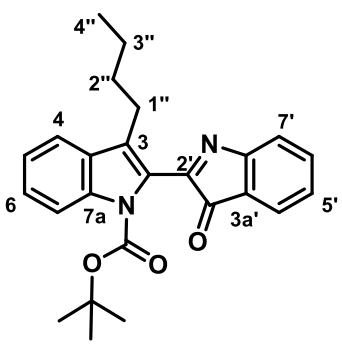

Prepared *via* ***General Procedure E***, using *n*-BuLi (1.95 M, 1.4 mL, 2.73 mmol) and TMEDA (333 mg, 2.86 mmol). Subsequent Boc-mediated dehydration (***General Procedure F***) of the crude product afforded a red-brown residue, which was fractionated on silica (75 g, using 10% EtOAc/hexane as eluent), and flash chromatography (30 g silica, 60% CH_2Cl_2/hexane) afforded the *N*-Boc indole **215** (162 mg, 80%) as a deep orange amorphous solid, mp 42–43 ˚C. R_f (10% EtOAc/hexane)

0.49. UV-Vis (acetone) λ_{max}/nm (ε, $M^{-1}cm^{-1}$) 331 (3679), 438 (2134), 500 (1810). ^{1}H NMR (400 MHz, $CDCl_3$) δ 8.17 (d, *J* = 8.4 Hz, 1H, H7), 7.65 (d, *J* = 7.7 Hz, 1H, H4), 7.62 – 7.53 (m, 2H, H4', H6'), 7.48 (d, *J* = 7.6 Hz, 1H, H7'), 7.42 (ddd, *J* = 8.4, 7.1, 1.3 Hz, 1H, H6), 7.34 – 7.26 (m, 2H, H5, H5'), 2.94 (d, *J* = 7.6 Hz, 2H, H1''), 1.74 – 1.64 (m, 2H, H2''), 1.51 (s, 9H, 3×Boc CH_3), 1.36 (h, *J* = 7.4 Hz, 2H, H3''), 0.90 (t, *J* = 7.3 Hz, 3H, H4''). ^{13}C NMR (101 MHz, $CDCl_3$) δ 191.9 (C3'), 160.7 (C7a'), 160.2 (C2'), 150.0 (Boc C=O), 137.2 (C7a), 136.6 (C6), 129.8 (C3a), 129.3 (C3), 128.2 (C5'), 126.4 (C6), 125.4 (C2), 124.8 (C4'), 122.9 (C5), 122.5 (C3a'), 122.2 (C7'), 120.3 (C4), 115.6 (C7), 84.7 (Boc Cq), 32.7 (C2''), 28.0 (Boc CH_3), 24.1 (C1''), 22.6 (C3''), 13.9 (C4''). IR (neat) 2957 (w), 2930 (w), 1734 (s), 1558 (m), 1319 (m) 1149 (s), 1105 (m), 761 (m), 745 (m) cm^{-1}. HRESI-MS calcd. for $C_{25}H_{27}N_2O_3^+$ 403.2022, found 403.2036.

3-methyl-1*H*,3'*H*-[2,2'-biindol]-3'-one (218)

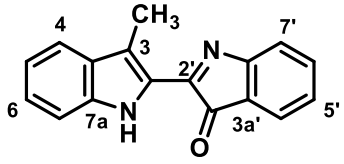

To a cooled (-84 ˚C) suspension of indigo (131 mg, 0.500 mmol) and TMEDA (320 mg, 2.75 mmol) in THF (20 mL) was added dropwise MeLi (2.74 M in DME, 0.90 mL, 2.47 mmol), and the mixture allowed to warm to RT over 1 h. The resulting intense-red solution was stirred at RT for a further hour, then sat. $NaHCO_3$ solution (3 mL) added, and the mixture transferred to a separatory funnel containing additional $NaHCO_3$ solution (40 mL). The aqueous phase was extracted with EtOAc (4×40 mL), and the combined organic phases washed with $NaHCO_3$ solution (40 mL) and brine (40 mL), dried ($MgSO_4$), and the solvent removed. The resulting golden residue was dissolved in CH_2Cl_2 (100 mL), then PPh_3 (159 mg, 0.606 mmol), imidazole (99 mg, 1.46 mmol), and I_2 (162 mg, 0.638 mmol) added sequentially. The deep brown mixture was stirred overnight, then diluted with water (50 mL) and transferred to a separatory funnel. The aqueous phase was extracted with CH_2Cl_2 (3×30 mL), and the combined organic phases washed with $NaHCO_3$ solution (40 mL) and brine (40 mL), dried ($MgSO_4$), and the solvent removed. The residue was subjected to flash chromatography (60 g silica, 60% CH_2Cl_2/pet spirit) and removal of the solvent from the intense deep-purple fraction afforded the desired indole **218** (97 mg, 74%) as feathery, dark purple crystals, mp 252–253 ˚C (dec.). R_f (60% CH_2Cl_2/pet spirit) 0.71. UV-Vis (acetone) λ_{max}/nm (ε, $M^{-1}cm^{-1}$) 326 (8389), 538 (4881). ^{1}H NMR (500 MHz, $CDCl_3$) δ 9.98 (s, 1H, NH), 7.68 (dd, *J* = 8.1, 1.0 Hz, 1H, H4), 7.58 – 7.50 (m, 2H, C4', C7'), 7.43 – 7.36 (m, 2H, H7, H6'), 7.32 (ddd, *J* = 8.2, 6.9, 1.1 Hz, 1H, H6), 7.22 – 7.16 (m, 1H, H5'), 7.16 –

7.11 (m, 1H, H5), 2.84 (s, 3H, Ar-CH_3). ^{13}C NMR (126 MHz, $CDCl_3$) δ 196.9 (C3'), 163.0 (C7a'), 154.8 (C2'), 138.4 (C7a), 137.7 (C6'), 128.8 (C3a), 127.4 (C5'), 126.3 (C6), 125.23 (C2), 125.19 (C4'), 124.3 (C3a'), 122.04 (C3), 121.95 (C7'), 120.7 (C4), 120.4 (C5), 112.0 (C7), 11.6 (Ar-CH_3). IR (neat) 3376 (m), 1708 (s), 1540 (s), 1452 (m), 1327 (s), 1241 (m), 1167 (s), 877 (m), 762 (s), 741 (s), 672 (s) cm^{-1}. HRESI-MS calcd. for $C_{17}H_{13}N_2O^+$ 261.1022, found 261.1022.

***tert*-butyl 3-benzyl-3'-oxo-1*H*,3'*H*-[2,2'-biindole]-1-carboxylate (219)**

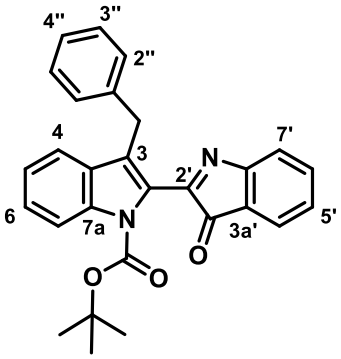

Prepared *via* ***General Procedure B*** using benzylmagnesium chloride (1.89 M, 1.10 mL, 2.08 mmol), and LiCl (106 mg, 2.50 mmol). Subsequent Boc-mediated dehydration (***General Procedure F***) of the crude product afforded a deep orange residue, which was separated by flash chromatography (100 g silica, 10% EtOAc/hexane) to give the *N*-Boc indole **219** (204 mg, 91%) as a deep orange powder, mp 85–86 ˚C. R_f (10% EtOAc/hexane) 0.27. UV-Vis (acetone) λ_{max}/nm (ε, $M^{-1}cm^{-1}$) 331 (3957), 409 (2129), 462 (1605), 499 (1561). ^{1}H NMR (500 MHz, $CDCl_3$) δ 8.16 (d, *J* = 8.4 Hz, 1H, H7), 7.58 (dd, *J* = 7.2, 0.6 Hz, 1H, H4'), 7.53 (td, *J* = 7.6, 1.2 Hz, 1H, H6'), 7.47 – 7.43 (m, 2H, H4, H7'), 7.38 (ddd, *J* = 8.4, 7.2, 1.2 Hz, 1H, H6), 7.31 (d, *J* = 7.6 Hz, 2H, H2", H6"), 7.28 – 7.24 (m, 1H, H4"), 7.22 (dd, *J* = 10.9, 4.1 Hz, 2H, H3", H5"), 7.19 – 7.16 (m, 1H, H5), 7.13 (t, *J* = 7.4 Hz, 1H, H4"), 4.32 (s, 2H, Ar-CH_2Ph), 1.53 (s, 9H, 3×Boc CH_3). ^{13}C NMR (126 MHz, $CDCl_3$) δ 191.9 (C3'), 160.5 (C7a'), 160.0 (C2'), 150.1 (Boc C=O), 139.7 (C1"), 137.3 (C7a), 136.8 (C6'), 129.6 (C3a), 128.7 (C2", C6"), 128.5 (C3", C5"), 128.4 (C5'), 126.7 (C3), 126.6 (C6), 126.4 (C2), 126.3 (C4"), 125.0 (C4'), 123.2 (C5), 122.5 (C7a'), 122.4 (C7'), 121.0 (C4), 115.6 (C7), 85.1 (Boc Cq), 30.6 (Ar-$\underline{CH_2}$Ph), 28.1 (Boc CH_3). IR (neat) 2979 (w), 1734 (s), 1558 (m), 1452 (m), 1319 (m) 1145 (s), 1105 (m), 762 (m), 745 (m), 698 (m) cm^{-1}. HRESI-MS calcd. for $C_{28}H_{25}N_2O_3^+$ 437.1865, found 437.1880.

***tert*-butyl 3-(4-methoxyphenyl)-3'-oxo-1*H*,3'*H*-[2,2'-biindole]-1-carboxylate (222)**

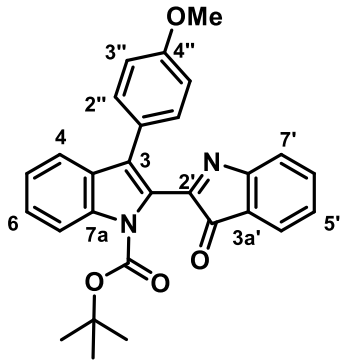

Prepared *via* ***General Procedure C***. The substituted Grignard reagent (4-methoxyphenylmagnesium chloride lithium chloride complex) was prepared using isopropylmagnesium chloride (1.08 M, 1.80 mL, 1.94 mmol), LiCl (106 mg, 2.50 mmol) and 4-iodoanisole (589 mg, 2.50 mmol), and the resulting mixture stirred at room temperature for 1.5 h prior to combining with indigo. Subsequent Boc-mediated dehydration (***General Procedure F***) of the crude product afforded a deep red-orange mixture, which was separated by flash chromatography (80 g silica, 10% EtOAc/pet spirit) to afford the title compound **222** (168 mg, 72%) as a bright orange powder, mp 79–80 ˚C (dec.). R_f (10% EtOAc/pet spirit) 0.25. UV-Vis (acetone) λ_{max}/nm (ε, $M^{-1}cm^{-1}$) 347 (2250), 412 (1222), 469 (1104), 504 (979). ^{1}H NMR (400 MHz, $CDCl_3$) δ 8.24 (d, *J* = 8.4 Hz, 1H, H7), 7.65 (d, *J* = 7.7 Hz, 1H, H4), 7.60 (d, *J* = 8.7 Hz, 2H, H2'', H6''), 7.55 (d, *J* = 7.1 Hz, 1H, H4'), 7.51 (td, *J* = 7.6, 1.3 Hz, 1H, H6'), 7.46 (ddd, *J* = 8.4, 7.2, 1.2 Hz, 1H, H6), 7.40 (d, *J* = 7.5 Hz, 1H, H7'), 7.30 (ddd, *J* = 8.1, 7.2, 1.0 Hz, 1H, H5), 7.26 – 7.21 (m, 1H, H5'), 6.97 (d, *J* = 8.7 Hz, 2H, H3'', H5''), 3.83 (s, 3H, -OCH_3), 1.52 (s, 9H, 3×Boc CH_3). ^{13}C NMR (101 MHz, $CDCl_3$) δ 191.9 (C3'), 160.6 (C7a'), 160.3 (C2'), 159.5 (C4''), 150.1 (Boc C=O), 136.9 (C7a), 136.7 (C6'), 132.2 (C2'', C6''), 129.8 (C3a), 128.5 (C5'), 128.0 (C3), 126.6 (C6), 125.0 (C4'), 124.9 (C2), 124.0 (C1''), 123.5 (C5), 122.7 (C3a'), 122.6 (C7'), 121.3 (C4), 115.7 (C7), 113.7 (C3'', C5''), 85.2 (Boc Cq), 55.4 (-OCH_3), 28.1 (Boc CH_3). IR (neat) 2956 (w), 2923 (m), 2853 (w), 1734 (s), 1506 (m), 1250 (s) 1151 (s), 763 (m) cm^{-1}. HRESI-MS calcd. for $C_{28}H_{25}N_2O_4^+$ 453.1809, found 453.1807.

***tert*-butyl 3-(3-methoxyphenyl)-3'-oxo-1*H*,3'*H*-[2,2'-biindole]-1-carboxylate (223)**

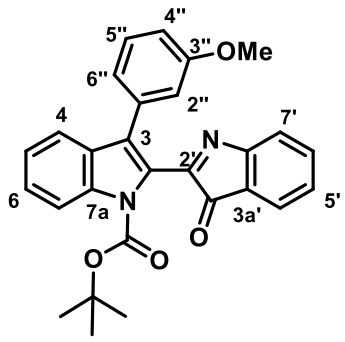

Prepared *via* ***General Procedure C***. The substituted Grignard reagent (3-methoxyphenylmagnesium chloride lithium chloride complex) was prepared using isopropylmagnesium chloride (1.08 M, 1.80 mL, 1.94 mmol), LiCl (106 mg, 2.50 mmol), and 3-iodoanisole (599 mg, 2.56 mmol), and the resulting mixture stirred at room temperature for 1.5 h prior to combining with indigo. Subsequent Boc-mediated dehydration (following ***General Procedure F***) of the crude

product afforded a deep red-orange residue, which was subjected to flash chromatography (95 g silica, 10% EtOAc/hexane), to afford the *N*-Boc indole **223** (167 mg, 72%) as deep orange crystals, mp 64–65 ˚C. R_f (10% EtOAc/hexane) 0.25. UV-Vis (acetone) λ_{max}/nm (ε, $M^{-1}cm^{-1}$) 327 (3430), 433 (1549), 467 (1357), 504 (1143). ^{1}H NMR (400 MHz, $CDCl_3$) δ 8.24 (d, *J* = 8.4 Hz, 1H, H7), 7.69 (d, *J* = 7.9 Hz, 1H, H4), 7.55 (d, *J* = 7.1 Hz, 1H, H4'), 7.51 (td, *J* = 7.6, 1.2 Hz, 1H, H6'), 7.48 – 7.42 (m, 1H, H6), 7.37 (d, *J* = 7.5 Hz, 1H, H7'), 7.34 – 7.22 (m, 4H, H5, H5', H2'', H5''), 7.20 – 7.16 (m, 1H, H6''), 6.91 (ddd, *J* = 8.2, 2.5, 0.8 Hz, 1H, H4''), 3.83 (s, 3H, -OCH_3), 1.52 (s, 9H, 3×Boc CH_3). ^{13}C NMR (101 MHz, $CDCl_3$) δ 191.7 (C3'), 160.43 (C7a' or C2'), 160.38 (C7a' or C2'), 159.5 (C3''), 150.1 (Boc C=O), 136.8 (C7a), 136.7 (C6'), 133.0 (C1''), 130.9 (C2), 129.5 (C3a), 129.2 (C5''), 128.6 (C5'), 127.9 (C3), 126.7 (C6), 125.0 (C4'), 123.6 (C5), 123.2 (C6''), 122.7 (C3a'), 122.6 (C7'), 121.2 (C4), 116.2 (C2''), 115.7 (C7), 114.4 (C4''), 85.4 (Boc Cq), 55.4 (-OCH_3), 28.1 (Boc CH_3). IR (neat) 2976 (w), 2361 (m), 2853 (w), 1734 (s), 1149 (s), 763 (m), 750 (m) cm^{-1}. HRESI-MS calcd. for $C_{28}H_{25}N_2O_4^+$ 453.1809, found 453.1808.

***tert*-butyl 3-(2-methoxyphenyl)-3'-oxo-1*H*,3'*H*-[2,2'-biindole]-1-carboxylate (224)**

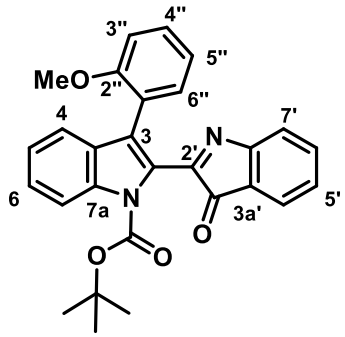

Prepared *via* ***General Procedure C***. The substituted Grignard reagent (2-methoxyphenylmagnesium chloride lithium chloride complex) was prepared using isopropylmagnesium chloride (1.08 M, 1.80 mL, 1.94 mmol), LiCl (106 mg, 2.50 mmol), and 2-iodoanisole (592 mg, 2.53 mmol), and the resulting mixture stirred at room temperature for 1.5 h prior to combining with indigo. Subsequent Boc-mediated dehydration (***General Procedure F***) of the crude product afforded a deep red-orange residue, which was subjected to flash chromatography (80 g silica, 10% EtOAc/hexane), to afford the *N*-Boc indole **224** (217 mg, 94%) as deep orange crystals, mp 159–160 ˚C (dec.). X-ray quality crystals were grown by slow evaporation of a 9:1 hexane:chloroform solution. R_f (10% EtOAc/hexane) 0.24. UV-Vis (acetone) λ_{max}/nm (ε, $M^{-1}cm^{-1}$) 329 (2794), 419 (1496), 505 (948). ^{1}H NMR (400 MHz, $CDCl_3$) δ 8.25 (d, *J* = 8.4 Hz, 1H, H7), 7.61 – 7.53 (m, 3H, H6'', H4, H4'), 7.47 (td, *J* = 7.8, 1.2 Hz, 1H, H6'), 7.42 (ddd, *J* = 8.4, 7.3, 1.2 Hz, 1H, H6), 7.34 – 7.22 (m, 4H, H5, H5', H7', H4''), 7.09 (td, *J* = 7.5, 0.9 Hz, 1H, H5''), 6.83 (d, *J* = 8.0 Hz, 1H, H3''), 3.37 (s, 3H, -OCH_3), 1.51 (s, 9H, 3×Boc CH_3). ^{13}C NMR (101 MHz, $CDCl_3$) δ 192.9 (C3'), 161.2 (C2'), 160.6 (C7a'), 155.5 (C2''), 149.9 (Boc C=O), 136.9 (C7a), 136.5 (C6'), 132.0 (C6''), 129.6 (C3a),

129.2 (C4''), 128.3 (C5'), 126.18 (C6), 126.15 (C2), 124.4 (C4'), 123.4 (C5), 122.8 (C3a'), 122.6 (C3), 122.3 (C7'), 121.1 (C1''), 121.0 (C5''), 120.9 (C4), 115.8 (C7), 111.4 (C3''), 85.1 (Boc Cq), 55.2 (-OCH_3), 28.1 (Boc CH_3). IR (neat) 2981 (w), 2358 (w), 1718 (s), 1323 (s), 1149 (s), 748 (s) cm^{-1}. HRESI-MS calcd. for $C_{28}H_{25}N_2O_4^+$ 453.1809, found 453.1808.

tert-butyl 3-(2,4-dimethoxyphenyl)-3'-oxo-1*H*,3'*H*-[2,2'-biindole]-1-carboxylate (228)

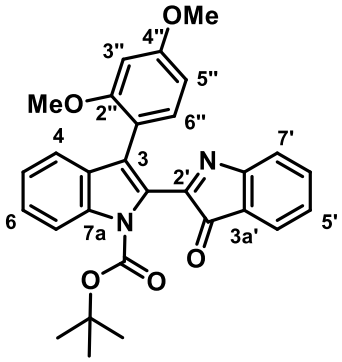

Prepared *via* ***General Procedure D***. The substituted Grignard reagent (2,4-dimethoxyphenylmagnesium chloride lithium chloride complex) was prepared using isopropylmagnesium chloride lithium chloride complex (0.45 M, 4.4 mL, 1.98 mmol), and 1-iodo-2,4-dimethoxybenzene (664 mg, 2.51 mmol), and the mixture stirred at 0 ˚C for 2 h prior to combining with indigo. Subsequent Boc-mediated dehydration (***General Procedure F***) of the crude product afforded a deep red-orange residue, which was subjected to flash chromatography (80 g silica, 20% EtOAc/hexane), to afford the *N*-Boc indole **228** (179 mg, 72%) as a deep orange solid, mp 89–90 ˚C (dec.). R_f (20% EtOAc/hexane) 0.35. UV-Vis (acetone) λ_{max}/nm (ε, $M^{-1}cm^{-1}$) 330 (3138), 400 (1623), 421 (1610), 507 (1127). ^{1}H NMR (500 MHz, $CDCl_3$) δ 8.24 (d, *J* = 8.5 Hz, 1H, H7), 7.59 (d, *J* = 7.1 Hz, 1H, H4'), 7.54 (d, *J* = 8.0 Hz, 1H, H4), 7.50 – 7.45 (m, 2H, H6', H6''), 7.41 (app t, *J* = 7.2 Hz, 1H, H6), 7.32 – 7.23 (m, 3H, H5, H5', H7'), 6.63 (dd, *J* = 8.4, 2.4 Hz, 1H, H5''), 6.40 (d, *J* = 2.4 Hz, 1H, H3''), 3.83 (s, 3H, C4''-OCH_3), 3.36 (s, 3H, C2''-OCH_3), 1.51 (s, 9H, 3×Boc CH_3). ^{13}C NMR (126 MHz, $CDCl_3$) δ 193.0 (C3'), 161.3 (C2'), 160.70 (C4'' or C7a'), 160.65 (C4'' or C7a'), 156.6 (C2''), 149.9 (Boc C=O), 136.9 (C7a), 136.5 (C6'), 132.5 (C6''), 129.8 (C3a), 128.2 (C5'), 126.1 (C6), 125.8 (C2), 124.4 (C4'), 123.3 (C5), 122.8 (C3a'), 122.6 (C3), 122.3 (C7'), 120.9 (C4), 115.8 (C7), 113.7 (C1''), 104.8 (C5''), 99.4 (C3''), 85.0 (Boc Cq), 55.5 (C4''-OCH_3), 55.2 (C2''-OCH_3), 28.1 (Boc CH_3). IR (neat) 2978 (w), 2933 (w), 2361 (w), 1734 (s), 1451 (m), 1323 (m), 1149 (s), 748 (s) cm^{-1}. HRESI-MS calcd. for $C_{29}H_{27}N_2O_5^+$ 483.1915, found 483.1914.

***tert*-butyl 3-(4-fluorophenyl)-3'-oxo-1*H*,3'*H*-[2,2'-biindole]-1-carboxylate (231)**

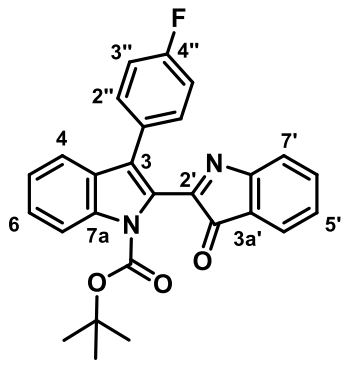

Prepared *via* ***General Procedure C***. The substituted Grignard reagent (4-fluorophenylmagnesium chloride lithium chloride complex) was prepared using isopropylmagnesium chloride (1.08 M, 1.70 mL, 1.84 mmol), LiCl (106 mg, 2.50 mmol), and 4-fluoroiodobenzene (567 mg, 2.56 mmol and the resulting mixture stirred at room temperature for 1.5 h prior to combining with indigo. Subsequent Boc-mediated dehydration (***General Procedure F***) of the crude product afforded a deep red-orange residue, which was subjected to flash chromatography (80 g silica, 10% EtOAc/hexane), to afford the *N*-Boc indole **231** (167 mg, 75%) as bright orange crystals, mp 137–138 ˚C (dec.). R_f (10% EtOAc/hexane) 0.53. UV-Vis (acetone) λ_{max}/nm (ε, $M^{-1}cm^{-1}$) 329 (3911), 418 (2023), 470 (1725), 503 (1448). ^{1}H NMR (500 MHz, $CDCl_3$) δ 8.24 (d, *J* = 8.4 Hz, 1H, H7), 7.64 – 7.57 (m, 3H, H4, H2", H6"), 7.56 (d, *J* = 7.1 Hz, 1H, H4), 7.52 (td, *J* = 7.6, 1.3 Hz, 1H, H6'), 7.47 (ddd, *J* = 8.4, 7.2, 1.2 Hz, 1H, H6), 7.38 (d, *J* = 7.5 Hz, 1H, H7'), 7.31 (app t, *J* = 7.1 Hz, 1H, H5), 7.29 – 7.22 (m, 1H, H5'), 7.11 (app tt, *J* = 8.8, 2.9 Hz, 2H, H3", H5"), 1.53 (s, 9H, 3×Boc CH_3). ^{13}C NMR (126 MHz, CDCl3) δ 191.7 (C3'), 162.7 (d, $^1J_{C\text{-}F}$ = 248.2 Hz, C4"), 160.4 (C2' or C7a'), 160.0 (C2' or C7a'), 150.2 (Boc C=O), 136.82 (C7a), 136.80 (C6'), 132.7 (d, $^3J_{C\text{-}F}$ = 8.1 Hz, C2", C6"), 129.5 (C3a), 128.6 (C5'), 127.7 (d, $^4J_{C\text{-}F}$ = 2.5 Hz, C1"), 127.2 (C3), 126.8 (C6), 125.3 (C2), 125.1 (C4'), 123.6 (C5), 122.7 (C3a'), 122.6 (C7'), 121.0 (C4), 115.8 (C7), 115.3 (d, $^2J_{C\text{-}F}$ = 21.3 Hz, C3", C5"), 85.5 (Boc Cq), 28.1 (Boc CH_3). ^{19}F NMR (470 MHz, $CDCl_3$, ^{1}H-decoupled) δ -114.0. IR (neat) 2980 (w), 2931 (w), 2367 (w), 1734 (s), 1506 (m), 1319 (m), 1149 (s), 748 (s) cm^{-1}. HRESI-MS calcd. for $C_{27}H_{22}FN_2O_3^+$ 441.1609, found 441.1608.

***tert*-butyl 3-(2-chlorophenyl)-3'-oxo-1*H*,3'*H*-[2,2'-biindole]-1-carboxylate (232)**

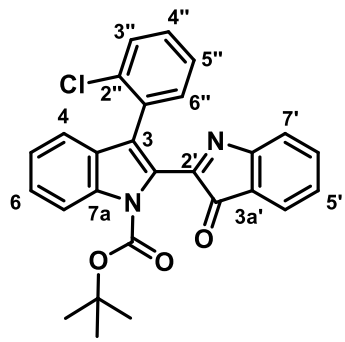

Prepared *via* ***General Procedure C***. The substituted Grignard reagent (2-chlorophenylmagnesium chloride lithium chloride complex) was prepared using isopropylmagnesium chloride (1.08 M, 1.80 mL, 1.94 mmol), LiCl (106 mg, 2.50 mmol), and 2-chloroiodobenzene (605 mg, 2.54 mmol), and the resulting mixture stirred at room temperature for 1.5 h prior to

combining with indigo. Subsequent Boc-mediated dehydration (***General Procedure F***) of the crude product afforded a deep red-orange residue, which was subjected to flash chromatography (80 g silica, 10% EtOAc/hexane), to afford the *N*-Boc indole **232** (182 mg, 79%) as deep red-orange crystals, mp 108–109 ˚C (dec.). X-ray quality crystals were grown by slow evaporation of a 9:1 hexane/chloroform solution. R_f (10% EtOAc/hexane) 0.30. UV-Vis (acetone) λ_{max}/nm (ε, $M^{-1}cm^{-1}$) 327 (3120), 401 (1619), 466 (1220), 500 (952). ^{1}H NMR (400 MHz, $CDCl_3$) δ 8.25 (d, *J* = 8.5 Hz, 1H, H7), 7.57 (d, *J* = 7.2 Hz, 1H, H4'), 7.52 (dd, *J* = 7.5, 1.7 Hz, 1H, H6''), 7.49 – 7.45 (m, 2H, H6, H6'), 7.43 (dd, *J* = 5.4, 1.3 Hz, 1H, H3''), 7.41 – 7.39 (m, 1H, H4), 7.35 (dd, *J* = 7.4, 1.6 Hz, 1H, H5''), 7.32 (dd, *J* = 7.6, 1.9 Hz, 1H, H4''), 7.30 – 7.27 (m, 3H, H5, H5', H7'), 1.53 (s, 9H, 3×Boc CH_3). ^{13}C NMR (101 MHz, $CDCl_3$) δ 191.8 (C3'), 160.5 (C7a'), 160.1 (C2'), 149.9 (Boc C=O), 136.8 (C7a), 136.6 (C6'), 133.6 (C2''), 133.0 (C6''), 131.3 (C1''), 130.0 (C3''), 129.4 (C4''), 129.2 (C3a), 128.5 (C5'), 128.4 (C2), 126.8 (C5''), 126.7 (C6), 126.6 (C3), 124.8 (C4'), 123.6 (C5), 122.54 (C3a'), 122.52 (C7'), 121.0 (C4), 115.8 (C7), 85.5 (Boc Cq), 28.3 (Boc CH_3). IR (neat) 2980 (w), 2931 (w), 2377 (w), 1734 (s), 1458 (m), 1320 (m), 1150 (s), 748 (s) cm^{-1}. HRESI-MS calcd. for $C_{27}H_{22}{}^{35}ClN_2O_3^+$ 457.1314, found 457.1313; calcd. for $C_{27}H_{22}{}^{37}ClN_2O_3^+$ 459.1284, found 459.1285.

***tert*-butyl 3'-oxo-3-(pyridin-3-yl)-1*H*,3'*H*-[2,2'-biindole]-1-carboxylate (233)**

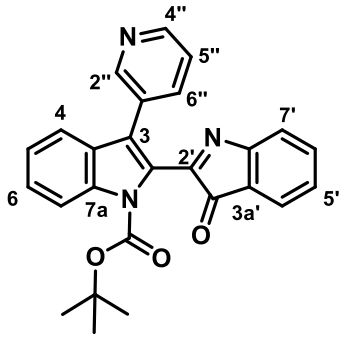

Prepared *via* ***General Procedure D***. The substituted Grignard reagent (pyridin-3-ylmagnesium chloride lithium chloride complex) was prepared using isopropylmagnesium chloride lithium chloride complex (0.45 M, 4.4 mL, 1.98 mmol), and 3-iodopyridine (534 mg, 2.60 mmol), and the mixture stirred at room temperature for 1.5 h prior to combining with indigo. Subsequent Boc-mediated dehydration (***General Procedure F***) of the crude product afforded a deep orange residue, which was subjected to flash chromatography (80 g silica, 10% EtOAc/CH_2Cl_2), to afford the *N*-Boc indole **233** (190 mg, 89%) as a bright orange powder, mp 123–124 ˚C. R_f (10% EtOAc/CH_2Cl_2) 0.35. UV-Vis (acetone) λ_{max}/nm (ε, $M^{-1}cm^{-1}$) 338 (2624), 431 (2240), 463 (2057), 500 (1593). ^{1}H NMR (500 MHz, $CDCl_3$) δ 8.90 (s, 1H, H2''), 8.60 (app s, 1H, H4''), 8.26 (d, *J* = 8.5 Hz, 1H, H7), 8.02 (d, *J* = 7.8 Hz, 1H, H6''), 7.60 (d, *J* = 7.9 Hz, 1H, H4), 7.56 (d, *J* = 7.0 Hz, 1H, H4'), 7.52 (d, *J* = 7.8 Hz, 1H, H6'), 7.48 (d, *J* = 8.3 Hz, 1H, H6), 7.40 – 7.35 (m, 2H, H7', H5''), 7.33 (app t, *J* = 7.5 Hz, 1H, H5), 7.28 – 7.23 (m, 1H,

H5'), 1.54 (s, 9H, 3×Boc CH_3). ^{13}C NMR (126 MHz, $CDCl_3$) δ 191.4 (C3'), 160.2 (C7a'), 159.6 (C2'), 151.4 (C2''), 149.9 (Boc C=O), 149.1 (C4''), 138.4 (C6''), 136.9 (C7a), 136.8 (C6'), 129.1 (C3a), 128.7 (C5'), 127.9 (C1''), 127.0 (C6), 126.1 (C2), 125.1 (C4'), 124.4 (C3), 123.9 (C5), 123.1 (C5''), 122.7 (C7'), 122.6 (C3a'), 120.6 (C4), 115.8 (C7), 85.7 (Boc Cq), 28.1 (Boc CH_3). IR (neat) 2978 (w), 2933 (w), 1734 (s), 1559 (m), 1318 (s), 1149 (s), 909 (m), 763 (s), 731 (s), 715 (s) cm^{-1}. HRESI-MS calcd. for $C_{26}H_{22}N_3O_3^+$ 424.1656, found 424.1655.

tert-butyl 3-(1-methyl-imidazol-2-yl)-3'-oxo-1*H*,3'*H*-[2,2'-biindole]-1-carboxylate (235)

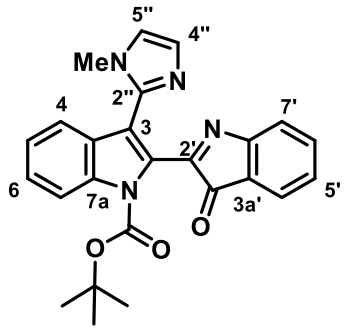

Prepared *via* ***General Procedure E***. The substituted organolithium reagent ((1-methyl-1*H*-imidazol-2-yl)lithium) was prepared using *n*-BuLi (1.95 M, 1.15 mL, 2.24 mmol), and *N*-methylimidazole (217 mg, 2.64 mmol), and the mixture stirred for 1.5 h prior to combining with indigo. Subsequent Boc-mediated dehydration (***General Procedure F***) of the crude product afforded a deep orange residue, which was subjected to flash chromatography (25 g silica, 20% EtOAc/CH_2Cl_2), to afford the *N*-Boc indole **235** (204 mg, 94%) as a deep orange-brown solid, mp 101–102 ˚C. R_f (10% MeCN/$CHCl_3$) 0.46. UV-Vis (acetone) λ_{max}/nm (ε, $M^{-1}cm^{-1}$) 334 (2215), 436 (1841), 465 (1653), 501 (1296). ^1H NMR (500 MHz, $CDCl_3$) δ 8.21 (d, J = 8.5 Hz, 1H, H7), 7.56 – 7.51 (m, 2H, H4, H4'), 7.51 – 7.43 (m, 2H, H6, H6'), 7.37 – 7.28 (m, 2H, H5, H7'), 7.25 (app t, J = 7.5 Hz, 1H, H5'), 7.16 (app s, 1H, H4''), 7.04 (app s, 1H, H5''), 3.68 (s, 3H, -NCH_3), 1.55 (s, 9H, 3×Boc CH_3). ^{13}C NMR (126 MHz, $CDCl_3$) δ 190.9 (C3'), 160.2 (C7a'), 159.7 (C2'), 149.8 (Boc C=O), 140.1 (C2''), 136.9 (C7a), 136.7 (C6'), 129.5 (C3a), 129.4 (C4''), 128.7 (C2), 128.6 (C5'), 127.0 (C6), 125.0 (C4'), 123.9 (C5), 122.6 (C7'), 122.4 (C3a'), 121.9 (C5''), 121.5 (C4), 117.0 (C3), 115.5 (C7), 85.7 (Boc Cq), 34.3 (-NCH_3), 28.1 (Boc CH_3). IR (neat) 2980 (w), 2933 (w), 1734 (s), 1559 (m), 1456 (m), 1369 (m), 1315 (s), 1149 (s), 909 (m), 763 (s), 748 (s), 731 (s) cm^{-1}. HRESI-MS calcd. for $C_{25}H_{23}N_4O_3^+$ 427.1765, found 427.1764.

***tert*-butyl 3'-oxo-3-(thiophen-2-yl)-1*H*,3'*H*-[2,2'-biindole]-1-carboxylate (237)**

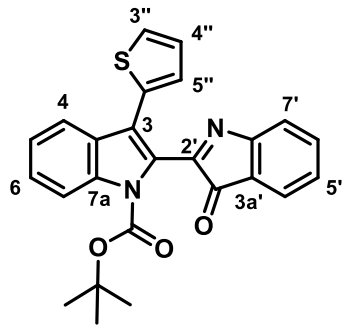

Prepared *via* ***General Procedure C***. The substituted Grignard reagent (thiophen-2-ylmagnesium chloride lithium chloride complex) was prepared using isopropylmagnesium chloride (1.08 M, 1.70 mL, 1.84 mmol), LiCl (106 mg, 2.50 mmol), and 2-iodothiophene (537 mg, 2.56 mmol), and the mixture stirred at room temperature for 1 h prior to combining with indigo. Subsequent Boc-mediated dehydration (***General Procedure F***) of the crude product afforded a deep orange residue, which was subjected to flash chromatography (80 g silica, 10% EtOAc/hexane), to afford the *N*-Boc indole **237** (210 mg, 95%) as bright orange crystals, mp 78–79 ˚C (dec.). X-ray quality crystals were grown by evaporating a saturated 9:1 hexane/chloroform (1 mL) solution to ¼ its original volume, then the mother liquor removed from the precipitated solids and diluted with fresh hexane, and the resulting solution slowly evaporated. R_f (10% EtOAc/hexane) 0.42. UV-Vis (acetone) λ_{max}/nm (ε, $M^{-1}cm^{-1}$) 328 (5623), 436 (1945), 466 (1796), 506 (1540). ^{1}H NMR (400 MHz, $CDCl_3$) δ 8.25 (d, *J* = 8.4 Hz, 1H, H7), 7.94 (d, *J* = 7.9 Hz, 1H, H4), 7.60 (dd, *J* = 3.6, 1.1 Hz, 1H, H5''), 7.59 – 7.52 (m, 2H, H4', H6'), 7.50 – 7.45 (m, 2H, H6, H7'), 7.40 (dd, *J* = 5.1, 1.1 Hz, 1H, H3''), 7.35 (app t, *J* = 7.2 Hz, 1H, H5), 7.28 (app t, *J* = 6.7 Hz, 1H, H5'), 7.14 (dd, *J* = 5.1, 3.6 Hz, 1H, H4''), 1.52 (s, 9H, 3×Boc CH_3). ^{13}C NMR (101 MHz, $CDCl_3$) δ 191.5 (C3'), 160.4 (C7a'), 159.6 (C2'), 149.9 (Boc C=O), 136.9 (C7a), 136.8 (C6'), 132.6 (C1''), 129.6 (C5''), 129.2 (C3a), 128.6 (C5'), 127.4 (C4''), 126.9 (C6), 126.8 (C3''), 125.5 (C2), 125.1 (C4'), 123.7 (C5), 122.9 (C3a'), 122.7 (C7'), 121.4 (C4), 121.1 (C3), 115.7 (C7), 85.6 (Boc Cq), 28.1 (Boc CH_3). IR (neat) 2979 (w), 2930 (w), 2373 (w), 1734 (s), 1558 (m), 1319 (s), 1148 (s), 841 (m), 761 (m), 747 (s), 700 (m) cm^{-1}. HRESI-MS calcd. for $C_{25}H_{21}N_2O_3S^+$ 429.1267, found 429.1267.

***tert*-butyl 3-(benzofuran-2-yl)-3'-oxo-1*H*,3'*H*-[2,2'-biindole]-1-carboxylate (239)**

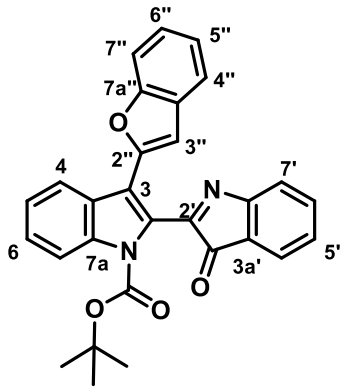

Prepared *via* ***General Procedure E***. The substituted organolithium reagent (benzofuran-2-yllithium) was prepared using *n*-BuLi (1.95 M, 1.2 mL, 2.34 mmol), and benzofuran (299 mg, 2.53 mmol), and the mixture stirred for 1 h prior to combining with indigo. Subsequent Boc-mediated dehydration (***General Procedure F***) of the crude product afforded a deep orange residue, which was fractionated on silica (80 g, using 10% EtOAc/hexane as eluent), and the resulting deep red-orange residue subjected to flash chromatography (40 g silica, 60% CH_2Cl_2/pet spirit), to afford the *N*-Boc indole **239** (200 mg, 85%) as a deep orange powder, mp 96–98 ˚C. R_f (10% EtOAc/hexane) 0.42. UV-Vis (acetone) λ_{max}/nm (ε, $M^{-1}cm^{-1}$) 332 (12256), 385 (3234), 436 (1841), 435 (2152), 510 (1797). ^{1}H NMR (500 MHz, $CDCl_3$) δ 8.29 – 8.23 (m, 2H, H4, H7), 7.64 – 7.59 (m, 2H, H4', H4''), 7.59 – 7.54 (m, 3H, H6', H7', H3''), 7.50 (app t, *J* = 7.7 Hz, 1H, H6), 7.45 (d, *J* = 8.1 Hz, 1H, H7''), 7.41 (app t, *J* = 7.6 Hz, 1H, H5), 7.33 – 7.25 (m, 2H, H5', H6''), 7.24 – 7.19 (m, 1H, H5''), 1.53 (s, 9H, 3×Boc CH_3). ^{13}C NMR (126 MHz, $CDCl_3$) δ 191.2 (C3'), 160.3 (C7a'), 159.8 (C2'), 155.1 (C7a''), 149.8 (Boc C=O), 149.6 (C2''), 137.0 (C7a), 136.8 (C6'), 128.8 (C5'), 128.7 (C3a''), 127.7 (C3a), 127.0 (C6), 125.8 (C3), 125.2 (C4'), 124.8 (C6''), 124.0 (C5), 123.0 (C5''), 122.8 (C3a'), 122.70 (C4), 122.66 (C7'), 121.4 (C4''), 117.2 (C2), 115.6 (C7), 111.2 (C7''), 108.1 (C3''), 85.8 (Boc Cq), 28.1 (Boc CH_3). IR (neat) 2977 (w), 2932 (w), 1734 (s), 1717 (m), 1559 (s), 1507 (m), 1317 (m), 1148 (s), 761 (m), 747 (s) cm^{-1}. HRESI-MS calcd. for $C_{29}H_{22}N_2O_4Na^+$ 485.1477, found 485.1479.

tert-butyl 1''-methyl-3-oxo-1'*H*,1''*H*,3*H*-[2,2':3',5''-terindole]-1'-carboxylate (245)

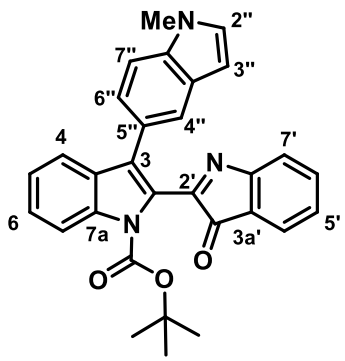

Prepared *via* ***General Procedure C***. The substituted Grignard reagent ((1-methyl-1*H*-indol-5-yl)magnesium chloride lithium chloride complex) was prepared using isopropylmagnesium chloride lithium chloride complex (0.512 M, 3.90 mL, 2.00 mmol), and 5-iodo-*N*-methylindole **243** (651 mg, 2.53 mmol), and the mixture stirred at 0 ˚C for 2 h prior to combining with indigo. Subsequent Boc-mediated dehydration (***General Procedure F***) of the crude product afforded a deep red-orange residue, which was subjected to flash chromatography (100 g silica, 10%

EtOAc/hexane), to afford the crude *N*-Boc terindole **245** (186 mg, 61% corrected NMR yield) as a bright orange amorphous solid, isolated alongside an unknown impurity which proved irresolute by all trialled separation techniques, including recrystallisation, PTLC separation and flash chromatographic separation. R_f (10% EtOAc/pet spirit) 0.28. ^{1}H NMR (500 MHz, $CDCl_3$) δ 8.26 (d, *J* = 8.4 Hz, 1H, H7), 7.93 (d, *J* = 1.0 Hz, 1H, H4''), 7.68 (d, *J* = 7.8 Hz, 1H, H4), 7.52 (d, *J* = 7.1 Hz, 1H, H4'), 7.49 – 7.42 (m, 3H, H6, H6', H6''), 7.37 – 7.32 (m, 2H, H7', H7''), 7.28 (app t, *J* = 7.1 Hz, 1H, H5), 7.21 (dd, *J* = 7.3, 0.8 Hz, 1H, H5'), 7.06 (d, *J* = 3.1 Hz, 1H, H2''), 6.52 (d, *J* = 2.3 Hz, 1H, H3''), 3.80 (s, 3H, N''CH_3), 1.52 (s, 9H, 3×Boc CH_3). ^{13}C NMR (126 MHz, $CDCl_3$) δ 192.0 (C3'), 160.5 (C7a'), 160.4 (C2'), 150.1 (Boc C=O), 136.9 (C7a or C7a''), 136.6 (C6'), 136.5 (C7a or C7a''), 130.2 (C3a), 129.7 (C2), 129.4 (C2''), 129.0 (C3), 128.4 (C5'), 128.1 (C3a''), 126.4 (C6), 124.9 (C4' or C6''), 124.8 (C4' or C6''), 123.5 (C4''), 123.2 (C5), 122.6 (C5''), 122.5 (C3a'), 122.4 (C7'), 121.5 (C4), 115.6 (C7), 109.0 (C7''), 101.6 (C3''), 84.9 (Boc Cq), 32.9 (N''CH_3), 27.3 (Boc CH_3). HRESI-MS calcd. for $C_{30}H_{26}N_3O_3^+$ 476.1969, found 476.1968.

7.4.7 ***General Procedure G*** for Boc Deprotection:

To a solution of the *tert*-butoxycarbonyl protected indole (*ca*. 0.1 mmol) in CH_2Cl_2 (0.1 M) was added neat trifluoroacetic acid (1 mL per 0.1 mmol of *N*-Boc indole). The resulting solution was stirred at room temperature for the indicated time, then diluted to *ca*. 20 mL with CH_2Cl_2, and transferred to a separatory funnel. The organic phase was repeatedly washed with sat. $NaHCO_3$ solution until foaming ceased (typically 2-3×20 mL), the organic layer dried (Na_2SO_4), and the solvent removed.

3-isopropyl-1*H*,3'*H*-[2,2'-biindol]-3'-one (209)

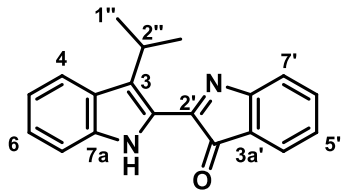

Prepared *via* ***General Procedure G***, using 48.4 mg (0.124 mmol) of **210**, and a 1 h reaction time. The resulting dark purple residue was subjected to flash chromatography (20 g silica, 10% EtOAc/hexane), and triturated with hot hexane to afford the desired indole **209** (33.0 mg, 92%) as an intense, black-purple powder, mp 168–170 ˚C (dec.). R_f (10% EtOAc/hexane) 0.56. UV-Vis (acetone) λ_{max}/nm (ε, $M^{-1}cm^{-1}$) 302 (7209), 552 (1594). ^{1}H NMR (400 MHz, $CDCl_3$) δ 10.11 (s, 1H, NH), 7.92 (d, *J* = 8.3 Hz, 1H, H4), 7.57 – 7.49 (m, 2H, H4', H6'), 7.42 (d, *J* = 8.3 Hz, 1H, H7), 7.37 (d, *J* = 7.5 Hz, 1H, H7'), 7.32 – 7.27 (m, 1H, H6), 7.18 (app t, *J* = 7.1 Hz, 1H, H5'), 7.11 – 7.05 (m, 1H, H5), 4.55 (hept, *J* = 7.0 Hz, 1H, H2''), 1.54 (d, *J* = 7.1 Hz, 6H, H1'', H3''). ^{13}C NMR (101 MHz, $CDCl_3$) δ 197.1 (C3'), 162.7 (C7a'), 154.6 (C2'), 138.8 (C7a), 137.5

(C6'), 135.0 (C3), 127.3 (C5'), 126.6 (C3a), 125.7 (C6), 125.1 (C4'), 123.8 (C2), 122.6 (C4), 121.9 (C7'), 121.7 (C3a'), 119.8 (C5), 112.3 (C7), 26.5 (C2''), 22.6 (C1'', C3''). IR (neat) 3378 (m), 1709 (s), 1540 (s), 1451 (m), 1329 (s), 1240 (m), 1168 (s), 875 (m), 761 (s), 741 (s), 672 (s) cm^{-1}. HRESI-MS calcd. for $C_{19}H_{17}N_2O^+$ 289.1341, found 289.1353.

3-phenyl-1*H*,3'*H*-[2,2'-biindol]-3'-one (214)

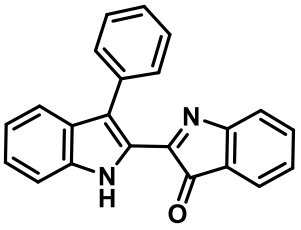

Prepared *via* ***General Procedure G***, using 51.1 mg (0.121 mmol) of **211**, and a 2 h reaction time. The resulting dark purple residue was subjected to flash chromatography (20 g silica, 10% EtOAc/pet spirit), and removal of the solvent gave the desired indole **214** (31.6 mg, 81%) as an intense, black-purple powder. Spectral and physical characteristics were identical to those reported above.

3-butyl-1*H*,3'*H*-[2,2'-biindol]-3'-one (250)

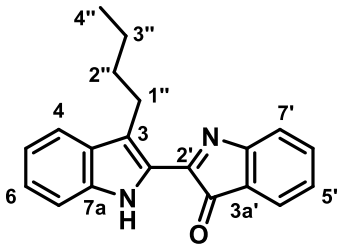

Prepared *via* ***General Procedure G***, using 43.6 mg (0.108 mmol) of **215**, and a 1.5 h reaction time. The resulting dark purple residue was subjected to flash chromatography (20 g silica, 10% EtOAc/hexane), and removal of the solvent afforded the desired indole **250** (29.8 mg, 91%) as an intense, black-purple powder, mp 131–132 ˚C. R_f (10% EtOAc/hexane) 0.45. UV-Vis (acetone) λ_{max}/nm (ε, $M^{-1}cm^{-1}$) 327 (2462), 542 (1654). ^{1}H NMR (400 MHz, $CDCl_3$) δ 10.00 (s, 1H, NH), 7.71 (dd, *J* = 8.2, 1.0 Hz, 1H, H4), 7.58 – 7.49 (m, 2H, H4', H6'), 7.41 (d, *J* = 8.3 Hz, 1H, H7), 7.36 (d, *J* = 7.6 Hz, 1H, H7'), 7.33 – 7.28 (m, 1H, H6), 7.22 – 7.13 (m, 1H, H5'), 7.12 (ddd, *J* = 8.0, 6.9, 1.0 Hz, 1H, H5), 3.37 (t, *J* = 7.7 Hz, 2H, H1''), 1.80 – 1.68 (m, 2H, H2''), 1.47 (h, *J* = 7.4 Hz, 2H, H3''), 0.97 (t, *J* = 7.4 Hz, 3H, H4''). ^{13}C NMR (101 MHz, $CDCl_3$) δ 197.0 (C3'), 163.0 (C7a'), 154.6 (C2'), 138.4 (C7a), 137.6 (C6'), 129.7 (C3), 128.4 (C3a), 127.3 (C5'), 126.2 (C6), 125.1 (C4'), 125.0 (C2), 122.1 (C3a'), 122.0 (C4), 120.9 (C7'), 120.3 (C5), 112.0 (C7), 32.7 (C2''), 25.4 (C1''), 23.0 (C3''), 14.2 (C4''). IR (neat) 3382 (m), 2955 (w), 2924 (w), 1715 (s), 1551 (s), 1449 (m), 1340 (w), 1237 (w), 1170 (m), 877 (w), 761 (m), 740 (m) cm^{-1}. HRESI-MS calcd. for $C_{20}H_{19}N_2O^+$ 303.1497, found 303.1508.

3-benzyl-1*H*,3'*H*-[2,2'-biindol]-3'-one (251)

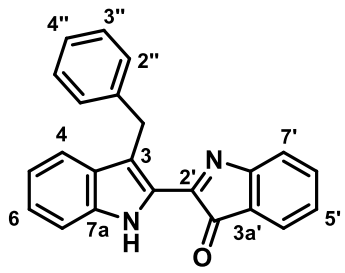

Prepared *via* ***General Procedure G***, using 65.3 mg (0.150 mmol) of **219**, and a 1.5 h reaction time. The resulting dark purple residue was subjected to flash chromatography (20 g silica, 10% EtOAc/hexane), and triturated with hexane to give the desired indole **251** (35.7 mg, 71%) as an intense, black-purple powder, mp 139–140 ˚C (dec.). R_f (10% EtOAc/hexane) 0.36. UV-Vis (acetone) λ_{max}/nm (ε, $M^{-1}cm^{-1}$) 327 (5752), 355 (4608), 537 (1655). ^{1}H NMR (500 MHz, $CDCl_3$) δ 10.09 (s, 1H), 7.59 (d, *J* = 8.2 Hz, 1H, H4), 7.54 (d, *J* = 7.0 Hz, 1H, H4'), 7.51 (td, *J* = 7.6, 1.3 Hz, 1H, H6'), 7.41 (d, *J* = 8.4 Hz, 1H, H7), 7.38 (d, *J* = 7.0 Hz, 2H, H2", H6"), 7.35 (d, *J* = 7.5 Hz, 1H, H7'), 7.29 (ddd, *J* = 8.2, 6.9, 1.1 Hz, 1H, H6), 7.23 (dd, *J* = 8.3, 6.9 Hz, 2H, H3", H5"), 7.18 (td, *J* = 7.5, 0.9 Hz, 1H, H5'), 7.16 – 7.12 (m, 1H, H4"), 7.08 (ddd, *J* = 8.0, 6.9, 1.0 Hz, 1H, H5), 4.81 (s, 2H, Ar-C$\underline{H_2}$Ph). ^{13}C NMR (126 MHz, $CDCl_3$) δ 196.7 (C3'), 162.6 (C7a'), 154.4 (C2'), 141.1 (C1"), 138.3 (C7a), 137.5 (C6'), 128.8 (C2"), 128.24 (C3"), 128.17 (C3a), 127.4 (C5'), 126.3 (C3), 126.1 (C6), 125.8 (C4"), 125.2 (C2), 125.1 (C4'), 122.0 (C4), 121.9 (C3a'), 121.1 (C7'), 120.5 (C5), 112.0 (C7), 31.3 (Ar-$\underline{C}H_2$Ph). IR (neat) 3421 (w), 2919 (w), 1734 (s), 1717 (s) 1558 (s), 1507 (s), 1457 (m), 1339 (w), 1237 (w), 1167 (m), 745 (s) cm^{-1}. HRESI-MS calcd. for $C_{23}H_{17}N_2O^+$ 337.1341, found 337.1326.

3-(4-methoxyphenyl)-1*H*,3'*H*-[2,2'-biindol]-3'-one (252)

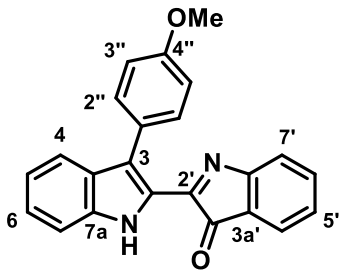

Prepared *via* ***General Procedure G***, using 31.8 mg (0.070 mmol) of **222**, and a 1.5 h reaction time. The resulting dark purple residue was subjected to flash chromatography (20 g silica, 10% EtOAc/hexane), and removal of the solvent gave the desired indole **252** (23.6 mg, 95%) as intense, black-purple crystals, mp 227–228 ˚C. R_f (10% EtOAc/hexane) 0.33. UV-Vis (acetone) λ_{max}/nm (ε, $M^{-1}cm^{-1}$) 327 (3173), 337 (3174), 390 (1478), 541 (1016). ^{1}H NMR (500 MHz, $CDCl_3$) δ 10.26 (s, 1H, NH), 7.70 – 7.65 (m, 3H, H4, H2", H6"), 7.52 (d, *J* = 7.1 Hz, 1H, H4'), 7.49 – 7.45 (m, 2H, H7, H6'), 7.35 (ddd, *J* = 8.2, 6.9, 1.0 Hz, 1H, H6), 7.24 (d, *J* = 7.6 Hz, 1H, H7'), 7.19 – 7.12 (m, 2H, H5, H5'), 7.04 (d, *J* = 8.8 Hz, 2H, H3", H5"), 3.91 (s, 3H, -OCH_3). ^{13}C NMR (126 MHz, $CDCl_3$) δ 196.6 (C3'), 162.4 (C7a'), 159.1 (C2'), 154.1 (C4"), 138.3 (C7a), 137.5 (C6'), 132.3 (C2", C6"), 128.2 (C3), 127.6 (C5'), 126.8 (C3a), 126.4 (C6), 126.1 (C2), 125.2 (C4'), 124.3 (C1"), 122.4

(C4), 122.2 (C3a'), 121.8 (C7'), 121.2 (C5), 113.6 (C3", C5"), 112.0 (C7), 55.4 (-OCH_3). IR (neat) 3374 (w), 3349 (w), 1710 (s), 1539 (s), 1444 (s), 1320 (m), 1251 (m), 1166 (s), 877 (m), 832 (s), 758 (m), 744 (s), 691 (s) cm^{-1}. HRESI-MS calcd. for $C_{23}H_{17}N_2O_2^+$ 353.1290, found 353.1280.

3-(2-methoxyphenyl)-1*H*,3'*H*-[2,2'-biindol]-3'-one (253)

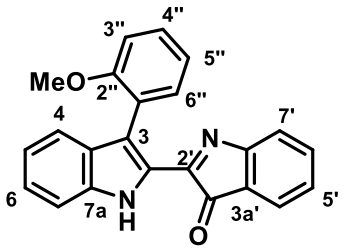

Prepared *via* ***General Procedure G***, using 70.9 mg (0.157 mmol) of **224**, and a 1.5 h reaction time. The resulting dark purple residue was subjected to flash chromatography (20 g silica, 10% EtOAc/hexane), and removal of the solvent gave the desired indole **253** (48.2 mg, 87%) as an intense, black-purple solid, mp 168–170 ˚C (dec.). R_f (10% EtOAc/hexane) 0.56. UV-Vis (acetone) λ_{max}/nm (ε, $M^{-1}cm^{-1}$) 328 (5039), 535 (2864). ^{1}H NMR (500 MHz, $CDCl_3$) δ 10.09 (s, 1H, NH), 7.56 (d, *J* = 8.2 Hz, 1H, H4), 7.51 – 7.48 (m, 2H, H4', H6"), 7.48 – 7.41 (m, 3H, H6, H7, H6'), 7.36 – 7.31 (m, 1H, H4"), 7.21 (d, *J* = 7.6 Hz, 1H, H7'), 7.18 – 7.08 (m, 3H, H5, H5', H5"), 7.04 (d, *J* = 7.3 Hz, 1H, H3"), 3.72 (s, 3H, -OCH_3). ^{13}C NMR (126 MHz, $CDCl_3$) δ 195.1 (C3'), 162.1 (C7a'), 157.6 (C2'), 154.9 (C2"), 138.1 (C7a), 137.3 (C6'), 132.1 (C6"), 129.1 (C4"), 128.5 (C3), 127.6 (C5'), 126.1 (C6), 125.6 (C3a), 125.0 (C4'), 123.4 (C2), 122.4 (C3a'), 122.1 (C4), 121.9 (C1"), 121.8 (C7'), 121.0 (C5"), 120.6 (C5), 111.9 (C7), 111.3 (C3"), 55.6 (-OCH_3). IR (neat) 3402 (m), 1718 (s), 1549 (s), 1451 (m), 1326 (s), 1257 (m), 1239 (s), 1026 (m), 875 (m), 793 (m), 745 (s), 691 (s) cm^{-1}. HRESI-MS calcd. for $C_{23}H_{17}N_2O_2^+$ 353.1290, found 353.1298.

3-(2,4-dimethoxyphenyl)-1*H*,3'*H*-[2,2'-biindol]-3'-one (254)

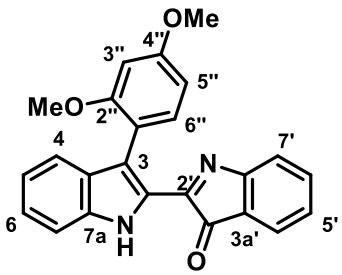

Prepared *via* ***General Procedure G***, using 29.1 mg (0.0603 mmol) of **228** in neat TFA (2 mL), and the mixture allowed to stir overnight. The resulting dark purple residue was triturated with hexane to give the desired indole **254** (18.9 mg, 82%) as an intense, black-purple solid, mp 119–120 ˚C. R_f (20% EtOAc/hexane) 0.25. UV-Vis (acetone) λ_{max}/nm (ε, $M^{-1}cm^{-1}$) 326 (4530), 546 (1547). ^{1}H NMR (400 MHz, $CDCl_3$) δ 10.15 (s, 1H, NH), 7.57 (d, *J* = 8.1 Hz, 1H, H4), 7.50 (d, *J* = 7.2 Hz, 1H, H4'), 7.48 – 7.40 (m, 3H, H7, H6', H6"), 7.32 (app t, *J* = 7.6 Hz, 1H, H6), 7.22 (d, *J* = 7.6 Hz, 1H, H7'), 7.17 – 7.08 (m, 2H, H5, H5'), 6.67 – 6.60 (m, 2H, H3", H5"), 3.91 (s, 3H, C4"-OCH_3), 3.70 (s, 3H, C2"-OCH_3). ^{13}C NMR (101 MHz, $CDCl_3$) δ 195.2 (C3'), 162.2 (C4"), 160.8 (C7a'), 158.6 (C2'), 154.8

(C2''), 138.2 (C7a), 137.2 (C6'), 132.5 (C6''), 128.6 (C3a), 127.4 (C5'), 126.1 (C6), 125.5 (C3), 125.0 (C4'), 122.4 (C2), 122.1 (C3a'), 122.0 (C4), 121.9 (C7'), 120.8 (C5), 116.2 (C1''), 111.9 (C7), 104.4 (C5''), 99.3 (C3''), 55.6 (C4''-OCH_3), 55.5 (C2''-OCH_3). IR (neat) 3414 (w), 2928 (m), 2360 (w), 1718 (s), 1612 (s), 1549 (s), 1451 (s), 1327 (m), 1301 (m), 1262 (m), 1209 (s), 1159 (s), 1032 (m), 876 (m), 746 (s), 692 (w) cm^{-1}. HRESI-MS calcd. for $C_{24}H_{18}N_2O_3Na^+$ 405.1215, found 405.1213.

3-(2-chlorophenyl)-1*H*,3'*H*-[2,2'-biindol]-3'-one (255)

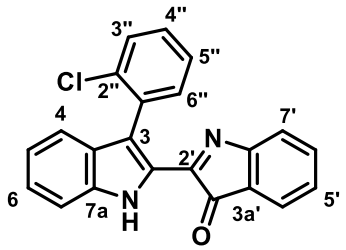

Prepared *via* ***General Procedure G***, using 41.4 mg (0.0906 mmol) of **232**, and the mixture allowed to stir overnight. The resulting deep burgundy residue was subjected to flash chromatography (20 g silica, 10% EtOAc/hexane), and triturated with hexane to give the desired indole (26.4 mg, 82%) as an intense, black-purple solid, mp 203–204 ˚C. R_f (10% EtOAc/hexane) 0.44. UV-Vis (acetone) λ_{max}/nm (ε, $M^{-1}cm^{-1}$) 328 (3113), 535 (2301). ^{1}H NMR (500 MHz, $CDCl_3$) δ 10.08 (s, 1H, NH), 7.57 – 7.54 (m, 1H, H6''), 7.52 – 7.44 (m, 4H, H4, H7, H4', H6'), 7.43 (dd, *J* = 8.1, 0.8 Hz, 1H, H3''), 7.41 – 7.34 (m, 3H, H6, H4'', H5''), 7.21 (d, *J* = 7.6 Hz, 1H, H7'), 7.20 – 7.13 (m, 1H, H5'), 7.17 – 7.11 (m, 1H, H5). ^{13}C NMR (126 MHz, $CDCl_3$) δ 194.8 (C3'), 161.8 (C7a'), 154.7 (C2'), 137.8 (C7a), 137.3 (C6'), 134.8 (C2''), 133.6 (C1''), 132.6 (C6''), 129.8 (C3''), 129.0 (C4''), 128.4 (C3), 127.9 (C5'), 126.6 (C5''), 126.3 (C6), 125.7 (C3a), 125.1 (C4'), 124.4 (C2), 122.6 (C3a'), 122.4 (C4), 121.5 (C7'), 121.3 (C5), 112.0 (C7). IR (neat) 3407 (w), 2924 (m), 1718 (m), 1554 (s), 1451 (m), 1327 (m), 1163 (w), 877 (m), 747 (m), 690 (w) cm^{-1}. HRESI-MS calcd. for $C_{22}H_{14}{}^{35}ClN_2O^+$ 357.0789, found 357.0795.

3-(4-fluorophenyl)-1*H*,3'*H*-[2,2'-biindol]-3'-one (256)

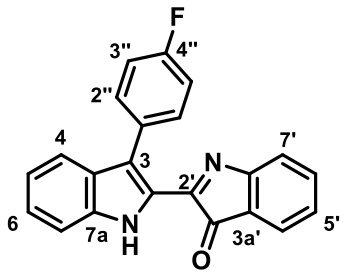

Prepared *via* ***General Procedure G***, using 33.7 mg (0.0765 mmol) of **231**, and a 2 h reaction time. The resulting dark purple residue was subjected to flash chromatography (20 g silica, 10% EtOAc/hexane), and triturated with hexane to afford the desired indole **256** (23.2 mg, 89%) as an intense, black-purple solid, mp 244–246 ˚C. R_f (10% EtOAc/hexane) 0.20. UV-Vis (acetone) λ_{max}/nm (ε, $M^{-1}cm^{-1}$) 326 (3668), 534 (2307). ^{1}H NMR (400 MHz, $CDCl_3$,^{19}F-decoupled) δ 10.27 (s, 1H, NH), 7.68 (d, *J* = 8.7 Hz, 2H, H2'', H6''), 7.64 (d, *J* = 8.2 Hz, 1H, H4), 7.53 (d, *J* = 7.1 Hz, 1H, H4'), 7.51 – 7.45 (m, 2H, H7, H6'), 7.36 (app

t, J = 7.7 Hz, 1H, H6), 7.23 (d, J = 7.6 Hz, 1H, H7'), 7.21 – 7.12 (m, 4H, H5, H5', H3'', H5''). ^{13}C NMR (101 MHz, $CDCl_3$) δ 196.2 (C3'), 162.3 (d, $^1J_{C\text{-}F}$ = 246.6 Hz, C4''), 162.0 (C7a'), 153.9 (C2'), 138.0 (C7a), 137.4 (C6'), 132.6 (d, $^3J_{C\text{-}F}$ = 8.0 Hz, C2''), 129.6 (d, $^4J_{C\text{-}F}$ = 3.3 Hz, C1''), 128.0 (C3a), 127.7 (C5'), 126.3 (C6), 125.4 (C3), 125.1 (C4'), 124.4 (C2), 122.3 (C4), 122.0 (C3a'), 121.3 (C7'), 121.2 (C5), 115.0 (d, $^2J_{C\text{-}F}$ = 21.4 Hz, C3''), 112.0 (C7). ^{19}F NMR (377 MHz, $CDCl_3$, ^{1}H-decoupled) δ -114.8. IR (neat) 3367 (w), 2998 (m), 1734 (m), 1714 (m), 1559 (s), 1507 (s), 1340 (m), 1255 (m), 879 (m), 834 (m), 746 (m), 692 (m) cm^{-1}. HRESI-MS calcd. for $C_{22}H_{14}N_2OF^+$ 341.1090, found 341.1098.

3-(thiophen-2-yl)-1*H*,3'*H*-[2,2'-biindol]-3'-one (257)

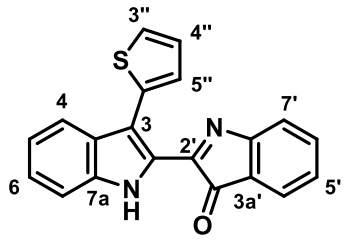

Prepared *via* ***General Procedure G***, using 49.0 mg (0.114 mmol) of **237**, and a 1.5 h reaction time. The resulting dark purple residue was subjected to flash chromatography (20 g silica, 10% EtOAc/hexane), and removal of the solvent gave the desired indole **257** (36.0 mg, 96%) as an intense, black-purple powder, mp >300 ˚C. R_f (10% EtOAc/hexane) 0.42. UV-Vis (acetone) λ_{max}/nm (ε, M^{-1}cm^{-1}) 328 (4194), 545 (1342). ^{1}H NMR (500 MHz, $CDCl_3$) δ 10.36 (s, 1H, NH), 7.97 (dd, J = 8.2, 0.9 Hz, 1H, H4), 7.76 (dd, J = 3.6, 1.2 Hz, 1H, H5''), 7.55 (ddd, J = 7.1, 1.4, 0.6 Hz, 1H, H4'), 7.53 – 7.46 (m, 3H, H7, H6', H3''), 7.37 (ddd, J = 8.1, 6.9, 1.1 Hz, 1H, H6), 7.33 (d, J = 7.6 Hz, 1H, H7'), 7.23 (dd, J = 5.1, 3.6 Hz, 1H, H4''), 7.22 – 7.17 (m, 2H, H5, H5'). ^{13}C NMR (126 MHz, $CDCl_3$) δ 196.4 (C3'), 162.1 (C7a'), 153.5 (C2'), 139.2 (C2''), 137.9 (C7a), 137.5 (C6'), 134.7 (C3), 129.5 (C5''), 127.8 (C3a), 127.7 (C4''), 127.1 (C5'), 126.4 (C3''), 126.2 (C6), 125.2 (C4'), 125.0 (C2), 122.4 (C7'), 122.0 (C4), 121.4 (C5), 119.2 (C3a'), 111.9 (C7). IR (neat) 3366 (w), 1734 (s), 1653 (s), 1558 (s), 1507 (s), 1340 (w), 1250 (w), 876 (w), 758 (w), 745 (m), 691 (m) cm^{-1}. HRESI-MS calcd. for $C_{20}H_{13}N_2OS^+$ 329.0749, found 329.0750.

3-(pyridin-3-yl)-1*H*,3'*H*-[2,2'-biindol]-3'-one (258)

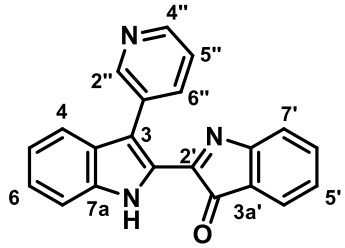

Prepared *via* ***General Procedure G***, using 36.8 mg (0.0869 mmol) of **233**, and the mixture allowed to stir overnight. The resulting deep burgundy residue was subjected to flash chromatography (20 g silica, 10% EtOAc/CH_2Cl_2), and triturated with hexane to give the desired indole **258** (26.4 mg, 94%) as an intense, black-purple powder, mp 276–277 ˚C (dec.). R_f (10% EtOAc/CH_2Cl_2) 0.46. UV-Vis (acetone) λ_{max}/nm (ε, M^{-1}cm^{-1}) 326 (5139), 530 (3061). ^{1}H

NMR (400 MHz, $CDCl_3$) δ 10.40 (s, 1H, NH), 8.95 (app s, 1H, H2''), 8.65 (app s, 1H, H4''), 8.04 (d, *J* = 7.8 Hz, 1H, H6''), 7.62 (d, *J* = 8.2 Hz, 1H, H4), 7.53 – 7.41 (m, 4H, H7, H4', H6', H5''), 7.36 (ddd, *J* = 8.2, 7.0, 0.9 Hz, 1H, H6), 7.23 – 7.12 (m, 3H, H5, H5', H7'). ^{13}C NMR (101 MHz, $CDCl_3$) δ 195.9 (C3'), 161.8 (C7a'), 153.9 (C2'), 151.6 (br, C2''), 148.2 (br, C4''), 138.3 (br, C6''), 138.1 (C7a), 137.6 (C6'), 127.94 (C5'), 127.92 (C3a), 127.7 (C3), 126.5 (C6), 125.3 (C4'), 125.0 (C1''), 123.1 (br, C5''), 122.5 (C5), 122.2 (C2), 122.0 (C3a'), 121.8 (C4), 120.9 (C7'), 112.3 (C7). IR (neat) 3393 (w), 1718 (s), 1556 (s), 1507 (w), 1452 (m), 1340 (w), 1261 (w), 1167 (w), 877 (m), 759 (w), 745 (m), 732 (m), 714 (w), 688 (m) cm^{-1}. HRESI-MS calcd. for $C_{21}H_{14}N_3O^+$ 324.1137, found 324.1142.

7.5 Biological testing

7.5.1. General considerations

All biological assays were performed by collaborators at Griffith University (Prof. Vicky Avery and Dr. Leonardo Lucantoni). The antiplasmodial activity of the experimental compounds was assessed against *Plasmodium falciparum* 3D7 (chloroquine sensitive) and Dd2 (drug resistant) parasite strains. Preliminary cytotoxicity assessment was carried out using Human Embryonic Kidney (HEK293) cells. The compounds were tested in a 22-point concentration-response range of 80 μM – 0.01 nM (160 μM – 0.02 nM for Compound **155**). Artesunate, dihydroartemisinin (DHA), chloroquine, puromycin and pyrimethamine were used as reference compounds / drugs, and were tested in both experiments using 22-point concentration-response range of 40 μM – 0.01 nM (10 μM – 0.003 nM for DHA and artesunate). 0.4% DMSO and 5 μM puromycin were used as negative and positive in-plate controls, respectively. Raw data from each assay was normalized using the in-plate positive and negative controls to obtain normalized % inhibition data, which was then used to calculate IC_{50} values, through a 4-parameter logistic curve fitting in Prism v 6.0 (GraphPad). All experiments were carried out in two biological replicates, each consisting of two technical repeats.

7.5.2. Antimalarial assay

Plasmodium falciparum 3D7 (chloroquine sensitive) and Dd2 (drug resistant) parasite strains were maintained in RPMI 1640 supplemented with 25 mM HEPES, 5% AB human male serum, 2.5 mg/ml Albumax II, and 0.37 mM hypoxanthine. Parasites were subjected to two rounds of sorbitol synchronization before undergoing compound treatment. Ring stage parasites at 2% parasitemia and 0.3% hematocrit were exposed to the experimental

compounds in 384-wells imaging CellCarrier microplates (PerkinElmer), as previously described.[191] Plates were incubated for 72 h at 37 °C, 90% N_2, 5% CO_2, 5% O_2, then the parasites were stained with 2-(4-amidinophenyl)-1*H*-indole-6-carboxamidine (DAPI) in permeabilization buffer (PBS, 5mM EDTA, 0.5ug/ml DAPI, 0.01% Triton X-100, and 0.001% saponin), and imaged with an Opera QEHS micro-plate confocal imaging system (PerkinElmer) using 20x water-immersion objective and 405 nm excitation, 450/50 nm emission filters. Images were analysed using a custom Acapella spot detection script to quantify DAPI-stained parasites in each well, as previously described.[191]

7.5.3. Cytotoxicity Assay

Human Embryonic Kidney cells (HEK293) were maintained in DMEM medium supplemented with 10% FBS. Cells were seeded at 2,000 cells/well in TC-treated 384-wells clear-bottom plates (Greiner), 24 h before the addition of compounds. Compounds were added to the plates as described above, then the plates were incubated for 72 h at 37 °C, 5% CO_2. At the end of the incubation, the media was removed from the wells and replaced with an equal volume of 44 µM resazurin. After an additional 5-6 hours incubation at standard conditions, the total fluorescence (excitation/emission: 530 nm / 595 nm) was measured using an Envision plate reader (PerkinElmer).

7.6 X-ray crystallographic data

7.6.1. Crystallographic data for compound **133**:

Crystal data

Compound **133**. $C_{34}H_{22}N_2O_2$, M = 490.56, T = 150 K, monoclinic, space group $P2_1/c$, Z = 4, a = 19.0715 (5), b = 14.3956 (5), c = 8.8496 (2), β = 98.221 (2) ˚, V = 2404.65 (12) Å^3, D_x = 1.355 Mg m^{-3}, Cu$K\alpha$ radiation, λ = 1.54184 Å, 35145 reflections measured (θ = 5–72˚), merged to 4690 unique data, R = 0.054 [for 4185 data with $I > 2\sigma(I)$], R_w = 0.062 [all data], S = 1.07.

Structure determination of compound 133

Images were measured on an Agilent SuperNova diffractometer (Cu $K\alpha$ radiation, mirror monochromator, λ = 1.54184 Å) and data extracted using the CrysAlis PRO package.[192] Structure solution was by direct methods (SIR92).[193] The structure was refined using the CRYSTALS program package.[194]

7.6.2. Crystallographic data for compounds **134** and **135**:

Crystal data

Compounds **134** and **135**. 0.688×($C_{36}H_{27}BrN_2O_4$)·0.312×($C_{36}H_{26}N_2O_4$)·0.172×(H_2O), M = 608.92, T = 150 K, Triclinic, space group $P1$, Z = 2, a = 9.4687 (3), b = 11.7407 (3), c = 13.5610 (3), α = 91.4143 (19) ˚, β = 100.6415 (19) ˚, γ = 109.760 (3) ˚, V = 1388.20 (7) Å^3, D_x = 1.457 Mg m^{-3}, Cu$K\alpha$ radiation, λ = 1.54184 Å, 22229 reflections measured (θ = 3–74 ˚), merged to 5600 unique data, R = 0.022 [for 5462 data with $I > 2\sigma(I)$], R_w = 0.045 [all data], S = 1.12.

Structure determination of compounds 133 and 135

Images were measured on an Agilent SuperNova diffractometer (Cu $K\alpha$ radiation, mirror monochromator, λ = 1.54184 Å) and data extracted using the CrysAlis PRO package.[192] Structure solution was by direct methods (SIR92).[193] The structure was refined using the CRYSTALS program package.[194]

7.6.3. Crystallographic data for compound **153**:

Crystal data

Compound **153**. $C_{19}H_{14}N_2O_3$, M = 318.33, T = 150 K, orthorhombic, space group $Pccn$, Z = 8, a = 10.8798(1), b = 18.4104(1), c = 14.5081(1) Å, V = 2905.99 (4) Å^3, D_x = 1.455 Mg m^{-3}, Cu$K\alpha$ radiation, λ = 1.54184 Å, 54126 reflections measured (θ = 5–72˚), merged to 2881 unique data, R = 0.030 [for 2749 data with $I > 2\sigma(I)$], R_w= 0.075 [all data], S = 1.00

Structure determination of compound 153

Images were measured on an Agilent SuperNova diffractometer (Cu $K\alpha$ radiation, mirror monochromator, λ = 1.54184 Å) and data extracted using the CrysAlis PRO package.[192] Structure solution was by direct methods (SIR92).[193] The structure was refined using the CRYSTALS program package.[194] Atomic coordinates, bond lengths and angles and displacement parameters have been deposited at the Cambridge Crystallographic Data Centre (CCDC no. 1590267). These data can be obtained free-of-charge via www.ccdc.cam.ac.uk/data_request/cif, by emailing data_request@ccdc.cam.ac.uk, or by contacting The Cambridge Crystallographic Data Centre, 12 Union Road, Cambridge CB2 1EZ, UK; fax: +44 1223 336033.

7.6.4. Crystallographic data for compound **154**:

Crystal data

Compound **154**. $C_{23}H_{18}N_2O_6$, M = 418.41, T = 150 K, monoclinic, space group $C2/c$, Z = 8, a = 23.9584 (7), b = 9.6484 (3), c = 16.0090 (6) Å, β = 90.165 (3)˚, V = 3700.6 (2) Å^3, D_x = 1.502 Mg m^{-3}, Mo$K\alpha$ radiation, λ = 0.71073 Å, 39146 reflections measured (θ = 2–29˚), merged to 4736 unique data, R = 0.044 [for 4495 data with $I > 2\sigma(I)$], R_w = 0.109 [all data], S = 1.03

Structure determination of compound 154

Images were measured on an Agilent SuperNova diffractometer (Mo $K\alpha$ radiation, mirror monochromator, λ = 0.71073 Å) and data extracted using the CrysAlis PRO package.[192] Structure solution was by direct methods (SIR92).[193] The structure was refined using the CRYSTALS program package.[194] Atomic coordinates, bond lengths and angles and displacement parameters have been deposited at the Cambridge Crystallographic Data Centre (CCDC no. 1590269). These data can be obtained free-of-charge via www.ccdc.cam.ac.uk/data_request/cif, by emailing data_request@ccdc.cam.ac.uk, or by contacting The Cambridge Crystallographic Data Centre, 12 Union Road, Cambridge CB2 1EZ, UK; fax: +44 1223 336033.

7.6.5. Crystallographic data for compound **155**:

Crystal data

Compound **154**. $C_{22}H_{18}N_2O_4$, M = 374.40, T = 150 K, orthorhombic, space group $P2_12_12_1$, Z = 4, a = 8.64640 (7), b = 11.41283 (8), c = 17.69376 (13) Å, V = 1746.02 (2) Å^3, D_x = 1.424 Mg m^{-3}, Cu$K\alpha$ radiation, λ = 1.54184 Å, 28445 reflections measured (θ = 5–72˚), merged to 3528 unique data, R = 0.030 [for 3486 data with $I > 2\sigma(I)$], R_w = 0.081 [all data], S = 1.00

Structure determination of compound 154

Images were measured on an Agilent SuperNova diffractometer (Cu $K\alpha$ radiation, mirror monochromator, λ = 1.54184 Å) and data extracted using the CrysAlis PRO package.[192] Structure solution was by direct methods (SIR92).[193] The structure was refined using the CRYSTALS program package.[194] Atomic coordinates, bond lengths and angles and displacement parameters have been deposited at the Cambridge Crystallographic Data Centre (CCDC no. 1590268). These data can be obtained free-of-charge via www.ccdc.cam.ac.uk/data_request/cif, by emailing data_request@ccdc.cam.ac.uk, or by contacting The Cambridge Crystallographic Data Centre, 12 Union Road, Cambridge CB2 1EZ, UK; fax: +44 1223 336033.

7.6.6. Crystallographic data for compound **180**:

Crystal data

Compound **180**. $C_{31}H_{25}N_3O_4S$, M = 535.62, T = 150 K, monoclinic, space group $P2_1/c$, Z = 4, a = 23.5193 (13), b = 11.6263 (7), c = 9.3856 (5) Å, β = 90.966(5)˚, V = 2566.1 (3) Å^3, D_x = 1.386 Mg m^{-3}, Cu$K\alpha$ radiation, λ = 1.54184 Å, 16907 reflections measured (θ = 4–72˚), merged to 4953 unique data, R = 0.071 [for 3162 data with $I > 2\sigma(I)$], R_w = 0.153 [all data], S = 1.01

Structure determination of compound 180

Images were measured on an Agilent SuperNova diffractometer (Cu $K\alpha$ radiation, mirror monochromator, λ = 1.54184 Å) and data extracted using the CrysAlis PRO package.[192] Structure solution was by direct methods (SIR92).[193] The structure was refined using the CRYSTALS program package.[194] Atomic coordinates, bond lengths and angles and displacement parameters have been deposited at the Cambridge Crystallographic Data Centre (CCDC no. 1590271). These data can be obtained free-of-charge via www.ccdc.cam.ac.uk/data_request/cif, by emailing data_request@ccdc.cam.ac.uk, or by contacting The Cambridge Crystallographic Data Centre, 12 Union Road, Cambridge CB2 1EZ, UK; fax: +44 1223 336033.

7.6.7. Crystallographic data for compound **183**:

Crystal data

Compound **183**. $2(C_{20}H_{16}N_2O_4).1.85(CH_2Cl_2).0.15(CHCl_3)$, M = 871.73, T = 150 K, orthorhombic, space group $P2_12_12_1$, Z = 4, a = 10.5565 (2), b = 14.9406 (2), c = 25.9563 (4) Å, V = 4093.84 (11) Å^3, D_x = 1.414 Mg m^{-3}, Cu$K\alpha$ radiation, λ = 1.54184 Å, 61022 reflections measured (θ = 3–64˚), merged to 7974 unique data, R = 0.068 [for 6934 data with $I > 2\sigma(I)$], R_w = 0.151 [all data], S = 0.98

Structure determination of compound 183.

Images were measured on an Agilent SuperNova diffractometer (Cu $K\alpha$ radiation, mirror monochromator, λ = 1.54184 Å) and data extracted using the CrysAlis PRO package.[192] Structure solution was by direct methods (SIR92).[193] The structure was refined using the CRYSTALS program package.[194] Atomic coordinates, bond lengths and angles and displacement parameters have been deposited at the Cambridge Crystallographic Data Centre (CCDC no. 1590270). These data can be obtained free-of-charge via www.ccdc.cam.ac.uk/data_request/cif, by emailing data_request@ccdc.cam.ac.uk, or by contacting The Cambridge Crystallographic Data Centre, 12 Union Road, Cambridge CB2 1EZ, UK; fax: +44 1223 336033.

7.6.8. Crystallographic data for compound **211**:

Crystal data
Compound **211**. $C_{27}H_{22}N_2O_3$, M = 422.28, T = 150 K, monoclinic, space group $P2_1/c$, Z = 4, a = 9.4461 (1), b = 10.2612 (1), c = 23.0912 (2), β = 100.4899 (8) ˚ V = 2200.78 (4) Å^3, D_x = 1.275 Mg m^{-3}, Cu$K\alpha$ radiation, λ = 1.54184 Å, 42054 reflections measured (θ = 4–74˚), merged to 4448 unique data, R = 0.031 [for 4255 data with $I > 2\sigma(I)$], R_w = 0.036 [all data], S = 1.00.

Structure determination of compound 211
Images were measured on an Agilent SuperNova diffractometer (Cu $K\alpha$ radiation, mirror monochromator, λ = 1.54184 Å) and data extracted using the CrysAlis PRO package.[192] Structure solution was by direct methods (SIR92).[193] The structure was refined using the CRYSTALS program package.[194]

7.6.9. Crystallographic data for compound **213**:

Crystal data
Compound **213**. $C_{26}H_{26}N_2O_6$, M = 462.50, T = 150 K, monoclinic, space group $C2/c$, Z = 4, a = 20.9084 (10), b = 7.3041 (2), c = 17.0572 (7), β = 100.4899 (8) ˚, V = 2383.40 (19) Å^3, D_x = 1.289 Mg m^{-3}, Mo$K\alpha$ radiation, λ = 0.71073 Å, 19845 reflections measured (θ = 2–30 ˚), merged to 3017 unique data, R = 0.033 [for 2600 data with $I > 2\sigma(I)$], R_w = 0.051 [all data], S = 1.04.

Structure determination of compound 213
Images were measured on an Agilent SuperNova diffractometer (Mo $K\alpha$ radiation, mirror monochromator, λ = 0.71073 Å) and data extracted using the CrysAlis PRO package.[192] Structure solution was by direct methods (SIR92).[193] The structure was refined using the CRYSTALS program package.[194]

7.6.10. Crystallographic data for compound **224**:

Crystal data
Compound **224**. $C_{28}H_{24}N_2O_4$, M = 452.51, T = 150 K, monoclinic, space group $P2_1/c$, Z = 4, a = 7.6361 (2), b = 13.7150 (3), c = 22.4168 (5), β = 98.156 (2) ˚, V = 2323.95 (10) Å^3, D_x = 1.293 Mg m^{-3}, Cu$K\alpha$ radiation, λ = 1.54184 Å, 4583 reflections measured (θ = 4–74˚), 4583 unique data, R = 0.062 [for 4398 data with $I > 2\sigma(I)$], R_w = 0.074 [all data], S = 1.00.

Structure determination of compound 224
Images were measured on an Agilent SuperNova diffractometer (Cu *K*α radiation, mirror monochromator, λ = 1.54184 Å) and data extracted using the CrysAlis PRO package.[192] Structure solution was by direct methods (SIR92).[193] The structure was refined using the CRYSTALS program package.[194]

7.6.11. Crystallographic data for compound **232**:

Crystal data
Compound **232**. $C_{27}H_{21}ClN_2O_3$, M = 456.93, T = 150 K, orthorhombic, space group $Pna2_1$, Z = 4, a = 18.76631 (12), b = 14.88559 (11), c = 7.88336 (7), V = 2202.21 (3) Å^3, D_x = 1.378 Mg m^{-3}, Cu$K\alpha$ radiation, λ = 1.54184 Å, 34133 reflections measured (θ = 2–74˚), merged to 4142 unique data, R = 0.024 [for 4091 data with $I > 2\sigma(I)$], R_w = 0.033 [all data], S = 1.01.

Structure determination of compound 232
Images were measured on an Agilent SuperNova diffractometer (Cu *K*α radiation, mirror monochromator, λ = 1.54184 Å) and data extracted using the CrysAlis PRO package.[192] Structure solution was by direct methods (SIR92).[193] The structure was refined using the CRYSTALS program package.[194]

7.6.12. Crystallographic data for compound **237**:

Crystal data
Compound **237**. $C_{25}H_{20}N_2O_3S$, M = 428.51, T=150 K, monoclinic, space group $P2_1/c$, Z = 4, a = 9.4271 (1), b = 10.0632 (1), c = 23.0963 (2), β = 101.1492 (11) ˚, V = 2149.72 (4) Å^3, D_x = 1.324 Mg m^{-3}, Cu$K\alpha$ radiation, λ = 1.54184 Å, 32752 reflections measured (θ = 5–72˚), merged to 4347 unique data, R = 0.034 [for 3948 data with $I > 2\sigma(I)$], R_w = 0.037 [all data], S = 1.00.

Structure determination of compound 237
Images were measured on an Agilent SuperNova diffractometer (Cu *K*α radiation, mirror monochromator, λ = 1.54184 Å) and data extracted using the CrysAlis PRO package.[192] Structure solution was by direct methods (SIR92).[193] The structure was refined using the CRYSTALS program package.[194]

Chapter 8:
References

[1] E. Stone, *Phil. Trans.* **1763**, *53*, 195-200.

[2] F. Sertürner, *Ann. Phys.* **1817**, *55*, 56-89.

[3] a) M. H. McCormick, J. M. McGuire, G. E. Pittenger, R. C. Pittenger, W. M. Stark, *Antibiot. Annu.* **1955**, *3*, 606-611; b) J. M. McGuire, R. N. Wolfe, D. W. Ziegler, *Antibiot. Annu.* **1955**, *3*, 612-618; c) R. S. Griffith, F. B. Peck, Jr., *Antibiot. Annu.* **1955**, *3*, 619-622; d) R. C. Anderson, H. M. Worth, P. N. Harris, K. K. Chen, *Antibiot. Annu.* **1956**, 75-81; e) C. C. Lee, R. C. Anderson, K. K. Chen, *Antibiot. Annu.* **1956**, 82-89.

[4] S. Omura, Y. Iwai, A. Hirano, A. Nakagawa, J. Awaya, H. Tsuchiya, Y. Takahashi, R. Asuma, *J. Antibiot.* **1977**, *30*, 275-282.

[5] D. S. Dalisay, B. I. Morinaka, C. K. Skepper, T. F. Molinski, *J. Am. Chem. Soc.* **2009**, *131*, 7552-7553.

[6] E. J. Corey, *Pure Appl. Chem.* **1967**, *14*, 19-38.

[7] J. Law, Z. Zsoldos, A. Simon, D. Reid, Y. Liu, S. Y. Khew, A. P. Johnson, S. Major, R. A. Wade, H. Y. Ando, *J. Chem. Inf. Model.* **2009**, *49*, 593-602.

[8] J. B. Hendrickson, *J. Am. Chem. Soc.* **1975**, *97*, 5784-5800.

[9] a) K. C. Nicolaou, C. K. Hwang, M. E. Duggan, D. A. Nugiel, Y. Abe, K. B. Reddy, S. A. DeFrees, D. R. Reddy, R. A. Awartani, *J. Am. Chem. Soc.* **1995**, *117*, 10227-10238; b) K. C. Nicolaou, E. A. Theodorakis, F. P. J. T. Rutjes, M. Sato, J. Tiebes, X. Y. Xiao, C. K. Hwang, M. E. Duggan, Z. Yang, *J. Am. Chem. Soc.* **1995**, *117*, 10239-10251; c) K. C. Nicolaou, F. P. J. T. Rutjes, E. A. Theodorakis, J. Tiebes, M. Sato, E. Untersteller, *J. Am. Chem. Soc.* **1995**, *117*, 10252-10263.

[10] G. Matsuo, K. Kawamura, N. Hori, H. Matsukura, T. Nakata, *J. Am. Chem. Soc.* **2004**, *126*, 14374-14376.

[11] K. C. Nicolaou, *Angew. Chem. Int. Ed.* **1996**, *35*, 588-607.

[12] a) M. D. Burke, S. L. Schreiber, *Angew. Chem. Int. Ed.* **2004**, *43*, 46-58; b) W. R. J. D. Galloway, A. Isidro-Llobet, D. R. Spring, *Nature Commun.* **2010**, *1*, 80.

[13] C. J. O' Connor, H. S. G. Beckmann, D. R. Spring, *Chem. Soc. Rev.* **2012**, *41*, 4444-4456.

[14] a) J. Kim, H. Kim, S. B. Park, *J. Am. Chem. Soc.* **2014**, *136*, 14629-14638; b) R. G. Doveston, P. Tosatti, M. Dow, D. J. Foley, H. Y. Li, A. J. Campbell, D. House, I. Churcher, S. P. Marsden, A. Nelson, *Org. Biomol. Chem.* **2015**, *13*, 859-865.

[15] D. G. Brown, J. Boström, *J. Med. Chem.* **2016**, *59*, 4443-4458.

[16] D. G. Brown, M. M. Gagnon, J. Boström, *J. Med. Chem.* **2015**, *58*, 2390-2405.

[17] R. Morgentin, M. Dow, A. Aimon, G. Karageorgis, T. Kalliokoski, D. Roche, S. Marsden, A. Nelson, *Drug Discov. Today* **2018**, *23*, 1578-1583.

[18] I. Colomer, C. J. Empson, P. Craven, Z. Owen, R. G. Doveston, I. Churcher, S. P. Marsden, A. Nelson, *Chem. Commun.* **2016**, *52*, 7209-7212.

[19] J. M. Rainard, G. C. Pandarakalam, S. P. McElroy, *SLAS DISCOVERY* **2018**, *23*, 225-241.

[20] A. Karawajczyk, F. Giordanetto, J. Benningshof, D. Hamza, T. Kalliokoski, K. Pouwer, R. Morgentin, A. Nelson, G. Müller, A. Piechot, D. Tzalis, *Drug Discov. Today* **2015**, *20*, 1310-1316.

[21] J. Meyers, M. Carter, N. Y. Mok, N. Brown, *Future Med. Chem.* **2016**, *8*, 1753-1767.

[22] a) A. L. Chandgude, D. Narducci, K. Kurpiewska, J. Kalinowska-Tłuścik, A.

Dömling, *RSC Adv.* **2017**, *7*, 49995-49998; b) E. M. M. Abdelraheem, R. Madhavachary, A. Rossetti, K. Kurpiewska, J. Kalinowska-Tłuścik, S. Shaabani, A. Dömling, *Org. Lett.* **2017**, *19*, 6176-6179; c) E. M. M. Abdelraheem, S. Khaksar, K. Kurpiewska, J. Kalinowska-Tłuścik, S. Shaabani, A. Dömling, *J. Org. Chem.* **2018**, *83*, 1441-1447; d) G. V. Janssen, J. A. C. van den Heuvel, R. P. Megens, J. C. J. Benningshof, H. Ovaa, *Bioorg. Med. Chem.* **2018**, *26*, 41-49; e) E. M. M. Abdelraheem, S. Khaksar, A. Dömling, *Synthesis* **2018**, *50*, 1027-1038; f) P. Patil, B. Mishra, G. Sheombarsing, K. Kurpiewska, J. Kalinowska-Tłuścik, A. Dömling, *ACS Comb. Sci.* **2018**, *20*, 70-74; g) T. Flagstad, C. M. G. Azevedo, G. Min, A. Willaume, R. Morgentin, T. E. Nielsen, M. H. Clausen, *Eur. J. Org. Chem.* **2018**, *2018*, 5023-5029.

[23] a) S. J. Cully, T. E. Storr, M. J. Rawling, I. R. Abeysena, D. Hamza, G. Jones, C. A. Pearce, A. Quddus, W. Lewis, R. A. Stockman, *Bioorg. Med. Chem.* **2016**, *24*, 5249-5257; b) B. D. Narhe, A. C. Breman, J. Padwal, D. A. L. Vandenput, J. M. Scheidt, J. C. J. Benningshof, G. A. van der Marel, H. S. Overkleeft, M. van der Stelt, D. V. Filippov, *Bioorg. Med. Chem.* **2017**, *25*, 5160-5170; c) G. C. Geary, A. Nortcliffe, C. A. Pearce, D. Hamza, G. Jones, C. J. Moody, *Bioorg. Med. Chem.* **2018**, *26*, 791-797; d) M. S. Santos, A. Nortcliffe, W. Lewis, T. D. Bradshaw, C. J. Moody, *Chem. Eur. J.* **2018**, *24*, 8325-8330; e) H. Hassan, S. P. Marsden, A. Nelson, *Bioorg. Med. Chem.* **2018**, *26*, 3030-3033; f) S. M. Wales, E. G. Merisor, H. V. Adcock, C. A. Pearce, I. R. Strutt, W. Lewis, D. Hamza, C. J. Moody, *Chem. Eur. J.* **2018**, *24*, 8233-8239; g) M. L. G. Borst, C. M. J. Ouairy, S. C. Fokkema, A. Cecchi, J. M. C. A. Kerckhoffs, V. L. de Boer, P. J. van den Boogaard, R. F. Bus, R. Ebens, R. van der Hulst, J. Knol, R. Libbers, Z. M. Lion, B. W. Settels, E. de Wever, K. A. Attia, P.-J. Sinnema, J. M. de Gooijer, K. Harkema, M. Hazewinkel, S. Snijder, K. Pouwer, *ACS Comb. Sci.* **2018**, *20*, 335-343; h) A. Aimon, G. Karageorgis, J. Masters, M. Dow, P. G. E. Craven, M. Ohsten, A. Willaume, R. Morgentin, N. Ruiz-Llamas, H. Lemoine, T. Kalliokoski, A. J. Eatherton, D. J. Foley, S. P. Marsden, A. Nelson, *Org. Biomol. Chem.* **2018**, *16*, 3160-3167.

[24] K. C. Nicolaou, D. Edmonds, P. Bulger, *Angew. Chem. Int. Ed.* **2006**, *45*, 7134−7186.

[25] L.-Q. Lu, J.-R. Chen, W.-J. Xiao, *Acc. Chem. Res.* **2012**, *45*, 1278-1293.

[26] a) K. C. Nicolaou, J. S. Chen, *Chem. Soc. Rev.* **2009**, *38*, 2993-3009; b) T. Newhouse, P. S. Baran, R. W. Hoffmann, *Chem. Soc. Rev.* **2009**, *38*, 3010-3021.

[27] R. Robinson, *J. Chem. Soc. Trans.* **1917**, *111*, 762-768.

[28] a) L. F. Tietze, *Chem. Rev.* **1996**, *96*, 115-136; b) K. Nicolaou, S. Snyder, T. Montagnon, G. Vassilikogiannakis, *Angew. Chem. Int. Ed.* **2002**, *41*, 1668-1698; c) L.-Q. Lu, J.-R. Chen, W.-J. Xiao, *Acc. Chem. Res.* **2012**, *45*, 1278–1293; d) Q. Liao, X. Yang, C. Xi, *J. Org. Chem.* **2014**, *79*, 8507-8515; e) L. J. Sebren, J. J. Devery, C. R. J. Stephenson, *ACS Catalysis* **2014**, *4*, 703-716.

[29] Z. Xiong, E. J. Corey, *J. Am. Chem. Soc.* **2000**, *122*, 4831-4832.

[30] Z. Xiong, E. J. Corey, *J. Am. Chem. Soc.* **2000**, *122*, 9328-9329.

[31] L. F. Tietze, U. Beifuss, *Angew. Chem. Int. Ed.* **1993**, *32*, 131-163.

[32] L.-F. Tietze, H. Stegelmeier, K. Harms, T. Brumby, *Angew. Chem. Int. Ed.* **1982**, *21*, 863-864.

[33] I. Ugi, *Angew. Chem. Int. Ed.* **1962**, *1*, 8-21.

[34] L. Kürti, B. Czakó, in *Strategic Applications of Named Reactions in Organic Synthesis*, Elsevier Academic Press, London, **2005**, pp. 462-463.

[35] D. Robbins, A. F. Newton, C. Gignoux, J.-C. Legeay, A. Sinclair, M. Rejzek, C.

A. Laxon, S. K. Yalamanchili, W. Lewis, M. A. O'Connell, R. A. Stockman, *Chem. Sci.* **2011**, *2*, 2232-2235.
[36] A. Sinclair, L. G. Arini, M. Rejzek, P. Szeto, R. A. Stockman, *Synlett* **2006**, *2006*, 2321-2324.
[37] M. S. Karatholuvhu, A. Sinclair, A. F. Newton, M.-L. Alcaraz, R. A. Stockman, P. L. Fuchs, *J. Am. Chem. Soc.* **2006**, *128*, 12656-12657.
[38] a) J.-C. Legeay, W. Lewis, R. A. Stockman, *Chem. Commun.* **2009**, 2207-2209; b) M. J. Rawling, T. E. Storr, W. A. Bawazir, S. J. Cully, W. Lewis, M. S. I. T. Makki, I. R. Strutt, G. Jones, D. Hamza, R. A. Stockman, *Chem. Commun.* **2015**, *51*, 12867-12870; c) T. E. Storr, S. J. Cully, M. J. Rawling, W. Lewis, D. Hamza, G. Jones, R. A. Stockman, *Bioorg. Med. Chem.* **2015**, *23*, 2621-2628.
[39] a) J. C. Splitstoser, T. D. Dillehay, J. Wouters, A. Claro, *Sci. Adv.* **2016**, *2*; b) C. Miliani, L. Monico, M. J. Melo, S. Fantacci, E. M. Angelin, A. Romani, K. Janssens, *Angew. Chem. Int. Ed.* **2018**, *57*, 7324-7334; c) A. E. Kramell, A. O. Brachmann, R. Kluge, J. Piel, R. Csuk, *RSC Adv.* **2017**, *7*, 12990-12997.
[40] a) H. Bauer, K. Kowski, H. Kuhn, W. Luttke, P. Rademacher, *J. Mol. Struct.* **1998**, *445*, 277−286; b) S. Yamazaki, A. L. Sobolewski, W. Domcke, *Phys. Chem. Chem. Phys.* **2011**, *13*, 1618-1628; c) H. Solís Correa, E. Ortiz, V. H. Uc, I. D. Barceló Quintal, J. L. Hernández Avila, *Mol. Simulat.* **2011**, *37*, 1085−1090.
[41] a) D. H. Rembert, *Econ. Bot.* **1979**, *33*, 128-134; b) R. J. H. Clark, C. J. Cooksey, M. A. M. Daniels, R. Withnall, *Endeavour* **1993**, *17*, 191-199; c) K. Hunger, in *Industrial Dyes: Chemistry, Properties, Applications* (Ed.: K. Hunger), Wiley-VCH, Darmstadt, Germany, **2003**, pp. 204-213; d) M. I. G. M. G. Travassob, P. C. S. Santosa, A. M. F. Oliveira-Camposa, M. M. M. Raposoa, N. Prasitpan, *Adv. Col. Sci. Tech.* **2003**, *6*, 95-99; e) S. P. Leite, J. R. Cardoso Vieira, P. Lys de Medeiros, R. M. Pereira Leite, *Evid.-Based Comp. Altern. Med.* **2006**, *3*, 261−265.
[42] a) A. Baeyer, *Ber. Dtsch. Chem. Ges.* **1878**, *11*, 1228-1229; b) A. Baeyer, V. Drewsen, *Ber. Dtsch. Chem. Ges.* **1882**, *15*, 2856-2864; c) A. Baeyer, *Chem. Ber.* **1883**, *16*, 2188-2204; d) A. de Meijere, *Angew. Chem. Int. Ed.* **2005**, *44*, 7836-7840.
[43] P. Miederer, in *Industrial Dyes: Chemistry, Properties, Applications* (Ed.: K. Hunker), Wiley VCH, Germany, **2003**, pp. 204-214.
[44] N. Stasiak, W. Kukula-Koch, K. Glowniak, *Acta. Pol. Pharm.* **2014**, *71*, 215-221.
[45] a) Y. Yoshihiro, I. Yoshihisa, T. Usaji, S. Hiroharu, *Bull. Chem. Soc. Jpn.* **2011**, *84*, 82-89; b) T. M. Hsu, D. H. Welner, Z. N. Russ, B. Cervantes, R. L. Prathuri, P. D. Adams, J. E. Dueber, *Nature Chem. Biol.* **2018**, *14*, 256.
[46] K. Heumann, *Ber. Dtsch. Chem. Ges.* **1890**, *23*, 3431-3435.
[47] a) Š. Komorsky-Lovrić, *J. Electroanal. Chem.* **2000**, *482*, 222-225; b) A. M. Bond, F. Marken, E. Hill, R. G. Compton, H. Hügel, *J. Chem. Soc., Perkin Trans. 2* **1997**, 1735-1742.
[48] A. Vuorema, *Ann. Univ. Turk. Ser. AI-388* **2008**, 1−72.
[49] a) M. Somei, H. Hayashi, S. Ohmoto, *Heterocycles* **1997**, *44*, 169-175; b) H. Hayashi, Y. Suzuki, M. Somei, *Heterocycles* **1999**, *51*, 1233-1235; c) M. Somei, F. Yamada, J. Kato, Y. Suzuki, Y. Ueda, *Heterocycles* **2002**, *56*, 81-84.
[50] a) O. L. Erdmann, *J. Prakt. Chem.* **1840**, *19*, 321-362; b) O. L. Erdmann, *J. Prakt. Chem.* **1841**, *24*, 1-18; c) W. C. Sumpter, F. M. Miler, in *Heterocyclic Compounds with Indole and Carbazole Systems*, Interscience Publishers, New York, **1954**, pp. 171-192; d) L. Kalb, *Ber. Dtsch. Chem. Ges.* **1909**, *42*, 3642–3652; e) J. v. Alphen, *Recl. Trav. Chim.* **1938**, *57*, 911-914.
[51] G. Beggiato, G. Casalboremiceli, A. Geri, D. Pietropaolo, *Anal. Chim.* **1993**, *83*,

355-363.
[52] A. J. Kettle, B. M. Clark, C. C. Winterbourn, *J. Biol. Chem.* **2004**, *279*, 18521–18525,.
[53] a) A. Binz, *Angew. Chem.* **1906**, *19*, 1415–1418; b) A. Binz, A. Kufferath, *Justus Liebigs Ann. Chem.* **1902**, *325*, 196–204; c) W. P. Bloxam, *J. Chem. Soc. Trans.* **1905**, *87*, 974-987.
[54] E. C. Nicholls-Allison, G. Nawn, B. O. Patrick, R. G. Hicks, *Chem. Commun.* **2015**, *51*, 12482-12485.
[55] J. E. Bailey, J. Travis, *Dyes Pigm.* **1985**, *6*, 135-154.
[56] E. Grandmougin, E. Dessoulavy, *Ber. Dtsch. Chem. Ges.* **1909**, *42*, 3636−3641.
[57] K. Christiane, B. Rainer, F. Manfred, G. Helmar, *J. Heterocyclic Chem.* **2006**, *43*, 1569−1574.
[58] S. Oakley, G. Nawn, K. Waldie, T. MacInnis, B. Patrick, R. Hicks, *Chem. Commun.* **2010**, *46*, 6753−6755.
[59] a) N. Kaltsoyannisa, P. Mountford, *J. Chem. Soc., Dalton Trans.* **1999**, 781-789; b) H. K. Hall, A. B. Padias, H. W. Boone, *J. Polym. Sci. A Polym. Chem.* **2007**, *45*, 4751−4763; c) O. Monaco, S. Tomas, M. Kirrane, A. Balija, *Beilstein J. Org. Chem.* **2013**, *9*, 2320−2327.
[60] G. Nawn, K. Waldie, S. Oakley, B. Peters, D. Mandel, B. Patrick, R. McDonald, R. Hicks, *Inorg. Chem.* **2011**, *50*, 9826−9837.
[61] a) S. Fortier, O. González-del Moral, C.-H. Chen, M. Pink, J. Le Roy, M. Murugesu, D. Mindiola, K. Caulton, *Chem. Commun.* **2012**, *48*, 11082−11084; b) G. Nawn, R. McDonald, R. Hicks, *Inorg. Chem.* **2013**, *52*, 10912−10919; c) G. Nawn, S. R. Oakley, M. B. Majewski, R. McDonald, B. O. Patrick, R. G. Hicks, *Chem. Sci.* **2013**, *4*, 612−621; d) M. Prasenjit, E. Fabian, B. Martina, D. Amit, M. M. Shaikh, K. Wolfgang, L. Goutam Kumar, *Inorg. Chem.* **2013**, *52*, 8467−8475.
[62] a) S. Hartmut, L. t. Wolfgang, *Angew. Chem. Int. Ed.* **1975**, *14*, 52; b) J. D. Thoburn, W. Lüttke, C. Benedict, H.-H. Limbach, *J. Am. Chem. Soc.* **1996**, *118*, 12459−12460.
[63] W. Borsche, R. Meyer, *Ber. Chem.* **1921**, *54*, 2854-2856.
[64] P. Seidel, *Ber. Chem. Dtsch. Ges.* **1945**, *77*, 788-797.
[65] J. Thiele, R. H. Pickard, *Ber. Chem.* **1898**, *31*, 1252-1253.
[66] W. Madelung, *Liebigs Ann.* **1914**, *405*, 58-95.
[67] F. Sachs, H. Kantorowicz, *Ber. Dtsch. Chem. Ges.* **1909**, *42*, 1565−1576.
[68] a) R. Pummerer, *Justus Liebigs Ann. Chem.* **1940**, *544*, 206-239; b) R. Pummerer, E. Stieglitz, *Ber. Dtsch. Chem. Ges.* **1942**, *75*, 1072-1085; c) C. D. Hurd, T. T. S. Wang, *J. Chem. Eng. Data* **1964**, *9*, 582-583.
[69] R. Pummerer, *Chem. Ber.* **1947**, *80*, 242-248.
[70] E. Grandmougin, *Ber. Dtsch. Chem. Ges.* **1909**, *42*, 4408–4411.
[71] T. L. Masterson, in *US Patent, Vol. 2036487* (Ed.: U. Patent), National Aniline & Chemical Company Inc., USA, p. 2.
[72] M. Darvekar, B. Ghorpade, P. S. Vankar, *Asian J. Chem.* **2004**, *16*, 965-970.
[73] E. Wolthuis, P. Nawiasky, *Vol. US 22700170 A*, United States, **1942**, pp. 1225-1125.
[74] L. Kalb, D. Berrer, *ibid* **1924**, *57*, 2105.
[75] J. van Alphen, *Recl. Trav. Chim. Pays-Bas* **1938**, *57*, 834-846.
[76] a) R. Crum, *Berz. Jahresb.* **1825**, *4*, 189; b) A. I. Vogel, *Ber. Dtsch. Chem. Ges.* **1878**, *11*, 1365.
[77] E. Grandmougin, *Comp. Rend.* **1921**, *173*, 586.
[78] K. Takeuchi, T. Ibusuki, *Anal. Chem.* **1989**, *61*, 619-623.

[79] J. D. Craik, D. Khan, R. Afifi, *J. Pelvic Med. Surg.* **2009**, *15*, 11-15.
[80] L. B. Jensen, *J. Near Eastern Stud.* **1963**, *22*, 104-118.
[81] P. E. McGovern, R. H. Michel, *Acc. Chem. Res.* **1990**, *23*, 152-165.
[82] a) A. Claus, M. E. Scheulen, *J. Prakt. Chem.* **1891**, *43*, 200-206; b) F. Sachs, R. Kempf, *Ber. Dtsch. Chem. Ges.* **1903**, *36*, 3299-3303; c) L. Ettinger, P. Friedlander, *Ber. Dtsch. Chem. Ges.* **1912**, *45*, 2074−2080; d) P. Friedländer, S. Bruckner, G. Deutsch, *Justus Liebigs Ann. Chem.* **1912**, *388*, 23-49; e) E. Grandmougin, P. Seyder, *Ber. Dtsch. Chem. Ges.* **1914**, *47*, 2365-2373; f) H. Waldmann, *J. Prakt. Chem.* **1930**, *126*, 65-68; g) R. Majima, M. Kotake, *Ber. Dtsch. Chem. Ges.* **1930**, *63B*, 2237-2245; h) F. Kröhnke, *Angew. Chem. Int. Ed.* **1963**, *2*, 380-393; i) G. Voss, H. Gerlach, *Chem. Ber.* **1989**, *122*, 1199-1201; j) P. Imming, I. Imhof, M. Zentgraf, *Synth. Commun.* **2001**, *31*, 153-159; k) C. J. Cooksey, *Molecules* **2001**, *6*, 736-739; l) Y. Tanoue, A. Terada, K. Sakata, M. Hashimoto, S. Morishita, M. Hamada, N. Kai, T. Nagai, *Fisheries Sci.* **2001**, *67*, 726-729; m) Y. Tanoue, K. Sakata, M. Hashimoto, M. Hamada, N. Kai, T. Nagai, *Dyes Pigm.* **2004**, *62*, 101-105.
[83] J. T. Baker, *Endeavor* **1974**, *33*, 11-17.
[84] W. Born, *Ciba Reu.* **1937**, *1*, 124-128.
[85] C. Cooksey, *Molecules* **2001**, *6*, 736-769.
[86] a) P. E. McGovern, R. H. Michel, *Acc. Chem. Res.* **1990**, *23*, 152-158; b) C. Christophersen, F. Wltjen, O. Buchardt, U. Anthoni, *Tetrahedron Lett.* **1977**, *20*, 1747-1748; c) C. Christophersen, F. Wätjen, O. Buchardt, U. Anthoni, *Tetrahedron* **1978**, *34*, 2779–2781.
[87] K. Benkendorff, J. B. Bremner, A. R. Davis, *J. Chem. Ecol.* **2000**, *26*, 1037-1050.
[88] a) K. Kunz, *Ber. Dtsch. Chem. Ges.* **1922**, *55*, 3688-3691; b) R. Kuhn, H. Machemer, *Ber. Dtsch. Chem. Ges.* **1928**, *61*, 118-127; c) H. Machemer, *J. Prakt. Chem.* **1930**, *127*, 109-168.
[89] W. Beck, C. Schmidt, R. Wienold, M. Steimunn, B. Wagner, *Angew. Chem. Int. Ed.* **1989**, *28*, 1529−1531.
[90] G. Boice, B. O. Patrick, R. McDonald, C. Bohne, R. Hicks, *J. Org. Chem.* **2014**, *79*, 9196-9205.
[91] P. Mondal, A. Das, G. K. Lahiri, *Inorg. Chem.* **2016**, *55*, 1208-1218.
[92] P. Mondal, M. Chatterjee, A. Paretzki, K. Beyer, W. Kaim, G. K. Lahiri, *Inorg. Chem.* **2016**, *55*, 3105-3116.
[93] M. Chatterjee, P. Ghosh, K. Beyer, A. Paretzki, J. Fiedler, W. Kaim, G. K. Lahiri, *Chem. Asian J.* **2018**, *13*, 118-125.
[94] R. Kuhn, H. Trischmann, *Chem. Ber.* **1961**, *94*, 2258−2263.
[95] T. Kitao, J. Sestune, *Kenkyu Hokoku - Asahi Garasu Kogyo Gijutsu Shoreikai* **1989**, *55*, 73-81.
[96] a) C. Liebermann, F. Dickhuth, *Ber. Dtsch. Chem. Ges.* **1891**, *24*, 4130-4136; b) J. Blanc, D. Ross, *J. Phys. Chem.* **1968**, *72*, 2817; c) T. Kitao, S.-i. Ishihara, J.-i. Setsune, K. Matsukawa, H. Wakemoto, R.-i. Yamamoto, *J. Chem. Soc., Chem. Commun.* **1982**, 1022-1023; d) E. D. Głowacki, G. Voss, K. Demirak, M. Havlicek, N. Sunger, A. C. Okur, U. Monkowius, J. Gasiorowski, L. Leonata, N. S. Sariciftcia, *Chem. Commun.* **2013**, *49*, 6063−6065; e) C. Guo, J. Quinn, B. Sun, Y. Li, *J. Mater. Chem. C* **2015**, *3*, 5226-5232.
[97] a) D. Farka, M. Scharber, E. D. Głowacki, N. S. Sariciftci, *J. Phys. Chem. A* **2015**, *119*, 3563-3568; b) C. Guo, J. Quinn, B. Sun, Y. Li, *Polym. Chem.* **2015**, *6*, 6998-7004; c) C.-Y. Huang, A. Bonasera, L. Hristov, Y. Garmshausen, B. M. Schmidt, D. Jacquemin, S. Hecht, *J. Am. Chem. Soc.* **2017**, *139*, 15205-15211.

[98] a) T. Posner, W. Kemper, *Ber. Dtsch. Chem. Ges.* **1924**, *57*, 1311-1315; b) T. Posner, R. Hofmeister, *Ber. Dtsch. Chem. Ges.* **1926**, *59*, 1827–1835.
[99] a) I. V. Klimovich, L. I. Leshanskaya, S. I. Troyanov, D. V. Anokhin, D. V. Novikov, A. A. Piryazev, D. A. Ivanov, N. N. Dremova, P. A. Troshin, *J. Mater. Chem. C* **2014**, *2*, 7621; b) O. Pitayatanakul, K. Iijima, M. Ashizawa, T. Kawamoto, H. Matsumotoa, T. Mori, *J. Mater. Chem. C* **2015**, *3*, 8612-8617.
[100] a) B. He, A. B. Pun, D. Zherebetskyy, Y. Liu, F. Liu, L. M. Klivansky, A. M. McGough, B. A. Zhang, K. Lo, T. P. Russell, L. Wang, Y. Liu, *J. Am. Chem. Soc.* **2014**, *136*, 15093-15101; b) B.-Y. Ren, Q. Xu, M. Kolaczkowski, C.-L. Sun, C.-J. Ou, Y.-G. Sun, L.-H. Xie, W. Huang, *Dyes Pigm.* **2019**, *160*, 25-27.
[101] J. van Alphen, *Recl. Trav. Chim. Pays-Bas* **1938**, *57*, 915-920.
[102] Y. Matsumoto, H. Tanaka, *Heterocycles* **2003**, *60*, 1805-1810.
[103] I. K. Kim, X. Li, M. Ullah, P. E. Shaw, R. Wawrzinek, E. B. Namdas, S.-C. Lo, *Adv. Mat.* **2015**, *27*, 6390-6395.
[104] a) P. Langer, M. Hein, D. Michalik, *Synthesis* **2005**, *2005*, 3531-3534; b) C. S. P. McErlean, J. Sperry, A. J. Blake, C. J. Moody, *Tetrahedron* **2007**, *63*, 10963-10970; c) J. Sperry, C. S. P. McErlean, A. M. Z. Slawin, C. J. Moody, *Tetrahedron Lett.* **2007**, *48*, 231-234; d) M. E. Zhidkov, A. V. Kantemirov, A. V. Koisevnikov, A. N. Andin, A. S. Kuzmich, *Tetrahedron Lett.* **2018**, *59*, 708-711.
[105] W. L. Mosby, in *Heterocyclic systems with bridgehead nitrogen atoms, part one*, Interscience Publishers Inc., New York, **1961**, pp. 239-451.
[106] R. Schwartz, *J. Prakt. Chem.* **1863**, *91*, 382.
[107] T. Posner, W. Zimmermann, S. Kautz, *Ber. Dtsch. Chem. Ges.* **1929**, *62*, 2150-2166.
[108] E. Dessoulavy, *Ber. Dtsch. Chem. Ges.* **1909**, *42*, 3636–3641.
[109] G. Engi, *Angew. Chem.* **1914**, *27*, 144-148.
[110] H. deDiesbach, E. Heppner, *Helv. Chim. Acta.* **1949**, *32*, 687-691.
[111] G. Rihs, A. Tzikas, *Dyes Pigm.* **1983**, *4*, 163-169.
[112] F. M. Lucius, B. Höchst, in *Frdl., Vol. 7* (Ed.: G. Pat.), Germany, **1903**, p. 637.
[113] B. D. Smith, D. E. Alonso, J. T. Bien, J. D. Zielinski, S. L. Smith, K. J. Haller, *J. Org. Chem.* **1993**, *58*, 6493−6496.
[114] B. D. Smith, D. E. Alonso, J. T. Bien, E. C. Metzler, M. Shang, J. M. I. Roosenberg, *J. Org. Chem.* **1994**, *59*, 8011−8014.
[115] a) M. K. Abdel-Hamid, J. B. Bremner, J. Coates, P. A. Keller, C. Miländer, Y. S. Torkamani, B. W. Skelton, A. H. White, A. C. Willis, *Tetrahedron Lett.* **2009**, *50*, 6947−6950; b) A. Shakoori, J. B. Bremner, M. K. Abdel-Hamid, A. C. Willis, R. Haritakun, P. A. Keller, *Beilstein J. Org. Chem.* **2015**, *11*, 481-492.
[116] a) A. Shakoori, J. B. Bremner, A. C. Willis, R. Haritakun, P. A. Keller, *J. Org. Chem.* **2013**, *78*, 7639−7647; b) A. Shakoori, Ph.D. thesis, University of Wollongong **2015**.
[117] a) F. Himo, T. Lovell, R. Hilgraf, V. V. Rostovtsev, L. Noodleman, K. B. Sharpless, V. V. Fokin, *J. Am. Chem. Soc.* **2005**, *127*, 210-216; b) H. C. Kolb, M. G. Finn, K. B. Sharpless, *Angew. Chem. Int. Ed.* **2001**, *40*, 2004-2021.
[118] L. Brandsma, *Synthesis of acetylenes, allenes and cumulenes: methods and techniques*, Elsevier Academic Press, Oxford, United Kingdom, **2004**.
[119] a) M. Bera, S. Roy, *J. Org. Chem.* **2009**, *74*, 8814-8817; b) X. Chen, T. Chen, Y. Zhou, C.-T. Au, L.-B. Han, S.-F. Yin, *Org. Biomol. Chem.* **2013**, *12*, 247-250; c) Y. Hu, C. Wang, D. Wang, F. Wu, B. Wan, *Org. Lett.* **2013**; d) G. J. Jiang, Q. H. Zheng, M. Dou, L. G. Zhuo, W. Meng, Z. X. Yu, *J. Org. Chem.* **2013**, *78*, 11783-11793; e) N. D. Schley, G. C. Fu, *J. Am. Chem. Soc.* **2014**, *136*, 16588-16593; f)

T. D. Montgomery, A. E. Nibbs, Y. Zhu, V. H. Rawal, *Org. Lett.* **2014**, *16*, 3480-3483; g) M. A. Omar, W. Frey, J. Conrad, U. Beifuss, *J. Org. Chem.* **2014**, *79*, 10367-10377; h) M. Dell'Acqua, V. Pirovano, G. Confalonieri, A. Arcadi, E. Rossi, G. Abbiati, *Org. Biomol. Chem.* **2014**, *12*, 8019-8030; i) Y. He, S. Guo, X. Zhang, X. Fan, *J. Org. Chem.* **2014**, *79*, 10611-10618; j) A. E. Nibbs, T. D. Montgomery, Y. Zhu, V. H. Rawal, *J. Org. Chem.* **2015**, *80*, 4928-4941.

[120] a) D. Tejedor, G. Méndez-Abt, L. Cotos, F. García-Tellado, *Chem. Soc. Rev.* **2013**, *42*, 458−471; b) K. Lauder, A. Toscani, N. Scalacci, D. Castagnolo, *Chem. Rev.* **2017**, *117*, 14091-14200; c) G. G. Melikyan, *Acc. Chem. Res.* **2015**, *48*, 1065-1079.

[121] a) N. Marion, R. S. Ramón, S. P. Nolan, *J. Am. Chem. Soc.* **2009**, *131*, 448-449; b) F. Li, N. Wang, L. Lu, G. Zhu, *J. Org. Chem.* **2015**, *80*, 3538-3546; c) N. Ghosh, S. Nayak, A. K. Sahoo, *J. Org. Chem.* **2011**, *76*, 500-511; d) W. Wang, B. Xu, G. B. Hammond, *J. Org. Chem.* **2009**, *74*, 1640-1643; e) L. Xie, Y. Wu, W. Yi, L. Zhu, J. Xiang, W. He, *J. Org. Chem.* **2013**, *78*, 9190-9195.

[122] S. Li, Z. Li, Y. Yuan, D. Peng, Y. Li, L. Zhang, Y. Wu, *Org. Lett.* **2012**, *14*, 1130-1133.

[123] H. Jin, L. Huang, J. Xie, M. Rudolph, F. Rominger, A. S. K. Hashmi, *Angew. Chem. Int. Ed.* **2016**, *55*, 794-797.

[124] H. Jin, B. Tian, X. Song, J. Xie, M. Rudolph, F. Rominger, A. S. K. Hashmi, *Angew. Chem. Int. Ed.* **2016**, *55*, 12688-12692.

[125] a) L. Jin, D. R. Tolentino, M. Melaimi, G. Bertrand, *Sci. Adv.* **2015**, *1*, e1500304; b) M. S. Ziegler, K. V. Lakshmi, T. D. Tilley, *J. Am. Chem. Soc.* **2017**, *139*, 5378-5386.

[126] B. T. Worrell, J. A. Malik, V. V. Fokin, *Science* **2013**, *340*, 457-460.

[127] P. M. McCosker, P. A. Keller, *Unpublished Results* **2019**.

[128] N. Miyaura, A. Suzuki, *Org. Synth.* **1990**, *68*, 130.

[129] a) M. Nendel, L. M. Tolbert, L. E. Herring, M. N. Islam, K. N. Houk, *J. Org. Chem.* **1999**, *64*, 976-983; b) K. J. Daoust, S. M. Hernandez, K. M. Konrad, I. D. Mackie, J. Winstanley, R. P. Johnson, *J. Org. Chem.* **2006**, *71*, 5708-5714; c) J. S. Barber, M. M. Yamano, M. Ramirez, E. R. Darzi, R. R. Knapp, F. Liu, K. N. Houk, N. K. Garg, *Nature Chem.* **2018**, *10*, 953-960.

[130] R. J. Gillespie, *Coord. Chem. Rev.* **2008**, *252*, 1315-1327.

[131] a) H. A. Bent, *Chem. Rev.* **1961**, *61*, 275-311; b) J. P. Foster, F. Weinhold, *J. Am. Chem. Soc.* **1980**, *102*, 7211-7218; c) I. V. Alabugin, S. Bresch, M. Manoharan, *J. Phys. Chem. A* **2014**, *118*, 3663-3677; d) I. V. Alabugin, S. Bresch, G. Passos Gomes, *J. Phys. Org. Chem.* **2015**, *28*, 147-162.

[132] A. Padwa, S. S. Murphree, *ARKIVOC* **2006**, 6-33.

[133] a) X. E. Hu, *Tetrahedron* **2004**, *60*, 2701-2743; b) P. Lu, *Tetrahedron* **2010**, *66*, 2549-2560; c) C.-Y. Huang, A. G. Doyle, *Chem. Rev.* **2014**, *114*, 8153-8198; d) G. Fumagalli, S. Stanton, J. F. Bower, *Chem. Rev.* **2017**, *117*, 9404-9432.

[134] P. Wyatt, S. Warren, in *Organic Synthesis: Strategy and Control*, John Wiley and Sons, Ltd., West Sussex, England, **2007**, pp. 465-503.

[135] a) H. M. I. Osborn, J. Sweeney, *Tetrahedron Asymm.* **1997**, *8*, 1693-1715; b) J. B. Sweeney, *Chem. Soc. Rev.* **2002**, *31*, 247-258; c) H. Pellissier, *Adv. Synth. Catal.* **2014**, *356*, 1899-1935.

[136] a) A. S. Pell, G. Pilcher, *Trans. Faraday Soc.* **1965**, *61*, 71-77; b) R. E. Parker, N. S. Isaacs, *Chem. Rev.* **1959**, *59*, 737-799.

[137] I. Vilotijevic, T. F. Jamison, *Mar. Drugs* **2010**, *8*, 763-809.

[138] a) A. Rolfe, T. B. Samarakoon, P. R. Hanson, *Org. Lett.* **2010**, *12*, 1216-1219; b)

J. Zhou, Y.-Y. Yeung, *Org. Lett.* **2014**, *16*, 2134-2137; c) L. Wei, L. Liu, J. Zhang, *Org. Biomol. Chem.* **2014**, *12*, 6869-6877; d) N. C. Ghosal, S. Santra, G. V. Zyryanov, A. Hajra, A. Majee, *Tetrahedron Lett.* **2016**, *57*, 3551-3555.

[139] a) M. D'hooghe, I. Kerkaert, M. Rottiers, N. De Kimpe, *Tetrahedron* **2004**, *60*, 3637-3641; b) M. D'hooghe, M. Rottiers, I. Kerkaert, N. De Kimpe, *Tetrahedron* **2005**, *61*, 8746–8751; c) M. D'hooghe, N. De Kimpe, *ARKIVOC* **2007**, 365-373; d) M. D'hooghe, N. De Kimpe, *ARKIVOC* **2008**, *9*, 6-19.

[140] a) M. J. Gresser, P. A. Keller, S. M. Wales, *Tetrahedron Lett.* **2009**, *50*; b) S. Wales, A. Willis, P. Keller, *Chem. Commun.* **2010**, *46*, 9226-9228; c) S. J. Bailey, S. M. Wales, A. C. Willis, P. A. Keller, *Org. Lett.* **2014**, *16*, 4344-4347; d) M. D. Kennedy, S. J. Bailey, S. M. Wales, P. A. Keller, *J. Org. Chem.* **2015**, *80*, 5992−5998.

[141] M. A. Robbins, P. N. Devine, T. Oh, *Org. Synth, Coll.* **2004**, *10*, 297.

[142] a) E. S. Shields, G. N. Merrill, *J. Phys. Org. Chem.* **2007**, *20*, 1058-1071; b) J. Gaca, G. Wejnerowska, P. Cysewski, *J. Phys. Org. Chem.* **2011**, *24*, 1045-1050.

[143] a) R. D. Adams, T. S. Barnard, K. Brosius, *J. Organomet. Chem.* **1999**, *582*, 358-361; b) B. N. Blackeit, J. M. Coxon, M. P. Hartshorn, A. J. Lewis, G. R. Littljz, G. J. Wright, *Tetrahedron* **1970**, *26*, 1311-1313; c) G. Li, B. Wanga, J. Wang, Y. Ding, L. Yan, J. Suo, *J. Mol. Catal. A. Chem.* **2005**, *236*, 72-76.

[144] S. Liang, H. Liu, T. Hiang, J. Song, G. Yang, B. Han, *Chem. Commun.* **2011**, *47*, 2131-2133.

[145] a) W. J. Gensler, *J. Am. Chem. Soc.* **1948**, *70*, 1843-1846; b) M. Karikomi, M. D'Hooghe, G. Verniest, N. De Kimpe, *Org. Biomol. Chem.* **2008**, *6*, 1902-1904.

[146] M. D'hooghe, B. De Meulenaer, N. De Kimpe, *Synlett* **2008**, 2437-2442.

[147] a) B. Zhao, W. Yuan, H. Du, Y. Shi, *Org. Lett.* **2007**, *9*, 4943-4945; b) S. De Jong, D. G. Nosal, D. J. Wardrop, *Tetrahedron* **2012**, *68*, 4067-4105; c) E. L. Ingalls, P. A. Sibbald, W. Kaminsky, F. E. Michael, *J. Am. Chem. Soc.* **2013**, *135*, 8854-8856; d) C. Röben, J. A. Souto, E. C. Escudero-Adán, K. Muñiz, *Org. Lett.* **2013**, *15*, 1008-1011; e) D. E. Olson, J. Y. Su, D. A. Roberts, J. Du Bois, *J. Am. Chem. Soc.* **2014**, *136*, 13506-13509; f) M. W. Danneman, K. B. Hong, J. N. Johnston, *Org. Lett.* **2015**, *17*, 2558-2561; g) C. Martínez, E. G. Pérez, Á. Iglesias, E. C. Escudero-Adán, K. Muñiz, *Org. Lett.* **2016**, *18*, 2998-3001; h) K. Muñiz, L. Barreiro, R. M. Romero, C. Martínez, *J. Am. Chem. Soc.* **2017**, *139*, 4354-4357.

[148] a) K. B. Sharpless, D. W. Patrick, L. K. Truesdale, S. A. Biller, *J. Am. Chem. Soc.* **1975**, *97*, 2305-2307; b) T. Katsuki, K. B. Sharpless, *J. Am. Chem. Soc.* **1980**, *102*, 5974-5976; c) K. Morikawa, J. Park, P. G. Andersson, T. Hashiyama, K. B. Sharpless, *J. Am. Chem. Soc.* **1993**, *115*, 8463-8464.

[149] a) E. M. Gerstenzang, *J. Chem. Educ.* **1931**, *8*, 1187-1189; b) S. Sussman, *J. Chem. Educ.* **1932**, *9*, 1652-1653.

[150] a) I. Ungureanu, P. Klotz, A. Mann, *Angew. Chem. Int. Ed.* **2000**, *39*, 4615-4617; b) Y.-M. Huang, C.-W. Zheng, L. Pan, Q.-W. Jin, G. Zhao, *J. Org. Chem.* **2015**, *80*, 10710-10718; c) J. Yin, C. J. T. Hyland, *Asian J. Org. Chem.* **2016**, *5*, 1368-1377.

[151] D. X. Hu, P. Grice, S. V. Ley, *J. Org. Chem.* **2012**, *77*, 5198-5202.

[152] P. Atkins, J. De Paula, *Atkins' Physical Chemistry*, 9th ed., Oxford University Press, Oxford, UK, **2010**.

[153] D. Seyferth, *Organometallics* **2009**, *28*, 1598-1605.

[154] P. Knochel, W. Dohle, N. Gommermann, F. F. Kneisel, F. Kopp, T. Korn, I. Sapountzis, V. A. Vu, *Angew. Chem. Int. Ed.* **2003**, *42*, 4302-4320.

[155] a) L. Boymond, M. Rottländer, G. Cahiez, P. Knochel, *Angew. Chem. Int. Ed.*

1998, *37*, 1701-1703; b) I. Sapountzis, H. Dube, R. Lewis, N. Gommermann, P. Knochel, *J. Org. Chem.* **2005**, *70*, 2445-2454; c) N. M. Barl, V. Werner, C. Saemann, P. Knochel, *Heterocycles* **2014**, *88*, 827-844; d) D. S. Ziegler, B. Wei, P. Knochel, *Chem. Eur. J.* **2019**, *25*, 2695-2703.

[156] a) A. Krasovskiy, P. Knochel, *Angew. Chem. Int. Ed.* **2004**, *43*, 3333-3336; b) D. Hauk, S. Lang, A. Murso, *Org. Proc. Res. Dev.* **2006**, *10*, 733-738.

[157] a) V. Snieckus, *Chem. Rev.* **1990**, *90*, 879-933; b) A. Unsinn, C. J. Rohbogner, P. Knochel, *Adv. Synth. Catal.* **2013**, *355*, 1553-1560.

[158] a) D. R. Armstrong, W. Clegg, S. H. Dale, E. Hevia, L. M. Hogg, G. W. Honeyman, R. E. Mulvey, *Angew. Chem. Int. Ed.* **2006**, *45*, 3775-3778; b) A. J. Martínez-Martínez, A. R. Kennedy, R. E. Mulvey, C. T. O'Hara, *Science* **2014**, *346*, 834-837; c) C. J. Rohbogner, G. C. Clososki, P. Knochel, *Angew. Chem. Int. Ed.* **2008**, *47*, 1503-1507; d) J. P. Flemming, M. B. Berry, J. M. Brown, *Org. Biomol. Chem.* **2008**, *6*, 1215-1221; e) R. J. Phipps, M. J. Gaunt, *Science* **2009**, *323*, 1593-1597; f) B. Chen, X.-L. Hou, Y.-X. Li, Y.-D. Wu, *J. Am. Chem. Soc.* **2011**, *133*, 7668-7671; g) G. Yang, P. Lindovska, D. Zhu, J. Kim, P. Wang, R.-Y. Tang, M. Movassaghi, J.-Q. Yu, *J. Am. Chem. Soc.* **2014**, *136*, 10807-10813; h) L. Fang, T. G. Saint-Denis, B. L. H. Taylor, S. Ahlquist, K. Hong, S. Liu, L. Han, K. N. Houk, J.-Q. Yu, *J. Am. Chem. Soc.* **2017**, *139*, 10702-10714; i) J. Gorecka, C. Heiss, R. Scopelliti, M. Schlosser, *Org. Lett.* **2004**, *6*, 4591-4593; j) C. Heiss, E. Marzi, M. Schlosser, *Eur. J. Org. Chem.* **2003**, *2003*, 4625-4629.

[159] Commissioner, U.S. Food and Drug Administration, Press Release, https://www.fda.gov/newsevents/newsroom/pressannouncements/ucm555778.htm, retrieved 22/01/2019, **2017**.

[160] a) N. L. Segraves, S. J. Robinson, D. Garcia, S. A. Said, X. Fu, F. J. Schmitz, H. Pietraszkiewicz, F. A. Valeriote, P. Crews, *J. Nat. Prod.* **2004**, *67*, 783-792; b) X. Qi, H. Bao, U. K. Tambar, *J. Am. Chem. Soc.* **2011**, *133*, 10050-10053; c) S. Han, K. C. Morrison, P. J. Hergenrother, M. Movassaghi, *J. Org. Chem.* **2014**, *79*, 473-486; d) K. Daniel, K. Eva, D. Eric, S. Birgitta, S. P. H., B. Jan, *Eur. J. Org. Chem.* **2016**, 1389-1396.

[161] a) A. Z. Britten, G. F. Smith, *J. Chem. Soc. Perkin Trans. 1* **1972**, 418-420; b) S. B. Mahato, N. B. Mandal, S. Chattopadhyay, P. Luger, M. Weber, *Tetrahedron* **1995**, *51*, 12667-12676; c) T. Benincori, E. Brenna, F. Sannicolb, L. Trimarco, P. Antognazza, E. Cesarotti, F. Demartin, T. Pilati, G. Zotti, *J. Organomet. Chem.* **1997**, *529*, 445-453; d) C. Charlet-Fagnere, W.-Q. Jiang, L. Jean-Yves, *Tetrahedron Lett.* **1999**, *40*, 1685-1688; e) Y. Deng, T. Haimowitz, M. G. LaPorte, S. R. Rippin, M. D. Alexander, P. T. Kumar, M. S. Hendi, Y.-H. Lee, S. M. Condon, *ACS Med. Chem. Lett.* **2016**, *7*, 318-323.

[162] A. C. Lindsay, I. K. H. Leung, J. Sperry, *Org. Lett.* **2016**, *18*, 5404-5407.

[163] a) K. Hayashi, S. Hiki, T. Kumagai, Y. Nagao, *Heterocycles* **2002**, *56*, 433-442; b) R. Gianatassio, D. Kadish, *Org. Lett.* **2019**, *Article ASAP, DOI: 10.1021/acs.orglett.9b00321*.

[164] a) R. Gianatassio, J. M. Lopchuk, J. Wang, C.-M. Pan, L. R. Malins, L. Prieto, T. A. Brandt, M. R. Collins, G. M. Gallego, N. W. Sach, J. E. Spangler, H. Zhu, J. Zhu, P. S. Baran, *Science* **2016**, *351*, 241-246; b) J. M. Lopchuk, K. Fjelbye, Y. Kawamata, L. R. Malins, C.-M. Pan, R. Gianatassio, J. Wang, L. Prieto, J. Bradow, T. A. Brandt, M. R. Collins, J. Elleraas, J. Ewanicki, W. Farrell, O. O. Fadeyi, G. M. Gallego, J. J. Mousseau, R. Oliver, N. W. Sach, J. K. Smith, J. E. Spangler, H. Zhu, J. Zhu, P. S. Baran, *J. Am. Chem. Soc.* **2017**, *139*, 3209-3226.

[165] a) E. Najahi, A. Valentin, P.-L. Fabre, K. Reybier, F. Nepveu, *Eur. J. Med. Chem.*

2014, *78*, 269-274; b) S. Guo, F. Wang, L. Tao, X. Zhang, X. Fan, *J. Org. Chem.* **2018**, *83*, 3889-3896.
[166] C. F. Macrae, I. J. Bruno, J. A. Chisholm, P. R. Edgington, P. McCabe, E. Pidcock, L. Rodriguez-Monge, R. Taylor, J. van de Streek, P. A. Wood, *J. Appl. Cryst.* **2008**, *41*, 466-470.
[167] E. D. Glowacki, G. Voss, K. Demirak, M. Havlicek, N. Sunger, A. C. Okur, U. Monkowius, J. Gasiorowski, L. Leonat, N. S. Sariciftci, *Chem. Commun.* **2013**, *49*, 6063-6065.
[168] P. Calí, M. Begtrup, *Synthesis* **2002**, *2002*, 63-66.
[169] J. E. Smyth, N. M. Butler, P. A. Keller, *Nat. Prod. Rep.* **2015**, *32*, 1562-1583.
[170] a) G. S. Reddy, R. T. Hobgood, J. H. Goldstein, *J. Am. Chem. Soc.* **1962**, *84*, 336-340; b) R. E. Wasylishen, G. Tomlinson, *Biochem. J.* **1975**, *147*, 605-607; c) S. Burling, L. D. Field, B. A. Messerle, S. L. Rumble, *Organometallics* **2007**, *26*, 4335-4343.
[171] a) C. Li, Y. Go, Z. Mao, K. Koyano, Y. Kai, N. Kanehisa, Q. Zhu, Z. Zhou, S. Wu, *Bull. Chem. Soc. Jpn.* **1996**, *69*, 1621-1627; b) J.-Y. Shim, Y.-J. Chang, S.-U. Kim, *Biotechnol. Lett.* **1998**, *20*, 1139-1143; c) R. Hoessel, S. Leclerc, J. A. Endicott, M. E. M. Nobel, A. Lawrie, P. Tunnah, M. Leost, E. Damiens, D. Marie, D. Marko, E. Niederberger, W. Tang, G. Eisenbrand, L. Meijer, *Nat. Cell Biol.* **1999**, *1*, 60-67; d) T. Kunikata, T. Tatefuji, H. Aga, K. Iwaki, M. Ikeda, M. Kurimoto, *Eur. J. Pharmacol.* **2000**, *410*, 93-100; e) D. Marko, S. Schatzle, A. Friedel, A. Genzlinger, H. Zankl, L. Meijer, G. Eisenbrand, *Br. J. Cancer* **2001**, *84*, 283-289; f) L. Meijer, A.-L. Skaltsounis, P. Magiatis, P. Polychronopoulos, M. Knockaert, M. Leost, X. P. Ryan, C. A. Vonica, A. Brivanlou, R. Dajani, C. Crovace, C. Tarricone, A. Musacchio, S. M. Roe, L. Pearl, P. Greengard, *Chem. Biol.* **2003**, *10*, 1255-1266; g) G. Eisenbrand, F. Hippe, S. Jakobs, S. Muehlbeyer, *J. Cancer Res. Clin. Oncol.* **2004**, *130*, 627-635; h) P. Polychronopoulos, P. Magiatis, A.-L. Skaltsounis, V. Myrianthopoulos, E. Mikros, A. Tarricone, A. Musacchio, S. M. Roe, L. Pearl, M. Leost, P. Greengard, L. Meijer, *J. Med. Chem.* **2004**, *47*, 935-946; i) R. Jautelat, T. Brumby, H. Briem, S. Schwahn, O. Prien, G. Eisenbrand, M. Kruger, G. Siemeister, *ChemBioChem* **2005**, *6*, 531 –540; j) S.-G. Ahn, J. I. Kim, S. W. Kim, T. S. Kim, Y.-C. Kim, S. K. Lee, M. J. Moon, J.-H. Yoon, **2005**; k) M. J. Moon, S. K. Lee, J. W. Lee, W. K. Song, S. W. Kim, J. I. Kim, C. Cho, S. J. Choi, Y. C. Kim, *Bioorg. Med. Chem.* **2006**, *14*, 237-246; l) Y. Ferandin, K. Bettayeb, M. Kritsanida, O. Lozach, P. Polychronopoulos, P. Magiatis, A.-L. Skaltsounis, L. Meijer, *J. Med. Chem.* **2006**, *49*, 4638-4649; m) A. Beauchard, Y. Ferandin, S. Frere, O. Lozach, M. Blairvacq, L. Meijer, V. Thiery, T. Besson, *Bioorg. Med. Chem.* **2006**, *14*, 6434-6443; n) L. Meijer, J. Shearer, K. Bettayeb, Y. Ferandin, *Int. Congr. Ser.* **2007**, *1304*, 60-74; o) S. Libnow, K. Methling, M. Hein, D. Michalik, M. Harms, K. Wende, A. Flemming, M. Koeckerling, H. Reinke, P. J. Bednarski, M. Lalk, P. Langer, *Bioorg. Med. Chem.* **2008**, *16*, 5570-5583; p) K. Vougogiannopoulou, Y. Ferandin, K. Bettayeb, V. Myrianthopoulos, O. Lozach, Y. Fan, C. H. Johnson, P. Magiatis, A.-L. Skaltsounis, E. Mikros, L. Meijer, *J. Med. Chem.* **2008**, *51*, 6421-6431; q) Z. Wang, Y. Wang, M. Feng, X. Tan, J. Cheng, W. Hua, Q. Yao, *Chin. J. Org. Chem.* **2009**, *29*, 1606-1610; r) M. Kritsanida, P. Magiatis, A.-L. Skaltsounis, Y. Peng, P. Li, L. P. Wennogle, *J. Nat. Prod.* **2009**, *72*, 2199-2202; s) S. Zhang, Y. Zhang, L. Xu, X. Lin, J. Lu, Q. Di, J. Shi, J. Xu, *Neurosci. Lett.* **2009**, *450*, 142-146; t) S.-J. Choi, J.-E. Lee, S.-Y. Jeong, I. Im, S.-D. Lee, E.-J. Lee, S. K. Lee, S.-M. Kwon, S.-G. Ahn, J.-H. Yoon, S.-Y. Han, J.-I. Kim, Y.-C. Kim, *J. Med. Chem.*

2010, *53*, 3696-3706; u) X. Cheng, P. Rasque, S. Vatter, K.-H. Merz, G. Eisenbrand, *Bioorg. Med. Chem.* **2010**, *18*, 4509-4515; v) T. C. Wang, J. Z. Wei, C. S. Guo, H. B. Zhang, H. X. Fan, *Chin. Chem. Lett.* **2010**, *21*, 1407-1410; w) A. V. Schwaiberger, E. H. Heiss, M. Cabaravdic, T. Oberan, J. Zaujec, D. Schachner, P. Uhrin, A. G. Atanasov, J. M. Breuss, B. R. Binder, V. M. Dirsch, *Arterioscler., Thromb., Vasc. Biol.* **2010**, *30*, 2475-2481; x) D. Alex, I. K. Lam, Z. X. Lin, S. M. Y. Lee, *J. Ethnopharmacol.* **2010**, *131*, 242-247; y) M. Kunz, K. M. Driller, M. Hein, S. Libnow, I. Hohensee, R. Ramer, B. Hinz, A. Berger, J. Eberle, P. Langer, *ChemMedChem* **2010**, *5*, 534-539; z) S.-A. Kim, S.-M. Kwon, J.-A. Kim, K. W. Kang, J.-H. Yoon, S.-G. Ahn, *Cancer Lett.* **2011**, *306*, 197-204; aa) S. P. Williams, M. O. Nowicki, F. Liu, R. Press, J. Godlewski, M. Abdel-Rasoul, B. Kaur, S. A. Fernandez, E. A. Chiocca, S. E. Lawler, *Cancer Res.* **2011**, *71*, 5374-5380; ab) H. Saito, K. Tabata, S. Hanada, Y. Kanda, T. Suzuki, S. Miyairi, *Bioorg. Med. Chem. Lett.* **2011**, *21*, 5370-5373; ac) G. Karapetyan, K. Chakrabarty, M. Hein, P. Langer, *ChemMedChem* **2011**, *6*, 25-37; ad) L. Martin, A. Magnaudeix, C. M. Wilson, C. Yardin, F. Terro, *J. Neurosci. Res.* **2011**, *89*, 1802-1811; ae) H. M. Riepl, C. Urmann, *Helv. Chim. Acta* **2012**, *95*, 1461-1477; af) F. Erben, D. Kleeblatt, M. Sonneck, M. Hein, H. Feist, T. Fahrenwaldt, C. Fischer, A. Matin, J. Iqbal, M. Plotz, J. Eberle, P. Langer, *Org. Biomol. Chem.* **2013**, *11*, 3963-3978; ag) X. Cheng, K. H. Merz, S. Vatter, J. Christ, S. Wolfl, G. Eisenbrand, *Bioorg. Med. Chem.* **2014**, *22*, 247-255.

[172] R. P. Maskey, I. Grun-Wollny, H. H. Fiebig, H. Laatsch, *Angew. Chem. Int. Ed.* **2002**, *41*, 597-599.

[173] X. Y. Wei, C. Y. Leung, C. K. C. Wong, X. L. Shen, R. N. S. Wong, Z. W. Cai, N. K. Mak, *J. Nat. Prod.* **2005**, *68*, 427-429.

[174] K. P. Lai, N. K. Mak, X. Wei, R. N. S. Wong, M. H. Wong, C. K. C. Wong, *Toxicology* **2006**, *226*, 188-196.

[175] N. T. H. Yen, H. Ibrahim, K. Reybier, P. Perio, F. Souard, E. Najahi, P.-L. Fabre, F. Nepveu, *J. Inorg. Biochem.* **2013**, *126*, 7-16.

[176] F. Nepveu, S. Kim, J. Boyer, O. Chatriant, H. Ibrahim, K. Reybier, M.-C. Monje, S. Chevalley, P. Perio, B. H. Lajoie, J. Bouajila, E. Deharo, M. Sauvain, R. Tahar, L. Basco, A. Pantaleo, F. Turini, P. Arese, A. Valentin, E. Thompson, L. Vivas, S. Petit, J.-P. Nallet, *J. Med. Chem.* **2010**, *53*, 699-714.

[177] A. Pantaleo, E. Ferru, R. Vono, G. Giribaldi, O. Lobina, F. Nepveu, H. Ibrahim, J.-P. Nallet, F. Carta, F. Mannu, P. Pippia, E. Campanella, P. S. Low, F. Turrini, *Free Rad. Biol. Med.* **2012**, *52*, 527-536.

[178] D. J. Henry, C. J. Parkinson, P. M. Mayer, L. Radom, *J. Phys. Chem. A* **2001**, *105*, 6750-6756.

[179] G. Harms, E. Schaumann, G. Adiwidjaja, *Synthesis* **2001**, 577-580.

[180] D. A. Evans, M. M. Faul, M. T. Bilodeau, B. A. Anderson, D. M. Barnes, *J. Am. Chem. Soc.* **1993**, *115*, 5328-5329.

[181] M. Rottmann, C. McNamara, B. K. S. Yeung, M. C. S. Lee, B. Zou, B. Russell, P. Seitz, D. M. Plouffe, N. V. Dharia, J. Tan, S. B. Cohen, K. R. Spencer, G. E. González-Páez, S. B. Lakshminarayana, A. Goh, R. Suwanarusk, T. Jegla, E. K. Schmitt, H.-P. Beck, R. Brun, F. Nosten, L. Renia, V. Dartois, T. H. Keller, D. A. Fidock, E. A. Winzeler, T. T. Diagana, *Science* **2010**, *329*, 1175-1180.

[182] J. Wolfard, J. Xu, H. Zhang, C. K. Chung, *Org. Lett.* **2018**, *20*, 5431-5434.

[183] a) H. S. Mosher, L. Turner, A. Carlsmith, *Org. Synth.* **1953**, *33*, 79; b) R. S. Varma, K. P. Naicker, *Org. Lett.* **1999**, *1*, 189-192.

[184] R. M. Letcher, D. W. M. Sin, K.-K. Cheung, *J. Chem. Soc. Perkin Trans. 1* **1993**,

939-944.
[185] W. Zhang, L. Ma, S. Li, Z. Liu, Y. Chen, H. Zhang, G. Zhang, Q. Zhang, X. Tian, C. Yuan, S. Zhang, W. Zhang, C. Zhang, *J. Nat. Prod.* **2014**, *77*, 1887-1892.
[186] R. Bernini, S. Cacchi, G. Fabrizi, G. Forte, F. Petrucci, A. Prastaro, S. Niembro, A. Shafir, A. Vallribera, *Green Chem.* **2010**, *12*, 150-158.
[187] Y.-J. Shang, L.-B. Ren, D.-M. Wang, *Chin. J. Chem.* **2007**, *25*, 1202-1206.
[188] A. C. Huitric, W. P. Gordon, S. D. Nelson, *J. Chem. Eng. Data* **1982**, *27*, 474-475.
[189] T. Ando, D. Kano, S. Minakata, I. Ryu, M. Komatsu, *Tetrahedron* **1998**, *54*, 13485-13494.
[190] P. W. Feit, O. T. Nielsen, *J. Med. Chem.* **1970**, *13*, 447-452.
[191] S. Duffy, V. M. Avery, *Am. J. Trop. Med. Hyg.* **2012**, *86*, 84-92.
[192] CrysAlis PRO, Agilent Technologies, Version 1.171.37.21t, Yarnton, Oxfordshire, England, **2013**
[193] A. Altomare, G. Cascarano, C. Giacovazzo, A. Guagliardi, M. C. Burla, G. Polidori, M. Camalli, *J. Appl. Crystallogr.* **1994**, *27*, 435.
[194] P. W. Betteridge, J. R. Carruthers, R. I. Cooper, K. Prout, D. J. Watkin, *J. Appl. Crystallogr.* **2003**, *36*, 1487.